

**STUDY OF MANGROVE ROOT ARCHITECTURE,
ANATOMICAL ADAPTATIONS AND MANGROVE
MICROBE INTERACTIONS IN THE RHIZOSPHERE
CONTRIBUTING TO THE SOIL ENVIRONMENT
UNDER DEGRADED AND NON-DEGRADED
MANGROVE HABITATS.**

**Thesis submitted for the Degree of
Doctor of Philosophy (Science)**

**In
Microbiology**

by

Biswajit Biswas

Post Graduate and Research Department of Microbiology

St. Xavier's College (Autonomous)

Kolkata

**[Affiliated to the University of Calcutta (Regulation for the
Degree of Doctor of Philosophy, Ph.D.), Regulations 2015]**

2024



ST. XAVIER'S COLLEGE (AUTONOMOUS), KOLKATA
KOLKATA – 700 016

DECLARATION BY SUPERVISOR

I, certify, that the thesis entitled “study of mangrove root architecture, anatomical adaptations and mangrove microbe interactions in the rhizosphere contributing to the soil environment under degraded and non-degraded mangrove habitats” submitted by Biswajit Biswas for the degree of Doctor of Philosophy (Ph.D.) in Science in the area of Microbiology is the record of research work carried out by him during the period from May 2017 to April 2024 under my guidance and supervision, and that this work has not formed the basis for the award of any Degree, Diploma, Associateship, Fellowship, Titles in this University or any other University or other similar institution of Higher learning.

Sandip Kumar Basak

Principal
Sarat Centenary College
Dhaniakhali, Hooghly

Signature of Co-Supervisor

Signature of the Supervisor

Place: Kolkata

Date:

Post Graduate and Research Department: Microbiology

Address: St. Xavier's College (Autonomous), Kolkata

PLAGIARISM CERTIFICATE
DECLARATION BY CANDIDATE

I, Biswajit Biswas (Ph.D Registration No. **PhD/16/MCB/02**) hereby declare that I am the sole author of the thesis entitled study of mangrove root architecture, anatomical adaptations and mangrove microbe interactions in the rhizosphere contributing to the soil environment under degraded and non-degraded mangrove habitats and that neither any part of the thesis nor the whole of the thesis has been submitted to any University or Institution for obtaining any degree / diploma / academic award.

I declare, to the best of my knowledge that my thesis work is free of any kind of plagiarism and does not breach upon anyone's ideas, techniques, copyright or quotations. The materials from the work of other people which has been included in my study have been acknowledged according to the standard reference practices.

I declare that this is the ORIGINAL thesis.

I shall be solely responsible for any dispute or plagiarism issue arising out of the doctoral thesis.

The doctoral thesis was scanned using iThenticate software for similarity detection by the Ph.D Office of St. Xavier's College (Autonomous) Kolkata and the similarity index¹ is as follows:

Similarity Index: 2%

Name of the Candidate : Biswajit Biswas

Signature of the Candidate :

Name of the Supervisor (s) : Dr. Mahashweta Mitra Ghosh (PI)

Dr. Sandip Kumar Basak (Co-PI)

Signature of the Supervisor (s) :

Sandip Kumar Basak
Principal
Sarat Censenary College
Dhanakhal, Nooghly

Name of the Ph.D Coordinator : Dr. Samrat Roy

Signature of Ph.D Coordinator (With Seal):

¹ Plagiarism Report is attached herewith.

PAPER NAME

Thesis_Biswajit Biswas.pdf

AUTHOR

THESIS BISWAJIT BISWAS

WORD COUNT

51140 Words

CHARACTER COUNT

278198 Characters

PAGE COUNT

274 Pages

FILE SIZE

25.5MB

SUBMISSION DATE

Apr 15, 2024 7:06 PM GMT+5:30

REPORT DATE

Apr 15, 2024 7:09 PM GMT+5:30

● 2% Overall Similarity

The combined total of all matches, including overlapping sources, for each database.

- 1% Internet database
- 1% Publications database
- Crossref database
- Crossref Posted Content database

● Excluded from Similarity Report

- Quoted material
- Small Matches (Less than 14 words)

Acknowledgement

I would like to extend my sincere gratitude to my Ph.D. supervisor Dr. Mahashweta Mitra Ghosh, Department of Microbiology, St. Xavier's College (Autonomous) Kolkata. Her guidance and continuous support have been precious throughout my research. Her constructive criticism, motivation and immense knowledge helped me in research and writing the thesis. I shall be forever grateful to her throughout my life.

I would also wish to convey my gratitude to my Ph.D. co-supervisor Dr. Sandip Kumar Basak, Principal of Sarat Centenary College, Dhaniakhali, Hooghly, West Bengal. His guidance and continuous support have been precious throughout my research. His constructive criticism, motivation and immense knowledge helped me in research and writing the thesis. I shall be forever grateful to him throughout my life.

I would also wish to convey my gratitude to Dr. Krishna Ray, Department of Botany, West Bengal State University, Barasat, West Bengal for providing me motivation and support during my research work. Her guidance and continuous support have been precious throughout my research. Her constructive criticism, motivation and immense knowledge helped me in research and writing the thesis. I shall be forever grateful to her throughout my life.

I am thankful to the Department Microbiology, St. Xavier's College (Autonomous) Kolkata for providing me opportunities to pursue my research work. I would like to express thanks to Dr. Sudeshna Shyam Chowdhury and all the faculty members especially Dr. Arup Kumar Mitra of the Department of Microbiology for valuable suggestions during my research work.

I am thankful to all my lab members of St. Xaviers College and West Bengal State University.

My heartfelt thanks go to Dr. Chandan Mukherjee, my senior labmate for his continuous support throughout my research work. His working knowledge has guided me to solve the experimental problems during hard times in my research work. I learned a lot from him. We have spent lots of time together during laboratory work and his patience for consistently guiding me in the laboratory work is commendable.

I am thankful to my senior labmate, Dr. Tapan Sutradhar for his support during research work and without his support, carrying out fieldwork would not have been possible. We have spent a lot memorable time together during field work and in the laboratory.

I am thankful to my senior labmate, Dr. Rajojit Chowdhury for his support during research work and without his support, carrying out fieldwork would not have been possible. We have spent a lot memorable time together during field work and in the laboratory.

Many sincere thanks also go to my senior labmate Dr. Momtaj Begam for valuable suggestions and kind co-operation during my research work. She had been our great support during the field visits and also in the laboratory.

Many sincere thanks also go to my dear friend and labmate Mrs. Sumana Mondal for valuable suggestions and kind co-operation during my research work. She took a very important role in my whole research work. Her valuable suggestions and cooperation help me many ways to complete my research. So, I am grateful to her and I would like to thank her heartily.

I would like to express my sincere thanks to all my junior labmates Subhajit, Ipsita, Anup, Hemendra, Rudranil, Chayan and Anjali for their assistance and support. They always extended their co-operation whenever I required.

I express my sincere thanks for all our field staff Ranjan Da, Shuvra Da, Sirsendu Da, Susanta Da, Tarun Da, Ashish da and Vedprakash Da for their immense help during root and pneumatophore sample collection from several mangroves of Indian Sundarbans and Rice field experiment and *Avicennia officinalis* nursery experiment of Indian Sundarbans for carrying out my research.

I am grateful for the financial support I received in the form of a fellowship along with necessary funding for chemicals, lab equipments and travel from The Rajiv Gandhi National Fellowship (RGNF) Scheme for Scheduled Caste and Scheduled Tribes funded by Ministry of Social Justice & Empowerment and Ministry of Tribal Affairs.

I could not progress an inch in my life without the continuous support of my father Bipul Chandra Biswas and mother Rita Biswas. Their continuous support and determination helped me to pursue my research work.

I would also express my thanks to my wife Priya Biswas for her strong support and motivation during my research period. I would also express my thanks to my daughter Aitri Biswas, my son Aitihya Biswas and all of my family members and well-wishers especially my friend Sujit Sarkar for supporting me throughout the research work.

Lastly, I would like to convey my thanks to everyone, whoever has extended co-operation and support during my Ph.D work.

Thus said I hereby submit the record of my observations for evaluation for the award of the degree of Doctor of Philosophy in Science.

Date:

Place: Kolkata

(Biswajit Biswas)

Contents

I: Introduction	1-20
1. Introduction.	2
1.1 Unique adaptability of diverse root niches of mangrove ecosystem.	2
1.2 Ultrafiltration of hypersaline water via roots for intake - a unique adaptation across mangroves.	4
1.3 Mangrove-microbe interaction in the rhizosphere for growth promotion amid hypersaline intertidal environment - another challenge faced by mangrove ecosystem.	4
1.4 Root endospheres of mangroves as the reservoir of PGPR endophytic bacteria from mangrove ecosystems.	6
1.5 Endophytes in agriculture and other beneficial roles of PGP endophytes for plant hosts.	8
1.6 Growth promoting traits of endophytic bacteria.	10
1.6.a. Phosphate-solubilization.	12
1.6.b. Siderophore production.	12
1.6.c. IAA production.	13
1.6.d. ACC deaminase production.	13
1.6.e. Nitrogen fixation.	14
1.7 Hypotheses of the present study.	17
1.8 Objectives undertaken in this study.	17
II: Materials and Methods	21-80
2. Materials and Methods.	22
2.1 Collection of root and pneumatophore samples.	22
2.2 Storage and transportation of collected samples.	23
2.3 Establishment of pure endophytic bacterial strains from mangrove roots and pneumatophores.	24
2.4 Establishment of pure endophytic bacterial colonies.	24
2.5 Gram staining technique.	25
2.6 Maintenance of pure endophytic bacterial colonies.	26
2.7 Preparation of Glycerol stock.	26
2.8 Endophytic bacterial genomic DNA isolation.	26

2.9 Bacterial sequence grade DNA preparation.	28
2.10 PCR amplification of genomic DNA.	29
2.11 Agarose gel electrophoresis.	29
2.12 Sequence submission to NCBI database.	29
2.13 Checking the growth of pure isolates on different nutrient cycling media.	30
2.13.a. Media composition for cellulose-degrading bacteria.	30
2.13.b. Media composition for phosphate solubilizing bacteria.	30
2.13.c. Media composition for free-living nitrogen-fixing bacteria.	31
2.13.d. Media composition for sulfur-oxidizing bacteria.	31
2.13.e. Media composition for preliminary selection of iron-oxidizing bacteria.	31
2.13.f. Confirmational study of Iron oxidizing bacteria (IOB).	32
2.13.g. Confirmation of iron-oxidizing endophytic bacteria (with ferric precipitate) by ammonium thiocyanate assay.	32
2.14 The determination of exchangeable sodium in plant tissue.	33
2.15. The determination of exchangeable potassium in plant tissue.	34
2.16 Determination of plant growth-promoting properties of endophytic bacterial strains.	35
2.16.a. IAA production assay.	35
2.16.b. Preparation of standard curve of IAA production assay.	35
2.16.c. IAA production assay from different endophytic bacterial strains (with Tryptophan).	36
2.16.d. IAA production assay from different endophytic bacterial strains (without Tryptophan).	37
2.17 Phosphate solubilization activity study.	37
2.17.a. Preparation of standard curve of phosphate solubilization assay.	37
2.17.b. Phosphate solubilization activity study from different endophytic bacterial strains.	38
2.18 Quantitative estimation of siderophore from different endophytic bacterial strains.	40
2.19. 1-aminocyclopropane-1-carboxylic acid deaminase (ACC deaminase) assay.	42
2.19.a. α -ketobutyrate standard curve preparation.	43
2.19.b. Protein standard curve preparation.	44
2.19.c. 1-aminocyclopropane-1-carboxylic acid deaminase (ACC deaminase) assay from different endophytic bacterial strains.	44

2.19.d. Protein concentration determination.	46
2.20. Nitrogenase assay from different endophytic bacterial strains.	46
2.21. Screening of salt tolerance properties of endophytic bacteria.	48
2.22. Histological study of mangrove roots and pneumatophores.	51
2.27. Conductivity determination from soil and water.	56
2.27.a. Conductivity determination from soil.	56
2.27.b. Conductivity determination from water.	56
2.28. pH determination from soil and water.	57
2.28.a. pH determination from soil.	57
2.28.b. pH determination from water.	57
2.29. Plant available phosphorus estimation from soil.	57
2.29.a. Plant-available phosphorus standard curve.	57
2.29.b. Plant-available phosphorus (P) extraction from soil.	59
2.29.c. Plant-available phosphorus determination from soil.	59
2.30. Soil organic carbon estimation.	59
2.30.a. Organic carbon standard curve preparation.	59
2.30.b. Organic carbon determination from soil.	61
2.31. Ammonia-nitrogen estimation.	61
2.31.a. Ammonia-nitrogen standard curve preparation.	62
2.31.b. Ammonia-nitrogen extraction from soil.	63
2.31.c. Ammonia-nitrogen determination from soil.	63
2.32. Nitrate-nitrogen estimation.	63
2.32.a. Nitrate-nitrogen standard curve preparation.	64
2.32.b. Nitrate-nitrogen extraction and determination from soil.	65
2.33. The determination of exchangeable sodium and potassium in soil.	65
2.34. Estimation of starch content from rice grains.	65
2.34.a. Starch standard curve preparation.	66
2.34.b. Estimation of starch content from rice grains.	67
2.35. Estimation of total protein content from rice grains.	67
2.35.a. Protein standard curve preparation.	68
2.35.b. Estimation of total protein content from rice grains.	68
2.36. Antioxidant assay of endophytic bacterial culture filtrates.	69

2.36.a. Free radical scavenging assay by spectrophotometric method.	69
2.36.b. Extraction of antioxidants from endophytic bacterial culture.	69
2.36.c. Superoxide anion scavenging assay by spectrophotometric method.	72
2.36.d. Extraction of antioxidants from endophytic bacterial culture filtrates.	72
2.36.e. Hydroxyl radical scavenging assay by spectrophotometric method.	74
2.36.f. Extraction of antioxidant from endophytic bacterial culture.	74
2.36.g. Nitric oxide scavenging assay by spectrophotometric method.	76
2.36.h. Extraction of antioxidants from endophytic bacterial culture.	76
2.37. Next Generation Sequencing method to measure the bacterial community abundance.	78
2.38. Precautions.	79
2.39. Instruments and chemicals used.	79

III: Results and Discussion

81-257

Objective 1:

3. Study of morphological/histological niches, anatomical adaptations, Na ⁺ /K ⁺ ratio in endospheres of roots and pneumatophores of mangrove species from degraded and non-degraded habitats of Sundarban mangrove ecosystem.	82
3.1. Morphological adaptations of roots/pneumatophores of mangrove species.	82
3.2. Histological adaptations of roots/pneumatophores of mangrove species.	85
3.3. NA ⁺ /K ⁺ ratio estimation in endospheric environments of roots, leaves and shoots of different mangrove species.	101

Objective 2:

4. Establishment of pure endophytic bacterial strains from mangrove roots and pneumatophores and their molecular identification by 16S rRNA sequencing.	105
4.1. Gram-staining microscopic pictures of some Gram-positive and Gram-negative endophytic bacteria.	106
4.2. Molecular identification of pure bacterial isolates.	106
4.3. Establishment of pure endophytic bacterial strains from mangrove roots and pneumatophores.	107
4.4. Testing of all 78 strains on differential nutrient cycling media for possible plant growth promotion potential.	11

Objective 3:

5. Plant growth promotion profiling of the established/accessioned endophytic bacterial strains.	117
--	-----

5.1. IAA production by different endophytic bacterial strains isolated from mangrove roots and pneumatophores.	117
5.2. Calibration curve of IAA.	117
5.3. Evaluation of IAA production potential of 78 endophyte accessions.	118
5.4. Analysis of IAA production by endophytic bacterial isolates against their source niches of diverse species of mangrove roots and pneumatophores.	119
5.6. Evaluation of IAA production potential (without addition of tryptophan precursor) of some endophyte accessions.	119
5.7. Phosphate solubilization by different endophytic bacterial strains isolated from mangrove roots and pneumatophores.	121
5.8. Calibration curve of plant-available phosphorus for phosphate solubilization assay.	122
5.9. Evaluation of phosphorus solubilization potential of 78 endophyte accessions.	123
5.10. Analysis of phosphorus solubilization by endophytic bacterial isolates against their source niches of diverse species of mangrove roots and pneumatophores.	124
5.11. Siderophore production activity by different endophytic bacterial strains isolated from mangrove roots and pneumatophores.	124
5.12. Evaluation of siderophore production potential of 78 endophyte accessions.	125
5.13. Analysis of siderophore production by endophytic bacterial isolates against their source niches of diverse species of mangrove roots and pneumatophores.	126
5.14. Quantitative estimation of siderophore by universal CAS assay.	127
5.15. ACC deaminase production activity by different endophytic bacterial strains isolated from mangrove roots pneumatophores.	127
5.16. Calibration curve preparation for ACC deaminase assay:	128
5.16.a. Calibration curve of α -ketobutyrate for ACC deaminase assay.	128
5.16.b. Calibration curve of protein for ACC deaminase assay.	128
5.17. Evaluation of ACC deaminase production potential of 78 endophyte accessions.	129
5.18. Analysis of ACC deaminase production by endophytic bacterial isolates against their source niches of diverse species of mangrove roots and pneumatophores.	130
5.19. Free nitrogen-fixation by different endophytic bacterial strains isolated from mangrove roots and pneumatophores.	131
5.20. Evaluation of free nitrogen-fixing potential of 78 endophyte accessions.	131
5.21. Analysis of free nitrogen-fixation by endophytic bacterial isolates against their source niches of diverse species of mangrove roots and pneumatophores.	132

5.22. Some chromatograms of the high acetylene reducers are presented below.	134
5.23. Testing of salt tolerance profile of some best PGP endophytic bacterial strains developed in this study.	140
5.24. Testing of salt tolerance profile of some best PGP endophytic bacterial strains on free nitrogen-fixing medium (FNFM).	141
5.25. Testing of salt tolerance profile of some best PGP endophytic bacterial strains on cellulose degrading medium (CDM).	142
5.26. Testing of salt tolerance profile of some best PGP endophytic bacterial strains on phosphate solubilizing medium (PSM).	143

Objective 4:

6. Selection of PGP endophytic bacterial consortia based on growth promotion criteria and growth curves for nursery/greenhouse/field applications.	145
6.1. Selection of endophytic bacterial consortia for the application of nursery/greenhouse/field on the basis of plant growth promoting (PGP) potential.	145
6.2. Plant growth promotion profile of different consortium.	148
6.3. Antioxidant assay profile from different consortia of endophytic bacterial strains.	150
6.3.a. Free radical scavenging profile (DPPH scavenging activity) from different consortium of endophytic bacterial strains.	150
6.3.b. Superoxide anion scavenging profile from different consortium of endophytic bacterial strains.	151
6.3.c. Hydroxyl radical scavenging profile from different consortium of endophytic bacterial strains.	151
6.3.d. Nitric oxide scavenging assay profile from different consortium of endophytic bacterial strains.	151
6.4. Preparation of growth curve of the 3 consortia with its PGP members for 96 hrs to find out the common exponential growth phase for large scale culture preparation.	152
6.4.a. Growth curve of consortium BC1 for 96 hours.	152
6.4.b. Growth curve of consortium BC2 for 96 hours.	153
6.4.c. Growth curve of consortium BC3 for 96 hours.	153

Objective 5:

7. Application of selected PGP endophytic bacterial consortia on <i>Avicennia officinalis</i> saplings in mangrove nursery at Sundarbans for observing their effect on mangrove growth modulation.	154
7.1. Analysis of soil pH across the experimental time period.	156

7.2. Analysis of soil electrical conductivity (EC) across the experimental time period.	157
7.3. Analysis of soil organic carbon (SOC) across the experimental time period.	158
7.3.a. Calibration curve Organic carbon.	159
7.3.b. Analysis of soil organic carbon.	159
7.4. Analysis of available nitrogen (N) in pot soil across the experimental time.	160
7.4.a. Calibration curve of nitrate-nitrogen.	160
7.4.b. Analysis of soil nitrate-nitrogen.	160
7.5. Analysis of soil ammonia-nitrogen across the experimental time period.	161
7.5.a. Calibration curve of ammonia-nitrogen.	162
7.5.b. Analysis of soil ammonia-nitrogen.	162
7.6. Analysis of soil phosphorus content across the period of the experiment.	163
7.6.a. Calibration curve of plant-available phosphorus.	163
7.6.b. Analysis of plant-available phosphorus in soil.	164
<u>Objective 6:</u>	
8. Application of selected PGP endophytic bacterial consortia on cultivated rice of Sundarbans at the greenhouse for observing their effect on rice growth modulation.	166
8.1. A few pictures from 2nd greenhouse experiment are depicted in the next pages.	168
8.2. Growth parameters from both 1st and 2nd greenhouse pot experiment.	176
8.3. Analysis of pot soil pH during the experimental period.	180
8.4. Analysis of pot soil conductivity across the experimental period.	184
8.5. Analysis of soil organic carbon (SOC) content during the experimental period.	188
8.6. Analysis of soil nitrate-nitrogen over the experimental time.	192
8.7. Analysis of soil ammonia-nitrogen across the experimental period.	196
8.8. Analysis of plant available phosphorus over the experimental period.	200
8.8.a. Analysis of plant-available rhizosphere pot soil phosphorus from the 1st greenhouse experiment over the experimental period.	200
8.8.b. Analysis of plant-available rhizosphere pot soil phosphorus from the 2nd greenhouse experiment over the experimental period.	203

Objective 7:

9. Application of selected PGP endophytic bacterial consortia on cultivated rice at fields at Sundarbans for observing their effect on rice growth and yield modulation.	208
9.1. Preparation of large-scale culture for field experiments.	208
9.2. 1 st field experiment details in Sundarban rice field.	209
9.2.a. Different growth parameters of rice plants observed in the 1 st field experiment at Sundarbans.	211
9.2.b. Different yield parameters of cultivated rice in the 1 st field experiment at Sundarbans.	212
9.2.c. Importance of rice grains with its starch and protein contents.	213
9.2.d. Calibration curve of starch.	214
9.2.e. Starch content analysis in rice grains.	214
9.2.f. Calibration curve of protein.	215
9.2.g. Protein content analysis.	215
9.2.h. Analysis of soil pH during the experimental period.	216
9.2.i. Analysis of soil electrical conductivity (EC) during the experimental period.	216
9.2.j. Analysis of soil exchangeable Na ⁺ /K ⁺ ratio during the experimental period.	217
9.2.k. Analysis of soil organic carbon (SOC) during the experimental period.	218
9.2.l. Analysis of soil nitrate-nitrogen during the experimental period.	219
9.2.m. Analysis of soil ammonia-nitrogen during the experimental period.	219
9.2.n. Analysis of plant-available phosphorus during the experimental period.	220
9.3. 2 nd field experiment details in Sundarban rice field (Field no. 1).	221
9.3.a. Field no. 2 details.	221
9.3.b. Different growth parameters of cultivated rice observed in the 2 nd field experiment, field no. 2 at Sundarbans.	223
9.3.c. Different yield parameters of cultivated rice in the 2 nd field experiment, field no. 2 at Sundarbans.	224
9.3.d. Starch content analysis in the harvested rice grains.	225
9.3.e. Protein content analysis in harvested rice grains.	226
9.3.f. Analysis of soil pH during the experimental period.	228
9.3.g. Analysis of soil electrical conductivity (EC) during the experimental period.	229
9.3.h. Analysis of soil organic carbon (SOC) during the experimental period.	230

9.3.i. Analysis of soil nitrate-nitrogen during the experimental period.	231
9.3.j. Analysis of soil ammonia-nitrogen during the experimental period.	232
9.3.k. Analysis of plant-available phosphorus in soil during the experimental period.	233
9.4. 2 nd field experiment details in Sundarban rice field (Field no. 2).	235
9.4.a. Field no. 2 details.	235
9.4.b. Different growth parameters of cultivated rice observed in the 2nd field experiment, field no. 2 at Sundarbans.	236
9.4.c. Different yield parameters of cultivated rice in the 2nd field experiment, field no. 2 at Sundarbans.	237
9.4.d. Starch content analysis in the harvested rice grains.	238
9.4.e. Protein content analysis in harvested rice grains.	239
9.4.f. Analysis of soil pH during the experimental period.	241
9.4.g. Analysis of soil electrical conductivity (EC) during the experiment time.	242
9.4.h. Analysis of soil organic carbon (SOC) during the experimental period.	243
9.4.i. Analysis of soil nitrate-nitrogen during the experimental period.	244
9.4.j. Analysis of soil ammonia-nitrogen during the experimental period.	245
9.4.k. Analysis of plant-available phosphorus in soil during the experimental period.	246
9.5. Data collected from neighbouring rice fields of Sundarban cultivated with conventional fertilizers after harvest.	248
9.5.a. Starch content analysis in harvested grains.	248
9.5.b. Protein content analysis in harvested grains.	248
9.5.c. Analysis of soil pH in neighboring rice fields.	249
9.5.d. Analysis of soil electrical conductivity (EC).	249
9.5.e. Analysis of soil organic carbon (SOC).	250
9.5.f. Analysis of soil nitrate-nitrogen in neighbouring rice fields at Sundarbans.	250
9.5.g. Analysis of soil ammonia-nitrogen in the neighbouring rice fields at Sundarbans.	251
9.5.h. Analysis of plant-available phosphorus from the neighbouring rice fields at Sundarbans.	251

Objective 8:

10. Observation of bacterial community abundances by Next Generation Sequencing (NGS) from rice fields before and after rice cultivation with PGP endophytic bacterial consortia.	252
10.a. Comparative account of relative abundances at phylum level.	254
10.b. Comparative account of relative abundances at class level.	255
10.c. Comparative account of relative abundances at family level.	256
10.d. Comparative account of relative abundances at genus level.	257

IV. Conclusion **259-260****References** **262-269****Publications** **271-274**

LIST OF FIGURES:

Sl. No.	Figure Legend	Page No.
Figure 1.1:	Phytohormone production by endophytes.	13
Figure 2.1:	Location map of 5 mangrove forests with sampling sites for root and pneumatophore.	23
Figure 3.1:	Different mangroves roots and pneumatophores (a) <i>Avicennia</i> spp. (b) <i>Ceriops decandra</i> (c) <i>Ceriops tagal</i> (d) <i>Bruguiera gymnorrhiza</i> .	83
Figure 3.2:	Different mangroves roots and pneumatophores (e) <i>Excoecaria agallocha</i> (f) <i>Heritiera fomes</i> (g) <i>Xylocarpus</i> sp. (h) <i>Rhizophora</i> sp.	84
Figure 3.3:	Leguminous mangrove associate species (a) Below ground root with root nodules of <i>Dalbergia spinosa</i> , (b) <i>Derris trifoliata</i> .	84
Figure 3.4:	Transverse section of <i>Avicennia alba</i> pneumatophore.	85
Figure 3.5:	Transverse section of <i>Avicennia marina</i> pneumatophore.	85
Figure 3.6:	Transverse section of <i>Avicennia marina</i> root.	86
Figure 3.7:	Transverse section of <i>Avicennia officinalis</i> pneumatophore.	87
Figure 3.8:	Transverse section of <i>Avicennia officinalis</i> root.	87
Figure 3.9:	Transverse section of <i>Bruguiera cylindrica</i> pneumatophore.	88
Figure 3.10:	Transverse section of <i>Bruguiera cylindrica</i> root.	89
Figure 3.11:	Transverse section of <i>Bruguiera gymnorrhiza</i> root.	89
Figure 3.12:	Transverse section of <i>Bruguiera gymnorrhiza</i> pneumatophore.	90
Figure 3.13:	Transverse section of <i>Ceriops</i> sp. root.	91
Figure 3.14:	Transverse section of <i>Excoecaria agallocha</i> root.	92
Figure 3.15:	Transverse section of <i>Heritiera fomes</i> root.	93
Figure 3.16:	Transverse section of <i>Xylocarpus</i> sp. root.	94
Figure 3.17:	Transverse section of <i>Myriostachya wightiana</i> root.	95
Figure 3.18:	Transverse section of <i>Porteresia cortata</i> root.	96
Figure 3.19:	Transverse section of <i>Dalbergia spinosa</i> root.	97
Figure 3.20:	Transverse section of <i>Derris trifoliata</i> root.	98
Figure 3.21:	Transverse section of <i>Rhizophora</i> sp. root.	99
Figure 3.22:	Na ⁺ /K ⁺ ratio was estimated in root endosphere niches of different mangrove species from Indian Sundarban. Data were represented in this graph -----	101
Figure 3.23:	Na ⁺ /K ⁺ ratio was estimated in shoot endosphere niches of different mangrove species from Indian Sundarban. Data were represented in this graph -----	102
Figure 3.24:	Na ⁺ /K ⁺ ratio was estimated in leaf endosphere niches of different mangrove species from Indian Sundarban. Data were represented in this graph -----	103
Figure 4.1:	Figure 4.1: A) Root and pneumatophore samples of different mangroves were inoculated in LB broth. B) From LB broth 50 µl culture spread on LB plate and single colonies obtained.	105

Sl. No.	Figure Legend	Page No.
Figure 4.2:	Gram-staining microscopic pictures of some Gram-positive and Gram-negative Endophytic bacteria -----	106
Figure 4.3:	Agarose (0.8%) gel picture of Partial 16S rRNA gene amplification of some endophytic bacterial isolates.	107
Figure 4.4:	Relative distribution of different bacterial genera among total 78 accessioned root endophytic bacterial strains developed as pure isolates.	111
Figure 4.5:	Number of accessioned isolates growing on different nutrient cycling media. The iron oxidizing bacterial isolates represent -----	115
Figure 4.6:	Confirmational test of Iron oxidizing bacteria at sub-neutral pH of 6 (Ghosh et. al., 2014).	116
Figure 5.1:	The calibration curve of IAA was done to measure the unknown concentration of IAA produced by different endophytic bacterial strains.	117
Figure 5.2:	IAA production by different endophytic bacterial strains isolated from mangrove roots pneumatophores -----	118
Figure 5.3:	Best 15 IAA-producing endophyte bacterial strains from mangrove roots and pneumatophores. Data -----	118
Figure 5.4:	Diverse mangrove root environments as source of differential IAA producing endophytic bacterial strains. -----	119
Figure 5.5:	Best 15 IAA-producing (without tryptophan) endophyte bacterial strains from mangrove roots and pneumatophores. Data -----	120
Figure 5.6:	Other 7 IAA-producing (without tryptophan) endophyte bacterial strains from mangrove roots and pneumatophores. Data -----	120
Figure 5.7:	The calibration curve of plant available phosphorus for phosphorus solubilization assay was done to measure -----	122
Figure 5.8:	Phosphorus solubilization by endophytic bacterial strains isolated from mangrove roots pneumatophores from Indian -----	122
Figure 5.9:	Best 15 P-solubilizer endophyte bacterial strains isolated from mangrove roots and pneumatophores. Data -----	123
Figure 5.10:	Diverse mangrove root environments as source of differential P-solubilizing endophytic bacterial strains. -----	124
Figure 5.11:	Siderophore activity by endophytic bacterial strains isolated from mangrove roots pneumatophores from -----	125
Figure 5.12:	Best 15 siderophore producing endophyte bacterial strains from mangrove roots and pneumatophores. Data -----	125
Figure 5.13:	Diverse mangrove root environments as source of differential siderophore producing endophytic bacterial strains.	126
Figure 5.14:	Quantitative estimation of siderophore by universal CAS assay	127
Figure 5.15:	The calibration curve of ACC deaminase was done to measure the unknown concentration -----	128
Figure 5.16:	The calibration curve of protein for ACC deaminase was done to measure the unknown concentration -----	128

Sl. No.	Figure Legend	Page No.
Figure 5.17:	ACC deaminase assay by endophytic bacterial strains isolated from mangrove roots pneumatophores from Indian -----	129
Figure 5.18:	Best 15 ACC deaminase producing endophyte bacterial strains from mangrove roots and pneumatophores. -----	129
Figure 5.19:	Diverse mangrove root environments as source of differential ACC deaminase producing endophytic bacterial strains from Indian Sundarban. Data -----	130
Figure 5.20:	Best 11 free nitrogen fixing endophyte bacterial strains from mangrove roots and pneumatophores from Indian -----	132
Figure 5.21:	Diverse mangrove root environments as source of differential free nitrogen fixing endophytic bacterial strains.	132
Figure 5.22:	CFU per 100 µl of FNFM for best 14 free nitrogen fixing endophyte bacterial strains from mangrove roots and pneumatophores	133
Figure 5.23:	Diverse mangrove root environments as source of differential free nitrogen fixing endophytic bacterial strains in terms of CFU per 100 µl of FNF broth.	134
Figure 5.24:	Chromatogram of <i>Staphylococcus epidermis</i> strain DAL6 (MT422044) from <i>Dalbergia spinosa</i> root.	135
Figure 5.25:	Chromatogram of <i>Pseudomonas stutzeri</i> strain BCY5 (MT422041) from <i>Bruguiera cylindrica</i> root.	135
Figure 5.26:	Chromatogram of <i>Bacillus thuringiensis</i> strain CRL3 (MT421996) from <i>Ceriops</i> sp. root.	136
Figure 5.27:	Chromatogram of <i>Bacillus subtilis</i> strain RRP6 (MT422018) from <i>Rhizophora mucronata</i> root.	136
Figure 5.28:	Chromatogram of <i>Pseudomonas stutzeri</i> strain BCY9 (MT422043) from <i>Bruguiera cylindrica</i> root.	137
Figure 5.29:	Chromatogram of <i>Bacillus oceanisediminis</i> strain BCY3 (MT422040) from <i>Bruguiera cylindrica</i> root.	137
Figure 5.30:	Chromatogram of <i>Aeromonas allosaccharophila</i> strain DAL2 (MT422027) from <i>Dalbergia spinosa</i> root.	138
Figure 5.31:	Chromatogram of <i>Pseudomonas fulva</i> strain DER9 (MT422023) from <i>Derris trifoliata</i> root.	138
Figure 5.32:	Chromatogram of <i>Citrobacter freundii</i> strain ERS1 (MT422008) from <i>Excoecaria agallocha</i> root.	139
Figure 5.33:	Chromatogram of <i>Pseudocitrobacter faecalis</i> strain HRR5 (MT422004) from <i>Heritiera fomes</i> root.	139
Figure 5.34:	Growth of free nitrogen fixers on FNFM broth in different NaCl concentration after 72 hours.	141
Figure 5.35:	Growth of cellulose degraders on CDM broth in different NaCl concentration after 72 hours.	142
Figure 5.36:	Growth of P-solublizers on PSM broth in different NaCl concentration after 72 hours.	143

Sl. No.	Figure Legend	Page No.
Figure 6.1:	Indole acetic acid production profile and phosphate solubilization profile of Consortium-1, Consortium-2, and Consortium-3.	148
Figure 6.2:	Siderophore production profile and ACC deaminase production profile of Consortium-1, Consortium-2, and Consortium-3.	148
Figure 6.3:	Acetylene reduction profile of Consortium-1, Consortium-2, and Consortium-3.	149
Figure 6.4:	Colony forming unit (CFU) count on the nitrogen-fixing medium profile of Consortium-1, Consortium-2, and Consortium-3.	149
Figure 6.5:	Free radical scavenging profile (DPPH) of Consortium-1, Consortium-2, and Consortium-3.	150
Figure 6.6:	Superoxide anion scavenging profile Consortium-1, Consortium-2, and Consortium-3.	151
Figure 6.7:	Growth curve of individual endophytic bacterial strains from consortium (BC1).	152
Figure 6.8:	Growth curve of individual endophytic bacterial strains from consortium (BC2).	153
Figure 6.9:	Growth curve of individual endophytic bacterial strains from consortium (BC3).	153
Figure 7.1:	Geo-tagged pictures of <i>Avicennia officinalis</i> saplings at mangrove nursery under ongoing experiment.	154
Figure 7.2:	95 days' old <i>Avicennia officinalis</i> saplings at mangrove nursery. In control plots where no bacterial culture was applied. Plot BC1 -----	155
Figure 7.3:	The above figures are the results observed for growth promotion of <i>Avicennia officinalis</i> saplings in comparison to control saplings. Figure (a): Consortium BC3 -----	156
Figure 7.4:	Soil sediment pH profile was studied from control (without bacteria) and different consortia added rhizospheric soil. Analysis was done for <i>Avicennia Officinalis</i> -----	157
Figure 7.5:	Soil sediment conductivity profile was studied from control (without bacteria) and different consortia added rhizospheric soil. Analysis was done for <i>Avicennia Officinalis</i> -----	158
Figure 7.6:	The calibration curve of Organic carbon was done to measure the unknown concentration of Organic carbon from the soil.	159
Figure 7.7:	Soil Organic carbon profile was studied from control (without bacteria) and different consortia added rhizospheric soil. Analysis was done for <i>Avicennia Officinalis</i> -----	159
Figure 7.8:	The calibration curve of Nitrate-nitrogen was done to measure the unknown concentration of Nitrate-nitrogen from the soil.	160
Figure 7.9:	Soil Nitrate-nitrogen profile was studied from control (without bacteria) and different consortia added rhizospheric soil. Analysis was done for <i>Avicennia Officinalis</i> -----	161
Figure 7.10:	The calibration curve of Ammonia-nitrogen was done to measure the unknown concentration of Ammonia-nitrogen from the soil.	162

Sl. No.	Figure Legend	Page No.
Figure 7.11:	Soil Ammonia-nitrogen profile was studied from control (without bacteria) and different consortia added rhizospheric soil. Analysis was done for <i>Avicennia Officinalis</i> -----	162
Figure 7.12:	The calibration curve of plant available phosphorus was done to measure the unknown concentration of plant available phosphorus from the soil.	163
Figure 7.13:	Soil phosphorus solubilization or plant available phosphorus profile was studied from control (without bacteria) and different consortia added rhizospheric soil. Analysis was done for <i>Avicennia Officinalis</i> -----	164
Figure 8.1:	Because of the very high salinity of saline soil, all transplanted rice seedlings died at initial days after transplantation. Therefore, rest of the 1 st greenhouse experiment and 2 nd greenhouse -----	167
Figure 8.2:	The greenhouse experiment being conducted.	167
Figure 8.3:	Checking of soil salinity and growth parameters at the greenhouse.	168
Figure 8.4:	The status of 85-days' post transplanted control (without bacteria) rice seedlings from 2 nd greenhouse experiment.	168
Figure 8.5:	The status of 85-days' post transplanted NPK added rice seedlings from 2 nd greenhouse experiment.	169
Figure 8.6:	The status of 85-days' post transplanted BC1 added rice seedlings from 2 nd greenhouse experiment.	169
Figure 8.7:	The status of 85-days' post transplanted BC2 added rice seedlings from 2 nd greenhouse experiment.	170
Figure 8.8:	The status of 85-days' post transplanted BC3 added rice seedlings from 2 nd greenhouse experiment.	170
Figure 8.9:	The status of 85-days' post transplanted SRC3+BEC3 added rice seedlings from 2 nd greenhouse experiment.	171
Figure 8.10:	The status of 85-days' post transplanted SRC5+BEC2 added rice seedlings from 2 nd greenhouse experiment.	171
Figure 8.11:	The status of 85-days' post transplanted SRC4+BEC2 added rice seedlings from 2 nd greenhouse experiment.	172
Figure 8.12:	The status of 85-days' post transplanted SRC1+BEC3 added rice seedlings from 2 nd greenhouse experiment.	172
Figure 8.13:	The status of 85-days' post transplanted SRC2+BEC2 added rice seedlings from 2 nd greenhouse experiment.	173
Figure 8.14:	The status of 85-days' post transplanted SRC6+BEC1 added rice seedlings from 2 nd greenhouse experiment.	173
Figure 8.15:	The status of 85-days' post transplanted SRC6+BEC3 added rice seedlings from 2 nd greenhouse experiment.	174
Figure 8.16:	The status of 85-days' post transplanted SRC1+BEC1 added rice seedlings from 2 nd greenhouse experiment.	174
Figure 8.17:	The status of 85-days' post transplanted SRC4+BEC1 added rice seedlings from 2 nd greenhouse experiment.	175

Sl. No.	Figure Legend	Page No.
Figure 8.18:	The above figure depicts the comparison study of shoot heights of 1 st and 2 nd greenhouse experiment on rice plants of Lunishree on 85 days post transplantation. Data were plotted as mean \pm standard error (n=10) in the graph.	176
Figure 8.19:	The above figure depicts the comparison study of shoot heights of 1 st and 2 nd greenhouse experiment on rice plants of Dudheswar on 85 days post transplantation. Data -----	177
Figure 8.20:	The above figure depicts the comparison study of leaf width of 1 st and 2 nd greenhouse experiment on rice plants of Lunishree on 85 days post transplantation. Data -----	178
Figure 8.21:	The above figure depicts the comparison study of leaf width of 1 st and 2 nd greenhouse experiment on rice plants of Dudheswar on 85 days post transplantation. Data -----	179
Figure 8.22:	The above figure depicts the comparison study of soil sediment pH from control (without bacteria) ----- 1 st greenhouse experiment on rice plants of Lunishree.	180
Figure 8.23:	The above figure depicts the comparison study of soil sediment pH from control (without bacteria) ----- 1 st greenhouse experiment on rice plants of Dudheswar.	181
Figure 8.24:	The above figure depicts the comparison study of soil sediment pH from control (without bacteria) ----- 2 nd greenhouse experiment on rice plants of Lunishree.	182
Figure 8.25:	The above figure depicts the comparison study of soil sediment pH from control (without bacteria) ----- 2 nd greenhouse experiment on rice plants of Dudheswar.	183
Figure 8.26:	The above figure depicts the comparison study of soil sediment conductivity from control (without bacteria) ----- -----1 st greenhouse experiment on rice plants of Lunishree.	184
Figure 8.27:	The above figure depicts the comparison study of soil sediment conductivity from control (without bacteria), NPK ----- ----- 1 st greenhouse experiment on rice plants of Dudheswar.	185
Figure 8.28:	The above figure depicts the comparison study of soil sediment conductivity from control (without bacteria), NPK ----- ----- 2 nd greenhouse experiment on rice plants of Lunishree.	186
Figure 8.29:	The above figure depicts the comparison study of soil sediment conductivity from control (without bacteria), NPK ----- -----2 nd greenhouse experiment on rice plants of Dudheswar.	187
Figure 8.30:	The above figure depicts the comparison study of soil organic carbon from control (without bacteria), NPK ----- ----- 1 st greenhouse experiment on rice plants of Lunishree.	188
Figure 8.31:	The above figure depicts the comparison study of soil organic carbon from control (without bacteria), NPK -----	189

Sl. No.	Figure Legend	Page No.
	----- 1 st greenhouse experiment on rice plants of Dudheswar.	
Figure 8.32:	The above figure depicts the comparison study of soil organic carbon from control (without bacteria), NPK ----- ----- 2 nd greenhouse experiment on rice plants of Lunishree.	190
Figure 8.33:	The above figure depicts the comparison study of soil organic carbon from control (without bacteria), NPK ----- ----- 2 nd greenhouse experiment on rice plants of Dudheswar.	191
Figure 8.34:	The above figure depicts the comparison study of soil Nitrate-nitrogen from control (without bacteria), ----- ----- 1 st greenhouse experiment on rice plants of Lunishree.	192
Figure 8.35:	The above figure depicts the comparison study of soil Nitrate-nitrogen from control (without bacteria), NPK ----- ----- 1 st greenhouse experiment on rice plants of Dudheswar.	193
Figure 8.36:	The above figure depicts the comparison study of soil Nitrate-nitrogen from control (without bacteria), NPK ----- ----- 2 nd greenhouse experiment on rice plants of Lunishree.	194
Figure 8.37:	The above figure depicts the comparison study of soil Nitrate-nitrogen from control (without bacteria), NPK ----- ----- 2 nd greenhouse experiment on rice plants of Dudheswar.	195
Figure 8.38:	The above figure depicts the comparison study of soil Ammonia-nitrogen from control (without bacteria), NPK ----- ----- 1 st greenhouse experiment on rice plants of Lunishree.	196
Figure 8.39:	The above figure depicts the comparison study of soil Ammonia-nitrogen from control (without bacteria), NPK ----- ----- 1 st greenhouse experiment on rice plants of Dudheswar.	197
Figure 8.40:	The above figure depicts the comparison study of soil Ammonia-nitrogen from control (without bacteria), NPK ----- ----- 2 nd greenhouse experiment on rice plants of Lunishree.	198
Figure 8.41:	The above figure depicts the comparison study of soil Ammonia-nitrogen from control (without bacteria), NPK ----- ----- 2 nd greenhouse experiment on rice plants of Dudheswar.	199
Figure 8.42:	The above figure depicts the comparison study of plant available phosphorus from control (without bacteria), NPK ----- ----- 1 st greenhouse experiment on rice plants of Lunishree.	200
Figure 8.43:	The above figure depicts the comparison study of plant available phosphorus from control (without bacteria), NPK -----	201

Sl. No.	Figure Legend	Page No.
	----- 1 st greenhouse experiment on rice plants of Dudheswar.	
Figure 8.44:	The above figure depicts the comparison study of plant available phosphorus from control (without bacteria), NPK ----- ----- 2 nd greenhouse experiment on rice plants of Lunishree.	203
Figure 8.45:	The above figure depicts the comparison study of plant available phosphorus from control (without bacteria), NPK ----- ----- 2 nd greenhouse experiment on rice plants of Dudheswar.	205
Figure 9.1:	The above figure depicts different steps in large culture preparation and large-scale PGP bacterial cultures brought to the rice field location in Sundarbans-----	208
Figure 9.2:	Bacterial cultures are being diluted for application in field.	210
Figure 9.3:	1 st field experiment at Sundarbans in 2021. (a) In control plots where no bacterial culture was added. (b) BC1 plots where Consortium BC1 -----	210
Figure 9.4:	The above figure depicts the growth parameters of rice plants (Dudheswar) after 1 st field experiment on 80 days post transplantation. A comparison -----	211
Figure 9.5:	The above figure depicts the yield parameters of rice plants (Dudheswar) after 1 st field experiment on 100 days post transplantation. A comparison -----	212
Figure 9.6:	The above figure depicts a comparison study of Quintal/bigha grain harvest between control (without bacteria), consortia added plot and neighbouring -----	213
Figure 9.7:	The calibration curve of starch was done to measure the unknown concentration of starch from the rice.	214
Figure 9.8:	The above figure depicts a comparative study of starch content analysis from rice grains of control (without bacteria) and different consortia added plots of 1 st field -----	214
Figure 9.9:	The calibration curve of protein was done to measure the unknown concentration of protein from the rice.	215
Figure 9.10:	The above figure depicts a comparative study of protein content analysis from rice grains of control (without bacteria) and different consortia added plots of 1 st -----	215
Figure 9.11:	The above figure depicts the Soil sediment pH was studied from control (without bacteria) and different consortia -----	216
Figure 9.12:	The above figure depicts the Soil sediment conductivity was studied from control (without bacteria) and different consortia -----	216
Figure 9.13:	The above figure depicts the Soil sediment Na/K ratio was studied from control (without bacteria) and different consortia -----	217
Figure 9.14:	The above figure depicts the Soil Organic carbon was studied from control (without bacteria) and different consortia ----- ----- Dudheswar.	218

Sl. No.	Figure Legend	Page No.
Figure 9.15:	The above figure depicts the Soil Nitrate-nitrogen was studied from control (without bacteria) and different consortia -----Dudheswar.	219
Figure 9.16:	The above figure depicts the Soil Ammonia-nitrogen was studied from control (without bacteria) and different -----Dudheswar.	219
Figure 9.17:	The above figure depicts the plant available phosphorus was studied from control (without bacteria) and different consortia -----Dudheswar	220
Figure 9.18:	2 nd field experiment at Sundarbans. (a) control plots (b) BC3 plots (c) SRC2+BEC2 (d) SRC3+BEC3 plots	222
Figure 9.19:	The above figure depicts the growth parameters of rice plants (Dudheswar) after 2 nd field experiment, field number 1 on 92 days post transplantation. A comparison study -----	223
Figure 9.20:	The above figure depicts the yield parameters of rice plants (Dudheswar) after 2 nd field experiment, field number 1 on 110 days post transplantation. A comparison study -----	224
Figure 9.21:	The above figure depicts a comparative study of starch content analysis from rice grains of control (without bacteria) and different consortia added plots of 2 nd field experiment at field number 1	225
Figure 9.22:	The above figure depicts a comparative study of starch content analysis from rice grains of neighbouring rice ----- 2 nd field experiment at field number 1.	225
Figure 9.23:	The above figure depicts a comparative study of protein content analysis from rice grains ----- 2 nd field experiment at field number 1.	226
Figure 9.24:	The above figure depicts a comparative study of protein content analysis from rice grains of neighbouring rice ----- 2 nd field experiment at field number 1.	227
Figure 9.25:	The above figure depicts the Soil sediment pH was studied from control (without bacteria) and different consortia ----- Dudheswar. 2 nd field experiment (field number 1).	228
Figure 9.26:	The above figure depicts the Soil sediment conductivity was studied from control (without bacteria) and different consortia -----Dudheswar 2 nd field experiment (field number 1).	229
Figure 9.27:	The above figure depicts the Soil Organic carbon was studied from control (without bacteria) and different consortia ----- Dudheswar. 2 nd field experiment (field number 1).	230
Figure 9.28:	The above figure depicts the Soil Nitrate-nitrogn was studied from control (without bacteria) and different consortia ----- Dudheswar. 2 nd field experiment (field number 1).	231
Figure 9.29:	The above figure depicts the Soil Ammonia-nitrogn was studied from control (without bacteria) and different consortia -----	232

Sl. No.	Figure Legend	Page No.
	-----Dudheswar. 2 nd field experiment (field number 1) in the graph.	
Figure 9.30:	The above figure depicts the comparison study of plant available phosphorus from control (without bacteria), NPK ----- -----2 nd field experiment (field number 1) on rice plants of Dudheswar.	233
Figure 9.31:	The above figure depicts the growth parameters of rice plants (Dudheswar) after 2 nd field experiment, field number 2 on 97 days post transplantation. -----	236
Figure 9.32:	The above figure depicts the yield parameters of rice plants (Dudheswar) after 2 nd field experiment, (field number 2) on 110 days post -----	237
Figure 9.33:	The above figure depicts a comparative study of starch content analysis from rice grains of control (without bacteria) and different consortia added plots of 2 nd field experiment at field number 2.	238
Figure 9.34:	The above figure depicts a comparative study of starch content analysis from rice grains of neighbouring ----- -----2 nd field experiment at field number 2.	238
Figure 9.35:	The above figure depicts a comparative study of protein content analysis from rice grains of control (without bacteria) and different consortia added plots of 2 nd field experiment at field number 2.	239
Figure 9.36:	The above figure depicts a comparative study of protein content analysis from rice grains of neighbouring ----- ----- 2 nd field experiment at field number 2.	240
Figure 9.37:	The above figure depicts the Soil sediment pH was studied from control (without bacteria) and different consortia ----- ----- Dudheswar. 2 nd field experiment (field number 2).	241
Figure 9.38:	The above figure depicts the Soil sediment conductivity was studied from control (without bacteria) and different consortia ----- -----Dudheswar. 2 nd field experiment (field number 2).	242
Figure 9.39:	The above figure depicts the Soil Organic carbon was studied from control (without bacteria) and different consortia ----- -----Dudheswar. 2 nd field experiment (field number 2).	243
Figure 9.40:	The above figure depicts the Soil Nitrate-nitrogen was studied from control (without bacteria) and different consortia ----- -----Dudheswar. 2 nd field experiment (field number 2).	244
Figure 9.41:	The above figure depicts the Soil Ammonia-nitrogen was studied from control (without bacteria) and different ----- -----Dudheswar. 2 nd field experiment (field number 2).	245
Figure 9.42:	The above figure depicts the comparison study of plant available phosphorus from control (without bacteria), NPK added ----- -----2 nd field experiment (field number 2) on rice plants of Dudheswar.	246

Sl. No.	Figure Legend	Page No.
Figure 9.43:	The percentage of starch (ranges 74.52-78.11 percent) observed overall same for 12 different neighbouring rice fields at Sundarbans with conventional fertilizers.	248
Figure 9.44:	The percentage of protein (ranges 6.12- 8.40 percent) observed more or less same for 12 different neighbouring rice fields at Sundarbans with conventional fertilizers.	248
Figure 9.45:	The soil sediment pH varied (4.17-5.46) for 12 different regions neighbouring rice fields at Sundarbans with conventional fertilizers.	249
Figure 9.46:	The soil sediment conductivity varied (0.353-1.976 ds/m) for 12 different regions neighbouring rice fields at Sundarbans with conventional fertilizers.	249
Figure 9.47:	The percentage of organic carbon (ranges 2.45- 3.03 percent) observed more or less same for 12 different neighbouring rice fields at Sundarbans with conventional fertilizers.	250
Figure 9.48:	The Nitrate-nitrogen content (ranges 13.50- 24.09 mg/kg of soil) varied for 12 different neighbouring rice fields at Sundarbans with conventional fertilizers.	250
Figure 9.49:	The Ammonia-nitrogen content (ranges 1.14- 3.52 mg/kg of soil) varied for 12 different neighbouring rice fields at Sundarbans with conventional fertilizers.	251
Figure 9.50:	The solubilized-P (ranges 35.25- 58.30 mg/kg of soil) varied for 12 different neighbouring rice fields at Sundarbans with conventional fertilizers	251
Figure 10.1:	Comparative account of relative abundances at phylum level	254
Figure 10.2:	Comparative account of relative abundances at class level	255
Figure 10.3:	Comparative account of relative abundances at family level	256
Figure 10.4:	Comparative account of relative abundances at genus level	257

LIST OF TABLES:

Sl. No.	Table Legend	Page No.
Table 1.	Some endophytic bacteria possessing host plants.	11
Table 2:	Some common plant growth promotion traits by endophytic/rhizospheric bacteria.	14
Table 3:	Moderately degraded mangrove forests and samples collected.	22
Table 4:	Pristine mangrove forests/non-degraded ecosystems and samples collected.	22
Table 5:	Highly degraded mangrove forests and samples collected.	22
Table 6:	Name of mangrove forests and their GPS locations.	23
Table 7:	Preparation of Na ⁺ standards.	33
Table 8:	Preparation of K ⁺ standards.	34
Table 9:	Reaction set up for preparation IAA standard curve.	35
Table 10:	Reaction set up for preparation of phosphorus standard curve.	38
Table 11:	Reaction set up for preparation of α ketobutyrate standard curve.	43
Table 12:	Reaction set up for preparation of BSA standard curve.	43
Table 13:	Reaction set up for preparation of phosphorus standard curve.	58
Table 14:	Reaction set up for preparation of organic carbon standard curve.	60
Table 15:	Reaction set up for ammonium-nitrogen standard curve.	62
Table 16:	Reaction set up for preparation of nitrate-nitrogen standard curve.	64
Table 17:	Reaction set up for preparation of glucose standard curve.	66
Table 18:	Reaction set up for preparation of BSA standard curve.	68
Table 19:	Reaction set up for preparation of Free radical scavenging assay.	71
Table 20:	Reaction Mixture preparation of Hydroxyl radical scavenging assay.	76
Table 21:	Name of the identified bacteria with accession numbers.	107
Table 22:	Endophytic bacterial growth on different nutrient cycling media.	112
Table 23:	Selection of best PGP Consortia for nursery/field/green-house application.	145
Table 24:	Showing Quantitative PGP profile of 3 consortia each of 6-7 endophytic bacterial strains with high plant growth promoting potential at laboratory level.	146
Table 25:	Initial physical and chemical parameters of both the soil types that were used for pot experiment before starting the experiment were as follows.	166
Table 26:	The details of the accessioned NGS data are enlisted in the following table.	252

List of Abbreviations

%	Percentage
°C	Degree Celsius
±	Both plus and minus
µg	Microgram
µl	Microlitre
µM	Micromolar
aq.	Aqueous
BLAST	Basic local alignment search tool
conc.	Concentration
DNA	Deoxyribonucleic acid
DW	Dry weight
EDTA	Ethylenediamine tetra acetic acid
g	Gram
hrs	Hours
kg	Kilogram
l	Litre
m	Meter
M	Molar
mg	Milligram
min	Minute
ml	Milliliter
mM	Millimolar
mm	Millimeter
N	Normality
nm	Nanometer
NCBI	National Center for Biotechnology
Ng	Nanogram
nM	Nanomole
OD	Optical density
PCR	Polymerase chain reaction
RNA	Ribonucleic acid

RNase	Ribonuclease
rpm	Revolutions per minute
rRNA	Ribosomal RNA
soln.	Solution
SD	Standard deviation
SE	Standard error
T_m	Melting temperature
Tris	Tris (hydroxymethyl)aminomethane
U	Unit
UV	Ultraviolet

Summary

Summary of the thesis

The sites selected were both non-degraded and degraded mangrove environments for my study. Among them, Shiber Ghat (21°50'29.30"N 88°21'23.95"E), Atharogazi (21°50'45.90"N 88°23'18.44"E) and Ramganga (21°47'34.30"N 88°22'53.01"E) are moderately to highly degraded mangrove ecosystems. Whereas Lakhipur (21°49'12.74"N 88°23'19.65"E) and Patharprotima (21°47'34.70"N 88°22'7.18"E) are pristine mangrove forests or non-degraded mangrove ecosystems. The below-ground and above-ground biomass ratio for mangroves is observed to be high, compared to other terrestrial communities suggesting that mangrove trees share a greater proportion of net primary production for their root growth as compared to other terrestrial tree communities. Although mangroves are well adapted to maintain oxygen availability in root cells under waterlogged conditions (negatively geotropic pneumatophores), anaerobicity being predominant in the rhizosphere compels roots to function under stress. My hypothesis was that mangrove roots should harbor endophytic microbes that interact with root cells, and promote growth, facilitating nutrient availability to the cells even under external anoxic ambiance. Endophytes can colonize the internal tissues of their host plant, including symbiotic, mutualistic, and trophobiotic relationships. Most endophytic bacteria originate from the rhizosphere. In this study mangrove species involved are *Avicennia alba*, *Avicennia marina*, *Avicennia officinalis*, *Heritiera fomes*, *Dalbergia* sp., *Bruguiera cylindrica*, *Bruguiera gymnorrhiza*, *Rhizophora mucronate*, *Xylocarpus* sp., *Derris trifoliata*, *Ceriops tagal*, *Excoecaria agallocha*, *Myriostachya wightiana*, *Porteresia coarctata*, from Indian Sundarbans, world's largest mangrove ecosystem. Root and pneumatophore samples from these mangrove species were studied for their anatomical adaptations, pure endophytic bacterial strains were established, genomic DNA was isolated from isolated bacteria, and PCR amplification of 16S rRNA gene from genomic DNA of bacteria was carried out. Partial 16S rRNA gene sequences were submitted to the NCBI database and accession numbers for the same was obtained. I have been successful in the establishment of 78 pure isolates of cultivable endophytic bacteria (NCBI Accession no. MT421976 to MT422053) from roots and pneumatophores of different mangroves and mangrove associate species of Indian Sundarbans. The study was conducted with the following objectives:

Objective-1: Study of morphological/histological niches, anatomical adaptations, Na^+/K^+ ratio in endosphere of roots and pneumatophores of mangrove species from degraded and non-degraded habitats of Sundarbans

For the study of anatomical adaptations and Na^+/K^+ ratio, I have selected *Avicennia alba*, *Avicennia marina*, *Avicennia officinalis*, *Heritiera fomes*, *Dalbergia* sp., *Bruguiera cylindrica*, *Bruguiera gymnorrhiza*, *Rhizophora mucronate*, *Xylocarpus* sp., *Derris trifoliata*, *Ceriops tagal*, *Excoecaria agallocha*, *Myriostachya wightiana*, *Porteresia coarctata*, from Indian Sundarbans. In histological transverse sections of roots and pneumatophores the following anatomical adaptive features are observed such as secondary cork tissues, aerenchymatous cortex, distinct endodermis, well developed vascular xylem and phloem with parenchyma rays, central pith tissues with parenchymatous cells etc.

Na^+/K^+ ratio of roots, shoots and leaves of the above mangrove species was carried out by flame photometry. Na^+/K^+ ratio was estimated in root endosphere niches of the above mangrove species that maintained a low ratio of Na^+/K^+ (<5) in roots. However, *Bruguiera gymnorrhiza* and *Ceriops* spp. showed higher (>5) Na^+/K^+ ratio in roots.

Na^+/K^+ ratio was estimated in shoot endosphere niches of the above mangrove species that maintained a low ratio of Na^+/K^+ (<5) in shoot except *Bruguiera gymnorrhiza* showed higher (>5) Na^+/K^+ ratio in shoot.

Na^+/K^+ ratio was estimated in leaf endosphere niches of the above mangrove species that maintained a low ratio of Na^+/K^+ (<5) in leaf. However, *Bruguiera gymnorrhiza* and *Myriostachya wightiana* showed higher (>5) Na^+/K^+ ratio in leaf.

Objective-2: Establishment of pure endophytic bacterial strains from mangrove roots and pneumatophores and their molecular identification by sequencing of 16S rRNA gene

Roots and pneumatophore samples of different mangrove species collected were cut into small pieces. After that surface sterilization was done by 0.1% HgCl_2 solution. Then the samples were incubated in LB broth medium. From there 50 μl of cultures were spread on LB plate and single colony was isolated after incubation. After that each single colony was identified. All total 78 bacterial colonies were identified as endophytes till date by me. The culturable community of endophytes comprises species of 12 genera viz. *Bacillus*, *Aeromonas*, *Pseudomonas*, *Staphylococcus*, *Vibrio*, *Gallacimonas*, *Serratia*, *Enterobacter*, *Pseudocitrobacter*, *Citrobacter*, *Acinetobacter*, *Mangrovibacter*. Bacterial endophytes were selected repeatedly on differential nutrient cycling media.

Objective-3: Plant growth promotion profiling of the established/accessioned endophytic bacterial strains

All 78 endophytic bacteria were tested for their plant growth-promoting potential under laboratory conditions through assays for indole-3-acetic acid production, phosphate solubilization, siderophore production, free nitrogen fixation (**Acetylene reduction assay for demonstration of nitrogenase activity *in vitro* for free nitrogen fixer endophytes**), 1-aminocyclopropane-1-carboxylate deaminase (ACC) synthesis.

For indole-3-acetic acid production activity the best IAA producer strains are found and their IAA production ranged between 9-17 µg/ml. The best IAA producer strains are as follows, such as *Pseudomonas sp.*, *Aeromonas sp.*, *Bacillus sp.* and *Staphylococcus sp.* The best 15 high IAA producer strains were also tested for their IAA production without adding tryptophan to the assay reaction. The IAA production without adding tryptophan ranged between 4.5-10 µg/ml.

The phosphorus (P) solubilization potential activity among the best P-solubilizer strains ranged between 90-160 µg of plant-available P released/ml of PSM. The best P-solubilizer strains found were *Aeromonas sp.*, *Pseudomonas sp.*, *Staphylococcus sp.*, *Gallacimonas sp.*, *Vibrio sp.*, and *Serratia sp.*

In case of siderophore production activity, the best siderophore-producing strains demonstrated siderophore production between 80%-95% in iron-free media. The best siderophore-producing strains observed are *Aeromonas sp.*, *Pseudomonas sp.*, *Staphylococcus sp.*, *Bacillus sp.*, *Mangrovibacter sp.*, and *Citrobacter sp.*

All 78 endophytic bacterial strains were tested for their ACC deaminase production potential. The best ACC deaminase-producing strains demonstrated ACC deaminase production units between 1.8-9. The best ACC deaminase-producing strains are as follows, such as *Aeromonas sp.*, *Pseudomonas sp.*, *Staphylococcus sp.*, *Bacillus sp.*, and *Citrobacter sp.*

Regarding the free nitrogen fixing potential of 78 endophytes, the best free nitrogen-fixing strains demonstrated reduced ethylene synthesis in the range of 0.4-14 nmole/100 µl/24 hour. The best reduced ethylene synthesis demonstrating strains are *Aeromonas sp.*, *Pseudomonas sp.*, *Staphylococcus sp.*, *Bacillus sp.*, *Pseudocitrobacter sp.* and *Citrobacter sp.*

Objective-4: Selection of PGP endophytic bacterial consortia on the basis of growth promotion criteria and growth curves for nursery/greenhouse/field applications

After analysing the plant growth promotion activity and salt tolerance profile via quantifying growth by measuring absorbance at 600 nm for some promising endophytic free nitrogen fixers, cellulose degraders and P-solubilizers on FNFM/CDM/PSM normal broth (3.99-5.44 dS/m), and also normal FNFM/CDM/PSM with additional 0.3M NaCl (25.23-31.94 dS/m), with additional 0.5 M NaCl (36.15-45.72 dS/m), and 0.7 M (45.09-56.73 dS/m), for 72 hrs starting at 0.1 OD at 0 hr. However, in most of the cases, the growth on FNFM/CDM/PSM broth without or with NaCl decreased in absorbance rather than increase after 72 hrs. On the basis of PGPR activity and salt tolerance profile, 18 bacterial strains were selected for making 3 combinations. The combinations are as follows:

A. Consortium BC1: *Aeromonas dhakensis* strain HPR7 (MT422007), *Mangrovibacter plantisponcer* strain BCRP5 (MT422011), *Pseudomonas stutzeri* strain BCY5 (MT422041), *Pseudomonas stutzeri* strain BCY7 (MT422042), *Bacillus subtilis* strain AOR5 (MT421976) and *Serratia marcescens* strain AOR4 (MT422009).

B. Consortium BC2: *Aeromonas allosaccharophila* strain DAL2 (MT422027), *Pseudomonas* sp. strain DER1 (MT422045), *Pseudomonas putida* strain DER3 (MT422020), *Pseudomonas fulva* strain DER9 (MT422023), *Aeromonas veronii* strain POT3 (MT422035), *Aeromonas veronii* strain POT7 (MT422025) and *Serratia marcescens* strain HPR4 (MT422006).

C. Consortium BC3: *Bacillus subtilis* strain AMR4 (MT421979), *Aeromonas hydrophila* strain HER3 (MT422047), *Bacillus altitudinis* strain XYL1 (MT422037), *Pseudocitrobacter faecalis* strain HRR5 (MT422004) *Serratia marcescens* strain HPR4 (MT422006) and *Enterobacter kobei* strain HRR1 (MT421989).

Objective-5: Application of selected PGP endophytic bacterial consortia on *Avicennia officinalis* saplings in mangrove nursery at Sundarbans for observing their effect on mangrove growth modulation.

The 3 selected consortia were applied twice on 23 days-old *Avicennia officinalis* saplings, 80 saplings for each consortium, and 80 saplings were used as control where no bacteria were applied in the mangrove nursery at Ramganga village of Sundarbans. Bacterial cultures were applied twice at 30 days intervals. Final shoot height, leaf width, and number of leaves per plant were measured from 95 days-old saplings and their effect on mangrove growth modulation was observed. Among 3 combinations consortium BC3 showed significant shoot

height improvement of *Avicennia officinalis* saplings. No significant difference in no. of leaves per sapling was observed among all the categories. BC1 and BC2 consortia-applied saplings showed a significant increase in leaf length. No significant difference in leaf width per sapling was observed among all the categories.

Objective-6: Application of selected PGP endophytic bacterial consortia on cultivated rice of Sundarbans at greenhouse for observing their effect on rice growth modulation.

Two selected rice varieties, Lunishree (N) and Dudheswar (D), were used for plant growth promotion studies at greenhouse pot experiments with control set where no bacterial culture was applied and also with conventional fertilizer NPK (20:20:20) applied in conventional doses for approximately 0.8 Kg of soil per pot used in the experiment.

A total of 12 bacterial consortia were used for the pot experiment; 5 pots for NPK with 3-4 seedlings per pot and 5 pots for control with 3-4 seedlings per pot were used for both the rice varieties. Among 12 bacterial consortia applied, 3 consortia belonged to only endophytic bacterial consortia BC1, BC2, and BC3. The remaining 9 consortia were made combining 6 rhizospheric consortia from halophytic native grasses from Sundarbans developed in another study. The greenhouse experiments were performed twice and the consortia were applied two times in both experiments. From both experiments we could obtain some significant results in shoot heights and leaf lengths of the two selected rice varieties, Lunishree (N) and Dudheswar (D). In addition, significant improvement was observed in terms of N and P enrichment in the consortia-added pot rhizosphere soil in comparison to the control pots where no bacterial consortia were added and also the NPK-added pot soil.

The same 3 root endophytic consortia were also applied in combination with PGP native halotolerant grass rhizobacteria in two consecutive greenhouse experiments. Tracking of P-solubilization profile at rhizospheres after addition of bacteria revealed enrichment of added consortia validated through increase of soluble-P release at rhizosphere even at the time of maximum utilization by the plants.

Objective-7: Application of selected PGP endophytic bacterial consortia on cultivated rice of Sundarbans at the field at Sundarbans for observing their effect on rice growth and yield modulation.

After the greenhouse experiments, 3 combinations of 18 selected growth-promoting bacteria out of these 78 accessions were applied to the rice field of Dudheswar landrace (IC No. 593998), widely cultivated at Sundarbans and also known to be an ideal salt tolerant variety

for growing at low lands. Field experiments were performed for twice to date, indicating significantly increased yield for the consortia-added plots in comparison to the control plots where bacterial consortia were not added and also compared to the rice grain yield data collected from several other neighbouring rice fields grown by local farmers where rice was cultivated with conventional fertilizers.

1st Field application of Consortium BC1 showed a yield of an average of 9.58 quintal/bigha, Consortium BC2 showed a yield of an average of 11.2 quintal/bigha, and Consortium BC3 showed a yield of an average of 11.3 quintal/bigha in comparison to control fields (without bacteria) yielding average of 7.52 quintal/bigha. The data collected from local farmers' field in the Sundarban western part in Patharpratima block exhibited only a yield of average of 3.7 quintal/bigha. The results of the study is found to be significant with respect to the control.

From the observation of 1st rice field experiment significant results, 2nd rice field experiment was conducted with the selected bacterial consortia where one endophytic consortium as BC3/BEC3 and two mixed combinations such as BEC2+SRC2 and BEC3+SRC3 were applied. 2nd rice field experiment conducted in two rice field plots such as field 1 and field 2.

In field 1 of 2nd field application, Consortium BC3 showed an yield of average 3.57 quintal/bigha, Consortium BEC2+SRC2 showed a yield of average 28.97 quintal/bigha and BEC3+SRC3 showed a yield of average 4.18 quintal/bigha in comparison to control fields (without bacteria) yielding average 0.66 quintal/bigha.

In field 2 of 2nd field application of Consortium BC3 showed a yield of average 18.94 quintal/bigha, Consortium BEC2+SRC2 showed a yield of average 16.14 quintal/bigha and BEC3+SRC3 showed a yield of average 13.96 quintal/bigha in comparison to control fields (without bacteria) yielding average 9.27 quintal/bigha. In this case the yield demonstrated significant increase in quintal/bigha as compared to the control both in field 1 and field 2.

Tracking of P-solubilization profile at rhizospheres in both the field experiments at Sundarbans after addition of bacteria revealed enrichment of added consortia validated through increase of soluble-P release at rhizosphere even at the time of maximum utilization by the plants. N-enrichment was also observed at rice rhizospheres in field where bacterial consortia were applied.

Objective-8: Observation of bacterial community abundances by Next Generation Sequencing (NGS) from rice field before and after rice cultivation with PGP endophytic bacterial consortia

The next generation metagenomic sequencing of rhizobacterial community from the collected rhizospheric soil from the 1st field experiment of Indian Sundarbnas, established noticeable enrichment of the applied bacterial consortia through analysing the relative abundance of the constituent bacterial members by amplicon based V3-V4 16S rRNA metagenomic sequencing through Illumina MiSeq platform. When the data was compared on the basis of phylum level, it showed enrichment of Firmicutes at BC1, BC2, BC3 consortia added soil as well as when all root endophyte consortia added soil was sampled in a mixed way. The constituent genus of root endophyte consortia *Bacillus* spp. belongs to the phylum Firmicutes. When the data was compared on the basis of class level it showed enrichment of Bacilli at BC1, BC2, BC3 consortia added soil as well as enrichment of Gammaproteobacteria at BC1, BC2, BC3 consortia added soil and when all root endophyte consortia added soil was sampled in a mixed way. The constituent genus of root endophyte consortia *Bacillus* spp. belongs to the class Bacilli, whereas *Aeromonas*, *Mangrovibacter*, *Pseudomonas*, *Serratia*, *Pseudocitrobacter*, *Enterobacter* spp. all belong to the class Gammaproteobacteria. When we the data was compared on the basis of family level it showed enrichment of Bacillaceae at BC1, BC2, BC3 consortia added soil. The family Prevotellaceae possesses the genus *Prevotella_9* and *Prevotella* which are signature sequences of soil manured with cow-dung as *Prevotella_9/Prevotella* has been reported to be present in gut microbiome of these animals. Relative abundance of Prevotellaceae was observed to be higher in control rhizosphere as compared to BC1, BC2, BC3 consortia added soil. However, the referred abundance is observed to be very high when all root endophyte consortia added soil was sampled in a mixed way (might be due to sampling error).

Comparative account of relative abundances at genus level shows the following features:

- Abundance enrichment of *Aeromonas* at BC2, BC3 consortia added soil
- Noticeable abundance enrichment of *Bacillus* at BC1, BC2, BC3 consortia added soil
- Consistent relative abundance of *Pseudomonas* observed in all the samples with highest abundance observed when all root endophyte consortia added soil was sampled in a mixed way

- Decrease in abundance of *Prevotella_9* at BC1, BC2, BC3 consortia added soil. However, the referred abundance is observed to be very high when all root endophyte consortia added soil was sampled in a mixed way (might be a cause of sampling error).
- Noticeable abundance of *Mangrovibacterium* at BC2, BC3 consortia added soil, all root endophyte consortia added soil as well as all halo-grass rhizosphere bacterial consortia added soil.
- The constituent genera of root endophyte consortia are *Aeromonas* spp., *Bacillus* spp. *Pseudomonas* spp., *Mangrovibacter* spp.

I. Introduction

1. Introduction:

1.1 Unique adaptability of diverse root niches of mangrove ecosystem:

The mangrove ecosystem is characterized by its disproportionately large uniquely integrated above and below-ground conspicuous root architecture as compared to its above-ground canopy with foliage (Ola et al, 2019). The extensive network of spreading horizontal cable roots interconnecting between aerial and below-ground root biomass, massive buttress roots anchoring the tree trunks, cone roots, knee root, and stilt/prop roots assisting in both anchorage, aerial gas exchange via negatively geotropic pencil-like pneumatophore roots, complemented with rhizopsheric nutrient absorption and water intake through root ultra-filtration restricting sodium chloride inside the plant system, are characteristic of root biomass of intertidal mangrove ecosystem (Takarina, 2020). The periodic dynamicity of low-tide and high-tide conditions, variability in sediment texture composition, long periods of complete submergence of mangrove root system under hypersaline water, extremely anaerobic niches, tidal hydrodynamic forces, cyclonic wind speed, all these environmental criteria led the intertidal mangrove community to develop unique adaptive features of their root systems, to survive and flourish in this unambiguously stressful habitat.

The complex root networks including aerial root systems provide anchorage and facilitate gaseous exchange in the halophytic mangrove environment in oxygen-poor, submerged soil (Okello et al, 2020). The porous interior structure of mangrove roots, consisting of a series of interconnected vents or channels collectively named as the aerenchyma is maintained as a reservoir of oxygen for mangrove plants. This unique tissue allows for gaseous exchange between the exposed above-ground plant structure and the submerged, oxygen-deprived roots. Typical specialized aerial roots are highly variable viz. buttress roots, flying buttresses, prop roots, surface roots, stilt roots or plank roots, spreading roots, cable roots with pneumatophores, pencil roots, cone roots, knee roots. Pneumatophores facilitate air storage and transport oxygen to belowground roots at low tide conditions (Srikanth et al, 2016; Okello et al, 2020). The widespread lenticels on the pneumatophore surface and a spongy cortex made up of large aerenchyma lacunae help mangroves with efficient internal oxygen transfer (Okello et al, 2020). They also provide mechanical support to withstand high tidal force as well as high wind velocity at the shoreline (Srikanth et al, 2016).

The below-ground to above-ground biomass ratio for mangroves is highly different from terrestrial plant communities. In mangroves, a larger proportion of net primary production is

consumed for their root growth. Extremely unstable substratum conditions also add to the reasons behind maintaining such a high root-to-shoot ratio (Saintilan, 1997).

A narrowed cortex reducing the distance between the epidermis and vascular tissue, the absence of root hairs, the presence of pronounced Casparian strips, significant endodermis, presence of superficial wide exodermis in roots, are typical traits of the ultra-filtration mechanism via roots existing in mangrove ecosystem, while the distinct anatomical transition from below-ground to aerial pneumatophores are also adaptive signatures of mangrove root systems to support an integrative functional network for survival of these mangrove communities in such a harsh external environment (Chen et al, 2011; Tomlinson, 2016). In aerial roots the initial exarch orientation of protoxylem (typical of roots), gradually transforms into mesarch and finally endarch type (typical of shoots) along with well-developed periderm, lenticels, secondary thickening, abundant trichosclereids, to acclimate for aerial mode of sustenance (Tomlinson, 2016). However, entering into the substratum, the same roots develop the exarch protoxylem vasculature, reduced cortex, little-developed phellogen, limited secondary thickening, airy spongy ground tissue like aerenchyma – an interesting enigma of root developmental process demonstrated by the mangrove plants (Tomlinson, 2016).

Mangrove tree trunks having massive above-ground root systems not only offer structural support, nutrient provision, and gas exchange, nevertheless it creates a highly favourable integral environment for the native fauna and flora in the habitat (Brooks and Bells, 2005). A minor variation in root architecture could contribute to change in habitat function and structure (Brooks and Bells, 2005). As observed in the mangrove *Rhizophora stylosa*, sediment bulk density (BD) also could influence the stilt root morphology below-ground (Ola et al, 2019). Root biomass enhanced in higher BD soils, with reduced primary root length, whereas root diameter increased in higher BD soils as compared to the low BD soils. Physical hindrance in high soil BD reduces the aerenchyma, available oxygen, instead increased structural stability with fibrous cell development, finally leading to more carbon sequestration (Ola et al, 2019). The intertwining pneumatophore network topologies observed in mangroves across the salt-stress gradient, where the lack of resource exchange results in random root network formation patterns, was found to be another adaptive strategy of mangroves positively facilitating in reduction of stress and enhanced resource exchange (Vovides et al, 2021).

1.2 Ultrafiltration of hypersaline water via roots for intake - a unique adaptation across mangroves:

Solutes from water move through the roots in apoplastic, symplastic, and cell-to-cell pathways. The apoplastic pathway is known to get blocked by hydrophobic barriers present in both the endo- and exodermis, while the plasma membranes are selectively permeable for the solutes. With these inherent features of plant transport via roots, the presence of a conspicuous endodermal membrane with the dense hydrophobic suberin and lignin deposited on Casparian strips acts as a barrier regulating the apoplastic pathway, and the entry of solutes through it (Chen et al, 2011). The plasma membrane of the endodermal cell remains tightly attached to the primary cell wall at the Casparian strips and allows reduced amounts of ions like Na^+ , Ca^{2+} , K^+ , Zn^{2+} to enter into the roots, performing the critical role of ultrafiltration mechanism (Chen et al, 2011). In *Arabidopsis thaliana* mutants, defective in suberin deposition and Casparian strip development, increased entry of solute with indirectly reduced root hydraulic conductivity was observed, proving the significance of this Casparian strip acting as an apoplastic barrier regulating the hydro-mineral transport via root, that in turn controls the shoot and overall above-ground growth (Calvo-Polanco et al, 2021). A cytochrome P450 gene was reported to regulate suberin biosynthesis and observed to be up-regulated when mangrove *Avicennia officinalis* roots were treated with saline water and showed increased suberin deposition. This developmental trait maintained low levels of Na^+ in the xylem sap and helped to filter ~99% of salt from the surrounding saline water (Krishnamurthy et al, 2014). In addition to prominent endodermis and Casparian strips in mangrove roots, periderm tissue also having suberin deposition on it, acts as an efficient barrier in mangrove *Sonneratia* spp. to the entry of water to root cells excluding the salt ion from saline water (Tatongjai et al, 2021).

1.3 Mangrove-microbe interaction in the rhizosphere for growth promotion amid hypersaline intertidal environment - another challenge faced by mangrove ecosystem:

Chemical profiling of non-sterile rhizosphere soil of abiotically and biotically stressed below-ground habitat revealed an interesting scenario to establish a below-ground “cry-for-help” model (Rolfe et al, 2019; Rizaludin et al, 2021). This “cry-for-help” theory postulates, that under stressed rhizo-environments, plant roots exude several metabolites like carbohydrates, amino acids, organic acids, membrane lipids, in the rhizosphere and these root exudates cause specific signaling effects attracting a specific rhizobiome microbiota, that help the plants to

overcome the stressed situation. While under biotic stress, “cry-for-help” via root exudates resulted in the recruitment/root colonization of beneficial microbes that restrain the development of pathogens, via secretion of antimicrobial exudates against susceptible microbial pathogens, leading to the enrichment of a disease-suppressive, disease-tolerant microbiome in and around the roots of the stressed plant (both in endosphere of the plant root as root endophytes and in rhizosphere of the plant species as rhizphytes or rhizosphere microbiota) (Rolfe et al, 2019). It was also reported that this plant-microbe interaction at rhizoplane also involves the enrichment/recruitment of plant growth-promoting rhizobacteria (PGPR), mediated by chemical signaling via organic acids exudates of the stressed roots. This specific group of PGPR was identified by the presence of plant-beneficial function-contributing (PBFC) genes in Proteobacterial PGPR (Rolfe et al, 2019). This “cry-for-help” hypothesis demonstrates the initiation of the mechanism for a long-term adaptation strategy via plant-microbe interactions under challenged environments (Rolfe et al, 2019). In addition to soluble root exudate metabolites, several volatile organic compounds (VOC) are also known to be emitted by stressed plant roots as an adaptive strategy of “cry-for-help”, where via emission of these VOCs plants can also warn neighboring plants to activate their defenses so that invading pathogens could be minimized leading to the recruitment of beneficial microbes (Rizaludin et al, 2021). However, studying root exudate metabolites below-ground is a very challenging task in a heterogeneous soil bed with water- and air-filled pores recalcitrant to chemical profiling thus creating a knowledge gap in establishing a “cry-for-help” strategy being applicable across irrespective of stress types (Rizaludin et al, 2021). Additionally, this “cry-for-help” theory contributes greatly to the rhizosphere colonization of the non-symbiotic beneficial bacteria (Liu et al, 2024). This root colonization by beneficial non-symbiotic rhizobacteria is a very complex process that initiates with rhizosphere chemotaxis, and root attachment, followed by rhizoplane biofilm formation, and may also involve subsequent endophytic colonization for some rhizobacteria (Liu et al, 2024). Utilization of root exudates as the sole carbon source of energy and rapid proliferation becomes very important in this process of colonization. Simultaneously, some bacteria colonized on the root surface also start penetrating the plant tissues and begin an endophytic lifestyle helping plants acquiesce nutrients in a facultative/obligatory symbiotic or non-symbiotic plant–microbe relationship (Liu et al, 2024).

Amid the abiotically stressed environment, like nutrient-deficient, high saline soil habitat of mangrove rhizosphere, this “cry-for-help” theory might become more evident, where PGPR bacteria are found to get enriched selectively both in the rhizospheres and root endospheres (as

root endophytic bacteria) of the stressed plants. Root endophytic bacteria are components of the soil-microbe-plant continuum and are known to be bidirectional in their movement from soil-to-plant and plant-to-soil (Verma et al, 2021). Evolution of such a complex relationship from rhizospheric to endophytic mode shifting, from free-living to symbiotic lifestyle transition, again represents a crucial plant-microbe interaction continuum. The nutrient acquisition “rhizophagy cycle” of root PGPR endophytic microbes in their free-living mode enriches the rhizosphere with nutrients and makes these nutrients available to the plants after entering into the root cells surviving and flourishing in endophytic mode (Verma et al, 2021). Moreover, especially for mangrove plants, the extensive “root system architecture” (RSA), the spatial configuration of elaborate root network consisting of primary and secondary, both aerial and underground roots and pneumatophores, branch roots, root hairs, root meristems and root caps that sense the abiotic stressors under soil habitat could also be influenced greatly by the root endophytic PGPR community. The PGPR by auxin production, may enhance the auxin level in roots, auxins can cross-talk with other phytohormones like cytokinins and ethylene, and ACC-deaminase synthesis could reduce ethylene, and all these phytohormone-mediated PGPR root endophytes have great potential to regulate the root development finally modifying the “root system architecture” (RSA) (Verma et al, 2021).

1.4 Root endospheres of mangroves as the reservoir of PGPR endophytic bacteria from mangrove ecosystems:

Mangrove habitats serve as a rich source of endophytic microbes. The root tips and lateral root emergence sites are the main colonization sites of endophytic bacteria. The important entry sites are differentiation and elongation zones above the root tip. Intercellular colonization of endophytes into living root tissues occurs after their entry. Within root cells intracellular colonization of periplasmic spaces has been observed (Verma et al, 2021). These endophytes have significant role in regulating the physiology of the host plants. Plant roots rich in endophytes are considered to have better health than the plants without endophytes (Waller et al, 2005). Endophytic bacteria colonizing the host plants’ internal tissues happen to be in mutualistic, commensalistic, symbiotic or trophobiotic relationships with the plants, essentially imposing no negative impact on their host plants (Ryan et al, 2008). PGPR endophytes play a very important role in plant growth and development in different ways such as the production of phytohormones, sequestration of iron by siderophore, solubilization of inorganic phosphate, nitrogen fixation, promoting the growth of the host plants, even in adverse environmental conditions (Chanway, 1996; Bent and Chanway, 1998). Different endophytic bacterial genera

like *Pseudomonas*, *Burkholderia*, *Azotobacter*, *Azospirillum*, *Alcaligenes*, *Klebsiella*, *Arthrobacter* and *Serratia* help in plant growth promotion by the PGPR activities viz. production of siderophore, production of indole-3-acetic acid (IAA), and solubilization of calcium phosphate (Mukherjee et al, 2017). Different genera of plant growth promoting bacteria (PGPB) such as *Bacillus*, *Pseudomonas*, *Enterobacter*, *Burkholderia*, *Paenibacillus*, *Agrobacterium*, *Azospirillum* and *Azotobacter* enter from the rhizospheric region, initially colonize on the root surface and finally enter into plants' internal tissues and start colonizing there (Puri et al, 2017).

Endophytic PGPB colonized in mangrove roots have a special role in regulating the mangrove forest community's chemical environment. Nutrient-limited mangrove muds are the result of subsurface bacterial populations and epibenthic microalgae sequestering nutrients; the primary decomposers in anoxic mangrove sediments, the sulfate-reducing bacteria such as *Desulfosarcina*, *Desulfotomaculum*, *Desulfovibrio*, and *Desulfococcus* majorly limit phosphorus, iron, and sulfur dynamics under mangrove environment (Alongi et al, 1993; Rivera-Monroy and Twilley, 1996). Under this condition, root endophytic PGPB can help mangroves in supplying nutrients for plants' metabolism. From the pneumatophores of *Avicennia* in the Beachwood Mangrove Reserve (South Africa), the N₂-fixing cyanobacterial endophytes were isolated which can supply an annual 24.3% nitrogen necessity of that mangrove ecosystem. It was reported that cyanobacteria as mangrove root endophytes fix N₂ at a faster rate in comparison to its growth in N-free artificial growing media (Toledo et al, 1995). The 18 isolates of endophytic bacteria from mangrove leaves of *Avicennia marina* showed inhibition against the pathogen *Stenotrophomonas maltophilia* that causes ice-ice disease on seaweed (Rahman et al., 2019). 18 isolates belonged to Gammaproteobacteria, Firmicutes, and Enterobacteria. Among them, *Bacillus subtilis* (AMS-11), *Pseudomonas* sp. (AMS-08), and *Vibrio* sp. (AMS-05) showed the best inhibitions against *Stenotrophomonas maltophilia* (Rahman et al., 2019). Plant growth-promoting (PGP) root endophytes adapted in high salinity conditions like from mangrove habitats, have high potential for improving crop production under saline soil conditions both directly and indirectly. In this regard, Sundarbans mangrove ecosystem have turned out as a natural source of endophytic PGPR adapted to high salinity conditions (Pallavi et al, 2023). It was reported that the accumulation of glycine betaine-like compounds in higher concentrations leads to enhanced salinity tolerance in rice induced by endophytic bacteria *Pseudomonas pseudoalcaligenes* (Jha et al, 2011). The co-inoculation of endophytic bacteria from various ecological niches is a promising substitute for

individual PGPR inoculation as were shown in some cases. The nitrogen-fixing *Phyllobacterium* sp. and the phosphate solubilizing *Bacillus licheniformis* when co-inoculated in the rhizospheres, *Laguncularia racemosa*, *Avicennia germinans*, and *Rhizophora mangle* mangrove plants displayed excellent phosphorous and nitrogen assimilation as compared to the plants with those endophytes inoculated individually (Rojas et al, 2001). Deivanai et al, 2014 isolated endophytic bacteria *Pantoea ananatis* (1MSE1) and *Bacillus amyloliquefaciens* (3MPE1) from the mangrove plants *Rhizophora apiculata*, that were applied on rice seedlings and a significant increase in chlorophyll content, root and shoot height, fresh weight were observed. The use of endophytes as bio-fertilizers that are eco-friendly, showing improved crop production, is gaining importance among agronomists and environmentalists. This alternative use of endophytic bacteria as bio-fertilizer reduces chemical input into the environment (Mukherjee et al, 2017).

1.5 Endophytes in agriculture and other beneficial roles of PGP endophytes for plant hosts:

In developing countries, agriculture is the principal economic activity and livelihood of people (Miliute et al, 2015). Exploitation and exploration of beneficial soil bacteria viz. endophytes inhabiting the plant tissues may be a good strategy to boost crop yield and reduce negative impacts to ensure the enhancement of the productivity of agriculture (Dheeman et al, 2017). Compared to rhizospheric bacteria, endophytic bacteria are better at nitrogen fixation. In comparison with the soil environment, they provide direct nitrogen to the host plant in fixed form due to low oxygen pressure within the plant cells (Marella, 2014). Endophytic bacteria can promote plant growth and development by simplifying mobilization and uptake of both micronutrients and macronutrients (Shakeel et al, 2015). In modern agricultural practices, the use of chemicals and fertilizer to control pests and pathogens alters the relationship between endophytes and their host crop plants across different soil structures and flourish well only in their wild relatives, where such an external chemical environment is not present (Minz et al, 2013). Biotic and abiotic factors such as environmental conditions, plant genotype, plant–microbe interactions, and microbe–microbe interactions influence the community structure of endophytes. The major effect on the structure and function of endophytic bacterial diversity depends upon agricultural practices, such as soil tillage, irrigation, use of fertilizers, and pesticides. Therefore, the maintenance of plant endophytic bacterial natural diversity depends upon agricultural practices, and exploiting the plant endophytic bacterial diversity to secure the

productivity and agricultural production quality of crop species, is required for sustainable agriculture (Jain and Pundir, 2017).

Endophytic microorganism has many beneficial effects on host plants such as promoting plant growth (Okon and Labandera-Gonzalez 1994), systemic resistance induction (Hallmann et al, 1997), siderophore production (Burd et al, 1998), plant diseases and pests control (Mariano et al, 2004), biological nitrogen fixation (Dobereiner and Boddey 1981), and antibiotic production (Strobel and Daisy 2003). Endophytic bacteria modulate the host plant's physiological condition and facilitate them to tolerate abiotic stresses, growth, and development (Conrath et al, 2006; Rodriguez et al, 2008). *Paenibacillus polymyxa* (endophytic diazotroph) in Cupressaceae, was considered for 36% foliar nitrogen derived from the atmosphere that helped *Thuja plicata* to show significant improvement of growth in nitrogen-limited soil conditions (Anand and Chanway, 2013). Endophytic bacteria help plant growth promotion in two ways, via direct and indirect methods. Direct promotion of plant growth occurs when endophytes facilitate the acquisition of essential nutrients such as sequestration of iron by siderophore, solubilization of inorganic phosphate, nitrogen fixation or modulate the hormone levels of a plant. Hormone levels modulation may include synthesizing one to many phytohormones such as auxin, gibberellin and cytokinin. Some PGPBs synthesize an enzyme, ACC deaminase (1-aminocyclopropane-1-carboxylate) which can lessen the phytohormone ethylene level. ACC deaminase split the ACC compound, immediate precursor of ethylene in all higher plant groups. PGPR can help plant growth and development indirectly through the production of cell wall-degrading enzymes, antibiotics, induced systemic resistance, reducing the quantity of iron obtainable to pathogens, and the formation of volatile compounds essential for pathogen-inhibition to minimize or stop plant damage created by pathogenic organisms such as fungus, bacteria, and nematodes (Santoyo et al, 2016). More than 20 genera of PGPB such as *Bacillus*, *Pseudomonas*, *Paenibacillus*, *Burkholderia*, *Enterobacter*, *Agrobacterium*, *Azospirillum*, and *Azotobacter* are known to be derived from the rhizosphere, colonize the root surface and also can penetrate the plants and colonize the internal tissues, as endophytes showing growth-promoting effects on plants (Puri et al, 2017). Phytohormone producing some endophytic bacterial genera are *Erwinia*, *Pseudomonas*, *Gluconacetobacter*, *Azospirillum*, *Herbaspirillum*, and *Pantoea* (Kuklinsky-Sobral et al, 2004; Maheshwari et al, 2015). Plant endophytic bacteria were isolated from soybeans as good phosphate solubilizers (Kuklinsky-Sobral et al, 2004). In association with sugarcane, various nitrogen-fixing endophytes can fix nitrogen from the atmosphere, up to 30-80 kg N/ha/year (Boddey et al, 1995). Various

endophytic bacteria such as *Stenotrophomonas*, *Pseudomonas*, and *Burkholderia* that can fix nitrogen from the atmosphere, helped various grasses to grow in low nitrogen-containing soil. Endophytes can also act as a biocontrol agent stimulating plant growth, development, and productivity (Shiomi et al, 2006).

ALKahtani et al, (2020) stated that bacterial endophytes *Bacillus* spp. and *Brevibacillus* spp. identified from desert plants showed that when these bacteria were inoculated in maize rhizosphere *in-vitro*, they increased the growth, and significantly increased P and N contents in maize shoots.

Bhattacharyya and Jha (2012) also proposed that various crops like maize, wheat, potato, tomato, etc. significantly increased their root length, plant height, and dry biomass production by most PGPR isolates. EL-Deeb et al, (2012) showed that endophytes help rose plants increase their root length so that they can penetrate their roots deep in the soil to absorb more water and can survive under harsh conditions. Pallavi et al, (2023) found that several salt-tolerant rhizobacteria from the Sundarbans mangrove ecosystem, help in plant growth promotion activity by phosphate solubilization, zinc solubilization, IAA production, and production of siderophores, which also impart salinity tolerance for pea seedling growth and seed germination. In another study by Prihatiningsih et al, (2023) endophytic bacterial consortium was developed and applied on a rice field and significant improvement of the tiller number, grain weight, and grain yield per clump was observed to increase by 37.85%, 39.50%, 52.76%, respectively. Another study by Shabanamol et al (2020) observed that growth improvement like root and shoot height increase of rice plants by endophytic diazotrophic bacteria *Lysinibacillus sphaericus* was observed under greenhouse conditions.

1.6 Growth promoting traits of endophytic bacteria

The beneficial effects of endophytes include phytohormone production, increased nutrients availability, phytoremediation and rhizoremediation, plant pathogen suppression and imparting of stress resistance to host plants. Some endophytic bacteria and their host plant are described below-

Table 1: Some endophytic bacteria possessing host plants:

Sl. No.	Endophytic bacteria	Host plant	References
1	<i>Bacillus</i> sp. SLS18	<i>Sorghum bicolor</i>	Luo et al, (2012)
2	<i>Paenibacillus</i>	Orchid	Feria et al, (2013)
3	<i>Enterobacter</i> sp., <i>Bacillus subtilis</i> , <i>Enterobacter ludwigii</i> , <i>Bacillus</i> sp., <i>Pseudomonas</i> sp., <i>Curtobacterium citreum</i> , <i>Lactobacillus plantarum</i> , and <i>Pantoea punctata</i> .	<i>Fragaria ananassa</i>	de Melo Pereira et al, (2012)
4	<i>Bacillus subtilis</i>	<i>Ocimum sanctum</i>	Tiwari et al, (2010)
5	<i>Bacillus pumilus</i> and <i>Acromobacter xylosoxidans</i>	<i>Helianthus annuus</i>	Forchetti et al, (2010)
6	<i>Enterobacter</i> sp. FD17; <i>Bacillus</i> spp.	<i>Zea mays</i>	Naveed et al, (2014); Gond et. al, (2015)
7	<i>Paenibacillus polymyxa</i>	<i>Panicum virgatum</i> L.	Ker et al, (2012)
8	<i>Pseudomonas</i> spp.	<i>Solanum melongena</i>	Ramesh & Phadke (2012)
9	<i>Neofusicoccum austral</i>	<i>Myrtus communis</i>	Nicoletti et al, (2014)
10	<i>Bacillus</i> sp.; <i>Phomopsis liquidambari</i>	<i>Oryza sativa</i> L.	Rangjaroen et al, (2015); Yang et al, (2010)
11	<i>Sphingomonas</i> sp. LK11	<i>Lycopersicon esculentum</i>	Khan et al, (2014)
12	<i>Bacillus</i> sp.	Poplar and willow	Kandel et al, (2010)
13	<i>Salmonella</i> , <i>Escherichia fergusonii</i> , <i>Bacillus megaterium</i> , <i>Enterica</i> , <i>Acinetobacter calcoaceticus</i> , <i>Pectobacterium</i> , <i>Cedecea davisae</i> , <i>Brevibacillus choshinensis</i> , and <i>Escherichia fergusonii</i>	<i>Coffea</i> sp.	Silva et al, (2012)
14	<i>Pseudomonas</i> , <i>Microbacterium</i> , <i>Sphingobacterium</i> , <i>Erwinia</i> , <i>Stenotrophomonas</i> , <i>Agrobacterium</i> , and <i>Herbaspirillum</i>	<i>Sorghum bicolor</i>	Maropola et al, (2015)

Plant intake of vital nutrients is facilitated by endophytes. Abiotic and biotic stress tolerance as well as enhanced plant nutrition may be linked to the plant growth promoters' stimulations of plant nutrient absorption and development (Machungo et al, 2009). According to some reports, *Festuca rubra* increased its phosphorus absorption after being injected with the endophytic fungi *Epichloe festucae* (Zabalgogezcoa et al, 2006; Pineda et al, 2010). Similar to this, it was demonstrated that the nitrogen fixation by the *Heteroconium chaetospira* (root endophyte) greatly increases the biomass output of Chinese cabbage (Usuki and Narisawa 2007). A small number of endophytic bacteria use the enzymes phytase, C-P lyase, and nonspecific phosphatases to convert organic phosphate into inorganic phosphate.

1.6.a. Phosphate-solubilization:

The endophytic bacteria are referred to as phosphate solubilizers because inorganic phosphates in the soil are solubilized by them and making it available for the plants is a well-known mechanism (Walia et al, 2017). Phosphate solubilization is thought to occur via several organic acids, including acetate, gluconate, glycolate, ketogluconate, lactate, tartrate, oxalate, succinate, and citrate secreted by the endophytic bacteria (Jain and Pundir, 2017). Phosphorus is present in soil both inorganic and organic forms. Inorganic phosphorous complexes (including iron, aluminium, and calcium cations) are found in the negatively charged environment. These compounds are comparatively insoluble, and their segregation is dependent upon pH. The pH between 6 and 7 is suitable for plants and microorganisms. Under these conditions phosphate rapidly converts to its organic form by endophytes, and it becomes available to plants. Organic P solubilization is a mineralization process (Walia et al, 2017). *Enterobacter*, *Burkholderia*, *Pantoea*, *Azotobacter*, and *Pseudomonas*, these endophytic bacteria have the capability to solubilize phosphate and enhance plant development (Park et al, 2010).

1.6.b. Siderophore production:

Siderophores are iron chelating agents, also known as low molecular weight secondary metabolites, which are synthesized by different groups of microbes which facilitate the plants in scavenging iron under iron-limited conditions. Siderophores function as chelating or solubilizing agents for iron from insoluble forms of iron. Iron is an important trace metal needed for microbial and plant life. In aerobic conditions, iron is found mainly as Fe^{3+} , converted to oxyhydroxides and hydroxides which are insoluble and unavailable to microbes. Iron oxidizing bacteria play a very important role in solubilizing this metal and the formation

of Fe^{3+} which are easily available to plants via chelation of siderophore compounds (Rajkumar et al, 2010; Andrews and Duckworth, 2016).

1.6.c. IAA production:

Indoleacetic acid (IAA) is a phytohormone and the most important natural auxin. IAA plays several growth functions in plants such as cell expansion, organogenesis, differentiation, tropic responses, division, and gene regulation (Patel and Patel, 2014). Hormone level modulations may include synthesizing one to more than one phytohormones such as cytokinin, auxin, and gibberellin by PGPB (Santoyo et al, 2016). Many endophytic bacteria can produce the auxin phytohormone IAA. IAA may be produced by microorganisms in the presence of the precursor L-tryptophan. IAA produced by endophytic bacteria gets utilized by the plant host which enhances plant growth and yield. Different *Bacillus* and *Pseudomonas* species are found for their IAA production ability (Patel and Patel, 2014). The three phytohormones i.e. IAA, gibberellic acid (GA), and cytokinin (CK) are particularly important in alleviating salt stress effects.

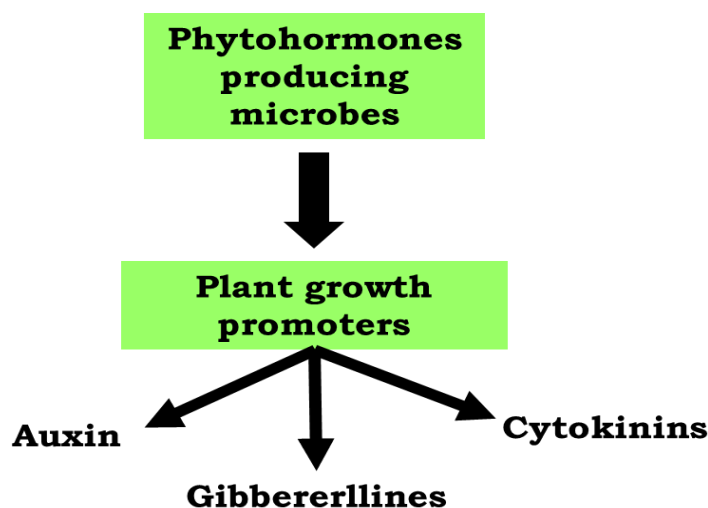


Figure 1.1: Phytohormone production by endophytes.

1.6.d. ACC deaminase production:

Some plant growth-promoting endophytic bacteria can produce 1-aminocyclopropane-1-carboxylate (ACC) deaminase enzyme. This enzyme promotes plant growth and development by decreasing plant ethylene levels under several abiotic and biotic stresses such as high light, extreme temperatures, drought, flooding, high salt, and different pathogens like bacteria, viruses, fungi, etc. When ethylene level is high then it affects plant growth and development. Ethylene is known as an anti-growth hormone. 1-aminocyclopropane-1-carboxylate (ACC)

deaminase enzyme helps decrease plant ethylene levels via the decomposition of ACC, the precursor of ethylene (Glick et al, 2007). When ethylene levels are decreased by the ACC deaminase enzyme, it simultaneously allows the stimulation of IAA causing cell elongation and proliferation without imposing any negative effects on increased ACC synthase and decreased levels of plant ethylene (Glick et al, 2007).

1.6.e. Nitrogen fixation:

Nitrogen is one of the very important macronutrients for plants. In the biological nitrogen fixation process, the atmospheric nitrogen is transformed into plants. In this process, nitrogen-fixing bacteria use the nitrogenase enzyme to convert nitrogen to ammonia (Kim and Rees 1994). Nitrogen-fixing bacteria are classified as non-symbiotic and symbiotic nitrogen-fixing bacteria. Non-symbiotic nitrogen-fixing bacteria *Azotobacter*, are well-known free-living nitrogen-fixing bacteria. Rhizobia are the best example of the symbiotic nitrogen-fixing bacteria (Ahemad and Kibret, 2014).

Table 2: Some common plant growth promotion traits by endophytic/rhizospheric bacteria.

Sl. No.	Bacterial genera	Plant growth promoting traits	References
1	<i>Azoarcus</i> sp.	Fixation of nitrogen	Krause et al, (2006)
2	<i>Aeromonas veronii</i> , <i>Enterobacter cloacae</i>	IAA synthesis	Bhattacharyya & Jha, (2012)
3	<i>Azospirillum</i> sp.	Fixation of nitrogen, Secretion of phytohormone	Kaneko et al, (2010)
4	<i>Azospirillum lipoferum</i>	Fixation of nitrogen, Secretion of phytohormone	Wisniewski-Dyé et al, (2011)
5	<i>Burkholderia</i> spp.	nif gene cluster, ACC deaminase, antifungal action (indirect PGP)	Kwak et al, (2012)
6	<i>Enterobacter</i> sp.	IAA synthesis, Siderophore, synthesis of acetoin and 2,3-butanediol, antifungal action (indirect PGP)	Taghavi et al, (2009)
7	<i>Burkholderia phytofirmans</i>	ACC deaminase, IAA synthesis	Weilharter et al, (2011)

Sl. No.	Bacterial genera	Plant growth promoting traits	References
8	<i>Gluconacetobacter diazotrophicus</i>	Fixation of nitrogen, IAA synthesis	Bertalan et al, (2009)
9	<i>Pseudomonas stutzeri</i>	Fixation of nitrogen	Yan et al, (2008)
10	<i>Klebsiella pneumoniae</i>	Fixation of nitrogen	Fouts et al, (2008)
11	<i>Pseudomonas putida</i> , <i>Stenotrophomonas maltophilia</i>	ACC deaminase, IAA synthesis	Taghavi et al, (2009)
12	<i>Serratia proteamaculans</i>	ACC deaminase, IAA synthesis, synthesis of acetoin and 2,3-butanediol	Taghavi et al, (2009)
13	<i>Acinetobacter</i> spp.	IAA synthesis, Siderophore, Phosphate solubilization	Rokhbakhsh-Zamin et al, (2011)
14	<i>Acinetobacter</i> sp., <i>Pseudomonas</i> sp.	ACC deaminase, IAA synthesis, antifungal activity, Phosphate solubilization, Fixation of nitrogen,	Indiragandhi et al. (2008)
15	<i>Azospirillum amazonense</i>	Nitrogenase activity, IAA synthesis	Rodrigues et al, (2008)
16	<i>Bacillus</i> sp.	IAA synthesis, HCN, Siderophore, production of ammonia	Ahmad et al, (2008)
17	<i>Bacillus subtilis</i>	Phosphate solubilization, IAA synthesis	Zaidi et al, (2006)
18	<i>Burkholderia</i> spp.	ACC deaminase, Siderophore, IAA synthesis, Phosphate and heavy metal solubilization	Jiang et al, (2008)
19	<i>Enterobacter asburiae</i>	Siderophore, IAA synthesis, Phosphate solubilization, production of ammonia, HCN, exo-polysaccharides	Ahemad & Khan (2010a,b)
20	<i>Klebsiella oxytoca</i>	IAA synthesis, nitrogenase activity, Phosphate solubilization	Jha & Kumar (2007)

Sl. No.	Bacterial genera	Plant growth promoting traits	References
21	<i>Enterobacter</i> sp.	ACC deaminase, Siderophore, IAA synthesis, Phosphate solubilization	Kumar et al, (2008)
22	<i>Klebsiella</i> sp.	Siderophore, IAA synthesis, Phosphate solubilization, production of ammonia, HCN, exo-polysaccharides	Ahemad & Khan (2011b,f,g)
23	<i>Kluyvera ascorbata</i>	Siderophore, ACC deaminase, metal resistance	Genrich et al, (1998)
24	<i>Pseudomonas aeruginosa</i>	Siderophore, ACC deaminase, IAA synthesis, Phosphate solubilization	Ganesan (2008)
25	<i>Rhizobium ciceri</i>	Siderophore	Berraho et al, (1997)
26	<i>Pseudomonas jessenii</i>	ACC deaminase, IAA synthesis, heavy metal solubilization, Siderophore, Phosphate solubilization	Rajkumar & Freitas (2008)
27	<i>Serratia marcescens</i>	IAA synthesis, Siderophore, HCN	Selvakumar et al, (2008)
28	<i>Pseudomonas</i> sp.	Siderophore, ACC deaminase, IAA synthesis, Phosphate solubilization, HCN, biocontrol potentials	Poonguzhali et al, (2008)
29	<i>Rhizobium meliloti</i>	Siderophore	Arora et al, (2001)
30	<i>Pseudomonas fluorescens</i>	Siderophore, ACC deaminase, Phosphate solubilization	Shaharoon et al, (2008)
31	<i>Rhizobium</i> sp.	Siderophore, exo-polysaccharides, IAA synthesis, production of ammonia, HCN	Ahemad & Khan (2011e,j)
32	<i>Pseudomonas putida</i>	Siderophore, IAA synthesis, Phosphate solubilization, HCN	Pandey et al, (2006)

1.7 Hypotheses of the present study:

Based on the background of this study presented here, the following hypotheses were proposed:

1. To strive under the extreme adversities of mangrove habitat, mangroves species with extensive root system may harbor some PGP endophytic bacteria that colonize the root surface in the rhizosphere as an outcome of “cry for help” responses from the mangrove roots, subsequently enter in the root cells and proliferate internally within the root cells, becoming an **endophytic member**.
2. These **root endophytic bacteria** may become crucial for mangroves in **promoting their growth and development, reshaping the root structures, facilitating nutrient availability** in the cells even under external anoxic, hypersaline ambience.
3. A cultivation-dependent approach could be undertaken to cultivate these root endophytes in pure culture, identify them, study their plant growth promotion ability under laboratory conditions and later best consortia of the best plant growth promoting root endophytic bacteria can be tested for lowland rice cultivars growing in lowland saline fields adjacent to mangrove shoreline, for their future applicability as an alternative to chemical fertilizers.

1.8 Objectives undertaken in this study:

Based on these hypotheses the presented research study was centered on the following objectives:

1. Study of morphological/histological niches, anatomical adaptations, Na^+/K^+ ratio in endospheres of roots and pneumatophores of mangrove species from degraded and non-degraded habitats of Sundarban mangrove ecosystem.
2. Establishment of pure endophytic bacterial strains from mangrove roots and pneumatophores and their molecular identification by 16S rRNA sequencing.
3. Plant growth promotion profiling of the established/accessioned endophytic bacterial strains.
4. Selection of PGP endophytic bacterial consortia based on growth promotion criteria and growth curves for nursery/greenhouse/field applications.
5. Application of selected PGP endophytic bacterial consortia on *Avicennia officinalis* saplings in mangrove nursery at Sundarbans for observing their effect on mangrove growth modulation.

- 6. Application of selected PGP endophytic bacterial consortia on cultivated rice of Sundarbans at the greenhouse for observing their effect on rice growth modulation.**
- 7. Application of selected PGP endophytic bacterial consortia on cultivated rice at fields at Sundarbans for observing their effect on rice growth and yield modulation.**
- 8. Observation of bacterial community abundances by Next Generation Sequencing (NGS) from rice fields before and after rice cultivation with PGP endophytic bacterial consortia.**

This study started with survey and study of root structures, their anatomy after collection of pieces of roots and pneumatophores from several mangrove and mangrove associate species from both degraded and non-degraded/pristine mangrove ecosystems from western part of Indian Sundarbans viz. Shiber Ghat (21°50'29.30"N 88°21'23.95"E), Atharogazi (21°50'45.90"N 88°23'18.44"E) and Ramganga (21°47'34.30"N 88°22'53.01"E) (moderately to highly degraded mangrove ecosystems), Lakkhipur (21°49'12.74"N 88°23'19.65"E) and Patharprotima (21°47'34.70"N 88°22'7.18"E) (non-degraded mangrove ecosystems). From these five-mangrove patches, 14 mangrove and associate species were studied for their root structure and anatomy. These studied species are *Avicennia alba*, *Avicennia marina*, *Avicennia officinalis*, *Heritiera fomes*, *Dalbergia spinosa*, *Bruguiera cylindrica*, *Bruguiera gymnorhiza*, *Rhizophora mucronata*, *Xylocarpus* sp., *Derris trifoliata*, *Ceriops tagal*, *Excoecaria agallocha*, *Myriostachya wightiana*, and *Porteresia coarctata*. Root and pneumatophore samples of these mangroves were studied for their anatomical adaptations initially. These root and pneumatophore pieces were surface sterilized and were further processed for the establishment of pure endophytic bacterial cultures. Genomic DNA was isolated from pure bacterial isolates and PCR amplification of 16S rRNA gene with bacterial genomic DNA as a template was carried out. The 16S rRNA gene amplicons were sequenced by Sanger's sequencing method and these 16S rRNA gene sequences were blasted against NCBI database, matched with the closest strains to identify these pure isolates, and subsequently the sequences were submitted to the NCBI GenBank and obtained the accession numbers for the same. 78 pure isolates of cultivable endophytic bacteria (NCBI Accession no. MT421976 to MT422053) from roots and pneumatophores of different mangroves and associate species of Indian Sundarbans were finally established. The culturable community of bacterial endophytes comprised species of 12 genera viz. *Bacillus*, *Aeromonas*, *Pseudomonas*, *Staphylococcus*, *Vibrio*, *Gallacimonas*,

Serratia, *Enterobacter*, *Pseudocitrobacter*, *Citrobacter*, *Acinetobacter*, *Mangrovibacter*. Bacterial endophytes were selected repeatedly on differential nutrient cycling media. All endophytic bacteria isolated were tested for their plant growth-promoting capability under the laboratory conditions through assays for indole-3-acetic acid production, phosphate solubilization, siderophore production, free nitrogen fixation, 1-aminocyclopropane-1-carboxylate deaminase (ACC) synthesis. Salt tolerance profile was also tested by quantifying the bacterial growth by measuring absorbance at 600 nm for some promising endophytic free nitrogen fixers, cellulose degraders, and P-solubilizers on different NaCl concentrations.

Based on PGPR activity and salt tolerance profile, 18 endophytic bacterial strains were selected for making 3 combinations named BC1, BC2, and BC3. Individual strain of bacterium under each consortium was tested for their growth curve and their exponential growth phase were observed first. Depending on the common exponential growth phase of these consortial members, large scale cultures were prepared and applied on lowland indigenous rice cultivar named Dudheswar landrace IC No. 593998 and Lunishree, under both greenhouse conditions and also in lowland saline fields of Indian Sundarbans. *Avicennia officinalis* mangrove saplings were also applied with these established BC1, BC2, and BC3 bacterial endophytic consortia at the onsite nursery at Sundarbans to find out their growth promotion activity.

Consortium BC1 comprised of bacteria viz. *Aeromonas dhakensis* strain HPR7, *Mangrovibacter plantisponcer* strain BCRP5, *Pseudomonas stutzeri* strain BCY5, *Pseudomonas stutzeri* strain BCY7, *Bacillus subtilis* strain AOR5, *Serratia marcescens* strain AOR4. Consortium BC2 comprised of *Aeromonas allosaccharophila* strain DAL2, *Pseudomonas* sp. strain DER1, *Pseudomonas putida* strain DER3, *Pseudomonas fulva* strain DER9, *Aeromonas veronii* strain POT3, *Aeromonas veronii* strain POT7, *Serratia marcescens* strain HPR4. Consortium BC3 comprised of *Bacillus subtilis* strain AMR4, *Aeromonas hydrophilia* strain HER3, *Bacillus altitudinis* strain XYL1, *Pseudocitrobacter faecalis* strain HRR5, *Serratia marcescens* strain HPR4, and *Enterobacter kobei* strain HRR1.

Field experiments were performed twice to date, indicating significantly increased yield in comparison to the control where bacteria were not added and yield was found to be significantly greater also when compared to the rice grain yield data collected from several neighboring rice fields grown by local farmers. Field application of consortium BC1 showed a yield of an average 9.58 quintal/bigha, consortium BC2 showed a yield of an average 11.2 quintal/bigha and consortium BC3 showed a yield of an average 11.3 quintal/bigha in comparison to control fields (without bacteria) yielding average 7.52 quintal/bigha. The data collected from local

farmers' fields in the western part of Sundarbans in Patharpratima block exhibited only a yield of an average 3.7 quintal/bigha.

Consortia of these bacteria when applied to the *Avicennia officinalis* saplings in mangrove nurseries in Indian Sundarbans, the observed increase of shoot height in saplings after bacterial application was significant. The same 3 root endophytic consortia were also tested in combination with PGP native halotolerant grass rhizobacteria in two consecutive greenhouse experiments. Tracking of P-solubilization profile at rhizospheres after the addition of bacteria revealed enrichment of added consortia validated through the increase of soluble-P release at the rhizosphere even at the time of maximum utilization by the plants.

The next-generation metagenomic sequencing of the rhizobacterial community from the collected rhizospheric soil from the 1st field experiment of Indian Sundarbans establishes noticeable enrichment of the applied bacterial consortia by analyzing the relative abundance of the constituent bacterial members by amplicon-based V3-V4 16S rRNA metagenomic sequencing through Illumina MiSeq platform.

II. Materials and Methods

2. Materials and Methods:

2.1 Collection of root and pneumatophore samples:

Root and pneumatophore samples of mangroves were collected from different places in Sundarbans. The details are follows-

Table 3: Moderately degraded mangrove forests and samples collected:

Moderately degraded mangrove forests	Name of mangrove species collected
Shiber Ghat	<i>Excoecaria agallocha</i> root.

Table 4: Pristine mangrove forests/non-degraded ecosystems and samples collected:

Pristine mangrove forests/non-degraded ecosystems	Name of mangrove species collected
Lakhipur	<i>Ceriops</i> sp. root.

Table 5: Highly degraded mangrove forests and samples collected:

Highly degraded mangrove forests	Name of mangrove species collected
Atharogazi	<i>Rhizophora mucronata</i> root.
Patharprotima	<i>Bruguiera cylindrica</i> root/pneumatophore, <i>Bruguiera gymnorrhiza</i> root/pneumatophore.
Ramganga	<i>Avicennia alba</i> root/pneumatophore, <i>Avicennia marina</i> root/pneumatophore, <i>Avicennia officinalis</i> root/pneumatophore, <i>Dalbergia</i> sp. root, <i>Derris</i> sp. root, <i>Heritiera fomes</i> root/pneumatophore, <i>Xylocarpus</i> sp. root, <i>Myriostachya</i> sp. root, <i>Porteresia</i> sp. root.

Table 6: Name of mangrove forests and their GPS locations.

Serial no.	Name of mangrove forests	Location
1	Shiber Ghat	(21°50'29.30"N 88°21'23.95"E)
2	Lakhipur	(21°49'12.74"N 88°23'19.65"E)
3	Atharogazi	(21°50'45.90"N 88°23'18.44"E)
4	Patharprotima	(21°47'34.70"N 88°22'7.18"E)
5	Ramganga	(21°47'34.30"N 88°22'53.01"E)

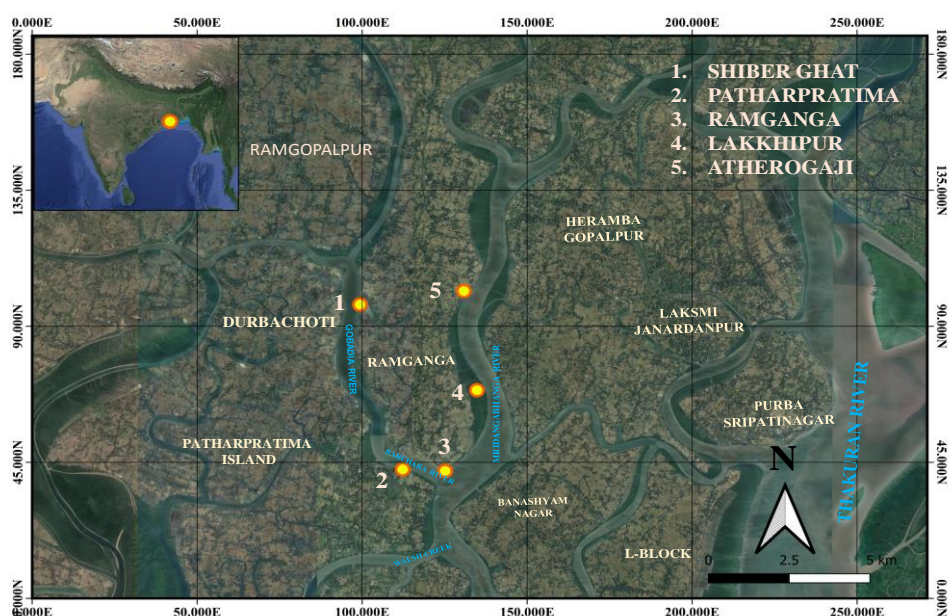


Figure 2.1: Location map of 5 mangrove forests with sampling sites for root and pneumatophore.

2.2 Storage and transportation of collected samples:

The collected samples (mangrove root and pneumatophore) were carried in sterile bags. The temperature was maintained 4°C in an ice-box while transporting the samples from the field to the laboratory.

The whole samples were divided into two parts. One part of these samples was preserved at 4°C for isolation of endophytic bacterial strains from them. The rest of the parts of the samples were preserved in FAA for the microtome section.

Composition of FAA:

FAA composition	Percentage
Formaldehyde	10
Alcohol	50
Acetic Acid	5
Water	10

2.3 Establishment of pure endophytic bacterial strains from mangrove roots and pneumatophores:

Establishment of pure endophytic bacterial strains from mangrove roots and pneumatophores was followed by the protocol of Boruah (2020).

Reagents:

1. **0.1% HgCl₂ solution:** 1 gm HgCl₂ dissolved in 1000 ml of distilled water.

Procedure:

1. The mangrove root and pneumatophore samples were first cleaned well by tap water.
2. Then the samples were cut into small pieces (2-5 mm.) with the help of sterilized blades.
3. After that the samples were dipped into the 0.1% HgCl₂ solution for 2 minutes.
4. Then the samples were washed 2 to 3 times with autoclaved distilled water for 2 to 3 minutes.
- 5.

2.4 Establishment of pure endophytic bacterial colonies:**Reagents:****Composition of LB (Luria-Bertani) agar medium:**

LB (Luria-Bertani) agar medium	
Sodium chloride	10g
Yeast extract	5g
Tryptone	10g
Distilled water (up to)	1000 ml
pH	7.0
Agar	10g

Procedure:

1. The surface sterilized small pieces of root and pneumatophore samples were inoculated in LB broth (Luria-Bertani without agar) medium.
2. Then the LB broth medium was kept overnight (24 hours) at 37°C in the incubator for incubation.
3. After incubation, 50µl LB broth culture was spread on an LB plate (Luria-Bertani with agar) medium.
4. Then the LB plate medium was kept overnight (24 hours) at 37°C in the incubator for incubation.
5. After incubation, the single colonies were isolated from the LB plate medium.
6. The various single colonies with apparently different colony morphology were picked up and re-inoculated on LB plate medium and kept overnight (24 hours) at 37°C in the incubator for incubation.
7. Then each single colony was checked for its purity by the Gram staining technique.

2.5 Gram staining technique:

Gram staining technique was followed by standard staining protocol of Rollins (2000).

Reagents:

1. Crystal violet
2. Gram's iodine
3. 95% ethyl alcohol
4. Safranin

Procedure:

1. A few drops of sterile water were added in the middle of a clean glass slide.
2. The bacterial culture was taken and an oval-shaped smear was prepared on the slide and then heat fixed.
3. Crystal violet solution was put on the smear and allowed to wait for 1 minute, then gently washed with tap water.
4. Gram's iodine was added on the smear and allowed to wait for 1 minute then gently washed by tap water.
5. 95% ethyl alcohol was added dropwise on the smear till the colour was decolorized then immediately, the slide was washed gently with tap water.

6. Safranin solution was put on the smear and waited for 30 seconds then gently washed with tap water.
7. The slide was kept for air drying and then was observed under the microscope.

2.6 Maintenance of pure endophytic bacterial colonies:

The pure single colony checked by Gram staining technique was re-inoculated on LB plate medium and kept overnight (24 hours) at 37°C in the incubator for incubation. The re-inoculated culture was placed in the refrigerator at 4-5°C for 20-25 days only. From these pure endophytic bacterial isolates, glycerol stocks were also prepared for future uses.

2.7 Preparation of Glycerol stock:

Glycerol stock preparation was essential for endophytic bacterial isolates for long-term storage.

Procedure:

1. The pure bacterial cultures were inoculated in LB broth medium for overnight (24 hours) in shaking incubator at 37°C for incubation.
2. Then 500 µl of overnight incubated culture was taken in a 2ml pre-autoclaved cryovial.
3. After that 500 µl of glycerol was added with it from 50% glycerol stock.
4. Bacterial culture and glycerol mixture were mixed properly by vortexing.
5. The glycerol stock was ready for further use and kept it in -80°C for future storage.

2.8 Endophytic bacterial genomic DNA isolation:

The endophytic bacterial genomic DNA isolation method was finalized after some modifications (Moore et al, 2004; Mahansaria et al, 2015).

Reagents:

1. **10 mM Tris-HCl (pH 8):** 157.5 mg of Tris-HCl was dissolved in 80 ml of water (distilled). pH 8 was maintained and finally volume was made up to 100 ml with distilled water.
2. **Lysozyme (100 mg/ml):** 100 mg Lysozyme was dissolved in 1ml molecular grade water.

3. **10% SDS:** The solution was freshly prepared before use. 0.1 g SDS was dissolved in 1 ml molecular grade water.
4. **RNase & Proteinase K:** Cold Spring Harbor Laboratory protocols (Cold Spring Harb Protoc, 2014; 2006) were followed.
5. **5M NaCl:** 29.22 g NaCl was dissolved in 100ml distilled water and autoclaved.
6. **CTAB and NaCl:** 4.1g NaCl and 10 g CTAB were dissolved in 100 ml distilled water and autoclaved.
7. **24:1 chloroform: isoamyl alcohol:** 24ml chloroform and 1ml isoamyl alcohol were mixed.
8. **70% ethanol:** In 70 ml ethanol, 30 ml molecular grade water were added and mixed.

Procedure:

1. The bacterial cultures were inoculated in LB broth medium for overnight (24 hours) in shaking incubator at 37°C for incubation.
2. Then the culture was taken in a microcentrifuge tube and centrifuged at 5000 rpm for 10 minutes. For accumulation of cell pellet the culture was centrifuged at 3-4 times.
3. Approx. 100 mg of glass beads was added to the cell pellet and crushed well by micro pestles.
4. After crushing the cell pellet was washed with 200µl of 10 mM Tris-HCl, pH 8, and centrifuged at 5000 rpm for 10 minutes.
5. Then 200 µl of 10 mM Tris-HCl was added with bacterial cell pellet and mixed well.
6. 20µl lysozyme (100 mg/ml) was added and mixed well and incubated for 1 hour at 37°C.
7. After incubation 22µl of 10% SDS (freshly prepared) was added into the microcentrifuge tube and vortexed well and incubated in the ice box for 10 minutes.
8. Then 5µl of RNase was added to the microcentrifuge tube, mixed well, and incubated for 1 hour at 37°C.
9. 4µl of proteinase K was added to the microcentrifuge tube, mixed well, and incubated overnight at 37°C.
10. After overnight incubation 100µl 5M NaCl + 80µl CTAB and NaCl were added and incubated for 10 minutes at 65°C in a water bath.
11. 200µl of phenol (Tris-saturated) was added, mixed well and centrifuged at 8000 rpm for 5 minutes.

12. Then the upper aqueous layer was collected very carefully and transferred to another microcentrifuge tube. An equal volume of 24:1 chloroform: isoamyl alcohol was added to the microcentrifuge tube, mixed well, and centrifuged at 8000 rpm for 5 minutes.
13. The aqueous layer was collected very carefully and transferred to another microcentrifuge tube. Then an equal volume of isopropanol was added and mixed properly and kept overnight at -20°C.
14. Next day the microcentrifuge tube was centrifuged at 10000 rpm for 15 minutes. Then DNA pellet was collected and washed with 70% ethanol at least two times at 10000 rpm for 10 minutes.
15. The pellet (DNA) was air dried.
16. Then the DNA was dissolved in 20µl molecular grade water.

2.9 Bacterial sequence grade DNA preparation:

If cell debris or other unwanted substance was still associated present in DNA pellet, to avoid problems in PCR reactions and further sequencing, bacterial sequence grade DNA preparation protocol was followed.

Reagents:

1. **4M NaCl:** 23.376 g NaCl was dissolved in 100ml distilled water and autoclaved.
2. **13% PEG 8000:** 1.3 g PEG 8000 was dissolved in 10ml molecular grade water.
3. **70% ethanol**

Procedure:

1. 8µl of 4M NaCl and 40µl of 13% PEG 8000 were added to the DNA solution and kept in ice for 20 minutes.
2. After that the solution was centrifuged at 13000 rpm for 15 minutes in room temperature.
3. The pellet was collected and washed twice with 500µl of 70% ethanol at 13000 rpm for 5 minutes.
4. The pellet (DNA) was air dried.
5. Then the DNA was dissolved with 20µl of molecular grade water.

2.10 PCR amplification of genomic DNA:

For molecular identification of bacterial strains, PCR amplification of the partial 16S rRNA gene of bacterial DNA was done.

Polymerase chain reaction:

Two universal primers 27F (5' AGAGTTTGATCMTGGCTCAG 3') and 1492R (L) (5'GGTTACCTTGTTACGACTT 3') were used for Polymerase chain reaction to amplify partial 16S rRNA gene. The polymerase chain reaction process also requires buffer, dNTPs, molecular grade water, genomic DNA, Taq polymerase, etc. The PCR amplification steps were - initial denaturation at 94°C for 5 min repeated by 35 cycles of 94°C for 1 min, 1 min at 50°C and 1 min at 72°C, and a final step of extension of 10 min at 72°C.

2.11 Agarose gel electrophoresis:

On 0.8% agarose gel containing ethidium bromide stain the amplified PCR product was electrophoresed and interpreted with the presence of 1kb DNA ladder. For preparation of agarose gel and tank buffer the TBE buffer (1X) was required.

TBE (5X) electrophoresis buffer composition:

TBE (5X) electrophoresis buffer composition (400 ml)	
Tris-base	21.6 g
Boric acid	11g
EDTA (disodium salt)	2.98 g

2.12 Sequence submission to NCBI database:

The amplified PCR products were sent for sequencing. Partial 16S rRNA gene sequencing was done. Sequencing results were interpreted through BioEdit software and blasted through NCBI database. Sequence submission to NCBI database and obtaining accession numbers for the same.

2.13 Checking the growth of pure isolates on different nutrient cycling media:

2.13.a. Media composition for cellulose-degrading bacteria:

Media of cellulose-degrading bacteria (cellulose decomposers) (Thatoi et al, 2012)	
MgSO ₄ ·7H ₂ O	0.2 g
CaCl ₂	0.1 g
FeCl ₃	0.02 g
K ₂ HPO ₄	1 g
NaCl	0.1 g
Precipitated cellulose	4 g
NaNO ₃	2 g
pH	7.0
Distilled water (up to)	1000 ml
Agar	12 g

2.13.b. Media composition for phosphate solubilizing bacteria:

Media of phosphate solubilizing bacteria NBRIP (Nautiyal, 1999)	
Glucose	10 g
(NH ₄) ₂ SO ₄	0.1 g
Ca ₃ (PO ₄) ₂	5 g
KCl	0.2 g
MgCl ₂	5 g
MgSO ₄ ·7H ₂ O	0.25 g
pH	6.8-7.0
Distilled water (up to)	1000 ml
Agar	15 g

2.13.c. Media composition for free-living nitrogen-fixing bacteria:

Media of free-living nitrogen fixing bacteria (Thatoi et al, 2012)	
Mannitol	15 g
MgSO ₄ ·7H ₂ O	0.2 g
K ₂ HPO ₄	0.5 g
NaCl	0.2 g
CaSO ₄	0.1 g
CaCO ₃	5 g
pH	8.3
Distilled water (up to)	1000 ml
Agar	15 g

2.13.d. Media composition for sulfur-oxidizing bacteria:

Media of sulfur-oxidizing bacteria <i>Thiobacillus</i> medium (Thatoi et al, 2012)	
Na ₂ S ₂ O ₃	0.5 g
(NH ₄) ₂ SO ₄	0.4 g
MgSO ₄ ·7H ₂ O	0.5 g
KH ₂ PO ₄	4 g
FeSO ₄	0.01 g
CaCl ₂	0.25 g
pH	6.8
Distilled water (up to)	1000 ml
Agar	18 g

2.13.e. Media composition for preliminary selection of iron-oxidizing bacteria:

Modified YBMI media (Ghosh et al, 2014)	
Sodium citrate	0.3 g
Ferrous ammonium sulfate	0.3 g
Manganous sulfate	0.02 g
Yeast extract	0.15 g
Beef extract	2 g
pH	6.0
Distilled water (up to)	1000 ml
Agar	15 g

The sterilization process for all media was for 15 minutes at 15 lbs pressure (121°C), except phosphate solubilizing media where sterilization process was done for 10 minutes at 10 lbs pressure.

2.13.f. Confirmational study of Iron oxidizing bacteria (IOB):

The selected IOB culture was inoculated in modified YMI media with a lowered amount of yeast and no beef extracts for re-confirmation of Iron oxidizing bacteria. The starting OD was 0.1. This stringent selection of IOBs occurs after lowering the main source of carbohydrate (yeast extract) and nitrogen (beef extract) in the medium. For that reason, the bacteria could only derive energy by converting ferrous salt to ferric and could grow in this medium.

Stringent selection of Iron oxidizing bacteria:

Modified YMI media with a low yeast and no beef extracts (Ghosh et al, 2014)	
Yeast extract	0.05 g
Sodium citrate	0.3 g
Ferrous ammonium sulfate	0.3 g
Manganous sulfate	0.02 g
pH	6.0
Distilled water (up to)	1000 ml

2.13.g. Confirmation of iron-oxidizing endophytic bacteria (with ferric precipitate) by ammonium thiocyanate assay:

Reagents:

1. **1M Ammonium thiocyanate:** 76.122 g ammonium thiocyanate was dissolved in 1 liter distilled water.

Procedure:

1. The IOB selected bacterial culture was grown in 15 ml Modified YMI media, a pH of media was maintained at 6 (Ghosh et al, 2014).
2. When the final OD reached 1-2 OD at 37°C then 3 ml ammonium thiocyanate (1 mole/liter) was added.
3. The experimental setup was kept at room temperature for 15 minutes for incubation.
4. If brick red or blood red colored precipitate developed instantaneously then the bacterium was finally selected as an Iron oxidizing bacterium.

2.14 The determination of exchangeable sodium in plant tissue:

The determination of exchangeable sodium in plant tissue was followed according to Toth and Prince (1949).

Reagents:

1. **1 M Ammonium Acetate solution:** 77 g of ammonium acetate ($\text{NH}_4\text{C}_2\text{H}_3\text{O}_2$) dissolved in 1000 ml of distilled water, the pH 7.0 was maintained either ammonium hydroxide or acetic acid.

2. **Sodium chloride ("Anal R" grade):** 22.99 gm Na present in 58.44 gm NaCl

So, 1 gm of Na is present in $(58.44/22.99) = 2.542$ gm NaCl

2.542 gm NaCl (1 gm of Na) dissolved in 1000 ml 1 M Ammonium Acetate solution i.e., 1000 ppm of Na^+ .

0.254 gm/254 mg NaCl dissolved in 1000 ml 1 M Ammonium Acetate solution i.e., **100 ppm of Na^+** .

Table 7: Preparation of Na^+ standards:

PPM of Na^+	Amount of Na^+ in μg in 25 ml.	Amount taken from stock in ml	Dissolved in 1 M ammonium acetate solution	Final Volume
0	Blank	0	25	25
10	250	2.5	22.5	25
20	500	5	20	25
30	750	7.5	17.5	25
40	1000	10	15	25
50	1250	12.5	12.5	25

Procedure:

1. The plant tissue extracts were prepared by grinding 0.5-1 gm of dried plant tissue in 10 ml of 1 M ammonium acetate solution in a mortar and pestle.
2. The homogenate was centrifuged at 5000 rpm for 15 min.
3. Then the aqueous layer was filtered by normal filter paper.
4. The detection was done by flame photometer.
5. First, the standards were calibrated in a flame photometer.
6. Then the readings were recorded from plant tissue samples based on this calibration.
7. For each plant, 3 tissue samples were made and 3 readings were recorded.

8. All dilutions were done by 1M ammonium acetate solution.
9. The whole experiment was done only with de-ionized water.

2.15. The determination of exchangeable potassium in plant tissue:

The determination of exchangeable potassium in plant tissue was followed according to Toth and Prince (1949).

Reagents:

1. **1 M Ammonium Acetate solution:** 77 g of ammonium acetate ($\text{NH}_4\text{C}_2\text{H}_3\text{O}_2$) dissolved in 1000 ml of distilled water, the pH 7.0 was maintained either ammonium hydroxide or acetic acid.
2. **Potassium chloride (“Anal R” grade):** 39 gm K present in 74.55 gm KCl

So, 1 gm of K is Present in $(74.55/39) = 1.911$ gm KCl

1.911 gm KCl (1gm K) dissolved in 1000 ml 1M Ammonium Acetate i.e., 1000 ppm of K^+ .

0.1911 gm/ 191.1 mg KCl dissolved in 1000 ml 1M Ammonium Acetate i.e., **100 ppm of K^+** .

Table 8: Preparation of K^+ standards:

PPM of K^+	Amount of K^+ in μg in 25 ml	Amount taken from stock in ml	Dissolved in 1 M ammonium acetate solution	Final Volume
0	Blank	0	25	25
10	250	2.5	22.5	25
20	500	5	20	25
30	750	7.5	17.5	25
40	1000	10	15	25
50	1250	12.5	12.5	25

Procedure:

1. The plant tissue extracts were prepared by grinding 0.5 - 1 gm of dried plant tissue in 10 ml of 1 M ammonium acetate solution in a mortar and pestle.
2. The homogenate was centrifuged at 5000 rpm for 15 min.
3. Then the aqueous layer was filtered by normal filter paper.
4. The detection was done by flame photometer.
5. First, the standards were calibrated in a flame photometer.

6. Then the readings were recorded from plant tissue samples based on this calibration.
7. For each plant, 3 tissue samples were made and 3 readings were recorded.
8. All dilutions were done by 1M ammonium acetate solution.
9. The whole experiment was done only with de-ionized water.

2.16. Determination of plant growth-promoting properties of endophytic bacterial strains:

2.16.a. IAA production assay:

IAA production assay was followed according to Gordon and Weber, 1951; Singh and Jha, 2015.

2.16.b. Preparation of standard curve of IAA production assay:

Procedure:

1. **1 mg /ml IAA stock preparation:** 10 mg IAA powder was dissolved in 10 ml distilled water. Here few drops of 0.1N NaOH was added to IAA stock to dissolve IAA powder.
2. **0.1 mg /ml IAA stock preparation:** In 9 ml distilled water 1 ml of 1 mg/ml IAA stock was added and mixed well.

Table 9: Reaction set up for preparation IAA standard curve.

Set no.	IAA in mg	IAA in μ l	Water added in μ l	Final volume in ml	Salkowski's reagent in ml
1	0	0	1000	1	2
2	0.001	10	990	1	2
3	0.003	30	970	1	2
4	0.005	50	950	1	2
5	0.010	100	900	1	2
6	0.020	200	800	1	2
7	0.003	300	700	1	2
8	0.004	400	600	1	2
9	0.006	600	400	1	2

3. The reaction set up was incubated in the dark at room temperature for 25 minutes.
4. Then the absorbance was measured at 530 nm.

2.16.c. IAA production assay from different endophytic bacterial strains (with Tryptophan):

Reagents:

1. **10 mg/ml Tryptophan stock preparation:** 200 mg L-tryptophan was dissolved in 20 ml autoclaved distilled water. Approximately 6 hours were required to dissolve L-tryptophan. Filter sterilization was done for further use.
2. Salkowski's reagent preparation:
 - a. 2 ml of 0.5 M FeCl_3 and 100 ml of 35% Perchloric acid (HClO_4) were mixed in 1:50 (v/v) proportion.
 - b. **0.5M FeCl_3 stock preparation:** (MW of FeCl_3 = 162.21 g) 405.52 mg was dissolved in 5 ml distilled water to prepare 5 ml of 0.5M FeCl_3 stock solution.
 - c. **35% Perchloric acid (HClO_4) solution preparation:** 50ml of 70% Perchloric acid (HClO_4) was mixed with 50ml of distilled water.
3. IAA powder
4. 0.1N NaOH
5. Nutrient broth (commercial)

Procedure:

1. Bacterial cultures were inoculated in nutrient broth medium for overnight (24 hours) at 30°C in shaking incubator for incubation.
2. Then the bacterial culture turbidity was measured individually at 600 nm. The un-inoculated nutrient broth medium was used as control.
3. 0.1 OD bacterial culture was inoculated in another 10 ml of NB broth (containing 100µl L-tryptophan, conc. 100 µg/ml) for 72 hours at 30°C in shaking incubator for incubation.
4. After incubation, the culture was taken in a microcentrifuge tube and centrifuged at 8,000 rpm for 10 min.
5. From here 1ml supernatant was taken in a glass tube and 2 ml of Salkowski's reagent was added to it.
6. 1ml of un-inoculated NB broth and 2ml of Salkowski's reagent was used as a control.
7. The reaction set up was incubated at room temperature in dark for 25 minutes.
8. Then the absorbance was taken at 530 nm.

2.16.d. IAA production assay from different endophytic bacterial strains (without Tryptophan):

The procedure was same as above but here 100µl L-tryptophan (conc. 100 µg/ml) was not used.

2.17 Phosphate solubilization activity study:

The phosphate solubilization activity study was done according to Nautiyal, 1999. Soluble phosphorus estimation was done with the molybdenum blue method (Krishnaswamy et al, 2009).

2.17.a. Preparation of standard curve of phosphate solubilization assay:

Reagents:

- A. Ammonium molybdate solution:** 5 g of $(\text{NH}_4)_6\text{Mo}_7\text{O}_{24} \cdot 4\text{H}_2\text{O}$ was dissolved in 40 ml distilled water in a bottle. 56 ml of conc. H_2SO_4 was added to the 90 ml distilled water in another bottle very carefully. The two bottles of solution were mixed. The final volume was made up upto 200 ml of distilled water. The prepared solution was kept in a dark bottle to prevent decomposition.
- B. Stannous chloride solution:** 2.5 g of $\text{SnCl}_2 \cdot 2\text{H}_2\text{O}$ was dissolved in 100 ml glycerol and stored in a dark bottle.
- C. Di-potassium hydrogen phosphate.**

Procedure:

1. Phosphorous standard stock solution calculations:

Mol. wt. of K_2HPO_4 (anhydrous) = 174.18 g;

Mol. wt. of Phosphorous (P) = 30.97 g.

In K_2HPO_4 , 30.97 g P is present in 174.18 g of K_2HPO_4 .

Therefore, 1 g P is present in $174.18/30.97 = 5.62$ g of K_2HPO_4 .

1000 ppm stock i.e. 1 g P was present in 1 L distilled water.

So, 5.62 g of K_2HPO_4 was present in 1 L water, i.e. 1000 ppm of P.

0.0562 g = 56.2 mg was present in 10 ml = 1000 ppm P stock, conc. = 1mg/ml.

1 ml was taken from the above solution and 9 ml of water was added to it =100 ppm P stock, conc. = 100 µg/ml.

5 ml was taken from the above solution and 95 ml of water was added to it =5 ppm P stock, conc. = 5 µg/ml.

Table 10: Reaction set up for preparation of phosphorus standard curve.

Set no.	Amount of 5 ppm stock (ml)	Amount of P in solution (µg)	Volume made up to (ml)	Ammonium molybdate solution added (ml)	Stannous chloride solution added (with a 1 ml micropipette)	Final volume (ml)	P in diluted standard (ppm)
1	-	-	25	2	4 drops	50	0.0
2	1	5	25	2	4 drops	50	0.1
3	2	10	25	2	4 drops	50	0.2
4	3	15	25	2	4 drops	50	0.3
5	4	20	25	2	4 drops	50	0.4
6	5	25	25	2	4 drops	50	0.5
7	6	30	25	2	4 drops	50	0.6
8	7	35	25	2	4 drops	50	0.7
9	8	40	25	2	4 drops	50	0.8
10	10	50	25	2	4 drops	50	1.0
11	14	70	25	2	4 drops	50	1.4

2. The measurements of color were estimated after 11 minutes.
3. Then the absorbance was taken at 660 nm.

2.17.b. Phosphate solubilization activity study from different endophytic bacterial strains:

Reagents:

1. Nutrient broth (commercial)
2. Physiological saline (0.85% NaCl)
3. Phosphate solubilization media

Media of phosphate solubilizing bacteria NBRIP (Nautiyal, 1999)	
Glucose	10g
(NH ₄) ₂ SO ₄	0.1 g
Ca ₃ (PO ₄) ₂	5 g
MgCl ₂	5 g
KCl	0.2 g
MgSO ₄ ·7H ₂ O	0.25 g
pH	6.8-7.0
Distilled water (up to)	1000 ml

Procedure:

1. Bacterial cultures were grown in nutrient broth medium for overnight (24 hours) at 30°C in shaking incubator for incubation.
2. Then the culture was taken in a microcentrifuge tube and centrifuged at 5000 rpm for 10mins. For accumulation of cell pellet the culture was centrifuged at 2-3 times.
3. The cell pellet was washed with saline water (0.85% NaCl solution) three times at 5000 rpm for 10 mins each to remove nutrient broth.
4. The accumulated culture was diluted by the addition of 500µl 0.85% saline water.
5. The turbidity measurement was done at 600 nm and 0.85% NaCl solution was taken as blank.
6. Then 0.25 OD cultures were inoculated in 10ml liquid NBRIP medium.
7. The cultures were incubated at 30°C for 5 days. After 5 days the cultures were centrifuged at 10,000 rpm for 10 min.
8. The supernatant was taken for soluble Phosphorus estimation.
9. 500 µl supernatant was added to 20 ml distilled water. Then 2ml ammonium molybdate solution and 4 drops of stannous chloride solution were added.
10. Then wait for 11 minutes and color measurements were taken at 660 nm.

2.18 Quantitative estimation of siderophore from different endophytic bacterial strains:

The siderophore production assay was followed based on the protocols of Andrews and Duckworth, 2016.

Reagents:

1. **1 mM CAS stock solution:** 0.06 g of Chrome Azurol S (CAS) to dissolved in 100 ml distilled water.
2. **1 mM Fe (NO₃)₃:** 24.2mg of Iron (III) nitrate to dissolved in 100 ml distilled water.
3. **10 mM DDAPS:** 0.334 gm of DDAPS (N-dodecyl-N, N-dimethyl-3-ammonia-1-propanesulfonate) was dissolved in 100 ml distilled water. It was a zwitterionic surfactant.
4. **1mM NH₄Ac buffer:** 0.077 g of ammonium acetate was added to 900 ml distilled water in a 1 L volumetric flask. The pH of the solution is to be made to **6.8** by adding glacial acetic acid/NaOH. Final volume was made up to 1 L mark.

The standard succinate medium (iron free)	
Succinic acid	4 g
KH ₂ P0 ₄	3 g
MgSO ₄ .7H ₂ O	0.2 g
(NH ₄) ₂ S0 ₄	1 g
K ₂ HP0 ₄	6 g
MES	10mM (final concern.)
pH	7.0
Distilled water (up to)	1000 ml

Procedure:

1. Bacterial cultures were grown in LB broth medium for overnight (24 hours) at 30°C in shaking incubator for incubation.
2. 0.1 OD bacterial culture was inoculated in 10 ml standard succinate medium.
3. The cultures were incubated at 28°C for 24 to 30 hours. Only succinate medium was used as a control. The pH was maintained in the range of 7.0 to 7.3.
4. After incubation, the cultures were centrifuged at 10,000 rpm at 4°C for 10 minutes and the supernatant was collected.

The CAS assay was made as follows to prepare a 20 μM final assay concentration:

CAS Assay Solution: The sequential order of addition of its components for the CAS assay is very sensitive. So it is essential to add in the following order:

- a. First add $\text{Fe}(\text{NO}_3)_3$ to CAS
- b. Then add the surfactant (DDAPS)
- c. Then add the buffer solution. The addition of each component resulted in a series of color changes in every time.

1 mM $\text{Fe}(\text{NO}_3)_3$ 20 μL + 1mM CAS 120 μL + 10 mM DDAPS 380 μL (excess surfactant was required) + 1mM NH_4Ac buffer 380 μL

Iron solution (colour is clear) + CAS solution (colour is yellow) = turned the solution colour to deep purple; + DDAPS solution (colour clear) = turned the solution colour to dark blue; + buffer to change pH to 6.8 = turned the solution colour to lighter blue.

The CAS assay solution was prepared for 10–15 min before use.

5. 100 μL of bacterial culture supernatant was added directly to 900 μL of CAS assay solution and kept 1 hour to react before analysis.
6. For reference blank, CAS assay solution (900 μL) and uninoculated media (100 μL) was maintained for 1 hour.
7. Absorbance for both sample and reference blank were measured at 630 nm.
8. Units of Siderophore were written as $[(\text{Ar} - \text{As}) / \text{Ar}] * 100 = \% \text{ of siderophore units}$. The siderophore unit percentage was calculated as the proportion of CAS assay solution color shifted. Here, Ar = Reference absorbance (CAS assay solution + uninoculated media) and As = Sample absorbance (CAS assay solution + cell-free supernatant).
9. The Fe–CAS–DDAPS complex (CAS assay solution), samples contained CAS assay solution and bacterial culture, and only free CAS (100 μL 1 mM) in 10 mM DDAPS (900 μL) were simultaneously scanned for absorbance from 350 nm to 750 nm.
10. Fe–CAS–DDAPS complex (CAS assay solution) showed the highest peak/absorbance at 630 nm with almost no peak at 425 nm. Samples containing CAS assay solution and bacterial culture had a lower peak at 630 nm with a peak also at 425 nm for free CAS relieved by siderophore–Fe binding. Free CAS had only one peak at 425 nm without any peak at 630 nm.

2.19. 1-aminocyclopropane-1-carboxylic acid deaminase (ACC deaminase)

assay:

The ACC deaminase assay was done according to Saravanakumar and Samiyappan, 2007; Penrose and Glick, 2003; Ali et al, 2014.

Reagents:

1. **0.56 mol/l HCl**
2. **2 mol/l HCl**
3. **2, 4 dinitrophenyl hydrazine preparation:** 0.1g of 2, 4 dinitrophenyl hydrazine was dissolved in 50 ml of 2 mol/l HCl.
4. **Bradford reagent preparation:** First Coomassie Brilliant Blue (G-250) 100 mg was dissolved in 50 ml of 95% ethanol. Then 85% (w/v) phosphoric acid 100 ml was added to it. Finally, the volume was made up to 1 Liter when the dye has completely dissolved. After dissolving the dye properly, the solution was filtered through Whatman #1 paper. The final solution was kept in dark bottle at 4°C (Bradford, 1976).
5. Bovine Serum Albumin (BSA)

2.19.a. α -ketobutyrate standard curve preparation:

Procedure:

1. 102.09 mg of α ketobutyrate was dissolved in 10ml of 0.1 mol/l Tris-HCl (pH 8.5) to prepare stock solution of 1 mmol α -ketobutyrate.
2. Stock solution of (1 mmol α -ketobutyrate) 1ml was mixed with 9 ml of 0.1 mol/l Tris- HCl (pH 8.5) to prepare 0.1 mmol α -ketobutyrate solution.
3. Stock solution of (0.1 mmol α -ketobutyrate) 1ml was mixed with 9 ml of 0.1 mol/l Tris- HCl (pH 8.5) to prepare 0.01 mmole α -ketobutyrate solution.
4. In 10 ml 0.1mol /l Tris-HCl (pH 8.5) contained 0.01mmol α -ketobutyrate
10000 μ l 0.1mol /l Tris-HCl (pH 8.5) contained 0.01*1000000 nmol α -ketobutyrate
1 μ l 0.1 mol /l Tris-HCl (pH 8.5) contained= (0.01*1000000)/10000 nmol α -ketobutyrate
1 μ l 0.1 mol /l Tris-HCl (pH 8.5) contained= 1 nmol α -ketobutyrate solution.

Table 11: Reaction set up for preparation of α -ketobutyrate standard curve.

Set no.	α -ketobutyrate in nmol	α -ketobutyrate in μ l	0.1 mol/l Tris–HCl (pH 8.5) added	Final volume made up to in μ l	2,4 dinitrophenyl hydrazine in μ l	2M NaOH in μ l
1	-	-	450	450	75	500
2	1	1	449	450	75	500
3	5	5	445	450	75	500
4	10	10	440	450	75	500
5	20	20	430	450	75	500
6	50	50	400	450	75	500
7	100	100	350	450	75	500
8	200	200	250	450	75	500
9	250	250	200	450	75	500

- According to the table different conc. of α -ketobutyrate solution was prepared and final volume of solution 450 μ l was prepared with 0.1 mol/l Tris–HCl (pH 8.5).
- Then 75 μ l of 2, 4 dinitrophenyl hydrazine reagents were added and the solution was kept for 30 min at 30°C.
- After that 0.5 ml of 2 M NaOH was added and mixed properly and absorbance was taken at 540 nm.

2.19.b. Protein standard curve preparation:

Procedure:

- Preparation of 1 mg/ml of BSA stock:** 5 mg Bovine serum albumin (BSA) was dissolved 5 ml of 0.1 mol/l Tris–HCl (pH 8.5).
- Preparation of 0.1 mg/ml of BSA stock:** 100 μ l of BSA stock (1mg/ml) was mixed with 900 μ l 0.1 mol/l Tris–HCl (pH 8.5).

Table 12: Reaction set up for preparation of BSA standard curve.

Set no.	Final stock of protein (mg/ml)	BSA in mg in 50 μ l	BSA (0.1mg/ml stock) taken in μ l	0.1 mol/l Tris–HCl (pH 8.5) added in μ l	0.1 mol/l Tris–HCl (pH 8.5) added (μ l)	0.1 N NaOH added (μ l)	Bradford added (μ l)
1	-	-	-	50	200	250	250
2	0.01	0.0005	5	45	200	250	250
3	0.02	0.001	10	40	200	250	250
4	0.03	0.0015	15	35	200	250	250

5	0.04	0.002	20	30	200	250	250
6	0.05	0.0025	25	25	200	250	250
7	0.075	0.00375	37.5	12.5	200	250	250
8	0.1	0.005	50	0	200	250	250

3. After preparation of different concentration BSA stock according to the table, 0.1 mol/l Tris-HCl and 0.1 N NaOH were added sequentially.
4. Then Bradford reagent was added.
5. After 5 min incubation at room temperature the absorbance was measured at 595 nm.

2.19.c. 1-aminocyclopropane-1-carboxylic acid deaminase (ACC deaminase) assay from different endophytic bacterial strains:

Reagents:

1. Tryptic soya broth (commercial)
2. DF salts preparation

Composition of DF salts (Saravanakumar and Samiyappan, 2007)	
KH ₂ PO ₄	4 g
Na ₂ HPO ₄	6 g
MgSO ₄ ·7H ₂ O	0.2 g
Glucose (dextrose)	2 g
Citric acid	2 g
Gluconic acid	2 g
H ₃ BO ₃	10 mg
FeSO ₄ ·7H ₂ O	1 mg
ZnSO ₄ ·7H ₂ O	124.6 mg
MnSO ₄ ·H ₂ O	11-19mg
MoO ₃	10 mg
CuSO ₄ ·5H ₂ O	78.22 mg
pH	7.2
Distilled water (up to)	1000 ml

- 3. 1-aminocyclopropane-1-carboxylic acid (ACC) preparation:** 50.55 mg of ACC (1-aminocyclopropane-1-carboxylic acid) was dissolved in 1 ml pre- autoclaved distilled water to prepare 0.5 mol/lit conc. of ACC.

Procedure:

1. Bacterial cultures were grown in 15 ml of tryptic soya broth medium for overnight (24 hours) at 30°C in shaking incubator for incubation.
2. The next day, 5 ml of bacterial culture suspension was transferred into 25 ml centrifuge tubes.
3. Then the bacterial culture was incubated overnight (24 hours) at 30°C in a shaking water bath at 150-170 rpm.
4. Next day the bacterial culture was centrifuged at 8000 rpm for 10 minutes at 4°C.
5. The bacterial cell pellet was dissolved with 2.5 ml DF minimal salt medium after washed twice with 5 ml DF salts.
6. Then 15 µl of 0.5M (0.5 mol/lit) ACC solution was added and mixed to the DF minimal salts medium containing bacterial cell pellet.
7. The bacterial culture was incubated overnight (24 hours) at 30°C in a shaking water bath at 150-170 rpm.
8. Next day the bacterial cell suspension was centrifuged at 8000 rpm for 10 minutes. The supernatant was removed and 200 µl of 0.1 mol /l Tris–HCl, pH 8.5 was added with bacterial cell pellet and mixed well.
9. Then in the cell suspension 10µl of toluene was added and mixed properly.
10. Then the mixture was divided into two parts i.e., 100 µl each. One part of 100µl bacterial cell suspension was used for ACC deaminase activity assay and the rest part was kept at 4°C for protein analysis.
11. 100µl of bacterial cell suspension was taken and 10µl of 0.5M ACC was added and mixed properly and incubated for 15 minutes at 30°C.
12. Then 0.5 ml of 0.56 mol/l HCl was added, mixed well, and centrifuged for 5 min at 14,000 rpm at room temperature.
13. 250µl of the supernatant was taken in a glass tube and 200µl of 0.56 mol/l HCl was added to it. Next, 75µl of the 2,4dinitrophenyl hydrazine reagent was added, mixed well and incubated at 30°C for 30 minutes.
14. After that, 0.5 ml of 2 N NaOH was added to it and the absorbance was taken at 540 nm.

2.19.d. Protein concentration determination:

Procedure:

1. From another part of the 100µl, 25 µl aliquot of the toluenized cells was taken.
2. Then 225µl of 0.1M (0.1mol /l) Tris–HCl, pH 8.5, and 250 µl NaOH (0.1M) were added to it.
3. The solution was mixed well and boiled for 10 min on a boiling water bath.
4. After cooling at room temperature, the cell suspensions were centrifuged for 6000 rpm for 1 min.
5. After centrifuged, 15-25 µl of cell supernatants were taken. Volume was made up to 250µl by the addition of 0.1M (0.1mol /l) Tris–HCl, pH 8.5 solutions.
6. Then 250µl of 0.1M NaOH solution was added.
7. At last, 250µl Bradford reagent was added and mixed properly.
8. After waiting for 5 min for incubation at room temperature the absorbance was measured at 595 nm immediately.

2.20. Nitrogenase assay from different endophytic bacterial strains:

The Nitrogenase assay was done according to Kifle and Laing (2016).

Reagents:

1.

Luria-Bertani (LB): Composition of LB (Luria-Bertani) agar medium	
Sodium chloride	10g
Yeast extract	5g
Tryptone	10g
Distilled water (up to)	1000ml
pH	7.0
Agar	10g

2. Tryptone Soya Broth (TSB):

30.0 g of Soyabean Casein Digest medium or Tryptone Soya Broth was dissolved in 1000 ml distilled water. Then autoclaved at 121°C for 15 minutes.

3. N- free medium (FNF): Three types of FNF medium are required-

- a. Liquid N- free medium
- b. Solid N- free medium
- c. Semi-solid N- free medium

N- free medium composition: 1L	
Glucose	5 g
CaCl ₂	0.15 g
Yeast extract	0.1 g
KH ₂ PO ₄	0.4 g
Na ₂ MoO ₄	0.025 g
FeSO ₄ ·7H ₂ O	0.04 g
MgSO ₄ ·7H ₂ O	0.2 g
K ₂ HPO ₄	0.5 g
CaCO ₃	1.0 g
pH	7.0
Distilled water (up to)	1000 ml

- 1. No agar was used for liquid media preparation.**
- 2. 1% agar was used for solid media preparation.**
- 3. 0.385% agar was used for semi-solid media preparation.**

Procedure:

- Bacterial cultures were grown in LB broth medium and incubated overnight (24 hours) at 30°C in shaking incubator.
- Then 0.1 OD culture of bacteria was inoculated in 5 ml TSB (Tryptic Soya Broth) medium and incubated at 30°C for 48 hours.
- After incubation, transfer the calculated volume of 0.2 OD culture to a sterile 1.5 ml micro centrifuge tube and spin the cells down in a centrifuge, wash two times with sterile water, and suspend in **200µl** of sterile water.
- Then **200µl** of 0.2 OD bacterial culture was inoculated in 10 ml of N- free liquid medium and incubated at 30°C for 72 hours.
- After incubation, all liquid media of 10 ml vol. was transferred into 25 ml centrifuge tubes and centrifuged at 6000 rpm for 10 minutes at 4°C. Then remove the supernatant.
- Add **200 µl** of sterile water to the pellet and mix. **100 µl suspended cells were taken for CFU counting at 4°C.**

7. Another **100 µl suspended cells** were inoculated to an N- free semi-solid medium (10 ml semi-solid media poured into transparent GC vials with cotton plug made with non-absorbent cotton) and incubated at 30°C for 72 hours.
8. Then cotton plug was replaced by septa and foil cap on it and sealed.
9. Then 1 ml of air from the headspace of the vial was replaced by 1 ml of acetylene gas (1000-2000ppm).
10. And again, incubated for 24 hrs at 29°C, then finally analysed for ARA assay by GC machine (6000 series Gas Chromatograph System) against a standard of ethylene if there was any conversion of acetylene to ethylene.
11. After that, **100 µl suspended cells** were taken at 4°C then serially diluted and spread on solid N-free media plates (1% Agar) and **CFU** count was recorded.

2.21. Screening of salt tolerance properties of endophytic bacteria:

Bacterial isolates were screened to check the ability of salt tolerance. Three media i.e., phosphate

solubilizing, free-living nitrogen fixing, cellulose-degrading, and three NaCl concentrations (0.3M, 0.5M, and 0.7M) were used with different combinations. The preparation of combinations of three media is mentioned below.

Medium Phosphate solubilizing bacteria (PSB): NBRIP medium (Nautiyal, 1999)	
Glucose	10 g
(NH ₄) ₂ SO ₄	0.1 g
Ca ₃ (PO ₄) ₂	5 g
MgSO ₄ ·7H ₂ O	0.25 g
KCl	0.2 g
MgCl ₂	5 g
pH	6.8-7.0
Distilled water (up to)	1000 ml

Three NaCl concentrations (0.3M, 0.5M and 0.7M) with normal PSB medium were prepared. Different NaCl concentrations were added as follows:

0.3M = 17.532 g NaCl/L, 0.5M = 29.22 g NaCl/L, 0.7M = 40.924 g NaCl/L and normal PSB medium where no NaCl was added.

Procedure:

1. Bacterial cultures were inoculated in 10 ml of LB broth medium and incubated at 37°C for 24 hours.
2. Then 0.1 OD culture of bacteria was inoculated in 10 ml normal PSB broth medium and incubated for 72 hours at 30°C.
3. After that the bacterial culture was taken in a microcentrifuge tube and turbidity was measured at 600 nm.
4. Then 0.1 OD bacterial culture was inoculated in 10 ml normal PSB broth medium, 0.3M NaCl PSB broth, 0.5M NaCl PSB broth, 0.7M NaCl PSB broth and incubated at 30°C for 72 hours.
5. After that bacterial culture turbidity was measured at 600 nm individually.

Media of cellulose-degrading bacteria (CDB) (cellulose decomposers) (Thatoi et al, 2012)	
Precipitated cellulose	4 g
CaCl ₂	0.1 g
K ₂ HPO ₄	1 g
FeCl ₃	0.02 g
NaCl	0.1 g
NaNO ₃	2 g
MgSO ₄ ·7H ₂ O	0.2 g
pH	7.0
Distilled water (up to)	1000 ml

Three NaCl concentrations (0.3M, 0.5M and 0.7M) with normal CDB medium were prepared. Different NaCl concentrations were added as follows:

0.3M = 17.532 g NaCl/L, 0.5M = 29.22 g NaCl/L, 0.7M = 40.924 g NaCl/L and normal CDB medium.

Procedure:

1. Bacterial cultures were inoculated in 10 ml of LB broth medium and incubated at 37°C for 24 hours.

2. Then 0.1 OD culture of bacteria was inoculated in 10 ml normal CDB broth medium and incubated for 72 hours at 30°C.
3. After that the bacterial culture was taken in a microcentrifuge tube and turbidity was measured at 600 nm.
4. Then 0.1 OD bacterial culture was inoculated in 10 ml normal CDB broth, 0.3M NaCl CDB broth, 0.5M NaCl CDB broth, 0.7M NaCl CDB broth and incubated at 30°C for 72 hours.
5. After that bacterial culture turbidity was measured at 600 nm individually.

Nitrogen fixing medium (FNF): Jensen's Medium (Sahadevan et al, 2016)	
Sucrose	20 g
K ₂ HPO ₄	1 g
MgSO ₄	0.5 g
FeSO ₄	0.1 g
CaCO ₃	2 g
Na ₂ MoO ₄	0.005 g
Distilled water (up to)	1000 ml

Three NaCl concentrations (0.3M, 0.5M and 0.7M) with normal FNF medium were prepared. Different NaCl concentrations were added as follows:

0.3M = 17.532 g NaCl/L, 0.5M = 29.22 g NaCl/L, 0.7M = 40.924 g NaCl/L and normal FNF medium

where no NaCl was added.

Procedure:

1. Bacterial cultures were inoculated in 10 ml of LB broth medium and incubated at 37°C for 24 hours.
2. Then 0.1 OD culture of bacteria was inoculated in 10 ml normal FNF broth medium and incubated for 72 hours at 30°C.
3. After that the bacterial culture was taken in a microcentrifuge tube and turbidity was measured at 600 nm.
4. Then 0.1 OD bacterial culture was inoculated in 10 ml normal FNF broth, 0.3M FNF broth, 0.5M FNF broth, 0.7M FNF broth, and incubated at 30°C for 72 hours.
5. After that bacterial culture turbidity was measured at 600 nm individually.

2.22. Histological study of mangrove roots and pneumatophores:

Histological studies of mangrove roots and pneumatophores were done according to Canene-Adams, 2013.

Root and pneumatophore samples of mangroves were collected from different places in Sundarbans and preserved in FAA. Root and pneumatophore samples were used for histological study by following the protocol described below:

STEP – 1: WASHING:

Initially, it was necessary to wash out the fluid (FAA required for fixation) thoroughly before progressing with dehydration and infiltration. Tissues should be treated with hot water for 5-6 hours with a regular interval of 40-50 minutes.

STEP – 2: DEHYDRATION:

After eliminating the fixing fluid and air from the tissues, they were now treated with the following reagents to dehydrate and clear.

1. 30% ethanol for 6 hours
2. 50% ethanol for 6 hours
3. 70% ethanol for 24 hours
4. 80% ethanol for 6 hours
5. 90% ethanol for 6 hours
6. 95% ethanol for 6 hours
7. Absolute ethanol for 24 hours (overnight)
8. 25% chloroform in ethanol for 6 hours
9. 50% chloroform in ethanol for 6 hours
10. 75% chloroform in ethanol for 6 hours
11. Absolute chloroform for 24 hours.

STEP – 3: INFILTRATION:

After dehydrating and clearing, the material was now ready for infiltration with paraplast. One chip of paraplast plus was added from time to time to clearing reagent where the tissues were dipped until the solution was saturated with partially dissolved paraplast. Now the vial was placed in the hot air oven and the temperature ranging from 58°C to 60°C was maintained. This step of infiltration took at least 6 hours. Now, after removal of the screw cap from the vial, it was left for 16 hours in the oven. Then, the mixture of chloroform and paraplast was drained out and replaced immediately with pure melted paraplast. Within the next 24 hours or so, at least two more changes of pure melted paraplast were made.

STEP – 4: EMBEDDING:

After the infiltration of pure melted paraplast, the next step was embedding. The steps were as follows:

1. A minimal amount of liquid paraplast was poured into the mold, from the paraplast reservoir.
2. The processed tissue was then transferred into the mold and oriented longitudinally to obtain transverse sections.
3. When the tissue was in the appropriate orientation, some more melted paraplast was poured on top of it up to the brink of the mold.
4. When it was solidified the paraplast block could be easily removed from the mold and it should not stick to the mold.

The blocks were now ready for sectioning or they could be stored at room temperature for years.

STEP – 5: SECTIONING:

Tissues were sectioned using a Leica RM2125 RTS rotary microtome. The steps were as follows–

1. The tissue blocks were chilled on ice before sectioning. Cold paraplast was used for thinner sections.
2. The water bath was turned on and the temperature was set at 40-45°C.
3. A fresh blade was placed on the blade holder of the microtome.
4. The Blade Clearance Angle was set optimally. For Leica blade holders this was normally between 1° and 5°.
5. The block was inserted into the block holder of the microtome and it was oriented properly, so the block would cut straight across by the blade.
6. The block was trimmed. Trimming was done generally at a thickness of 10-30 µm. After trimming the sections were cut at a thickness of about 7-12 µm.
7. When the block was ribboning in the desired plane and desired thickness, the ribbons of sections were picked up and they were floated on the surface of the water (40-45°C).
8. When the ribbons were completely flattened, adhesive-coated microscope slides were used to take the sections out of the water bath and the excess water was drained out from the slide.

STEP – 6: STAINING:

Series was to be prepared in coupling jars/staining jars for removing paraplast and staining the slides by treating them with the following reagents –

1. Deparaffinized in xylene (pure) for 40 minutes
2. Deparaffinized again in xylene and absolute ethanol in a 1:1 ratio for 15 minutes
3. Treated in absolute ethanol for 15 minutes
4. Hydrated in 90% ethanol for 15 minutes
5. Hydrated in 70% ethanol for 15 minutes
6. Hydrated in 50% ethanol for 15 minutes
7. Hydrated in 30% ethanol for 15 minutes
8. Hydrated in water for 15 minutes
9. Stained with 0.05% Toluidine Blue dye for 15-25 seconds.
10. Washing out of the excess stain with water.
11. Mounting of the tissue sections with DPX and then observed under the microscope.

2.23. Selection of the best PGP bacteria as consortium:

On the basis of the comprehensive PGP profiles of all the 78-mangrove root endophytic bacterial strains were observed, finally 19 bacterial strains were selected for making 3 combinations of large-scale bacterial cultures for the application of the same in rice fields and on *Avicennia officinalis* saplings at Sundarbans for studying plant growth promotion by mangrove root endophytes.

Consortium BC-1:

- a. *Aeromonas dhakensis* strain HPR7 (MT422007)
- b. *Mangrovibacter plantisponcer* strain BCRP5 (MT422011)
- c. *Pseudomonas stutzeri* strain BCY5 (MT422041)
- d. *Pseudomonas stutzeri* strain BCY7 (MT422042)
- e. *Bacillus subtilis* strain AOR5 (MT421976)
- f. *Serratia marcescens* strain AOR4 (MT422009)

Consortium BC-2:

- a. *Aeromonas allosaccharophila* strain DAL2 (MT422027)
- b. *Pseudomonas* sp. strain DER1 (MT422045)
- c. *Pseudomonas putida* strain DER3 (MT422020)
- d. *Pseudomonas fulva* strain DER9 (MT422023)

- e. *Aeromonas veronii* strain POT3 (MT422035)
- f. *Aeromonas veronii* strain POT7 (MT422025)
- g. *Serratia marcescens* strain HPR4 (MT422006)

Consortium BC-3:

- a. *Bacillus subtilis* strain AMR4 (MT421979)
- b. *Aeromonas hydrophilia* strain HER3 (MT422047)
- c. *Bacillus altitudinis* strain XYL1 (MT422037)
- d. *Pseudocitrobacter faecalis* strain HRR5 (MT422004)
- e. *Serratia marcescens* strain HPR4 (MT422006)
- f. *Enterobacter kobei* strain HRR1 (MT421989)

2.24. Optimization of growth curve of endophytic bacteria for preparation of consortium:

1. The selected endophytic bacteria were inoculated in nutrient broth and incubated overnight at 30°C.
2. Then, 0.1 OD bacterial culture was inoculated in another 10 ml of NB broth.
3. The cultures were incubated at 37°C for 96 hours, their growth profile had been recorded individually on 6hrs, 12hrs, 24hrs, 48hrs, 72hrs and 96 hrs at 600 nm.

2.25. Optimization of large-scale culture of all PGP bacterial combinations for application in rice field at Sundarbans and on *Avicennia officinalis* saplings in onsite mangrove nursery also at Sundarbans:

1. The growth of individual bacteria was continued for 96 hours, their growth profile was recorded on 6hrs, 12hrs, 24hrs, 48hrs, 72hrs and 96hrs. Depending on their common exponential phase the cultures were prepared for application in the field.
2. It was found that all the bacteria usually attained exponential phase within a 48-72 hrs period.
3. Individual bacterial member from each of the combinations was initially inoculated in a small culture of 100 ml and then raised to 600 ml of large volume with a final OD between 2-3 within 48-72 hrs.
4. The culture media used was Nutrient Broth (NB) of conductivity ~8-9 dS/m.
5. Finally, an equal volume of each of the large-volume cultures of bacterial members of each combination was mixed.

6. Approximately 8–9-liter culture volume was developed for each bacterial combination to be applied in equal volume in 4 m² area of each 4 replica plots after 3 times dilution with pond water with conductivity of ~ **2.256 dS/m**. Here each replica plot was added with approx. 7 liters of diluted culture.
7. The lowland indigenous rice cultivar used for the field experiments was **Dudheswar landrace IC No. 593998**.
8. In the case of *Avicennia officinalis* approximately **3–4-liter** culture volume was developed for each bacterial combination to be applied in equal volume in **1 m² pots** after **3** times dilution with river water. Here **80, 28-day-old *Avicennia* sp.** saplings were used for each combination.
Each plant was grown in individual plastic nursery bags. Here 50 ml of diluted culture was applied to each plant.

2.26. Development of large-scale culture of all PGP bacterial combinations for application in the 1st and 2nd greenhouse pot experiments:

1. **Selected rice varieties for pot experiment:** Lunishree and **Dudheswar** landrace IC No. 593998
2. **Details of NPK fertilizer used in the experiment:**

Name: RJ Shriram 20:20:20

Brand: **Shriram**

Required conventional dose of NPK 20:20:20 is 4.4 mg of NPK in 0.8 kg of soil (0.8 Kg of soil was approximately present in each pot used in the experiment).

3. **Bacterial combinations selected for pot experiments:**

A total of 18 bacterial combinations were used for the pot experiment. 2 sets of pot for NPK and 2 sets for control without any bacteria were used. Among 18 bacterial combinations, some combinations were of only rhizospheric bacterial isolates and some of only endophytic bacterial isolates, and other combinations were made by mixing both rhizospheric and endophytic bacterial isolates. Those used combinations were-

Sole endophytic bacterial combinations:

Consortium BC-1

Consortium BC-2

Consortium BC-3

Mixed bacterial combinations:

SRC1+BEC1, SRC2+BEC2, SRC3+BEC3, SRC4+BEC1, SRC5+BEC2, SRC6+BEC3, SRC4+BEC2, SRC1+BEC3, SRC6+BEC1

Where,

❑ BEC= root endophytic consortia

❑ SRC= native halophytic grass rhizospheric consortia

1. Initial culture preparation was already described earlier. Here 3 endophytic and 6 rhizospheric bacterial combinations were selected. For each consortium 600 ml culture was prepared.
2. **Mixed combinations** (600ml) containing both **rhizospheric & endophytic** bacterial isolates were prepared by mixing equal volumes (300ml+300ml) of two different combinations.
3. Then all types of cultures were stored for a few days at 4°C and the bacterial pellet was collected by removing the medium before application.
4. After that, the pellet was diluted by adding 240 ml tap water and the diluted culture was then applied in 12 pots equally (i.e., 20 ml/pot).

2.27. Conductivity determination from soil and water:**2.27.a. Conductivity determination from soil:**

The soil samples conductivity was measured by 1:2, soil: water suspension method (Gartley, 2011; Mangalassery et al, 2017).

Procedure:

1. 10 g dry sieved soil sample and 20 ml of distilled water were mixed.
2. After shaking for 30 minutes in a room-temperature shaker, soil suspension was made.
3. By the help of conductivity meter at 25°C, the conductivity of soil samples was measured and 0.1M KCl was used as standard.

2.27.b. Conductivity determination from water:**Procedure:**

The water conductivity was measured with conductivity meter at 25°C and 0.1M KCl was used as standard.

2.28. pH determination from soil and water:

2.28.a. pH determination from soil:

The soil samples pH was measured by 1:2, soil: water suspension method (Hossain et al, 2012; Mangalassery et al, 2017).

Procedure:

1. 10 g dry sieved soil sample was added in 20 ml of distilled water and mixed well.
2. After shaking for 30 minutes in a room-temperature shaker, soil suspension was made.
3. The soil samples pH was measured by a pH meter.
4. Proper calibration of the pH meter was essential for this analysis.

2.28.b. pH determination from water:

Procedure:

1. The pH of the water sample was measured by a pH meter.
2. Proper calibration of the pH meter was essential for this analysis.

2.29. Plant available phosphorus estimation from soil:

Plant-available phosphorus extraction was done by Modified Morgan extraction solution (McIntosh, 1969). Soluble phosphorus estimation was followed with the molybdenum blue method (Krishnaswamy et al, 2009).

2.29.a. Plant-available phosphorus standard curve:

Reagents:

1. Ammonium molybdate solution preparation was described earlier in the phosphate solubilization assay.
2. Stannous chloride solution preparation was described earlier in the phosphate solubilization assay.
3. Di-potassium hydrogen phosphate
4. Glacial acetic acid
5. Ammonia (NH₄OH) solution
6. Modified Morgan extraction solution (0.62 N NH₄OH and 1.25 N CH₃COOH) preparation
 - a. 14.37 ml glacial acetic acid was dissolved in 10 ml of distilled water.

- b. 9.125 ml of ammonia (NH₄OH) solution was added slowly in glacial acetic acid solution.
- c. pH was adjusted to 4.8± 0.05 with concentrated NH₄OH or acetic acid and the final volume was filled up to 200 ml with distilled water.

7. Activated charcoal.

Plant-available phosphorus standard curve procedure was already described earlier:

Table 13: Reaction set up for preparation of phosphorus standard curve.

Setno.	Amount of 5 ppm stock (ml)	Amount of P in solution (µg)	Volume made upto (ml)	Ammonium molybdate solution added (ml)	Stannous chloride solution added	Final volume (ml)	P in diluted standard (ppm)
1	-	-	25	2	4drops	50	0.0
2	0.25	1.25	25	2	4drops	50	0.025
3	0.5	2.5	25	2	4drops	50	0.05
2	1	5	25	2	4drops	50	0.1
3	2	10	25	2	4drops	50	0.2
4	3	15	25	2	4drops	50	0.3
5	4	20	25	2	4drops	50	0.4
6	5	25	25	2	4drops	50	0.5
7	6	30	25	2	4drops	50	0.6
8	7	35	25	2	4drops	50	0.7
9	8	40	25	2	4drops	50	0.8
10	9	45	25	2	4drops	50	0.9
11	10	50	25	2	4drops	50	1.0
12	15	75	25	2	4drops	50	1.5
13	20	100	25	2	4drops	50	2

2.29.b. Plant-available phosphorus (P) extraction from soil:

Procedure:

1. 2 g of air-dried, sieved soil was taken in 15 ml falcon.
2. Then 500 mg of activated charcoal and 10 ml of modified Morgan extraction solution were added.
3. After shaking at 180 rpm for 15 minutes on a shaker homogeneous soil slurry was produced.
4. Soil slurry was filtered through a normal filter paper.
5. Then the clear solution was taken for further P estimation.

2.29.c. Plant-available phosphorus determination from soil:

Procedure:

1. In 20 ml distilled water, 1 ml clear soil extract was added.
2. 2 ml ammonium molybdate solution and 4 drops of stannous chloride solution were added respectively.
3. Then wait for 11 minutes and absorbance was measured at 660 nm.

2.30. Soil organic carbon estimation:

Soil organic carbon estimation was determined by colorimetric procedure according to Datta et al, 1962.

Reagents:

- a) Standard potassium dichromate 1/6M (1N)
- b) Concentrated sulfuric acid containing 1.25% Ag_2SO_4
- c) Sucrose (AR quality)

2.30.a. Organic carbon standard curve preparation:

Procedure:

1. Sucrose was used as a primary carbon source for the preparation of the organic carbon standard curve. For the preparation of the standard curve, 500 mg of sucrose (A.R. grade) was dissolved in 500 μl water, **stock solution as 1mg/ μl .**

Table 14: Reaction set up for preparation of organic carbon standard curve.

Set no.	Distilled water added (µl)	Sucrose solution in µl	Sucrose (in mg)	Final volume in µl	Amount Organic Carbon (mg) (sucrose in mg*0.42)	Potassium dichromate 1/6M (1N) in ml	Concentrated sulfuric acid containing 1.25% Ag ₂ SO ₄ in ml
1	60	0	0	60	0	2.5	5
2	59	1	1	60	0.42	2.5	5
3	58	2	2	60	0.84	2.5	5
4	55	5	5	60	2.1	2.5	5
5	52	8	8	60	3.36	2.5	5
6	50	10	10	60	4.2	2.5	5
7	48	12	12	60	5.04	2.5	5
8	45	15	15	60	6.3	2.5	5
9	42	18	18	60	7.56	2.5	5
10	40	20	20	60	8.4	2.5	5
11	35	25	25	60	10.5	2.5	5
12	30	30	30	60	12.6	2.5	5
13	25	35	35	60	14.7	2.5	5
14	20	40	40	60	16.8	2.5	5
15	10	50	50	60	21	2.5	5
16	0	60	60	60	25.2	2.5	5

1. Sucrose solution was added in different conditions according to the table.
2. 2.5 ml 1/6M (1N) K₂Cr₂O₇ and 5 ml of H₂SO₄ (concentrated) containing 1.25% Ag₂SO₄ solutions were added respectively.
3. Then the total solution was mixed properly and left for 30 minutes.
4. After incubation, green color developed and absorbance was measured at 660 nm.
5. For the preparation of the organic carbon standard curve, the absorbance was plotted with mg of sucrose x 0.42 as a carbon source (carbon = weight of sucrose x 0.42, because 42% carbon content was present in sucrose).

2.30.b. Organic carbon determination from soil:

Procedure:

1. 1 g dry sieved soil sample and 60 µl distilled water were taken in a flask.
2. 2.5 ml of 1/6M (1N) K₂Cr₂O₇ and 5 ml of H₂SO₄ (concentrated) containing 1.25% of Ag₂SO₄ solutions were added respectively.
3. Then the total solution was mixed properly, and the green color developed. And the solution was left for 30 minutes.
4. 1.5 ml solution was taken in a microcentrifuge tube and centrifuged at 3000 rpm for 2 minutes.
5. The supernatant was taken and absorbance was measured at 660 nm.

2.31. Ammonia-nitrogen estimation:

Ammonia-nitrogen extraction from soil was followed as Dorich and Nelson, 1983; Keeney and Nelson, 1987. Ammonia-nitrogen content from soil was estimated by the Phenate method (Park et al, 2009; Solo´rzano, 1969; Dorich and Nelson, 1983).

Reagents:

1. **2M KCl extraction solution:** 74.55g KCl was taken in distilled water and dissolved, then final volume was filled 500 ml with distilled water.
2. **EDTA (6% w/v):** 6g EDTA was dissolved in 100 ml distilled water.
3. **Phenol solution (10 ml):** The liquefied phenol (89%) 1.11 ml and 8.89 ml of 95% ethyl alcohol was mixed.
4. **0.5% (w/v) Sodium nitroprusside solution:** 100 mg sodium nitroprusside was dissolved in 20 ml deionized water and stored in brown bottle or amber bottle.
5. **Alkaline citrate solution:** 10 g tri-sodium citrate and sodium hydroxide 0.5 g were mixed in 30 ml deionized water and dissolved properly. Then final volume filled up to 50 ml with deionized water.
6. **Sodium hypochlorite (commercial)**
7. **Oxidizing solution:** Alkaline citrate solution 4 ml and 1 ml sodium hypochlorite was mixed well.

2.31.a. Ammonia-nitrogen standard curve preparation:

Procedure:

- 1. Ammonium-nitrogen stock preparation (Standard stock solution, conc. = 1000 mg/L):** 3.821 g of anhydrous NH_4Cl (dried at 100°C for 1 hour) was dissolved in ammonia-free water of 1 L.

Mol. wt. of NH_4Cl is 53.49, Mol. wt. of N = 14

14 g N is present in 53.49 g NH_4Cl

1 g N is present in $53.49/14 = 3.8207 \sim 3.821$ g NH_4Cl .

So, 3.821g NH_4Cl contains 1 g of N = 1000 mg of N.

Ammonium-nitrogen standard stock solution calculations-

1 ml of 1000 ppm ammonium-nitrogen stock was taken and mixed with 9 ml water to prepare 100 ppm ammonium-nitrogen stock solution.

Again 1 ml of 100 ppm ammonium-nitrogen stock was taken and mixed with 9 ml water to prepare 10 ppm ammonium-nitrogen stock solution.

Table 15: Reaction set up for ammonium-nitrogen standard curve.

Set no.	Volume of 10 ppm stock in μl (0.01 $\mu\text{g}/\mu\text{l}$)	Amount of $\text{NH}_3\text{-N}$ (ppm)	Amount of $\text{NH}_3\text{-N}$ in μg	Water added (μl)	Final volume (ml)
1	0	0	0	10000	10
2	5	0.005	0.05	9995	10
3	10	0.01	0.1	9990	10
4	25	0.025	0.25	9975	10
5	50	0.05	0.5	9950	10
6	100	0.1	1	9900	10
7	200	0.2	2	9800	10
8	300	0.3	3	9700	10
9	400	0.4	4	9600	10
10	500	0.5	5	9500	10
11	600	0.6	6	9400	10
12	700	0.7	7	9300	10
13	800	0.8	8	9200	10
14	900	0.9	9	9100	10
15	1000	1	10	9000	10
16	2000	2	20	8000	10
17	3000	3	30	7000	10

2. From this 10 ml final solution 1000 µl was taken in a micro centrifuge tube.
3. Different concentration of ammonia stock solution was prepared in microcentrifuge tube.
4. Then phenol solution of 40 µl, sodium nitroprusside solution of 40 µl, and oxidizing solution of 100 µl were added and mixed respectively.
5. The reaction mixture was kept for 1 hour in depressed light at room temperature.
6. After 1 hour, color was produced and absorbance was read at 640 nm.

2.31.b. Ammonia-nitrogen extraction from soil:

Procedure:

1. In 2 g of air-dried, sieved soil 10 ml of 2M KCl solution was added.
2. After shaking at 180 rpm for 1 hour on a shaker homogeneous soil slurry was produced.
3. Soil slurry was filtered through a normal filter paper and a clear soil extract was prepared.

2.31.c. Ammonia-nitrogen determination from soil:

Procedure:

1. In the microcentrifuge tube 200µl clear soil extract, 100µl EDTA, and 700µl distilled water were taken.
2. Then phenol solution of 40 µl, sodium nitroprusside solution of 40 µl and oxidizing solution of 100 µl were added and mixed respectively.
3. The reaction mixture was kept for 1 hour in depressed light at room temperature.
4. After 1 hour, color was produced and absorbance was read at 640 nm.

2.32. Nitrate-nitrogen estimation:

Nitrate-nitrogen extraction from soil was followed according to Dorich and Nelson, 1983; Keeney and Nelson, 1987. Nitrate-nitrogen content from soil was estimated by the UV spectroscopy method (Edwards et al, 2001; Kaneko et al, 2010).

Reagents:

- A. Potassium nitrate (KNO_3)
- B. 2M KCl solution

2.32.a. Nitrate-nitrogen standard curve preparation:

Procedure:

1. Preparation of KNO₃ stock and standards:

Mol. wt. of KNO₃ is 101.11, Mol. wt. of N = 14

So, 14 g N present in 101.11 g of KNO₃ in 1 L 2M KCl solution.

So, 1 g N = 7.22 g KNO₃ in 1 L.

So, 7.22 g KNO₃/L = 1000 ppm of NO₃-N

So. 0.0722 g KNO₃ / 10 ml = 1000 ppm of NO₃-N

Therefore, 0.0722g KNO₃ in 10 ml of 2M KCl solution = 1000 ppm of NO₃-N (stock)

Table 16: Reaction set up for preparation of nitrate-nitrogen standard curve.

Set no.	Stock added (μ l)	2M KCl added (μ l)	Final ppm in terms of NO ₃ -N	Amount of NO ₃ -N in μ g in 10 μ l stock solution taken from 1 ml final stock volume
1	-	1000	0	0
2	1	999	1	0.01
3	3	997	3	0.03
4	5	995	5	0.05
5	10	990	10	0.10
6	15	985	15	0.15
7	20	980	20	0.20
8	25	975	25	0.25

2. From this 1 ml final solution 10 μ l was taken in a microcentrifuge tube.
3. Different concentration of nitrate-nitrogen stock solutions was prepared in micro centrifuge tube.
4. Then 990 μ l distilled water was added to it.
5. Absorbance was measured at 210 nm. The absorbance of reagent blank was subtracted from the sample absorbance.

2.32.b. Nitrate-nitrogen extraction and determination from soil:

Procedure:

1. In 2 g of air-dried, sieved soil 10 ml of 2M KCl solution was added.
2. After shaking at 180 rpm for 1 hour on a shaker homogeneous soil slurry was produced.
3. Soil slurry was filtered through a normal filter paper and a clear soil extract was prepared.
4. Then 10 μ l clear soil extract was taken and 990 μ l distilled water was added to it.
5. Absorbance was taken at 210 nm and 270 nm.
6. 2 times absorbance at 270 nm (due to dissolved organic matter) was subtracted from the absorbance of 210 nm.

2.33. The determination of exchangeable sodium and potassium in soil:

The determination of exchangeable sodium and potassium was described earlier for plant tissues. Here some differences in the same procedure while extracting from soil are described below:

Procedure:

1. 1g of air-dried, sieved soil was taken in 50 ml falcon.
2. Then 25 ml of 1 M ammonium acetate solution added to it.
3. After shaking at 180 rpm for 1 hour on a shaker homogeneous soil slurry was produced.
4. Soil slurry was filtered through a normal filter paper and a clear soil extract was prepared.
5. Detection was done by flame photometer.
6. First, the standards were calibrated in a flame photometer.
7. Then readings were recorded from soil samples based on this calibration.
8. For each soil type, 3 soil samples were made and 3 readings were recorded.
9. All dilutions were done by 1M ammonium acetate.
10. Only de-ionized water was used throughout the experiment.

2.34. Estimation of starch content from rice grains:

Estimation of starch content from rice grains were done as Dubois et al, 1951.

Estimation of the amount of starch from rice grains by Phenol–Sulfuric Acid method.

Reagents:

1. **Sulfuric acid:** 95.5% (reagent grade) specific gravity 1.84.

2. **Phenol:** 5% by weight, was made by adding dH₂O to 5 g of re-distilled phenol (reagent grade).
3. **2.5N HCL:** 20.83 mL of concentrated HCL (12 N) was added to 79.17 mL of sterile H₂O.

2.34.a. Starch standard curve preparation:

Procedure:

1 mg/ml or, 1 µg/µl of starch stock: 10 mg glucose was dissolved in 10 ml of distilled water to prepare 1mg/ml or, 1µg/µl of starch stock. Different concentrations of standard protein solutions were prepared from the stock solution into a numbers of test tubes and the volume was made up to 6.1 ml.

Table 17: Reaction set up for preparation of glucose standard curve.

Set no.	Concentration of starch (µg)	Volume of starch stock added (µl)	Volume of distilled water (µl)	5% phenol added(µl)	Conc. Sulfuric acid added (µl)	Final volume (µl)
1	0	0	100	1000	5000	6100
2	10	10	90	1000	5000	6100
3	20	20	80	1000	5000	6100
4	30	30	70	1000	5000	6100
5	40	40	60	1000	5000	6100
6	50	50	50	1000	5000	6100
7	60	60	40	1000	5000	6100
8	70	70	30	1000	5000	6100
9	80	80	20	1000	5000	6100
10	90	90	10	1000	5000	6100
11	100	100	0	1000	5000	6100

1. After waiting for 10 minutes, all the test tubes were kept in a water bath for 15 minutes at 25 to 30°C.
2. 1 ml of distilled water used as blank and the absorbance of per test tube was read at 490 nm.

2.34.b. Estimation of starch content from rice grains:

Procedure:

1. 100 mg of powder from rice grains was taken in test tube and 5 ml of 2.5N HCL was added to the sample.
2. Then test tubes were kept in a water bath for 3 hrs at 95°C.
3. After incubation the test tubes were removed from the water bath, and cooled.
4. After test tubes were cooled, it was neutralized by adding solid sodium carbonate until effervescence ceased.
5. The total volume was made upto 100 ml with distilled water.
6. Then 1 ml solution was taken in 1.5 ml centrifuge tube and centrifuged at 3000 rpm for 5 minutes, supernatant was used as a sample for estimation of starch.
7. 100 µl of the sample was taken and 1 ml of 5% phenol solution was added.
8. Then 5 ml of 95.5% sulphuric acid was added.
9. The reaction was continued for 10 minutes and all tubes were placed in a water bath for 15 minutes at 25-30°C.
10. Distilled water was used as blank.
11. Absorbance was read at 490 nm immediately after 15 min of incubation.
12. The amount of starch present in the sample was measured by the help of the standard curve.

2.35. Estimation of total protein content from rice grains:

Estimation of total protein content from rice grains were done according to Sadaiah et al, (2018).

Estimation of the amount of protein from rice grains by Bradford Assay.

Reagents:

1. BSA
2. Coomassie-Brilliant blue G250
3. 85% phosphoric acid
4. 95% Ethanol
5. Glycerol

Coomassie-Brilliant blue (G250) 100 mg was taken in 50 ml of 95% ethanol and dissolved properly. Then 100 ml of 85% phosphoric acid was added and volume was made up to 1000 ml by distilled water. The solution was filtered and this solution was used after 24 hrs.

2.35.a. Protein standard curve preparation:

Procedure:

1. **1mg/ml or, 1 μ g/ μ l of BSA stock:** 10 mg of BSA (Bovine serum albumin) was added in 10 ml of distilled water and dissolved properly to prepare 1mg/ml or, 1 μ g/ μ l of BSA stock. Different concentrations of standard protein solutions were prepared from the stock solution into several test tubes and the volume was made up to 5.1 ml.

Table 18: Reaction set up for preparation of BSA standard curve.

Set no.	Vol. of BSA (μ l)	Conc. of BSA (μ g)	BSA (mg/ml) stock taken in μ l	Volume of Bradford added (μ l)	Volume of distilled water (μ l)	Final volume (μ l)
1	0	0	0	5	100	5100
2	10	10	10	5	90	5100
3	20	20	20	5	80	5100
4	30	30	30	5	70	5100
5	40	40	40	5	60	5100
6	50	50	50	5	50	5100
7	60	60	60	5	40	5100
8	70	70	70	5	30	5100
9	80	80	80	5	20	5100
10	90	90	90	5	10	5100
11	100	100	100	5	0	5100

2. After the preparation of different concentrations of BSA stock, Bradford reagent was added.
3. Absorbance was measured immediately after 5 min of room temperature incubation at 595 nm.

2.35.b. Estimation of total protein content from rice grains:

Procedure:

NaOH extraction methods were followed-

1. 50 mg of powdered rice sample was taken into a 15 ml screw-capped tube.
2. Then 0.5 ml of ethanol was added and observed so that no precipitate was formed at the base of the tube.

3. After 2 minutes 4.5 ml of 1N NaOH was added and incubated for 15 min in a boiling water bath to ensure complete dissolution of the sample.
13. Then the tubes were taken out from the boiling water bath and cooled to room temperature.
4. From here 20 μ l of the sample was taken and the volume was filled up to 100 μ l by distilled water.
5. Then 5 ml of Coomassie-Brilliant blue was added and mixed by vortexing or inversion.
6. Distilled water was used as blank.
7. Absorbance was read at 595 nm immediately after 5 min of room temperature incubation.
8. The amount of protein present in the sample was determined by the help of a standard curve.

Calculation:

The percentage of protein present in rice grains was determined by the following equation:

20 μ l of sample contain X μ g of protein. Or, 20 ml of sample contain X mg of protein and 100 ml of sample contain $=X/20 * 100$ % of protein=Y% of protein.

This Y% of protein present in 50 mg of powder rice grains.

2.36. Antioxidant assay of endophytic bacterial culture filtrates:

2.36.a. Free radical scavenging assay by spectrophotometric method:

Free radical scavenging assay was followed according to Dhayanithy et al, 2019.

The free radical scavenging activity of endophytic bacterial extracts was measured with DPPH assay.

2.36.b. Extraction of antioxidants from endophytic bacterial culture:

The medium used: TSB medium or Tryptic Soy Broth - Tryptone Soya Broth (TSB):

30.0 g of TSB medium was suspended in 1000 ml distilled water and sterilized at 121°C for 15 minutes.

1. Bacterial cultures were grown in 5 ml of tryptic soya broth medium overnight at 30°C in a shaking incubator for incubation.
2. Then 0.2 OD bacterial culture was grown in 10 ml TSB (Tryptic Soya Broth) medium and incubated at 30°C for 48 hours.
3. After incubation, 10ml culture (well shaken) was taken into a 25ml centrifuge tube and centrifuged at 10000 rpm for 15 min.

4. Then the supernatant was collected into a 25ml centrifuge tube.
5. 1:1 v/v ethyl acetate and chloroform were added to the supernatant and vigorously shaken.
6. The organic solvent layer was collected in a new centrifuge tube.
7. The organic layer was concentrated with the help of a vacuum rotary evaporator (Concentrator Plus) at 40°C.
8. The extract was transferred into a 2 ml microcentrifuge tube and left to dry at room temperature.
9. The extract was to be dissolved in 2 ml methanol.

Reagents:

i) DPPH (2, 2-diphenyl-1-picrylhydrazyl) 100ml 0.1mM solution preparation:

DPPH dissolved in 95% Ethanol to prepare DPPH solution.

M.W. of DPPH = 394.32 g/mol

1M DPPH = 394.32 g of DPPH in 1000ml

0.1mM DPPH = 394.32/ 100000 g of DPPH in 100ml

= 0.0039432 g of DPPH in 100ml

= 3.9432 mg of DPPH in 100ml

So, **3.94 mg** of DPPH was dissolved in 100 ml 95% Ethanol.

ii) Tris-HCl buffer: 100ml 100mM, pH=7.4

- a. **Preparation of 500Mm 100ml Tris-HCl buffer-** Add 6.05gm of Tris-base (MW = 121.14gm/mol) in 50ml of distilled water and maintained the pH to 7.4 by adding 1M HCL (8.3ml HCL to 100ml distilled water) and then make the final volume of 100ml.

- b. Take 20ml of 500mM Tris-HCl buffer and 80ml of distilled water will finally make **100ml of 100mM Tris-HCl buffer.**

iii) Ascorbic acid: Add 5mg Ascorbic acid in 100ml Tris-HCL buffer to make a concentration of 50µg mL⁻¹.

Table 19: Reaction set up for preparation:

	Sample added (µl)	Ascorbic acid (µl)	Methanol added (µl)	0.1 mM of DPPH added (µl)	100 Mm Tris-HCl buffer added (µl)	Total volume (ml)
Sample	200	0	0	1000	800	2
Control	0	0	200	1000	800	2
Positive control	0	200	0	1000	800	2

Procedure:

1. Add 1ml of 0.1 mM of DPPH solution to 200µl of methanolic solution of bacterial extracts.
2. Add 800µl Tris-HCl buffer. So, the final DPPH concentration was converted to 0.05mM.
3. Vortex vigorously and incubate in dark at room temperature for 30 mins.
4. After incubation (Colour changed from purple to yellow), absorbance was taken at 517 nm by the help of a Spectrophotometer and ethanol is used as blank.
5. For reagent blank or control 200µl methanol was used instead of the sample.
6. The measurement of the radical scavenging activity was done by decreasing the absorbance of DPPH.
7. The free radical scavenging potential percentage was measured by the formula = $(1 - (\text{Abs (517 nm) of the sample} / \text{Abs (517 nm) of the control})) \times 100$.
8. For positive control ascorbic acid (dissolved in Tris-HCL buffer) at a concentration of 50µg mL⁻¹ was used.

2.36.c. Superoxide anion scavenging assay by spectrophotometric method:

Super oxide anion scavenging assay was followed according to Dhayanithy et al, 2019.

2.36.d. Extraction of antioxidants from endophytic bacterial culture filtrates:

The medium used: TSB medium or Tryptic Soy Broth - Tryptone Soya Broth (TSB):

30.0 g of TSB medium was suspended in 1000 ml distilled water and sterilized at 121°C for 15 minutes.

1. Bacterial cultures were grown in 5 ml of tryptic soya broth medium overnight at 30°C in a shaking incubator for incubation.
2. Then 0.2 OD bacterial culture was grown in 10 ml TSB (Tryptic Soya Broth) medium and incubated at 30°C for 48 hours.
3. After incubation, 10ml culture (well shaken) was taken into a 25ml centrifuge tube and centrifuged at 10000 rpm for 15 min.
4. Then the supernatant was collected into a 25ml centrifuge tube.
5. 1:1 v/v ethyl acetate and chloroform were added to the supernatant and vigorously shaken.
6. The organic solvent layer was collected in a new centrifuge tube.
7. The organic layer was concentrated with the help of a vacuum rotary evaporator (Concentrator Plus) at 40°C.
8. The extract was transferred into a 2 ml microcentrifuge tube and left to dry at room temperature.
9. The extract was to be dissolved in 2 ml of methanol.

Reagents:

i) Phosphate buffer (PB): 500ml, 100mM (pH 7.4)

a) 1M 100 ml Na₂HPO₄ solution (141.96gm/mol)

14.196 gm Na₂HPO₄ dissolved in 100ml of distilled water.

b) 1M 100ml NaH₂PO₄.2H₂O solution (156.01gm/mol)

Add 15.601 gm of NaH₂PO₄.2H₂O and it was dissolved in 100 ml of distilled water.

- c) **38.7ml of Na₂HPO₄ (1M) solution and 11.3ml of (1M) NaH₂PO₄.2H₂O solution** was taken and made a final volume of 50 ml 1M sodium phosphate buffer solution. Now the **pH was maintained at 7.4** and volume was made up to 500 ml by distilled water to prepare **500 ml 100mM sodium phosphate buffer (7.4)**.

ii) Nitroblue Tetrazolium (NBT) solution: 100ml, 150 μ M

M.W. of NBT = 817.64 gm/mol.

1M NBT = 817.64 gm in 1000ml

150 μ M NBT = 0.081764*150/1000 gm of NBT in **100ml**.

= 0.01226 gm of NBT in 100ml.

= 12.26 mg of NBT in 100ml.

So, 12.26 mg of NBT dissolved in 100 ml of 100 mM phosphate buffer (pH 7.4).

iii) NADH solution: 100ml, 468 μ M

M.W. of NADH-Na₂ = 709.40 gm/mol.

1M NADH-Na₂ = 709.40 gm in 1000ml

468 μ M NADH-Na₂ = 0.07094*468/1000 gm of NADH-Na₂ in **100ml**.

= 0.03319 gm of NADH-Na₂ in 100ml

= 33.19 mg of NADH-Na₂ in 100ml.

So, 33.19 mg of NADH-Na₂ dissolved in 100ml of 100 mM phosphate buffer (pH 7.4).

iv) Phenazine methosulphate (PMS) solution: 100ml, 60 μ M

a. 3.06 mg of PMS (306.34gm/mol) was dissolved in 1 ml of Potassium phosphate buffer (pH 7.4) to make a concentration of 10mM PMS stock solution.

b. 0.06ml (60 μ l) of 10mM PMS stock solution and 9.94ml of phosphate buffer was taken to make 10 ml 60 μ M PMS solution.

v) **Ascorbic acid:** Added 50 mg Ascorbic acid in 50 ml Phosphate buffer to make a concentration of 1mg mL⁻¹.

Procedure:

1. 1 ml of Nitroblue Tetrazolium solution added with 1 ml NADH.
2. 200 μ l methanolic solution of bacterial extracts was added to it.
3. Then the reaction was started with the addition of 100 μ l of PMS (Phenazine methosulphate solution) and incubated for 5 mins at 25 °C.
4. For **reagent blank or control** 200 μ l methanol was used instead of the sample.
5. The absorbance was measured at 560 nm against **Phosphate buffer solution as blank**.
6. Decreased absorbance indicated the increased superoxide anion scavenging activity.
7. The superoxide anion radical scavenging potential percentage was measured by the formula = (1-(Abs (560 nm) of the sample/ Abs (560 nm) of the control)) \times 100.
8. **Ascorbic acid** (dissolved in phosphate buffer) at a concentration of **1mg mL⁻¹** was used as a **Positive control**.

2.36.e. Hydroxyl radical scavenging assay by spectrophotometric method:

Hydroxyl radical scavenging assay was followed according to Singh and Raijin (2004).

2.36.f. Extraction of antioxidant from endophytic bacterial culture:

The medium used: TSB medium or Tryptic Soy Broth - Tryptone Soya Broth (TSB):

30.0 g of TSB medium was suspended in 1000 ml distilled water and sterilized at 121°C for 15 minutes.

1. Bacterial cultures were grown in 5 ml of tryptic soya broth medium overnight at 30°C in a shaking incubator for incubation.
2. Then 0.2 OD bacterial culture was grown in 10 ml TSB (Tryptic Soya Broth) medium and incubated at 30°C for 48 hours.
3. After incubation, 10ml culture (well shaken) was taken into a 25ml centrifuge tube and centrifuged at 10000 rpm for 15 min.
4. Then the supernatant was collected into a 25ml centrifuge tube.
5. 1:1 v/v ethyl acetate and chloroform were added to the supernatant and vigorously shaken.
6. The organic solvent layer was collected in a new centrifuge tube.
7. The organic layer was concentrated with the help of a vacuum rotary evaporator (Concentrator Plus) at 40°C.
8. The extract was transferred into a 2 ml microcentrifuge tube and left to dry at room temperature.
9. The extract was to be dissolved in 2 ml methanol.

Reagents:

i. Potassium phosphate buffer: 500ml, 20mM, pH 7.4

- a. 1.212 g of potassium phosphate dibasic (K_2HPO_4 , 174.18gm/mol) was dissolved in 400 ml of dH_2O .
- b. Then 414 mg of potassium phosphate monobasic (KH_2PO_4 , 136.09gm/mol) was added to the solution.
- c. pH was adjusted to 7.4 using HCl or KOH.
- d. Then the volume was made up to 500 ml by dH_2O .

ii. $FeCl_3$: 100ml, 100 μ M $FeCl_3$

- a. 16.22 mg of $FeCl_3$ (162.2gm/mol) was dissolved in 10 ml of potassium phosphate buffer to make a concentration of 10 mM $FeCl_3$ stock solution.

- b. 1ml of 10mM stock solution was taken and 99 ml of buffer was added to make 100 ml 100 μ M FeCl₃ solution.

iii. EDTA: 100ml, 100 μ M EDTA

- a. 37.22mg of EDTA.2H₂O (372.2gm/mol) in was dissolved 10 ml of potassium phosphate buffer to make a concentration of 10 mM EDTA.2H₂O stock solution.
- b. To 1ml of 10mM stock solution 99ml of buffer was added to make 100ml 100 μ M EDTA.2H₂O solution.

iv. 2-deoxyribose: 100ml, 3.75mM

- a. 134.13mg of 2-deoxyribose (134.13gm/mol) was dissolved in 100ml of potassium phosphate buffer to make a concentration of 10 mM 2-deoxyribose stock solution.
- b. To 37.5ml of 10mM stock solution, 62.5ml of buffer was added to make 100ml 3.75mM 2-deoxyribose solution.

v. H₂O₂: 100ml, 1mM

- a. Stock concentration: 30% H₂O₂ (w/w); density = 1.11 g/ml and Mt = 34.01 gm/mol
- b. Strength of H₂O₂ = $(1.11 \times 30 \times 1000) / 34.01 \times 100 = 9.79$ M
- c. To make 100ml, 1mM H₂O₂ add 0.01 ml (10 μ l) to 99.99ml of Potassium phosphate buffer was added.

vi. TCA (Trichloroacetic acid): 100ml, 2% w/v

2 g of trichloroacetic acid was dissolved in 100 ml distilled water and heated gently until complete dissolution.

vii. TBA (Thiobarbituric acid): 100ml, 1% w/v

1g of thiobarbituric acid was dissolved in 100ml of distilled water and heated gently until complete dissolution.

viii. Ascorbic acid: 100ml, 100 μ M

- a. 19.81 mg of ascorbic acid (198.11gm/mol) was dissolved in 100 ml of potassium phosphate buffer to make a concentration of 1mM ascorbic acid stock solution.
- b. To 10 ml of 1mM stock solution 90 ml of buffer was added to make 100 ml 100 μ M ascorbic acid solution.

Table 20: Reaction Mixture preparation:

20mM, pH 7.4 PB (ml)	10mM FeCl₃ (ml)	10mM EDTA (ml)	10mM 2- deoxyribose (ml)	1mM H₂O₂ (ml)	1mM Ascorbic acid (ml)	Final volume (ml)
50.49	1.0	1.0	37.50	0.01	10	100

Procedure:

1. 200µl methanolic solution of bacterial extracts was added to **1ml reaction mixture** (100µM FeCl₃, 100µM EDTA, 3.75mM 2-deoxyribose, 1mM H₂O₂ and 100µM ascorbic acid in potassium phosphate buffer 20 mM, pH 7.4).
2. The mixture was then kept at 37 °C for 60 min.
3. After incubation, 1ml of 2% Trichloroacetic acid (TCA) and 1mL of 1% Thiobarbituric acid (TBA) were added, then were again incubated for 15 mins in a boiling water bath.
4. For reagent blank or control 200µl methanol was used instead of the sample.
5. After cooling, absorbance was measured at 535 nm with **phosphate buffer as blank**.
6. Decreased absorbance of the reaction mixture indicated decreased oxidation of deoxyribose.
7. The hydroxyl radical scavenging potential percentage was measured by the formula = $(1 - (\text{Abs (535 nm) of the sample} / \text{Abs (535 nm) of the control})) \times 100$.

2.36.g. Nitric oxide scavenging assay by spectrophotometric method:

Nitric oxide scavenging assay was followed by Gupta et al, 2017.

2.36.h. Extraction of antioxidants from endophytic bacterial culture:

The medium used: TSB medium or Tryptic Soy Broth - Tryptone Soya Broth (TSB):

30.0 g of TSB medium was suspended in 1000 ml distilled water and sterilized at 121°C for 15 minutes.

1. Bacterial cultures were grown in 5 ml of tryptic soya broth medium overnight at 30°C in a shaking incubator for incubation.

2. Then 0.2 OD bacterial culture was grown in 10 ml TSB (Tryptic Soya Broth) medium and incubated at 30°C for 48 hours.
3. After incubation, 10ml culture (well shaken) was taken into a 25ml centrifuge tube and centrifuged at 10000 rpm for 15 min.
4. Then the supernatant was collected into a 25ml centrifuge tube.
5. 1:1 v/v ethyl acetate and chloroform were added to the supernatant and vigorously shaken.
6. The organic solvent layer was collected in a new centrifuge tube.
7. The organic layer was concentrated with the help of a vacuum rotary evaporator (Concentrator Plus) at 40°C.
8. The extract was transferred into a 2 ml microcentrifuge tube and left to dry at room temperature.
9. The extract was to be dissolved in 2 ml methanol.

Reagents:

i. Phosphate-buffer saline (PBS): 500ml, pH 7.4

4 g of NaCl (137mM), 0.1g of KCl (2.7mM), 0.72g of Na₂HPO₄ (10mM) and 0.12 g of KH₂PO₄ (1.8mM) was dissolved in 400 ml of distilled water. The pH was maintained at 7.4 with HCl. Added dH₂O to make the volume upto 500 ml. Autoclaved for 20 minutes at 15psi and stored at room temperature.

ii. Sodium nitroprusside: 100ml, 10 mM

M.W. of Sodium nitroprusside = 297.95 gm/mol.

1M Sodium nitroprusside = 297.95 gm of Sodium nitroprusside in 1000ml.

10 mM Sodium nitroprusside = $29.795 \times 10 / 1000$ gm of Sodium nitroprusside in 100ml.
= 0.29795 gm of Sodium nitroprusside in 100ml.

So, 0.298 gm of Sodium nitroprusside was dissolved in 100ml of phosphate buffered saline.

ii) Greiss reagent: Greiss reagent (1% sulphanilamide, 2% H₃PO₄, and 0.1% naphthyl ethylene diamine dihydrochloride).

iii) Ascorbic acid: Added 5 mg Ascorbic acid in 100 ml Phosphate-buffered saline to make a concentration of 50µg mL⁻¹.

Procedure:

1. 200µl of methanolic solution of bacterial extracts was added to 300µl of Phosphate-buffer saline.
2. Then added 500µl (10Mm) Sodium nitroprusside to get a final concentration of 5mM.

3. This reaction mixture was then kept for 120 mins at 25°C.
4. For reagent blank or control 200µl methanol was used instead of the sample.
5. After the incubation period, 500µL of Greiss reagent was added to 500µl of the reaction mixture.
6. Then the absorbance was measured at 546 nm with **PBS as blank**.
7. The percentage of nitric oxide scavenging potential was measured by the formula = $(1 - (\text{Abs (546 nm) of the sample} / \text{Abs (546 nm) of the control})) \times 100$.
8. For Positive control, **Ascorbic acid** (dissolved in phosphate-buffered saline) at a concentration of **50µg mL⁻¹** was used.

2.37. Next Generation Sequencing method to measure the bacterial community abundance:

Soil samples were collected in composite method from the rice field before the addition of culture and then was dried and mixed well. After the cultivation also, soil samples were collected in composite manner and then dried and mixed well. Then DNA was isolated by commercially available soil DNA extraction kit.

Detailed steps were as follows:

1. Composite soil samples were collected at 0-15 cm depth of different applied bacterial combinations and control sets from experimental field and then dried and mixed well.
2. Metagenomic DNA was isolated from these samples by the help of commercially available kits (Nucleospin soil). The isolated metagenomic DNA samples were quantified using Nanodrop.
3. Amplicon libraries were made by the help of Nextera XT Index kit as followed by the 16S Metagenomic sequencing library preparation protocol.
4. Primers for V3-V4 region were designed and amplification of V3-V4 was done. The QC passed amplicons with the Illumina adapter were amplified using i5 and i7 primers as followed by the standard Illumina protocol.
5. Quality and quantity check of the library was performed on the Agilent 4200 tape station.
6. Libraries were loaded on MiSeq at eligible concentrations for cluster generation and sequencing. Paired-end sequencing on MiSeq was performed and 2x 300 bp length of near about 1 lakh reads per sample were generated.

7. Dada2 pipeline was used for generating relative abundance and taxonomy assignment from paired-end Fastq format file.
8. Raw reads were first filtered and trimmed looking at plot quality profile. Generally, the first 20 bases were cut off and truncated at a tail portion where the mean quality of reads dropped (270 for forward and 220 for reverse). The Dada2 pipeline did not allow ambiguous bases, so maxN was kept at 0. Maximum expected error allowed 2.
9. Then error rates, dereplication, and sample inference steps were performed.
10. Now merging of forward and reverse reads was done if the minimum overlap was 12.
11. Then after the chimera removal step the taxonomy assignment was done with the Silva reference database at minimum bootstrap value 80.
12. One sequence table is also generated with unique ASV (Amplicon Sequence Variant) and their counts for relative abundance calculation.
<https://benjjneb.github.io/dada2/tutorial.html>

2.38. Precautions:

Roots and pneumatophore samples of mangroves were handled after wearing sterile plastic gloves or rubber gloves. Soil samples were handled after wearing sterile plastic gloves or rubber gloves. PGPR activity by endophytes from roots and pneumatophores were performed immediately, as early as possible. All types of analyses were made under sterile conditions. When working with bacteria, wearing gloves and mask was essential. Petri-plates containing cultures (sub culture was done before 1 month) were essential to be disposed properly. All the bacterial cultures were discarded only after autoclaving.

2.39. Instruments and chemicals used:

☐ Centrifuge

Model no. Remi, C24 Plus, rotor no. (R243M, R244M and R248M).

☐ Conductivity meter

Model no. Digital Conductivity Meter Chemiline CL 250, Labline Technology Pvt. Ltd, Ahmedabad, India.

☐ pH meter

Model no. μ C pH System 361, Systronics, Ahmedabad, India.

☐ Spectrophotometer

Model no. Bio-Rad, Smart Spec Plus Spectrophotometer, California, USA.

☐ PCR

Model no. Applied Biosystems, 2720 Thermal Cycler.

☐ Gel documentation instruments

Bio-Rad Gel Doc TM XR+ and GE Image Quant™ LAS 500 with compatible softwares.

☐ Microscope Dewinter Classic 1624424 from Dewinter India, Camera- DGI 510 CCD and Software -Digicam Dewinter India.

☐ Microscope Dewinter Technologies 1062 from Dewinter Italy.

☐ Stereo microscope

Dewinter Technologies, DEW/691

☐ Chemicals were purchased from Merck, Hi-media, Sigma, Fisher Scientific etc.

☐ Hanna Salinity tester.

☐ Vacuum concentrator Concentrator Plus from Eppendorf.

III. Results and Discussion

Objective 1

3. Study of morphological/histological niches, anatomical adaptations, Na⁺/K⁺ ratio in endospheres of roots and pneumatophores of mangrove species from degraded and non-degraded habitats of Sundarban mangrove ecosystem.

3.1. Morphological adaptations of roots/pneumatophores of mangrove species

The mangrove species from both degraded and non-degraded habitats of Indian Sundarbans are found to have extensive root and pneumatophore (aerial negatively geotropic roots) biomass in comparison to their above ground biomass. Following are some of the representatives of the appearance of roots and pneumatophores of mangrove species, from both degraded and non-degraded mangrove niche and both the habitats are inhabited by identical root morphology. Aerial root parts are basically meant for gaseous exchange to maintain oxygen balance in the inside root cell environments amid tidal flooding conditions of mangrove niche. The submerged root parts inside hypersaline anoxic/hypoxic tidal water/sediment maintain specific adaptive/acclimative anatomical and eco-physiological traits to exhibit exclusion/ultrafiltration/excretion phenomena to avoid entry/accumulation of saline salt species in the *in vivo* cell-environments of mangrove species. In addition to mangrove species, leguminous mangrove associates are also integral component of mangrove flora. These mangrove legumes are found to bear underground root nodules, validating their contribution through nitrogen fixation in mangrove sediments.



Figure 3.1: Different mangroves roots and pneumatophores. (a) *Avicennia* spp. pneumatophores. (b) *Ceriops decandra* aerial roots and pneumatophores. (c) Knee roots of *Ceriops tagal*. (d) *Bruguiera gymnorrhiza* roots and pneumatophores.



Figure 3.2: Different mangroves roots and pneumatophores. (e) *Excoecaria agallocha* aerial roots and pneumatophores. (f) *Heritiera fomes* buttress roots and pneumatophores. (g) *Xylocarpus* spp. pneumatophores. (h) Extensive stilt roots of *Rhizophora* sp.

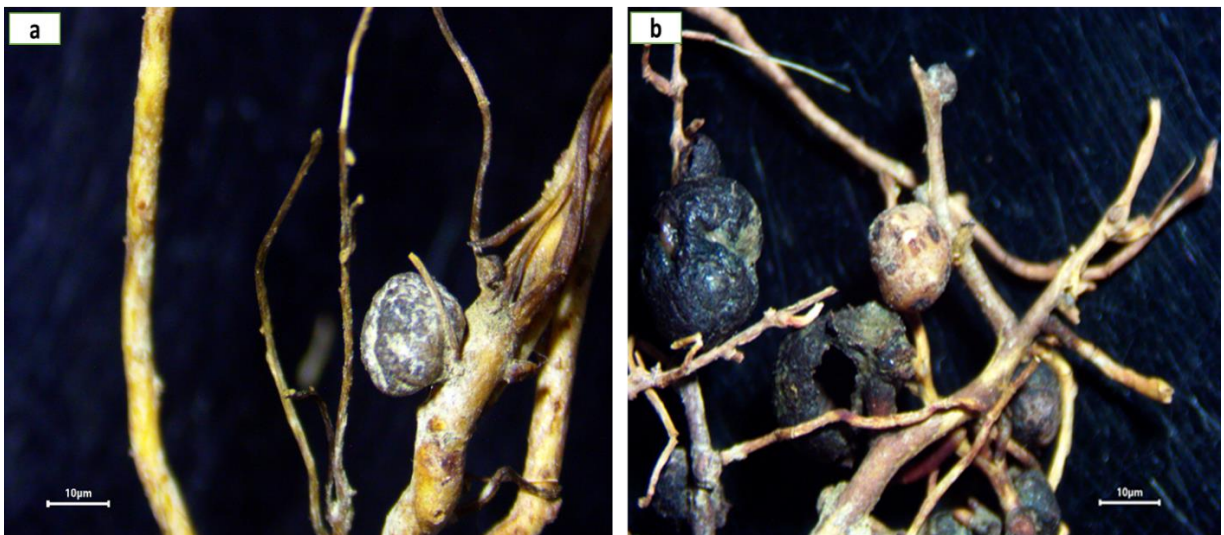


Figure 3.3: Leguminous mangrove associate species (a) Below ground root with root nodules of *Dalbergia spinosa*, (b) Below ground root with root nodules of *Derris trifoliata*.

3.2. Histological adaptations of roots/pneumatophores of mangrove species:

The major anatomical adaptations observed in histological transverse sections of roots and pneumatophores. The following figures represent the anatomical adaptations:

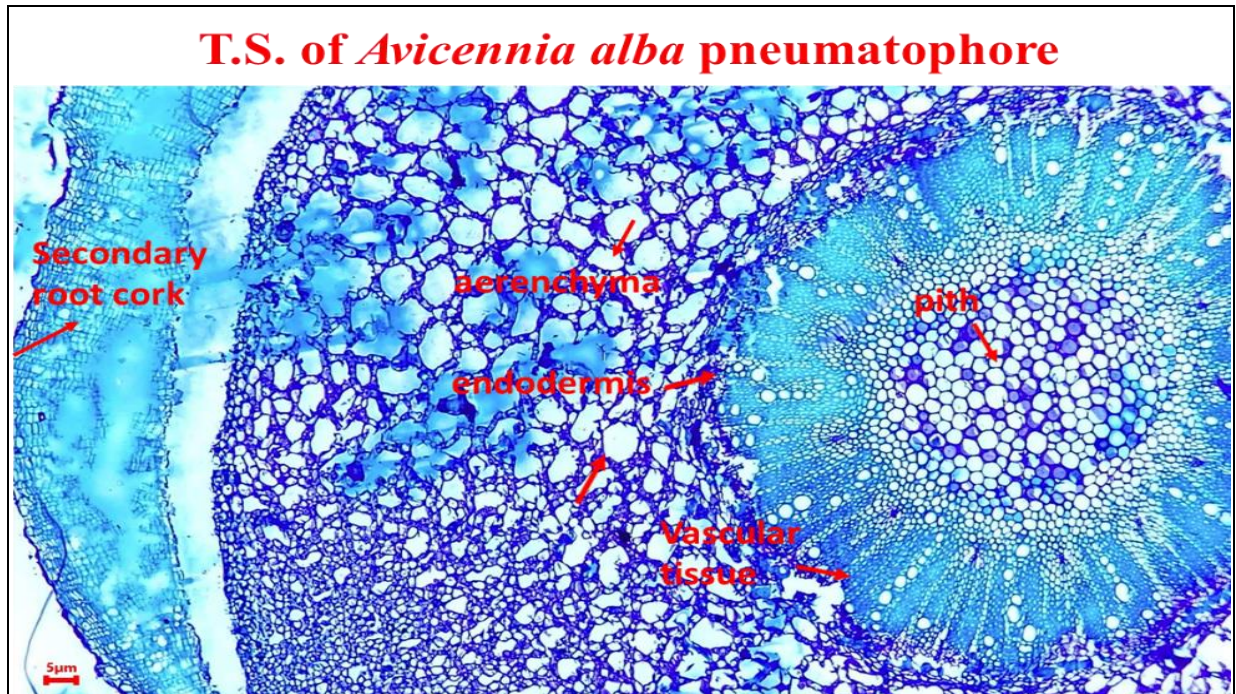


Figure 3.4: Transverse section of *Avicennia alba* pneumatophore.

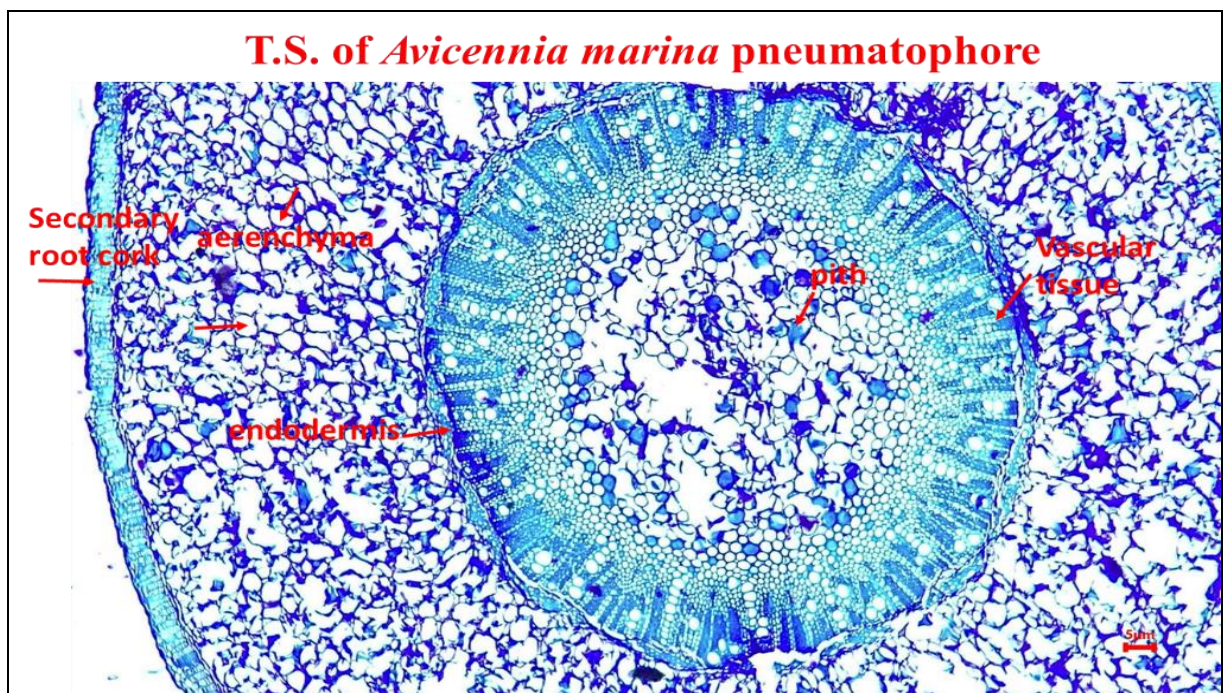


Figure 3.5: Transverse section of *Avicennia marina* pneumatophore.

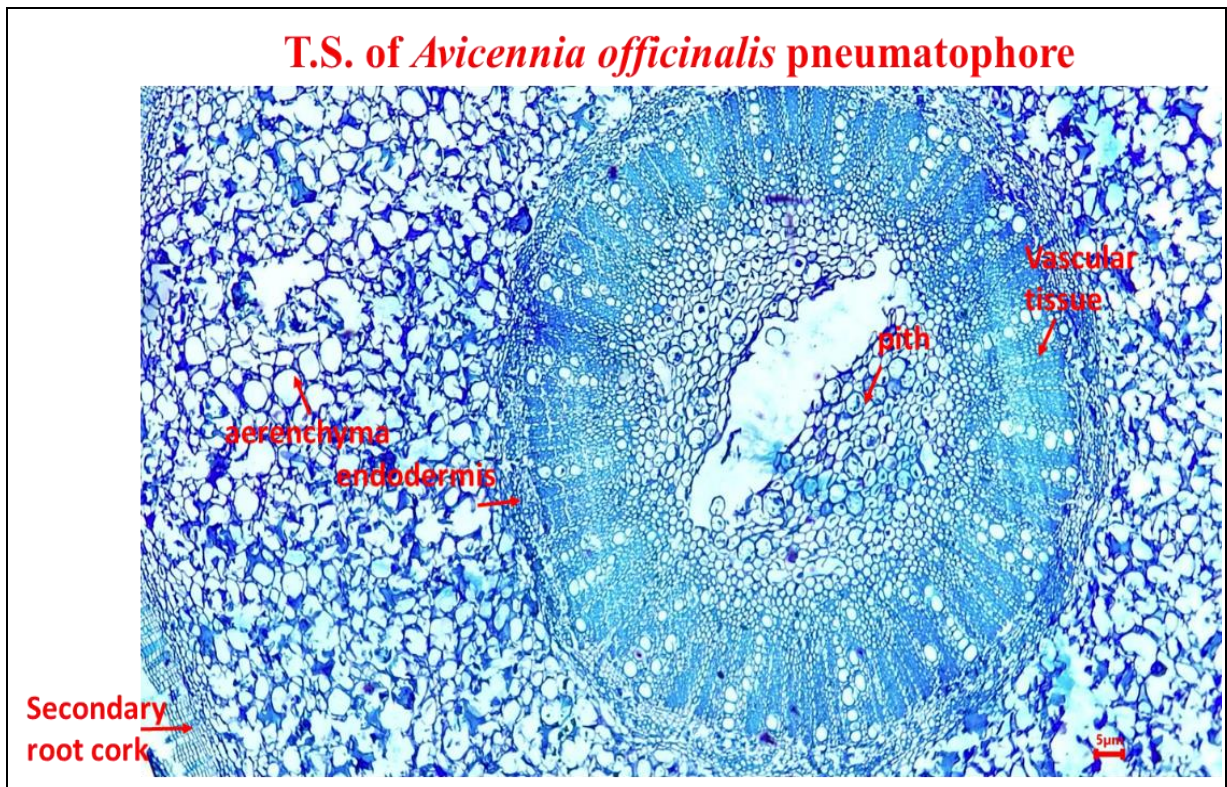


Figure 3.6: Transverse section of *Avicennia officinalis* pneumatophore.

Observations:

All three pneumatophore sections of *Avicennia* spp. distinctively showed the following common features:

1. Presence of secondary tissues like cork (phellogen), lenticels, and aerenchymatous cortex with a few sclereids to provide entry of air and mechanical support to stay upright under tidal pressure.
2. Distinct endodermis for ultrafiltration.
3. Endarch and mesarch xylem like aerial shoot parts, unlike below-ground roots.
4. Reduced pith area.

These features are very characteristic of mangrove species aerial roots like pneumatophores (Tomlinson, 2016).

T.S. of *Avicennia marina* root

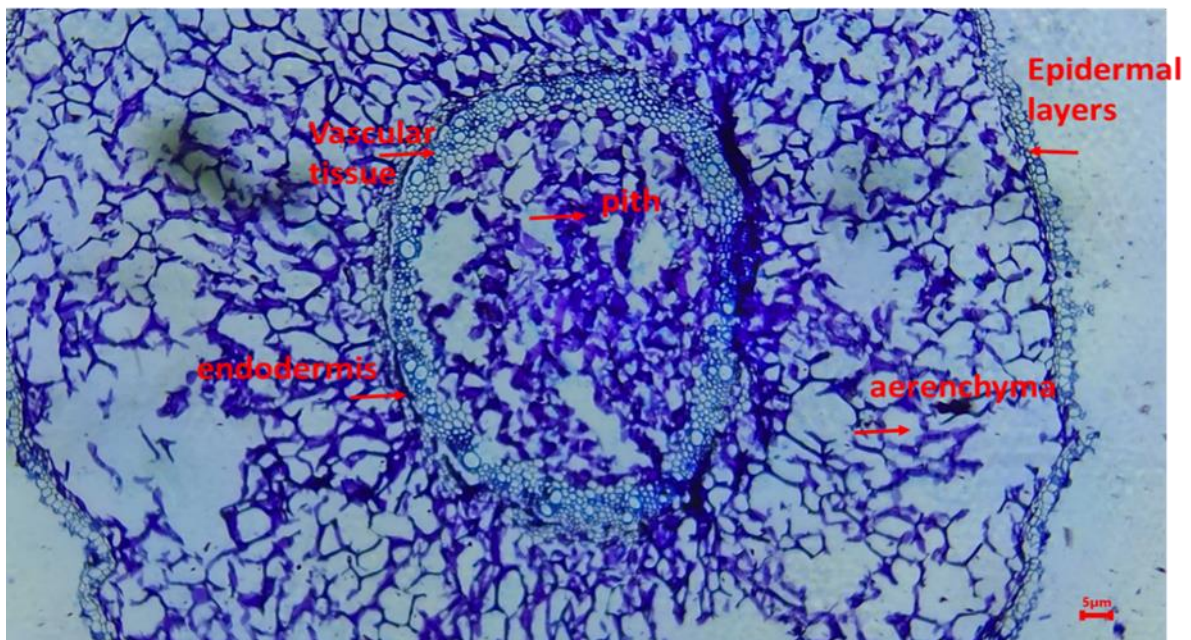


Figure 3.7: Transverse section of *Avicennia marina* root.

T.S. of *Avicennia officinalis* root

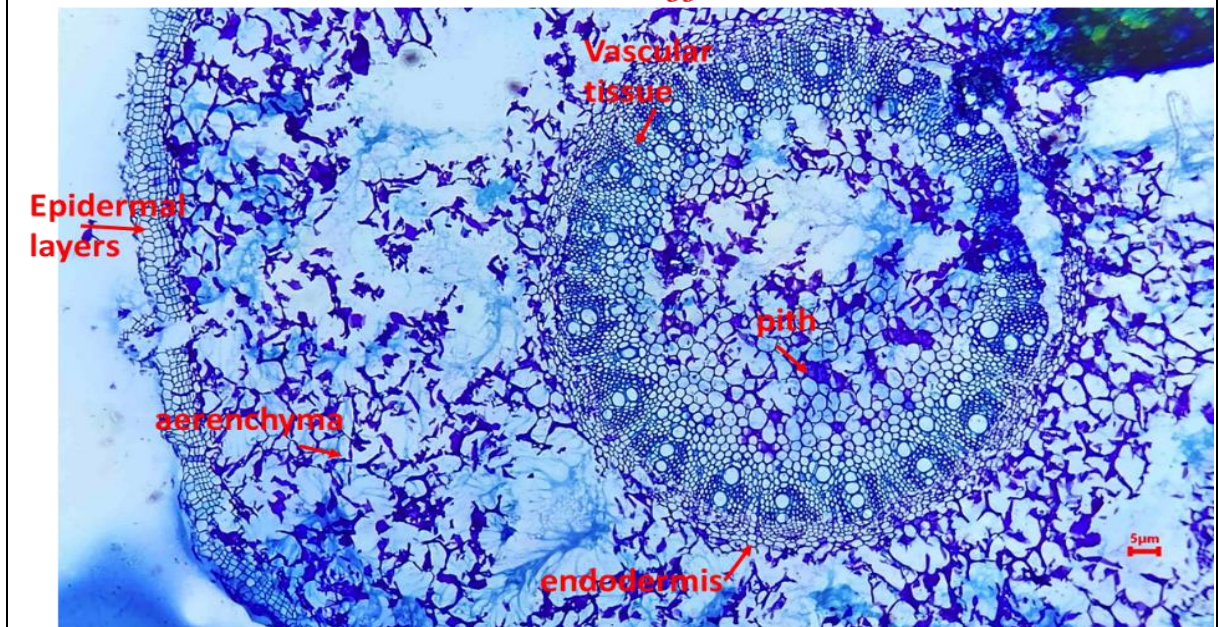


Figure 3.8: Transverse section of *Avicennia officinalis* root.

Observations:

The above sections of roots of *Avicennia* spp. showed some distinct differences in anatomy after entering into the substratum (Tomlinson, 2016). These are as follows:

1. The same roots develop the exarch protoxylem vasculature, reduced cortex, little-developed phellogen, and limited secondary thickening.
2. Pith and cortex both now have airy spongy tissue like aerenchyma – an interesting oxygen reservoir of mangrove roots under anaerobic submerged conditions.

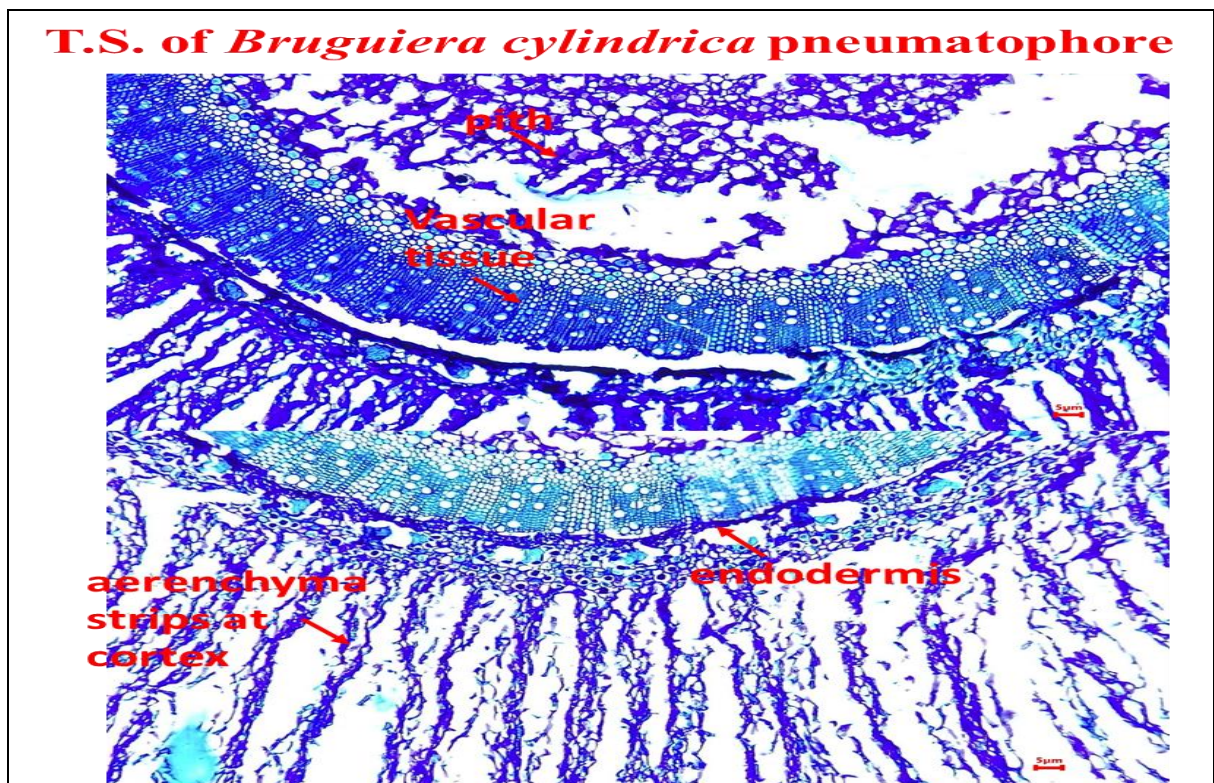


Figure 3.9: Transverse section of *Bruguiera cylindrica* pneumatophore.

Observations:

Bruguiera cylindrica pneumatophore section shows the following typical features:

1. Highly aerenchymatous cortex, with strip-like aerenchyma.
2. Distinct endodermis.
3. Reduced vasculature with mesarch xylem.

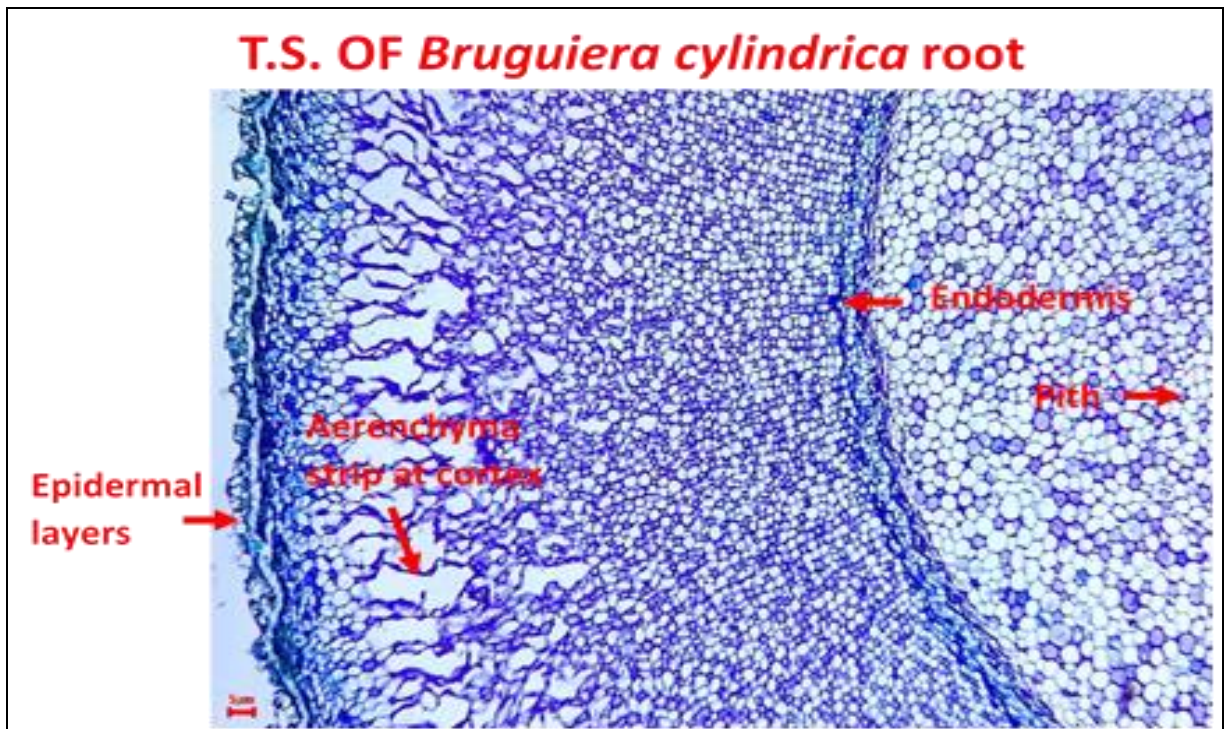


Figure 3.10: Transverse section of *Bruguiera cylindrica* root.

Observations:

The same *Bruguiera cylindrica* at below-ground root level shows the following characteristics:

1. Well-developed cortex with aerenchymatous strips just below the hypodermis.
2. Distinct endodermis.
3. Well-developed pith.

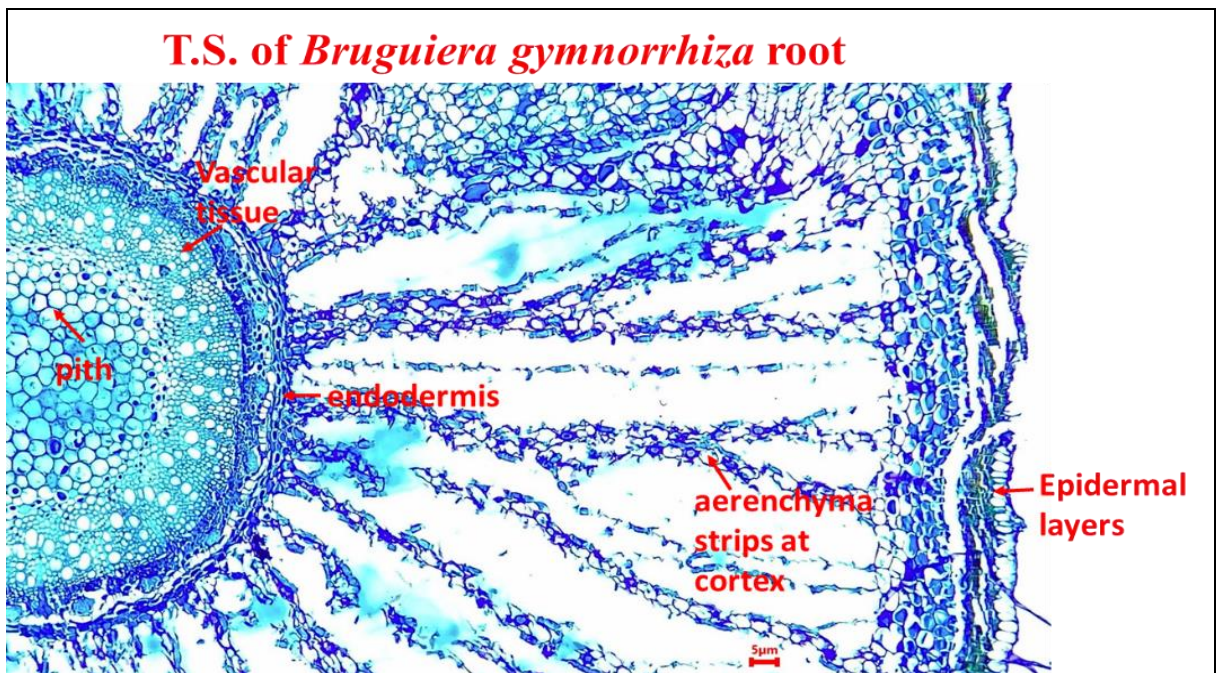


Figure 3.11: Transverse section of *Bruguiera gymnorrhiza* root.

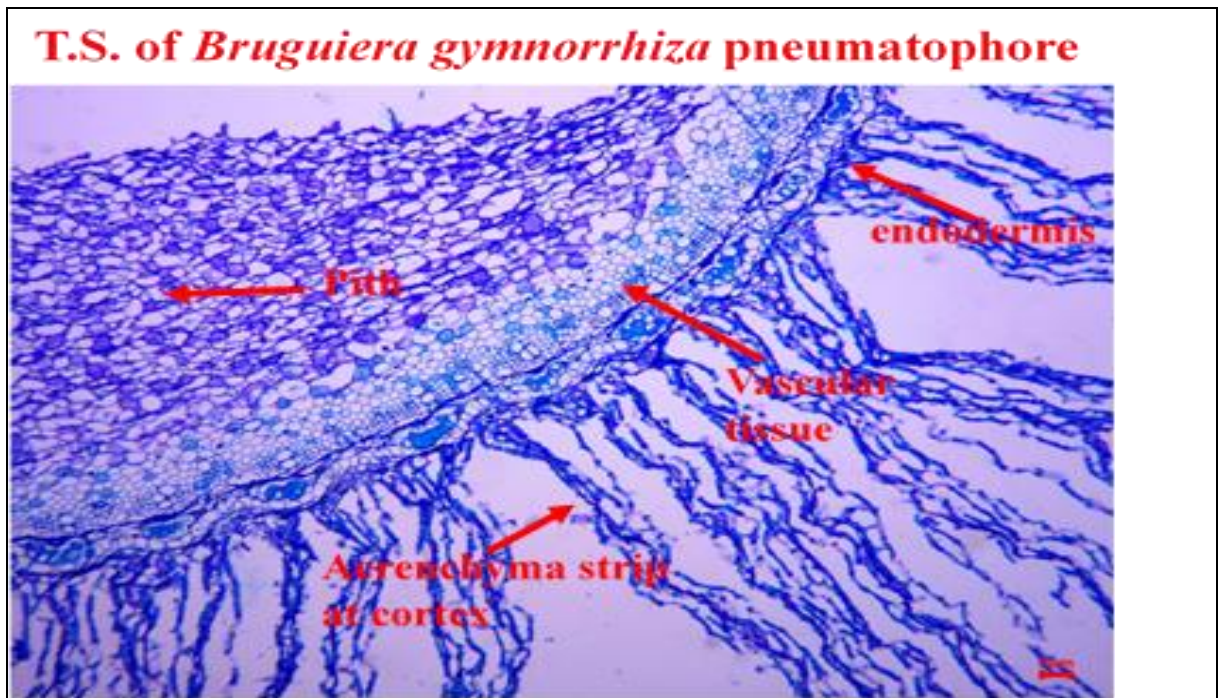


Figure 3.12: Transverse section of *Bruguiera gymnorrhiza* pneumatophore.

Observations:

The root and pneumatophore sections of *Bruguiera gymnorrhiza* both have some common traits described as follows:

1. Both root and pneumatophores have distinct well-developed aerenchymatous cortex having strips of aerenchyma.
2. Distinct endodermis.
3. Less-developed vascular tissue.

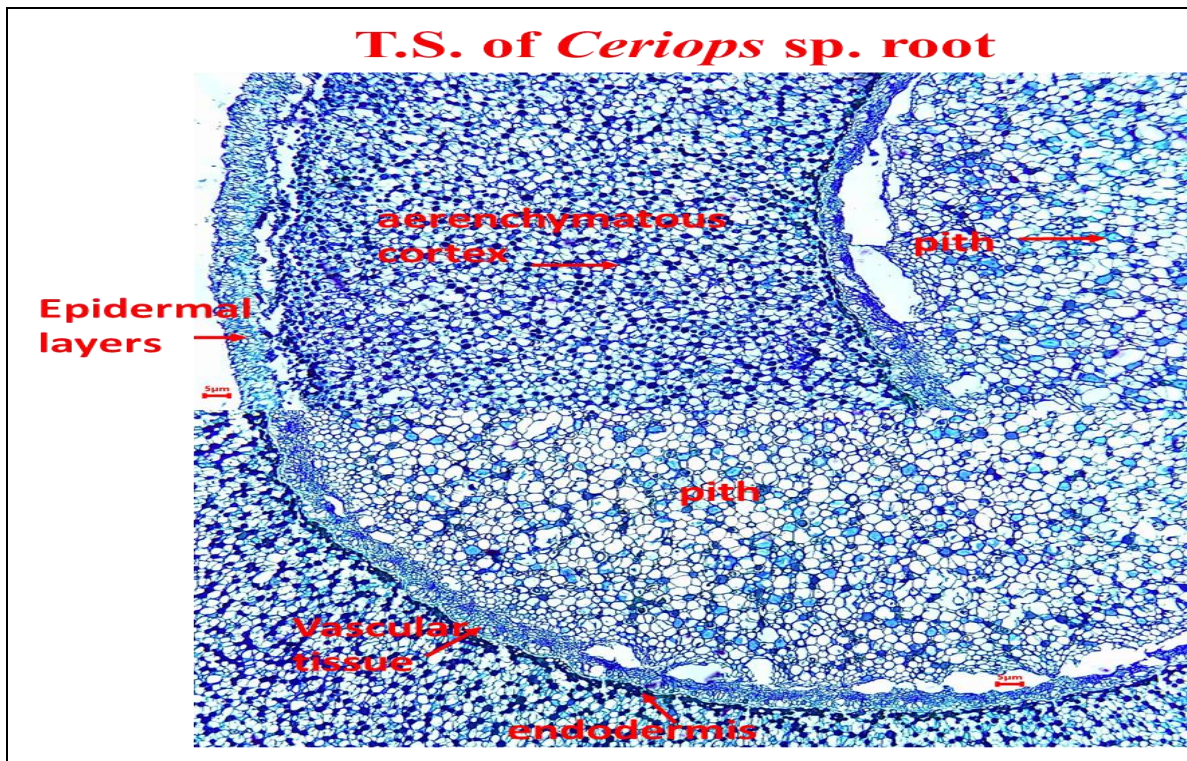


Figure 3.13: Transverse section of *Ceriops* sp. root.

Observations:

The *Ceriops* sp. root section shows extremely poor developed vascular tissue, distinct endodermis, and secondary cork at epidermal layers, as well as well-developed aerenchymatous cortex, all indicating that mangrove roots fight for oxygen underwater and therefore try to maintain well-developed aerenchyma to store air to meet oxygen deficit under water-logged conditions. Roots act as more of an oxygen reservoir and site of ultrafiltration rather than utilizing the vascular architecture for water uptake and transport.

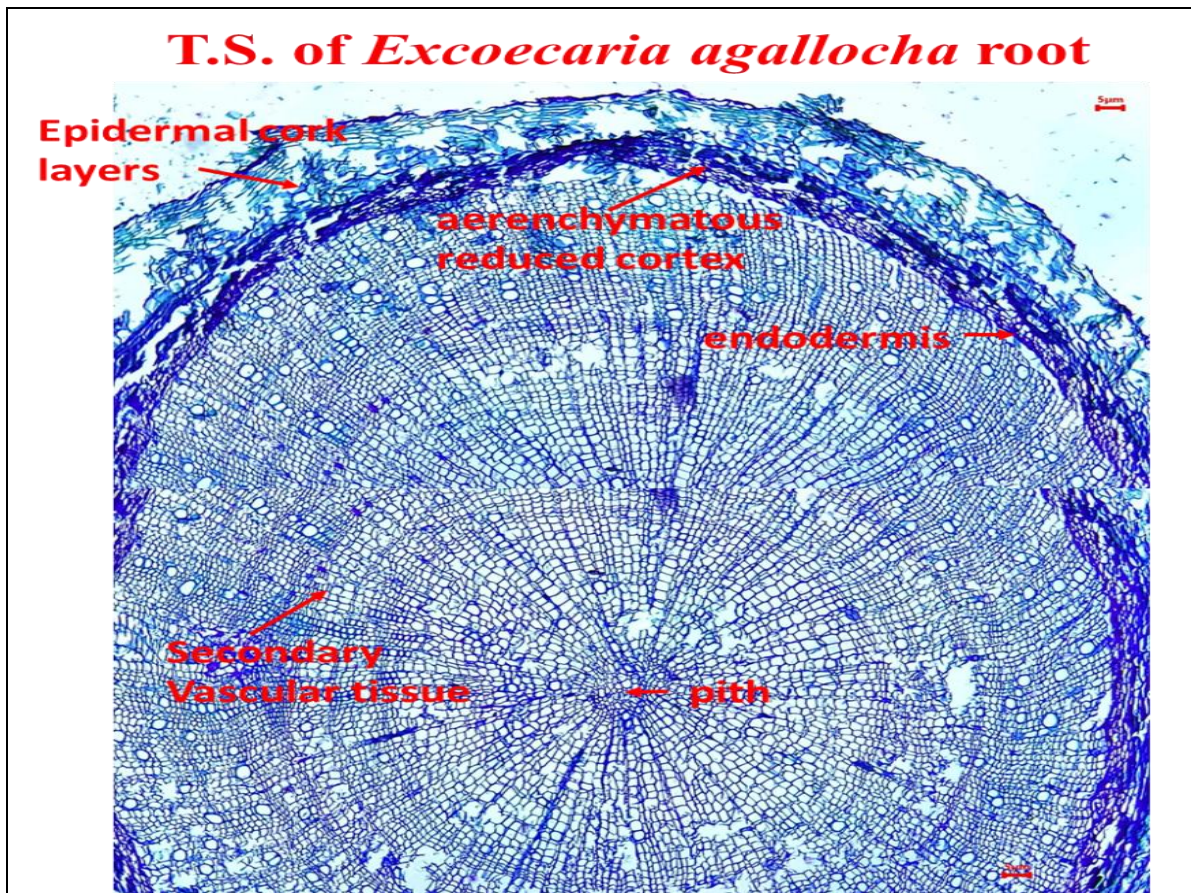


Figure 3.14: Transverse section of *Excoecaria agallocha* root.

Observations:

In contrast *Excoecaria agallocha* root section shows a very different anatomy. *Excoecaria agallocha*, known to be a back mangrove, does not always inhabit lower intertidal regions and hence does not face frequent tidal inundation. Therefore some distinct differences were observed in root anatomy for this species. These are:

1. Aerenchymatous cortex is much reduced.
2. Secondary vasculature is pronounced.
3. Cork tissues are present at the epidermis with lenticels.
4. Pith tissue is almost obliterated.

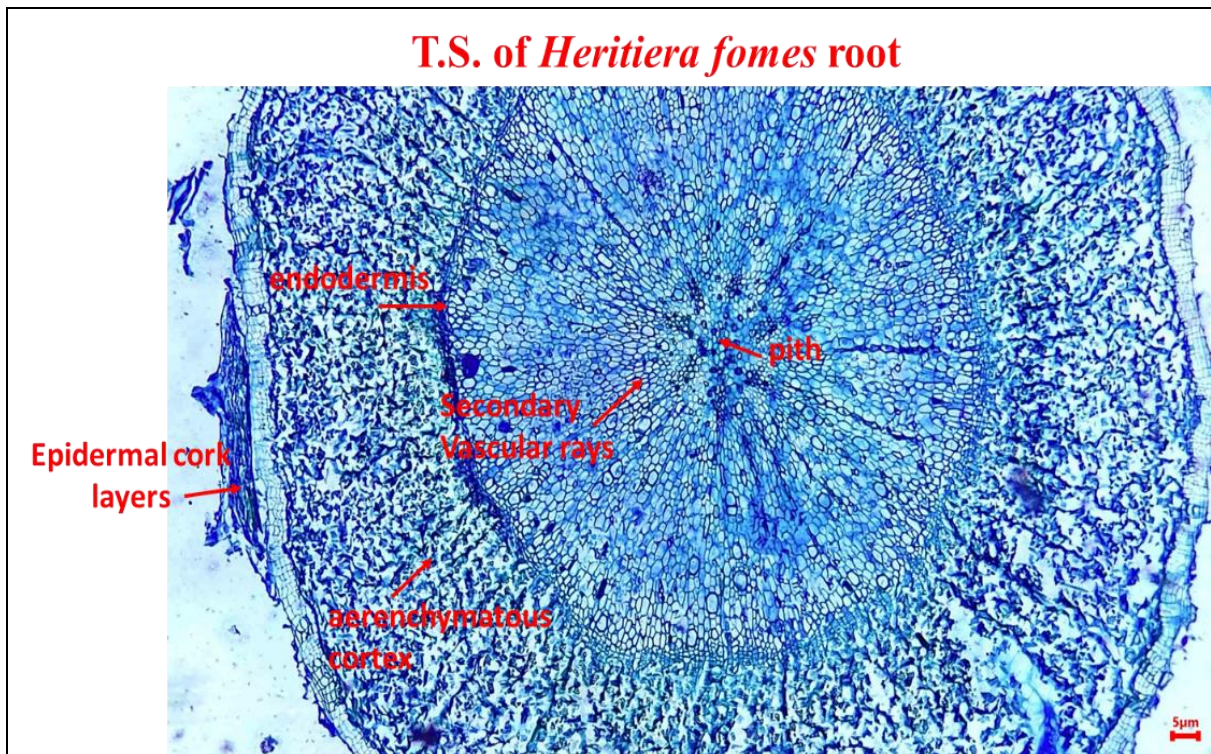


Figure 3.15: Transverse section of *Heritiera fomes* root.

Observations:

The *Heritiera fomes* root section has some similarities with *Excoecaria* root section. Like *Excoecaria*, *Heritiera fomes* also is a fresh-water-loving mangrove and inhabits the higher intertidal regions, thus does not face regular inundation. This difference from lower intertidal inhabiting mangrove species is strongly reflected in its anatomical features:

1. Epidermis with cork and lenticel.
2. Well-developed cortex with aerenchyma.
3. Distinct endodermis.
4. Well-developed extensive vasculature with reduced pith.

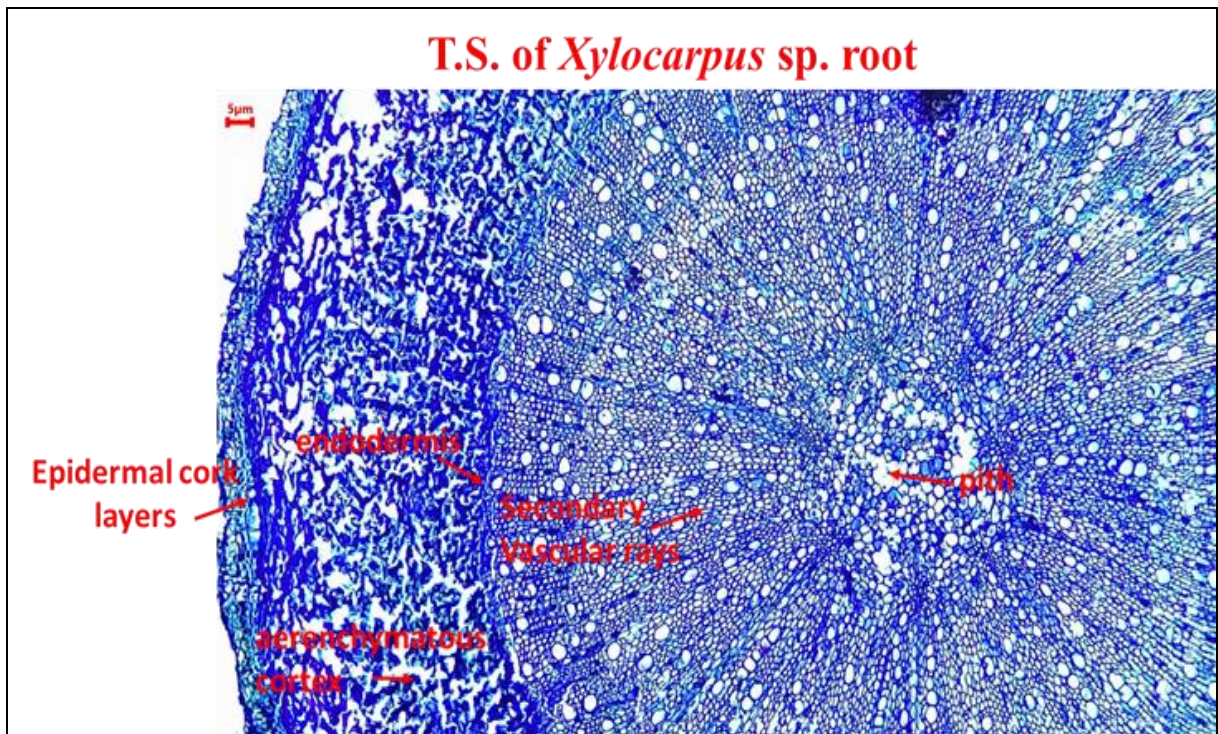


Figure 3.16: Transverse section of *Xylocarpus* sp. root.

Observations:

The *Xylocarpus* sp. root sections show the following distinctive traits:

1. Epidermal cork with lenticels.
2. Aerenchymatous cortex.
3. Distinct endodermis.
4. Well-developed extensive vascular tissue with much reduced parenchymatous pith.

This root anatomy with elaborate vascular tissue diagnostically signifies its role in water absorption and transport in a lower-mid intertidal zone inhabiting mangrove tree species like *Xylocarpus* sp.

T.S. of *Myriostachya wightiana* root

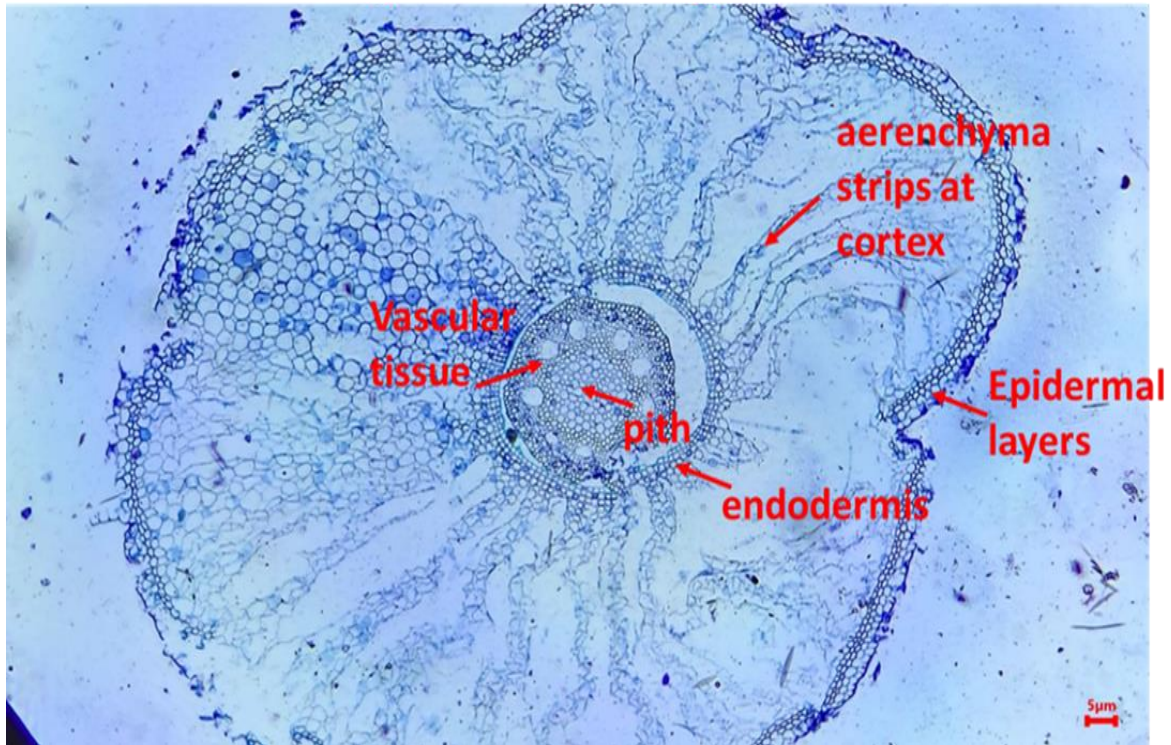


Figure 3.17: Transverse section of *Myriostachya wightiana* root.

Observations:

Myriostachya wightiana is a lower-mid intertidal mangrove grass species. The characteristic features of its root section are as follows:

1. Extensive aerenchymatous cortex with aerenchyma strips.
2. Distinct endodermis.
3. Reduced vascular tissue.
4. Reduced pith.
5. Complete absence of secondary tissues.

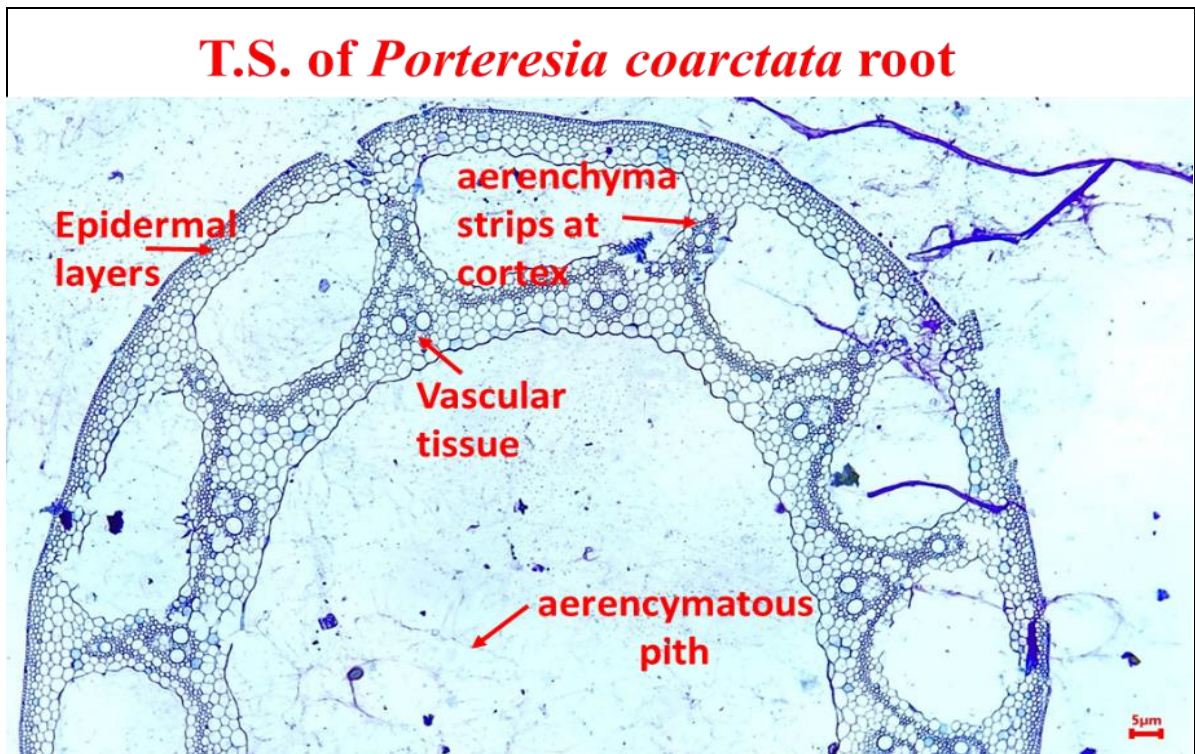


Figure 3.18: Transverse section of *Porteresia cortata* root.

Observations:

Porteresia coarctata, another lower intertidal mangrove grass shows typical root anatomical features helping the species to sustain under complete submergence for the larger period of the day. These observed traits are:

1. Elaborately air chambered aerenchymatous cortex and pith, symbolizing as a reservoir of air, a distinct contrivance to sustain underwater.
2. Poorly developed vascular tissue.
3. Absence of any secondary growth.

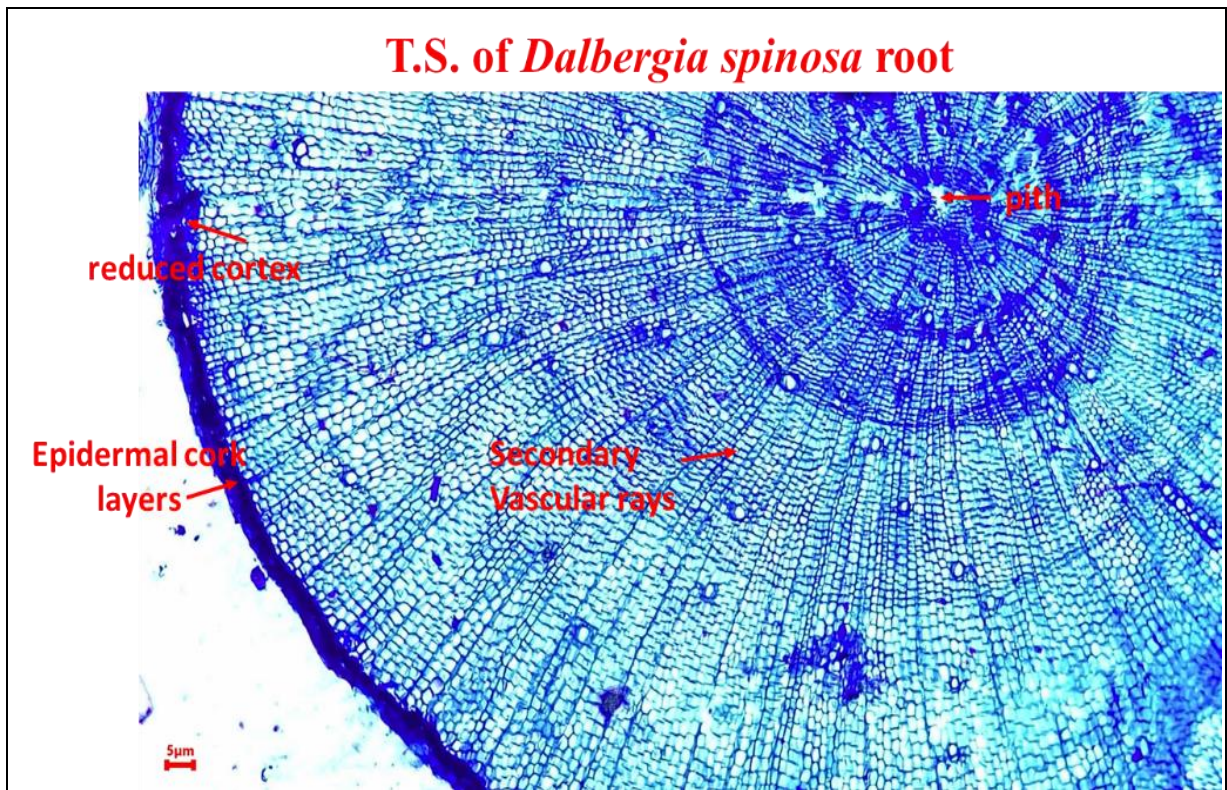


Figure 3.19: Transverse section of *Dalbergia spinosa* root.

Observations:

Dalbergia spinosa, a nodule-forming mangrove associate legume shows very interesting root anatomy. The features are as follows:

1. Extremely elaborate vascular rays with secondary cortical tissue.
2. Reduced pith.
3. Epidermal cork tissue with lenticels.

Dalbergia spinosa, being a shrub species, elaborate vasculature in root indicates its necessity for water uptake and transport.

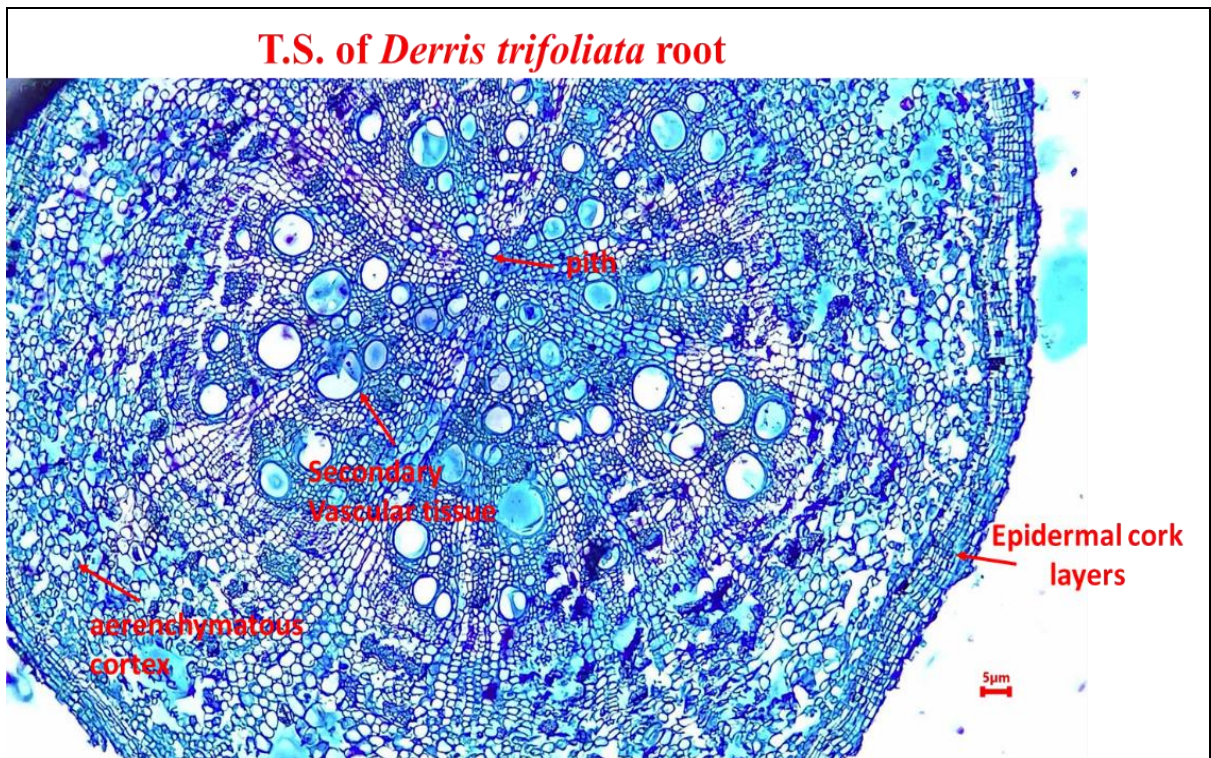


Figure 3.20: Transverse section of *Derris trifoliata* root.

Observations:

Derris trifoliata, another mangrove associate nodule-forming legume, shows its distinctive features in root anatomy. The plant being a climber, shows presence of well-developed endarch secondary xylem like stem. Cortex is aerenchymatous and epidermal cork layer with lenticels are observed. Pith is almost absent.

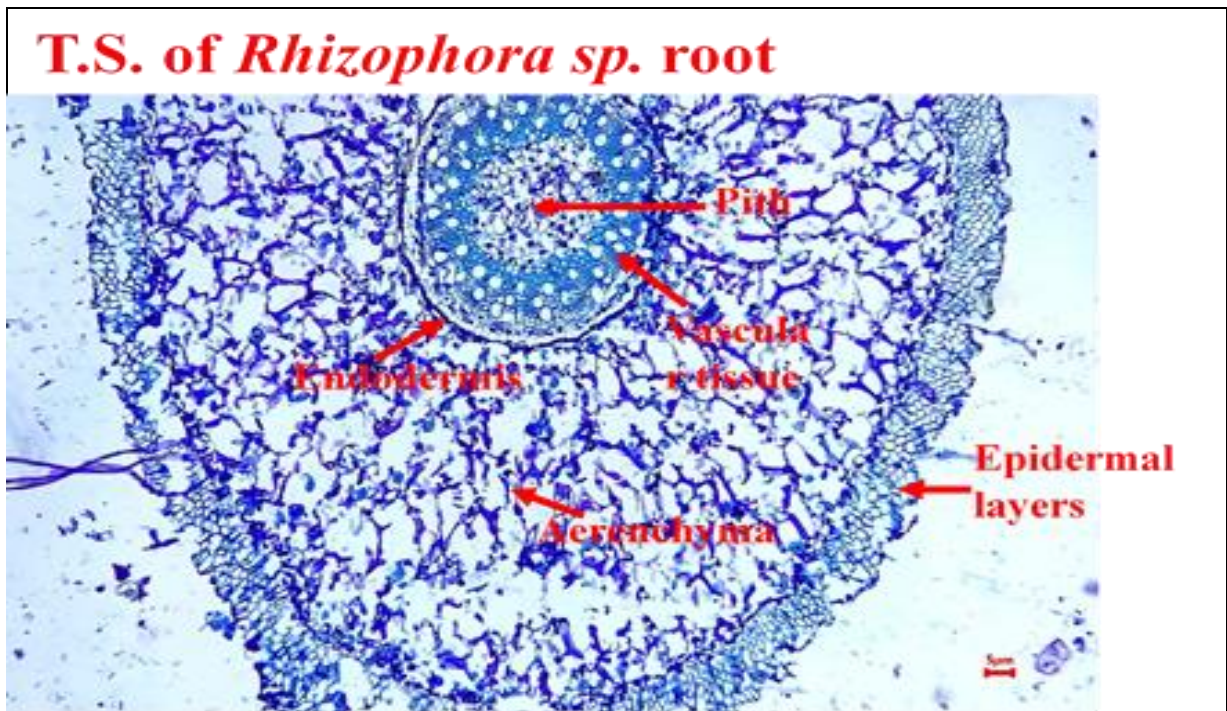


Figure 3.21: Transverse section of *Rhizophora* sp. aerial stilt root.

Observations:

Rhizophora sp. root section shows distinctively aerenchymatous cortex, distinct endodermis, large xylem cavities, scanty pith, and secondary cork tissue with lenticels as epidermal layers. These roots give mechanical support to the plant and face frequent inundation. Hence, the elaborate aerenchymatous cortex is needed for their survival under submergence.

All the observed root sections showed the following common features very characteristic of mangrove plants. These are:

1. Complete absence of root hairs.
2. Elaborate aerenchymatous tissues.
3. Cork epidermal layer with lenticels.
4. Distinct epidermis.

The function and adaptation capability of mangrove roots in waterlogged conditions to gain nutrients and interact with rhizospheric microbes is only partly realized.

Mangroves, with their exposed breathing roots, vast buttresses and support roots, salt-emitting leaves, and viviparous water-dispersed propagules, are extremely suited to the coastal environment. The pneumatophores of *Sonneratia*, *Avicennia*, and *Lumnitzera* spp., the stilt roots of *Rhizophora* spp., the root knees of *Ceriops*, *Bruguiera*, and *Xylocarpus* spp., and the buttress roots of *Heritiera* and *Xylocarpus* spp. are arguably the most amazing adaptations

found in mangroves. Many mangroves have roots that only reach a shallow depth in the anaerobic substrate. Like *Rhizophora*, roots can only generally penetrate soft substrates to a depth of around 1 m. Their roots become thinner and further develop into "capillary rootlets," having a narrow cortex and a basic diarch stele. The trees develop a large number of lateral roots to provide support. The large mangrove trees, located in Ecuador, which achieved heights of over 60 meters and possibly are 100 years old, their extensive root system serve as good examples of their amazingly unique potential (Emilio, 1997; Ong et al, 2004; Tomlinson, 2016). Mangroves do not have root hairs, just like aquatic plants. In stead, the endodermis functions as a useful absorbent layer.

Avicennia spp. have upward-directed pneumatophores that are endowed with lenticel, which allows oxygen to passively permeate through them. Lenticels can be closed, partially or fully opened based on the surrounding circumstances (Tomlinson, 1986; Ish-Shalom-Gordon and Dubinsky, 1993).

The root systems of mangroves show decreased cortex to reduce the separation between epidermis and stele. Saline marsh plants and mangroves when contrasted with mesophytes, the casparian strip is significantly found in these plants in more extensive form. Epidermis and exodermis (hypodermis with secondary thickening) provide mechanical support for the spiral flow of water and solutes from the cortex to the stele under the flowing situation.

The gases in mangrove roots have been analyzed by a few specialists. These roots circulate the air inside the mangrove tissue. While the external substratum possesses zero oxygen, the inner roots contain typically 16–18 % oxygen (Vinoth et al, 2019). Aerial root parts are basically meant for gaseous exchange to maintain oxygen balance inside root cell environments amid tidal flooding conditions of mangrove niche.

The submerged root parts inside hypersaline anoxic/hypoxic tidal water/sediment maintain specific adaptive/acclimative anatomical and eco-physiological traits to exhibit exclusion/ultrafiltration/excretion phenomena to avoid entry/accumulation of saline salt species in the *in vivo* cell-environments of mangrove species.

Among the major anatomical adaptations observed in histological transverse sections of roots and pneumatophores, distinctive traits are arranged in order from outermost surface to centre of the section as follows:

1. Secondary cork tissues allowing entry of air through lenticels
2. Aerenchymatous cortex, aerenchyma either in reticular/nested form or as parallel vertical strips, sometimes with large air cavities
3. Distinct endodermis

4. Well-developed vascular xylem and phloem with parenchyma rays in between, often extensive well developed secondary vascular tissues with very reduced cortex in some cases
5. Central pith tissues with parenchymatous cells, extremely reduced in some cases, in some pith is replaced by a central air cavity like in roots of *Porteresia coarctata*.

All the above anatomical adaptations establish that the roots and pneumatophores are well adapted for water-logged/flooded anoxic/hypoxic condition with ample in-built air-spaces with well-developed vascular tissues for transport.

3.3 Na⁺/K⁺ ratio estimation in endospheric environments of roots, leaves and shoots of different mangrove species:

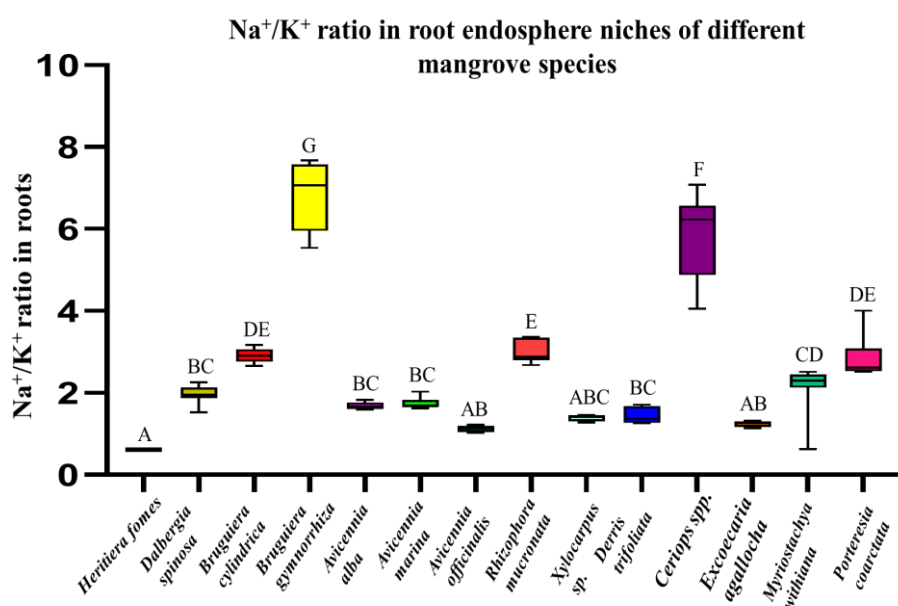


Figure 3.22: Na⁺/K⁺ ratio was estimated in root endosphere niches of different mangrove species from Indian Sundarban. Data were represented in this graph by the mean \pm standard error (n=8). Analysis of variance (ANOVA) by Tukey's honest significant difference (HSD) test (at 0.05 significance level) was performed to differentiate if there were significant differences present in the Na⁺/K⁺ ratio estimated in root endosphere

Observations:

1. Almost all mangrove species maintained a low Na⁺/K⁺ ratio (<5) in roots.
2. *Bruguiera gymnorrhiza* and *Ceriops* spp. are the only exceptions showing higher (>5) Na⁺/K⁺ ratio in roots.

3. Amid surrounding tidal water of about ~30-40 dS/m, the maintenance of such a low ratio of Na^+/K^+ is only possible if ultrafiltration/exclusion via endodermis in roots is efficiently functioning to allow selective entry of ions in the endosphere of roots.

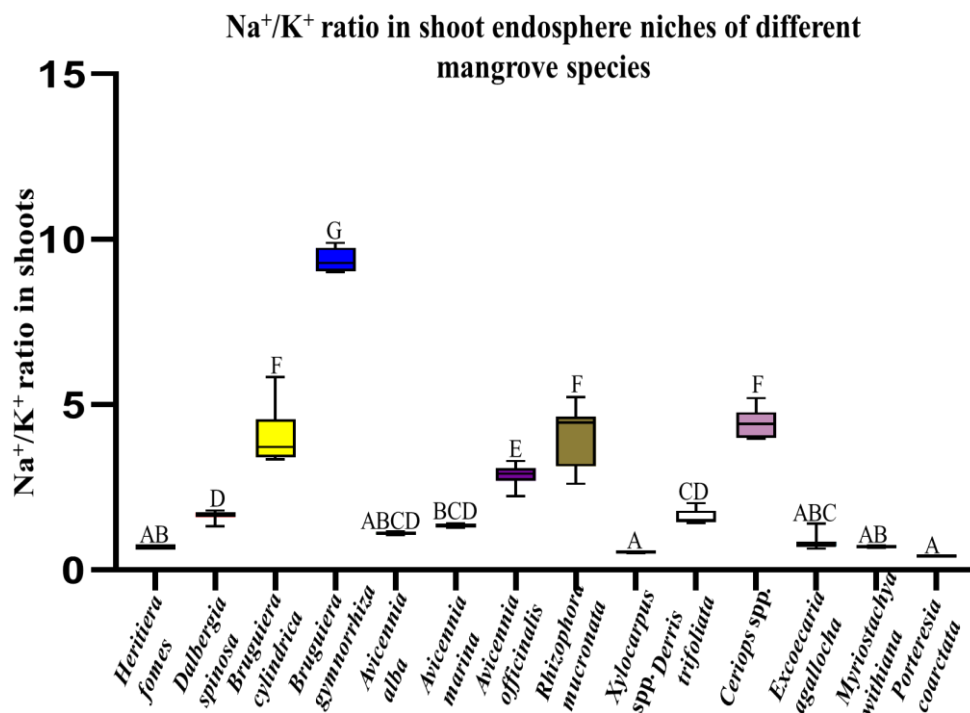


Figure 3.23: Na^+/K^+ ratio was estimated in shoot endosphere niches of different mangrove species from Indian Sundarban. Data were represented in this graph by the mean \pm standard error (n=8). Analysis of variance (ANOVA) by Tukey's honest significant difference (HSD) test (at 0.05 significance level) was performed to differentiate if there were significant differences present in the Na^+/K^+ ratio estimated in shoot endosphere niches from different mangrove species.

Observations:

1. Almost all mangrove species maintained a lower Na^+/K^+ ratio (<5) in shoot endosphere.
2. *Bruguiera gymnorhiza* is the only exception showing higher (~10) Na^+/K^+ ratio in shoots.
3. Amid surrounding tidal water of about ~30-40 dS/m, the maintenance of such a low ratio of Na^+/K^+ is only possible in shoots if ultrafiltration/exclusion via endodermis in roots is efficiently functioning to allow selective entry of ions in the endosphere of roots and salt excretion/exudation via salt glands over the stem surface is simultaneously occurring, leading to the maintenance of a lower Na^+/K^+ in shoot endospheres.

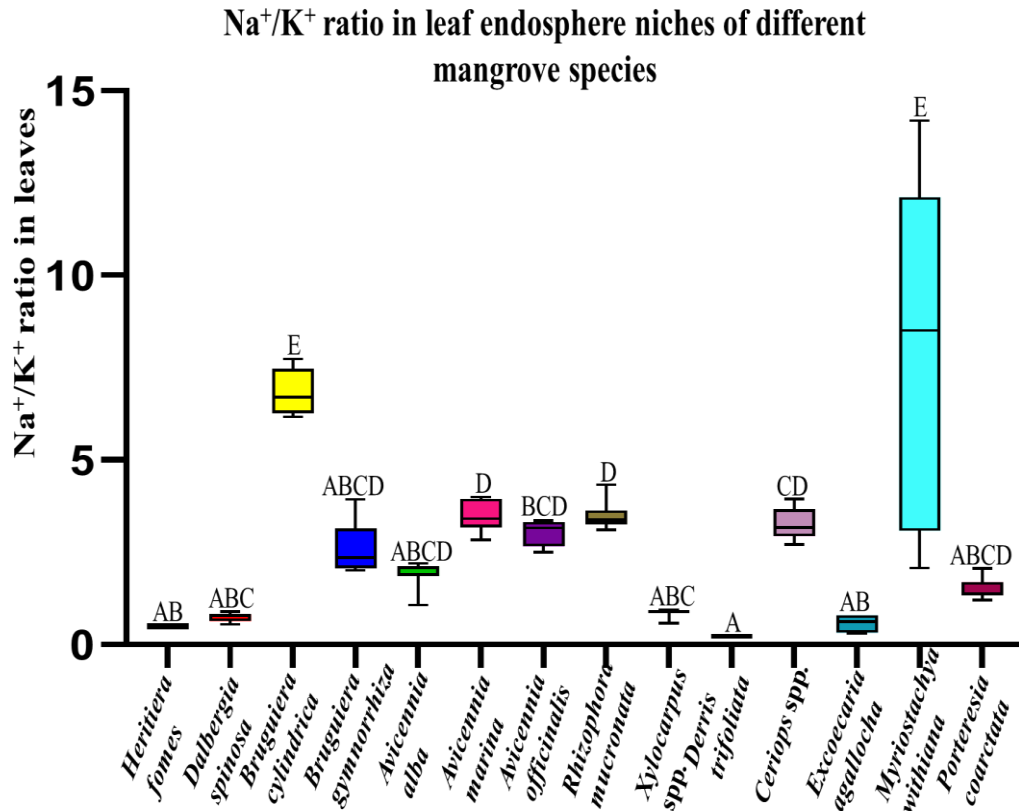


Figure 3.24: Na⁺/K⁺ ratio was estimated in leaf endosphere niches of different mangrove species from Indian Sundarban. Data were represented in this graph by the mean \pm standard error (n=8). Analysis of variance (ANOVA) by Tukey's honest significant difference (HSD) test (at 0.05 significance level) was performed to differentiate if there were significant differences present in the Na⁺/K⁺ ratio estimated in leaf endosphere niches from different mangrove species.

Observations:

1. Almost all mangrove species maintained a lower Na⁺/K⁺ ratio (<5) in leaf endospheres.
2. *Bruguiera gymnorhiza* and *Myriostachya wightiana* are the only exceptions showing higher (>5) Na⁺/K⁺ ratio in leaves. *Myriostachya wightiana* displayed a wide range of Na⁺/K⁺ ratio in leaves, spanning from below 5 to above 10.
3. Amid surrounding tidal water of about ~30-40 dS/m, the maintenance of such a low ratio of Na⁺/K⁺ is only possible in leaves if ultrafiltration/exclusion via endodermis in roots is efficiently functioning to allow selective entry of ions in the endosphere of roots and salt excretion/exudation via salt glands over the stem and leaf surface is collectively occurring, leading to the maintenance of a final lower Na⁺/K⁺ in leaf endospheres.

Na^+/K^+ ratio was estimated in endospheric environments of roots, shoots, and leaves of different mangrove species by flame photometry. The comparative analyses of Na^+/K^+ ratios, reveal that *in vivo* environments of almost all mangrove species maintain a low Na^+/K^+ ratio (<5) in roots, shoots, and leaves, leaving a few exceptions. In most of the cases *Bruguiera gymnorhiza* exhibited higher (>5) Na^+/K^+ ratio in roots, shoots and leaves. This maintenance of low internal Na^+/K^+ ratio in endospheric compartments makes them favourable niches for less halotolerant bacteria to survive and flourish as well as continue their unhindered metabolism amid hypersaline external environment.

Farooqui et al, (2016) established Na^+/K^+ ratios as the suitable screening tools for salt tolerance in mangrove species at specific level and concluded that salinity stress has an important role on growth and distribution pattern of mangrove trees. The leaf tissues *Avicennia marina*, *A. officinalis*, *Suaeda nudiflora* and *S. maritima* differentially absorb higher amount of K^+ ions over Na^+ thus reflecting their cause of dominance on saline substrata. *Avicennia alba* and *Suaeda monoica* have lower affinity for K^+ absorption, hence are sensitive to salinity stresses. *Acanthus ilicifolius* is reported to maintain moderately lower Na^+/K^+ ratios, thus being moderately salt tolerant. Thus, sodium and potassium ions have a powerful correlation with the salt tolerance potential in various mangrove species.

Objective 2

4. Establishment of pure endophytic bacterial strains from mangrove roots and pneumatophores and their molecular identification by 16S rRNA sequencing.

Roots and pneumatophore samples collected from different mangrove and mangrove associate species of Indian Sundarban were surface sterilized and were inoculated in LB broth for isolation of the root endophytic bacterial community. From LB broth 50 µl culture was spread on LB plate and single colonies were obtained. Each morphologically different single colony was Gram-stained by standard staining protocol.

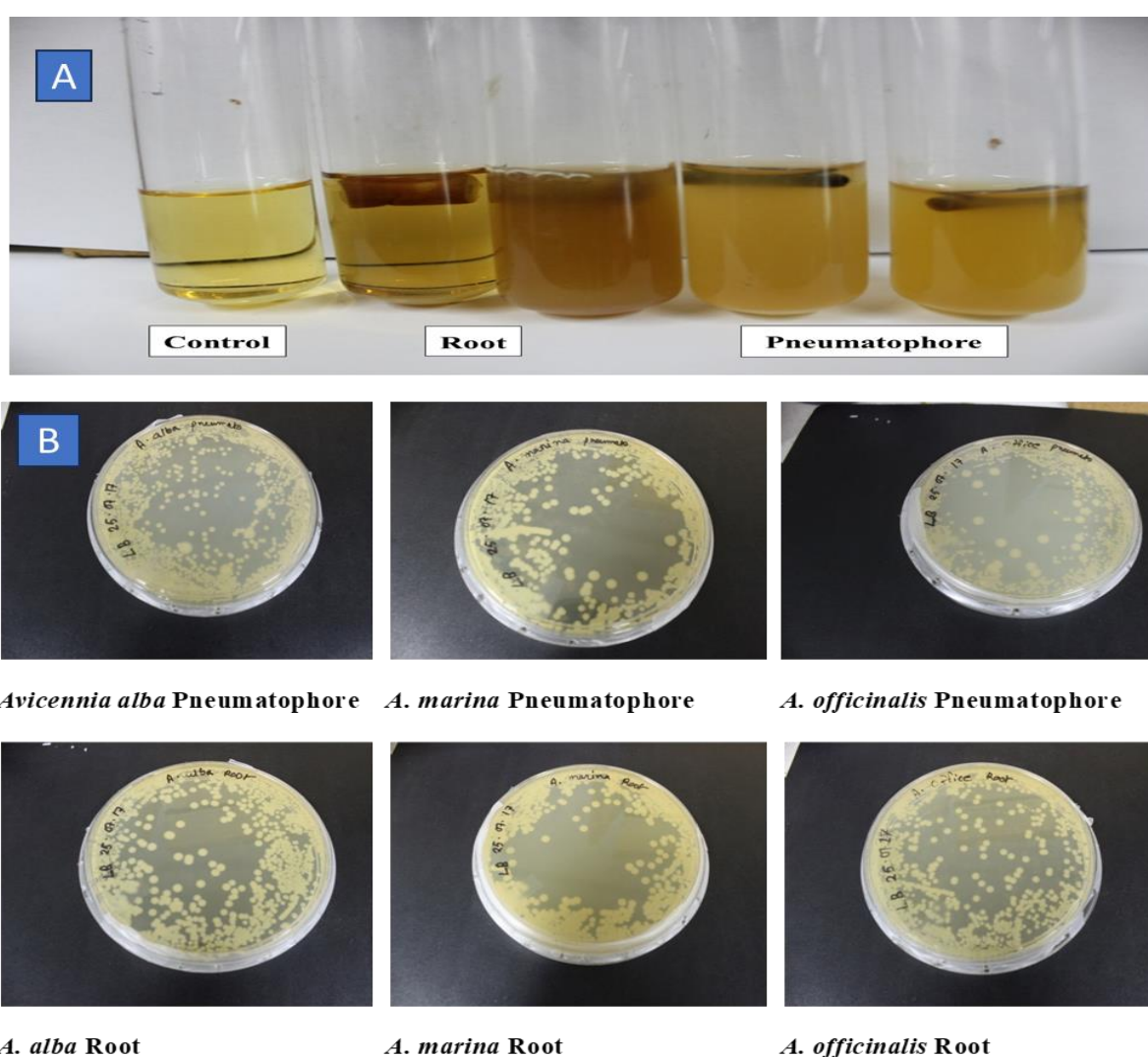


Figure 4.1: A) Root and pneumatophore samples of different mangrove and associate species were inoculated in LB broth. B) From LB broth 50 µl culture was spread on LB plate and single colonies are found to grow.

4.1. Gram-staining microscopic pictures of some Gram-positive and Gram-negative endophytic bacteria:

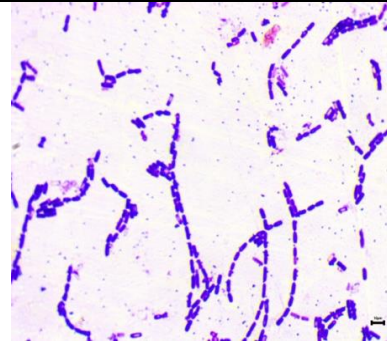
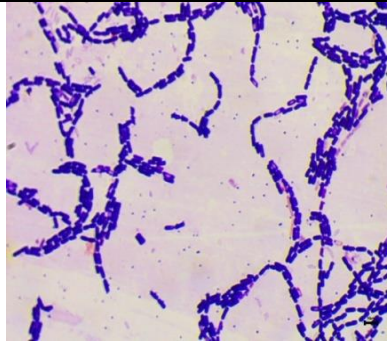
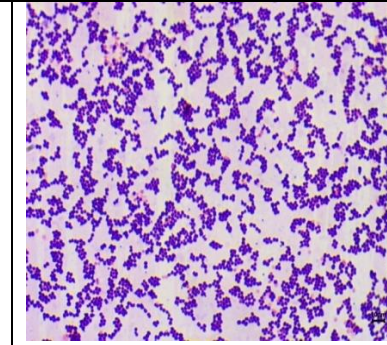
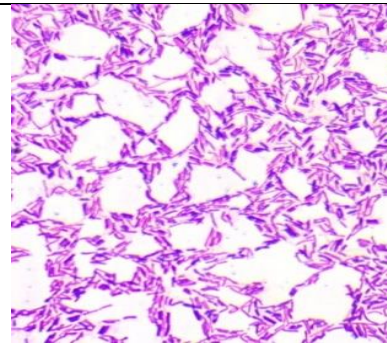
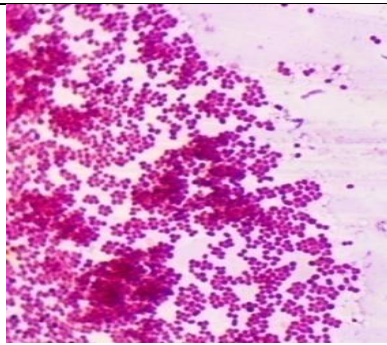
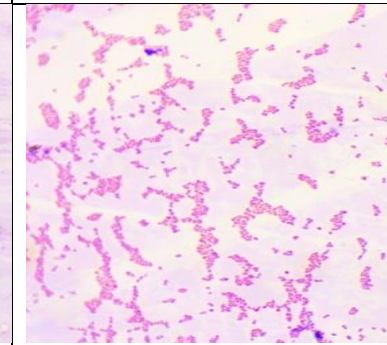
		
Fig. Isolate MYR9 Gram positive rod.	Fig. Isolate HPR4 Gram positive rod.	Fig. Isolate BCPP3 Gram positive cocci.
		
Fig. Isolate RRP6 Gram negative rod.	Fig. Isolate ERS2 Gram negative cocci.	Fig. Isolate ERS1 Gram negative cocci.

Figure 4.2: Gram-staining microscopic pictures of a few Gram-positive and Gram-negative endophytic bacteria isolated from roots and pneumatophores of different mangrove species from Indian Sundarbans. The bacterial isolates were observed under the microscopic light under 100x magnification with a scale bar of 5 μ m.

4.2. Molecular identification of pure bacterial isolates:

The purity of each bacterial isolate was initially checked via Gram staining observations. Then genomic DNA was isolated according to a standard protocol by using lysozyme/proteinase K. Identification of pure bacterial isolates were carried out at the molecular level using 16S rRNA sequencing procedure. The methods of PCR amplification technique have already been discussed in the materials and method section. The amplified PCR products were run through gel electrophoresis.

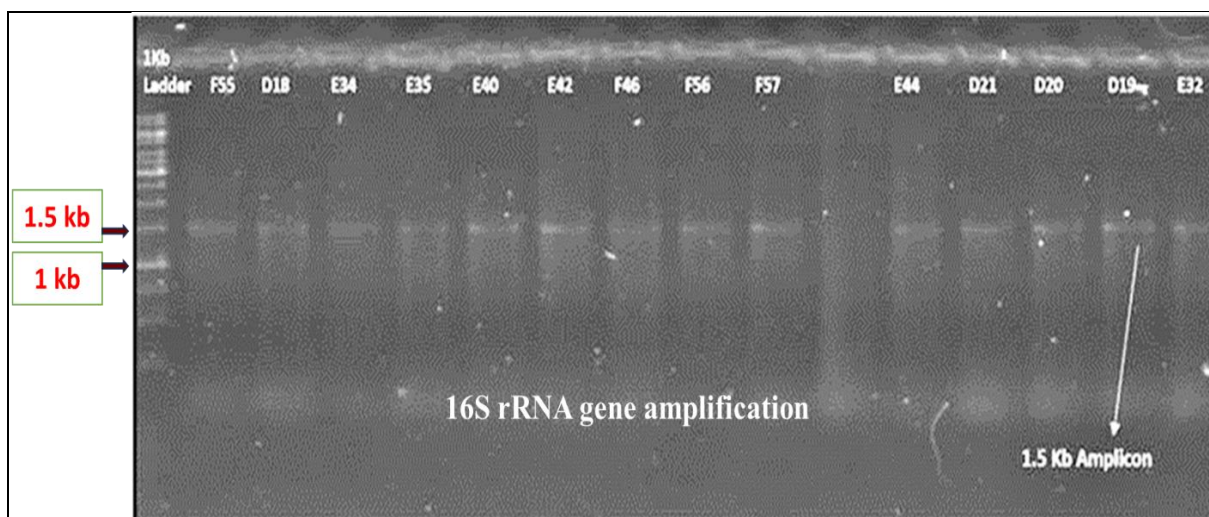


Figure 4.3: Agarose (0.8%) gel picture of partial 16S rRNA gene amplification of some endophytic bacterial isolates.

4.3. Establishment of pure endophytic bacterial strains from mangrove roots and pneumatophores:

In total 78 endophytic pure isolates of bacteria have been isolated, identified by 16S rRNA sequences and were accessioned in NCBI on submission of the sequences. The following Table comprises of the list of pure 78 isolates developed in this study.

Table 21: Name of the identified bacteria with accession numbers.

SL no.	PLACE	NAMES OF MANGROVE SPECIES AND ITS PLANT PARTS AS SOURCE OF ENDOPHYTIC BACTERIA	NAME OF THE IDENTIFIED BACTERIA	ACCESSION NO. s
1	Ramganga	<i>Avicennia officinalis</i> root	<i>Bacillus subtilis</i> strain AOR5	MT421976
2	Ramganga	<i>Avicennia officinalis</i> root	<i>Bacillus tequilensis</i> strain AOR8	MT421977
3	Ramganga	<i>Avicennia marina</i> pneumatophore	<i>Bacillus subtilis</i> strain AMP2	MT421978
4	Ramganga	<i>Avicennia marina</i> root	<i>Bacillus subtilis</i> strain AMR4	MT421979
5	Ramganga	<i>Avicennia alba</i> pneumatophore.	<i>Bacillus cereus</i> strain AAP2	MT421980
6	Ramganga	<i>Avicennia officinalis</i> pneumatophore	<i>Aeromonas veronii</i> strain AOP4	MT421981
7	Ramganga	<i>Avicennia marina</i> pneumatophore	<i>Aeromonas sobria</i> strain AMP4	MT421982
8	Ramganga	<i>Avicennia alba</i> root	<i>Bacillus subtilis</i> strain AAR1	MT421983

SL no.	PLACE	NAMES OF MANGROVE SPECIES AND ITS PLANT PARTS AS SOURCE OF ENDOPHYTIC BACTERIA	NAME OF THE IDENTIFIED BACTERIA	ACCESSION NO. s
9	Lakhipur	<i>Ceriops</i> sp. root	<i>Bacillus thuringiensis</i> strain CRL1	MT421984
10	Lakhipur	<i>Ceriops</i> sp. root	<i>Bacillus cereus</i> strain CRL2	MT421985
11	Lakhipur	<i>Ceriops</i> sp. root	<i>Bacillus</i> sp. strain CRL4	MT421986
12	Lakhipur	<i>Ceriops</i> sp. root	<i>Bacillus</i> sp. strain CRL5	MT421987
13	Lakhipur	<i>Ceriops</i> sp. root	<i>Bacillus</i> sp. strain CRL6	MT421988
14	Ramganga	<i>Heritiera fomes</i> root	<i>Enterobacter kobei</i> strain HRR1	MT421989
15	Shiber Ghat	<i>Excoecaria agallocha</i> root	<i>Acinetobacter lwoffii</i> strain ERS4	MT421990
16	Shiber Ghat	<i>Excoecaria agallocha</i> root	<i>Acinetobacter lwoffii</i> strain ERS6	MT421991
17	Patharprotima	<i>Bruguiera gymnorhiza</i> root	<i>Bacillus anthracis</i> strain BGRP8	MT421992
18	Patharprotima	<i>Bruguiera cylindrica</i> pneumatophore	<i>Aeromonas media</i> strain BCPP1	MT421993
19	Ramganga	<i>Heritiera fomes</i> pneumatophore	<i>Serratia marcescens</i> strain HPR1	MT421994
20	Patharprotima	<i>Bruguiera cylindrica</i> pneumatophore	<i>Staphylococcus hominis</i> strain BCPP2	MT421995
21	Lakhipur	<i>Ceriops</i> sp. root	<i>Bacillus thuringiensis</i> strain CRL3	MT421996
22	Ramganga	<i>Heritiera fomes</i> pneumatophore	<i>Serratia marcescens</i> strain HPR2	MT421997
23	Patharprotima	<i>Bruguiera cylindrica</i> pneumatophore	<i>Aeromonas finlandiensis</i> strain BCPP3	MT421998
24	Ramganga	<i>Heritiera fomes</i> pneumatophore	<i>Bacillus cereus</i> strain HPR3	MT421999
25	Ramganga	<i>Heritiera fomes</i> root	<i>Enterobacter</i> sp. HRR6	MT422000
26	Ramganga	<i>Heritiera fomes</i> pneumatophore	<i>Bacillus cereus</i> strain HPR8	MT422001
27	Shiber Ghat	<i>Excoecaria agallocha</i> root	<i>Acinetobacter lwoffii</i> strain ERS2	MT422002
28	Ramganga	<i>Heritiera fomes</i> root	<i>Pseudocitrobacter faecalis</i> strain HRR4	MT422003
29	Ramganga	<i>Heritiera fomes</i> root	<i>Pseudocitrobacter faecalis</i> strain HRR5	MT422004
30	Patharprotima	<i>Bruguiera gymnorhiza</i> root	<i>Aeromonas veronii</i> strain BGRP3	MT422005
31	Ramganga	<i>Heritiera fomes</i> pneumatophore	<i>Serratia marcescens</i> strain HPR4	MT422006
32	Ramganga	<i>Heritiera fomes</i> pneumatophore	<i>Aeromonas dhakensis</i> strain HPR7	MT422007
33	Shiber Ghat	<i>Excoecaria agallocha</i> root	<i>Citrobacter freundii</i> strain ERS1	MT422008

SL no.	PLACE	NAMES OF MANGROVE SPECIES AND ITS PLANT PARTS AS SOURCE OF ENDOPHYTIC BACTERIA	NAME OF THE IDENTIFIED BACTERIA	ACCESSION NO. s
34	Ramganga	<i>Avicennia officinalis</i> root	<i>Serratia marcescens</i> strain AOR4	MT422009
35	Ramganga	<i>Avicennia marina</i> pneumatophore	<i>Serratia marcescens</i> strain AMP1	MT422010
36	Patharprotima	<i>Bruguiera cylindrica</i> root	<i>Mangrovibacter plantisponsor</i> strain BCRP5	MT422011
37	Patharprotima	<i>Bruguiera gymnorrhiza</i> root	<i>Aeromonas bestiarum</i> strain BGRP7	MT422012
38	Ramganga	<i>Heritiera fomes</i> pneumatophore	<i>Aeromonas veronii</i> strain HPR5	MT422013
39	Ramganga	<i>Heritiera fomes</i> pneumatophore	<i>Aeromonas veronii</i> strain HPR6	MT422014
40	Shiber Ghat	<i>Excoecaria agallocha</i> root	<i>Citrobacter portucalensis</i> strain ERS3	MT422015
41	Shiber Ghat	<i>Excoecaria agallocha</i> root	<i>Acinetobacter lwoffii</i> strain ERS5	MT422016
42	Shiber Ghat	<i>Excoecaria agallocha</i> root	<i>Aeromonas hydrophila</i> strain ERS8	MT422017
43	Atharogazi	<i>Rhizophora mucronata</i> root	<i>Bacillus subtilis</i> strain RRP6	MT422018
44	Ramganga	<i>Dalbergia</i> sp. root	<i>Staphylococcus hominis</i> strain DAL4	MT422019
45	Ramganga	<i>Derris trifoliata</i> root	<i>Pseudomonas putida</i> strain DER3	MT422020
46	Ramganga	<i>Derris trifoliata</i> root	<i>Pseudomonas putida</i> strain DER6	MT422021
47	Ramganga	<i>Derris trifoliata</i> root	<i>Pseudomonas putida</i> strain DER8	MT422022
48	Ramganga	<i>Derris trifoliata</i> root	<i>Pseudomonas fulva</i> strain DER9	MT422023
49	Ramganga	<i>Myriostachya</i> sp. root	<i>Vibrio ruber</i> strain MYR10	MT422024
50	Ramganga	<i>Porteresia</i> sp. root	<i>Aeromonas veronii</i> strain POT7	MT422025
51	Ramganga	<i>Xylocarpus</i> sp. root	<i>Staphylococcus epidermidis</i> strain XYL9	MT422026
52	Ramganga	<i>Dalbergia</i> sp. root	<i>Aeromonas allosaccharophila</i> strain DAL2	MT422027
53	Ramganga	<i>Dalbergia</i> sp. root	<i>Staphylococcus hominis</i> strain DAL5	MT422028
54	Ramganga	<i>Dalbergia</i> sp. root	<i>Staphylococcus epidermidis</i> strain DAL9	MT422029
55	Ramganga	<i>Myriostachya</i> sp. root	<i>Vibrio ruber</i> strain MYR4	MT422030

SL no.	PLACE	NAMES OF MANGROVE SPECIES AND ITS PLANT PARTS AS SOURCE OF ENDOPHYTIC BACTERIA	NAME OF THE IDENTIFIED BACTERIA	ACCESSION NO. s
56	Ramganga	<i>Myriostachya</i> sp. root	<i>Gallaecimonas</i> sp. strain MYR5	MT422031
57	Ramganga	<i>Myriostachya</i> sp. root	<i>Gallaecimonas</i> sp. strain MYR7	MT422032
58	Ramganga	<i>Myriostachya</i> sp. root	<i>Vibrio ruber</i> strain MYR9	MT422033
59	Ramganga	<i>Porteresia</i> sp. root	<i>Aeromonas veronii</i> strain POT2	MT422034
60	Ramganga	<i>Porteresia</i> sp. root	<i>Aeromonas veronii</i> strain POT3	MT422035
61	Ramganga	<i>Porteresia</i> sp. root	<i>Aeromonas veronii</i> strain POT4	MT422036
62	Ramganga	<i>Xylocarpus</i> sp. root	<i>Bacillus altitudinis</i> strain XYL1	MT422037
63	Ramganga	<i>Xylocarpus</i> sp. root	<i>Staphylococcus epidermidis</i> strain XYL8	MT422038
64	Ramganga	<i>Xylocarpus</i> sp. root	<i>Staphylococcus hominis</i> strain XYL10	MT422039
65	Ramganga	<i>Bruguiera cylindrica</i> root	<i>Bacillus oceanisediminis</i> strain BCY3	MT422040
66	Ramganga	<i>Bruguiera cylindrica</i> root	<i>Pseudomonas stutzeri</i> strain BCY5	MT422041
67	Ramganga	<i>Bruguiera cylindrica</i> root	<i>Pseudomonas stutzeri</i> strain BCY7	MT422042
68	Ramganga	<i>Bruguiera cylindrica</i> root	<i>Pseudomonas stutzeri</i> strain BCY9	MT422043
69	Ramganga	<i>Dalbergia</i> sp. root	<i>Staphylococcus epidermidis</i> strain DAL6	MT422044
70	Ramganga	<i>Derris</i> sp. root	<i>Pseudomonas</i> sp. Strain DER1	MT422045
71	Ramganga	<i>Derris</i> sp. root	<i>Pseudomonas putida</i> strain DER10	MT422046
72	Ramganga	<i>Heritiera fomes</i> root	<i>Aeromonas hydrophila</i> strain HER3	MT422047
73	Ramganga	<i>Myriostachya</i> sp. root	<i>Vibrio ruber</i> strain MYR2	MT422048
74	Ramganga	<i>Porteresia</i> sp. root	<i>Aeromonas fluviialis</i> strain POT6	MT422049
75	Ramganga	<i>Porteresia</i> sp. root	<i>Aeromonas veronii</i> strain POT9	MT422050
76	Ramganga	<i>Xylocarpus</i> sp. root	<i>Staphylococcus epidermidis</i> strain XYL3	MT422051
77	Ramganga	<i>Xylocarpus</i> sp. root	<i>Staphylococcus epidermidis</i> strain XYL4	MT422052
78	Ramganga	<i>Xylocarpus</i> sp. root	<i>Staphylococcus epidermidis</i> strain XYL7	MT422053

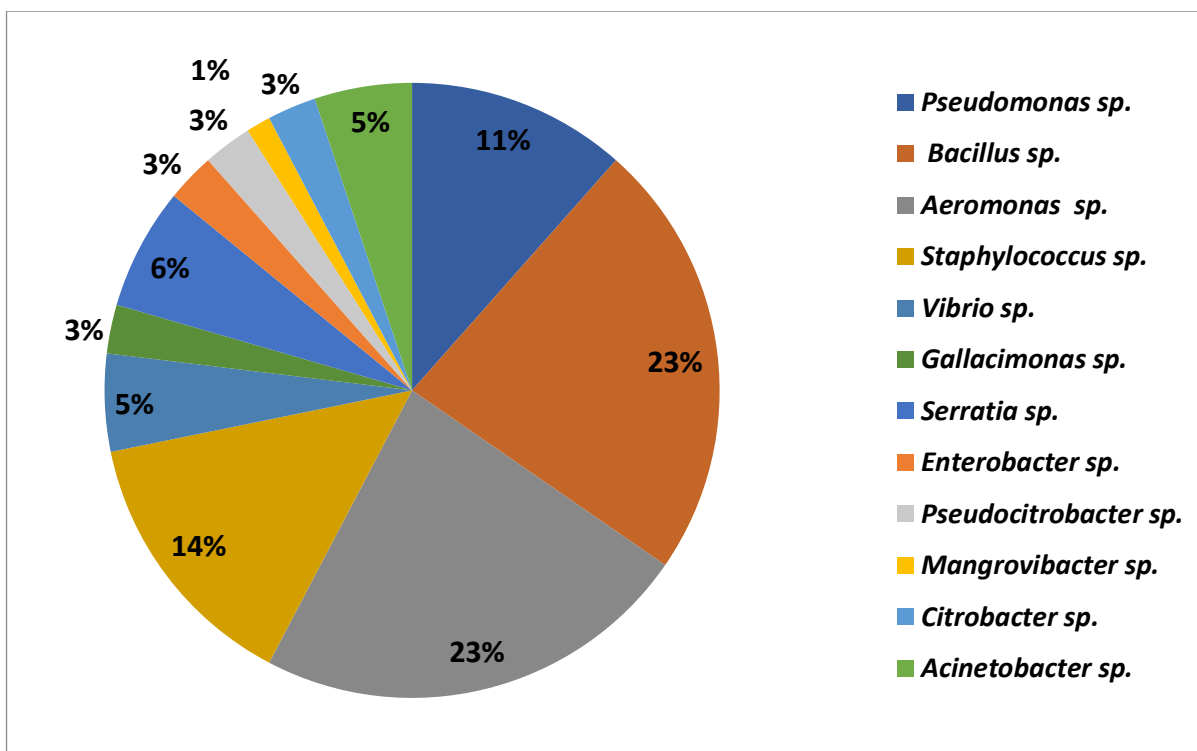


Figure 4.4: Relative distribution of different bacterial genera among total 78 accessioned root endophytic bacterial strains developed as pure isolates.

Observations:

The all 78 bacterial isolates comprise of 12 bacterial genera, out of which two bacterial genera *Bacillus* spp. and *Aeromonas* spp. were found out to be the most abundant genera inhabiting mangrove roots and pneumatophores, followed by *Staphylococcus* spp. and *Pseudomonas* spp. Rest of the other genera of isolates belong to spp. of *Serratia*, *Vibrio*, *Gallacimonas*, *Enterobacter*, *Pseudocitrobacter*, *Citrobacter*, *Acinetobacter*, *Mangrovibacter*, which occupy 1%-6% of the total 78 accessions distributed over 12 genera.

4.4. Testing of all 78 strains on differential nutrient cycling media for possible plant growth promotion potential

The following table demonstrates the positive or negative growth observed when all these 78 strains were allowed to grow on different nutrient cycling media viz. cellulose degrading medium (CDM), phosphorus solubilizing medium (PSM), free nitrogen fixing medium (FNFM), sulphur oxidizing medium (SOM) and stringent iron oxidizing medium (IOM). Positive growth on IOM was again reconfirmed by the presence of confirmed ferric salt precipitate (ppt.) obtained in the stringent IOM maintained at sub-neutral pH of 6 only.

Table 22: Endophytic bacterial growth on different nutrient cycling media.

S	ENDOPHYTIC BACTERIAL GROWTH ON DIFFERENT NUTRIENT CYCLING MEDIA						
	CDM=Cellulose degrading medium; PSM=Phosphorous solublizing medium; FNFM=Free nitrogen fixing medium; SOM=Sulfur oxidizing medium; IOM= Iron oxidizing medium. Negative growth is denoted as NA and +/++/+++ shows density of growth observed by naked eyes						
	NAME OF BACTERIAL ISOLATES	NAME OF MANGROVE SPECIES	ON CDM	ON PSM	ON FNFM	ON SOM	ON IOM
1	<i>Bacillus oceanisediminis</i> strain BCY3 (MT422040)	<i>Bruguiera cylindrica</i> root	+	++	+++	+++	ppt observed
2	<i>Pseudomonas stutzeri</i> strain BCY5 (MT422041)	<i>Bruguiera cylindrica</i> root	NA	+++	+++	NA	NA
3	<i>Pseudomonas stutzeri</i> strain BCY7 (MT422042)	<i>Bruguiera cylindrica</i> root	NA	NA	+++	NA	NA
4	<i>Pseudomonas stutzeri</i> strain BCY9 (MT422043)	<i>Bruguiera cylindrica</i> root	NA	NA	+++	NA	NA
5	<i>Aeromonas allosaccharophila</i> strain DAL2 (MT422027)	<i>Dalbergia</i> sp. root	+++	+++	++	NA	NA
6	<i>Staphylococcus hominis</i> strain DAL4 (MT422019crl3)	<i>Dalbergia</i> sp. root	NA	NA	NA	NA	NA
7	<i>Staphylococcus hominis</i> strain DAL5 (MT422028)	<i>Dalbergia</i> sp. root	NA	NA	NA	++	NA
8	<i>Staphylococcus epidermis</i> strain DAL6 (MT422044)	<i>Dalbergia</i> sp. root	NA	NA	NA	++	ppt observed
9	<i>Staphylococcus epidermis</i> strain DAL9 (MT422026)	<i>Dalbergia</i> sp. root	NA	NA	NA	++	NA
10	<i>Pseudomonas</i> sp. strain DER1 (MT422045)	<i>Derris trifoliata</i> root	NA	+++	NA	++	NA
11	<i>Pseudomonas putida</i> strain DER3 (MT422020)	<i>Derris trifoliata</i> root	NA	+++	NA	++	ppt observed
12	<i>Pseudomonas putida</i> strain DER6 (MT422021)	<i>Derris trifoliata</i> root	NA	+++	NA	++	NA
13	<i>Pseudomonas putida</i> strain DER8 (MT422022)	<i>Derris trifoliata</i> root	NA	+++	NA	+	NA
14	<i>Pseudomonas fulva</i> strain DER9 (MT422023)	<i>Derris trifoliata</i> root	++	+++	++	+	NA
15	<i>Pseudomonas putida</i> strain DER10 (MT422046)	<i>Derris trifoliata</i> root	NA	+++	NA	+	NA
16	<i>Aeromonas hydrophilia</i> strain HER3 (MT422047)	<i>Heritiera fomes</i> root	NA	NA	+++	+	ppt observed
17	<i>Vibrio ruber</i> strain MYR2 (MT422048)	<i>Myriostachya</i> sp. root	NA	NA	NA	++	NA
18	<i>Vibrio ruber</i> strain MYR4 (MT422030)	<i>Myriostachya</i> sp. root	NA	NA	NA	++	NA
19	<i>Gallacimonas</i> sp. strain MYR5 (MT422031)	<i>Myriostachya</i> sp. root	++	++	+	+++	NA
20	<i>Gallacimonas</i> sp. strain MYR7 (MT422032)	<i>Myriostachya</i> sp. root	++	+++	+	+++	NA

21	<i>Vibrio ruber</i> strain MYR9 (MT422033)	<i>Myriostachya</i> sp. root	++	++	+	+++	NA
22	<i>Vibrio ruber</i> strain MYR10 (MT422024)	<i>Myriostachya</i> sp. root	+	+++	NA	++	NA
23	<i>Aeromonas veronii</i> strain POT2 (MT422034)	<i>Porteresia</i> sp. root	+++	NA	NA	+++	NA
24	<i>Aeromonas veronii</i> strain POT3 (MT422035)	<i>Porteresia</i> sp. root	+++	NA	+++	++	NA
25	<i>Aeromonas veronii</i> strain POT4 (MT422036)	<i>Porteresia</i> sp. root	+	NA	+++	++	NA
26	<i>Aeromonas fluvialis</i> strain POT6 (MT422049)	<i>Porteresia</i> sp. root	+++	+++	NA	+++	NA
27	<i>Aeromonas veronii</i> strain POT7 (MT422025)	<i>Porteresia</i> sp. root	+	NA	++	++	NA
28	<i>Aeromonas veronii</i> strain POT9 (MT422050)	<i>Porteresia</i> sp. root	NA	NA	+++	++	NA
29	<i>Bacillus altitudinis</i> strain XYL1 (MT422037)	<i>Xylocarpus</i> sp. root	NA	+++	+++	++	NA
30	<i>Staphylococcus epidermis</i> strain XYL3 (MT422051)	<i>Xylocarpus</i> sp. root	NA	NA	NA	+++	NA
31	<i>Staphylococcus epidermis</i> strain XYL4 (MT422052)	<i>Xylocarpus</i> sp. root	NA	+++	NA	+++	NA
32	<i>Staphylococcus epidermis</i> strain XYL7 (MT422053)	<i>Xylocarpus</i> sp. root	NA	NA	NA	+++	NA
33	<i>Staphylococcus epidermis</i> strain XYL8 (MT422038)	<i>Xylocarpus</i> sp. root	+	+	NA	++	NA
34	<i>Staphylococcus epidermis</i> strain XYL9 (MT422026)	<i>Xylocarpus</i> sp. root	NA	+++	NA	++	NA
35	<i>Staphylococcus hominis</i> strain XYL10 (MT422039)	<i>Xylocarpus</i> sp. root	NA	++	+	++	NA
36	<i>Bacillus subtilis</i> strain AOR5 (MT421976)	<i>Avicennia officinalis</i> root	NA	+	NA	++	NA
37	<i>Bacillus tequilensis</i> strain AOR8 (MT421977)	<i>Avicennia officinalis</i> root	NA	NA	NA	++	NA
38	<i>Bacillus subtilis</i> strain AMP2 (MT421978)	<i>Avicennia marina</i> pneumatophore	++	NA	NA	+	NA
39	<i>Bacillus subtilis</i> strain AMR4 (MT421979)	<i>Avicennia marina</i> root	NA	NA	NA	++	NA
40	<i>Bacillus cerius</i> strain AAP2 (MT421980)	<i>Avicennia alba</i> pneumatophore.	+	NA	NA	++	NA
41	<i>Aeromonas sobria</i> strain AMP4 (MT421982)	<i>Avicennia marina</i> pneumatophore	NA	+	NA	++	NA
42	<i>Aeromonas veronii</i> strain AOP4 (MT421981)	<i>Avicennia officinalis</i> pneumatophore	NA	+++	NA	++	NA
43	<i>Serratia marcescens</i> strain AOR4 (MT422009)	<i>Avicennia officinalis</i> root	+	+++	NA	++	NA
44	<i>Serratia marcescens</i> strain AMP1 (MT422010)	<i>Avicennia marina</i> pneumatophore	NA	+++	NA	++	NA
45	<i>Bacillus subtilis</i> strain AAR1 (MT421983)	<i>Avicennia alba</i> root	NA	+	NA	++	NA
46	<i>Bacillus thuringiensis</i> strain CRL1 (MT421984)	<i>Ceriops</i> sp. Root	++	+	+	++	NA
47	<i>Bacillus cerius</i> strain CRL2 (MT421985)	<i>Ceriops</i> sp. Root	++	+	+	+++	NA
48	<i>Bacillus thuringiensis</i> strain CRL3 (MT421996)	<i>Ceriops</i> sp. Root	NA	+	NA	+++	ppt observe d

49	<i>Bacillus</i> sp. strain CRL4 (MT421986)	<i>Cerriops</i> sp. Root	+	+	+	+++	NA
50	<i>Bacillus</i> sp. strain CRL5 (MT421987)	<i>Cerriops</i> sp. Root	NA	NA	NA	NA	NA
51	<i>Bacillus</i> sp. strain CRL6 (MT421988)	<i>Cerriops</i> sp. Root	+++	NA	NA	NA	NA
52	<i>Enterobacter kobei</i> strain HRR1 (MT421989)	<i>Heritiera fomes</i> root	+++	+++	NA	NA	NA
53	<i>Pseudocitrobacter faecalis</i> strain HRR4 (MT422003)	<i>Heritiera fomes</i> root	++	NA	NA	NA	NA
54	<i>Pseudocitrobacter faecalis</i> strain HRR5 (MT422004)	<i>Heritiera fomes</i> root	+++	NA	NA	NA	ppt observed
55	<i>Enterobacter</i> sp. strain HRR6 (MT422000)	<i>Heritiera fomes</i> root	NA	NA	NA	++	NA
56	<i>Aeromonas veronii</i> strain BGRP3 (MT422005)	<i>Bruguiera gymnorrhiza</i> root	+	NA	+	+++	NA
57	<i>Aeromonas bestiarum</i> strain BGRP7 (MT422012)	<i>Bruguiera gymnorrhiza</i> root	NA	+++	NA	++	ppt observed
58	<i>Bacillus anthracis</i> strain BGRP8 (MT421992)	<i>Bruguiera gymnorrhiza</i> root	NA	NA	NA	++	NA
59	<i>Serratia marcescens</i> strain HPR1 (MT421994)	<i>Heritiera fomes</i> pneumatophore	NA	++	NA	+	NA
60	<i>Serratia marcescens</i> strain HPR2 (MT421997)	<i>Heritiera fomes</i> pneumatophore	++	+++	NA	+	NA
61	<i>Bacillus cereus</i> strain HPR3 (MT421999)	<i>Heritiera fomes</i> pneumatophore	NA	NA	NA	++	NA
62	<i>Serratia marcescens</i> strain HPR4 (MT422006)	<i>Heritiera fomes</i> pneumatophore	NA	NA	+++	+	ppt observed
63	<i>Aeromonas veronii</i> strain HPR5 (MT422013)	<i>Heritiera fomes</i> pneumatophore	NA	NA	NA	++	NA
64	<i>Aeromonas veronii</i> strain HPR6 (MT422014)	<i>Heritiera fomes</i> pneumatophore	NA	+++	NA	++	NA
65	<i>Aeromonas dhakensis</i> strain HPR7 (MT422007)	<i>Heritiera fomes</i> pneumatophore	++	+++	+	+++	ppt observed
66	<i>Bacillus cereus</i> strain HPR8 (MT422001)	<i>Heritiera fomes</i> pneumatophore	++	++	+	+++	NA
67	<i>Citrobacter freundii</i> strain ERS1 (MT422008)	<i>Excoecaria agallocha</i> root	++	++	+	+++	ppt observed
68	<i>Acinetobacter lowffi</i> strain ERS2 (MT422002)	<i>Excoecaria agallocha</i> root	+++	NA	NA	++	NA
69	<i>Citrobacter portucalensis</i> strain ERS3 (MT422015)	<i>Excoecaria agallocha</i> root	+	+	NA	++	NA
70	<i>Acinetobacter lowffi</i> strain ERS4 (MT421990)	<i>Excoecaria agallocha</i> root	+	+	NA	++	NA
71	<i>Acinetobacter lowffi</i> strain ERS5 (MT422016)	<i>Excoecaria agallocha</i> root	+++	++	++	+	NA
72	<i>Acinetobacter lowffi</i> strain ERS6 (MT421991)	<i>Excoecaria agallocha</i> root	+++	++	+	++	NA
73	<i>Aeromonas hydrophilia</i> strain ERS8 (MT422017)	<i>Excoecaria agallocha</i> root	NA	++	NA	+++	NA
74	<i>Mangrovibacter plantisponcer</i> strain BCRP5 (MT422011)	<i>Bruguiera cylindrica</i> root	+++	+++	+++	++	ppt observed

75	<i>Aeromonas media</i> strain BCPP1 (MT421993)	<i>Bruguiera cylindrica</i> pneumatophore	++	NA	NA	+++	NA
76	<i>Staphylococcus hominis</i> strain BCPP2 (MT421995)	<i>Bruguiera cylindrica</i> pneumatophore	++	++	NA	+++	NA
77	<i>Aeromonas finlandiensis</i> strain BCPP3 (MT421998)	<i>Bruguiera cylindrica</i> pneumatophore	+++	+	+++	++	NA
78	<i>Bacillus subtilis</i> strain RRP6 (MT422018)	<i>Rhizophora mucronata</i> root	+++	++	+++	+	ppt observed

The figure below demonstrates the overall view of no. of accessioned isolates and their possible potential for nutrient cycling. The highest no. of isolates showed high potential for sulfur oxidation to sulfate, followed by a good no. of phosphorus solubilizers, cellulose degraders, free nitrogen fixers as well as iron oxidizers. Several strains were observed to be multi-tasker, contributing to more than one nutrient cycling activities.

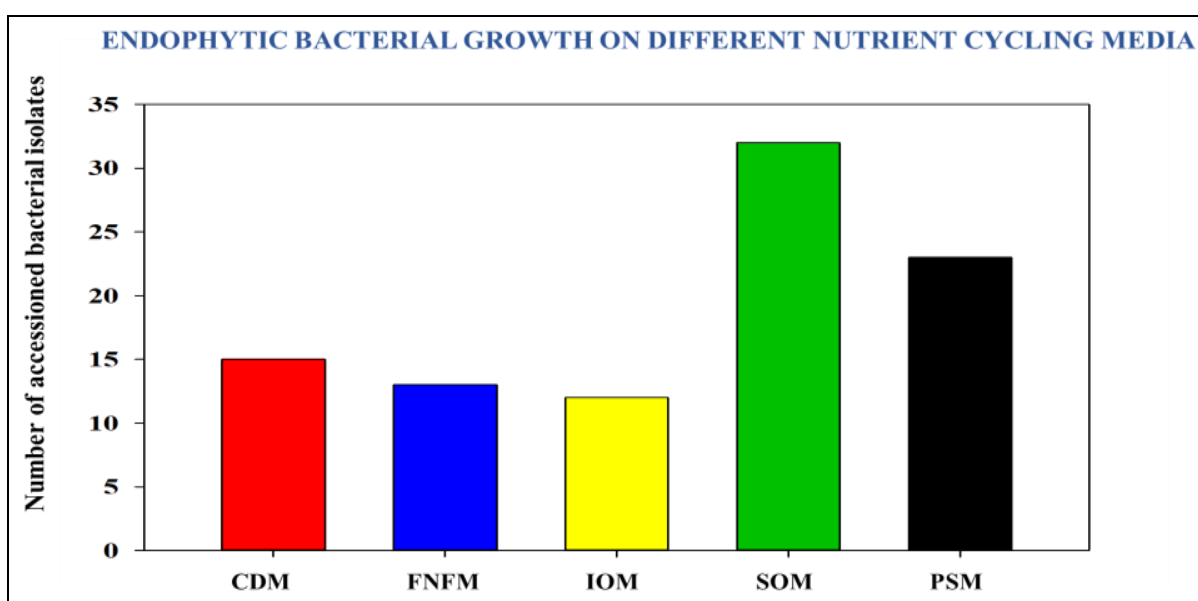
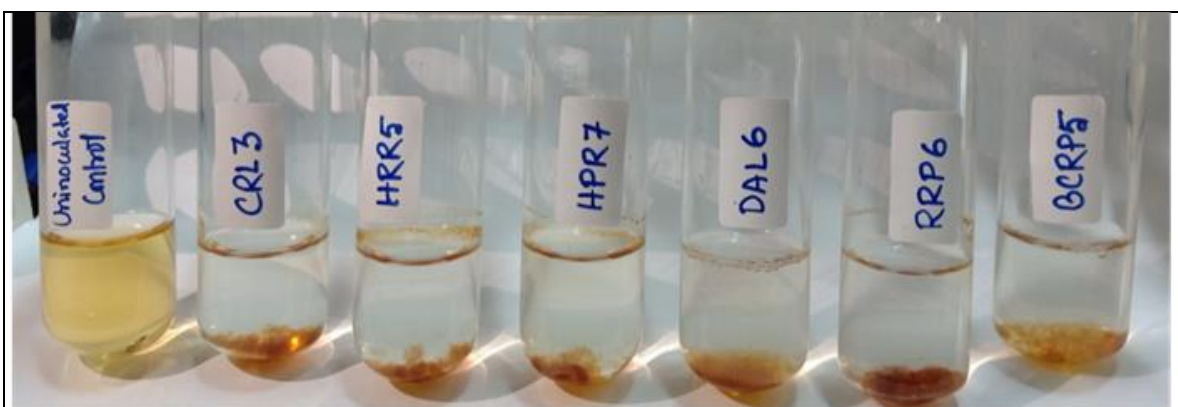


Figure 4.5: Number of accessioned isolates growing on different nutrient cycling media. The iron oxidizing bacterial isolates represent here displayed brown precipitation at pH 6 and further were confirmed as IOB after confirmed ferric salt precipitate (ppt.) obtained in the stringent IOM maintained at sub-neutral pH of 6 only (Figure-4.6).



Precipitation of iron (Ferric) oxide by iron oxidizers. pH of media was maintained at 6 (Ghosh et al, 2014).



Confirmatory test for iron ppt by ammonium thiocyanate (Ghosh et al, 2014)

Figure 4.6: Confirmational test of Iron oxidizing bacteria at sub-neutral pH of 6 (Ghosh et al, 2014).

Biswas et al, (2020) isolated *Pseudomonas* spp. and *Bacillus* spp. from Sundarban mangrove forest. Other endophytic bacterial genera like *Pseudomonas*, *Burkholderia*, *Azotobacter*, *Azospirillum*, *Alcaligenes*, *Klebsiella*, *Arthrobacter*, *Serratia* etc. were also reported from mangrove forests by Mukherjee et al, (2017). Except the finding of a few different endophytic bacteria like *Vibrio* spp., *Gallacimonas* spp., *Pseudocitrobacter* spp., *Mangrovibacter* spp. noticeable in this study, similar endophytic bacterial isolates were reported by other authors.

Objective 3:

5. Plant growth promotion profiling of the established/accessioned endophytic bacterial strains.

5.1. IAA production by different endophytic bacterial strains isolated from mangrove roots and pneumatophores:

Indoleacetic acid (IAA) is a phytohormone, the most important natural auxin. IAA plays several growth functions of plants such as tropic responses, organogenesis, cell expansion, differentiation, division, and gene regulation. Many endophytic bacteria have the ability to produce the auxin phytohormone IAA. IAA is produced by microorganisms in the presence of the precursor L-tryptophan. IAA is produced by endophytic bacteria and used by plants that enhances plant growth and yield. Different *Bacillus* and *Pseudomonas* species are found for their IAA production ability (Patel and Patel, 2014). In this study, IAA production assay was studied under laboratory conditions for 78 endophytic bacterial strains to speculate their plant growth facilitating activity under degraded and non-degraded mangrove habitats.

5.2. Calibration curve of IAA

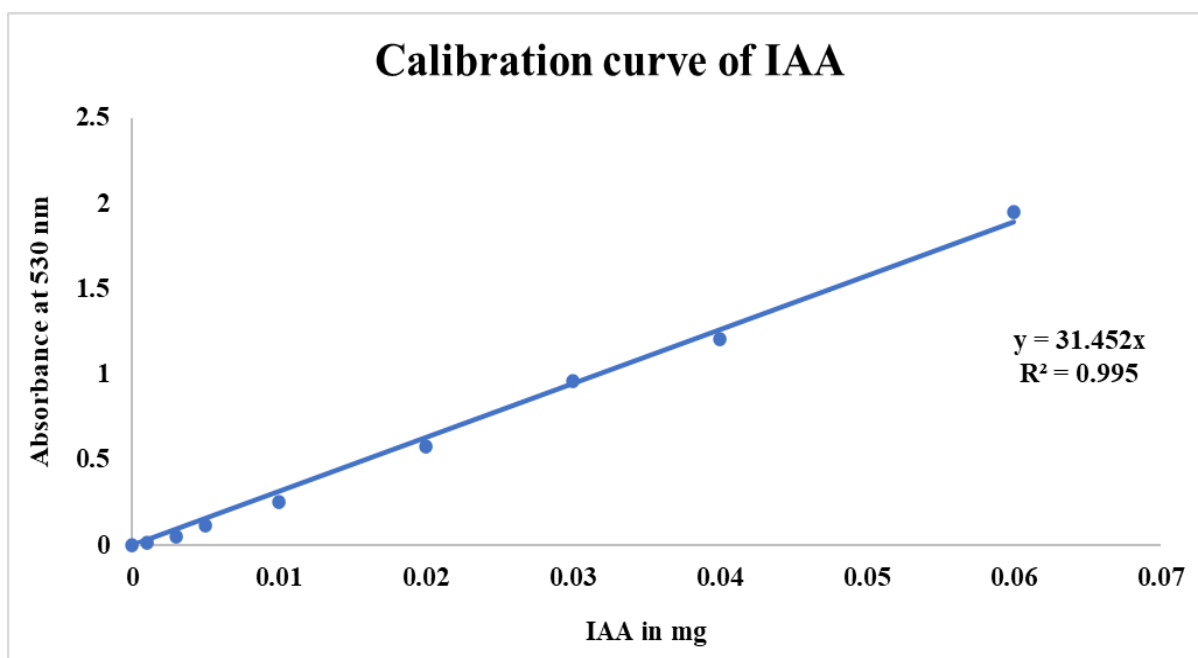


Figure 5.1: The calibration curve of IAA was made to measure the unknown concentration of IAA produced by different endophytic bacterial strains.

IAA production by isolated endophytic bacterial strains

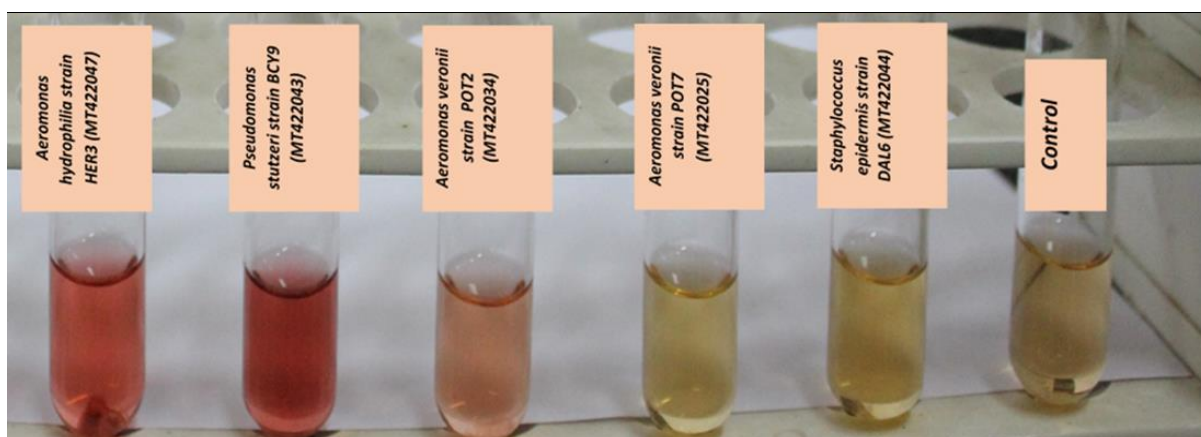


Figure 5.2: IAA production by different endophytic bacterial strains isolated from mangrove roots and pneumatophores from Indian Sundarbans. In this picture the red coloured culture filtrate indicated IAA production by endophytic bacterial strains.

5.3. Evaluation of IAA production potential of 78 endophyte accessions:

The all 78 endophytic bacteria were tested for their IAA production. The best 15 high IAA producer strains are represented below.

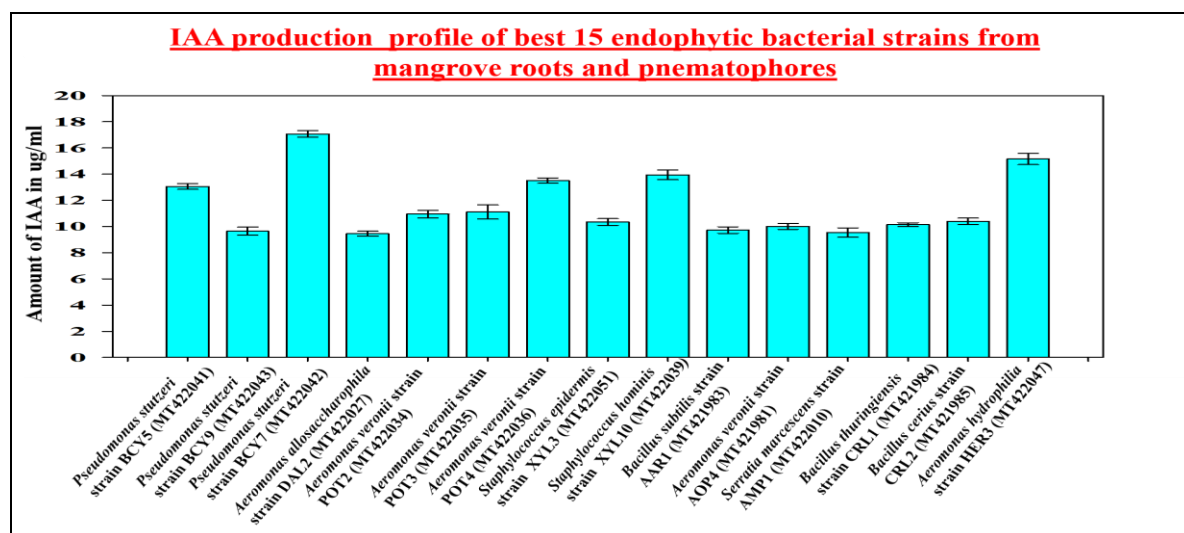


Figure 5.3: Best 15 IAA-producing endophyte bacterial strains from mangrove roots and pneumatophores. Data were represented as mean \pm standard deviation (n=3) in the above graph.

Observations:

Here all 15 best IAA-producing endophyte bacterial strains displayed IAA production activity in a range varied between 9-17 $\mu\text{g/ml}$.

5.4. Analysis of IAA production by endophytic bacterial isolates against their source niches of diverse species of mangrove roots and pneumatophores:

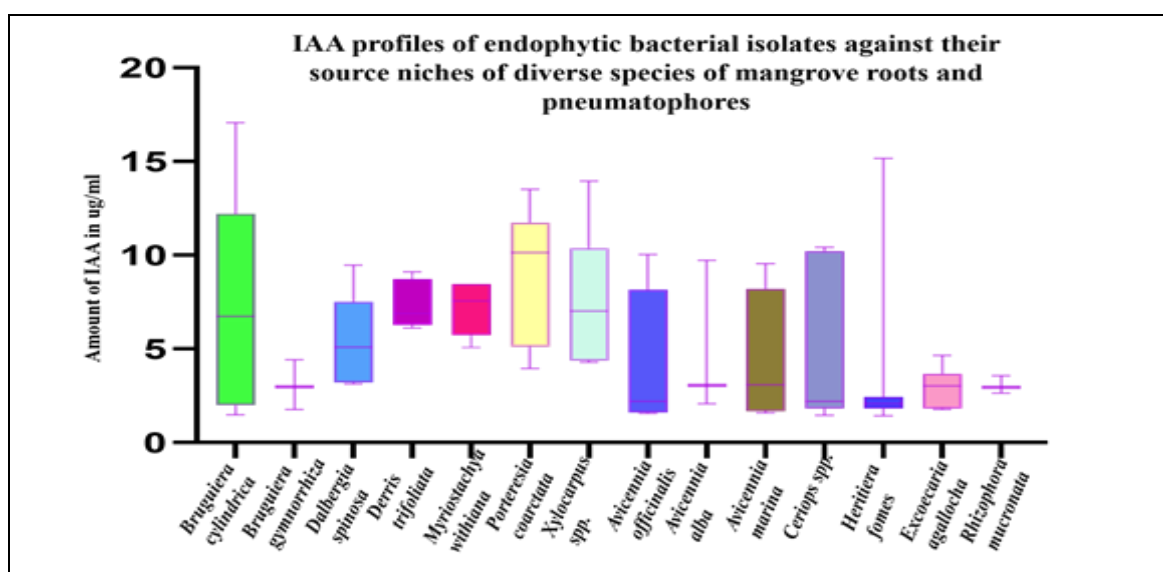


Figure 5.4: Diverse mangrove root environments as source of differential IAA producing endophytic bacterial strains. Data were represented as mean \pm standard deviation in above the graph.

Observations:

The above figure depicts the diverse mangrove root environments as resource niches of differential IAA producing traits of 78 accessioned strains. The high IAA producers could be isolated mostly from *Bruguiera cylindrica*, *Porteresia coarctata*, *Xylocarpus spp.*, *Avicennia officinalis*, *Avicennia marina* and *Ceriops spp.* roots and pneumatophores.

5.6. Evaluation of IAA production potential (without addition of tryptophan precursor) of some endophyte accessions:

Here the best 15 high IAA producer strains and some other high IAA producer strains of endophytic bacteria are tested for their IAA production without adding the precursor compound tryptophan in the assay reaction. The best 15 high IAA producer strains without adding tryptophan in the reaction are represented below and their range of IAA production varied between 4.5-10 µg/ml.

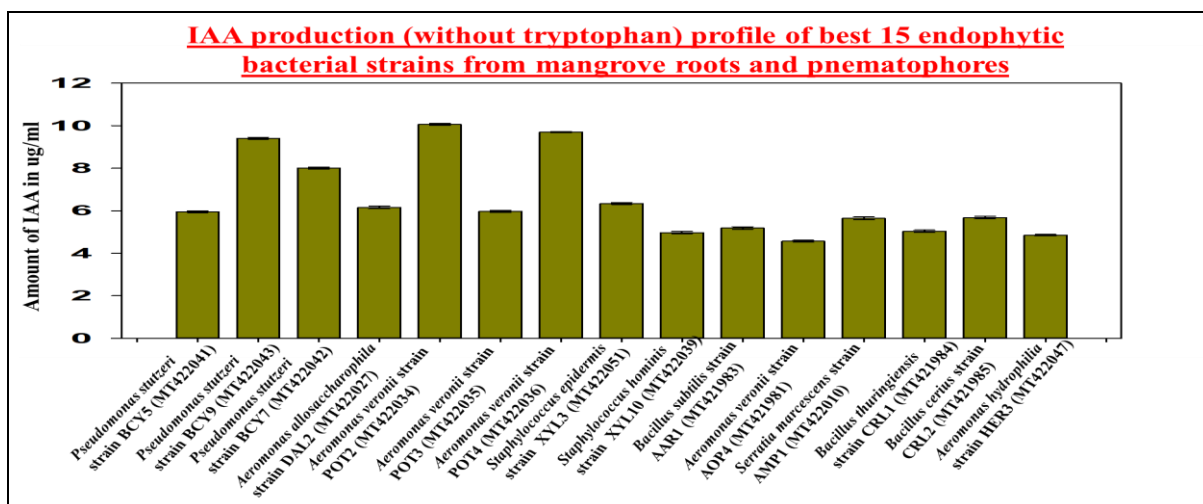


Figure 5.5: Best 15 IAA-producing endophyte bacterial strains (without adding tryptophan) from mangrove roots and pneumatophores. Data were represented as mean \pm standard deviation (n=3) in the above graph.

Other 7 high IAA producer strains are represented below that need not require the addition of tryptophan in the reaction medium and their range of IAA production varied between 1.4-6 μ g/ml.

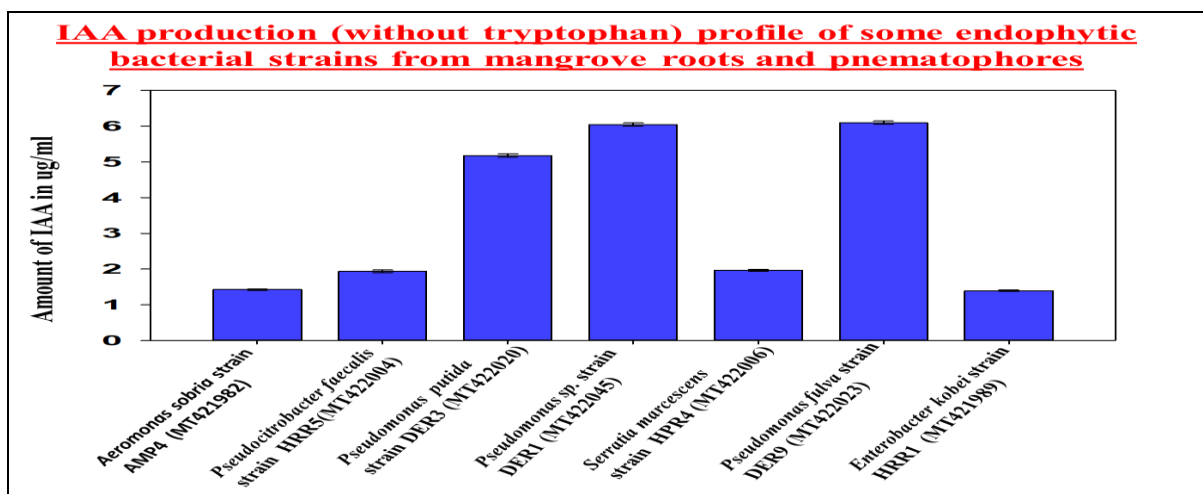


Figure 5.6: Other 7 IAA-producing (without adding tryptophan) endophyte bacterial strains from mangrove roots and pneumatophores. Data were represented as mean \pm standard deviation (n=3) in the above graph.

Observations:

1. The above figure 5.5 and figure 5.6 represents the total 22 endophytic bacterial isolates showing their IAA production activity without the addition of tryptophan in their reaction medium and their range of IAA production varied between 1.4-10 μ g/ml.

2. This finding indicated that about 28% isolated endophytic bacterial strains (22 out of 78) can synthesize the precursor amino acid tryptophan also to produce IAA. These endophytic strains seem to be independent in IAA production in root endosphere and can be the main regulators of root architecture and growth.
3. The other endophytic strains utilize the plant-synthesized tryptophan to produce IAA and thus modulate the root growth and development.

5.7. Phosphate solubilization by different endophytic bacterial strains isolated from mangrove roots and pneumatophores:

One of the important macronutrients for plant growth and development is phosphorus. The amount of phosphorus in average soils is about 0.05% (w/w). From these 0.05% (w/w) phosphorus content only 0.1% of the total P is available to the plants. It is fixed as insoluble form of phosphate. In acidic soils it is fixed as iron and aluminium phosphates and in alkaline soil it is fixed as calcium phosphates. These complexed forms are not available to the plants. Very small number of soil microorganisms have the ability to change insoluble phosphorus (P) to a plant-available form or soluble form. Plants absorb soluble phosphorus in monobasic (H_2PO_4^-) and the dibasic (HPO_4^{2-}) forms. These microorganisms are known as P-solubilizing microorganisms (PSM) including the plant growth-promoting rhizobacteria (PGPR). The utilization of PGPR promotes the phosphorus uptake for the plants and help increase crop yields. Endophytic bacteria are one kind of rhizobacteria that build up and lives their whole life cycle inside the plant roots. They do not show any negative impact on the host plants and build further close associations. Endophytic bacteria are also known as intracellular PGPR (iPGPR). Endophytic bacteria (iPGPR) originate from the outside region or rhizospheric environment and enter into the plant through lenticels, stomata, wounds, lateral roots and site of emergence of germinating radicals (Walia et al, 2017).

A few bacterial genera with known phosphate solubilizing potentials are already established such as *Mesorhizobium*, *Klebsiella*, *Rhizobium*, *Acinetobacter*, *Achromobacter*, *Erwinia*, *Enterobacter*, *Pseudomonas*, *Micrococcus* and *Bacillus* (Walia et.al. 2017). In this study, phosphate solubilization potential was studied under laboratory conditions for 78 endophytic bacterial strains to assume their activity under degraded and non-degraded mangrove habitats.

5.8. Calibration curve of plant-available phosphorus for phosphate solubilization assay.

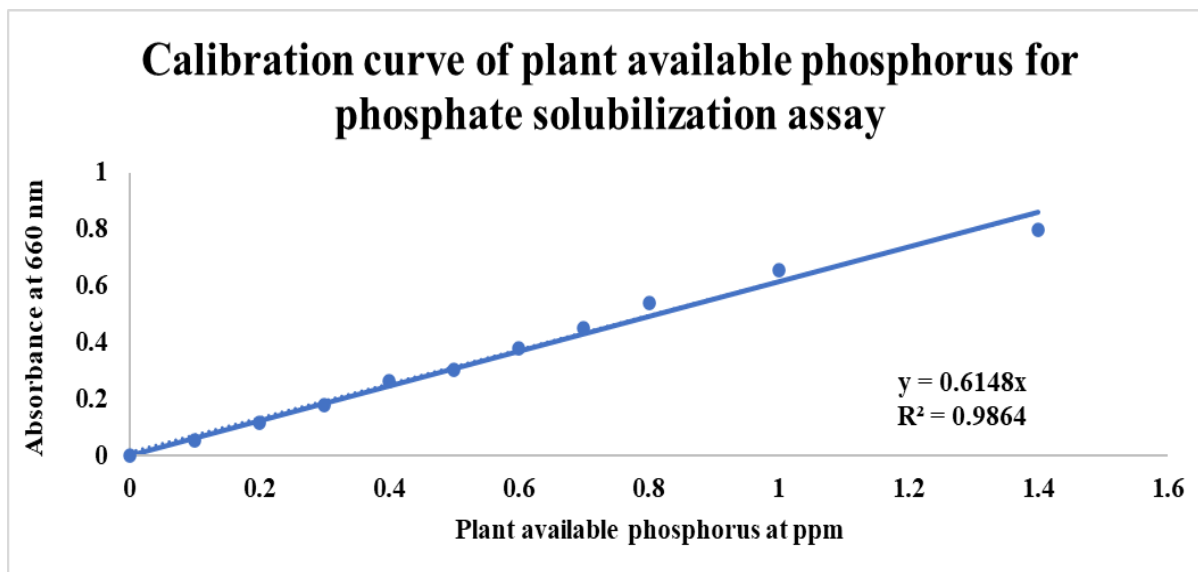


Figure 5.7: The calibration curve of plant-available phosphorus in phosphorus solubilization assay to measure the unknown concentration of plant-available phosphorus released by different endophytic bacterial strains.

Phosphate solubilization by isolated endophytic bacterial strains:

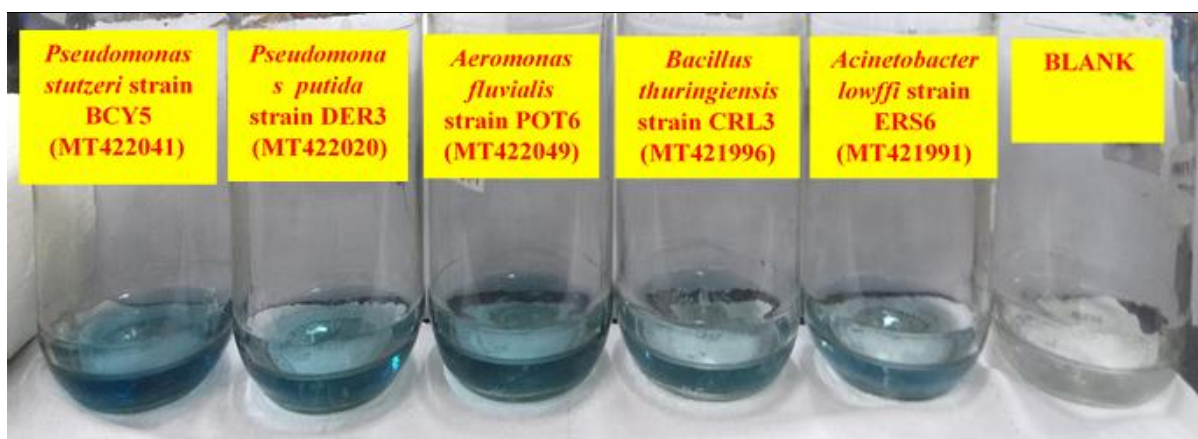


Figure 5.8: Phosphorus solubilization by endophytic bacterial strains isolated from mangrove roots and pneumatophores from Indian Sundarbans. In this picture the blue coloured culture filtrate indicated phosphate solubilization by endophytic bacterial strains.

5.9. Evaluation of phosphorus solubilization potential of 78 endophyte accessions:

The all 78 endophytic bacteria were tested for their phosphorus (P) solubilization potential. The best 15 high P-solubilizer strains are represented below.

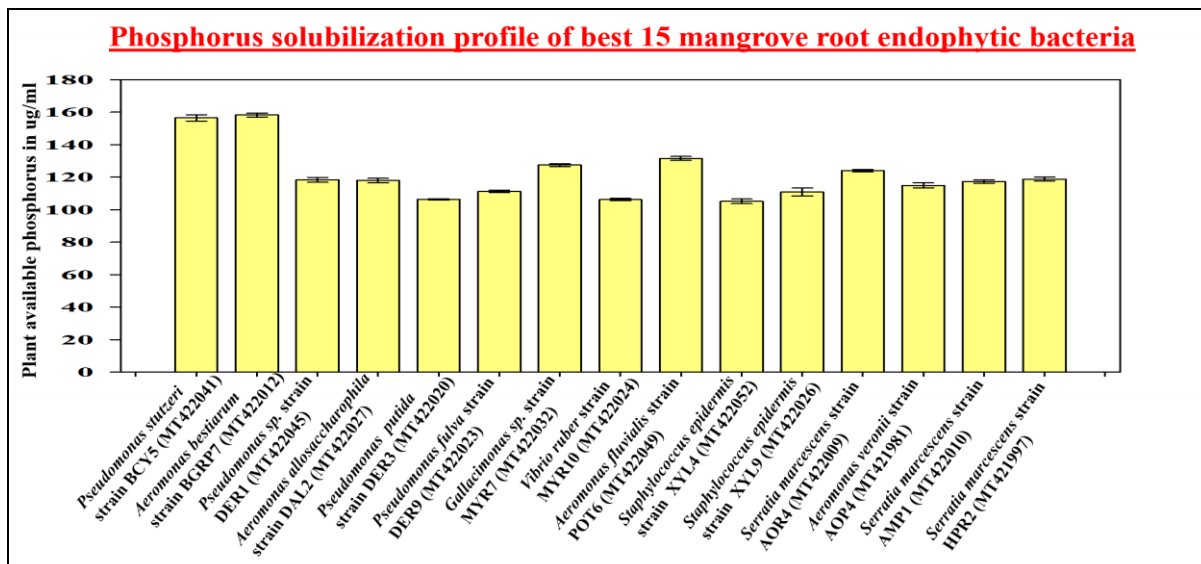


Figure 5.9: Best 15 P-solubilizer endophyte bacterial strains isolated from mangrove roots and pneumatophores. Data were represented as mean \pm standard deviation (n=3) in the above graph.

Observations:

The best 15 high P-solubilizer strains are represented above and their range of P-solubilization varied between 90-160 μ g of plant-available P released/ml of PSM.

5.10. Analysis of phosphorus solubilization by endophytic bacterial isolates against their source niches of diverse species of mangrove roots and pneumatophores

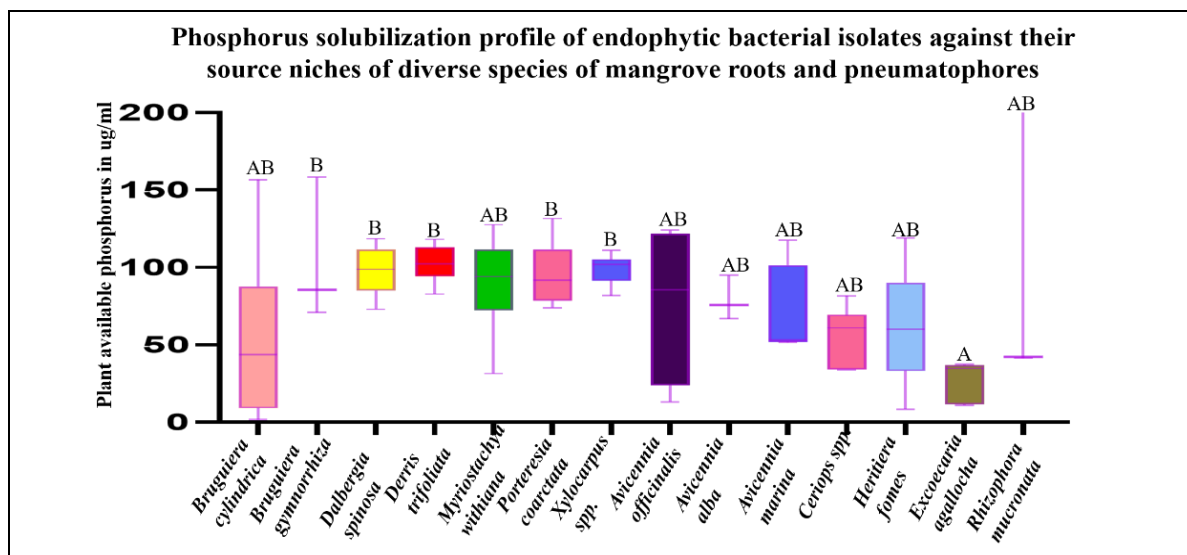


Figure 5.10: Diverse mangrove root environments as source of differential P-solubilizing endophytic bacterial strains. Data were represented as mean \pm standard deviation (n=3) in the above graph.

Observations:

The figure above depicts the diverse mangrove root environments as resource niches of differential P-solubilizing traits of 78 accessioned strains. The high P-solubilizers belong to almost all mangrove species studied here except *Excoecaria agallocha* and *Rhizophora mucronata* roots and pneumatophores.

5.11. Siderophore production activity by different endophytic bacterial strains isolated from mangrove roots and pneumatophores:

Siderophores function as solubilizing or chelating agents for iron from insoluble form of iron. Iron is an essential trace element which are necessary for plants and microbes both for their entire life-cycle. In the aerobic condition iron is found mainly as Fe^{3+} , converted to hydroxides and oxyhydroxides which are insoluble and unavailable to microorganisms. Iron oxidizing bacteria play a very important role to sequester this Fe^{3+} making them easily available to plants. One of the most common trait is siderophore production evolved by the bacteria, which play a very crucial role to chelate iron to make it easily available to others (Rajkumar et al, 2010 ; Andrews and Duckworth, 2016). In this study, siderophore production assay was studied under

laboratory conditions for 78 endophytic bacterial strains to assume their plant growth promoting activity under degraded and non-degraded mangrove habitats.

Siderophore production by isolated endophytic bacterial strains

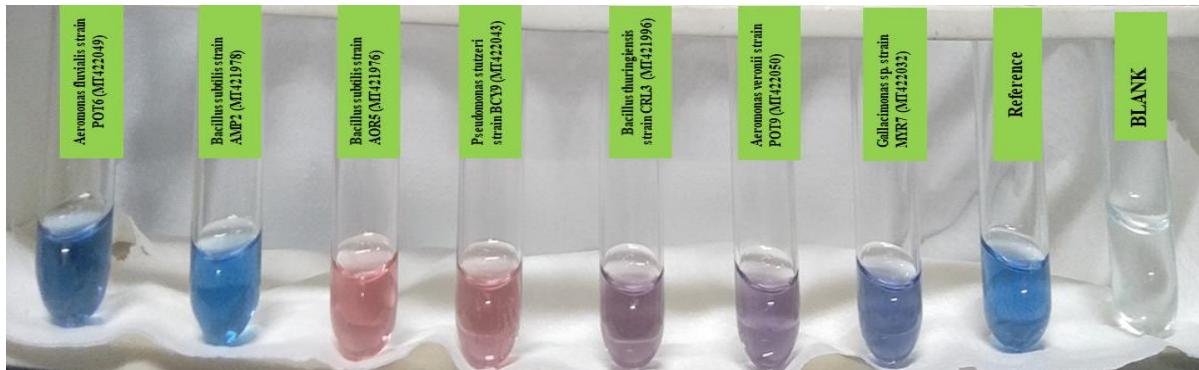


Figure 5.11: Siderophore activity by endophytic bacterial strains isolated from mangrove roots and pneumatophores from Indian Sundarbans. In this picture the pink coloured filtrates indicated siderophore production by bacterial strains.

5.12. Evaluation of siderophore production potential of 78 endophyte accessions:

The all 78 endophytic bacteria were tested for their siderophore production potential. The best 15 high siderophore producing strains are represented below.

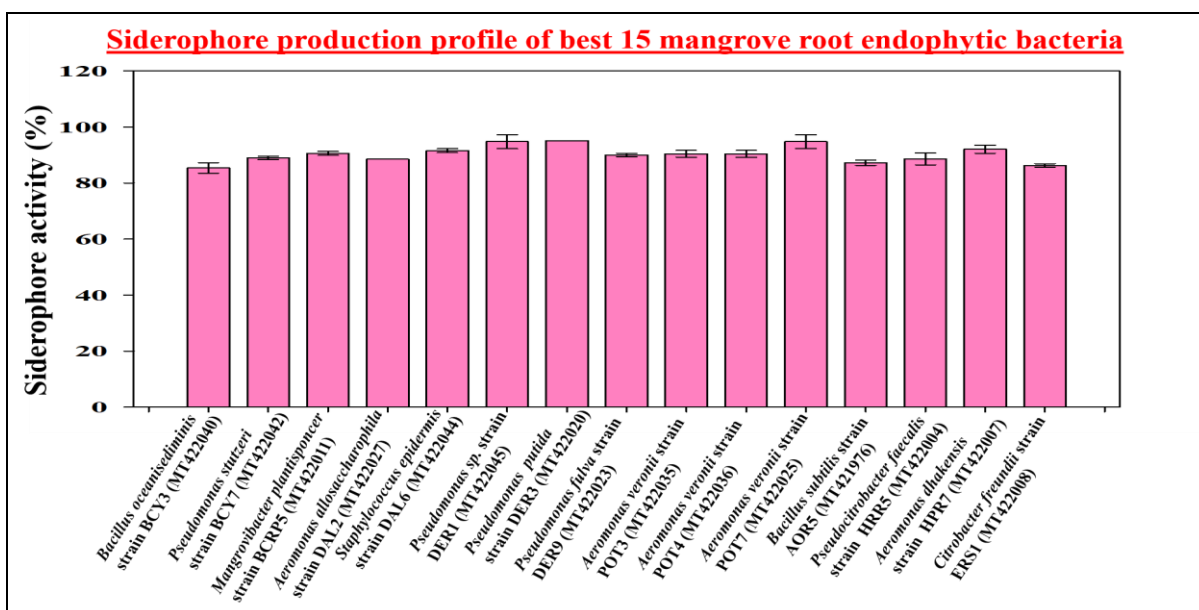


Figure 5.12: Best 15 siderophore producing endophyte bacterial strains from mangrove roots and pneumatophores. Data were represented as mean \pm standard deviation (n=3) in the above graph.

Observations:

The best 15 high siderophore producing strains are represented above and their range of siderophore production activity varied between 80%-95% in iron-free media.

5.13. Analysis of siderophore production by endophytic bacterial isolates against their source niches of diverse species of mangrove roots and pneumatophores

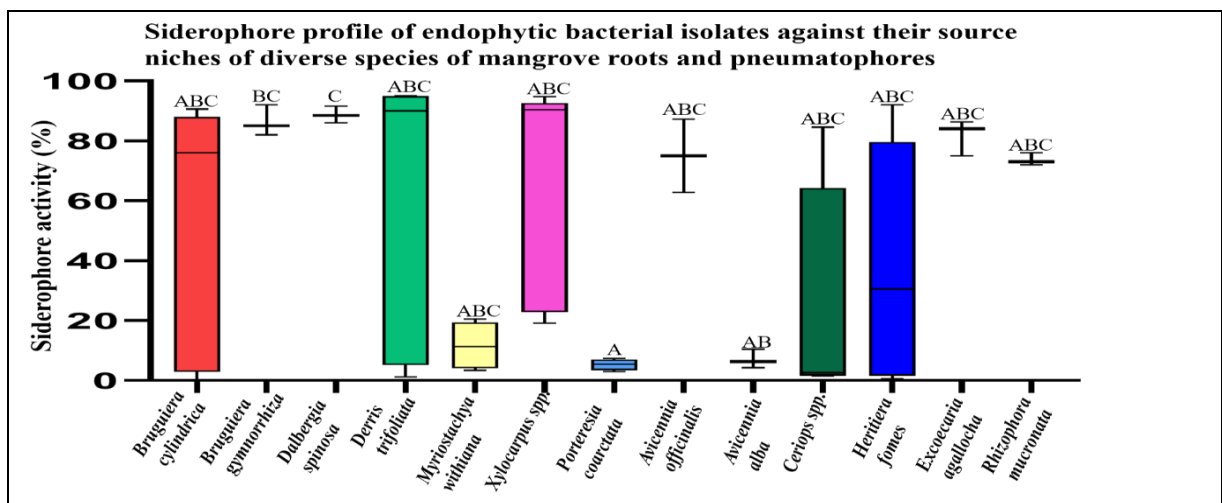


Figure 5.13: Diverse mangrove root environments as source of differential siderophore producing endophytic bacterial strains.

Observations:

The figure above depicts the diverse mangrove root environments as resource niches of differential siderophore producing traits of 78 accessioned strains. The range of siderophore production percentage varies from low to high in endophytic strains from *Bruguiera cylindrica*, *Derris trifoliata*, *Xylocarpus spp.*, *Ceriops spp.*, and *Heritiera fomes*. *Bruguiera gymnorhiza*, *Dalbergia spinosa*, *Avicennia officinalis*, *Excoecaria agallocha* and *Rhizophora mucronata* roots and pneumatophores seem to be niche of high siderophore producers while *Myriostachya*, *Porteresia* and *Avicennia alba* are found to harbour low siderophore producers.

5.14. Quantitative estimation of siderophore by universal CAS assay:

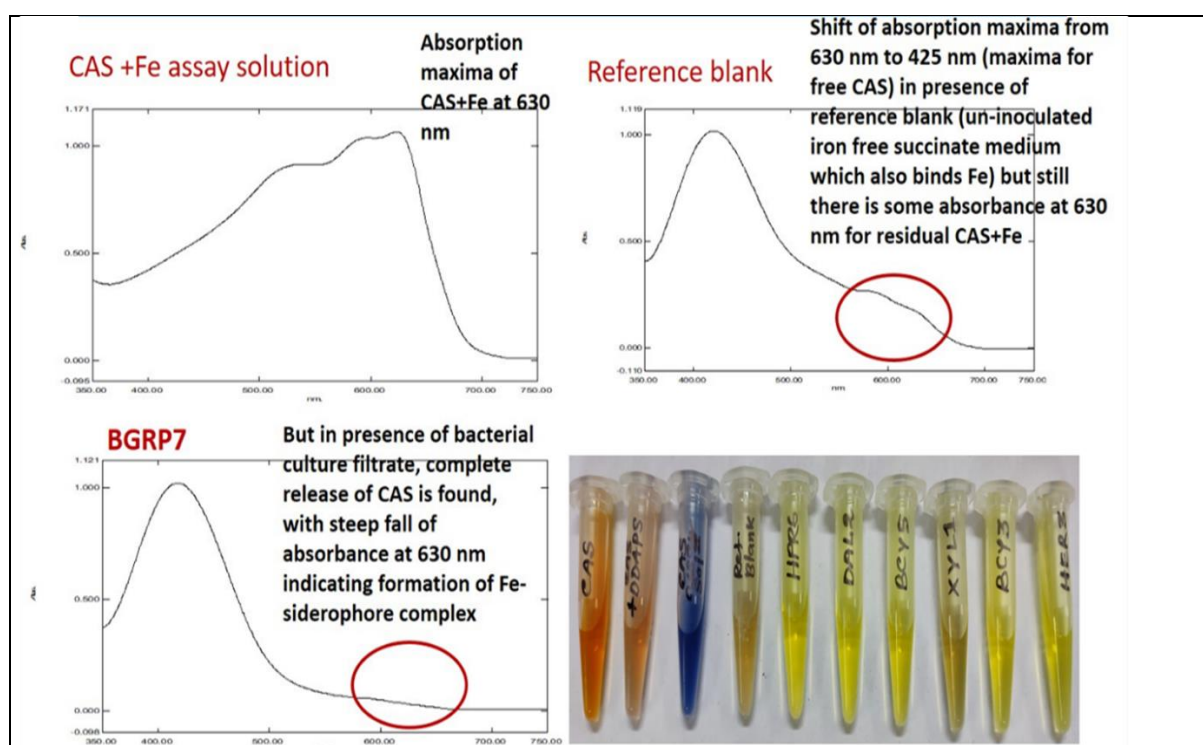


Figure 5.14: Quantitative estimation of siderophore by universal CAS assay. (i) Absorption maxima of CAS+Fe at 630nm; (ii) Shift of absorption maxima from 630 nm to 425 nm (maxima for free CAS) in the presence of reference blank (Un-inoculated iron free succinate medium which also binds Fe but still there is some absorbance at 630 nm for residual CAS+Fe; (iii) In presence of bacterial culture filtrate, complete release of CAS is found, with steep fall of absorbance at 630 nm that indicates the formation of Fe-siderophore complex; (iv) here the yellow colour indicates siderophore production by endophytic bacterial strains.

5.15. ACC deaminase production activity by different endophytic bacterial strains isolated from mangrove roots pneumatophores:

Some plant growth-promoting endophytic bacteria synthesize ACC (l-aminocyclopropane-l-carboxylate) deaminase enzyme (Glick et al, 2007). This enzyme promotes plant growth and development by decreasing the levels of ethylene of plants under several abiotic stresses such as high light, extremes of temperature, drought, flooding, high salt, and different biotic stresses like infection by pathogens including bacteria, viruses and fungi. When ethylene level is high then it affects plant growth and development. Ethylene is actually known as an anti-growth hormone or stress hormone as well as a plant growth regulator. l-aminocyclopropane-l-carboxylate (ACC) deaminase enzyme helps decreasing plant ethylene levels via decomposing ACC, the precursor of ethylene phytohormone. In this study, ACC deaminase activity assay

was studied for 78 endophytic bacterial strains under laboratory conditions to speculate on their plant growth facilitation activity under degraded and non-degraded mangrove habitats.

5.16. Calibration curve preparation for ACC deaminase assay:

5.16.a. Calibration curve of α -ketobutyrate for ACC deaminase assay:

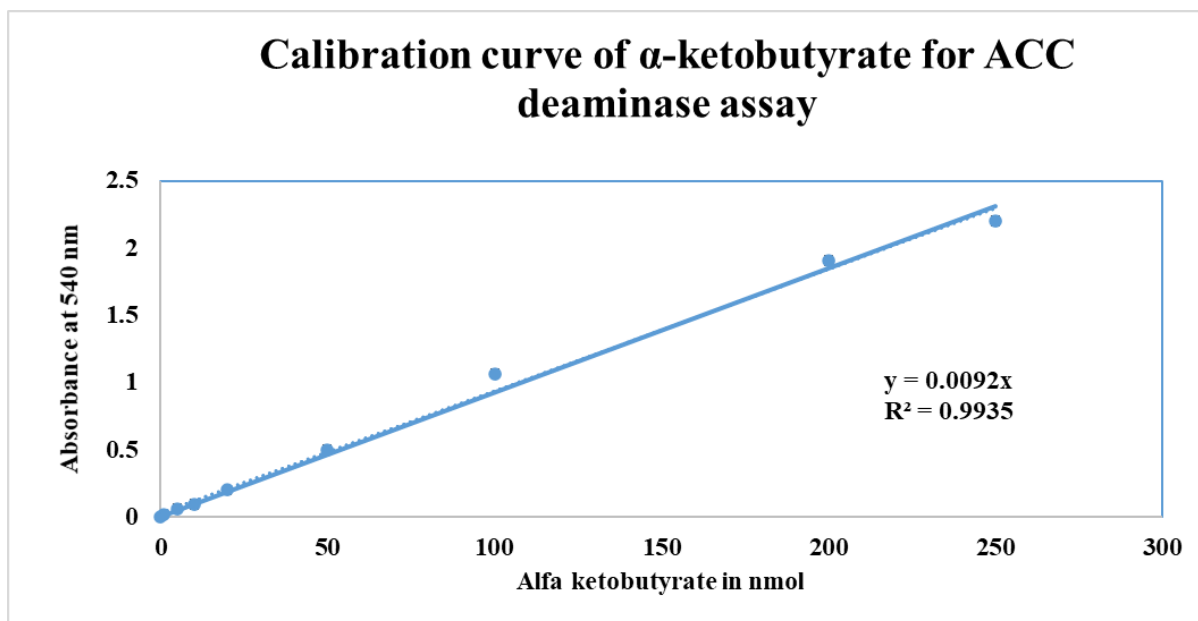


Figure 5.15: The calibration curve of ACC deaminase to measure the unknown concentration of α -ketobutyrate for evaluation of ACC deaminase activity from different endophytic bacterial strains.

5.16.b. Calibration curve of protein for ACC deaminase assay:

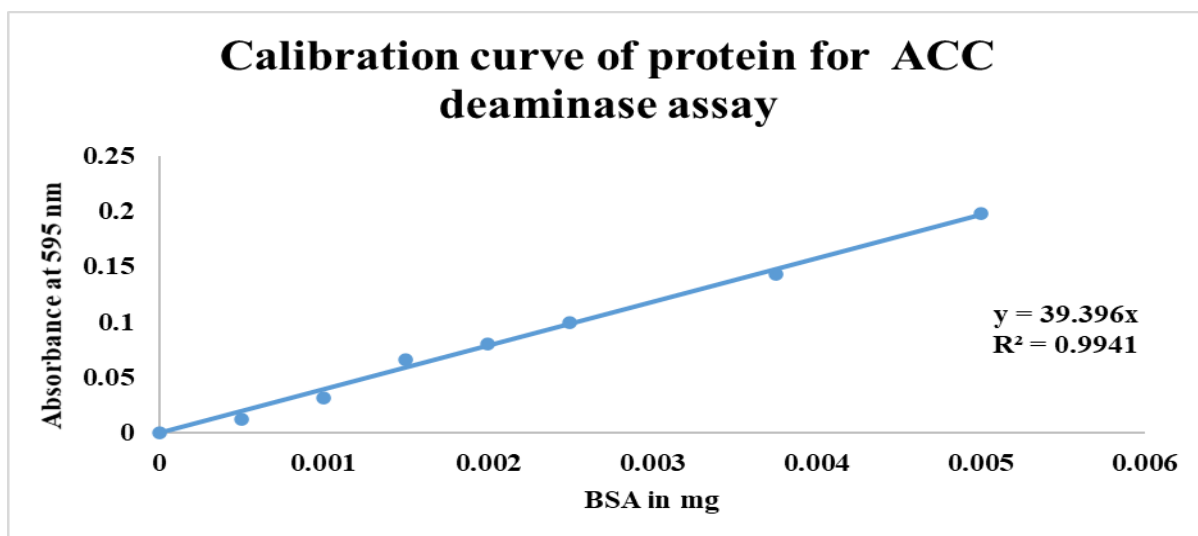


Figure 5.16: The calibration curve of protein for ACC deaminase assay to measure the unknown concentration of protein from different endophytic bacterial strains.

ACC deaminase production by isolated endophytic bacterial strains

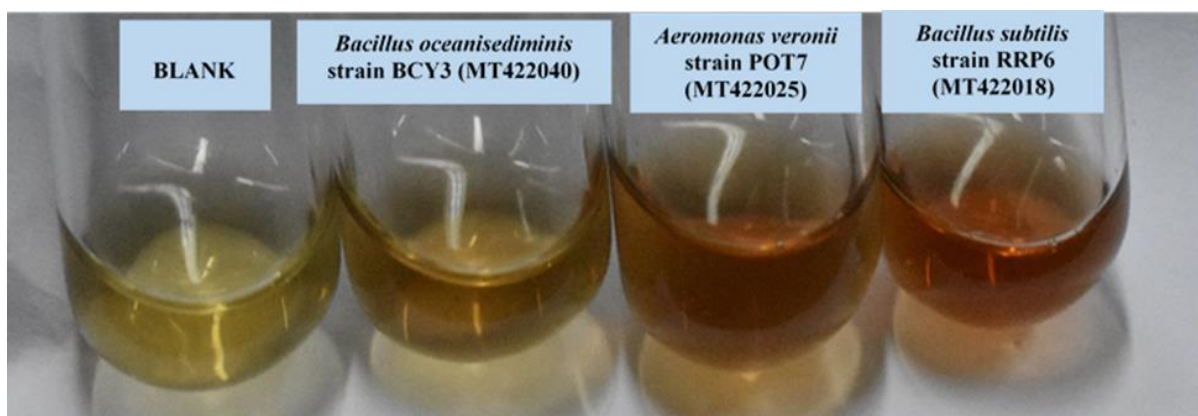


Figure 5.17: ACC deaminase assay by endophytic bacterial strains isolated from mangrove roots and pneumatophores from Indian Sundarbans. In this picture the dark brown colour indicated ACC deaminase production by endophytic bacterial strains.

5.17. Evaluation of ACC deaminase production potential of 78 endophyte accessions:

The all 78 endophytic bacteria were tested for their ACC deaminase production potential. The best 15 high ACC deaminase producing strains are represented below.

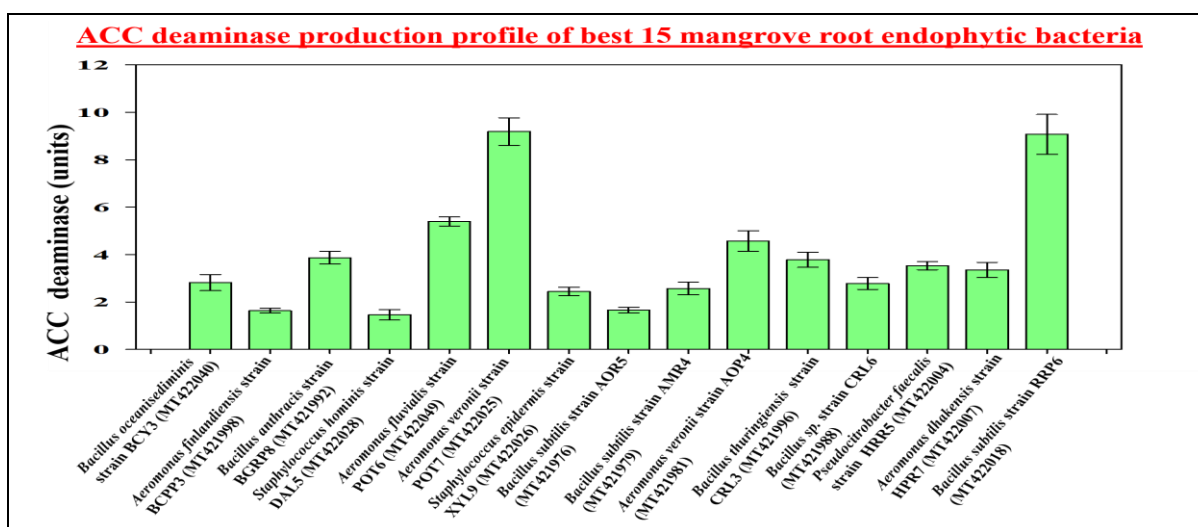


Figure 5.18: Best 15 ACC deaminase producing endophyte bacterial strains from mangrove roots and pneumatophores. Data were represented as mean \pm standard deviation (n=3) in the above graph. ACC deaminase (units) was expressed in $\mu\text{mol}/\text{mg}$ of protein/ hour.

Observations:

The best 15 high ACC deaminase producing strains are represented above and their range of ACC deaminase production units varied between 1.8-9 units.

5.18. Analysis of ACC deaminase production by endophytic bacterial isolates against their source niches of diverse species of mangrove roots and pneumatophores

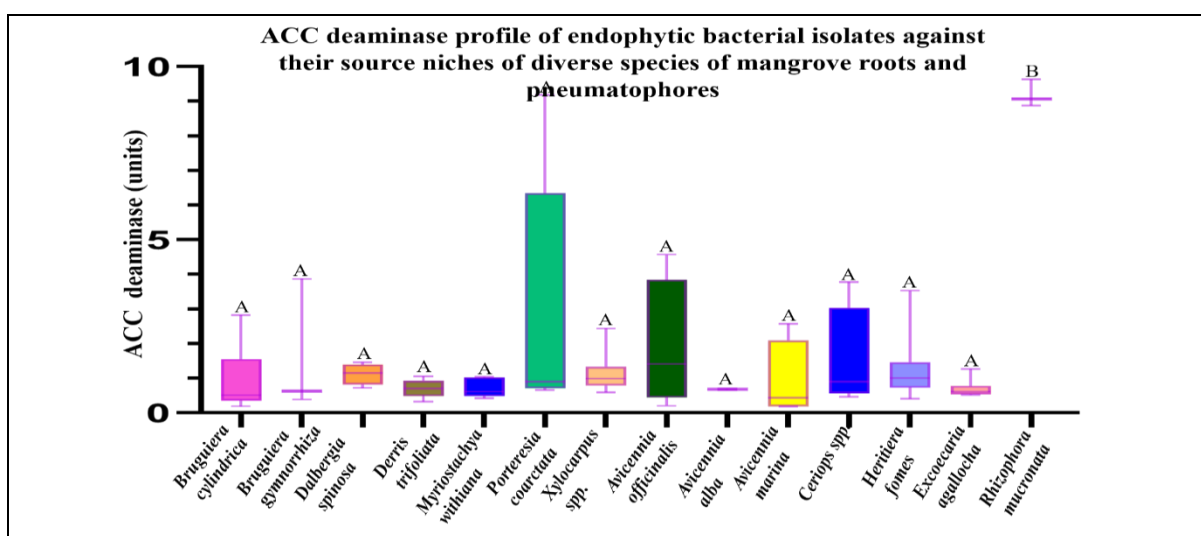


Figure 5.19: Diverse mangrove root environments as source of differential ACC deaminase producing endophytic bacterial strains from Indian Sundarban. Data were plotted as mean \pm standard deviation in the above graph.

Observations:

The figure above depicts the diverse mangrove root environments as resource niches of differential ACC deaminase producing traits of 78 accessioned strains. The range of ACC deaminase unit production is restricted within 3-5 units in most of the mangrove niches for endophytic bacterial strains except for *Porteresia coarctata* and *Rhizophora mucronata*.

5.19. Free nitrogen-fixation by different endophytic bacterial strains isolated from mangrove roots and pneumatophores:

Nitrogen is one of the most important macronutrients for plants for their growth and development. This element plays a very significant function in most plant metabolic processes. In biological nitrogen fixation process the atmospheric nitrogen is transformed into plant-available forms of N. In this process nitrogen-fixing bacteria use the nitrogenase enzyme to convert gaseous nitrogen to ammonia (Kim and Rees, 1994). Nitrogen-fixing bacteria are classified as symbiotic and non-symbiotic nitrogen-fixing bacteria.

The available form of nitrogen in mangrove ecosystem depends on a difficult pattern of bacterial activity. Nitrification occurs in both aerobic and anaerobic condition. Significant inputs of nitrogen (N) to mangrove sediments are provided by litter from the mangrove trees. Depending on the micrometeorological conditions, mangrove ecosystem uses atmospheric ammonia and NO_x as a nitrogen source and recycle various forms of aquatic and atmospheric nitrogen protecting from the negative impacts of nutrient affluence and atmospheric pollution of the coastal ecosystems (Ray et al, 2014).

In anaerobic condition, the organic matter-rich soils of the mangrove ecosystem become favoured niches of for nitrogen fixation and significant source of N. In case of both light-dependent and light-independent nitrogen fixation process, higher levels of nitrogen fixation have been observed in endophytic microbial associations in the tree leaves, roots, and pneumatophores and also in rhizospheric soil (Reef et al, 2010).

5.20. Evaluation of free nitrogen-fixing potential of 78 endophyte accessions:

The all 78 endophytic bacteria were tested under laboratory conditions for their free nitrogen fixing potential. The best 11 high free nitrogen-fixing strains are represented below:

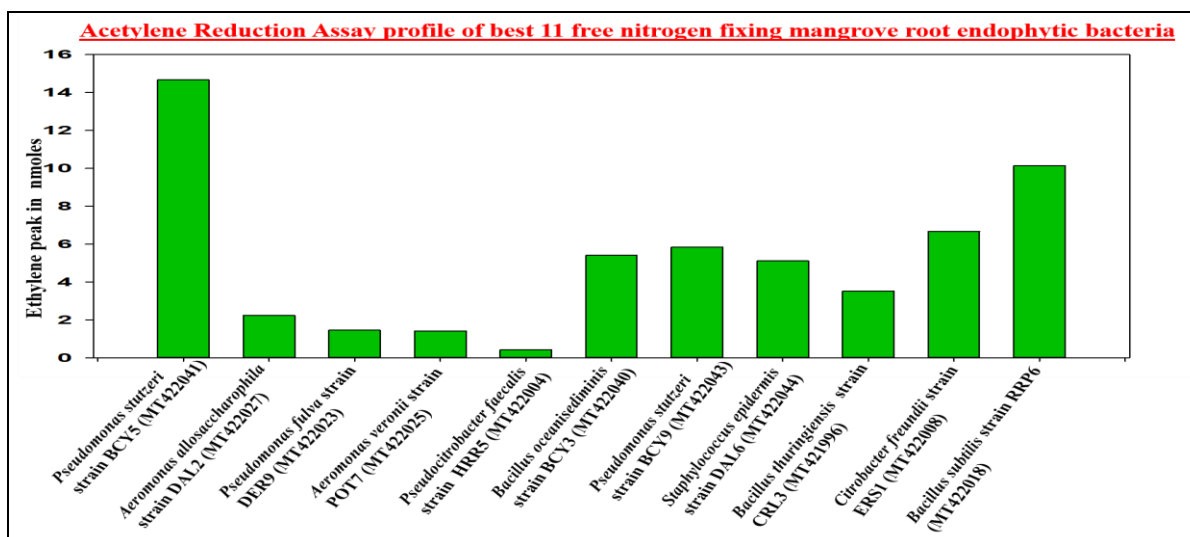


Figure 5.20: The best 11 free nitrogen-fixing endophyte bacterial strains from mangrove roots and pneumatophores from Indian Sundarbans. Acetylene reduction potential was expressed as nmol/100 μ l/24 hours.

Observations:

The best 11 high free nitrogen fixing strains are represented above with their range of reduced ethylene synthesis in the range of 0.4-14 nmoles.

5.21. Analysis of free nitrogen-fixation by endophytic bacterial isolates against their source niches of diverse species of mangrove roots and pneumatophores

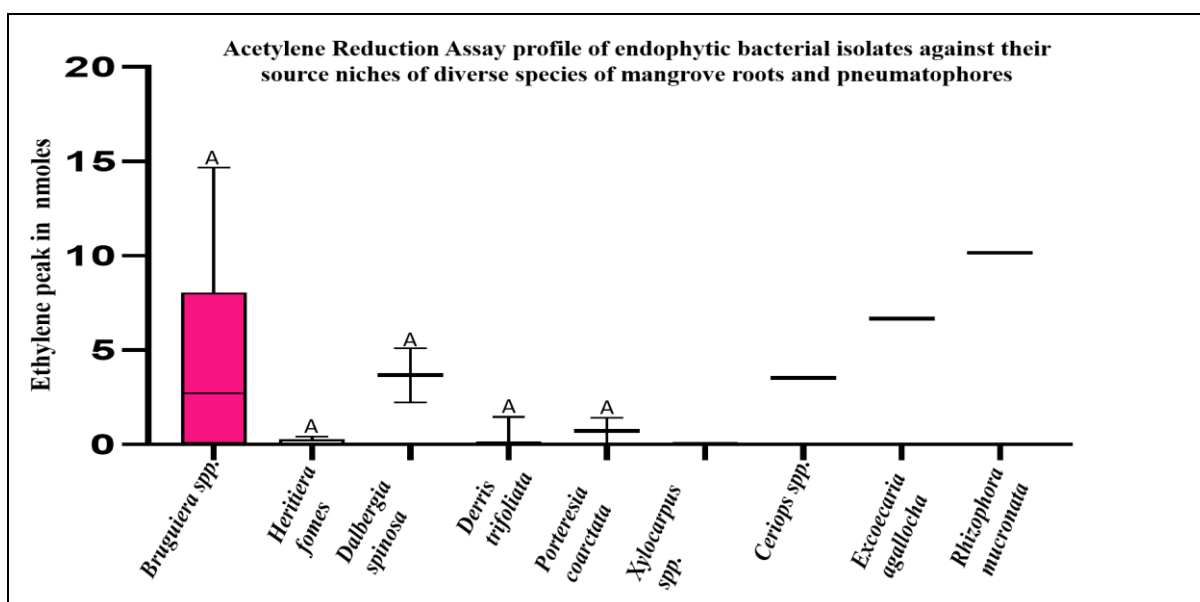


Figure 5.21: Diverse mangrove root environments as source of differential free nitrogen-fixing endophytic bacterial strains.

Observations:

The figure above depicts the diverse mangrove root environments as resource niches of differential free nitrogen-fixing traits of 18 accessioned strains in total. The range of free nitrogen-fixation activity demonstrated a wide range for strains isolated from *Bruguiera* spp. as source niches, with other mangrove species as abode of low to high acetylene reduction potential-having free nitrogen-fixers.

The all 18 strains were quantified for their growth on FNFM medium in terms of CFU (colony forming units) per 100 μ l of liquid FNFM. The results are depicted in the below figure. For the count of CFU on FNFM, bacterial cells were serially diluted by using sterile distilled water. Then petri plates containing bacterial cells were incubated for 3 days at (72 hours) $28 \pm 2^\circ\text{C}$ until bacterial colonies were found to grow. Then CFU was counted for every plate and recorded.

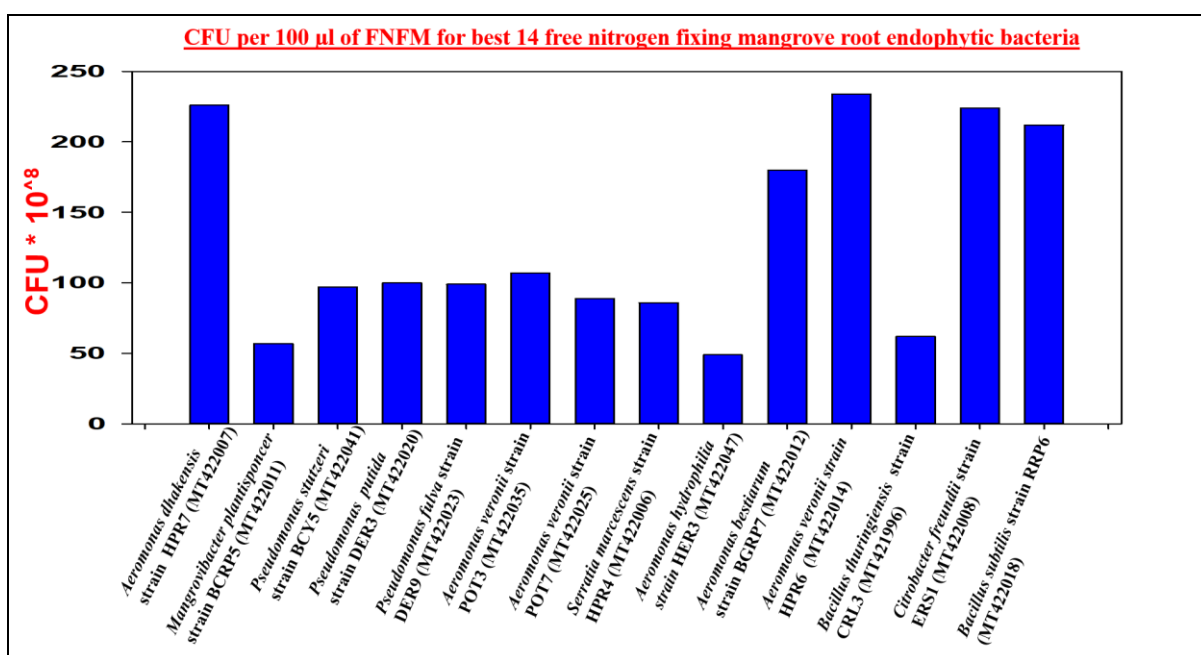


Figure 5.22: CFU per 100 μ l of FNFM for best 14 free nitrogen-fixing endophyte bacterial strains from mangrove roots and pneumatophores

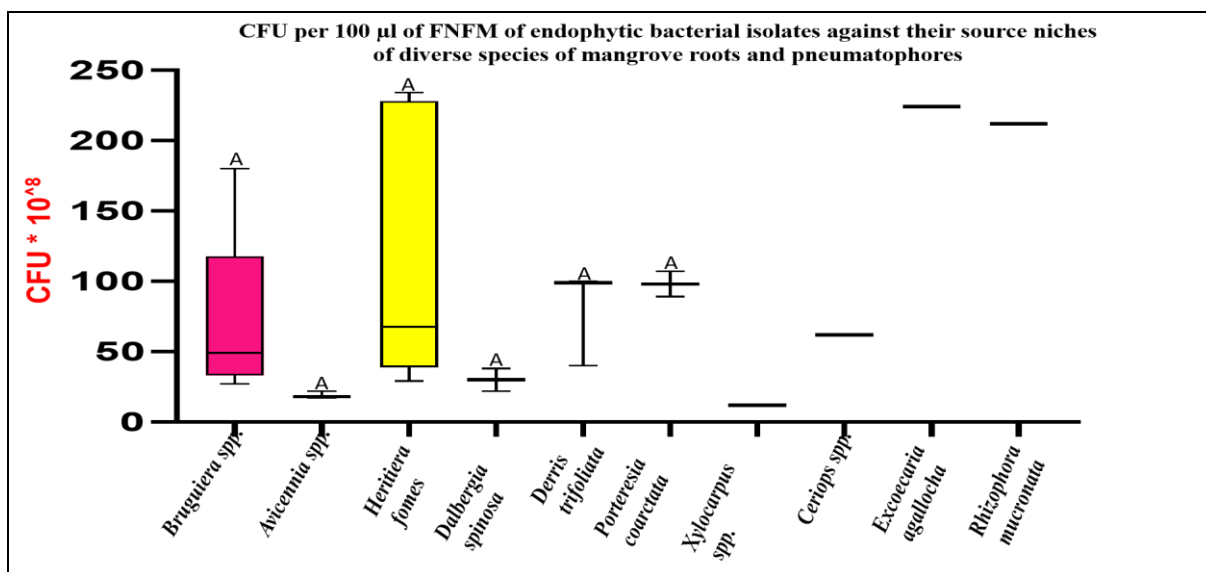


Figure 5.23: Diverse mangrove root environments as source of differential free nitrogen-fixing endophytic bacterial strains in terms of CFU per 100 µl of FNF broth.

Observations:

The figure above depicts the diverse mangrove root environments as resource niches of differential free nitrogen-fixing traits of 18 accessioned strains in terms of CFU per 100 µl of liquid FNFM. A wide range of CFU per 100 µl of liquid FNFM is observed for isolates from *Bruguiera* spp. and *Heritiera fomes* as source niches, with other mangrove species as abode of low to medium CFU per 100 µl of liquid FNFM except for *Excoecaria* and *Rhizophora* which harbour strains showing above 200*10⁸ CFU per 100 µl of liquid FNFM.

5.22. Some chromatograms of the high acetylene reducers are presented below:

The figures below demonstrate the chromatograms of some bacterial strains showing a high peak of ethylene (conversion of acetylene to ethylene). Un-inoculated medium or control medium was used as a reference blank where no conversion of acetylene to ethylene took place. Some chromatograms of the high acetylene reducers are presented below:

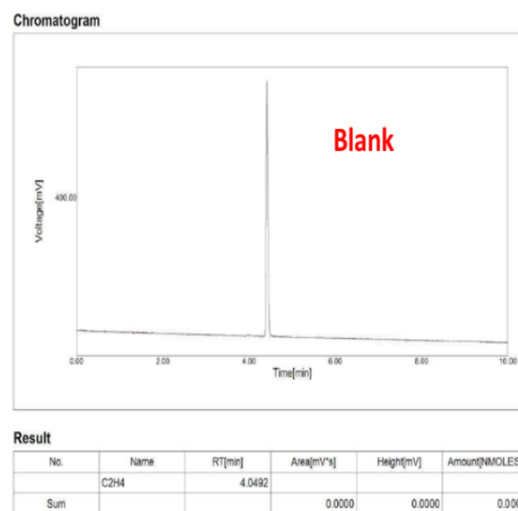
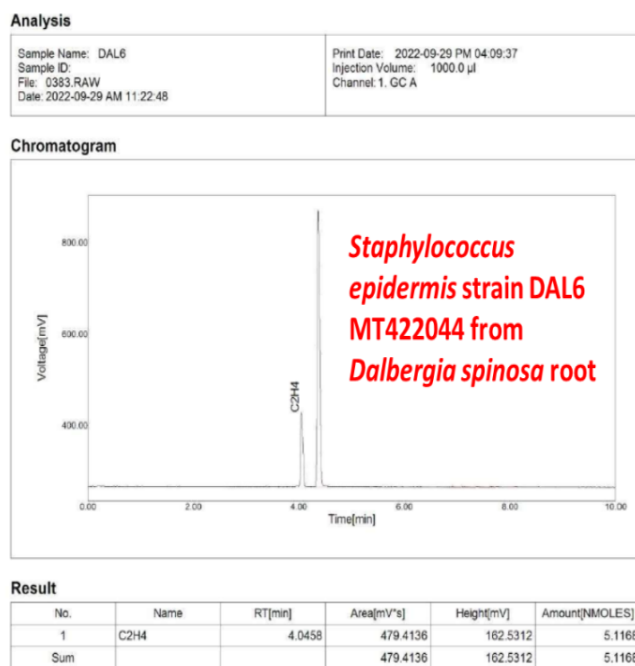


Figure 5.24: Chromatogram of *Staphylococcus epidermis* strain DAL6 (MT422044) from *Dalbergia spinosa* root. The amount of Acetylene Reduction is 5.116 nmol under lab condition.

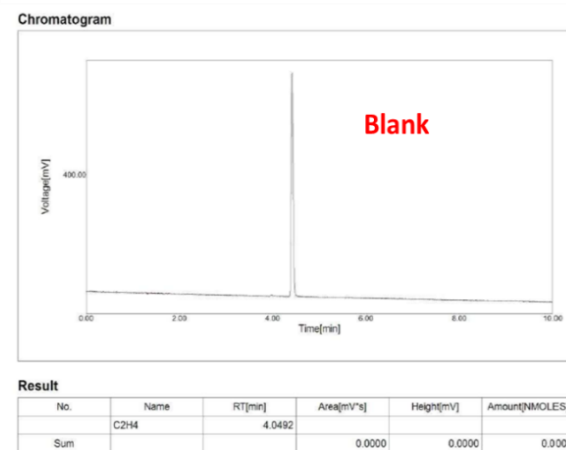
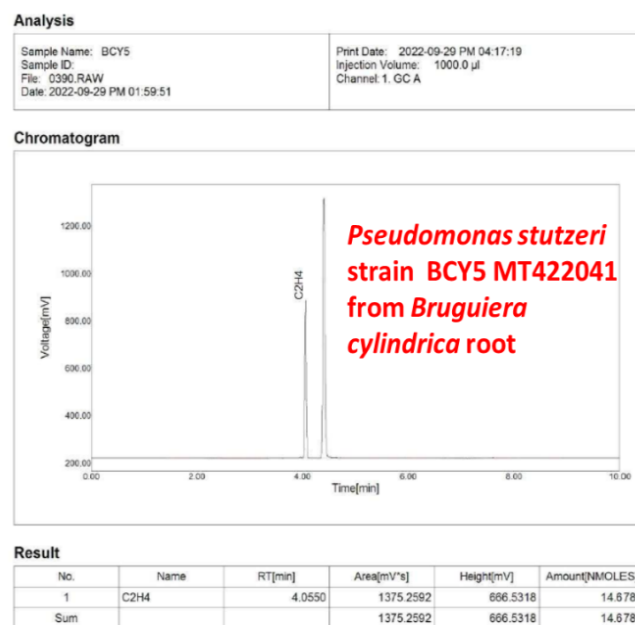


Figure 5.25: Chromatogram of *Pseudomonas stutzeri* strain BCY5 (MT422041) from *Bruguiera cylindrica* root. The amount of Acetylene Reduction is 14.678 nmol under lab condition.

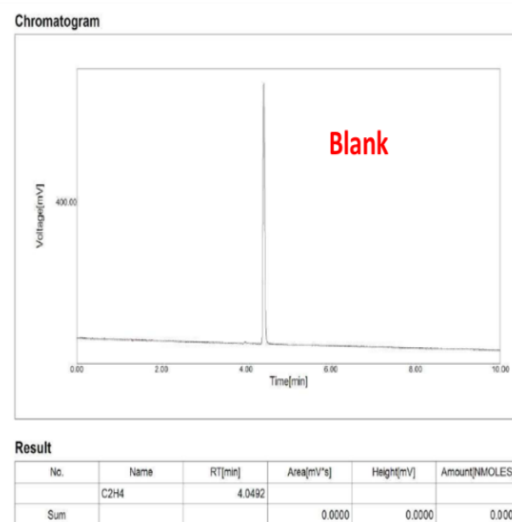
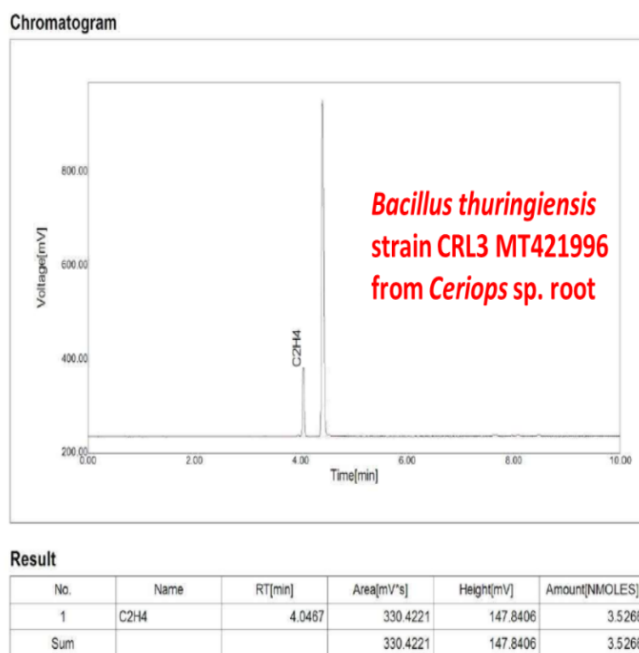


Figure 5.26: Chromatogram of *Bacillus thuringiensis* strain CRL3 (MT421996) from *Ceriops* sp. root. The amount of Acetylene Reduction is 3.526 nmol under lab condition.

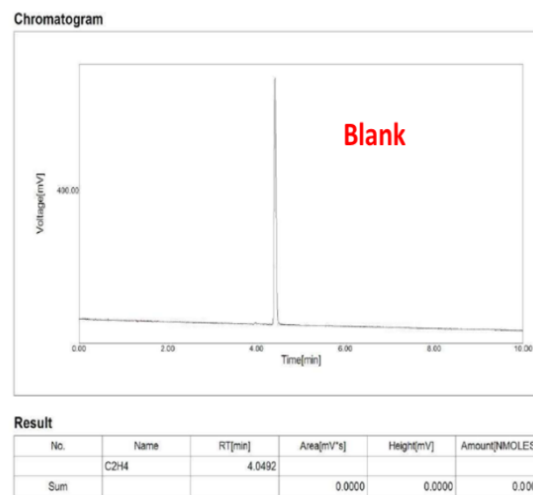
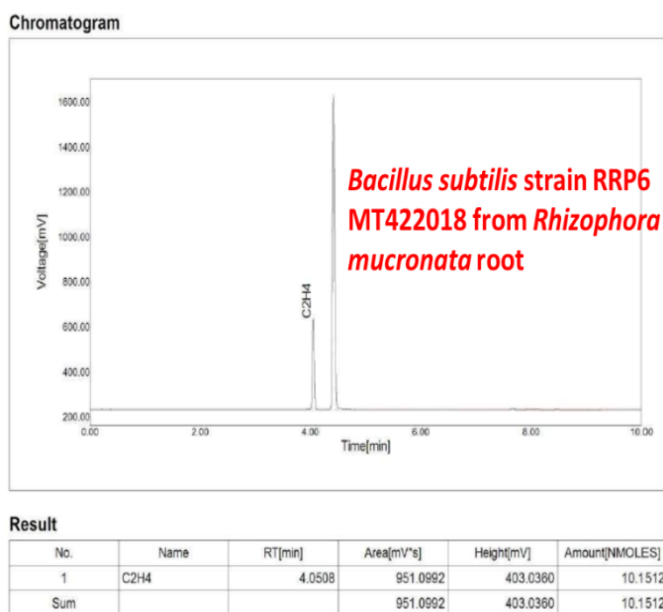


Figure 5.27: Chromatogram of *Bacillus subtilis* strain RRP6 (MT422018) from *Rhizophora mucronata* root. The amount of Acetylene Reduction is 10.151 nmol under lab condition.

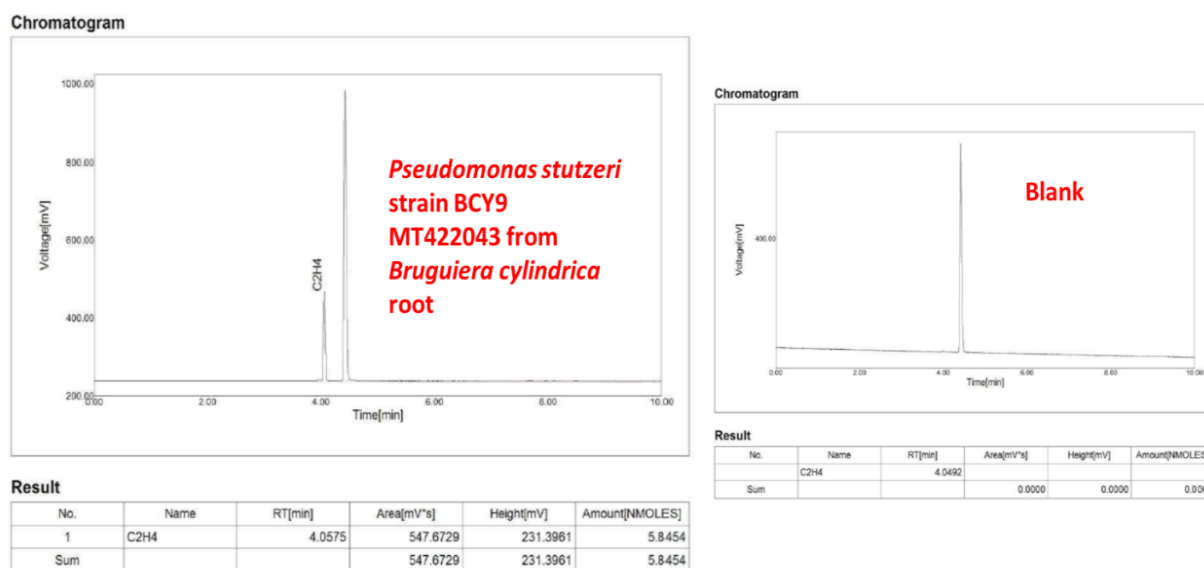


Figure 5.28: Chromatogram of *Pseudomonas stutzeri* strain BCY9 (MT422043) from *Bruguiera cylindrica* root. The amount of Acetylene Reduction is 5.845 nmol under lab condition.

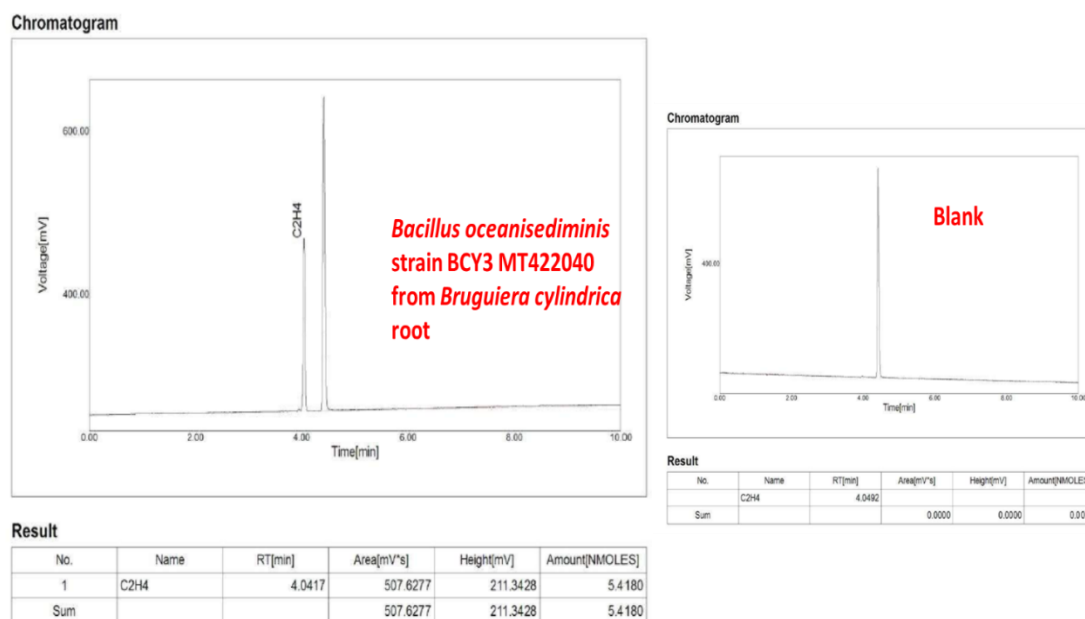


Figure 5.29: Chromatogram of *Bacillus oceanisediminis* strain BCY3 (MT422040) from *Bruguiera cylindrica* root. The amount of Acetylene Reduction is 5.418 nmol under lab condition.

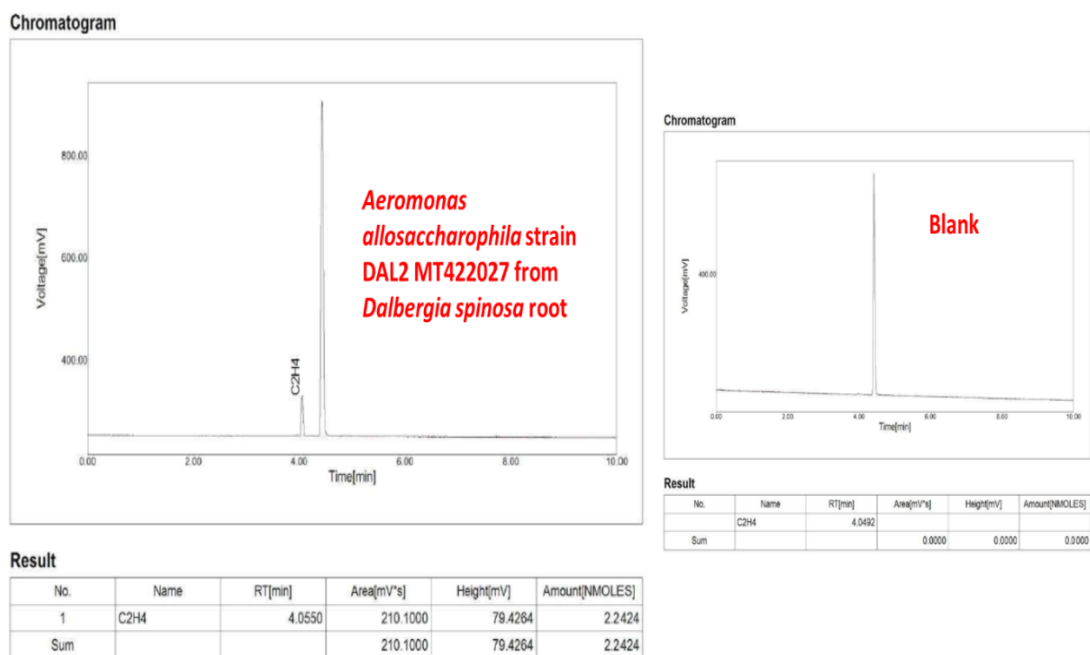


Figure 5.30: Chromatogram of *Aeromonas allosaccharophila* strain DAL2 (MT422027) from *Dalbergia spinosa* root. The amount of Acetylene Reduction is 2.242 nmol under lab condition.

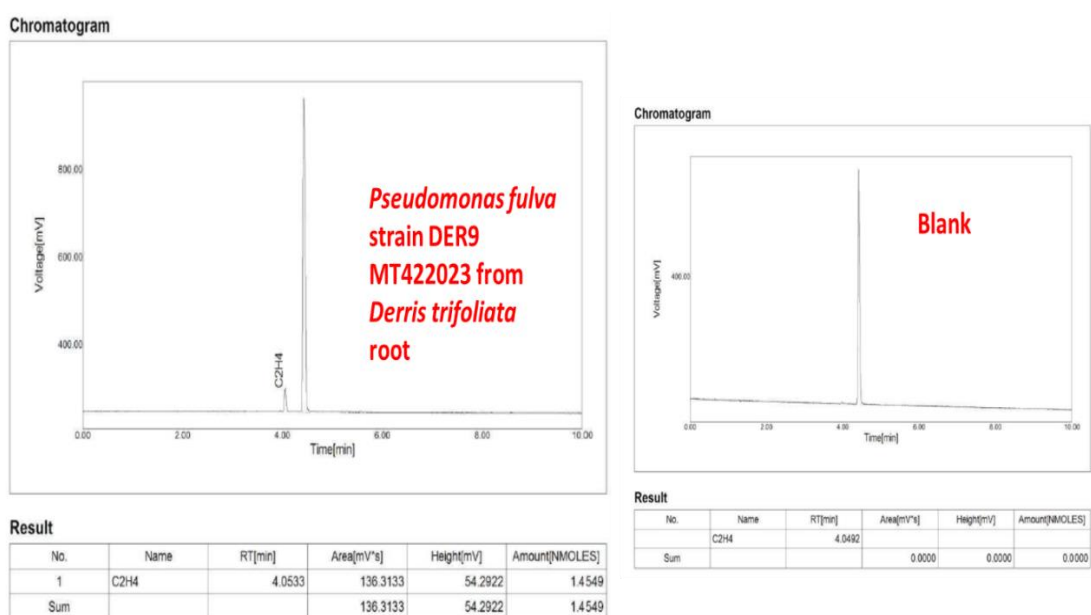


Figure 5.31: Chromatogram of *Pseudomonas fulva* strain DER9 (MT422023) from *Derris trifoliata* root. The amount of Acetylene Reduction is 1.455 nmol under lab condition.

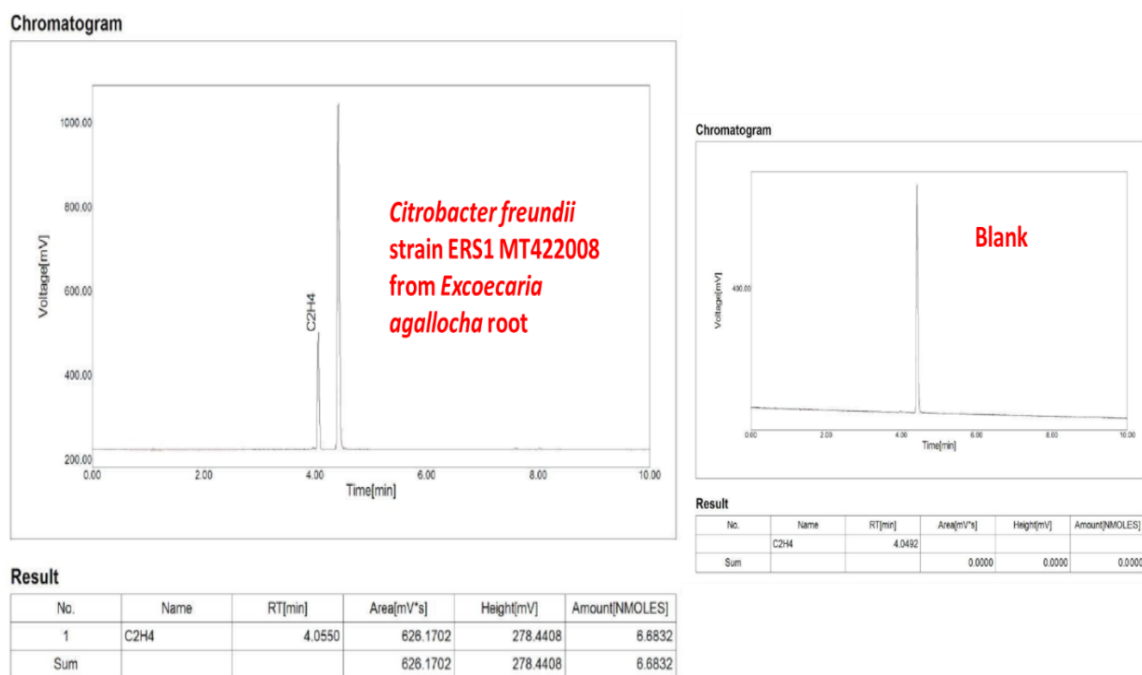


Figure 5.32: Chromatogram of *Citrobacter freundii* strain ERS1 (MT422008) from *Excoecaria agallocha* root. The amount of Acetylene Reduction is 6.683 nmol under lab condition.

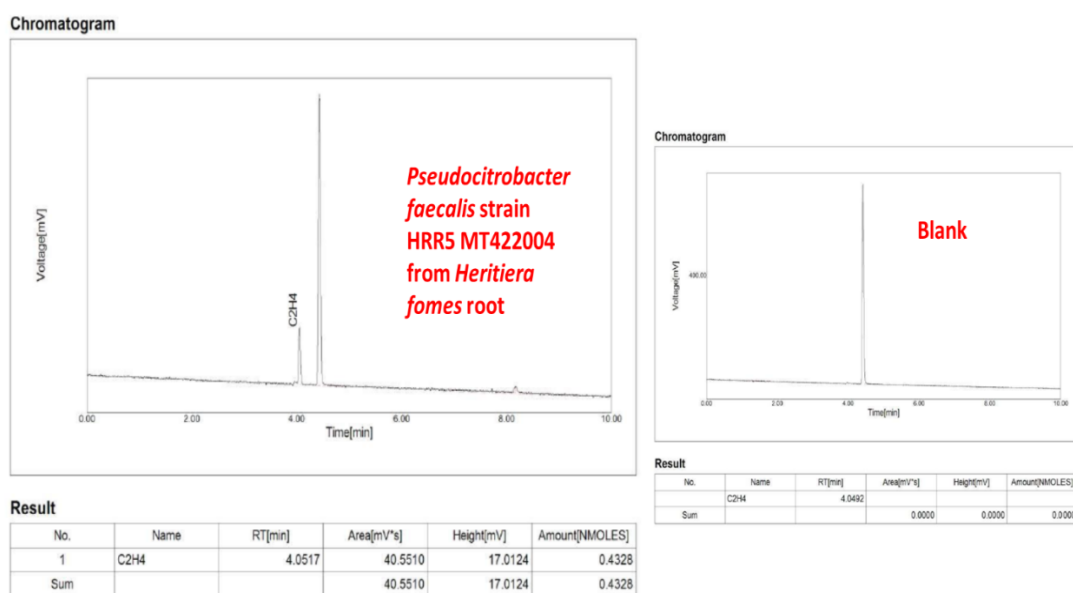


Figure 5.33: Chromatogram of *Pseudocitrobacter faecalis* strain HRR5 (MT422004) from *Heritiera fomes* root. The amount of Acetylene Reduction is 0.433 nmol under lab condition.

5.23. Testing of salt tolerance profile of some best PGP endophytic bacterial strains developed in this study:

Salt tolerance profile was tested by quantifying growth by measuring absorbance at 600 nm for some promising endophytic free nitrogen fixers, cellulose degraders and P-solubilizers on FNFM/CDM/PSM normal broth (3.99-5.44 dS/m), and also normal FNFM/CDM/PSM with additional 0.3M NaCl (25.23-31.94 dS/m), with additional 0.5 M NaCl (36.15-45.72 dS/m), and with additional 0.7 M (45.09-56.73 dS/m), for 72 hrs starting at 0.1 OD at 0 hr. However, in most of the cases, the growth on FNFM/CDM/PSM broth without or with NaCl decreased in absorbance rather than increase after 72 hrs. *Aeromonas veronii* strain POT3 (MT422035) showed noticeable increase in O.D. up to FNFM+ 0.5M NaCl and *Acinetobacter lowffi* strain ERS6 (MT421991) showed increase in O.D. up to CDM+ 0.5M NaCl. In contrast, several P-solubilizer strains showed high tolerance upto PSM+0.5M NaCl, even in some cases up to PSM+0.7M NaCl, viz. *Pseudomonas* sp. strain DER1 (MT422045), *Pseudomonas putida* strain DER3 (MT422020), *Pseudomonas putida* strain DER6 (MT422021), *Pseudomonas putida* strain DER8 (MT422022), *Pseudomonas fulva* strain DER9 (MT422023), *Pseudomonas putida* strain DER10 (MT422046), *Aeromonas veronii* strain HPR6 (MT422014), *Aeromonas dhakensis* strain HPR7 (MT422007), *Mangrovibacter plantisponcer* strain BCRP5 (MT422011), *Enterobacter kobei* strain HRR1 (MT421989), even after 72 hrs of continuous incubation. Below are the figures representing the results of salt tolerance tests.

5.24. Testing of salt tolerance profile of some best PGP endophytic bacterial strains on free nitrogen-fixing medium (FNFM):

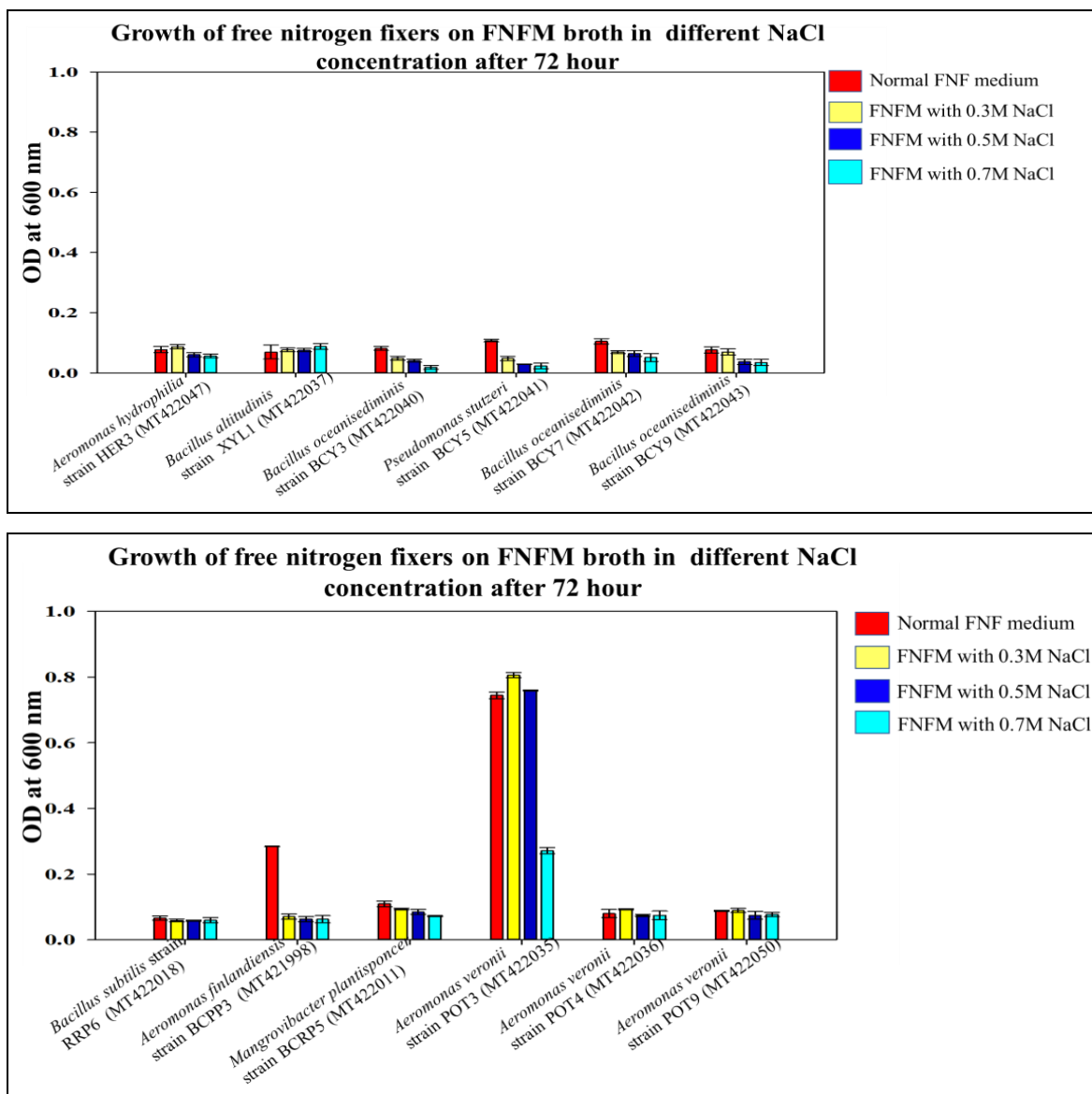


Figure 5.34: Growth of free nitrogen-fixers on FNFM broth in different NaCl concentration after 72 hours.

Observations:

A total of 12 representative N₂-fixing endophytic bacteria (out of 78) were screened that were isolated from mangrove roots and pneumatophores for their growth on free nitrogen-fixing medium (FNFM) at different strength of salinities. In most of the cases O.D. was observed to decrease in normal FNF media as well as FNFM with 0.3 M NaCl, FNFM with 0.5 M NaCl and FNFM with 0.7 M NaCl. Except *Aeromonas veronii* strain POT3 (MT422035) showed noticeable increase in O.D. up to FMFM+0.5M NaCl.

5.25. Testing of salt tolerance profile of some best PGP endophytic bacterial strains on cellulose degrading medium (CDM):

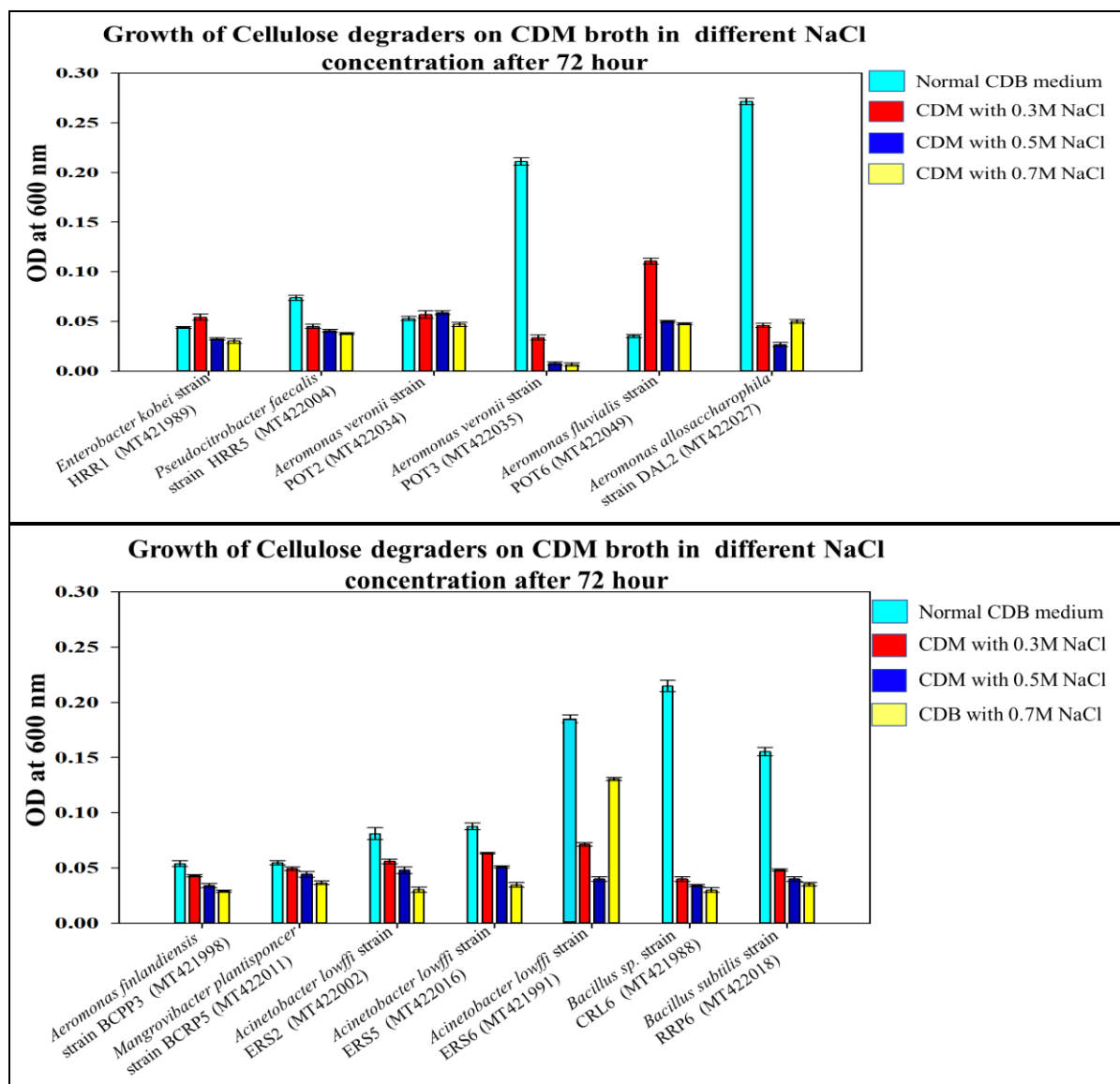


Figure 5.35: Growth of cellulose degraders on CDM broth in different NaCl concentration after 72 hours.

Observations:

A total of 13 representative endophytic bacteria (out of 78) were screened from mangrove roots and pneumatophores for their growth on cellulose degrading medium (CDM) at different salinity. Most of the cases O.D. was observed to decrease gradually from normal CDB media to CDM with 0.3 M NaCl, to CDM with 0.5 M NaCl and up to CDM with 0.7 M NaCl. *Acinetobacter lowffi* strain ERS6 (MT421991) only showed increase in O.D. up to CDM+0.5M NaCl.

5.26. Testing of salt tolerance profile of some best PGP endophytic bacterial strains on phosphate solubilizing medium (PSM):

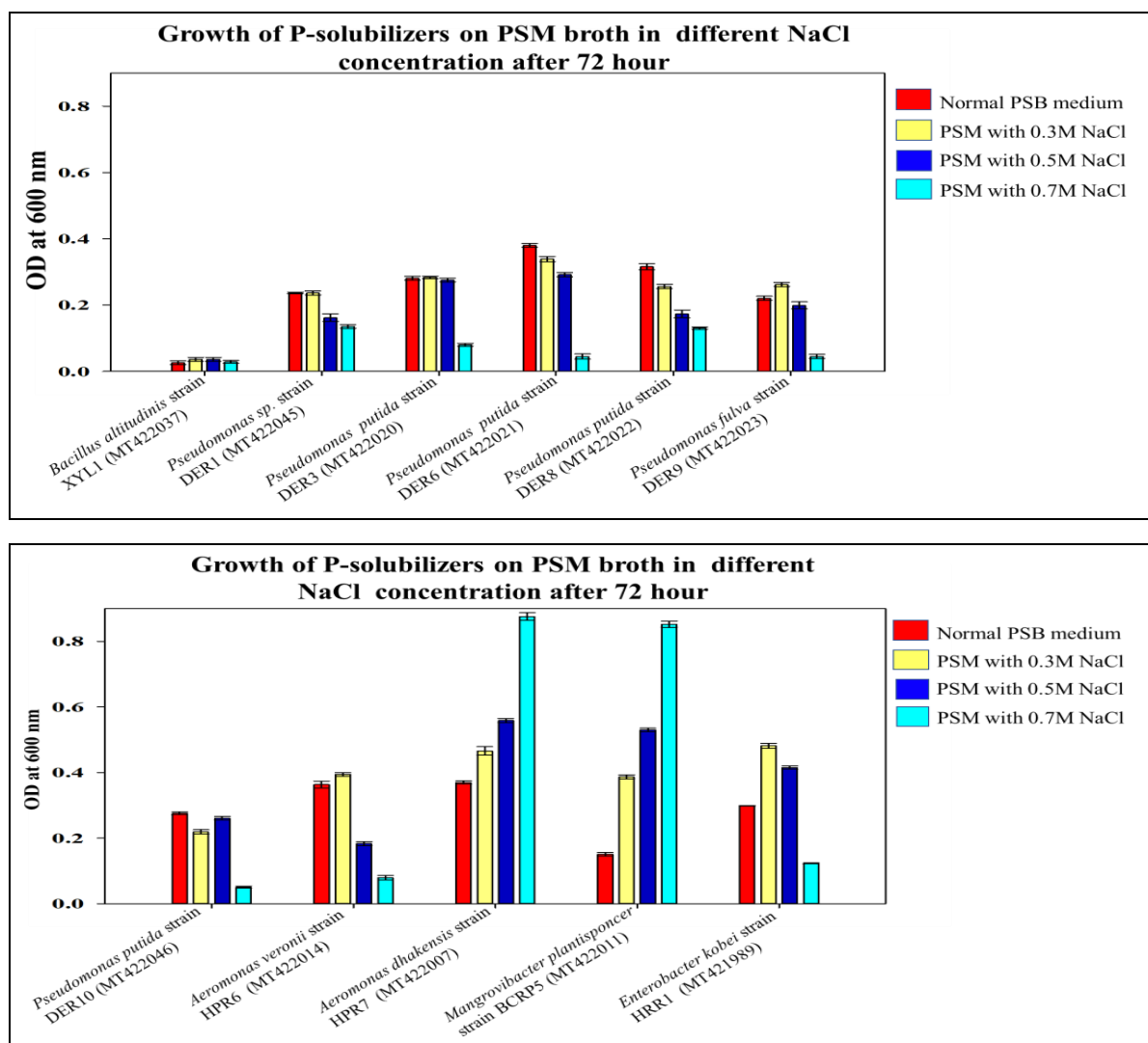


Figure 5.36: Growth of P-solublizers on PSM broth in different NaCl concentration after 72 hours.

Observations:

A total of 11 representative endophytic bacteria (out of 78) were screened from mangrove roots and pneumatophores for their growth on free phosphate solubilizing medium (PSM) at different strength of salinities. Most of the cases O.D. was found to incese on normal PSB media as well as PSM with 0.3 M NaCl and PSM with 0.5 M NaCl. *Aeromonas dhakensis* strain HPR7 (MT422007) and *Mangrovibacter plantisponcer* strain BCRP5 (MT422011) showed noticeable increase in O.D. up to PSM+ 0.7M NaCl.

Salt tolerance profile was tested by quantifying growth by measuring absorbance at 600 nm in differentially saline media. In most of the cases such as on free nitrogen-fixing medium (FNFM), cellulose degrading medium (CDM) and phosphate solubilizing medium (PSM) the endophytic bacteria showed their poor growth ability under increased salinity condition. It is assumed that the selected 78 bacteria are isolated from low-saline endosphere of mangrove roots and pneumatophores as endophytes. Therefore, these endophytes being already acclimatized under low-saline root endosphere (despite their possible origins at high-saline rhizospheres of mangrove species), they could not show better growth ability under increasingly saline conditions.

In similar studies

1. Puri et al, (2017) described different genera of plant growth promoting bacteria (PGPB) such as *Bacillus*, *Pseudomonas*, *Enterobacter*, *Burkholderia*, *Paenibacillus*, *Agrobacterium*, *Azospirillum* and *Azotobacter* from the rhizospheric region. They can colonize on the root surface but also can enter plants' internal tissue and colonize there.
2. Berg et al, (2005) stated that other bacterial strains e.g., *Enterobacter* sp., *Burkholderia* sp., *Herbaspirillum* sp., *Pseudomonas* sp., *Ochrobactrum* sp., *Staphylococcus* sp., *Ralstonia* sp., and *Stenotrophomonas* sp., were found inhabiting the plant rhizosphere.
3. Chanway (1996); Bent and Chanway, (1998) mentioned that endophytes play a very important role in plant growth and development in different ways such as the production of phytohormones, sequestration of iron by siderophore, solubilization of inorganic phosphate, nitrogen fixation, etc.
4. Mukherjee et al (2017) found that endophytic bacteria such as *Bacillus*, *Staphylococcus* and *Pseudomonas* could be isolated from *Ophioglossum reticulatum* L. and plant growth promoting activities by the solubilization of inorganic phosphate, phytohormones production, sequestration of iron by siderophore, fixation of nitrogen etc were observed for the isolates. Different endophytic bacterial genera like *Pseudomonas*, *Burkholderia*, *Azotobacter*, *Azospirillum*, *Alcaligenes*, *Klebsiella*, *Arthrobacter* and *Serratia* were found to augment plant growth promotion by the activities of production of siderophore, production of indole-3-acetic acid (IAA) and solubilization of calcium phosphates.

Objective 4

6. Selection of PGP endophytic bacterial consortia based on growth promotion criteria and growth curves for nursery/greenhouse/field applications.

6.1. Selection of endophytic bacterial consortia for the application of nursery/greenhouse/field on the basis of plant growth promoting (PGP) potential

The following **three consortia** were formulated based on plant growth promotion activities and salinity tolerance profiles of the 78 isolated endophytic PGP bacteria. Each consortium comprised of 6-7 endophytic bacterial strains with promising plant growth promotion profile observed at laboratory conditions. These 3 consortia were selected out of 78 accessioned endophytes to be applied in nursery/greenhouse/field applications, for further plant growth promotion studies. Below is the presented the PGP profile in both tabular and graphical formats.

Table 23: Selection of the 3 best PGP Consortia for nursery/field/green-house application.

Combinations of endophytic PGP strains	Sl No.	Name of bacterial strain	Accession no.	Source of mangrove species
Consortium BC1	1	<i>Aeromonas dhakensis</i> strain HPR7	MT422007	<i>Heritiera fomes</i> pneumatophore
	2	<i>Mangrovibacter plantisponcer</i> strain BCRP5	MT422011	<i>Bruguiera cylindrica</i> root
	3	<i>Pseudomonas stutzeri</i> strain BCY5	MT422041	<i>Bruguiera cylindrica</i> root
	4	<i>Pseudomonas stutzeri</i> strain BCY7	MT422042	<i>Bruguiera cylindrica</i> root
	5	<i>Bacillus subtilis</i> strain AOR5	MT421976	<i>Avicennia officinalis</i> root
	6	<i>Serratia marcescens</i> strain AOR4	MT422009	<i>Avicennia officinalis</i> root
Consortium BC2	1	<i>Aeromonas allosaccharophila</i> strain DAL2	MT422027	<i>Dalbergia</i> sp. root
	2	<i>Pseudomonas</i> sp. strain DER1	MT422045	<i>Derris trifoliata</i> root
	3	<i>Pseudomonas putida</i> strain DER3	MT422020	<i>Derris trifoliata</i> root
	4	<i>Pseudomonas fulva</i> strain DER9	MT422023	<i>Derris trifoliata</i> root
	5	<i>Aeromonas veronii</i> strain POT3	MT422035	<i>Porteresia</i> sp. root
	6	<i>Aeromonas veronii</i> strain POT7	MT422025	<i>Porteresia</i> sp. root
	7	<i>Serratia marcescens</i> strain HPR4	MT422006	<i>Heritiera fomes</i> pneumatophore
Consortium BC3	1	<i>Bacillus subtilis</i> strain AMR4	MT421979	<i>Avicennia marina</i> root
	2	<i>Aeromonas hydrophila</i> strain HER3	MT422047	<i>Heritiera fomes</i> root
	3	<i>Bacillus altitudinis</i> strain XYL1	MT422037	<i>Xylocarpus</i> sp. root
	4	<i>Pseudocitrobacter faecalis</i> strain HRR5	MT422004	<i>Heritiera fomes</i> root
	5	<i>Serratia marcescens</i> strain HPR4	MT422006	<i>Heritiera fomes</i> pneumatophore
	6	<i>Enterobacter kobei</i> strain HRR1	MT421989	<i>Heritiera fomes</i> root

Table 24: Showing Quantitative PGP profile of 3 consortia each of 6-7 endophytic bacterial strains with high plant growth promoting potential at laboratory level

18 identified bacterial strains were selected on the basis of plant growth promoting activities. consortium-1 and consortium-3 each comprises of 6 endophytic bacterial strains. Consortium-2 has 7 endophytic bacterial strains described in the following table:

Combinations of endophytic PGP strains	Sl No.	Name of bacterial strain	Accession no.	Source of mangrove species	IAA production ($\mu\text{g ml}^{-1}$)	Soluble phosphorus production ($\mu\text{g ml}^{-1}$)	% of siderophore production	ACC deaminase units production	Growth on stringent IOM at pH 6 with confirmed ppt	Ethylene peak at ARA (nmole)	CFU count per 100 μl FNFM broth
Consortium BC1	1	<i>Aeromonas dhakensis</i> strain HPR7	MT422007	<i>Heritiera fomes</i> pneumatophore	1.55 \pm 0.06	8.35 \pm 0.81	92.07 \pm 1.44	3.35 \pm 0.32	Yes	0.0118	226*10 ⁸
	2	<i>Mangrovibacter plantisponcer</i> strain BCRP5	MT422011	<i>Bruguiera cylindrica</i> root	1.9 \pm 0.18	26.95 \pm 1.03	90.59 \pm 0.71	0.19 \pm 0.05	Yes	0.0196	57*10 ⁸
	3	<i>Pseudomonas stutzeri</i> strain BCY5	MT422041	<i>Bruguiera cylindrica</i> root	13.06 \pm 0.22	156.52 \pm 1.87	67.70 \pm 2.13	0.35 \pm 0.01	Yes	14.6783	97*10 ⁸
	4	<i>Pseudomonas stutzeri</i> strain BCY7	MT422042	<i>Bruguiera cylindrica</i> root	9.65 \pm 0.31	94.08 \pm 0.81	88.94 \pm 0.63	0.36 \pm 0.03	Only FNF	0.0342	35*10 ⁸
	5	<i>Bacillus subtilis</i> strain AOR5	MT421976	<i>Avicennia officinalis</i> root	1.79 \pm 0.11	13.15 \pm 1.97	87.29 \pm 0.96	1.66 \pm 0.12	Yes	Below detection level	18*10 ⁸
	6	<i>Serratia marcescens</i> strain AOR4	MT422009	<i>Avicennia officinalis</i> root	2.58 \pm 0.14	124.08 \pm 0.82	62.83 \pm 1.39	1.17 \pm 0.17	Yes	Below detection level	22*10 ⁸
Consortium BC2	1	<i>Aeromonas allosaccharophila</i> strain DAL2	MT422027	<i>Dalbergia</i> sp. root	9.46 \pm 0.19	118.4 \pm 1.48	88.50 \pm 0.00	1.33 \pm 0.07	Only FNF	2.2424	38*10 ⁸
	2	<i>Pseudomonas</i> sp. strain DER1	MT422045	<i>Derris trifoliata</i> root	6.11 \pm 0.36	118.01 \pm 1.4	94.78 \pm 2.46	0.32 \pm 0.01	Yes	0.0694	40*10 ⁸
	3	<i>Pseudomonas putida</i> strain DER3	MT422020	<i>Derris trifoliata</i> root	6.33 \pm 0.26	106.46 \pm 0.39	95.09 \pm 0.01	0.54 \pm 0.04	Yes	0.011	100*10 ⁸

Combinations of endophytic PGP strains	Sl No.	Name of bacterial strain	Accession no.	Source of mangrove species	IAA production ($\mu\text{g ml}^{-1}$)	Soluble phosphorus production ($\mu\text{g ml}^{-1}$)	% of siderophore production	ACC deaminase units production	Growth on stringent IOM at pH 6 with confirmed ppt	Ethylene peak at ARA (nmole)	CFU count per 100 μl FNEM broth
	4	<i>Pseudomonas fulva</i> strain DER9	MT422023	<i>Derris trifoliata</i> root	6.73 \pm 0.19	111.31 \pm 0.73	90.00 \pm 0.61	0.8 \pm 0.07	Yes	1.4549	99*10 ⁸
	5	<i>Aeromonas veronii</i> strain POT3	MT422035	<i>Porteresia</i> sp. root	11.12 \pm 0.54	80.09 \pm 1	90.43 \pm 1.23	0.97 \pm 0.07	Yes	0.0291	107*10 ⁸
	6	<i>Aeromonas veronii</i> strain POT7	MT422025	<i>Porteresia</i> sp. root	3.96 \pm 0.35	104.75 \pm 1.18	94.78 \pm 2.46	9.19 \pm 0.58	Yes	1.4267	89*10 ⁸
	7	<i>Serratia marcescens</i> strain HPR4	MT422006	<i>Heritiera fomes</i> pneumatophore	2.14 \pm 0.13	35.46 \pm 0.47	79.65 \pm 1.25	0.79 \pm 0.01	Only FNF	0.0236	49*10 ⁸
Consortium BC3	1	<i>Bacillus subtilis</i> strain AMR4	MT421979	<i>Avicennia marina</i> root	1.98 \pm 0.06	53.22 \pm 0.45	0.00	2.57 \pm 0.26		Below detection level	17*10 ⁸
	2	<i>Aeromonas hydrophilia</i> strain HER3	MT422047	<i>Heritiera fomes</i> root	15.16 \pm 0.43	59.19 \pm 1.17	78.76 \pm 1.25	1.41 \pm 0.01	Only FNF	0.0161	86*10 ⁸
	3	<i>Bacillus altitudinis</i> strain XYL1	MT422037	<i>Xylocarpus</i> sp. root	5.85 \pm 0.32	81.75 \pm 0.96	0.00	1.33 \pm 0.17	Only FNF	0.0481	12*10 ⁸
	4	<i>Pseudocitrobacter faecalis</i> strain HRR5	MT422004	<i>Heritiera fomes</i> root	2.08 \pm 0.19	65.26 \pm 1.25	88.59 \pm 2.12	3.53 \pm 0.17	Yes	0.4328	42*10 ⁸
	5	<i>Serratia marcescens</i> strain HPR4	MT422006	<i>Heritiera fomes</i> pneumatophore	2.14 \pm 0.13	35.46 \pm 0.47	79.65 \pm 1.25	0.79 \pm 0.01	Only FNF	0.0236	49*10 ⁸
	6	<i>Enterobacter kobei</i> strain HRR1	MT421989	<i>Heritiera fomes</i> root	1.43 \pm 0.06	92.66 \pm 0.92	65.41 \pm 0.41	0.4 \pm 0.02	Yes	Below detection level	29*10 ⁸

6.2. Plant growth promotion profile of different consortium:

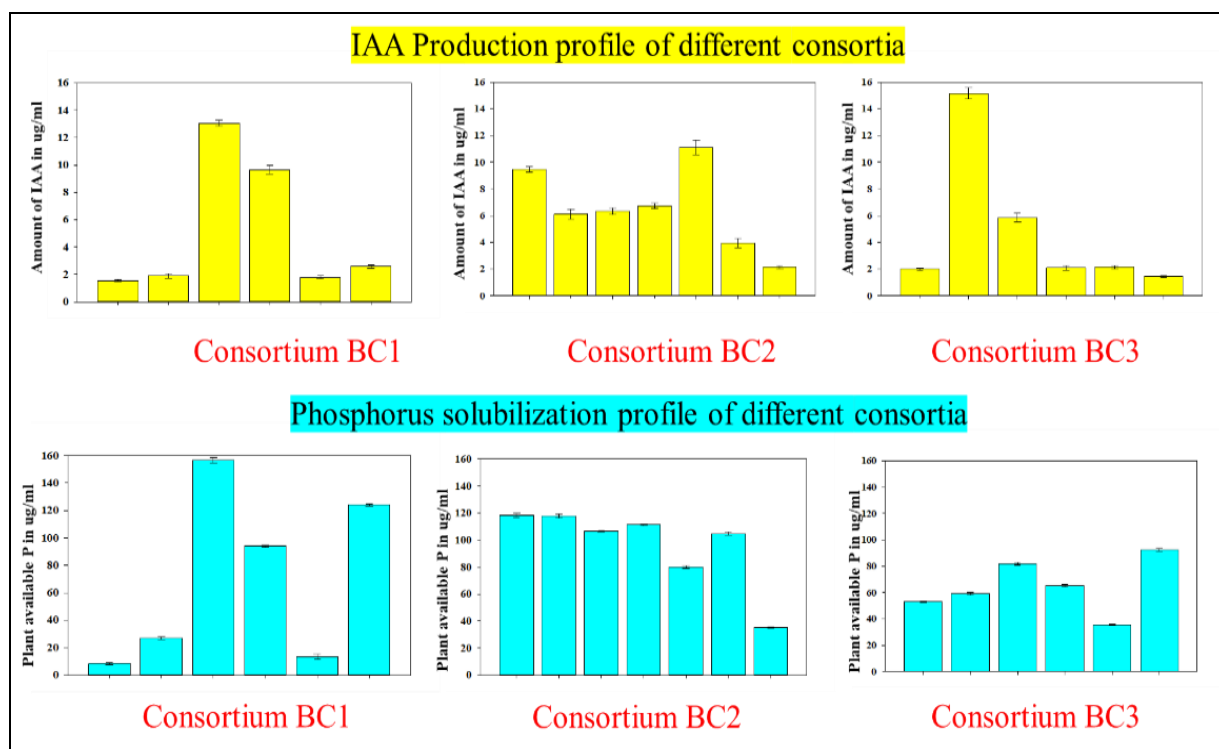


Figure 6.1: Indole acetic acid production profile and phosphate solubilization profile of Consortium-BC1, Consortium- BC2, and Consortium- BC3.

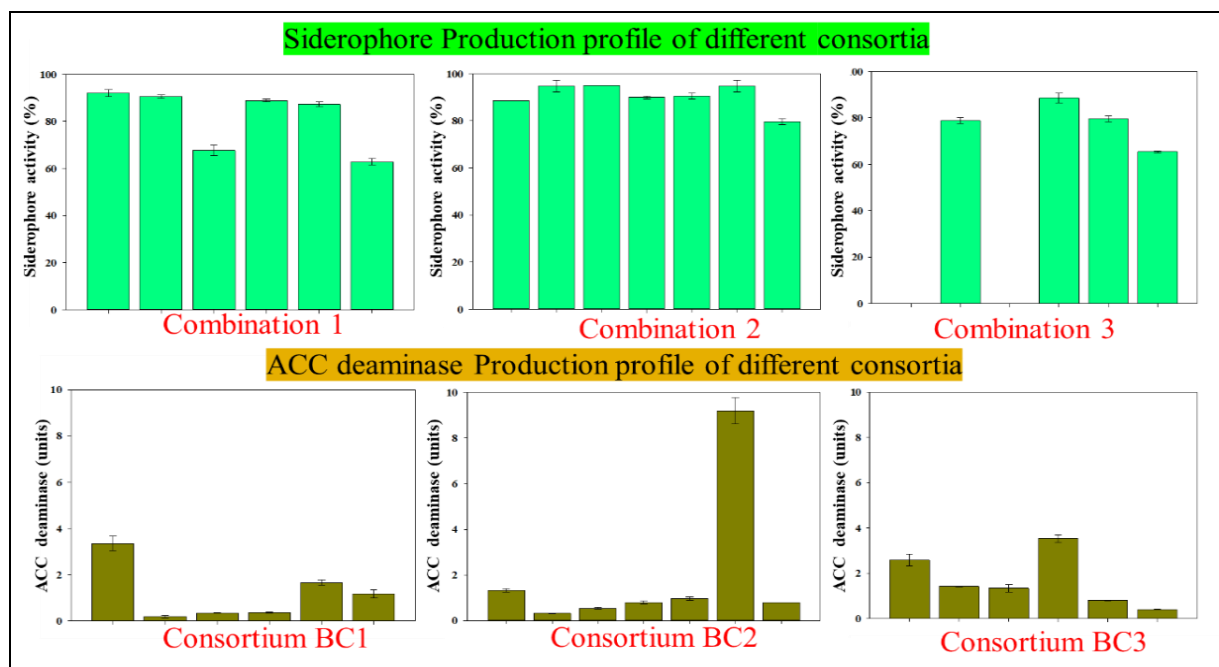


Figure 6.2: Siderophore production profile and ACC deaminase production profile of Consortium-BC1, Consortium- BC2, and Consortium- BC3.

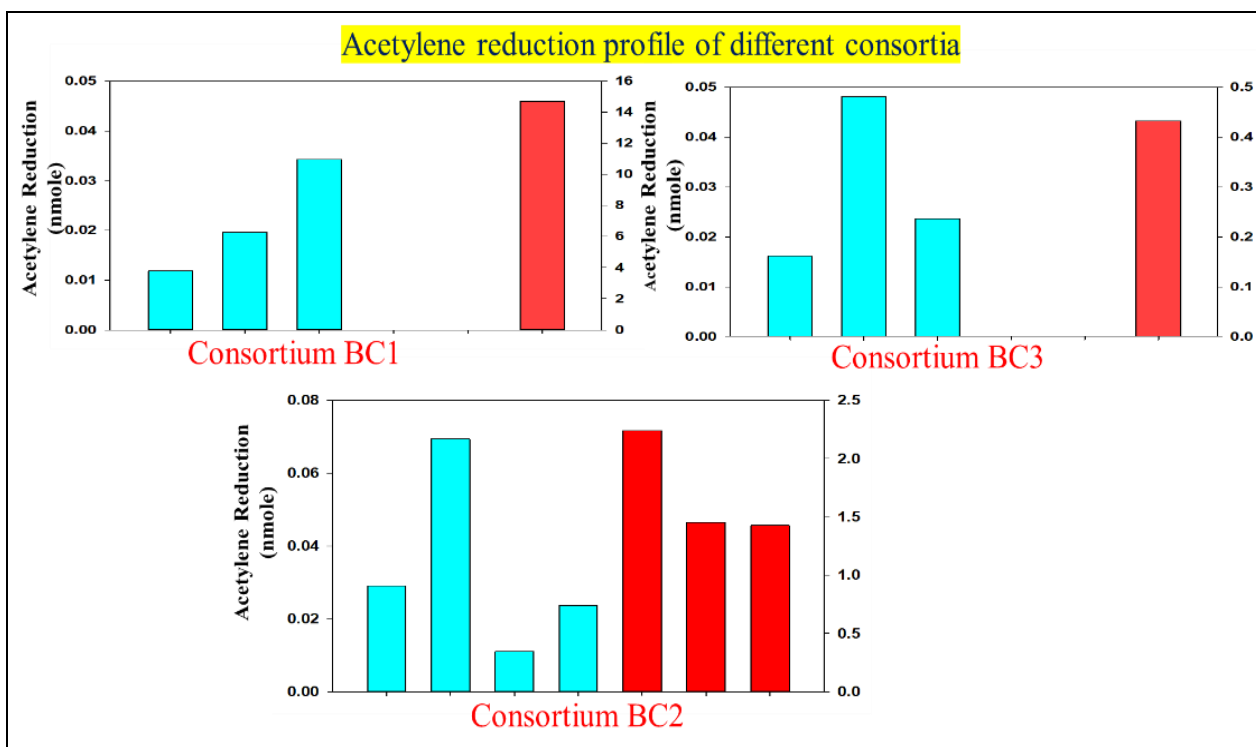


Figure 6.3: Acetylene reduction profile of Consortium-BC1, Consortium- BC2, and Consortium- BC3.

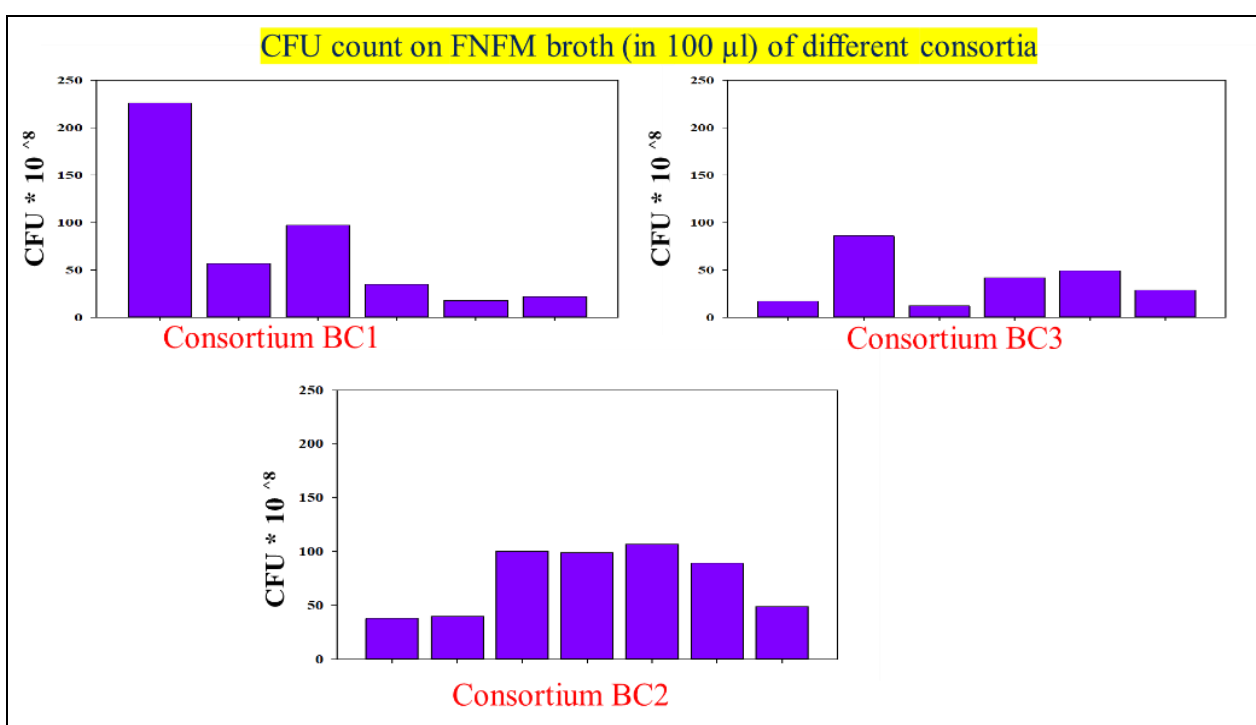


Figure 6.4: Colony forming unit (CFU) count on the nitrogen-fixing medium profile of Consortium-BC1, Consortium- BC2, and Consortium- BC3.

6.3. Antioxidant assay profile from different consortia of endophytic bacterial strains:

6.3.a. Free radical scavenging profile (DPPH scavenging activity) from different consortium of endophytic bacterial strains:

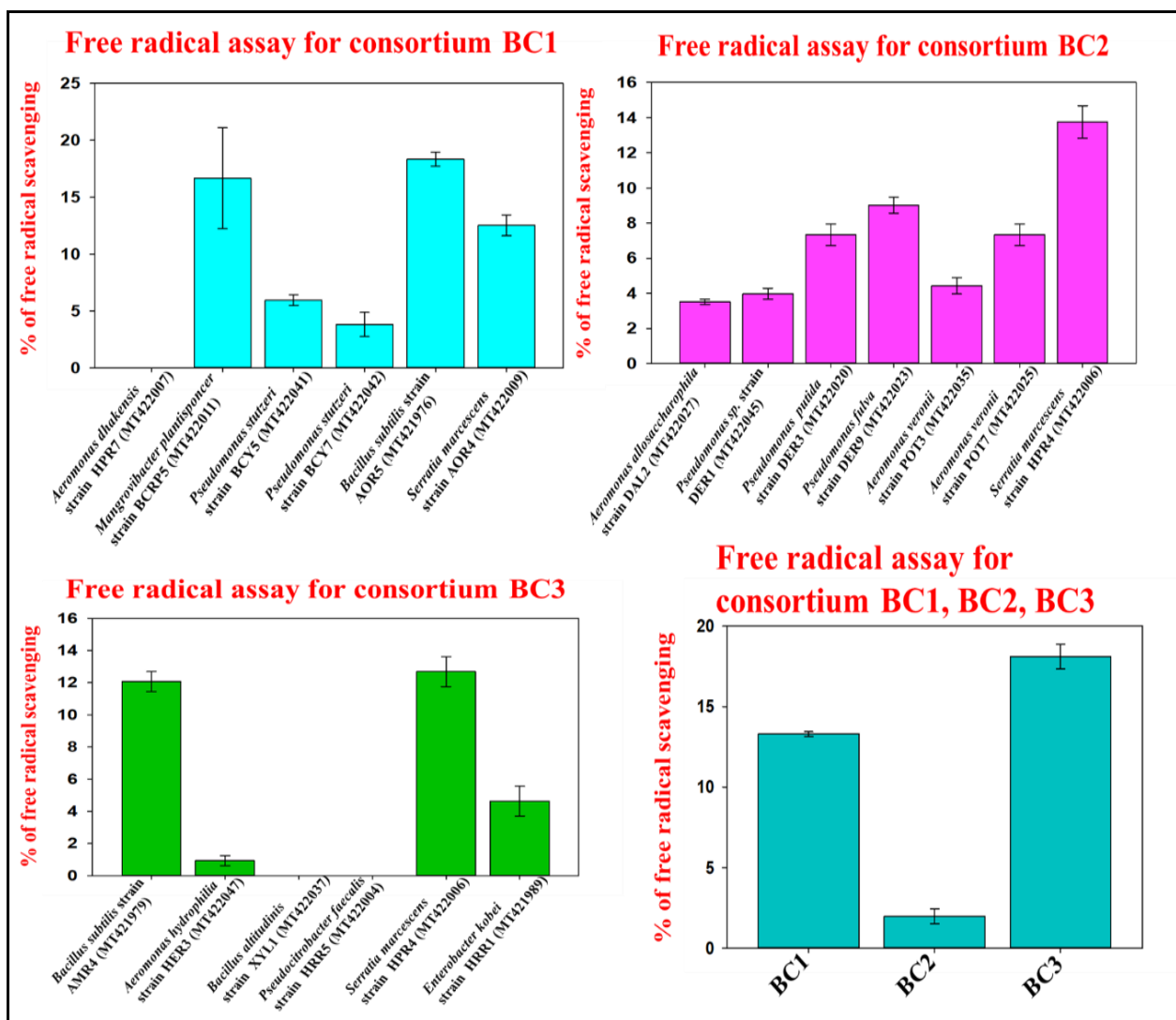


Figure 6.5: Free radical scavenging profile (DPPH) of Consortium-BC1, Consortium-BC2, and Consortium- BC3.

6.3.b. Superoxide anion scavenging profile from different consortium of endophytic bacterial strains:

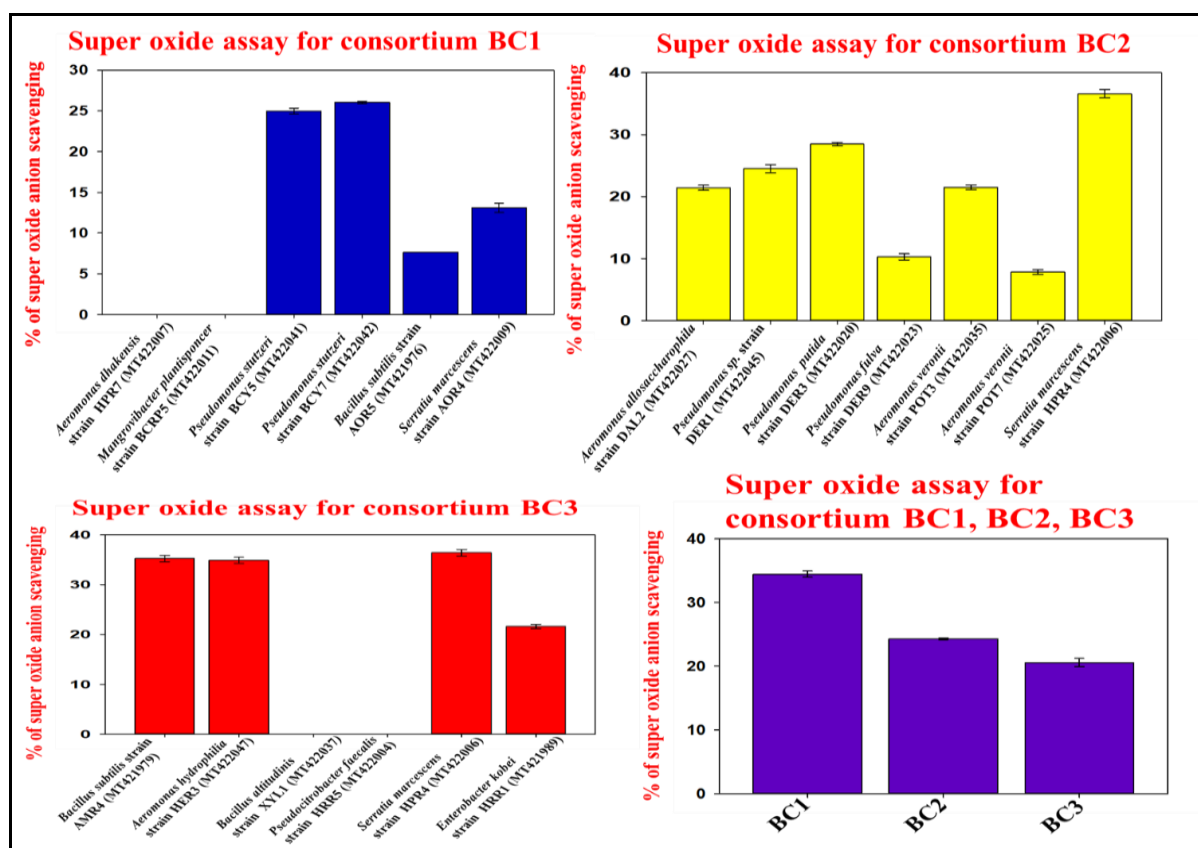


Figure 6.6: Superoxide anion scavenging profile Consortium-1, Consortium-2, and Consortium-3.

6.3.c. Hydroxyl radical scavenging profile from different consortium of endophytic bacterial strains:

Hydroxyl radical scavenging assays from different endophytic bacterial consortium when was carried out, no such activity could be observed. All endophytic bacterial consortium showed 0% of hydroxyl radical scavenging activity.

6.3.d. Nitric oxide scavenging assay profile from different consortium of endophytic bacterial strains:

Nitric oxide scavenging assay from different endophytic bacterial consortium when was carried out, no such activity could be observed. All endophytic bacterial consortia were negative for nitric oxide scavenging activity.

6.4. Prepration of growth curve of the 3 consortia with its PGP members for 96 hrs to find out the common exponential growth phase for large scale culture preparation

The consortia with their constituent PGP members were checked for growth in nutrient broth separately till 96 hrs to determine their overlapping exponential zone for further large-scale culture preparation for nursery/greenhouse and field applications. All the members of all 3 consortia showed 24-48 hr as their best exponential phase and hence it was decided to grow all consortia upto 48 hrs in large culture, after which the cultures were harvested for further application for growth plant promotion studies. Below are the growth curves prepared till 96 hrs for the 3 selected consortia.

6.4.a. Growth curve of consortium BC1 for 96 hours

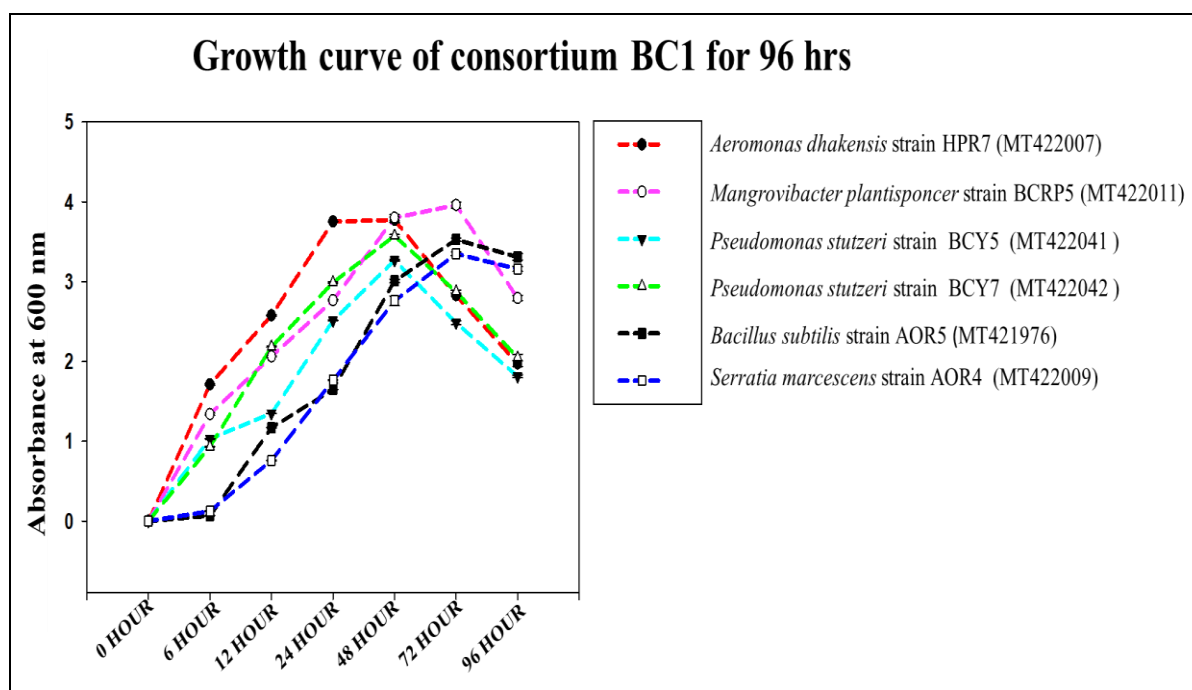


Figure 6.7: Growth curve of individual endophytic bacterial strains from consortium (BC1).

6.4.b. Growth curve of consortium BC2 for 96 hours

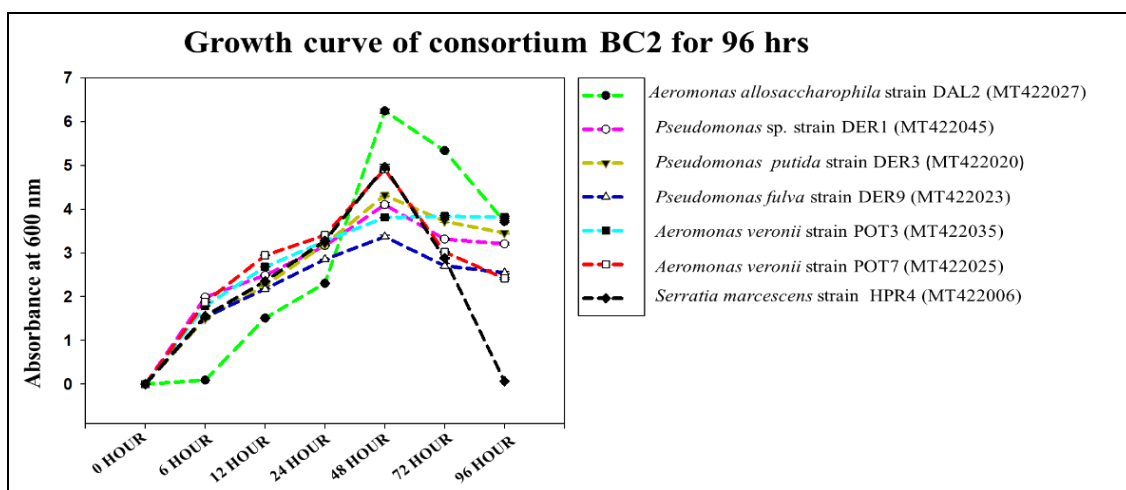


Figure 6.8: Growth curve of individual endophytic bacterial strains from consortium (BC2).

6.4.c. Growth curve of consortium BC3 for 96 hours

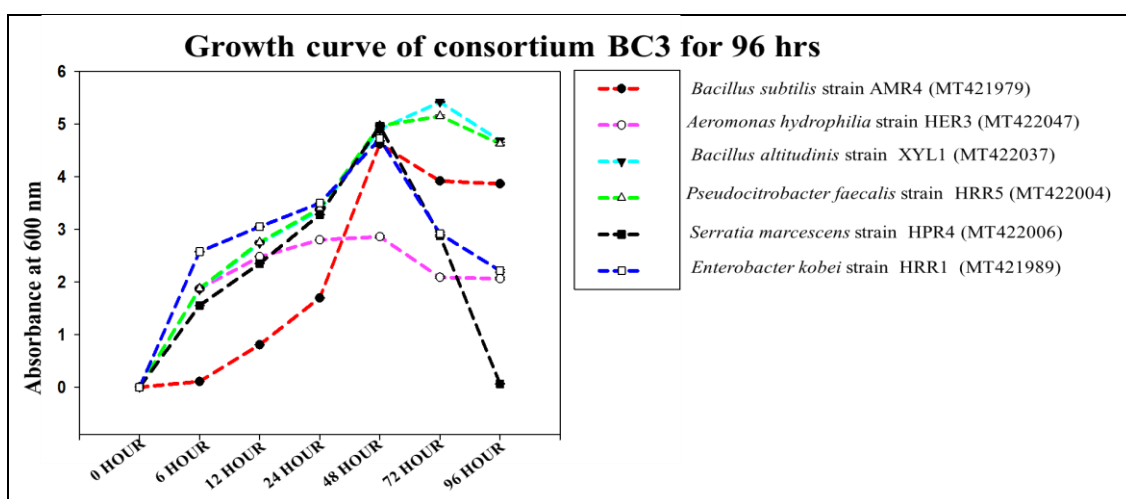


Figure 6.9: Growth curve of individual endophytic bacterial strains from consortium (BC3).

Observations:

All the members of all 3 consortia showed 24-48 hr as their best exponential phase and hence it was decided to grow all consortia up to 48 hrs in large culture, after which the cultures were harvested for further application for growth plant promotion studies.

Mukherjee et al (2017) mentioned that the use of endophytes as a bio-fertilizers is eco-friendly and is gaining importance among agronomists and environmentalists. The use of endophytic bacteria as bio-fertilizers showed improved crop production and quality. The alternative use of endophytic bacteria as bio-fertilizer significantly reduces chemical fertilizer inputs into the environment.

Objective 5

7. Application of selected PGP endophytic bacterial consortia on *Avicennia officinalis* saplings in mangrove nursery at Sundarbans for observing their effect on mangrove growth modulation.

The 3 selected consortia were applied twice on 23 days' old *Avicennia officinalis* saplings, 80 saplings for each consortium and 80 saplings were used as control where no bacteria were applied, in mangrove nursery at Ramganga village of Western Sundarbans (Patharpratima Block). Bacterial cultures were applied twice at 30 days' interval. Final shoot height, leaf length, leaf width and number of leaves per plant were measured from 95 days' old saplings.



Figure 7.1: Geo-tagged pictures of *Avicennia officinalis* saplings at mangrove nursery under ongoing experiments.



Figure 7.2: 95 days' old *Avicennia officinalis* saplings at mangrove nursery. Under control pots, saplings have no bacterial culture applied on them. Pot BC1 has BC1 bacterial consortium applied. In BC2 pots, BC2 bacterial consortium was applied. Pot BC3 has BC3 bacterial consortium applied. All the bacterial consortia were applied twice.

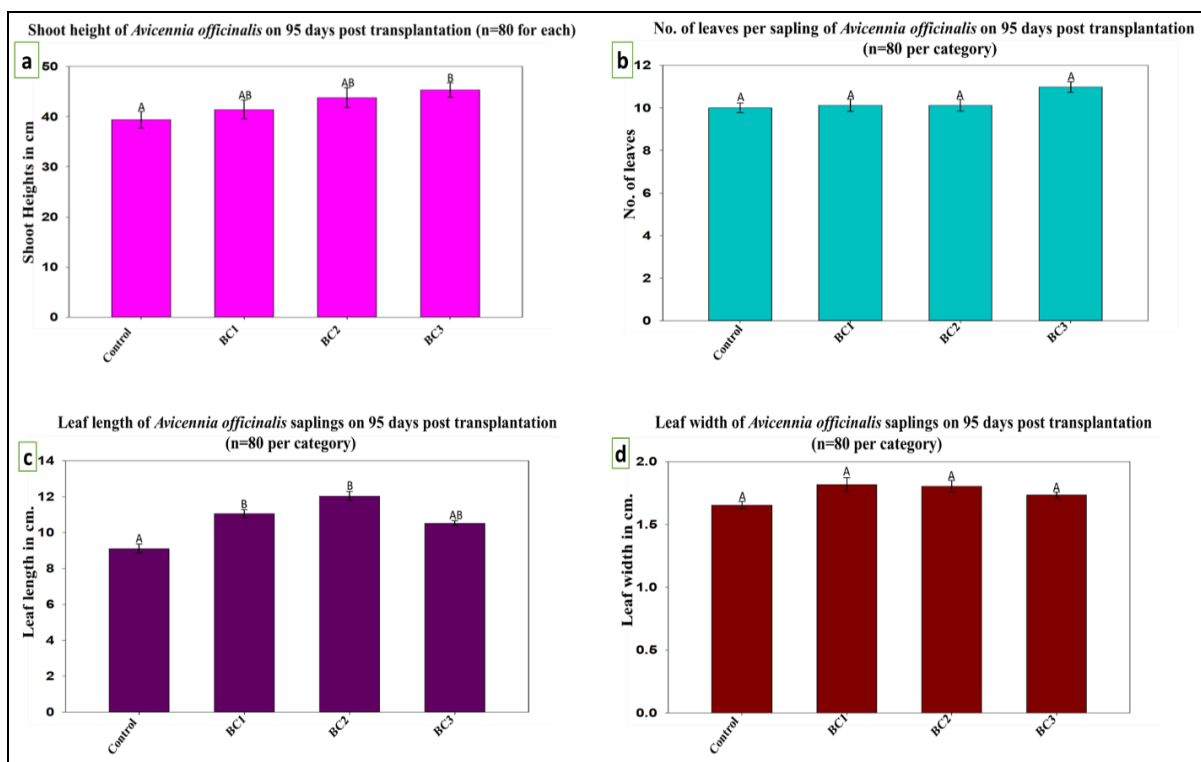


Figure 7.3: The above figures are the results observed for the growth promotion of *Avicennia officinalis* saplings in comparison to control saplings, after application of PGP endophytic consortia. (a) Consortium BC3 showed significant shoot height improvement of *Avicennia officinalis* saplings. (b) No significant difference in no. of leaves per sapling was observed among all the categories. (c) BC1 and BC2 consortia-applied-saplings showed significant increase in leaf length. (d) No significant difference in leaf width per sapling was observed among all the categories. Data were plotted as mean \pm standard error in the above graph (n=80).

7.1. Analysis of soil pH across the experimental time period:

pH has an important role for soil microbial community models. Nutrient availability in soil is directly related to soil pH (Msimbira and Smith 2020) via organic matter decomposition and microbial processes. However, the microbial processes get affected by the pH levels. Neutral pH is the optimal pH for microbial function that makes phosphorus, sulfur and nitrogen available for plants in the soil. Higher levels of pH causes available forms of elements like aluminium to generate that are toxic or lethal to the plants. When soil pH level is low, it directly affects the plant growth, making them suffer from nutrient deficiency.

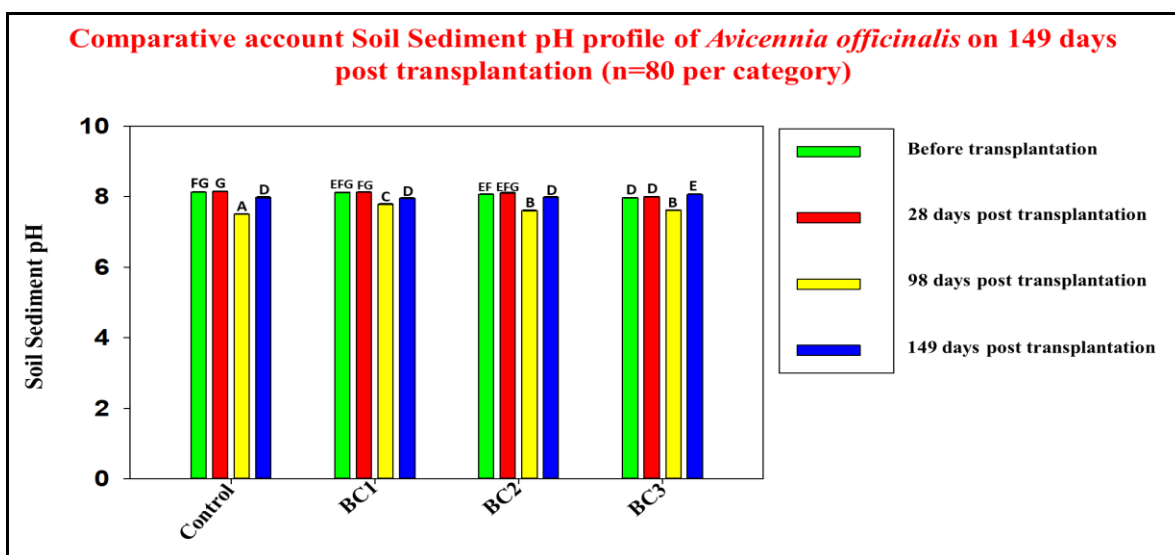


Figure 7.4: Soil sediment pH profile was studied from control (without bacteria) and different consortia-added pot rhizospheric soil. Analysis was carried out for *Avicennia officinalis* pot soils till 149 days post-transplantation. Data were plotted as mean \pm standard error in the above graph.

Observations:

The soil sediment pH remained the same for all consortia-added sapling pots as compared to control (without bacteria) in *Avicennia officinalis* nursery. On 98 days post-plantation a slight drop in pH was observed in all pots including controls. However, it again shot up as observed from 149 days post plantation data. Altogether an alkaline pH of about 8 was observed to be maintained across the experimental period in all the sapling pots including the control ones. Data were collected till 149 days post-transplantation.

7.2. Analysis of soil electrical conductivity (EC) across the experimental time period:

Soil salinity is measured by soil EC (electrical conductivity) or conductivity. Salinity is a very important factor in the development of mangroves. EC is commonly expressed as dS/m. The geophysical features of the ecosystem are reflected by soil salinity (Biswas et al, 2017). The increase in salinity results from excess chloride formation causing burning and firing of leaf tips and margins of mangrove plants. Excess sodium formation was also observed in necrotic areas on the tips, margins, or inter-venial areas of leaves. Other associated symptoms are smaller leaves due to slower growth, premature yellowing, bronzing, frequent chlorosis, abscission of leaves.

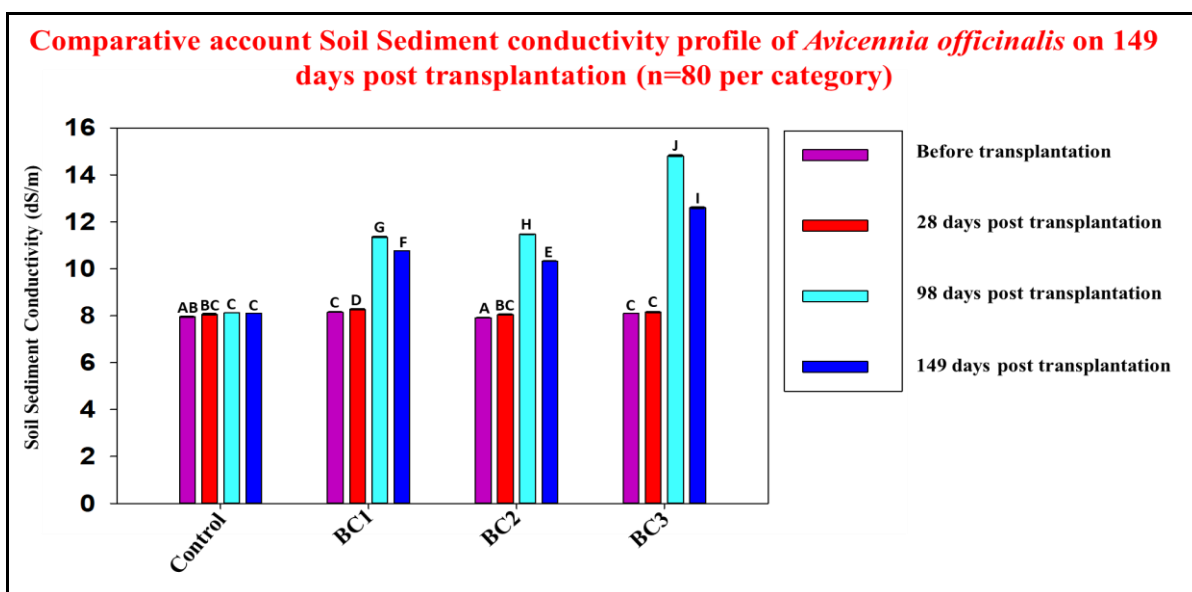


Figure 7.5: Soil sediment conductivity profile was studied from control (without bacteria) and different consortia-added pot rhizospheric soil. Analysis was carried out for *Avicennia officinalis* pot-soils till 149 days post-transplantation. Data were plotted as mean \pm standard error in the above graph.

Observations:

The soil sediment conductivity was observed to increase for all consortia-added pots as compared to control (without bacteria) from 98 days post-transplantation, however slightly decreased at 149 days post-transplantation in *Avicennia officinalis* nursery. *Avicennia officinalis* saplings could tolerate EC as high as 10-14 dS/m in soil, as observed from the presented data. This enhanced salinity in consortia-added pot soils might be due to addition of bacterial culture. Even under such a high salinity, consortia-added *Avicennia officinalis* saplings showed growth improvement in comparison to control saplings having soil EC of about 8 dS/m (comparatively lower salinity).

7.3. Analysis of soil organic carbon (SOC) across the experimental time period:

Soil organic carbon (SOC) has a major role in ecosystem maintenance. Higher amount of soil organic carbon enhances soil tilth and structure offering greater physical stability. Greater physical stability promotes soil aeration, oxygen in the soil, water retention and drainage capacity, and reduces the nutrient leaching and risk of erosion. Mangrove ecosystems are well-known for their carbon richness across the world. They sequester carbon into their both below-ground and above-ground biomass and soil. Approx. 85% of this carbon is stored within the soil. This huge

amount of stored carbon in soil has global importance and help mitigate unfavourable effects of climate change (Rahman et al, 2021). Significant inputs of organic carbon to mangrove sediments is provided by litter from the mangrove trees such as leaves, propagules and twigs, in addition to subsurface root growth. About one-third of the net primary production of carbon is represented by these litterfalls (Kristensen et al, 2008).

7.3.a. Calibration curve Organic carbon:

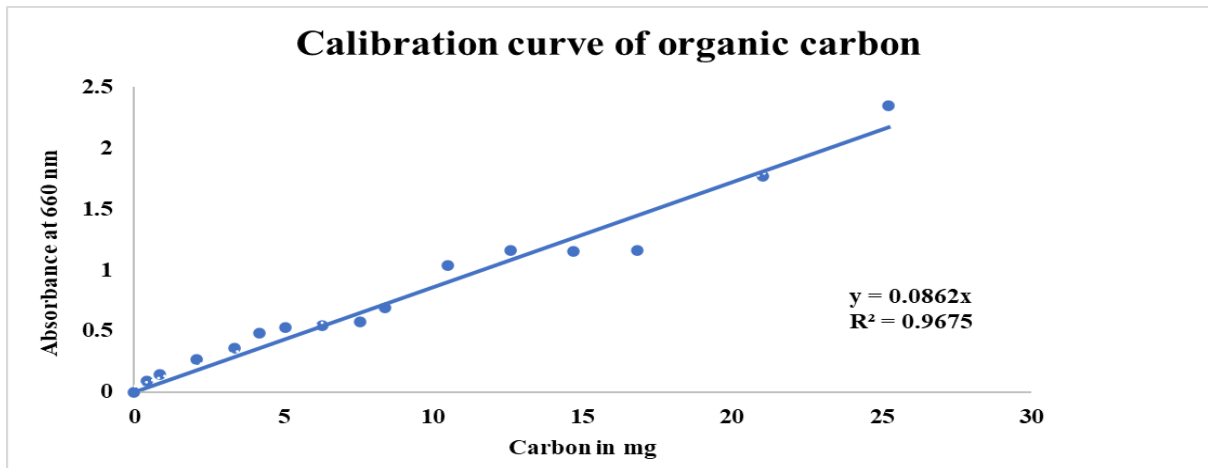


Figure 7.6: The calibration curve of organic carbon was carried out to measure the unknown concentration of organic carbon from the soil.

7.3.b. Analysis of soil organic carbon:

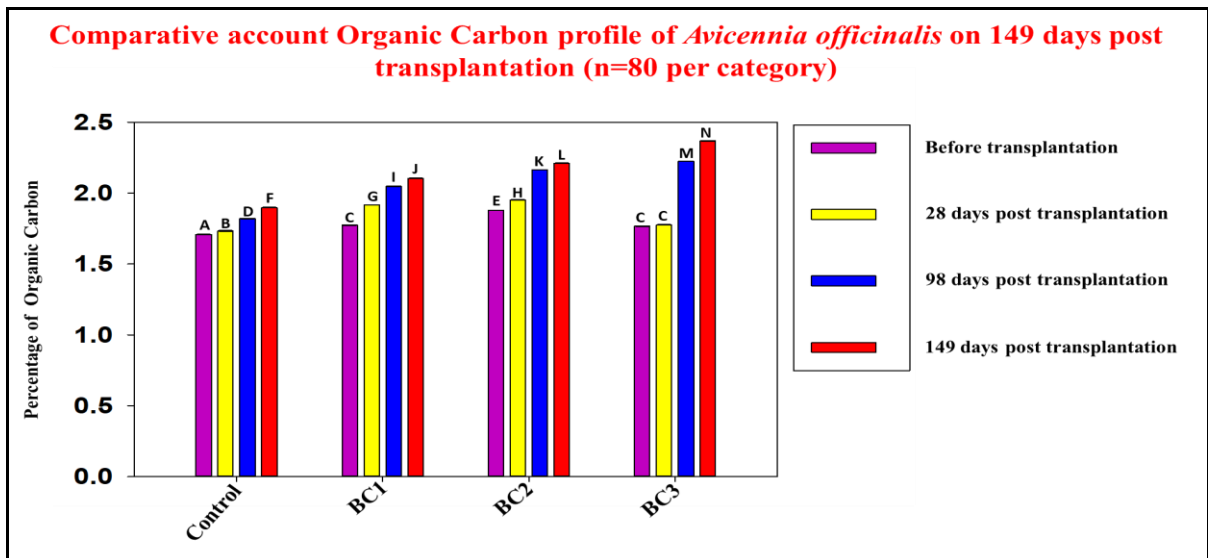


Figure 7.7: Soil organic carbon profile was studied from control (without bacteria) and different consortia-added pot rhizospheric soil. Analysis was carried out for *Avicennia officinalis* pot-soils till 149 days post transplantation. Data were plotted as mean \pm standard error in the above graph.

Observations:

The soil organic carbon was observed to increase for all consortia-added sapling pot soils, although a gradual increase in SOC of control (without bacteria) pot soil was also noticed till 149 days post-transplantation studies in *Avicennia officinalis* nursery. SOC increased and reached around 2-2.5% in BC2 & BC3 consortia-added pot soils, showing significant accumulation of SOC during the experimental period.

7.4. Analysis of available nitrogen (N) in pot soil across the experimental time:

The available form of nitrogen in the mangrove ecosystem depends on a difficult pattern of bacterial activity. Nitrification occurs in both aerobic and anaerobic conditions. Significant inputs of nitrogen (N) to mangrove sediments are provided by litter falls from the mangrove trees.

7.4.a. Calibration curve of nitrate-nitrogen:

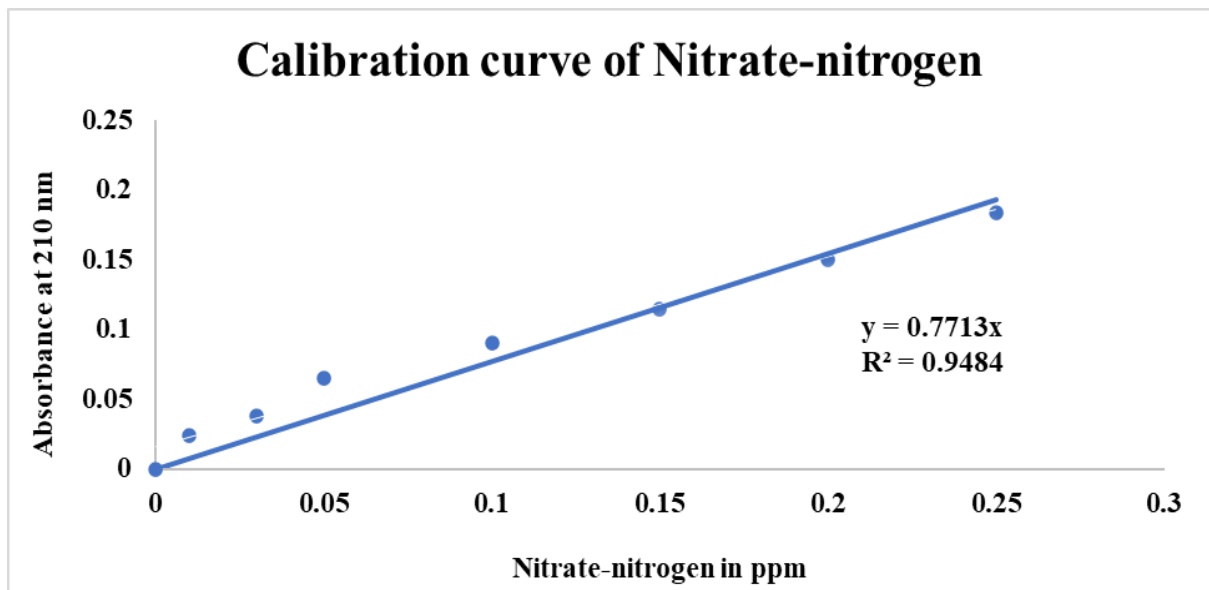


Figure 7.8: The calibration curve of nitrate-nitrogen was made to measure the unknown concentration of nitrate-nitrogen in the soil.

7.4.b. Analysis of soil nitrate-nitrogen:

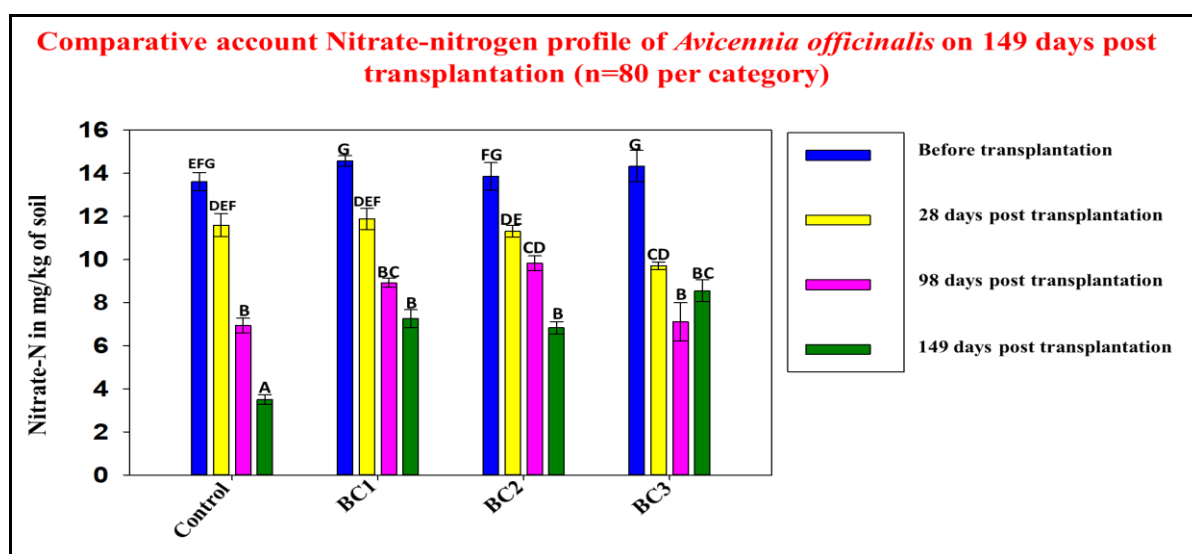


Figure 7.9: Soil nitrate-nitrogen profile was studied from control (without bacteria) and different consortia-added pot rhizospheric soil. Analysis was carried out for *Avicennia officinalis* pot soils till 149 days post-transplantation. Data were plotted as mean \pm standard error in the above graph.

Observations:

Interestingly the soil nitrate-nitrogen was found to gradually decrease for all consortia-added pots and also for control (without bacteria) till the 149 days post-transplantation studies in *Avicennia officinalis* nursery. However, it is noticed that the fall in nitrate-N content in consortia-added pots has slightly improved from 98 days post-transplantation results. The experimental results altogether showed lower rate of replenishment of nitrate-N in soil via soil/microbial processes, while consumption of nitrate-N by growing *Avicennia officinalis* outcompeted this replenishment process, again validating N-deficiency in mangrove soil, as observed by earlier researchers (Reef et al, 2010).

7.5. Analysis of soil ammonia-nitrogen across the experimental time period:

The primary form of nitrogen in mangrove sediments is ammonia-N (Reef et al, 2010). In anoxic soil conditions the growth of trees is mainly supported by ammonium uptake. Mangrove soils are rich in denitrifying bacteria. In anaerobic condition with high organic matter content, denitrification rates can be higher in mangrove soils. The higher rates of denitrification reduce the pools of nitrate and nitrite leaving ammonia-N, as the most common form of nitrogen. High

rates of ammonification and N-fixation also play a major role leading to the production of ammonium in mangrove soil (Reef et al, 2010).

7.5.a. Calibration curve of ammonia-nitrogen:

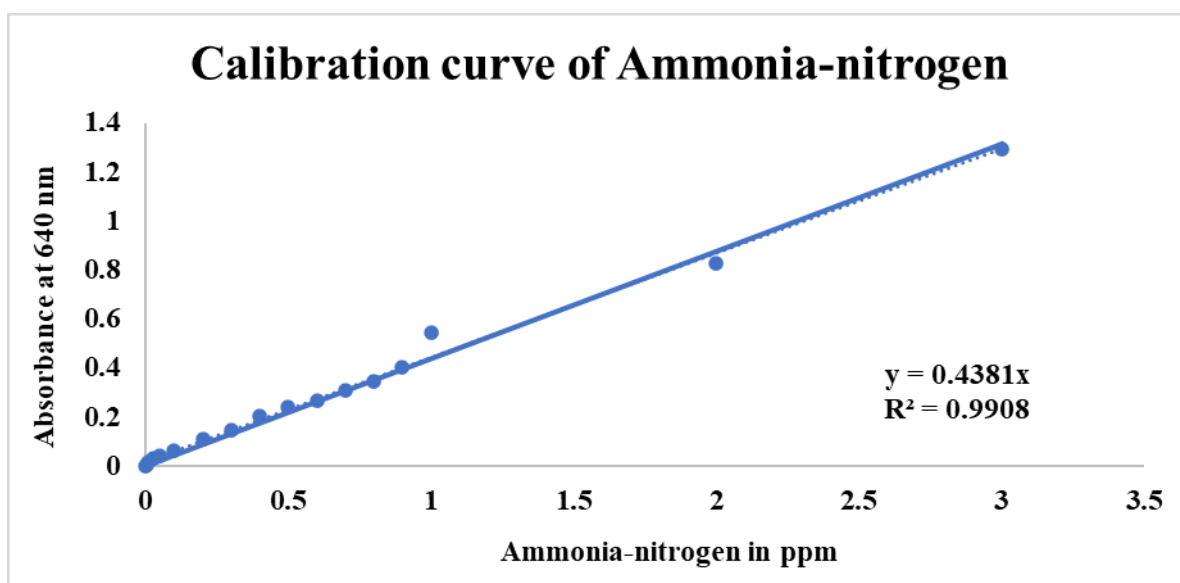


Figure 7.10: The calibration curve of ammonia-nitrogen was developed to measure the unknown concentration of ammonia-nitrogen from the soil.

7.5.b. Analysis of soil ammonia-nitrogen:

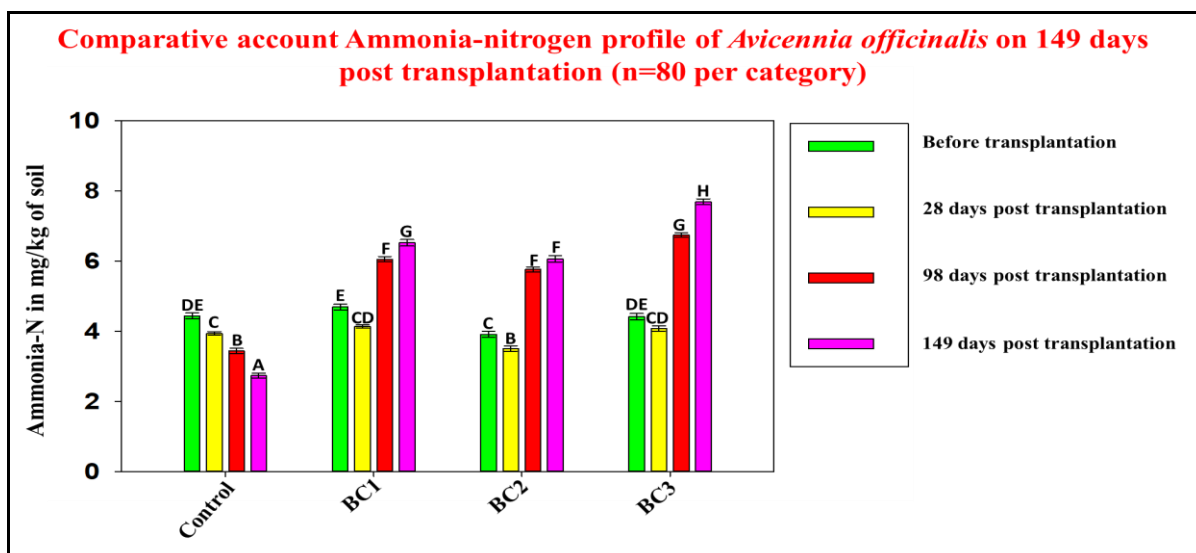


Figure 7.11: Soil ammonia-nitrogen profile was studied from control (without bacteria) and different consortia-added pot rhizospheric soil. Analysis was carried out for *Avicennia officinalis* pot soils till 149 days post-transplantation. Data were plotted as mean \pm standard error in the above graph.

Observations:

In contrast to nitrate-N, the soil ammonia-nitrogen was found to increase for all consortia-added pots as compared to control (without bacteria) observed from 98 days and 149 days post-transplantation data collected from *Avicennia officinalis* nursery. This increase in ammonia-nitrogen in consortia-added pot soils can be attributed to the free N₂-fixing consortial member bacteria, which might have caused improvement in ammonia-N content in consortia-added pots and this rate of replenishment of ammonia-N has outcompeted the consumption rate by the growing *Avicennia officinalis* saplings, finally, this higher ammonia-N accumulation was reflected in 149 days post-transplantation data.

7.6. Analysis of soil phosphorus content across the period of the experiment:

Phosphorus is an essential element for plant growth and development. The key plant functions like photosynthesis, energy transfer, and transformation of sugars and starches all are energy-dependent processes involving phosphorylation in several ways.

7.6.a. Calibration curve of plant-available phosphorus

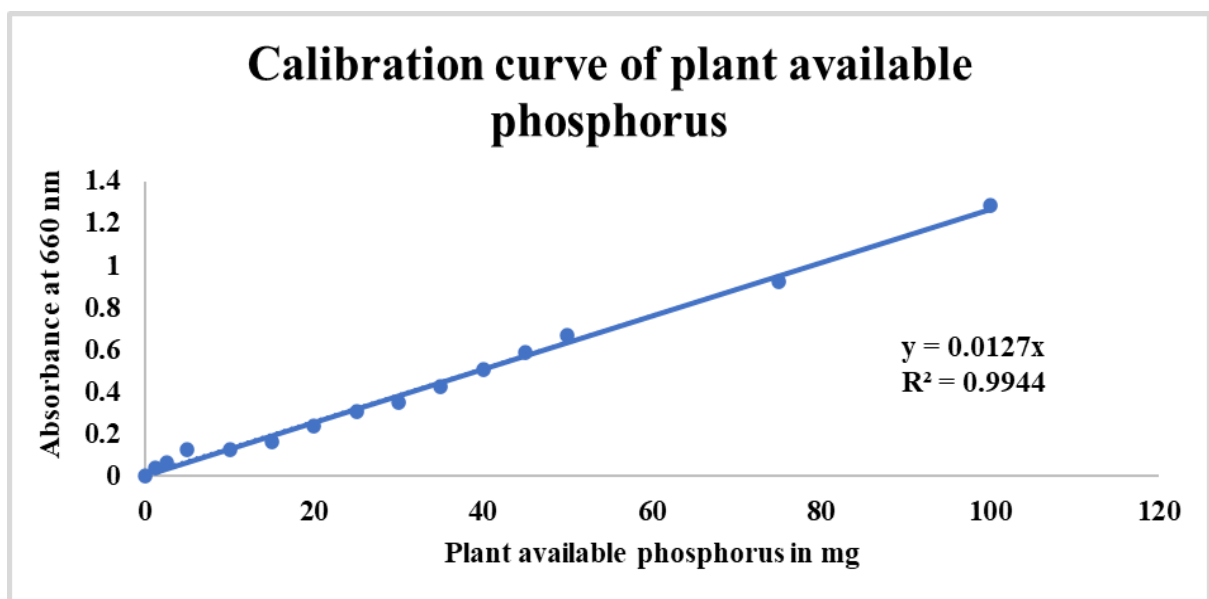


Figure 7.12: The calibration curve of plant-available phosphorus was made to measure the unknown concentration of plant-available phosphorus in the soil.

7.6.b. Analysis of plant-available phosphorus in soil:

P-solubilization profile at rhizosphere soils of experimental pots as indicator/metric of growth promotion/enrichment of consortia

Taking P-solubilization profile at rhizospheres of experimental pots as indicator/metric of growth promotion/enrichment of consortia, in *Avicennia officinalis* nursery, data were recorded before transplantation, at 28 days, 98 days and 149 days post transplantation. The data are represented in the following figure:

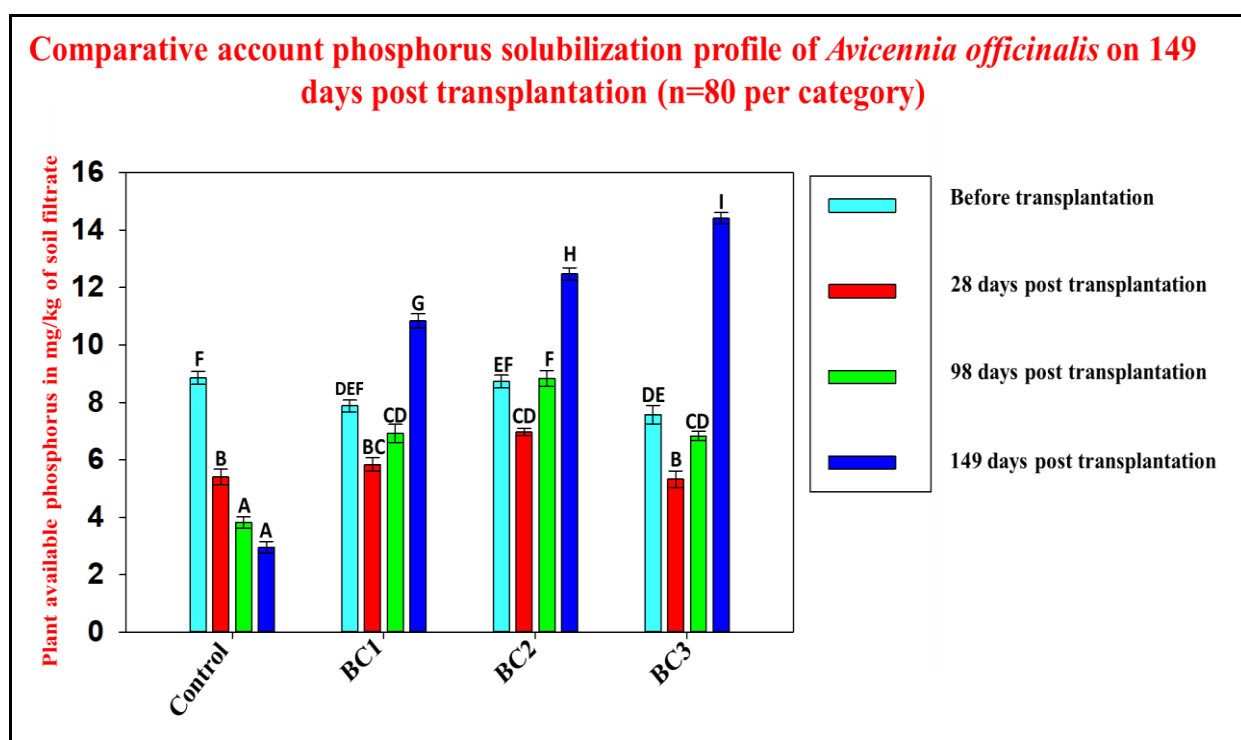


Figure 7.13: Soil plant-available phosphorus profile was studied from control (without bacteria) and different consortia added pot rhizospheric soil. Analysis was carried out for *Avicennia officinalis* pot soils till 149 days post-transplantation. Data were plotted as mean \pm standard error in the above graph.

Observations:

- In almost all consortia-added rhizosphere pot soils, the lowest level of soluble plant available phosphorus (P) is found to be at **28 days** post-transplantation after which it gradually increased as observed at **98 days** and **149 days** post transplantation rhizosphere soils. This increase in soluble plant available phosphorus (P) can be

attributed to the enrichment of PGP consortia at *Avicennia Officinalis* rhizosphere which have many a constituent member as high P-solubilizer

- In contrast, control (no bacteria added) pot soil rhizospheres, showed no significant increase in level of soluble plant available phosphorus (P) even after 149 days post-transplantation.
- BC1 and BC2 consortia-added rhizospheres of experimental *Avicennia Officinalis* plants showed increase in level of soluble plant-available phosphorus (P) as compared to control (no bacteria added) pot rhizosphere soil even on **28** days post transplantation, when the saplings showed maximum utilization of soil-P
- P-solubilization seems to be as promising growth promotion potential of the selected/added consortia (most members in each consortium were high P-solubilizers as observed earlier in laboratory experiments).
- Significant increase in solubilized-P was observed in consortia-added pot soil rhizospheres as compared to control (no bacterial addition) pot rhizospheric soils of *Avicennia officinalis* saplings even after 98-149 days post-transplantation as the data presented here.

Objective 6

8. Application of selected PGP endophytic bacterial consortia on cultivated rice of Sundarbans at the greenhouse for observing their effect on rice growth modulation.

Two selected rice varieties, Lunishree (N) and Dudheswar (D), were used for plant growth promotion studies at greenhouse pot experiments with control set where no bacterial culture was applied and also with conventional fertilizer NPK (20:20:20) applied in conventional doses for approximately 0.8 Kg of soil per pot used in the experiment.

A total of 12 bacterial consortia were used for the pot experiment; 5 pots for NPK with 3-4 seedlings per pot and 5 pots for control with 3-4 seedlings per pot were used for both the rice varieties. Among 12 bacterial consortia applied, 3 consortia belong to only endophytic bacterial consortia BC1, BC2 and BC3. Rest 9 consortia are made combining 6 rhizospheric consortia from halophytic native grasses from Sundarbans developed in another study and combining them with these 3 endophytic bacterial consortia in possible combinations. Those combinations are-

Sole endophytic bacterial consortia

BC1 as BEC1, BC2 as BEC2, BC3 as BEC3

And mixed bacterial consortia are-

SRC1+BEC1, SRC2+BEC2, SRC3+BEC3, SRC4+BEC1, SRC5+BEC2, SRC6+BEC3, SRC4+BEC2, SRC1+BEC3, SRC6+BEC1

Where, BEC= endophytic consortia & SRC= rhizospheric consortia

3 sets of pots with 3-4 seedlings were used per bacterial consortium for both the rice cultivars D and N, 7-days' old seedlings were transplanted on the pot, and bacterial cultures were applied twice at 15-20 days intervals. Initially, two soil types were used in the 1st greenhouse experiment, saline soil from Sundarbans and non-saline (sweet) soil also from Sundarbans area cultivated rice fields.

Table 25: Initial physical and chemical parameters of both the soil types that were used for the pot experiment before the start of the experiment were as follows:

Types of soil	Soil pH (mean \pm SE)	Soil conductivity (dSm ⁻¹) (mean \pm SE)	Plant available Phosphorus (mg kg ⁻¹) (mean \pm SE)	% soil organic carbon (mean \pm SE)	Ammonia-nitrogen (mg kg ⁻¹) (mean \pm SE)	Nitrate-nitrogen (mg kg ⁻¹) (mean \pm SE)
Saline soil	8.544 \pm 0.025	5.278 \pm 0.183	30.895 \pm 6.989	1.239 \pm 0.038	1.764 \pm 0.206	17.661 \pm 1.264
Sweet (non-saline) from cultivated rice fields of Sundarbans	7.455 \pm 0.089	0.452 \pm 0.028	55.250 \pm 3.948	2.212 \pm 0.014	2.324 \pm 0.466	17.396 \pm 1.510

The greenhouse experiment started off with these both soil types initially. However, after some days, due to high salinity in saline soil (EC rose from 5.27dS/m to 7.7dS/m), all rice seedlings started to wilt, and ultimately all the seedlings died. For this reason, we had to stop experimenting with saline soil and **continued with only sweet (non-saline, EC 0.452 dS/m)** cultivated rice field soil in subsequent experiments.

The whole experiment with 12 consortia for plant growth promotion of Dudheswar (D) and Lonanshree (N), rice cultivars was performed **twice** at the greenhouse along with control sets where no bacterial cultures were applied and with NPK fertilizer also at its conventional dose for comparison.

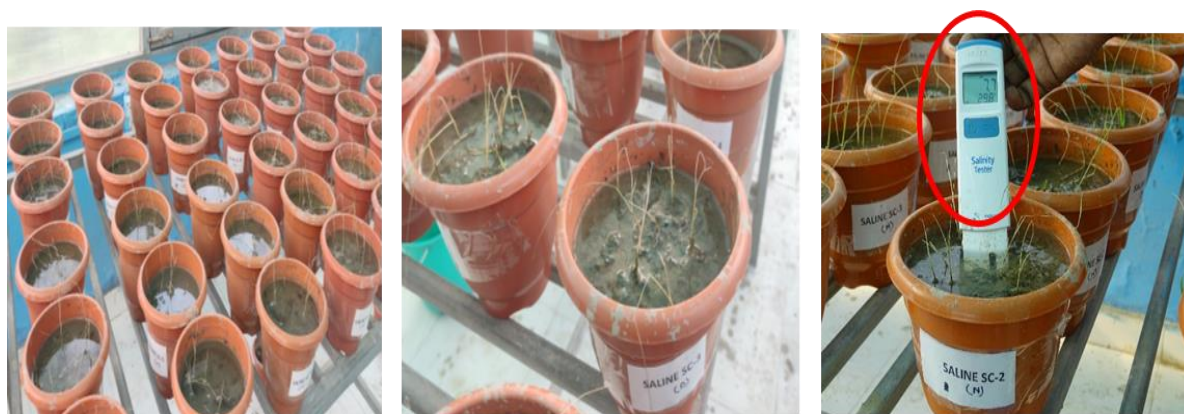


Figure 8.1: Because of the very high salinity of saline soil, all transplanted rice seedlings died in the initial days after transplantation. Therefore, the rest of the 1st greenhouse experiment and 2nd greenhouse experiment were conducted only with the rice seedlings growing on sweet soil (non-saline, EC 0.452 dS/m) brought from cultivated rice fields of Sundarbans.



Figure 8.2: The greenhouse experiment being conducted.



Figure 8.3: Checking of soil salinity and growth parameters at the greenhouse.

8.1. A few pictures from 2nd greenhouse experiment are depicted in the next pages:



Figure 8.4: The status of 85-day post-transplanted control (without bacteria) rice seedlings from 2nd greenhouse experiment.



Figure 8.5: The status of 85 days' post-transplanted NPK added rice seedlings from the 2nd greenhouse experiment.



Figure 8.6: The status of 85-days' post-transplanted BC1 added rice seedlings from the 2nd greenhouse experiment.



Figure 8.7: The status of 85-days' post-transplanted BC2 added rice seedlings from 2nd greenhouse experiment.

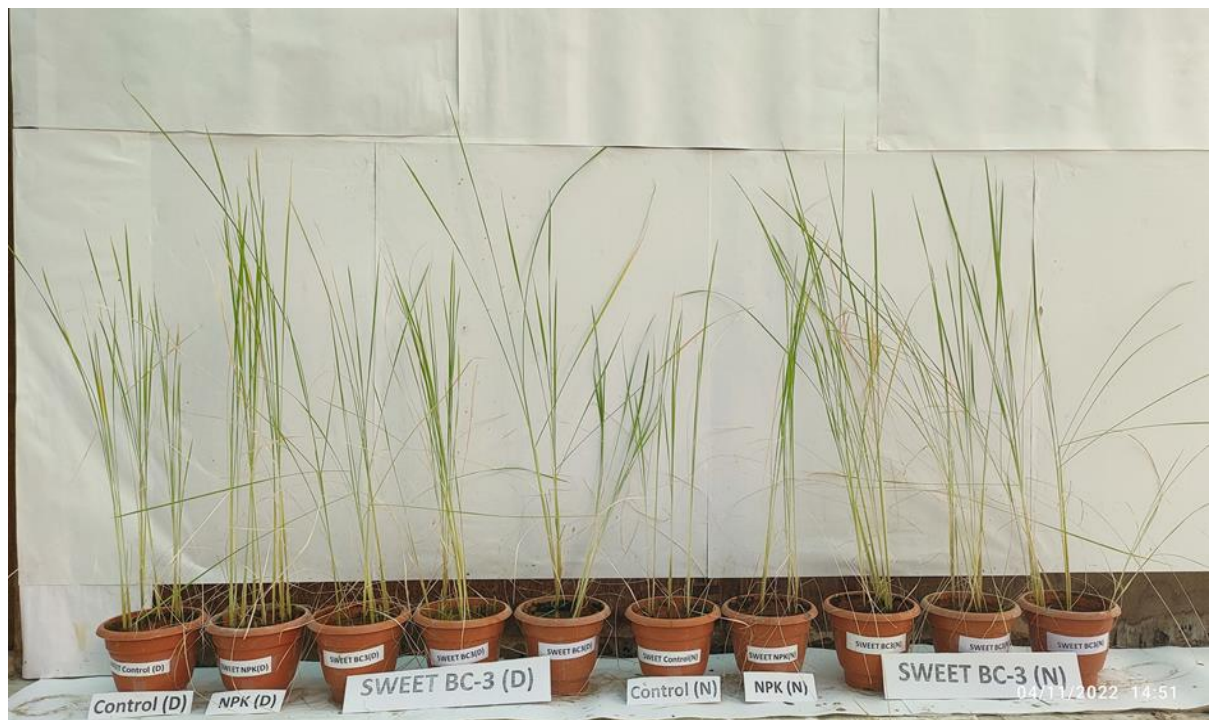


Figure 8.8: The status of 85-days' post-transplanted BC3 added rice seedlings from the 2nd greenhouse experiment.



Figure 8.9: The status of 85-days' post-transplanted SRC3+BEC3 added rice seedlings from the 2nd greenhouse experiment.



Figure 8.10: The status of 85-days post-transplanted SRC5+BEC2 added rice seedlings from the 2nd greenhouse experiment.



Figure 8.11: The status of 85-day post-transplanted SRC4+BEC2 added rice seedlings from the 2nd greenhouse experiment.



Figure 8.12: The status of 85-day post-transplanted SRC1+BEC3 added rice seedlings from the 2nd greenhouse experiment.



Figure 8.13: The status of 85-day post-transplanted SRC2+BEC2 added rice seedlings from the 2nd greenhouse experiment.

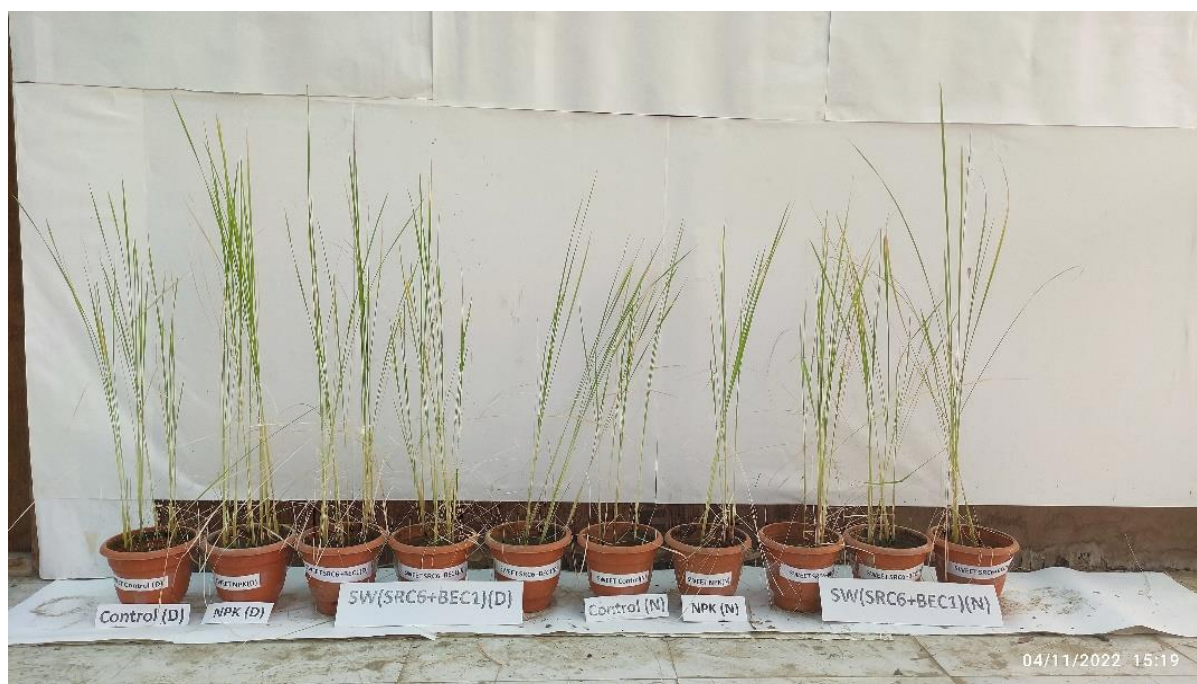


Figure 8.14: The status of 85-day post-transplanted SRC6+BEC1 added rice seedlings from the 2nd greenhouse experiment.



Figure 8.15: The status of 85-day post-transplanted SRC6+BEC3 added rice seedlings from the 2nd greenhouse experiment.

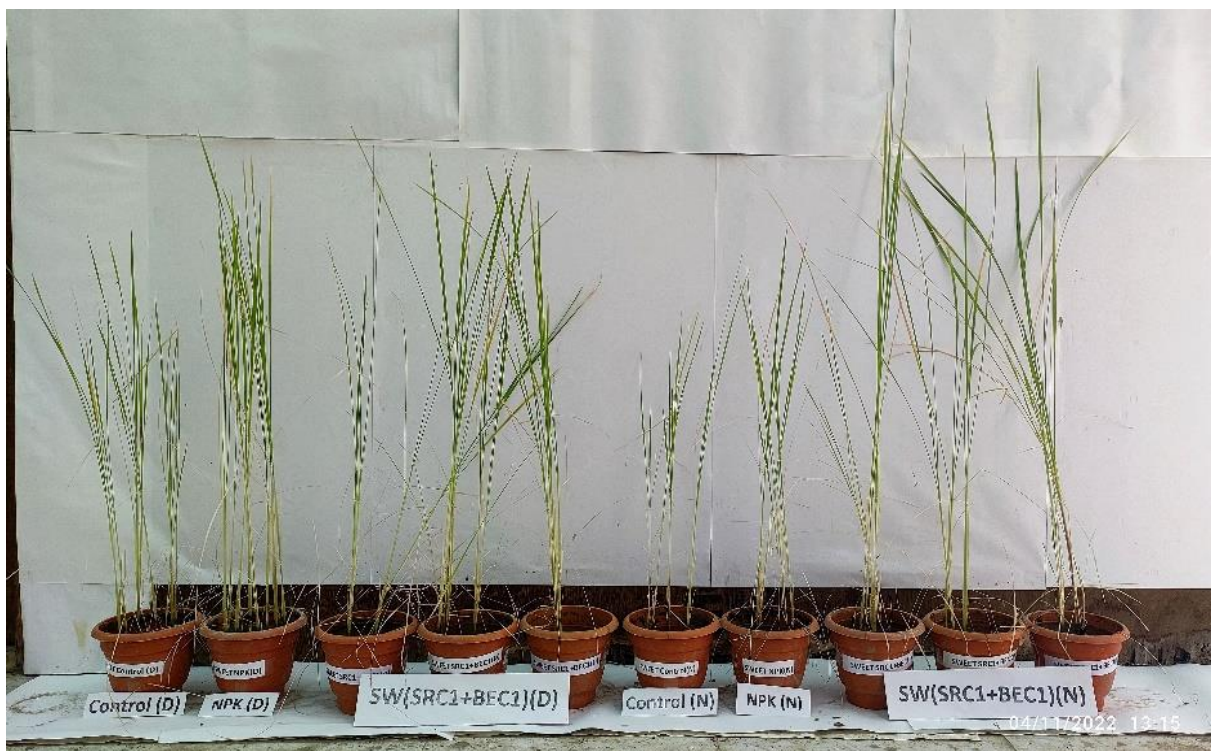


Figure 8.16: The status of 85-day post-transplanted SRC1+BEC1 added rice seedlings from the 2nd greenhouse experiment.



Figure 8.17: The status of 85-day post-transplanted SRC4+BEC1 added rice seedlings from the 2nd greenhouse experiment.

8.2. Growth parameters from both 1st and 2nd greenhouse pot experiment:

The comparative growth promotion results obtained from the 1st and 2nd greenhouse experiments performed with D (Dudheswar) and N (Lunishree) rice cultivars, 12 consortia, NPK and control (without any bacterial consortia) are presented below:

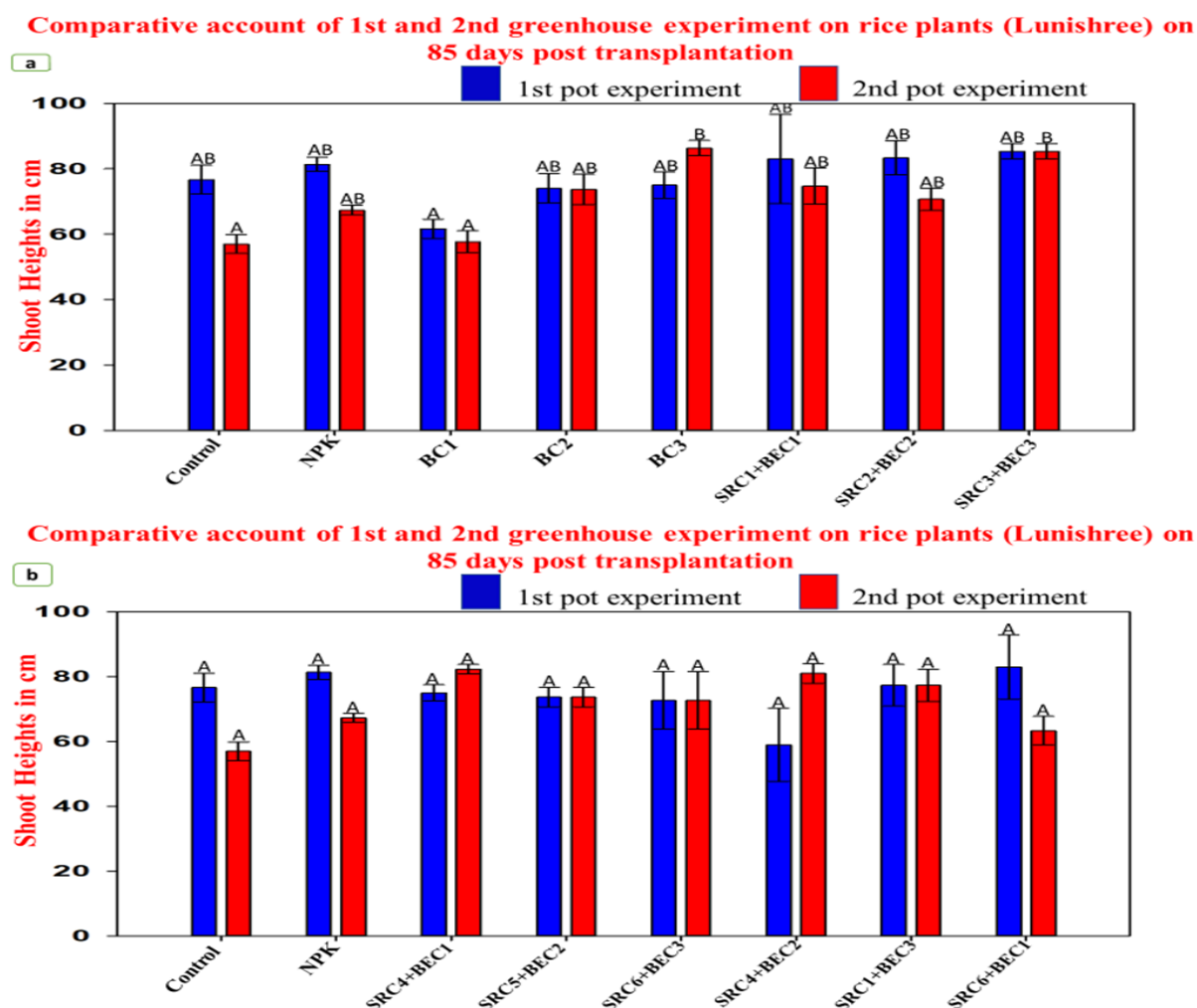
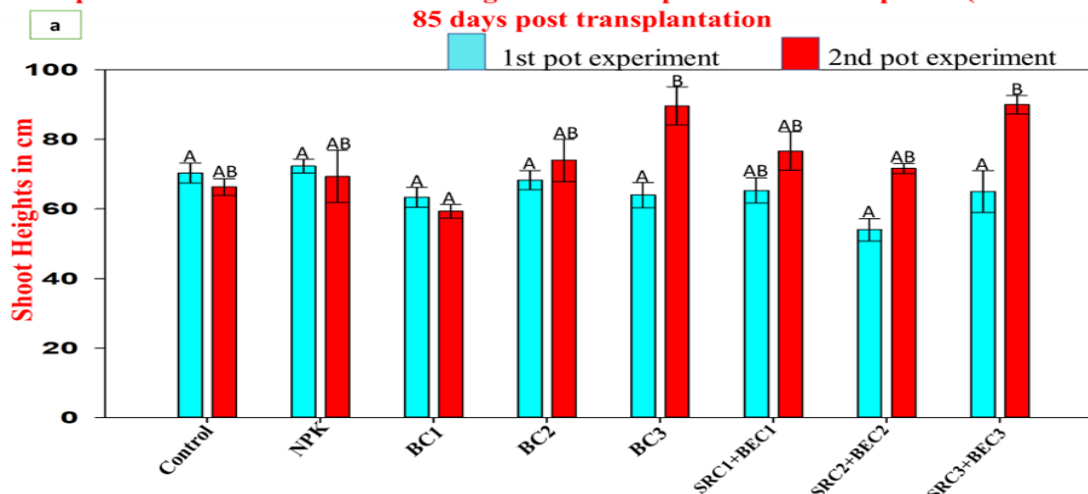


Figure 8.18: The above figure depicts the comparison study of shoot heights of 1st and 2nd greenhouse experiments on rice plants of Lunishree on 85 days post-transplantation. Data were plotted as mean \pm standard error (n=10) in the graph.

Observations:

In the above figures (a) and (b) no significant improvement in shoot heights was observed in 1st greenhouse and 2nd greenhouse experiments on rice plants of Lunishree as compared to control (without bacteria) and NPK-added pots. However, BC3 and SRC3+BEC3 combination-added pots showed significant shoot height improvements over control in the 2nd greenhouse experiment.

Comparative account of 1st and 2nd greenhouse experiment on rice plants (Dudheswar) on 85 days post transplantation



Comparative account of 1st and 2nd greenhouse experiment on rice plants (Dudheswar) on 85 days post transplantation

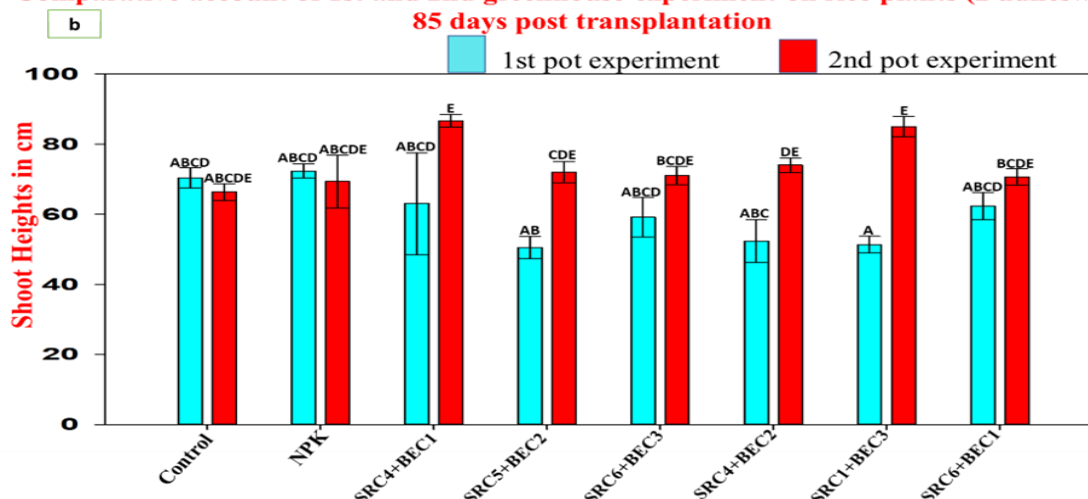


Figure 8.19: The above figure depicts the comparison study of shoot heights of 1st and 2nd greenhouse experiments on rice plants of Dudheswar on 85 days post-transplantation. Data were plotted as mean \pm standard error (n=10) in the graph.

Observations:

In the above figures (a) and (b) no significant improvement in shoot heights was observed in 1st greenhouse and 2nd greenhouse experiments on rice plants of Dudheswar as compared to control (without bacteria) and NPK-added pots. However, BC3, SRC3+BEC3, SRC4+BEC1, and SRC+BEC3 combinations added plants demonstrated significant shoot height improvements in the 2nd greenhouse experiment.

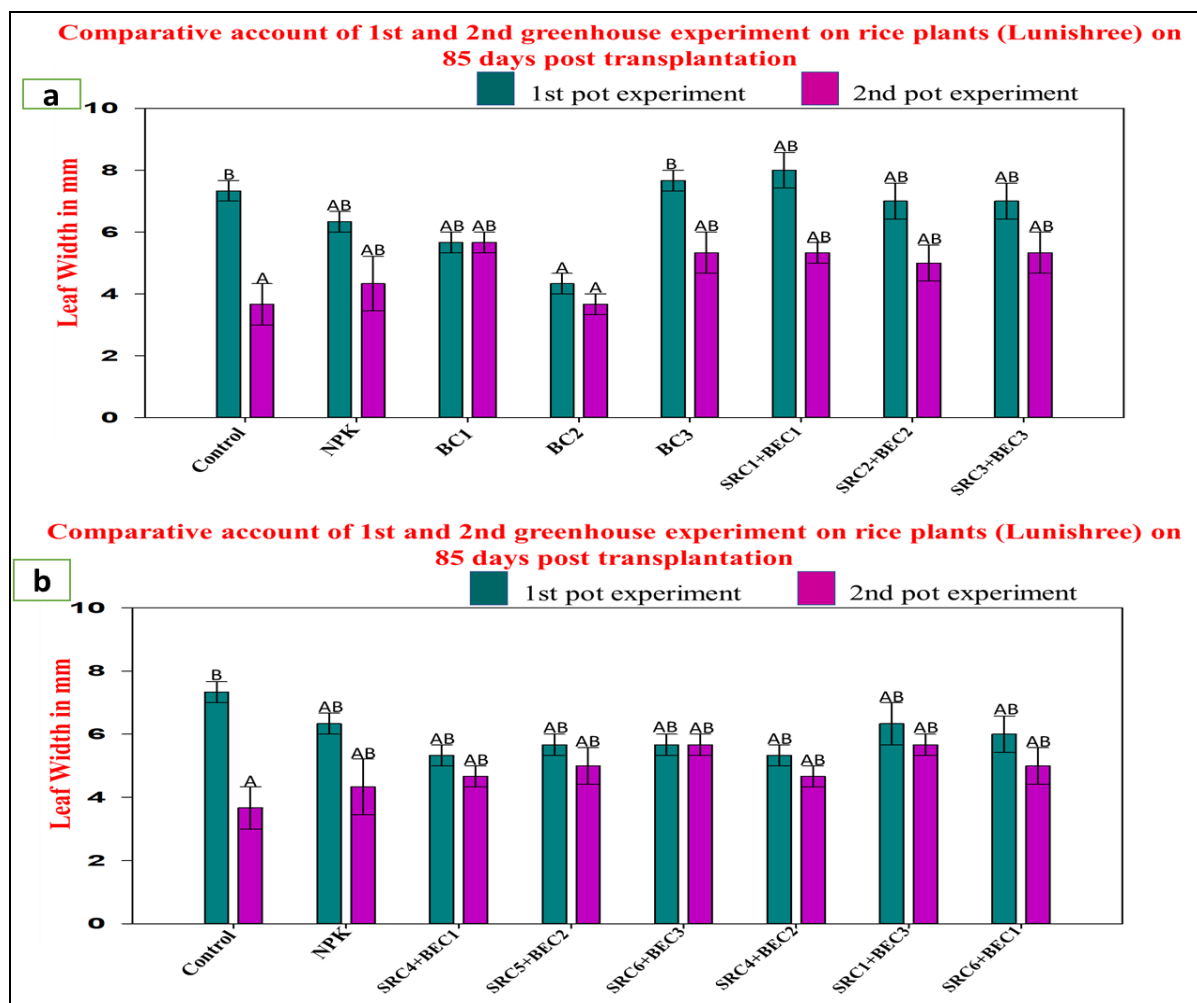


Figure 8.20: The above figure depicts the comparison study of leaf width of the 1st and 2nd greenhouse experiments on rice plants of Lunishree at 85 days post-transplantation. Data were plotted as mean \pm standard error (n=10) in the graph.

Observations:

In the above figures (a) and (b) not very significant improvement in leaf width was observed in the 1st greenhouse and 2nd greenhouse experiments on rice plants of Lunishree as compared to control (without bacteria) and NPK-added pots.

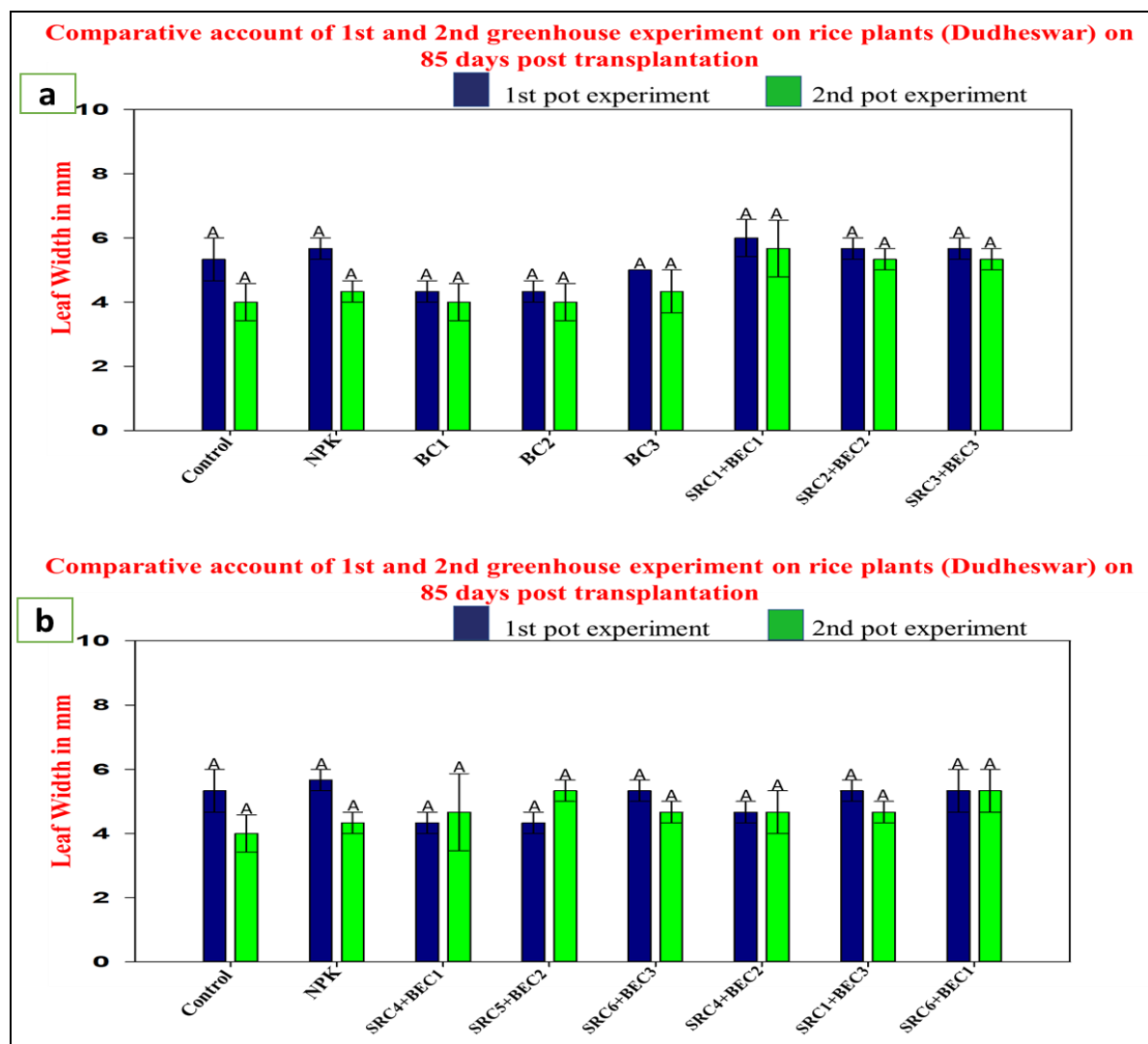


Figure 8.21: The above figure depicts the comparison study of leaf width of 1st and 2nd greenhouse experiments on rice plants of Dudheswar on 85 days post-transplantation. Data were plotted as mean \pm standard error (n=10) in the graph.

Observations:

In the above figures (a) and (b) no significant improvement in leaf width was observed in 1st greenhouse and 2nd greenhouse experiments on rice plants of Dudheswar as compared to control (without bacteria) and NPK-added pots.

8.3. Analysis of pot soil pH during the experimental period:

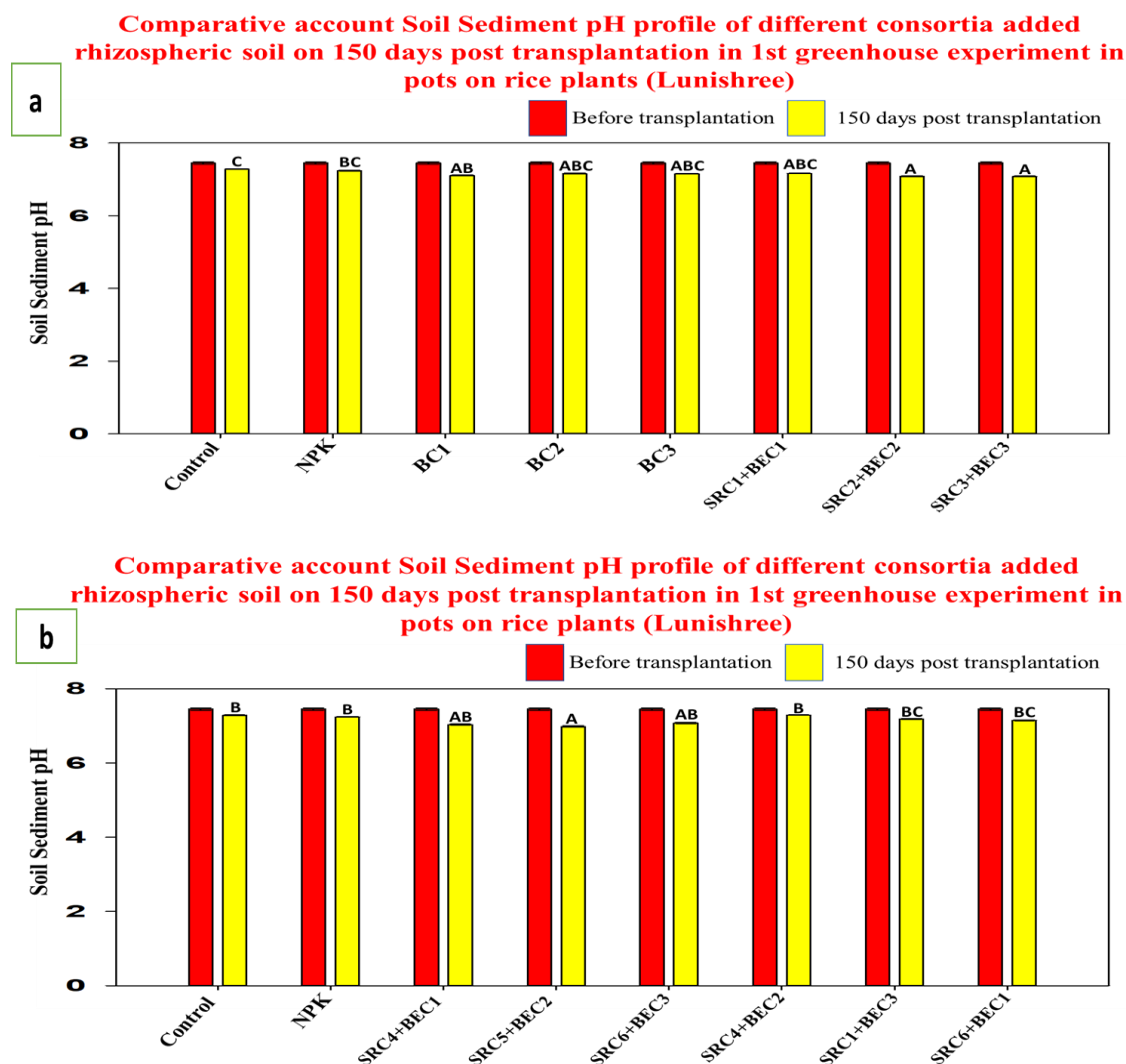


Figure 8.22: The above figure depicts the comparison study of soil pH from control (without bacteria), NPK-added and different consortia (prepared by mixing endophytic and rhizospheric bacterial strains) added rhizospheric soil in 1st greenhouse experiment on rice plants of Lunishree. Data were plotted as mean \pm standard error (n=3) in the graph.

Observations:

In the above figures (a) and (b) the pot soil pH was found to slightly decrease over 150 days post-transplantation as compared to before transplantation as found in control (without bacteria) and NPK-added pots, in 1st greenhouse experiment on rice plants of Lunishree.

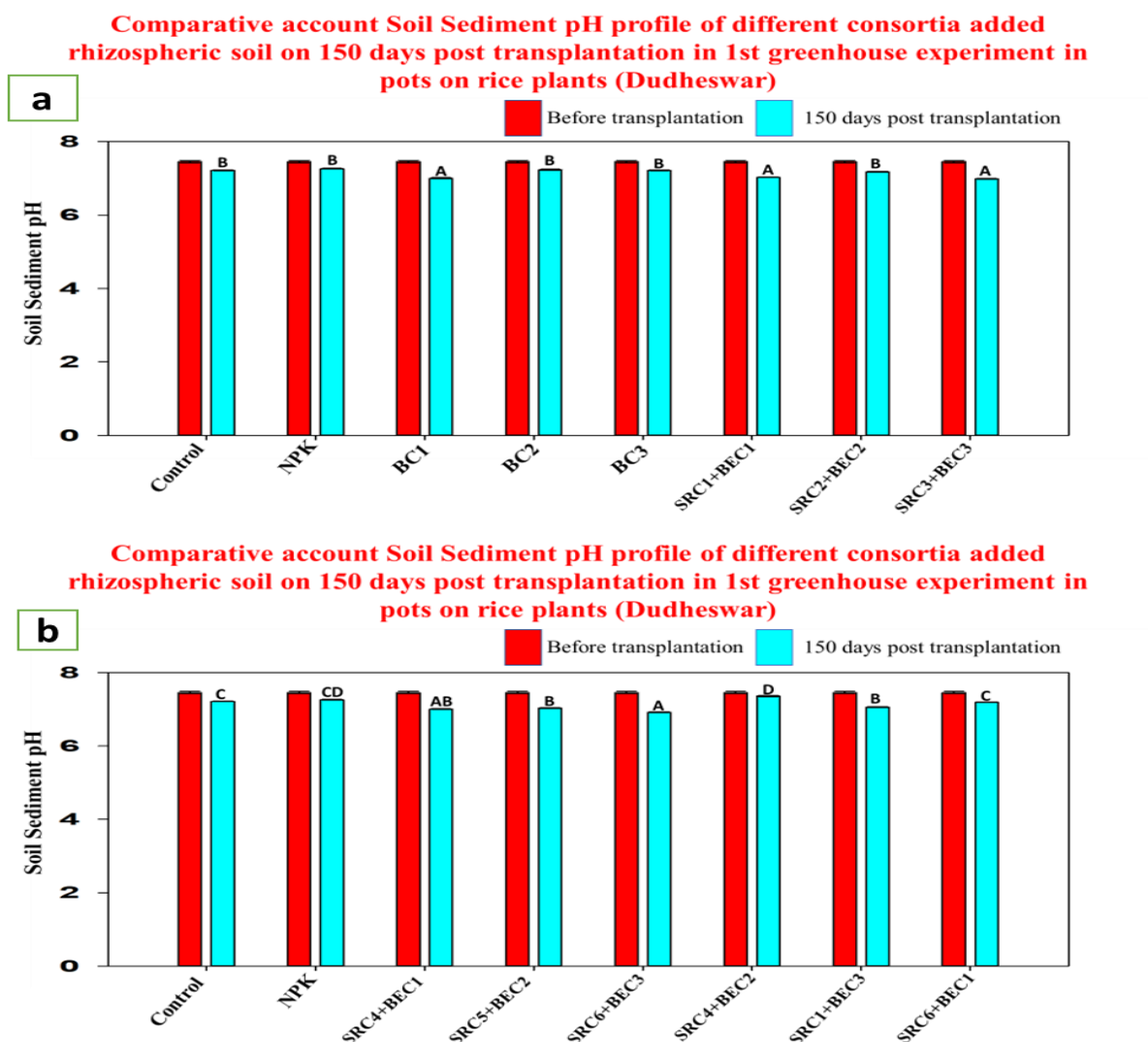


Figure 8.23: The above figure depicts the comparison study of soil pH from control (without bacteria), NPK-added and different consortia (prepared by mixing endophytic and rhizospheric bacterial strains) added rhizospheric pot soil in 1st greenhouse experiment on rice plants of Dudheswar. Data were plotted as mean \pm standard error (n=3) in the graph.

Observations:

In the above figures (a) and (b) the soil pH was observed to slightly decrease over 150 days post-transplantation as compared to before transplantation as found in control (without bacteria) and NPK-added pots, in 1st greenhouse experiment on rice plants of Dudheswar.

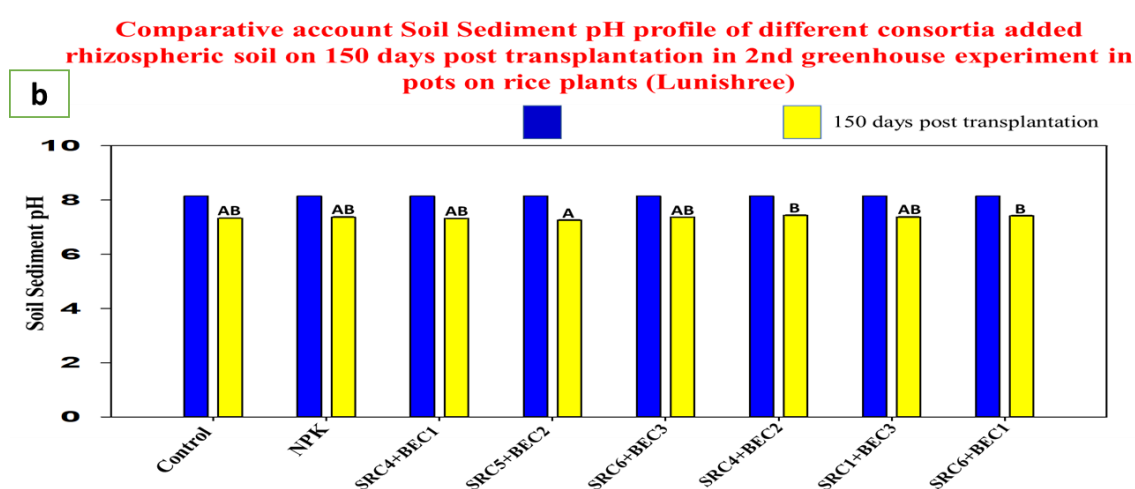
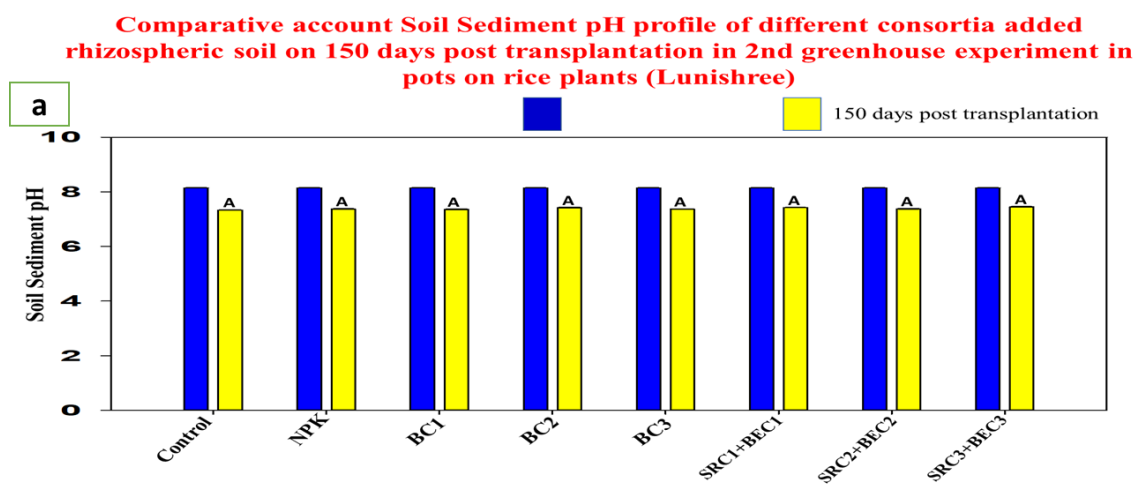


Figure 8.24: The above figure depicts the comparison study of soil pH from control (without bacteria), NPK-added, and different consortia (prepared by mixing endophytic and rhizospheric bacterial strains) added rhizospheric pot soil in the 2nd greenhouse experiment on rice plants of Lunishree. Data were plotted as mean \pm standard error (n=3) in the graph.

Observations:

In the above figures (a) and (b) the soil pH was observed to decrease over 150 days post-transplantation as compared to before transplantation as observed in control (without bacteria) and NPK-added pots, in the 2nd greenhouse experiment on rice plants of Lunishree.

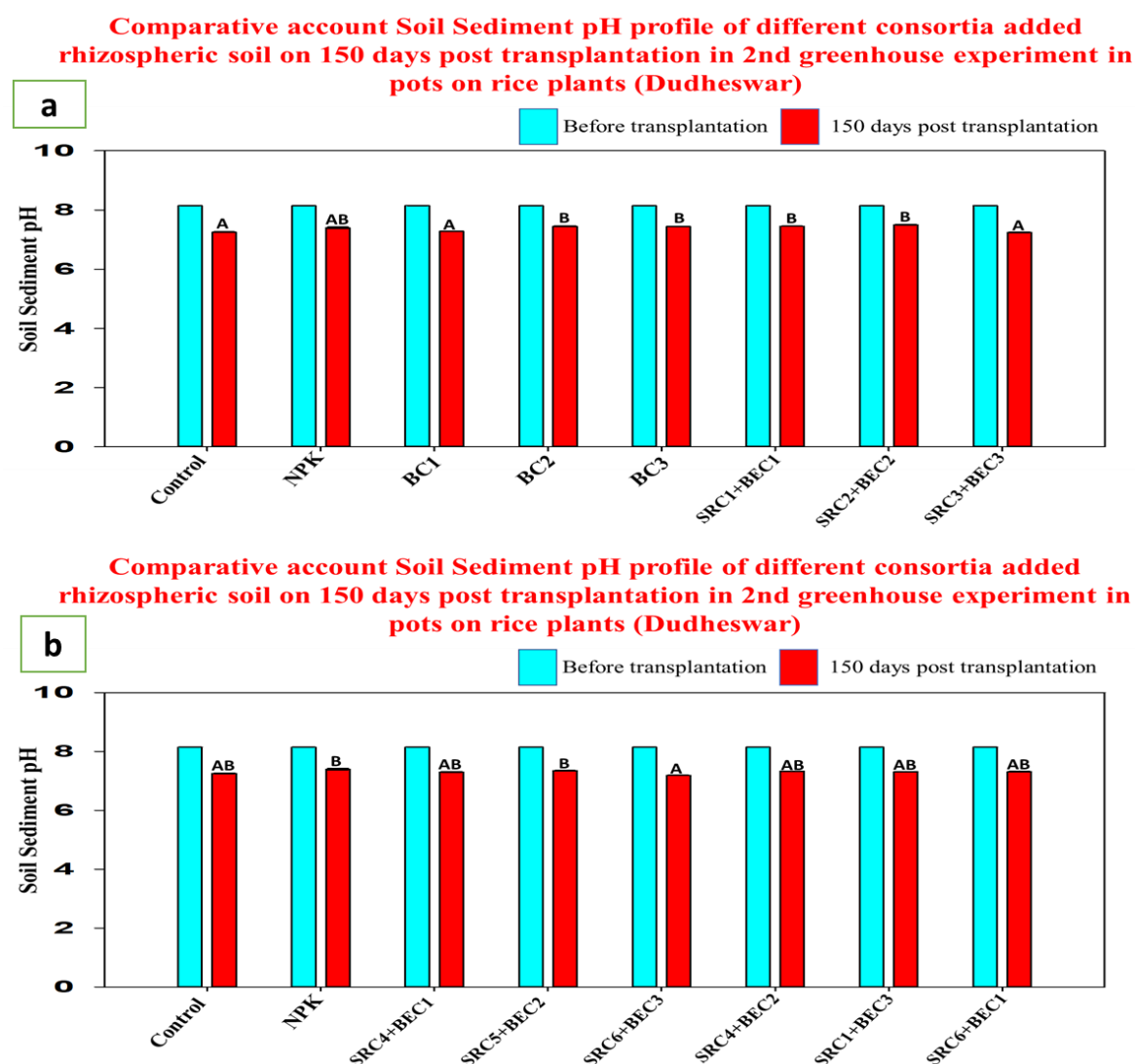


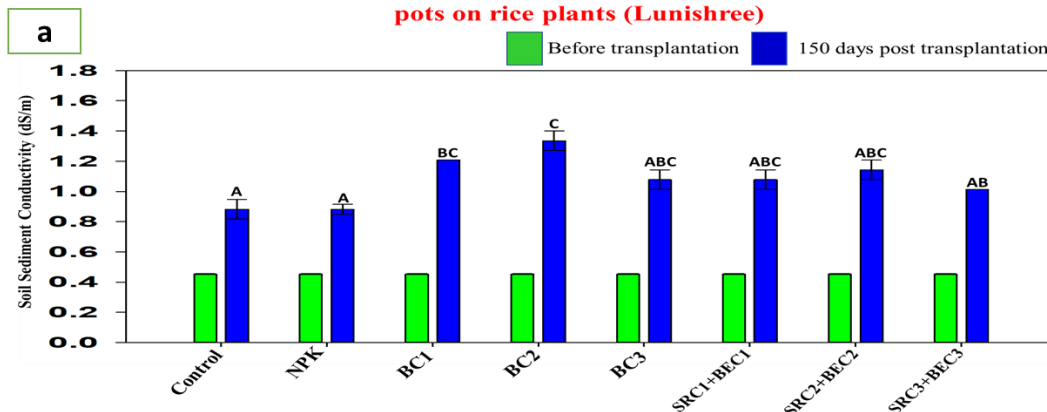
Figure 8.25: The above figure depicts the comparison study of soil pH from control (without bacteria), NPK-added and different consortia (prepared by mixing endophytic and rhizospheric bacterial strains) added rhizospheric pot soil in the 2nd greenhouse experiment on rice plants of Dudheswar. Data were plotted as mean \pm standard error (n=3) in the graph.

Observations:

In the above figures (a) and (b) the soil pH was observed to slightly decrease over 150 days post-transplantation period as compared to before transplantation as observed for control (without bacteria) and NPK-added pots, in the 2nd greenhouse experiment on rice plants of Dudheswar.

8.4. Analysis of pot soil conductivity across the experimental period:

Comparative account Soil Sediment Conductivity profile of different consortia added rhizospheric soil on 150 days post transplantation in 1st greenhouse experiment in pots on rice plants (Lunishree)



Comparative account Soil Sediment Conductivity profile of different consortia added rhizospheric soil on 150 days post transplantation in 1st greenhouse experiment in pots on rice plants (Lunishree)

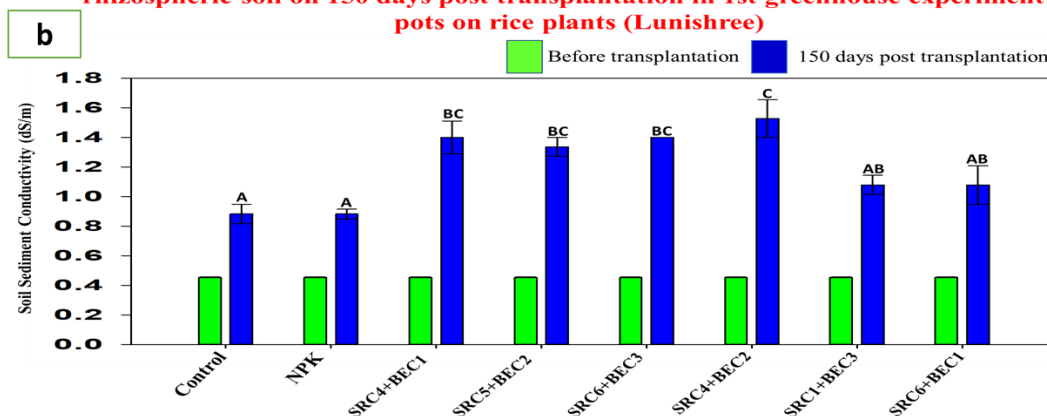
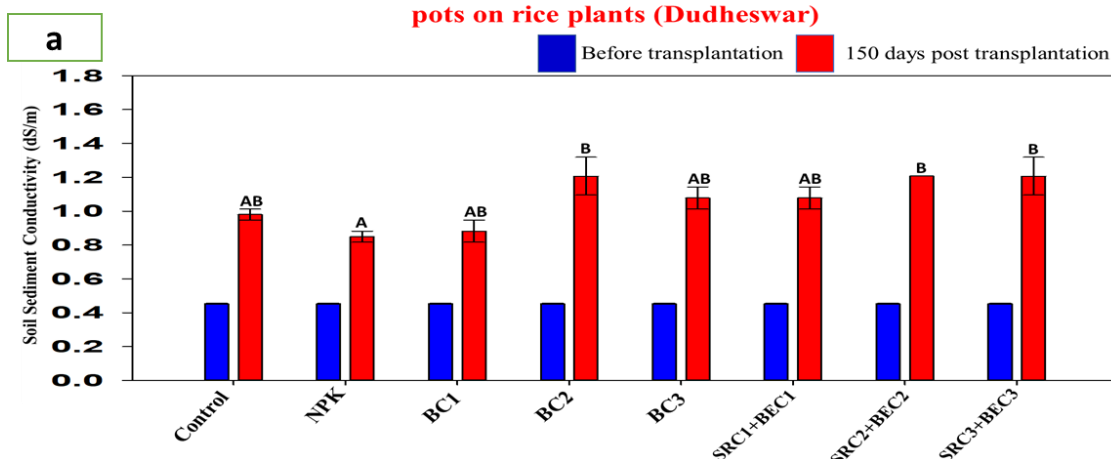


Figure 8.26: The above figure depicts the comparison study of soil conductivity from control (without bacteria), NPK-added and different consortia (prepared by mixing endophytic and rhizospheric bacterial strains) added rhizospheric pot soil in the 1st greenhouse experiment on rice plants of Lunishree. Data were plotted as mean \pm standard error (n=3) in the graph.

Observations:

In the above figures (a) and (b) the soil conductivity was found to increase considerably across 150 days post-transplantation period as compared to before transplantation as observed in control (without bacteria) and NPK-added pots, in the 1st greenhouse experiment on rice plants of Lunishree. The salinity increased from 0.4dS/m to 1.5dS/m over the 150 days experimental period, even in control and NPK-added pot soils also. This might be contributed to the reason of more dissolution of available ionic species in the pot soil over this 150-day time, because of regular watering.

Comparative account Soil Sediment Conductivity profile of different consortia added rhizospheric soil on 150 days post transplantation in 1st greenhouse experiment in pots on rice plants (Dudheswar)



Comparative account Soil Sediment Conductivity profile of different consortia added rhizospheric soil on 150 days post transplantation in 1st greenhouse experiment in pots on rice plants (Dudheswar)

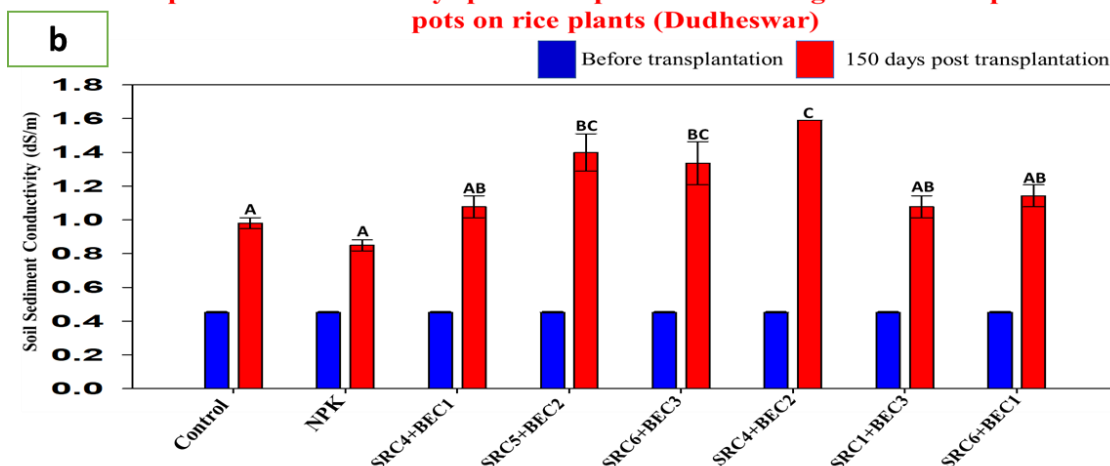


Figure 8.27: The above figure depicts the comparison study of soil conductivity from control (without bacteria), NPK-added and different consortia (prepared by mixing endophytic and rhizospheric bacterial strains) added rhizospheric pot soil in the 1st greenhouse experiment on rice plants of Dudheswar. Data were plotted as mean \pm standard error (n=3) in the graph.

Observations:

In the above figure (a) and (b) the soil conductivity was found to increase significantly over 150 days post-transplantation period as compared to before transplantation as observed in control (without bacteria) and NPK-added pots, in the 1st greenhouse experiment on rice plants of Dudheswar. The salinity increased from 0.4dS/m to 1.6dS/m during the 150 days experimental period, even in control and NPK-added pot soils also. This might be contributed to the reason of more dissolution of available ionic species in the pot soil over this 150-day time, because of regular watering.

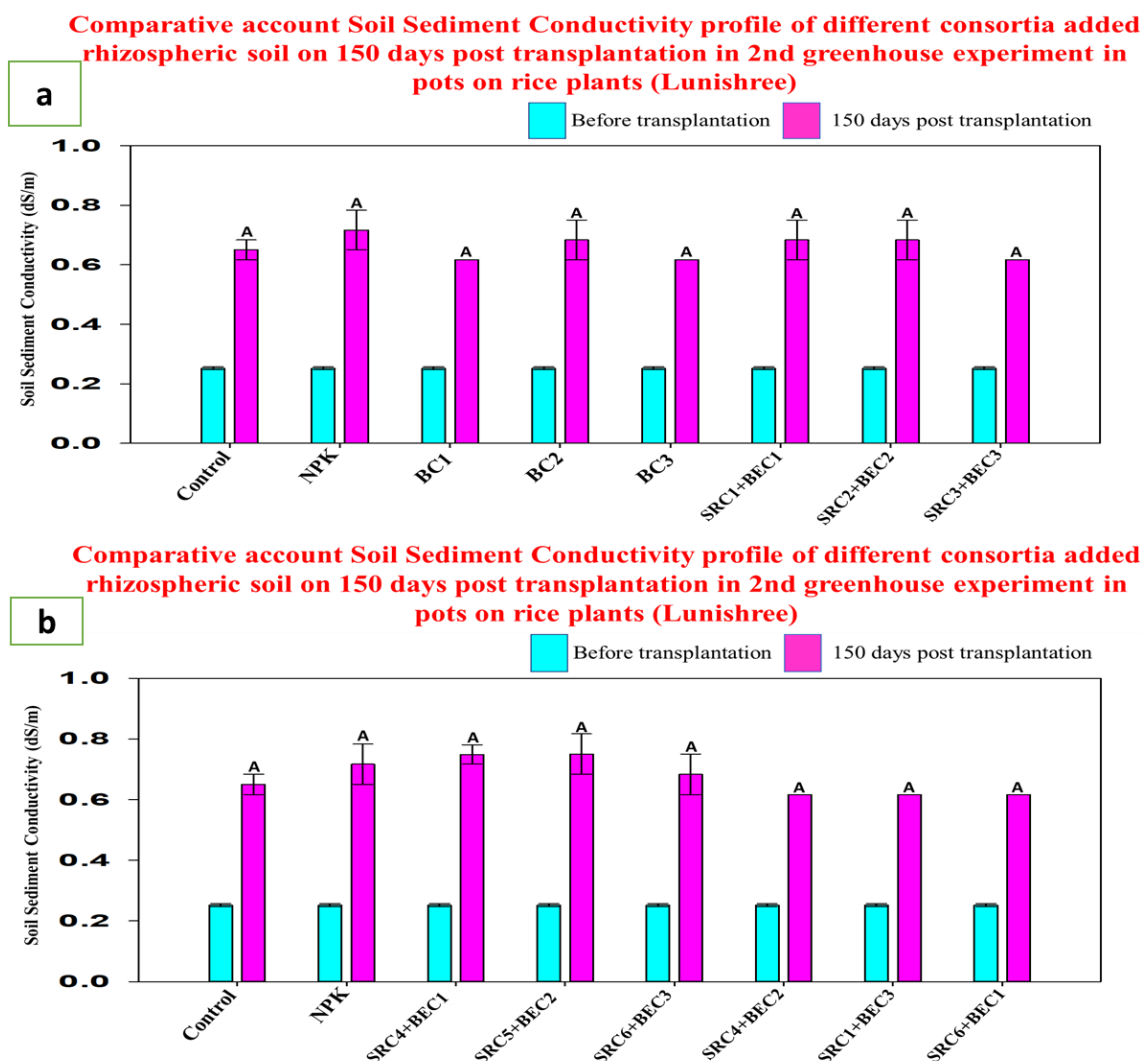


Figure 8.28: The above figure depicts the comparison study of soil conductivity from control (without bacteria), NPK-added and different consortia (prepared by mixing endophytic and rhizospheric bacterial strains) added rhizospheric pot soil in the 2nd greenhouse experiment on rice plants of Lunishree. Data were plotted as mean \pm standard error (n=3) in the graph.

Observations:

In the above figures (a) and (b) the soil conductivity was found to increase significantly during 150 days post-transplantation time as compared to before transplantation as observed in control (without bacteria) and NPK-added pots, in the 2nd greenhouse experiment on rice plants of Lunishree. The salinity increased from 0.2dS/m to 0.7dS/m over the 150 days experimental period, even in control and NPK-added pot soils also. This might be contributed to the reason of more dissolution of available ionic species in the pot soil over this 150-day time, because of regular watering.

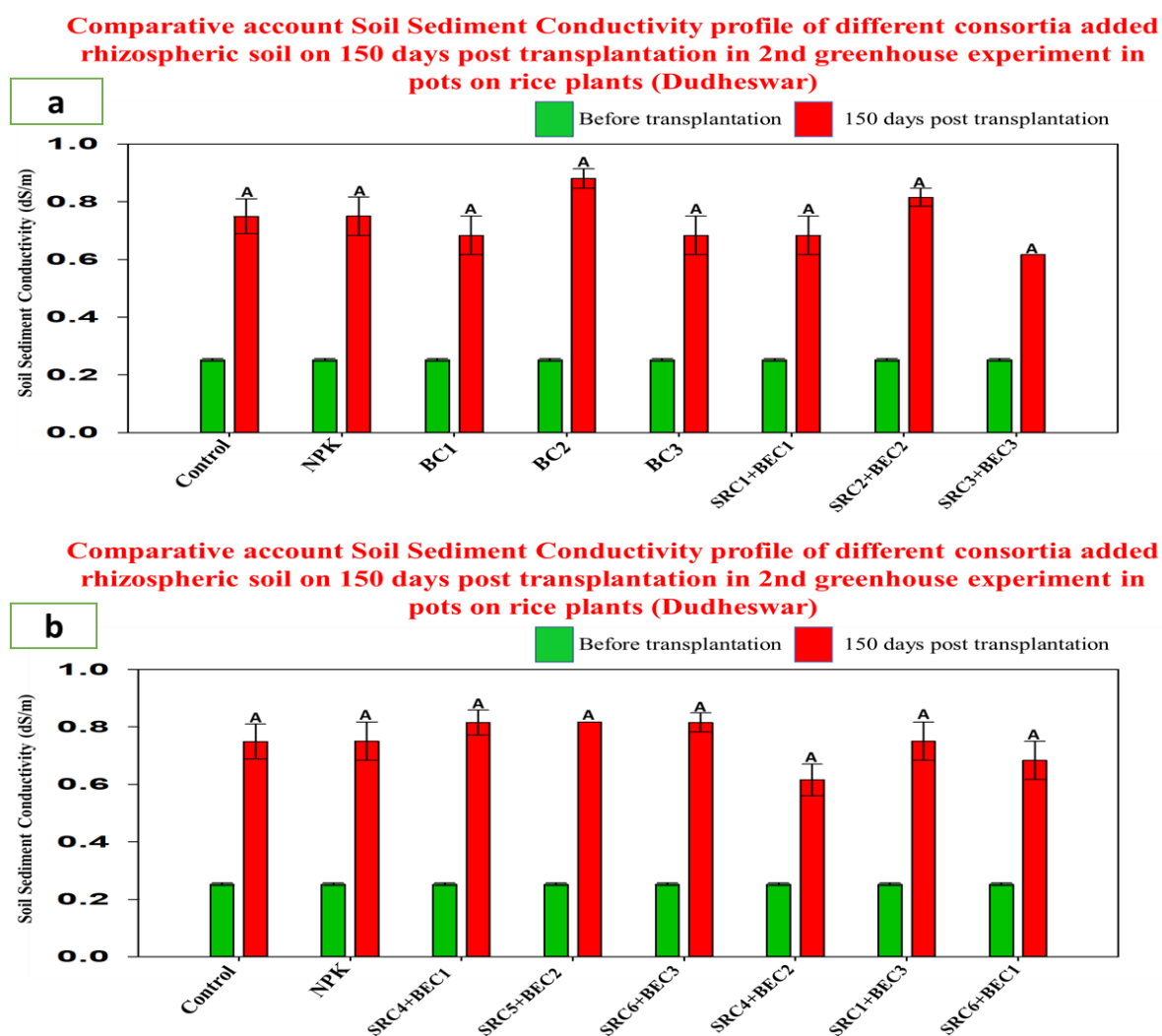


Figure 8.29: The above figure depicts the comparison study of soil sediment conductivity from control (without bacteria), NPK added and different consortia (prepared by mixing endophytic and rhizospheric bacterial strains) added rhizospheric soil in 2nd greenhouse experiment on rice plants of Dudheswar. Data were plotted as mean \pm standard error (n=3) in the graph.

Observations:

In the above figures (a) and (b) the soil conductivity was found to increase considerably during 150 days post-transplantation as compared to before transplantation as found in control (without bacteria) and NPK-added pots, in the 2nd greenhouse experiment on rice plants of Dudheswar. The salinity increased from 0.2dS/m to 0.9dS/m over the 150 days experimental period, even in control and NPK-added pot soils also. This might be contributed to the reason of more dissolution of available ionic species in the pot soil over this 150-day time, because of regular watering.

8.5. Analysis of soil organic carbon (SOC) content during the experimental period:

Calibration curve of organic carbon to be followed as described in the figure 7.6

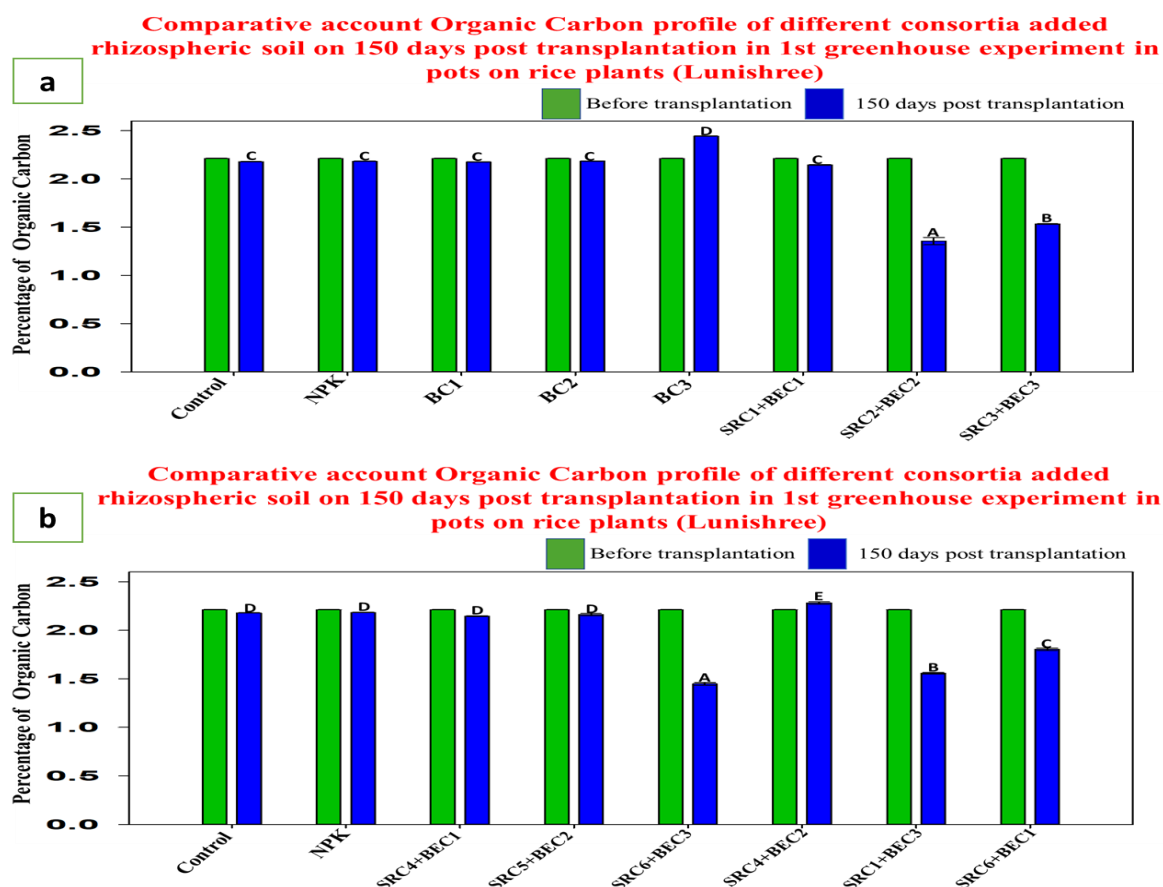


Figure 8.30: The above figure depicts the comparison study of soil organic carbon from control (without bacteria), NPK-added and different consortia (prepared by mixing endophytic and rhizospheric bacterial strains) added rhizospheric pot soil in the 1st greenhouse experiment on rice plants of Lunishree. Data were plotted as mean \pm standard error (n=3) in the graph.

Observations:

In the above figures (a) and (b) the soil organic carbon was found to be the same after 150 days post-transplantation as compared to before transplantation along with the control (without bacteria) and NPK-added pots, in the 1st greenhouse experiment on rice plants of Lunishree with the exceptions of BC3-added pot soil where soil organic carbon content was found to increase significantly as compared to before transplantation. However, it was also observed for SRC2+BEC2, SRC3+BEC3, SRC6+BEC3, SRC1+BEC3 and SRC6+BEC1-added pot soil where soil organic carbon content was found to decrease significantly as compared to before transplantation.

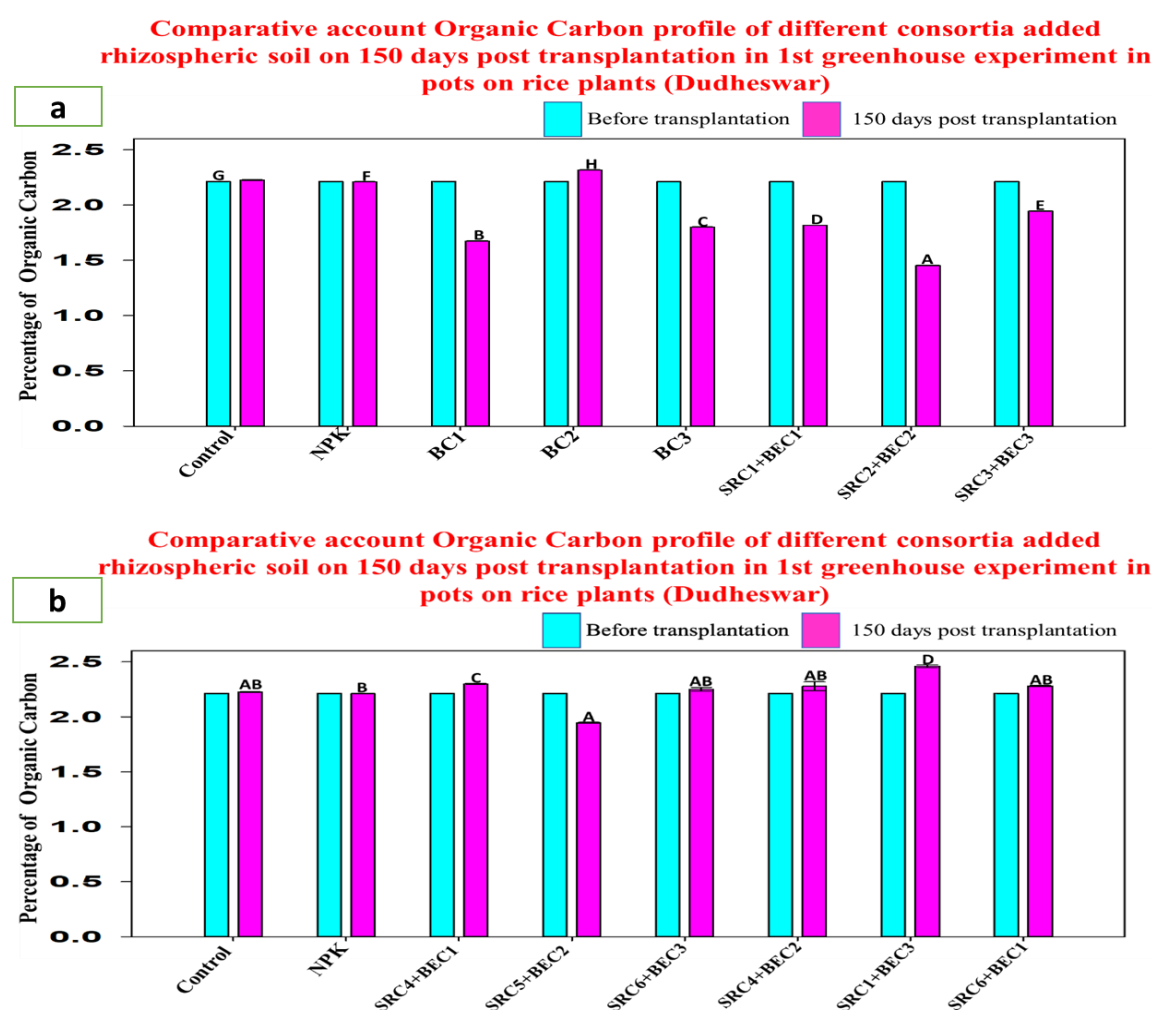


Figure 8.31: The above figure depicts the comparison study of soil organic carbon from control (without bacteria), NPK-added and different consortia (prepared by mixing endophytic and rhizospheric bacterial strains) added rhizospheric pot soil in the 1st greenhouse experiment on rice plants of Dudheswar. Data were plotted as mean \pm standard error (n=3) in the graph.

Observations:

In the above figures (a) and (b) the soil organic carbon was observed to be more or less the same after 150 days post-transplantation as compared to before transplantation along with the control (without bacteria) and NPK-added pots, in the 1st greenhouse experiment on rice plants of Dudheswar. However, in BC1, BC3, SRC1+BEC1, SRC2+BEC2, SRC3+BEC3 and SRC5+BEC2 consortia-added pot soils, soil organic carbon content was found to decrease significantly as compared to before transplantation. In contrast, in BC2 and SRC1+BEC3-added pot soil, soil organic carbon content increased significantly as compared to that of before transplantation.

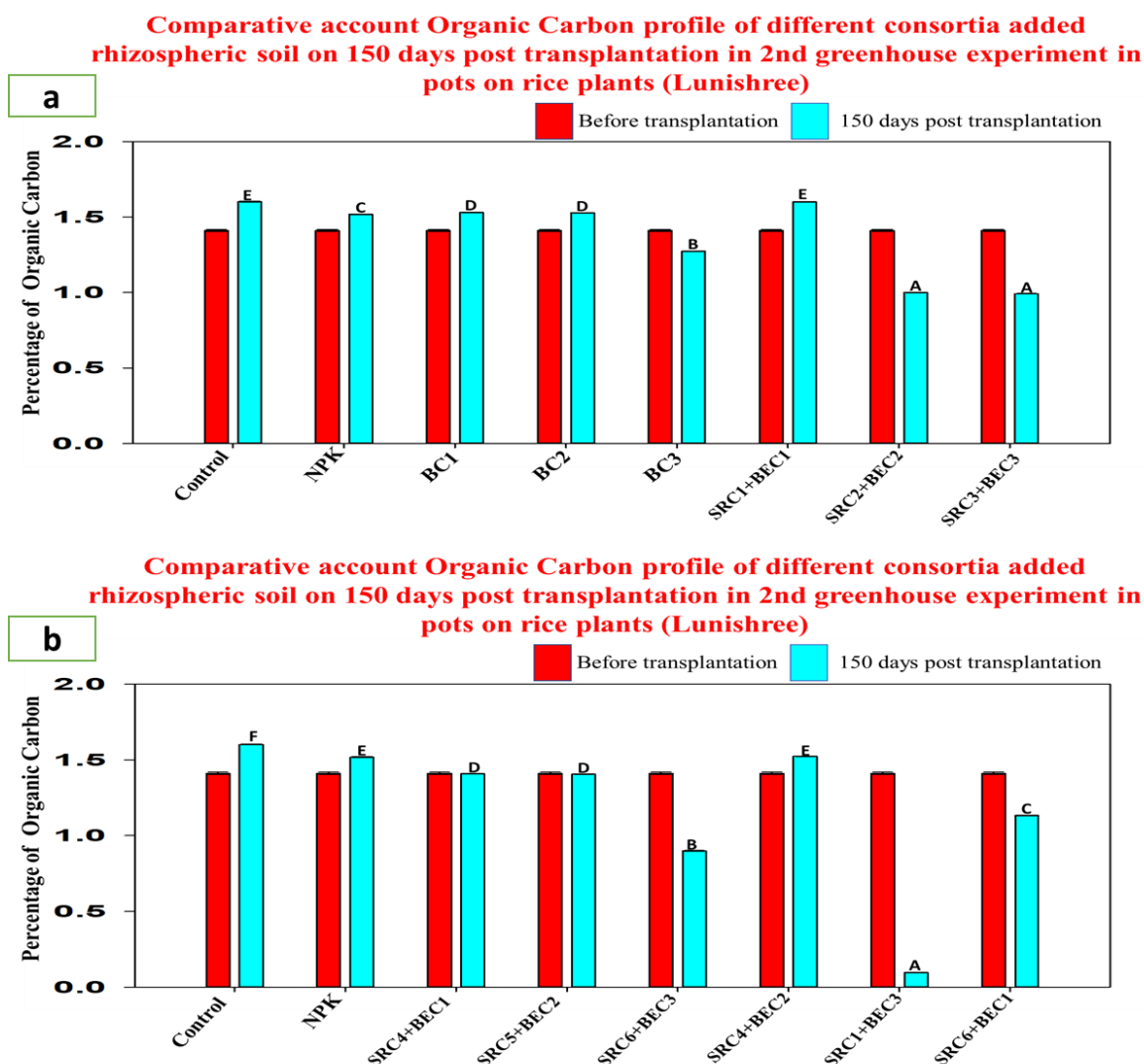


Figure 8.32: The above figure depicts the comparison study of soil organic carbon from control (without bacteria), NPK-added and different consortia (prepared by mixing endophytic and rhizospheric bacterial strains) added rhizospheric pot soil in the 2nd greenhouse experiment on rice plants of Lunishree. Data were plotted as mean \pm standard error (n=3) in the graph.

Observations:

In the above figures (a) and (b) the soil organic carbon content more or less increased significantly as compared to that of before transplantation in most cases along with the control (without bacteria) and NPK-added pots, in the 2nd greenhouse experiment on rice plants of Lunishree with the exceptions of BC3, SRC2+BEC2, SRC3+BEC3, SRC6+BEC3-added soils where SOC decreased significantly over 150 days. The decline of SOC from ~1.5% (before transplantation) to 0.1% (after 150 days of transplantation) as observed in SRC1+BEC3-added soil, as presented in the above figure might be an experimental error.

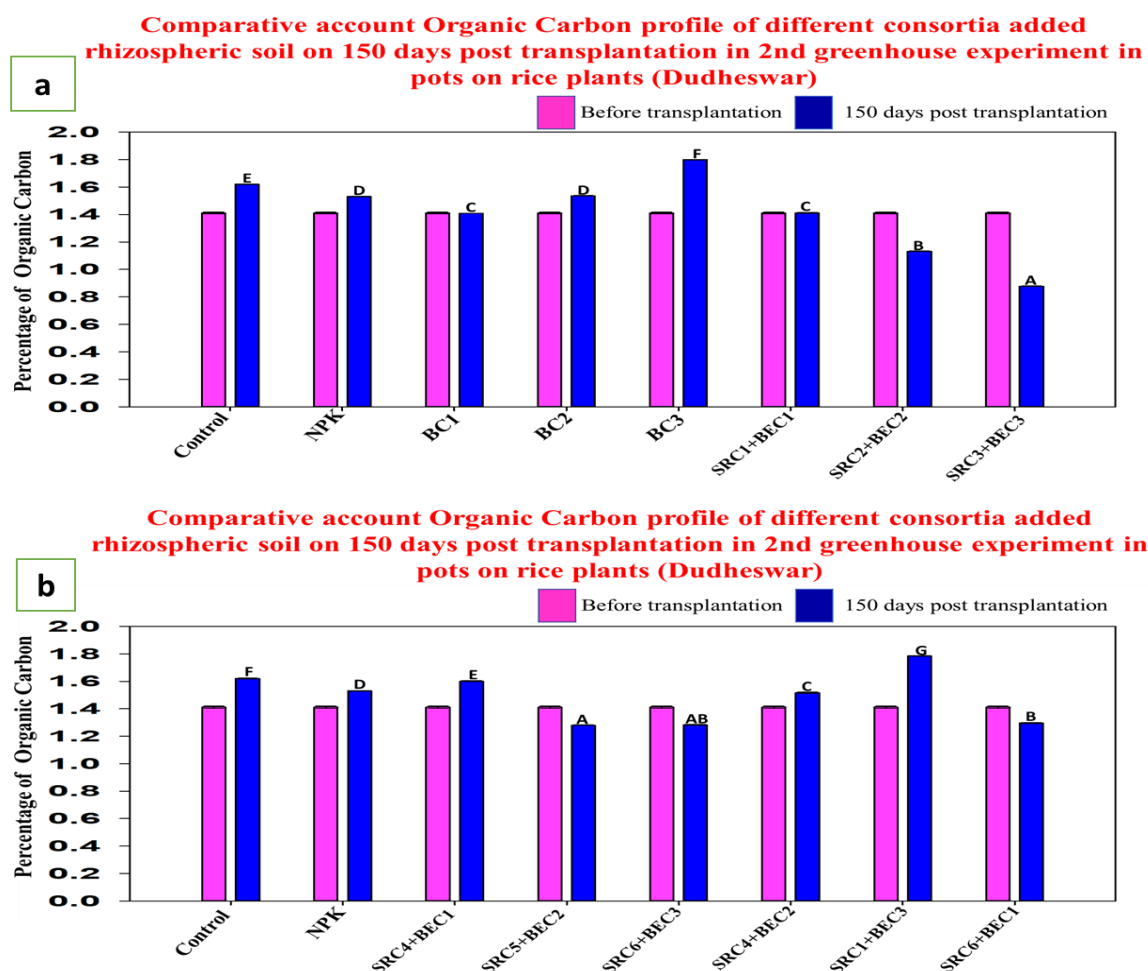


Figure 8.33: The above figure depicts the comparison study of soil organic carbon from control (without bacteria), NPK-added and different consortia (prepared by mixing endophytic and rhizospheric bacterial strains) added rhizospheric pot soil in the 2nd greenhouse experiment on rice plants of Dudheswar. Data were plotted as mean \pm standard error (n=3) in the graph.

Observations:

In the above figures (a) and (b) the soil organic carbon more or less increased significantly as compared to that of before transplantation after 150 days of transplantation, in most cases, along with control (without bacteria) and NPK-added pots, in the 2nd greenhouse experiment on rice plants of Dudheswar with exceptions for SRC2+BEC2, SRC3+BEC3, SRC6+BEC3 and SRC6+BEC1-added pots soils, where soil organic carbon content was found to decrease significantly as compared to before transplantation.

8.6. Analysis of soil nitrate-nitrogen over the experimental time:

Calibration curve of nitrate-nitrogen to be followed is described in figure 7.8.

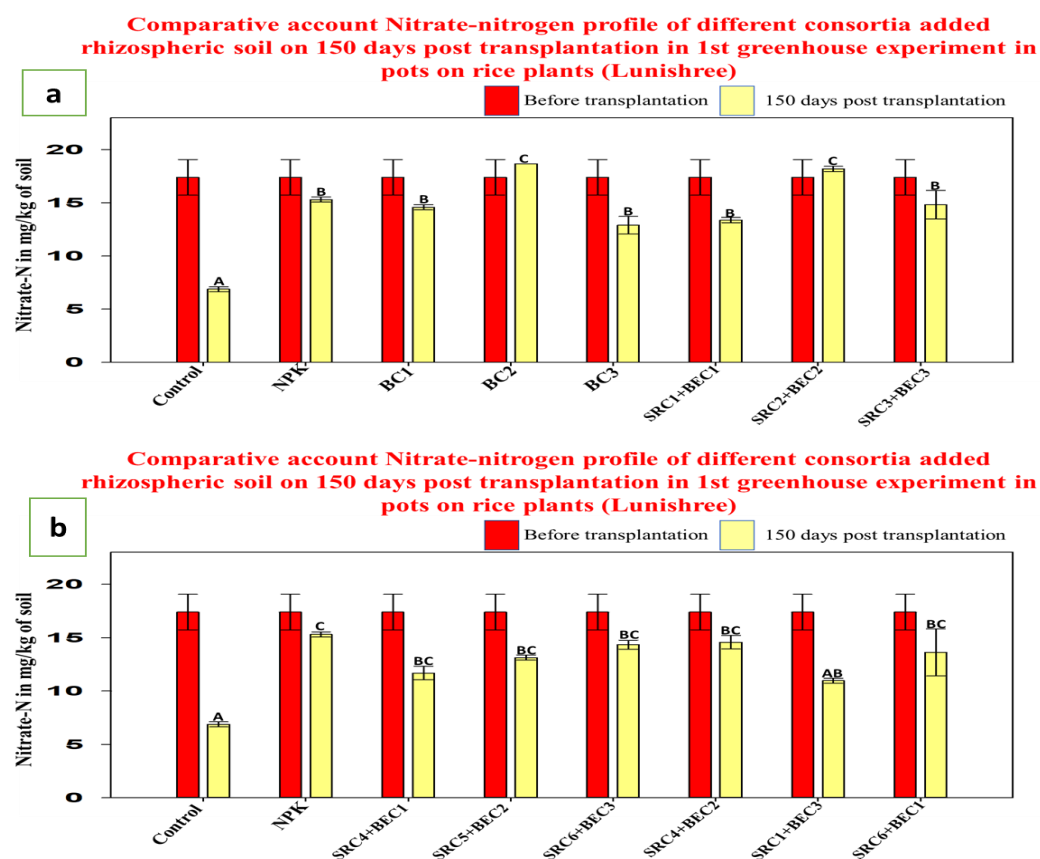


Figure 8.34: The above figure depicts the comparison study of soil nitrate-nitrogen from control (without bacteria), NPK-added, and different consortia (prepared by mixing endophytic and rhizospheric bacterial strains) added rhizospheric pot soil in the 1st greenhouse experiment on rice plants of Lunishree. Data were plotted as mean \pm standard error (n=3) in the graph.

Observations:

In the above figures (a) and (b) the consumption rate of soil nitrate-nitrogen by rice plants was found to be higher in comparison to its replenishment in pot soil via addition of NPK or bacterial consortia. As a result soil nitrate-nitrogen significantly decreased over 150 days of post-transplantation period in NPK-added pots as well as in bacterial consortia-added pots when compared to that of before transplantation. However, this decrease in soil nitrate-nitrogen was observed to be the highest in control pot soils (without bacteria), in the 1st greenhouse experiment on rice plants of Lunishree, while contrastingly BC2 and SRC2+BEC2 consortia added pots showed significant increase in soil nitrate-nitrogen over 150 days of post-transplantation period.

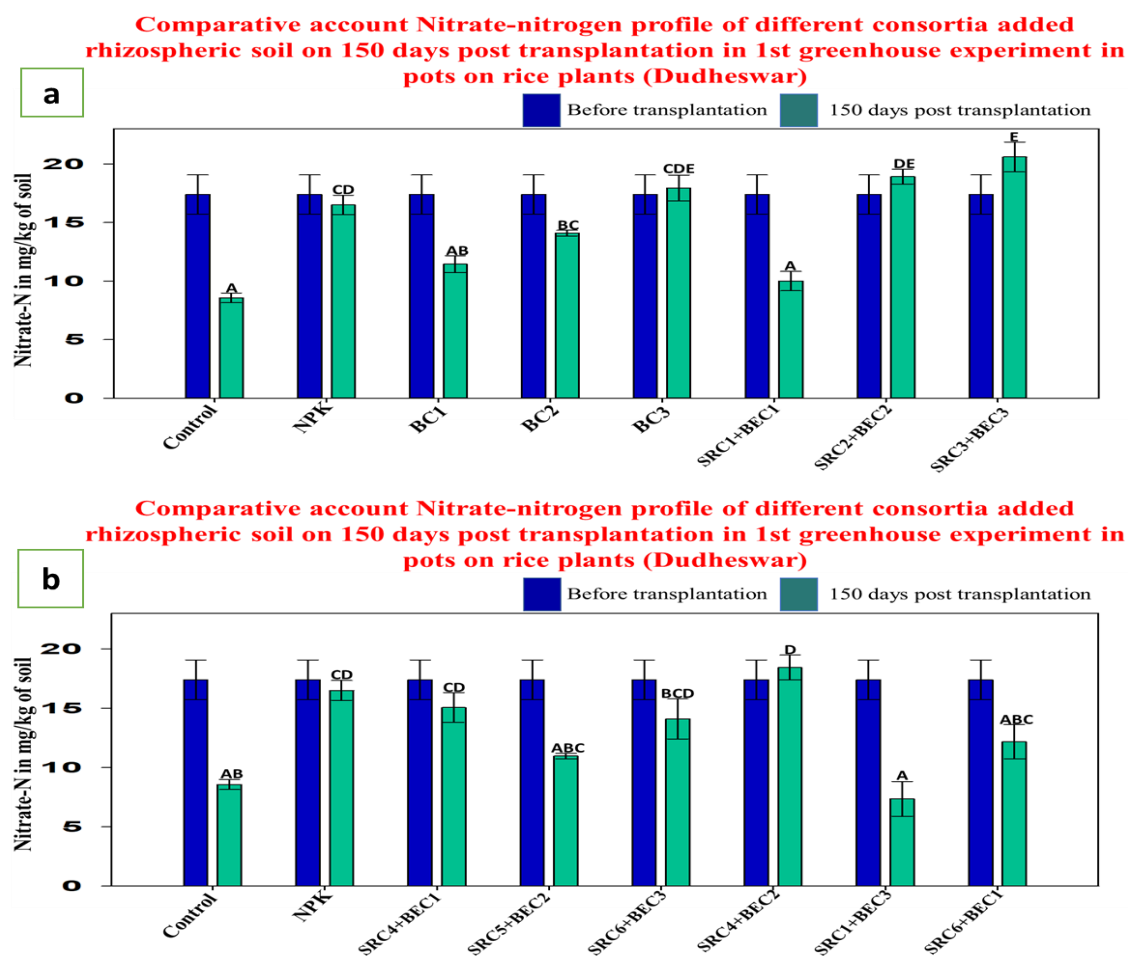


Figure 8.35: The above figure depicts the comparison study of soil nitrate-nitrogen from control (without bacteria), NPK-added and different consortia (prepared by mixing endophytic and rhizospheric bacterial strains) added rhizospheric pot soil in the 1st greenhouse experiment on rice plants of Dudheswar. Data were plotted as mean \pm standard error (n=3) in the graph.

Observations:

In the above figures (a) and (b) overall the consumption rate of soil nitrate-nitrogen by rice plants was found to be higher in comparison to its replenishment in pot soil via addition of NPK or bacterial consortia. As a result soil nitrate-nitrogen significantly decreased over 150 days of post-transplantation period in NPK-added pots as well as in bacterial consortia-added pots when compared to that of before transplantation. However, this decrease in soil nitrate-nitrogen was observed to be the highest in control pot soils (without bacteria), and a few consortia-added pot soils also in the 1st greenhouse experiment on rice plants of Dudheswar, while contrastingly BC3, SRC2+BEC2, SRC3+BEC3, and SRC4+BEC2 consortia-added pots showed significant increase in soil nitrate-nitrogen over 150 days of post-transplantation period.

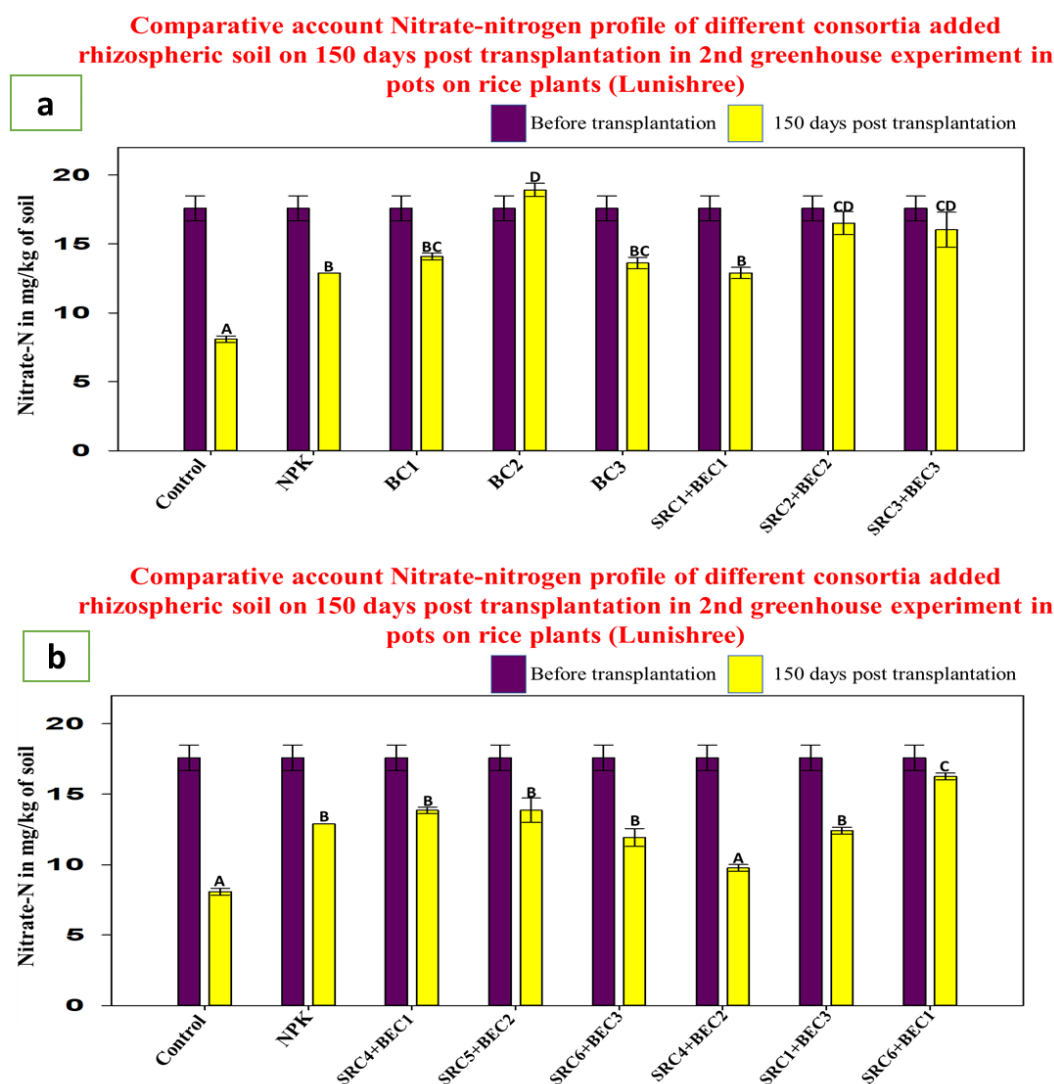


Figure 8.36: The above figure depicts the comparison study of soil nitrate-nitrogen from control (without bacteria), NPK-added and different consortia (prepared by mixing endophytic and rhizospheric bacterial strains) added rhizospheric pot soil in the 2nd greenhouse experiment on rice plants of Lunishree. Data were plotted as mean \pm standard error (n=3) in the graph.

Observations:

In the above figures (a) and (b) overall the consumption rate of soil nitrate-nitrogen by rice plants was found to be higher in comparison to its replenishment in pot soil via addition of NPK or bacterial consortia. As a result soil nitrate-nitrogen significantly decreased over 150 days of post-transplantation period in NPK-added pots as well as in bacterial consortia-added pots when compared to that of before transplantation. However, this decrease in soil nitrate-nitrogen was observed to be the highest in control pot soils (without bacteria), and a few consortia-added pot soils also in the 2nd greenhouse experiment on rice plants of Lunishree,

while contrastingly BC2 consortia-added pots showed significant increase in soil nitrate-nitrogen over 150 days of post-transplantation period.

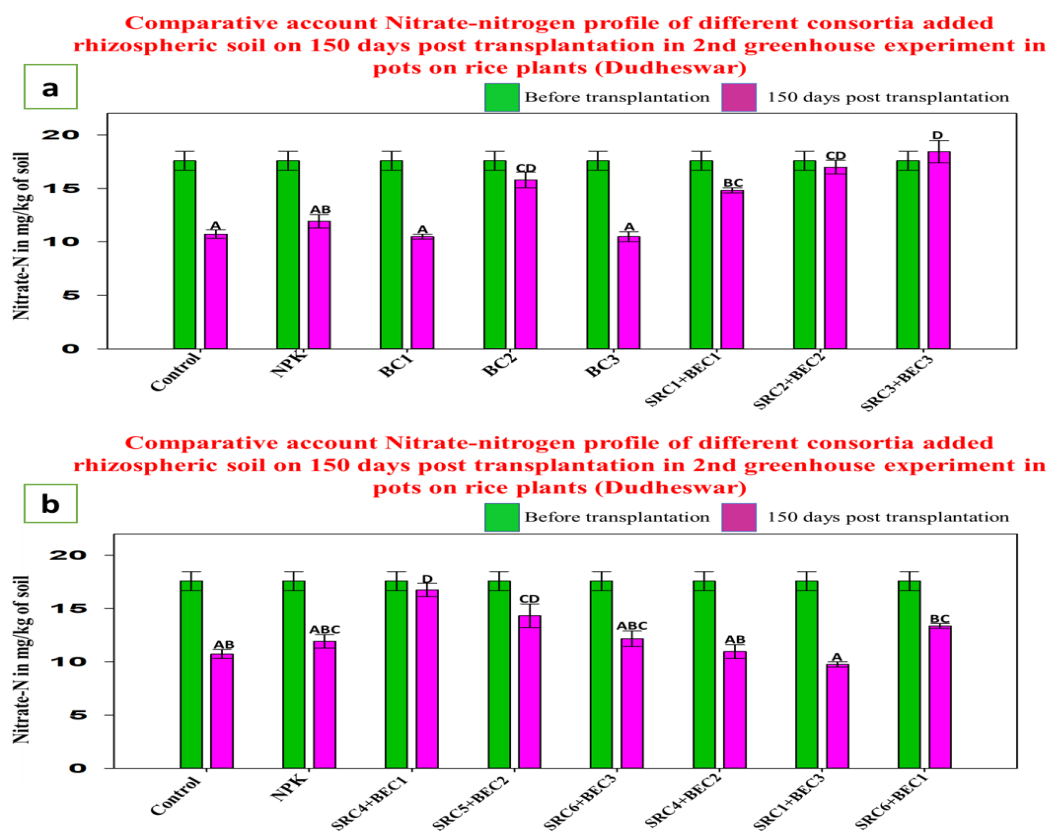


Figure 8.37: The above figure depicts the comparison study of soil nitrate-nitrogen from control (without bacteria), NPK-added and different consortia (prepared by mixing endophytic and rhizospheric bacterial strains) added rhizospheric pot soil in the 2nd greenhouse experiment on rice plants of Dudheswar. Data were plotted as mean \pm standard error (n=3) in the graph.

Observations:

In the above figures (a) and (b) overall the consumption rate of soil nitrate-nitrogen by rice plants was found to be higher in comparison to its replenishment in pot soil via addition of NPK or bacterial consortia. As a result soil nitrate-nitrogen significantly decreased over 150 days of post-transplantation period in NPK-added pots as well as in bacterial consortia-added pots when compared to that of before transplantation. However, this decrease in soil nitrate-nitrogen was observed to be the highest in control pot soils (without bacteria), and many consortia-added pot soils also in the 2nd greenhouse experiment on rice plants of Dudheswar, while contrastingly SRC3+BEC3 consortia-added pots showed significant increase in soil nitrate-nitrogen over 150 days of post-transplantation period.

8.7. Analysis of soil ammonia-nitrogen across the experimental period:

Calibration curve of ammonia-nitrogen to be followed as described in the figure 7.10

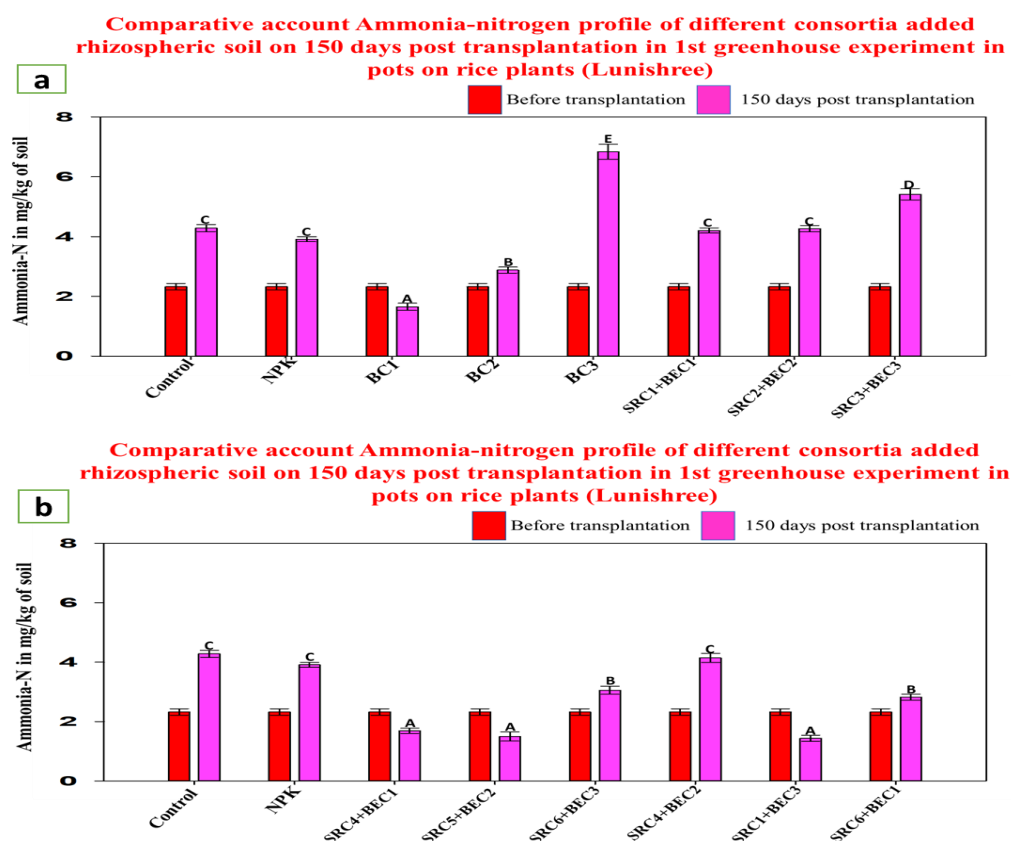


Figure 8.38: The above figure depicts the comparison study of soil ammonia-nitrogen from control (without bacteria), NPK-added and different consortia (prepared by mixing endophytic and rhizospheric bacterial strains) added rhizospheric pot soil in the 1st greenhouse experiment on rice plants of Lunishree. Data were plotted as mean \pm standard error (n=3) in the graph.

Observations:

In the above figures (a) and (b) overall the accumulation rate of soil ammonia-nitrogen in rhizospheric pot soil was found to be significantly higher in comparison to its consumption by rice plants even in control pot soils (without bacteria), NPK or bacterial consortia-added pot soils over 150 days of post-transplantation period when compared to that of before transplantation. However, this increase in soil ammonia-nitrogen was observed to be the highest in BC3 consortia-added pot soils in the 1st greenhouse experiment on rice plants of Lunishree, while contrastingly BC1, SRC4+BEC1, SRC5+BEC2, and SRC1+BEC3 consortia-added pots showed significant decrease in soil ammonia-nitrogen over 150 days of post-transplantation period.

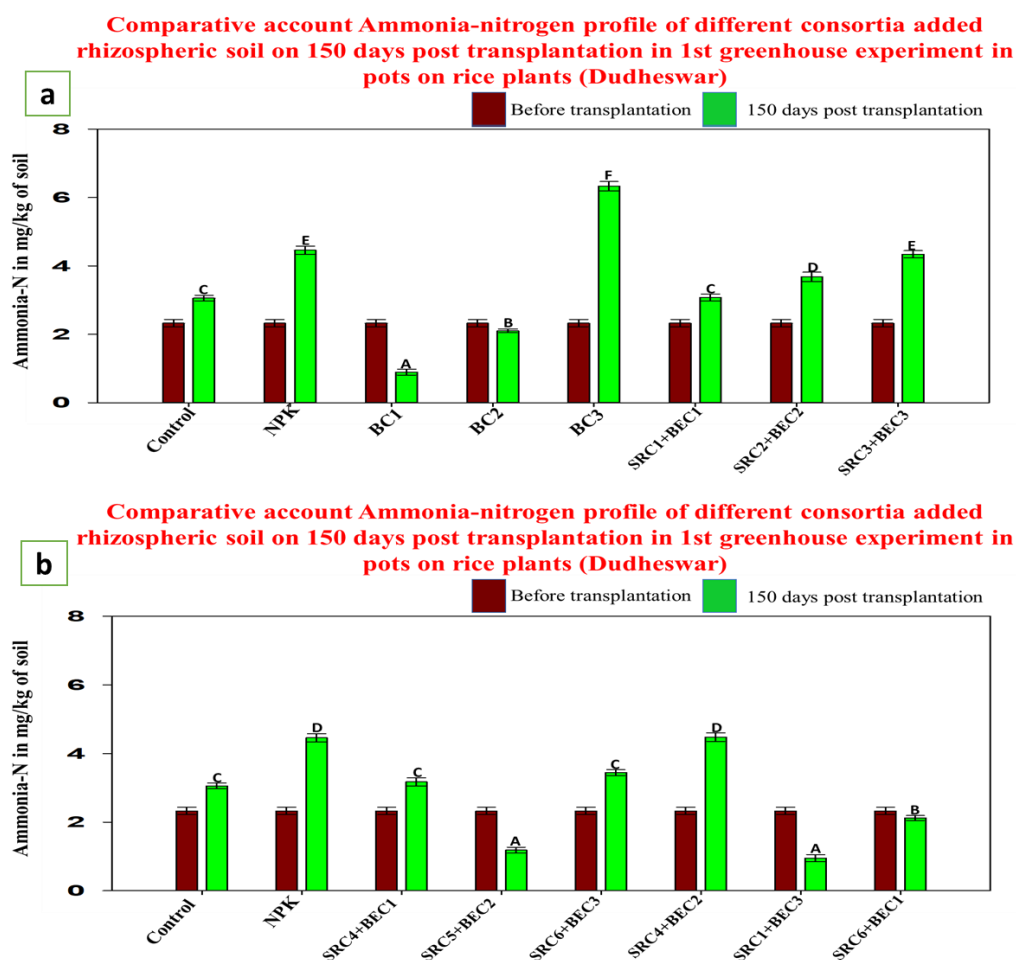


Figure 8.39: The above figure depicts the comparison study of soil ammonia-nitrogen from control (without bacteria), NPK-added and different consortia (prepared by mixing endophytic and rhizospheric bacterial strains) added rhizospheric pot soil in the 1st greenhouse experiment on rice plants of Dudheswar. Data were plotted as mean \pm standard error (n=3) in the graph.

Observations:

In the above figures (a) and (b) overall the accumulation rate of soil ammonia-nitrogen in rhizospheric pot soil was found to be significantly higher in comparison to its consumption by rice plants even in control pot soils (without bacteria), NPK or bacterial consortia-added pot soils over 150 days of post-transplantation period when compared to that of before transplantation. However, this increase in soil ammonia-nitrogen was observed to be the highest in BC3 consortia-added pot soils in the 1st greenhouse experiment on rice plants of Dudheswar, while contrastingly BC1, BC2, SRC5+BEC2, SRC1+BEC3 and SRC6+BEC1 consortia-added pots showed significant decrease in soil ammonia-nitrogen over 150 days of post-transplantation period.

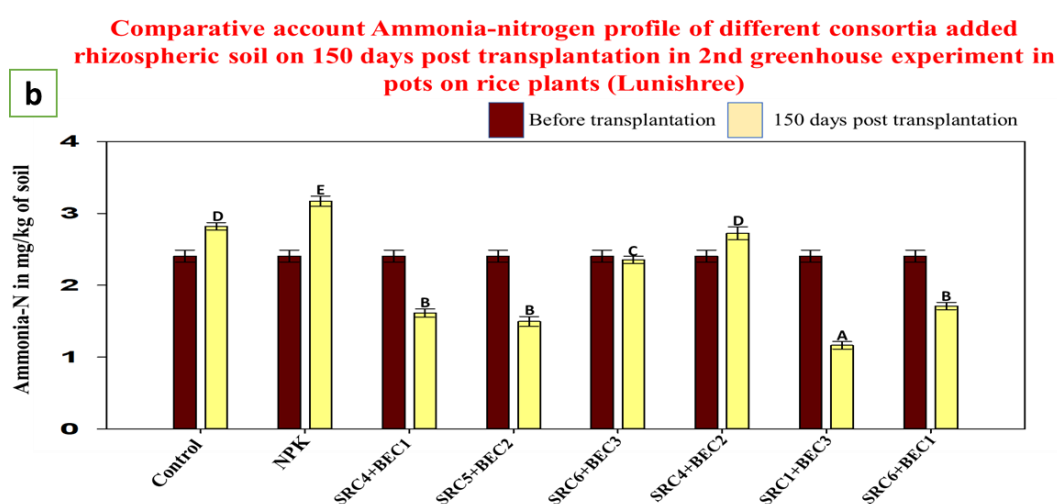
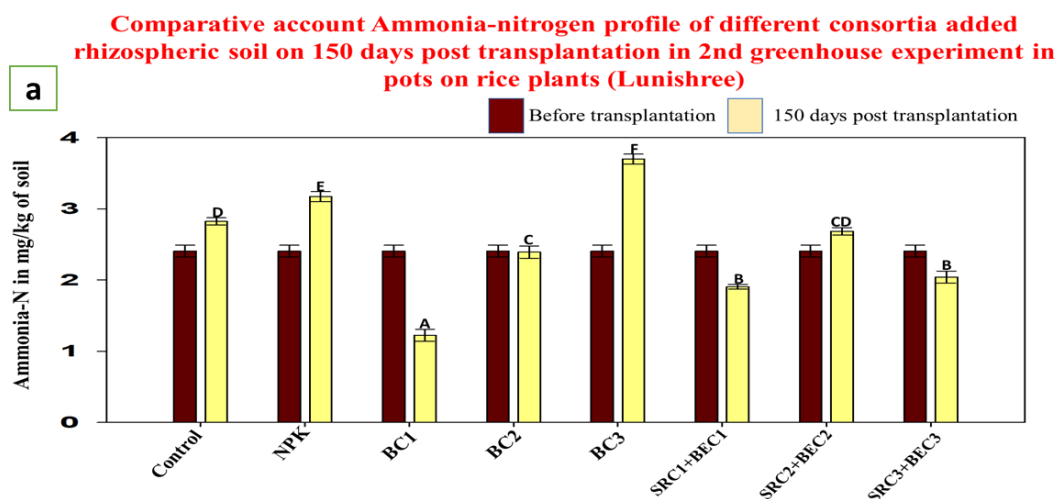


Figure 8.40: The above figure depicts the comparison study of soil ammonia-nitrogen from control (without bacteria), NPK-added and different consortia (prepared by mixing endophytic and rhizospheric bacterial strains) added rhizospheric soil in the 2nd greenhouse experiment on rice plants of Lunishree. Data were plotted as mean \pm standard error (n=3) in the graph.

Observations:

In the above figures (a) and (b) overall the accumulation rate of soil ammonia-nitrogen in rhizospheric pot soil was found to be significantly higher in comparison to its consumption by rice plants even in control pot soils (without bacteria), NPK or bacterial consortia-added pot soils over 150 days of post-transplantation period when compared to that of before transplantation. However, this increase in soil ammonia-nitrogen was observed to be the highest in BC3 consortia-added pot soils in the 2nd greenhouse experiment on rice plants of Lunishree, while contrastingly BC1, SRC3+BEC3, SRC1+BEC1, SRC4+BEC1, SRC5+BEC2, SRC1+BEC3 and SRC6+BEC1 consortia-added pots showed significant decrease in soil ammonia-nitrogen over 150 days of post-transplantation period.

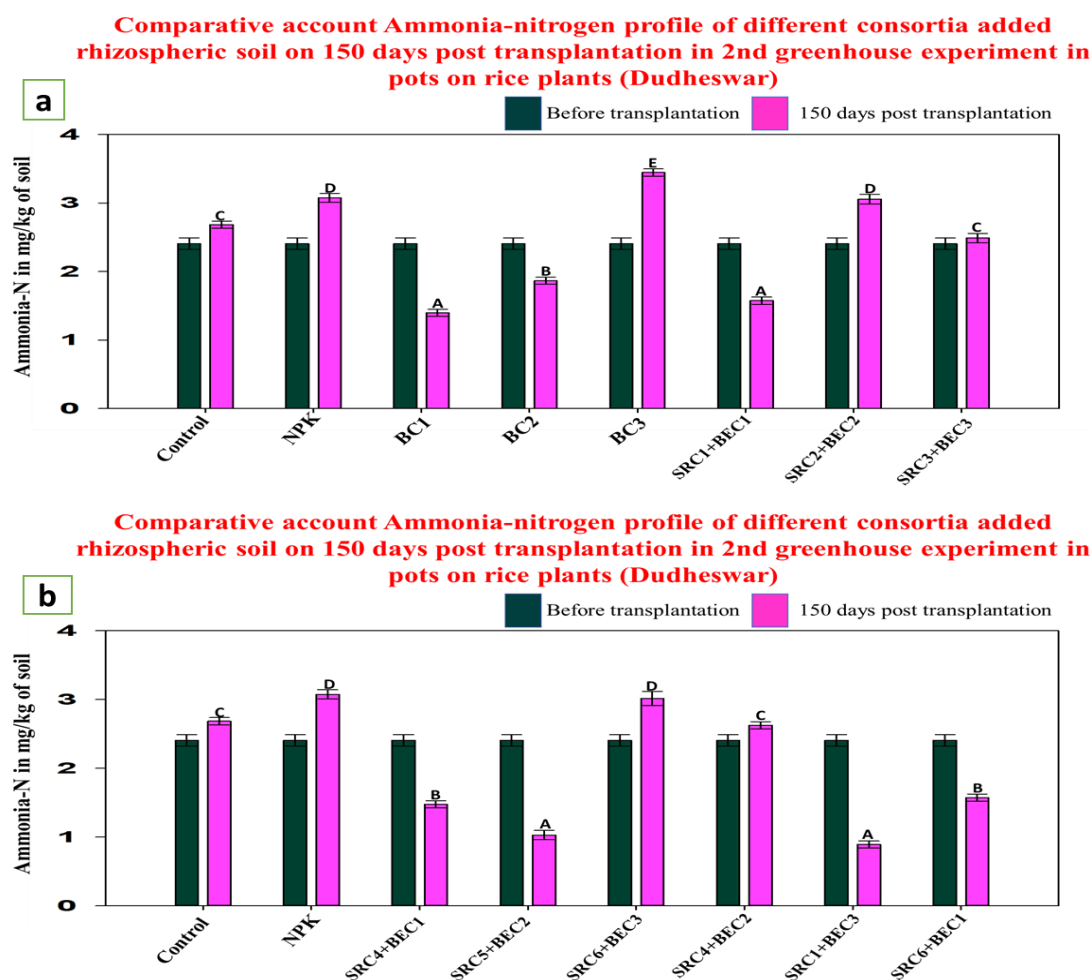


Figure 8.41: The above figure depicts the comparison study of soil ammonia-nitrogen from control (without bacteria), NPK-added and different consortia (prepared by mixing endophytic and rhizospheric bacterial strains) added rhizospheric pot soil in the 2nd greenhouse experiment on rice plants of Dudheswar. Data were plotted as mean \pm standard error (n=3) in the graph.

Observations:

In the above figures (a) and (b) overall the accumulation rate of soil ammonia-nitrogen in rhizospheric pot soil was found to be significantly higher in comparison to its consumption by rice plants even in control pot soils (without bacteria), NPK or bacterial consortia-added pot soils over 150 days of post-transplantation period when compared to that of before transplantation. However, this increase in soil ammonia-nitrogen was observed to be the highest in BC3 consortia-added pot soils in the 2nd greenhouse experiment on rice plants of Dudheswar, while contrastingly BC1, BC2, SRC1+BC1, SRC4+BC1, SRC5+BC2, SRC1+BC3 and SRC6+BC1 consortia-added pots showed significant decrease in soil ammonia-nitrogen over 150 days of post-transplantation period.

8.8. Analysis of plant available phosphorus over the experimental period:

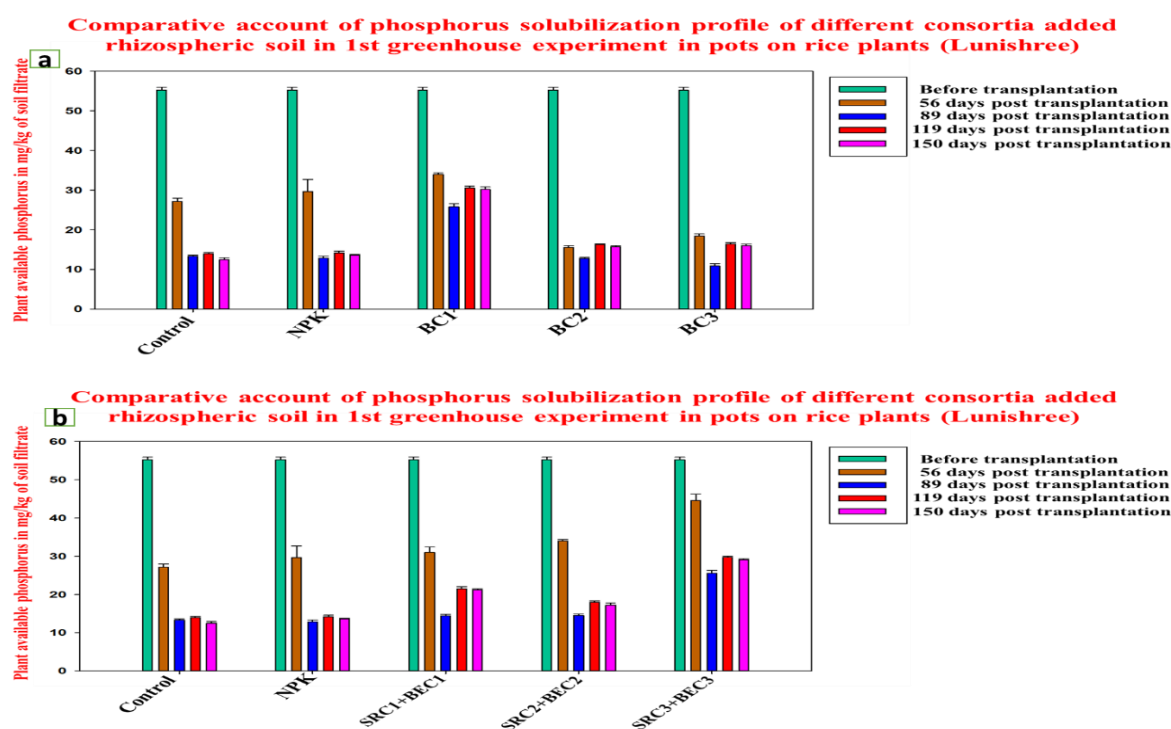
8.8.a. Analysis of plant-available rhizosphere pot soil phosphorus from the 1st greenhouse experiment over the experimental period:

Calibration curve of plant-available phosphorus to be followed as depicted in the figure 7.12

P-solubilization profile at rhizospheres of experimental pots as indicator/metric of growth promotion/enrichment of consortia

Taking P-solubilization profile at rhizospheres of experimental pots as indicator/metric of growth promotion/enrichment of consortia, in 1st greenhouse experiment, data were recorded at 56 days, 89 days, 119 days and 150 days post-transplantation for both rice cultivars D and N.

The data are represented in the following figures:



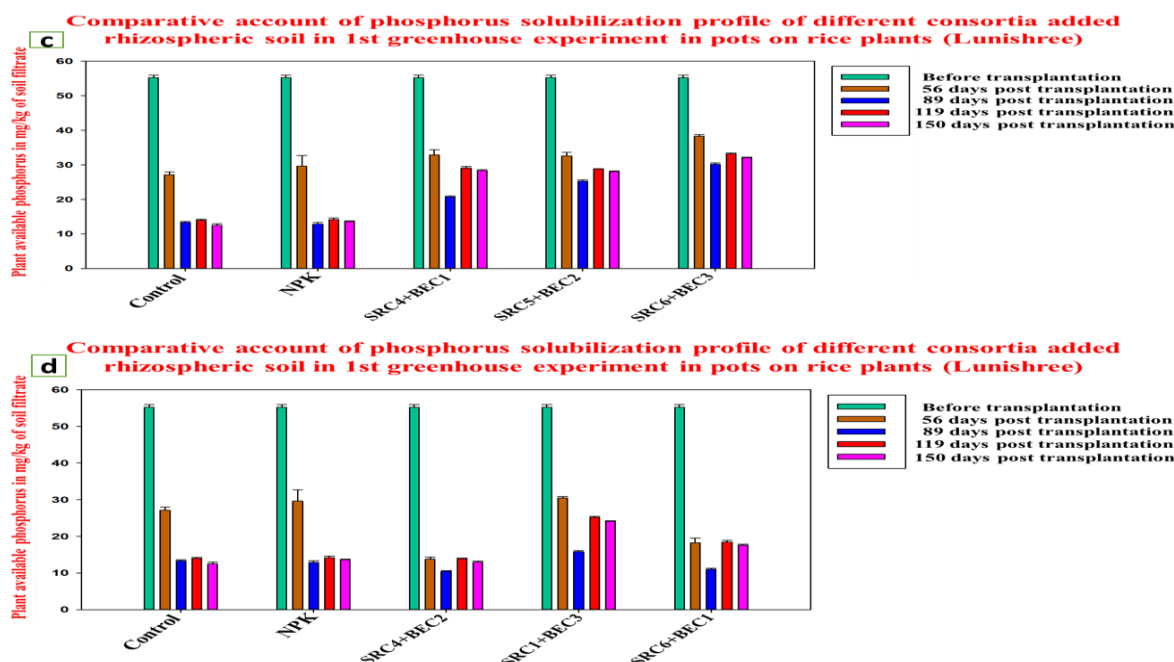
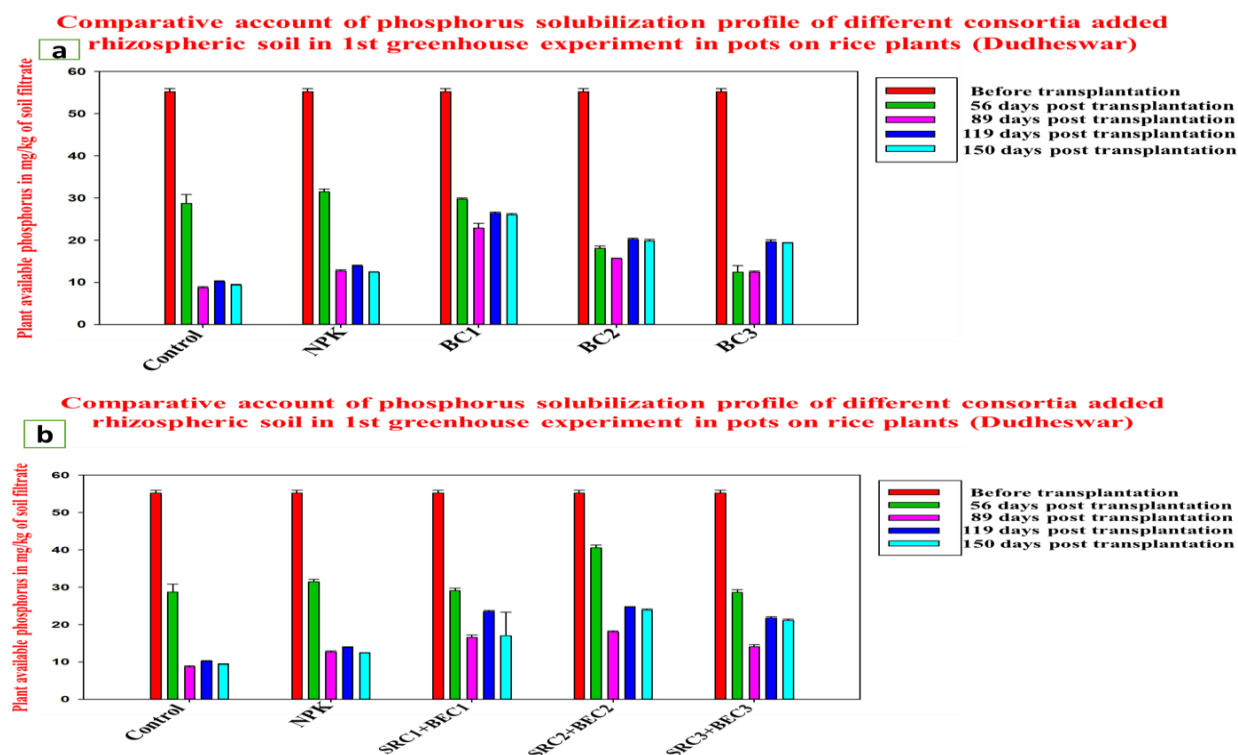


Figure 8.42: The above figure depicts the comparison study of plant-available phosphorus from control (without bacteria), NPK-added and different consortia (prepared by mixing endophytic and rhizospheric bacterial strains) added rhizospheric pot soil, up to 150 days post-transplantation at a specific time interval in the 1st greenhouse experiment on rice plants of **Lunishree**. Data were plotted as mean \pm standard error (n=3) in the graph.



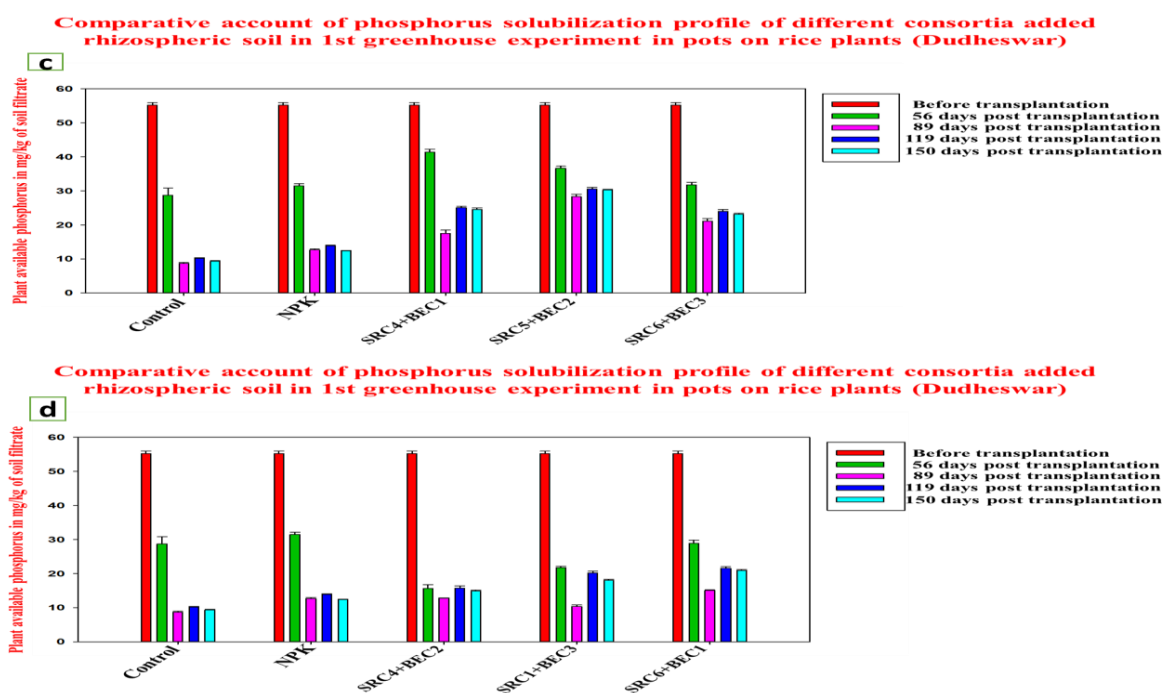


Figure 8.43: The above figure depicts the comparison study of plant-available phosphorus from control (without bacteria), NPK-added and different consortia (prepared by mixing endophytic and rhizospheric bacterial strains) added rhizospheric pot soil, up to 150 days post-transplantation at a specific time interval in the 1st greenhouse experiment on rice plants of **Dudheswar**. Data were plotted as mean \pm standard error (n=3) in the graph.

Observations:

- In almost all consortia-added rhizospheres, the lowest level of soluble plant available phosphorus (P) is found to be at **89 days** post-transplantation after which it gradually increased as observed at **119 days** and **150 days** post-transplantation rhizosphere soils. This increase in soluble plant available phosphorus (P) can be attributed to the enrichment of PGP consortia at rice rhizosphere which have many a constituent member as high P-solubilizer.
- In contrast, control (no bacteria added) and NPK fertilizer added rice rhizospheres, showed no significant increase in level of soluble plant available phosphorus (P) even after 89 days post-transplantation.
- Many of the consortia added rhizospheres of experimental rice plants showed the presence of higher level of soluble plant-available phosphorus (P) as compared to control (no bacteria added) and NPK fertilizer-added rice rhizospheres even on **89 days** post-transplantation, when the rice plants showed maximum utilization of soil-P.

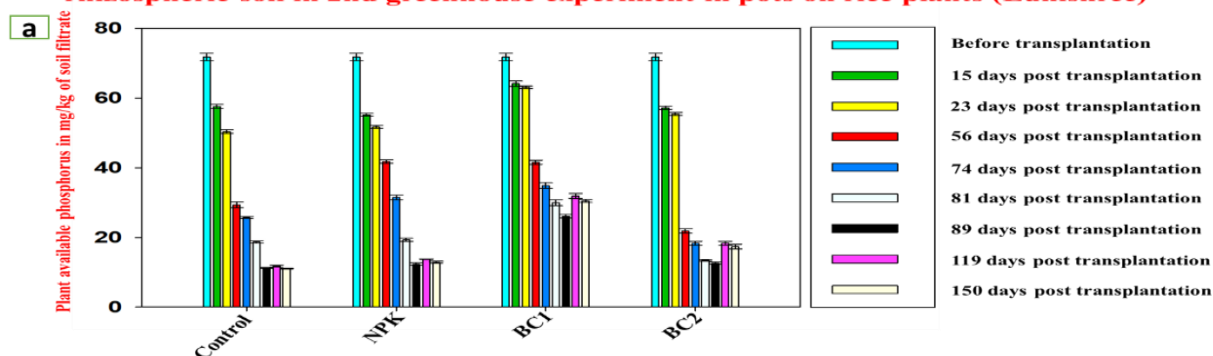
- P-solubilization seems to be a promising growth promotion potential of the selected/added consortia (most members in each consortium were high P-solubilizers as observed earlier in laboratory experiments).
- Significant increase in solubilized-P observed in consortia-added rhizospheres as compared to that of control (no bacterial addition) and NPK-added rhizospheric soils after 89 days post-transplantation is evident in all the above-presented figures.

8.8.b. Analysis of plant-available rhizosphere pot soil phosphorus from the 2nd greenhouse experiment over the experimental period:

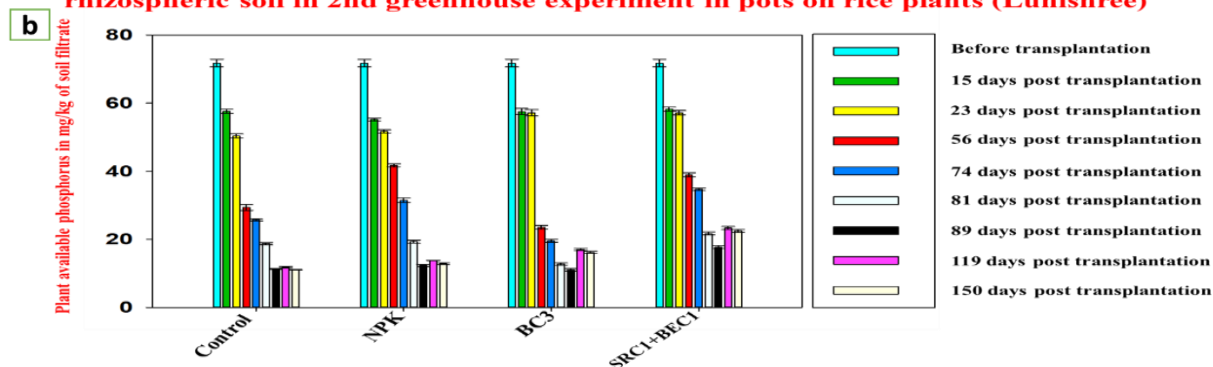
P-solubilization profile at rhizospheres of experimental pots as indicator/metric of growth promotion/enrichment of consortia

Taking P-solubilization profile at rhizospheres of experimental pots as indicator/metric of growth promotion/enrichment of consortia, in 2nd greenhouse experiment, data were recorded at 15 days, 23 days, 56 days, 74 days, 81 days, 89 days, 119 days and 150 days post-transplantation for both rice cultivars D and N. The data are represented in the following figures:

Comparative account of phosphorus solubilization profile of different consortia added rhizospheric soil in 2nd greenhouse experiment in pots on rice plants (Lunishree)



Comparative account of phosphorus solubilization profile of different consortia added rhizospheric soil in 2nd greenhouse experiment in pots on rice plants (Lunishree)



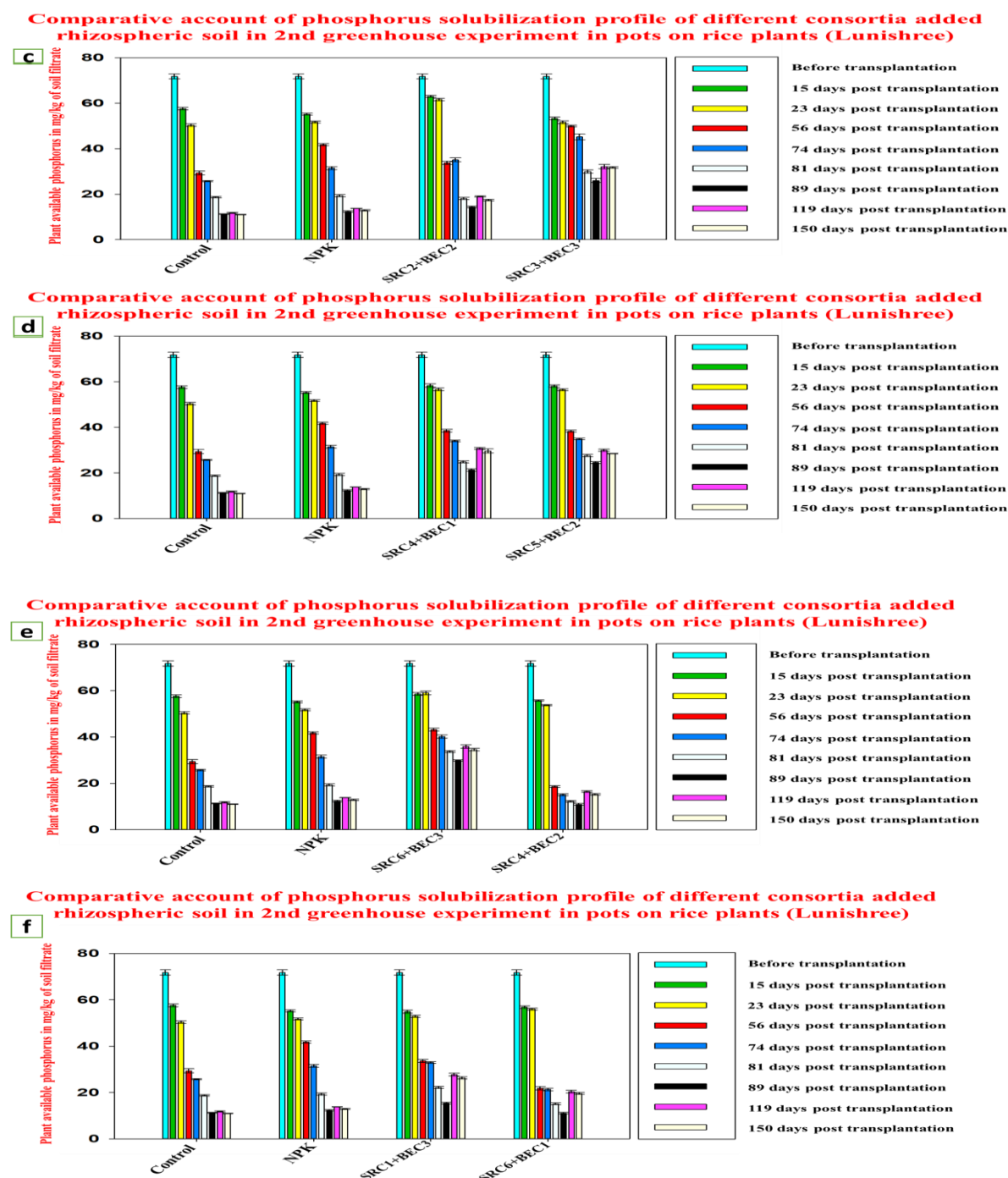
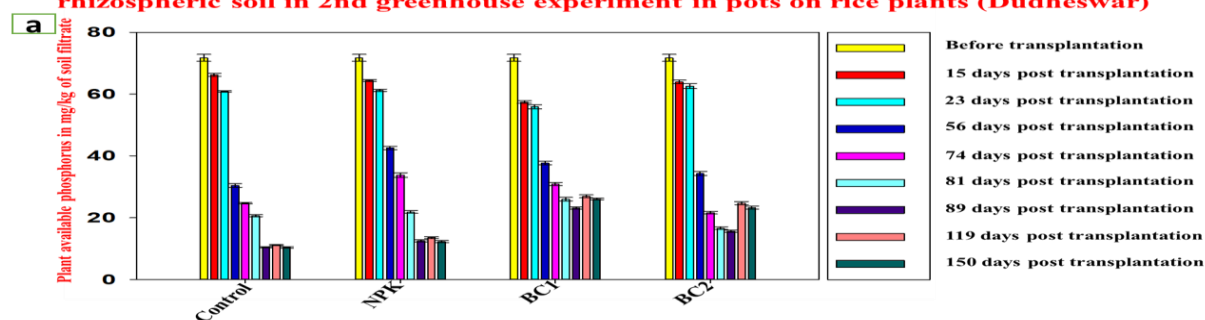
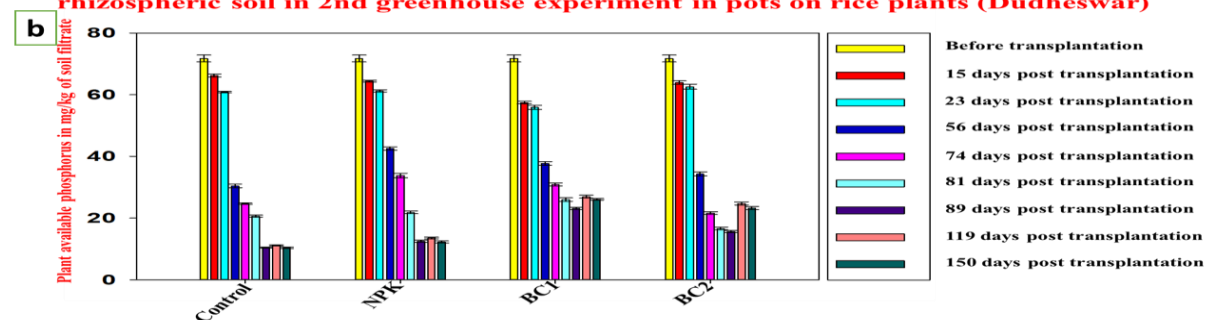


Figure 8.44: The above figure depicts the comparison study of plant-available phosphorus from control (without bacteria), NPK-added and different consortia (prepared by mixing endophytic and rhizospheric bacterial strains) added rhizospheric soil, up to 150 days post-transplantation at a specific time interval in the 2nd greenhouse experiment on rice plants of **Lunishree**. Data were plotted as mean \pm standard error (n=3) in the graph.

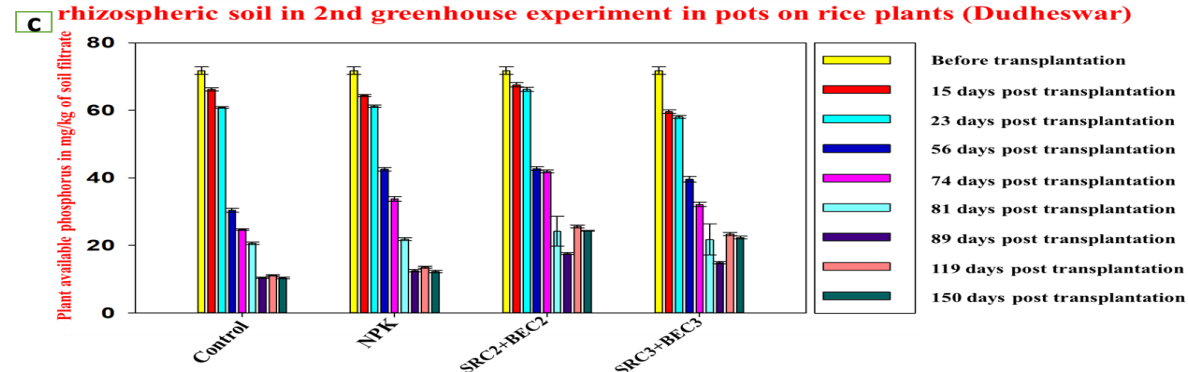
Comparative account of phosphorus solubilization profile of different consortia added rhizospheric soil in 2nd greenhouse experiment in pots on rice plants (Dudheswar)



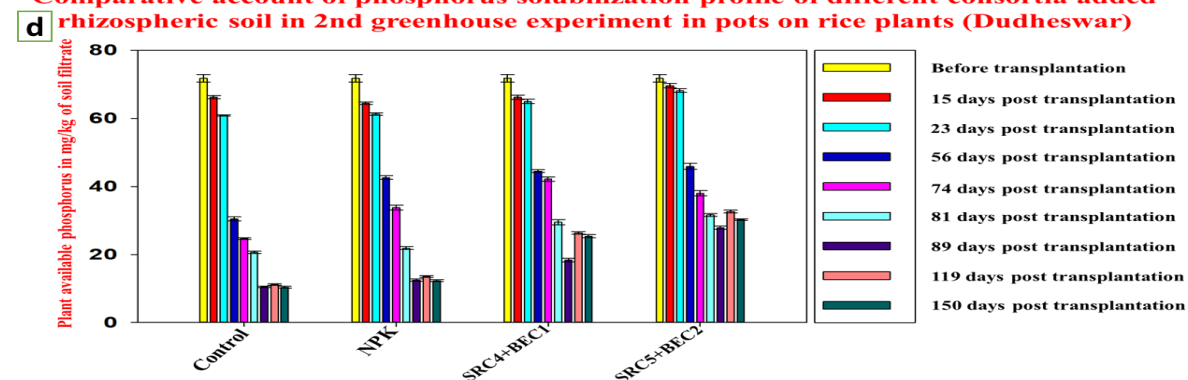
Comparative account of phosphorus solubilization profile of different consortia added rhizospheric soil in 2nd greenhouse experiment in pots on rice plants (Dudheswar)



Comparative account of phosphorus solubilization profile of different consortia added rhizospheric soil in 2nd greenhouse experiment in pots on rice plants (Dudheswar)



Comparative account of phosphorus solubilization profile of different consortia added rhizospheric soil in 2nd greenhouse experiment in pots on rice plants (Dudheswar)



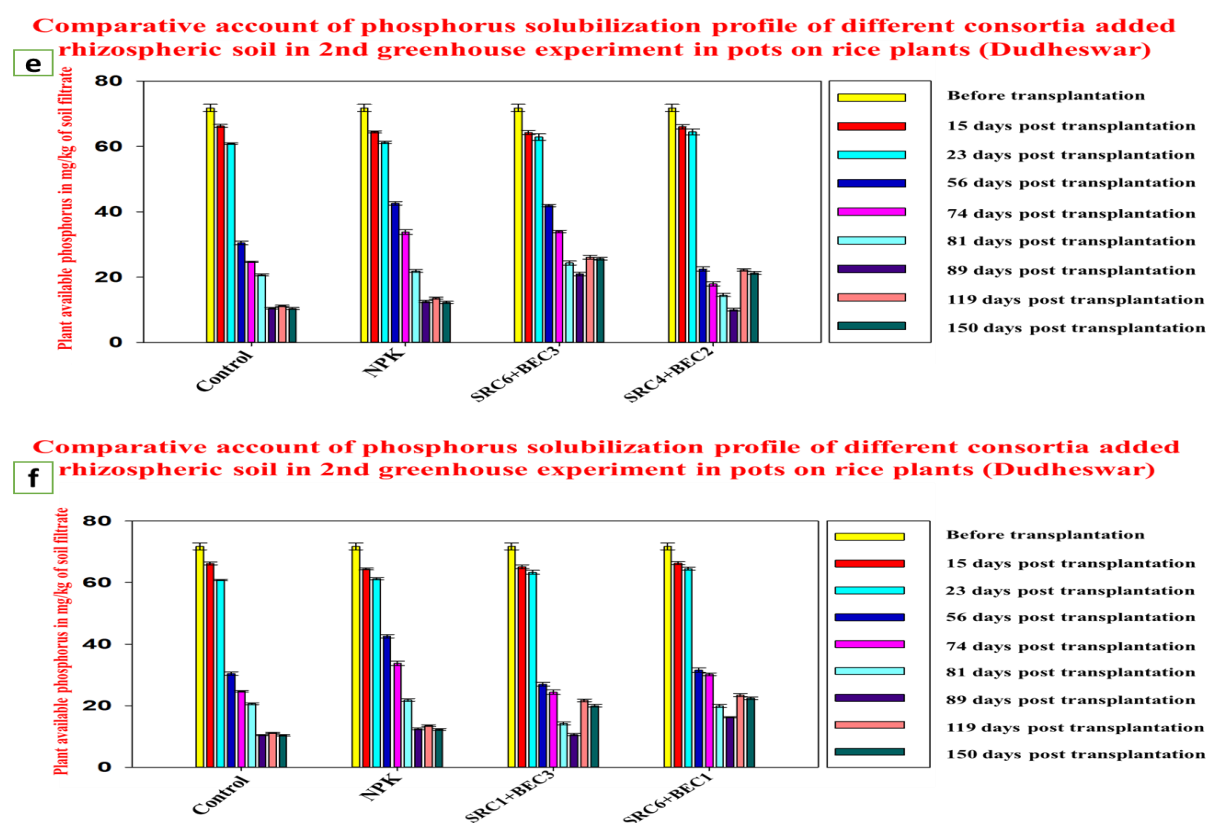


Figure 8.45: The above figure depicts the comparison study of plant available phosphorus from control (without bacteria), NPK-added and different consortia (prepared by mixing endophytic and rhizospheric bacterial strains) added rhizospheric soil, up to 150 days post-transplantation at a specific time interval in the 2nd greenhouse experiment on rice plants of **Dudheswar**. Data were plotted as mean \pm standard error (n=3) in the graph.

Observations:

- In almost all consortia added rhizospheres, the lowest level of soluble plant available phosphorus (P) is found to be at **89 days** post-transplantation after which it gradually increased as observed at **119 days** and **150 days** post-transplantation rhizosphere soils **similar to that observed in the 1st greenhouse experiment**. This increase in soluble plant-available phosphorus (P) can be attributed to the enrichment of PGP consortia at rice rhizosphere which have many a constituent member as high P-solubilizer.
- In contrast, control (no bacteria added) and NPK fertilizer added rice rhizospheres, showed no significant increase in level of soluble plant available phosphorus (P) even after 89 days post-transplantation.
- Many of the consortia added rhizospheres of experimental rice plants showed presence of higher level of soluble plant available phosphorus (P) as compared to control (no

bacteria added) and NPK fertilizer-added rice rhizospheres even on **89** days post-transplantation, when the rice plants showed maximum utilization of soil-P.

- P-solubilization seems to be a promising growth promotion potential of the selected/added consortia (most members in each consortium were high P-solubilizers as observed earlier in laboratory experiments).
- Significant increase in solubilized-P observed in consortia added rhizospheres as compared to control (no bacterial addition) and NPK-added rhizospheric soils after 89 days post-transplantation, similar to the 1st greenhouse experiment is evident in all the above-presented figures.

Similar studies by Shabanamol et al, (2020) observed growth improvement like root and shoot height of rice plants by endophytic diazotrophic bacteria *Lysinibacillus sphaericus* under greenhouse condition. Lally et al, (2017) also reported that endophytic bacteria *Pseudomonas fluorescens* significantly increases the height and biomass of the plant *Brassica napus* in a greenhouse experiment.

Objective 7

9. Application of selected PGP endophytic bacterial consortia on cultivated rice at fields at Sundarbans for observing their effect on rice growth and yield modulation.

Application of selected PGP endophytic bacterial consortia on cultivated rice of Sundarbans was carried out for two consecutive years at the fields at Sundarbans for observing their effect on rice growth and yield modulation.

9.1. Preparation of large-scale culture for field experiments:

Large scale culture preparation and details for the field experiments are already explained in the materials method sections.



Figure 9.1: The above figure depicts different steps in large culture preparation and large-scale PGP bacterial cultures brought to the rice field location in Sundarbans. These field experiments were initiated during the Covid 19 lockdown condition in 2021.

9.2. 1st field experiment details in Sundarban rice field:

- ☐ The rice cultivar: **Dudheswar IC 593998**
- ☐ Seeds sown on the seedbed: **05-07-2021**
- ☐ Seedlings transplantation: **17-08-2021**
- ☐ Age of the seedlings when transplantation was done: **43 days**
- ☐ Initial height of seedlings at the time of transplantation: **60cm to 83cm**
- ☐ Distance between the seedlings transplanted: **approx 30cm**
- ☐ Seedlings transplanted per replica plot: **49**
- ☐ Seedlings transplanted per consortium: **196**
- ☐ Leaf width at the time of transplantation: **0.2-0.5 cm**
- ☐ Number of tillers transplanted in a cluster: **5 to 8**
- ☐ 1st addition of bacterial culture: **04-09-2021**
- ☐ 2nd addition of bacterial culture: **29-10-2021**
- ☐ Conductivity of the water where rice seedlings had been transplanted:
mS/cm=1.3 ppt
- ☐ Conductivity of the soil where rice seedlings had been transplanted:
mS/cm=1 ppt
- ☐ Conductivity of water by which seedbed was maintained: **0.817 mS/cm=0.4 ppt**
- ☐ Conductivity of soil where seedbed was prepared: **0.817 mS/cm=0.4 ppt**
- ☐ Soil pH: **7.38-7.48**
- ☐ **4 Control rice plots of 4 m² each** (no bacterial culture added) used
- ☐ **4 replica rice plots of 4 m² each** used for each bacterial consortium

All growth parameters data were recorded after 80 days post-transplantation in rice fields and yield and harvest data were recorded after 100 days post-transplantation at Sundarban fields.



Figure 9.2: Bacterial cultures are being diluted for application in field.

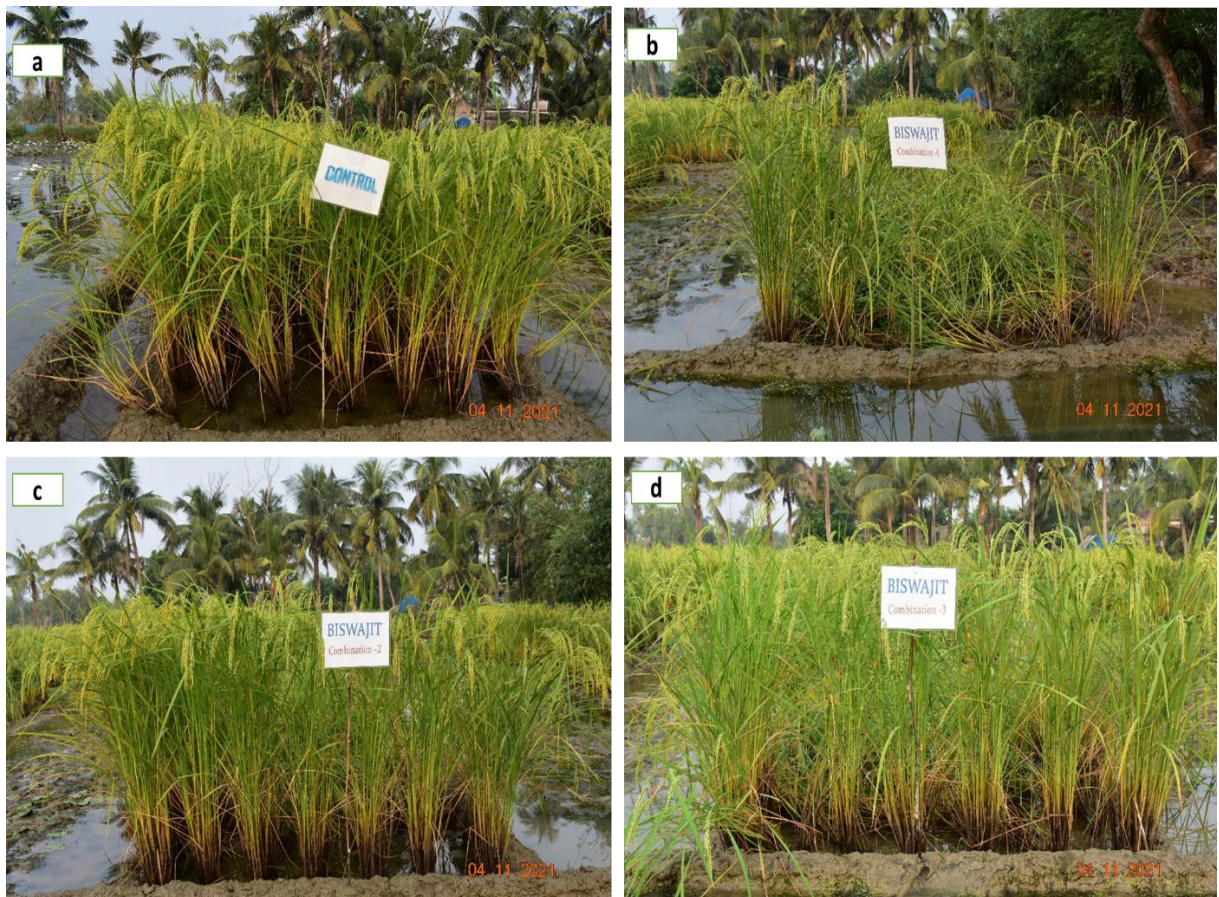


Figure 9.3: 1st field experiment at Sundarbans in 2021. (a) In control plots no bacterial culture was added (b) BC1 plots where Consortium BC1 was added (c) BC2 plots where Consortium BC2 was added (d) BC3 plots where Consortium BC3 was added.

9.2.a. Different growth parameters of rice plants observed in the 1st field experiment at Sundarbans:

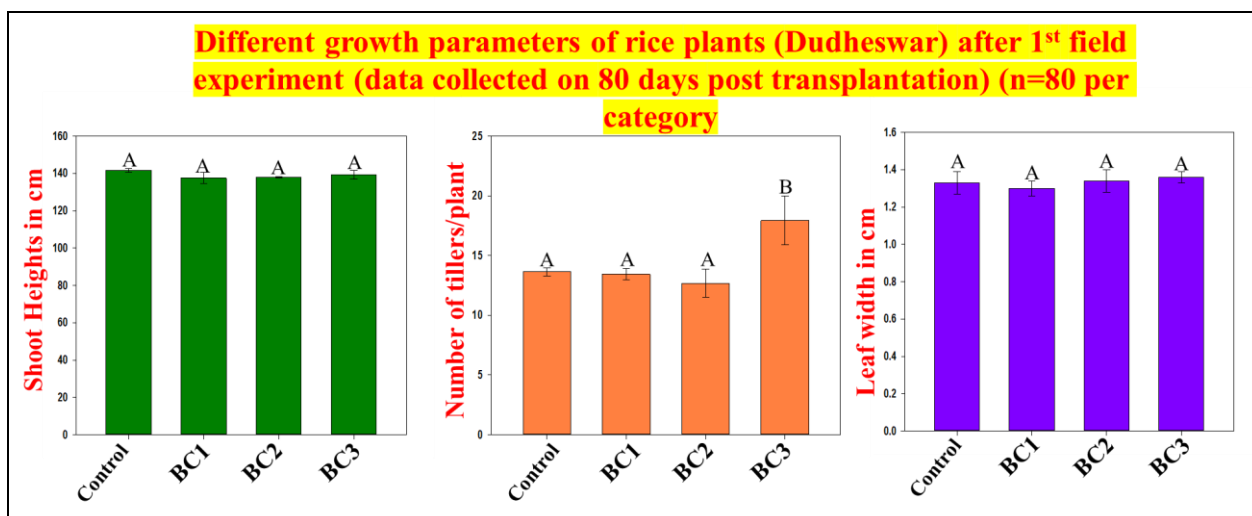


Figure 9.4: The above figure depicts the growth parameters of rice plants (Dudheswar) after 1st field experiment on 80 days post-transplantation. A comparison study of shoot height, number of tillers and the leaf width between control (without bacteria) and consortia added plots were observed. Data were plotted as mean \pm standard error (n=80 per category) in the graph.

Observations:

No significant difference was observed as compared to control at vegetative stages for shoot height and leaf width. However, a significant difference (increase) was observed between control and BC3 consortia-added plots for number of tillers.

9.2.b. Different yield parameters of cultivated rice in the 1st field experiment at Sundarbans:

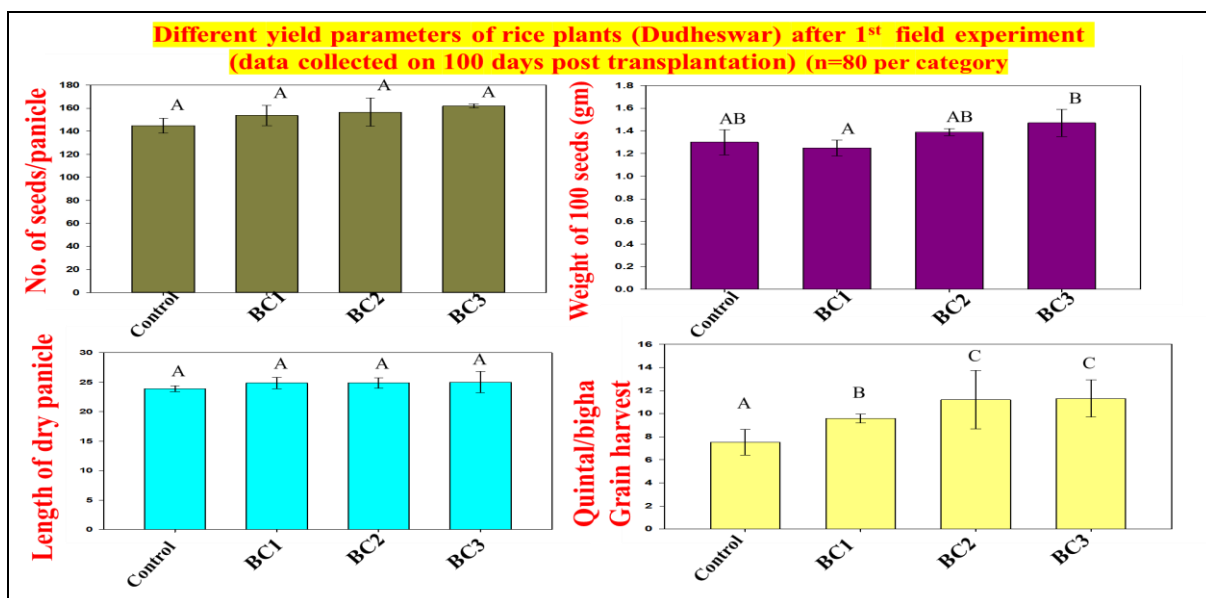


Figure 9.5: The above figure depicts the yield parameters of rice plants (Dudheswar) after 1st field experiment on 100 days post-transplantation. A comparison study of no. of seeds/panicles, weight of 100 seeds, length of dry panicle and quintal/bigha grain harvest between control (without bacteria) and consortia added plots were observed. Data were plotted as mean \pm standard error (n=80 per category) in the graph.

Observations:

The major significant increase is observed in grain yield in quintal per bigha in BC1, BC2, and BC3 consortia-added plots as compared to that of control plots where no bacterial consortia was added. Not much significant difference was observed for other yield traits like no. of seeds/panicles, weight of 100 seeds and length of dry panicle of the cultivated rice in the 1st field experiment.

Rice (Dudheswar) yield and different yield parameters of rice cultivars after harvest (data collected on 100 days post-transplantation). Below is the comparative account of the yield in quintal/bigha in 1st successful field experiment (1 bigha~0.25 ha, a unit used by common people in Sundarbans to measure land area under cultivation).

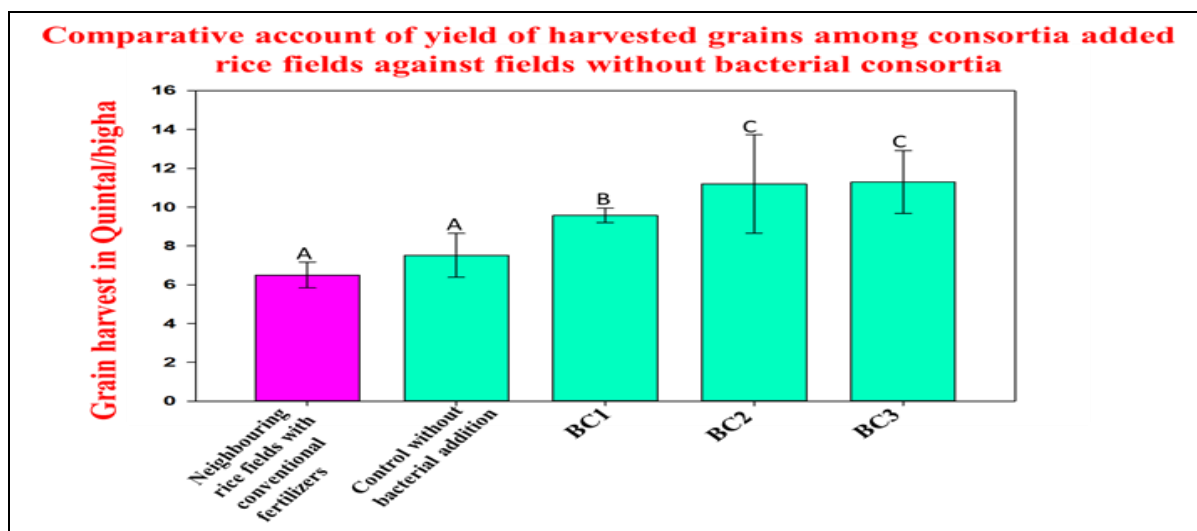


Figure 9.6: The above figure depicts a comparison study of quintal/bigha grain harvest across control (without bacteria), consortia-added plots and neighbouring rice fields cultivated with conventional fertilizers. Data were plotted as mean \pm standard error in the graph.

Observations:

Major significant improvement in yield of grains in quintal per bigha was observed for bacterial consortia-added rice plots as compared to control plots (without bacterial consortia) and neighbouring rice field cultivated with conventional fertilizers. In comparison to ~6 quintal per bigha grain yield from control plots (without bacterial consortia) and neighbouring rice fields, the BC2 and BC3 consortia-added rice plots yielded ~11 quintal per bigha rice grains, as calculated by us using our laboratory instruments.

9.2.c. Importance of rice grains with its starch and protein contents:

Rice is the most important cereal crop of the world. Almost half of the world's population consumes rice directly as staple food. Rice grains contain approximately, proteins 6-7 %, carbohydrates 76.2 %, fibre 3.6 %, lipids 0-3.2 %, energy 367 kcal. It contains vitamins A, B, E and also some other important nutrients. Rice protein is rich in lysine, valued for its nutrition and quality. Lysine is an important essential amino acid for growth and development. Rice protein is a competitive protein ingredient in the food market as it contains high nutritive quality and the hypoallergenic property. Total protein content ranges between 4.3-18.2 % in rice grain. Rice endosperm or milled rice contains 9.6–10.8% globulin, 3.8–8.8% albumin, 2.6–3.3% prolamin and 66–78% glutelin. Glutelin is the main storage protein in rice (Sadaiah et al, 2018). Rice grain is the major source of carbohydrates which provides metabolic energy, both for plants and animals.

9.2.d. Calibration curve of starch:

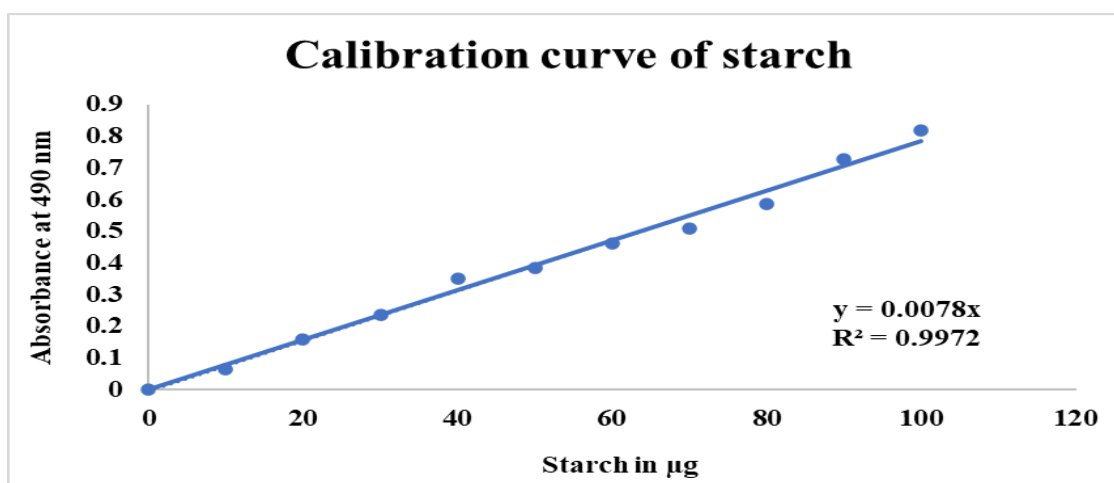


Figure 9.7: The calibration curve of starch was developed to measure the unknown concentration of starch in rice grains.

9.2.e. Starch content analysis in rice grains:

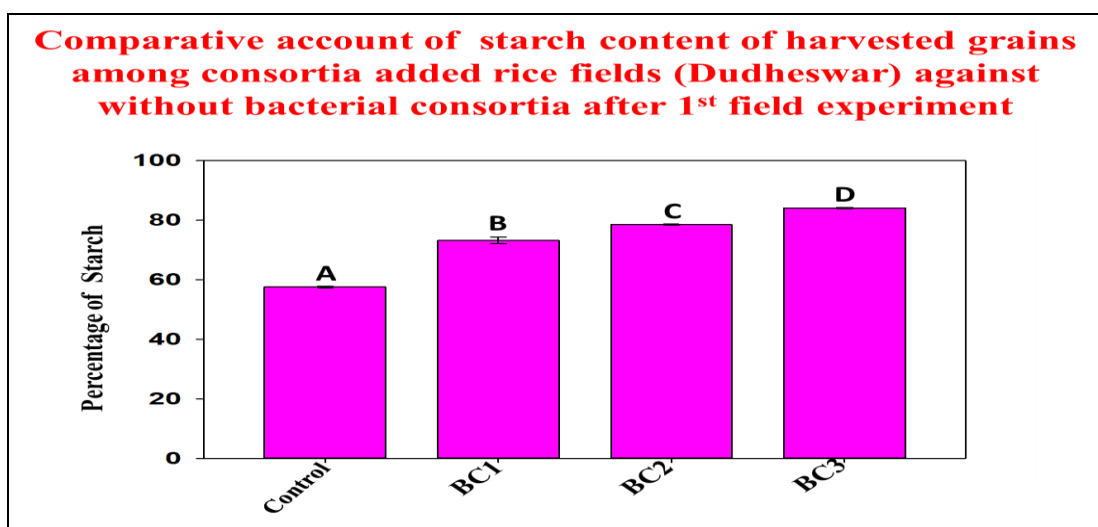


Figure 9.8: The above figure depicts a comparative study of starch content analysis from rice grains of control (without bacteria) and different consortia-added plots of the 1st field experiment. Data were plotted as mean \pm standard error (n=3) in the graph.

Observations:

Major significant improvement in starch% was observed for bacterial consortia-added rice plots of 1st field experiment over the grains harvested from control (without bacteria) rice plots. Control rice showed ~60% starch content in comparison to ~70-80% starch contained in the grains harvested from bacterial consortia-added fields.

9.2.f. Calibration curve of protein:

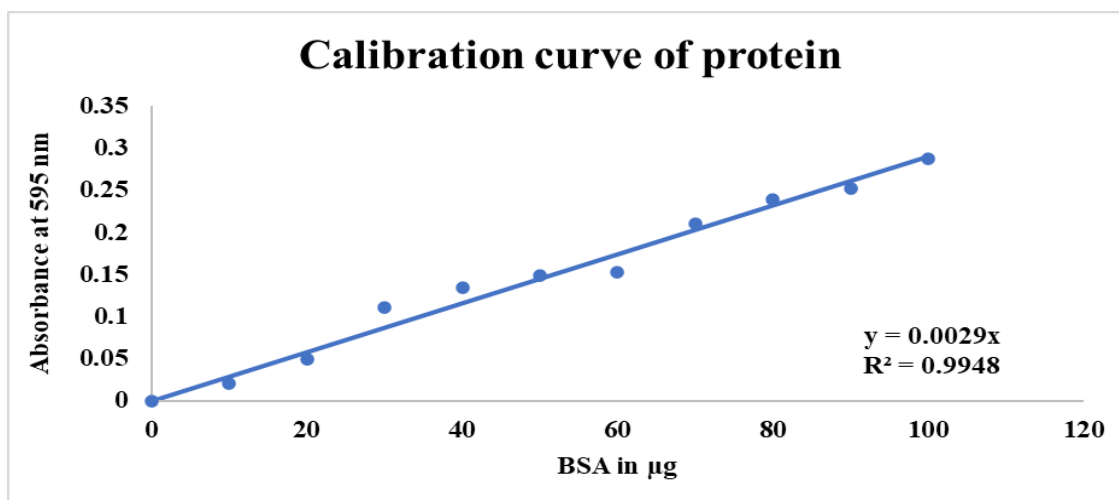


Figure 9.9: The calibration curve of protein was generated to measure the unknown concentration of protein in the harvested rice grains.

9.2.g. Protein content analysis:

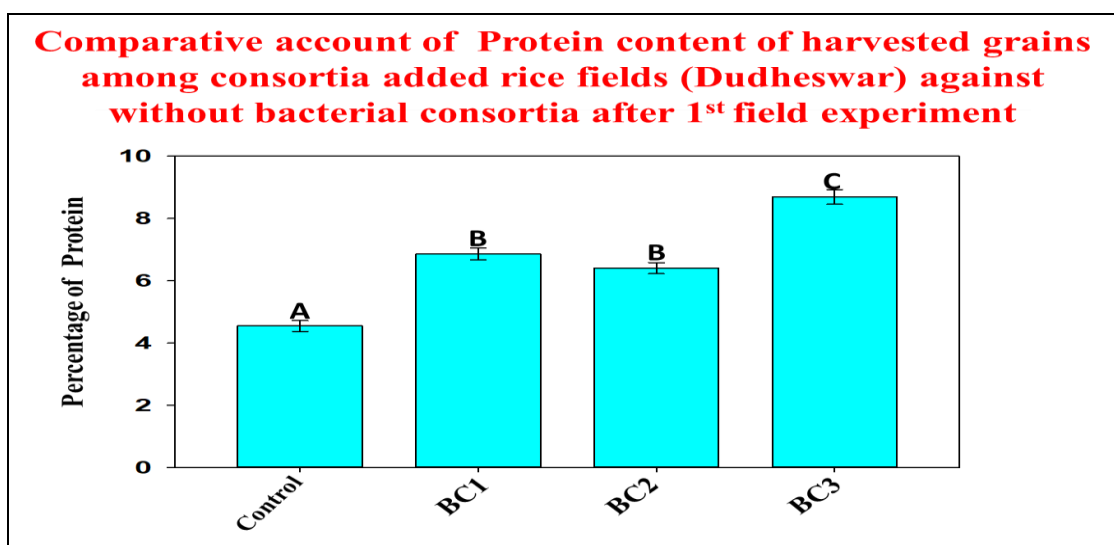


Figure 9.10: The above figure depicts a comparative study of protein content analysis from rice grains of control (without bacteria) and different consortia-added plots of the 1st field experiment. Data were plotted as mean \pm standard error (n=3) in the graph.

Observations:

Major significant improvement in protein% was observed for bacterial consortia-added rice plots of 1st field experiment over the grains harvested from control (without bacteria) rice plots. Control rice showed ~4-5% protein content in comparison to ~7-8% protein contained in the grains harvested from bacterial consortia-added fields.

Soil physical parameters and nutrient profiling in Sundarbans cultivated rice field soil (0-15 cm cores) before and after the 1st field experiment:

9.2.h. Analysis of soil pH during the experimental period:

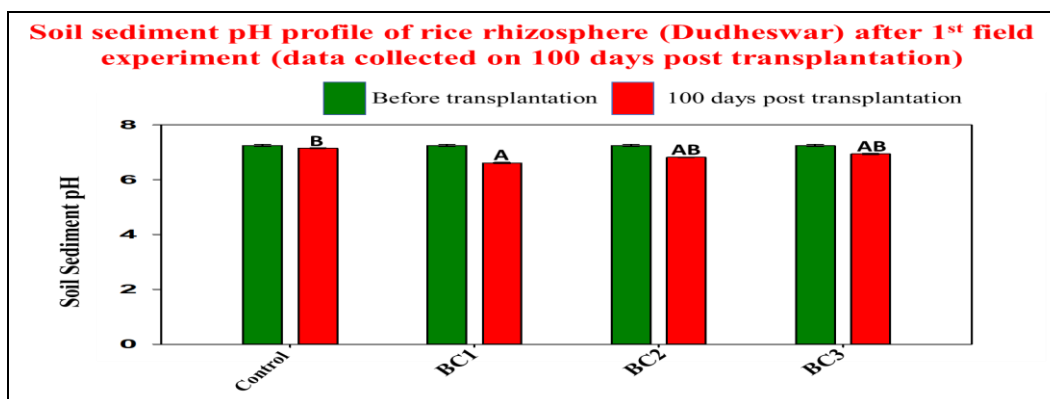


Figure 9.11: The above figure depicts the soil pH studied from control (without bacteria) and different consortia-added rhizospheric soil for rice varieties Dudheswar. Data were plotted as mean \pm standard error (n=3) in the graph.

Observations:

The soil pH decreased significantly for all consortia-added plots as compared to control (without bacteria) in the 1st field experiment when compared to before transplantation. Data were collected on 100 days post-transplantation.

9.2.i. Analysis of soil electrical conductivity (EC) during the experimental period:

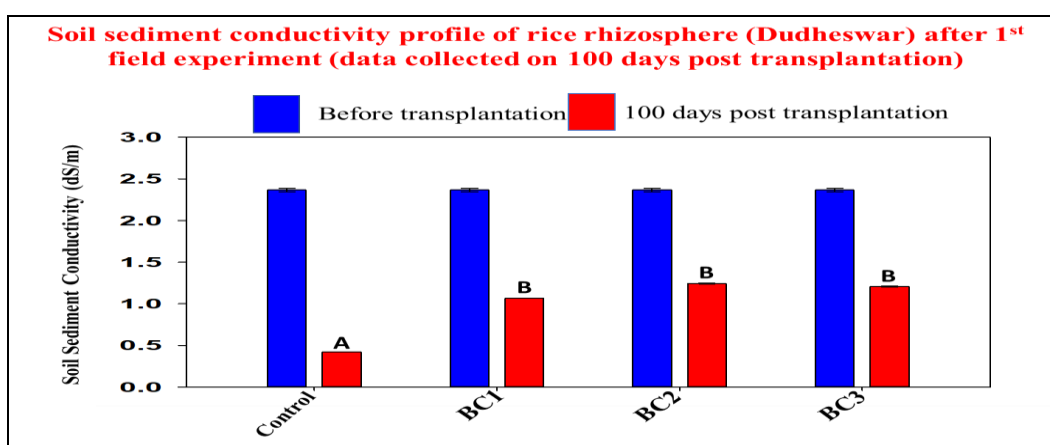


Figure 9.12: The above figure depicts the soil conductivity studied from control (without bacteria) and different consortia-added rhizospheric soil for rice varieties Dudheswar. Data were plotted as mean \pm standard error (n=3) in the graph.

Observations:

The soil conductivity decreased significantly for all consortia-added plots as well as control plots (without bacteria) in the 1st field experiment when compared to before transplantation. This happened probably due to the monsoon season experienced by the soil in its initial cultivation phase. Data were collected on 100 days post-transplantation.

9.2.j. Analysis of soil exchangeable Na⁺/K⁺ ratio during the experimental period:

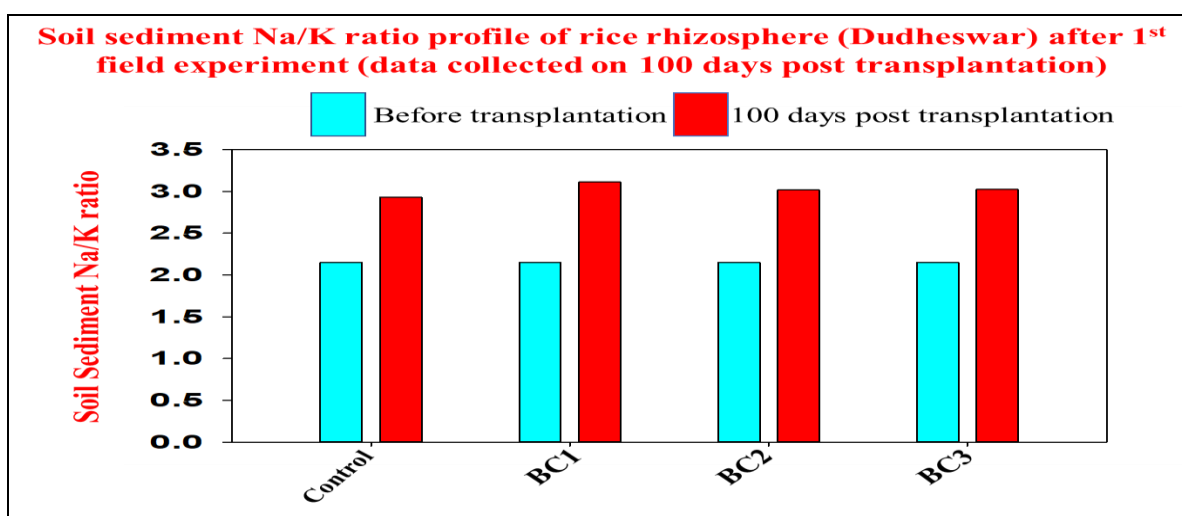


Figure 9.13: The above figure depicts the soil Na⁺/K⁺ ratio studied from control (without bacteria) and different consortia-added rhizospheric soil for rice varieties Dudheswar.

Observations:

The soil Na⁺/K⁺ ratio was found to increase significantly for all consortia-added soil as well as control plots after the 1st field experiment when compared to before transplantation. This might be because of higher dissolution and higher availability of ionic species in soil during the monsoon seasons and water-logged situations in rice fields. Data were collected on 100 days post-transplantation.

9.2.k. Analysis of soil organic carbon (SOC) during the experimental period:

Calibration curve of organic carbon to be followed as depicted in the figure 7.6

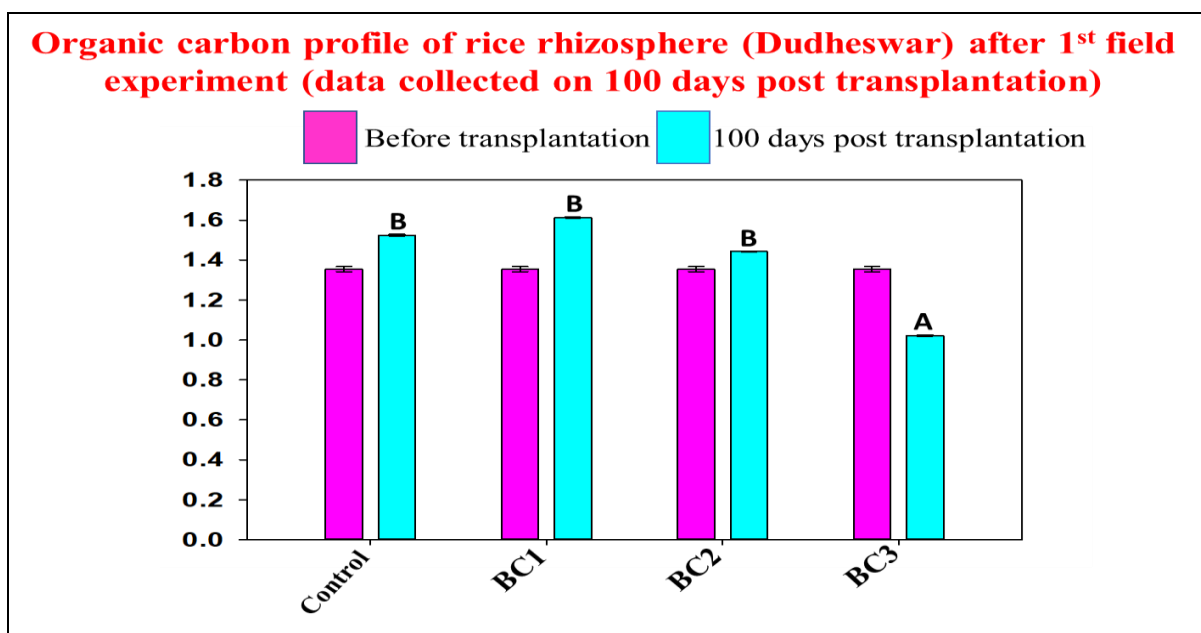


Figure 9.14: The above figure depicts the soil organic carbon studied from control (without bacteria) and different consortia-added rhizospheric soil for rice varieties Dudheswar. Data were plotted as mean \pm standard error (n=3) in the graph.

Observations:

Soil organic carbon was found to increase significantly for all consortia-added soil as well as control plots (without bacteria) after the 1st field experiment when compared to that of before transplantation. Contrastingly, BC3 consortia-added plots showed significant decrease in SOC. Data were collected on 100 days post-transplantation.

9.2.l. Analysis of soil nitrate-nitrogen during the experimental period:

Calibration curve of nitrate-nitrogen to be followed as depicted in the figure 7.8

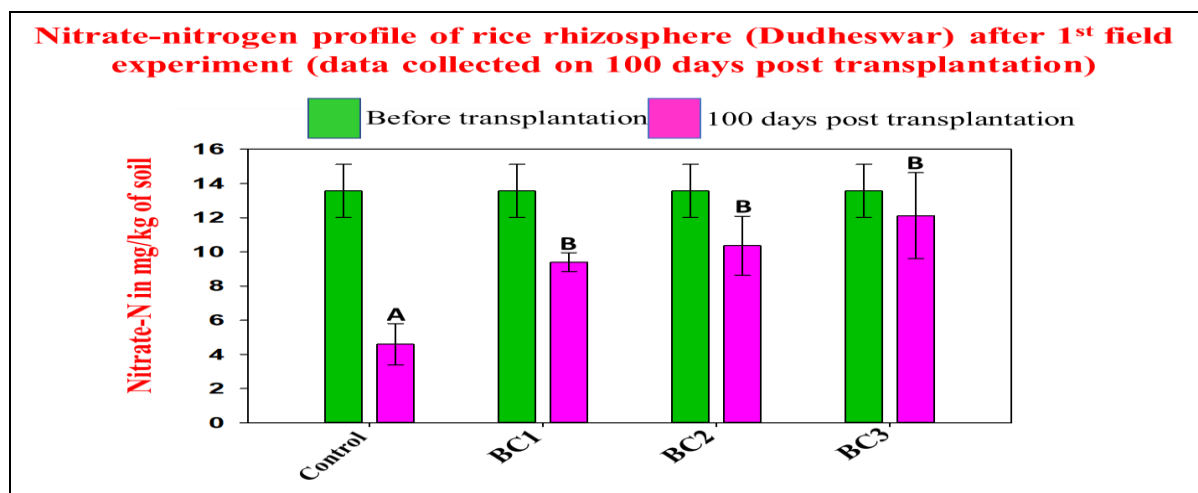


Figure 9.15: The above figure depicts the soil nitrate-nitrogen studied from control (without bacteria) and different consortia-added rhizospheric soil for rice varieties Dudheswar. Data were plotted as mean \pm standard error (n=3) in the graph.

Observations:

The nitrate-nitrogen content of soil was found to decrease significantly for all consortia-added soil as well as control plots after the 1st field experiment. Data were collected on 100 days post-transplantation.

9.2.m. Analysis of soil ammonia-nitrogen during the experimental period:

Calibration curve of ammonia-nitrogen to be followed as depicted in the figure 7.10

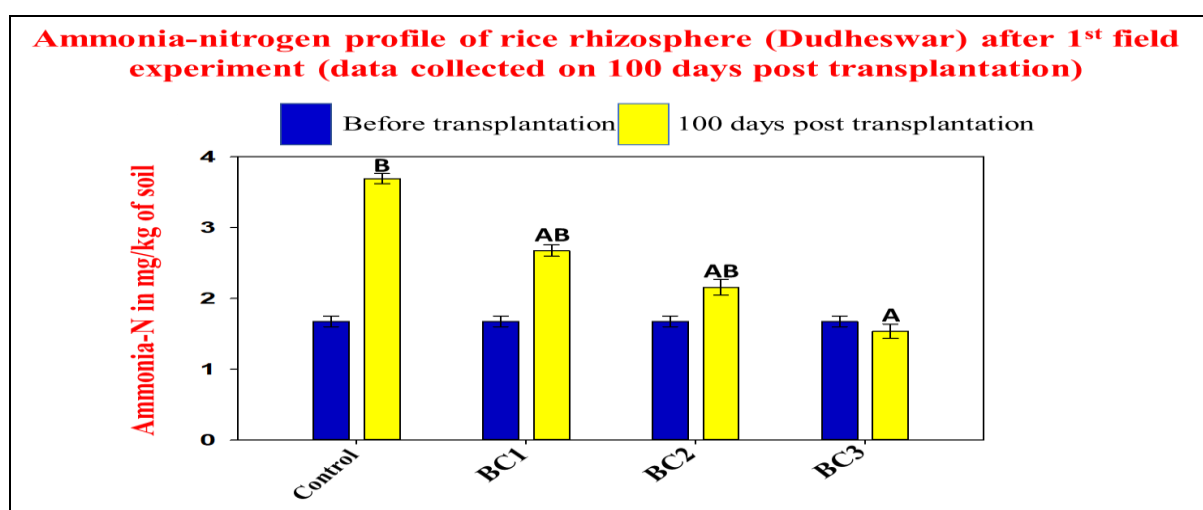


Figure 9.16: The above figure depicts the soil ammonia-nitrogen studied from control (without bacteria) and different consortia-added rhizospheric soil for rice varieties Dudheswar. Data were plotted as mean \pm standard error (n=3) in the graph.

Observations:

The ammonia-nitrogen content of soil was increased for all consortia added soil as well as control plot after 1st field experiment. Except BC3 consortia added plots where the Ammonia-nitrogen content was decreased. Data were collected on 100 days post-transplantation.

9.2.n. Analysis of plant-available phosphorus during the experimental period:

Calibration curve of plant-available phosphorus to be followed is depicted in the figure 7.12

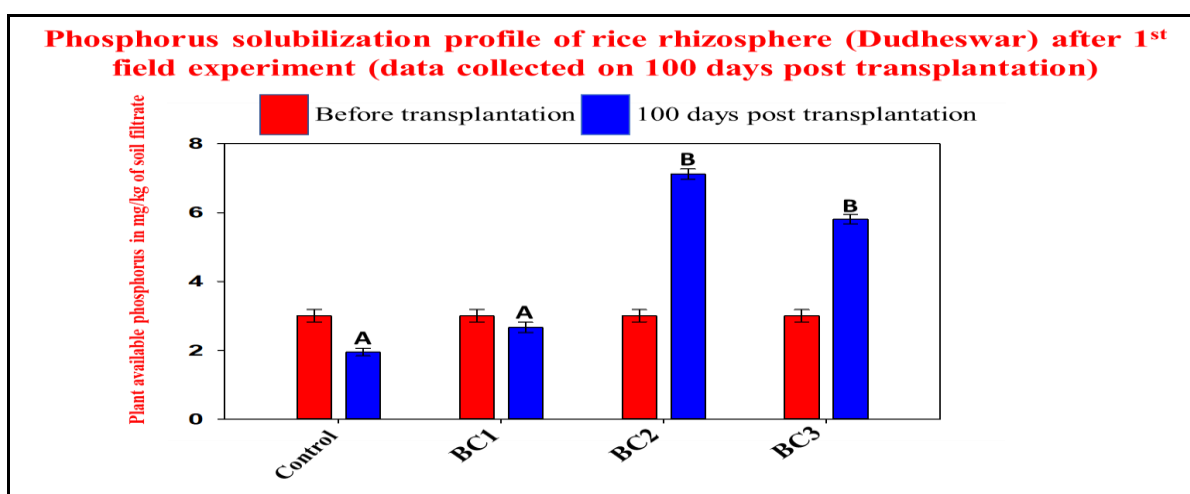


Figure 9.17: The above figure depicts the plant-available phosphorus studied from control (without bacteria) and different consortia-added rhizospheric soil for rice varieties Dudheswar. Data were plotted as mean \pm standard error (n=3) in the graph.

Observations:

Improved P-solubilization profile validates the enrichment of added consortia at rice rhizospheres in comparison to control plots where bacterial culture was not added. BC1 consortia-added plots was the exception where the plant-available phosphorus content significantly decreased. Data were collected on 100 days post-transplantation.

Based on the results obtained in 1st rice field experiments and two experiments conducted at greenhouse with 12 consortia, 2nd field experiment at Sundarbans was conducted only with the 3 best consortia, consortium BC3, consortium SRC2+BEC2 and consortium SRC3+BEC3 in two different rice fields with 8 replicate plots (4m² each) for each consortium tested along with control plots (8 replicate plots of 4m² each) where no bacterial culture was added. Consortium SRC2+BEC2 and consortium SRC3+BEC3 are made by mixing endophytic and rhizospheric bacterial strains.

9.3. 2nd field experiment details in Sundarban rice field (Field no. 1):

Two different rice plots were selected for 2nd rice field experiment viz. field no.1 and field no. 2. Details of field no.1 rice fields in Sundarbans are described below:

9.3.a. Field no. 1 details:

- ☐ The rice cultivar: **Dudheswar IC 593998**
- ☐ Seeds sown on the seedbed: **25-06-2022**
- ☐ Seedlings transplantation: **08-08-2022**
- ☐ Age of the seedlings when transplantation was done: **43 days**
- ☐ Initial height of roots at the time of transplantation: **10cm to 15cm**
- ☐ Initial height of seedlings at the time of transplantation: **60cm to 70cm**
- ☐ Distance between the seedlings transplanted: **approx. 30cm**
- ☐ Seedlings transplanted per replica: **50**
- ☐ Seedlings transplanted per consortium: **200**
- ☐ Leaf width at the time of plantation: **0.2-0.4 cm**
- ☐ Number of tillers transplanted in a cluster: **5 to 8**
- ☐ 1st addition of bacterial culture: **05-09-2022**
- ☐ 2nd addition of bacterial culture: **13-10-2022**
- ☐ Conductivity of the water where rice seedlings had been transplanted
0.414 mS/cm=0.2 ppt
- ☐ Conductivity of the soil where rice seedlings had been transplanted
1.78 mS/cm =0.9 ppt
- ☐ Conductivity of water by which seedbed was maintained: **0.414 mS/cm=0.2 ppt**
- ☐ Conductivity of soil where seedbed was prepared=**0.414 mS/cm =0.2 ppt**
- ☐ Soil sediment pH: **7.38-7.48**
- ☐ **4 Control rice plots of 4 m² each** (no bacterial culture added) used.
- ☐ **4 replica rice plots of 4 m² each** used for each bacterial consortium.

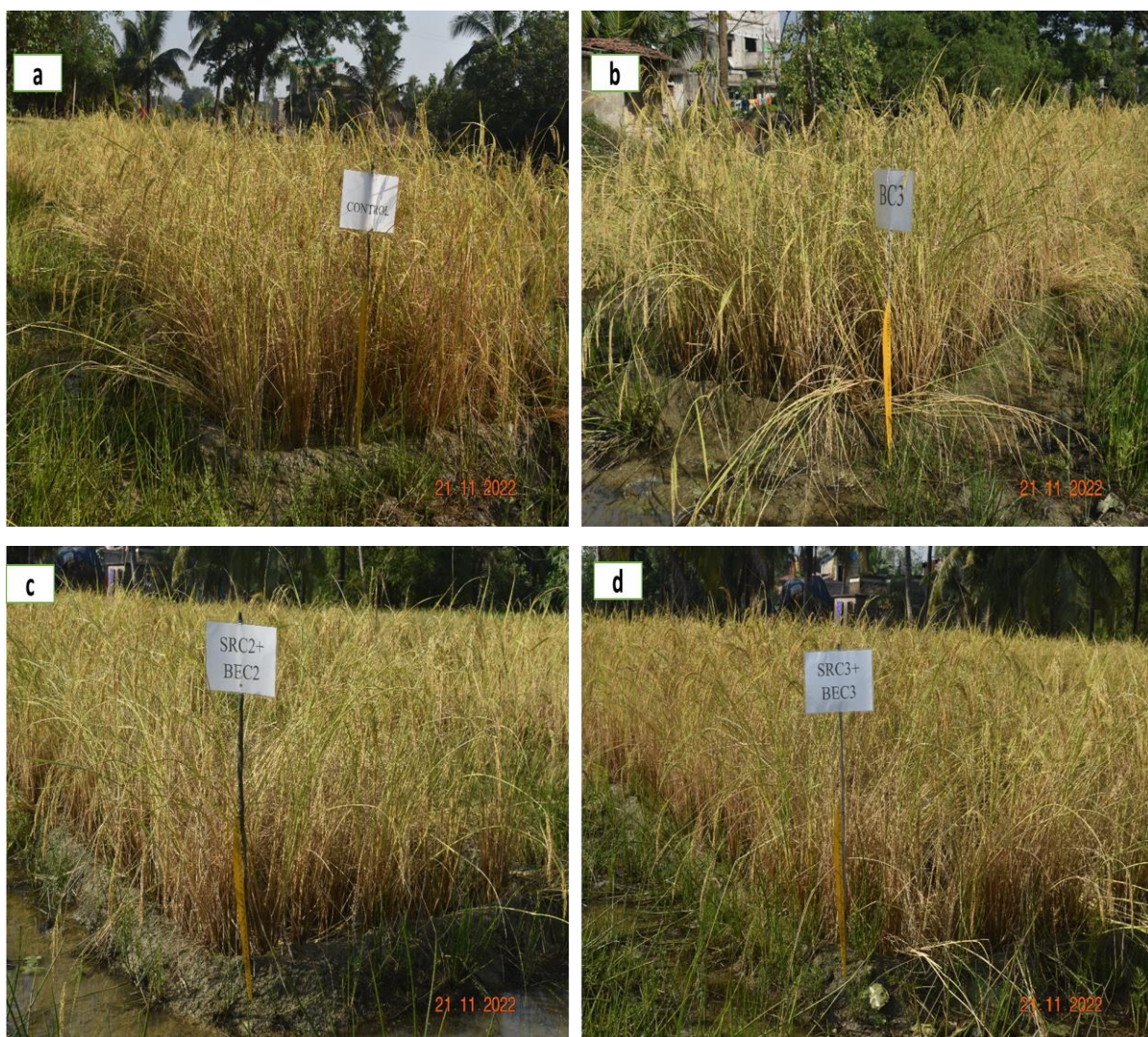


Figure 9.18: 2nd field experiment at Sundarbans. (a) Control plots where no bacterial culture was added (b) BC3 plots where Consortium BC3 was added (c) SRC2+BEC2 plots where Consortium SRC2+BEC2 was added (d) SRC3+BEC3 plots where Consortium SRC3+BEC3 was added.

9.3.b. Different growth parameters of cultivated rice observed in 2nd field experiment, **field no. 1** at Sundarbans:

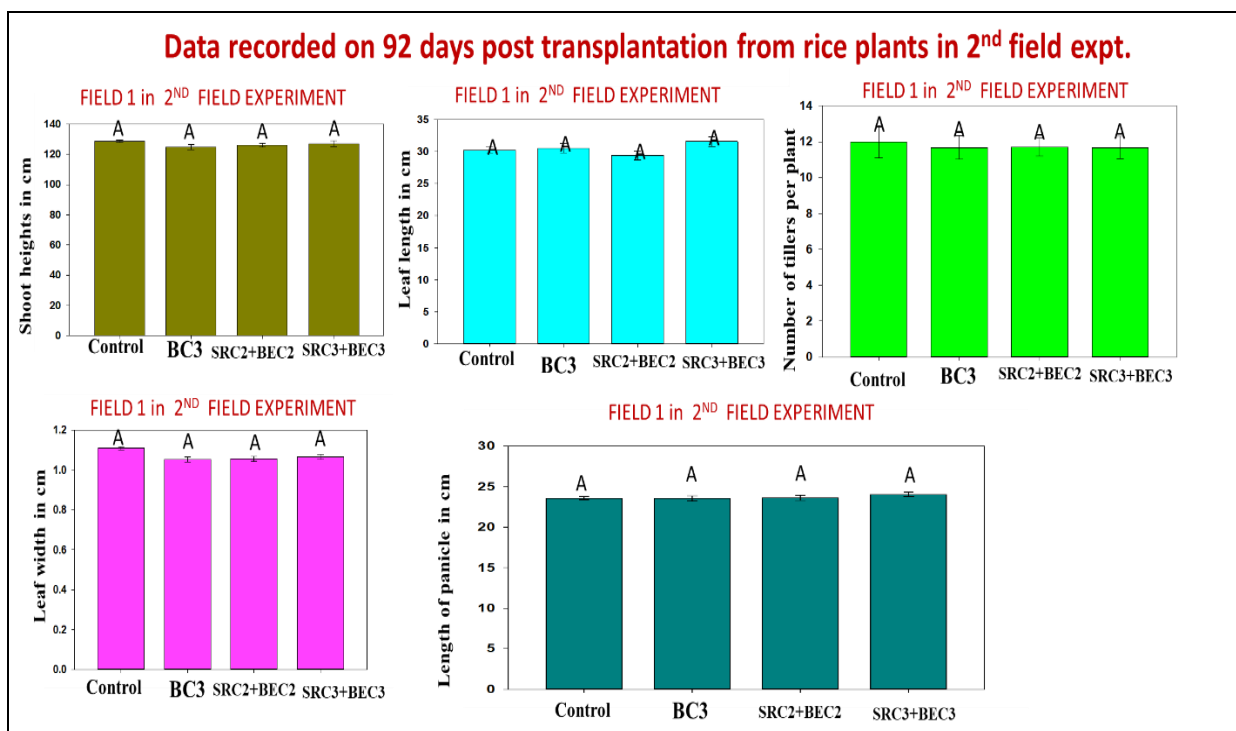


Figure 9.19: The above figure depicts the growth parameters of rice plants (Dudheswar) after 2nd field experiment, field no. 1 on 92 days post-transplantation. A comparison study of shoot height, leaf length, number of tillers, leaf width and length of panicle across control (without bacteria) and consortia-added plots was made. Data were plotted as mean \pm standard error (n=80 per category) in the graph.

Observations:

No significant difference was observed as compared to control at vegetative stages such as shoot height, leaf length, number of tillers, leaf width and length of panicle in cultivated rice at **field no. 1** in the 2nd field experiment.

9.3.c. Different yield parameters of the cultivated rice in 2nd field experiment, field no. 1 at Sundarbans:

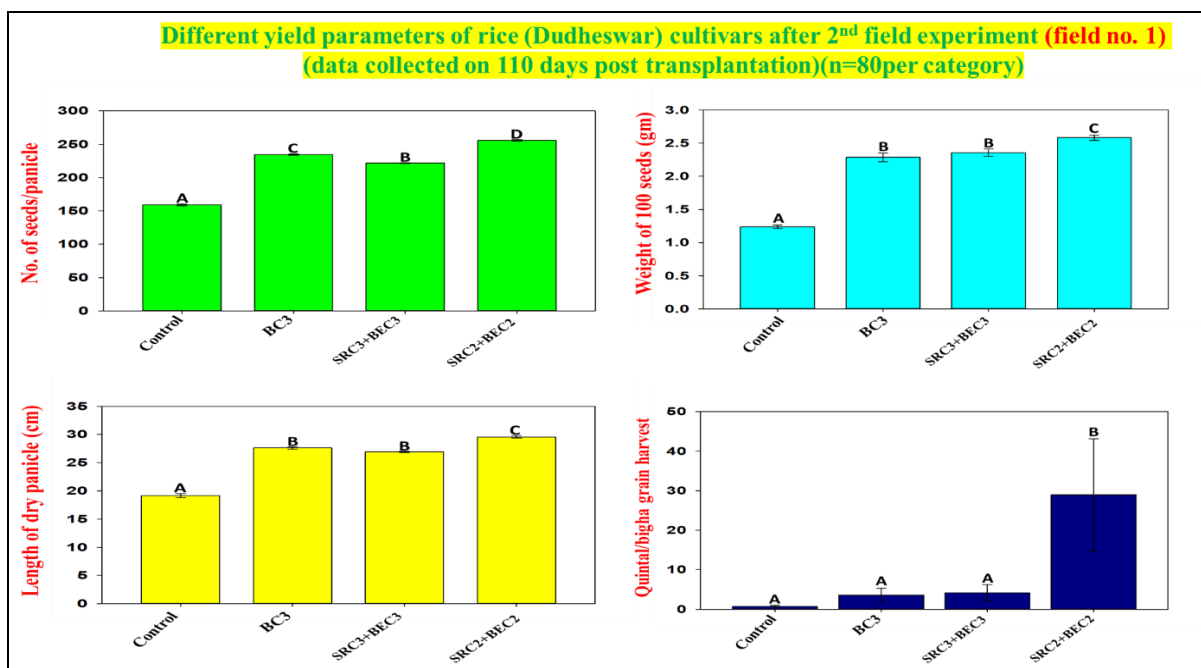


Figure 9.20: The above figure depicts the yield parameters of rice plants (Dudheswar) after the 2nd field experiment, field no. 1 on 110 days post-transplantation. A comparison study of no. of seeds/panicles, weight of 100 seeds, length of dry panicle and quintal/bigha grain harvest across control (without bacteria) and consortia-added plot was made. Data were plotted as mean \pm standard error (n=80 per category) in the graph.

Observations:

The significant increase is observed in all the above yield parameters such as number of seeds per panicle, weight of 100 seeds in gm and length of dry panicle in cm. However, major significant increase is observed in yield in quintal per bigha in SRC2+BEC2 consortia-added plots as compared to control where no bacterial consortia was added. A very high yield ~30 quintal/bigha grain yield was observed for these SRC2+BEC2 consortia-added plots.

9.3.d. Starch content analysis in harvested grains:

Calibration curve of starch to be followed was depicted in the figure 9.7.

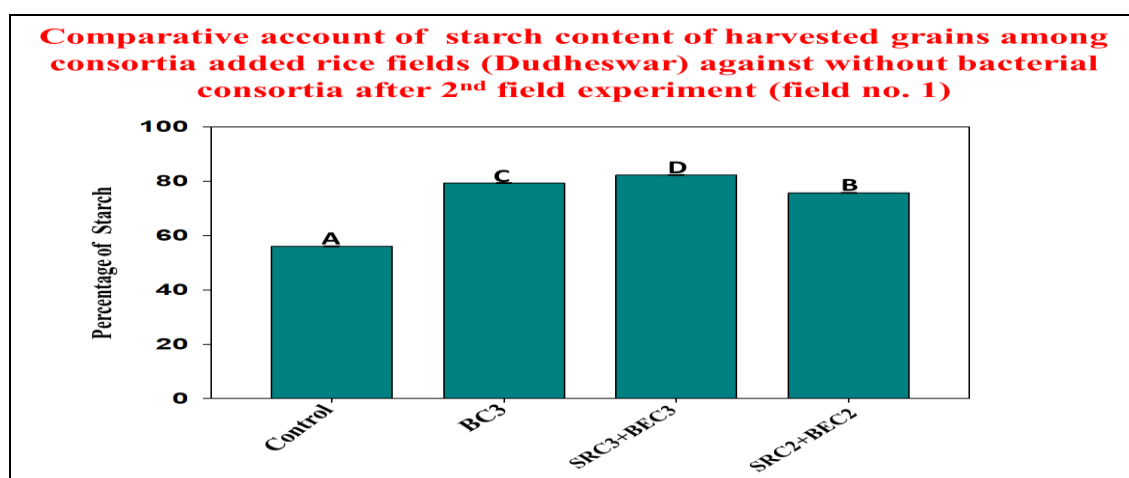


Figure 9.21: The above figure depicts a comparative study of starch content analysis from rice grains of control (without bacteria) and different consortia-added plots of the 2nd field experiment at field no. 1. Data were plotted as mean \pm standard error (n=3) in the graph.

Observations:

Major significant improvement in starch% in harvested grains was observed for all bacterial consortia-added rice plots especially BC3 and SRC3+BEC3 (80% starch content) consortia-added plots as compared to that of the control plots (~60% starch content) where no bacterial consortia was added.

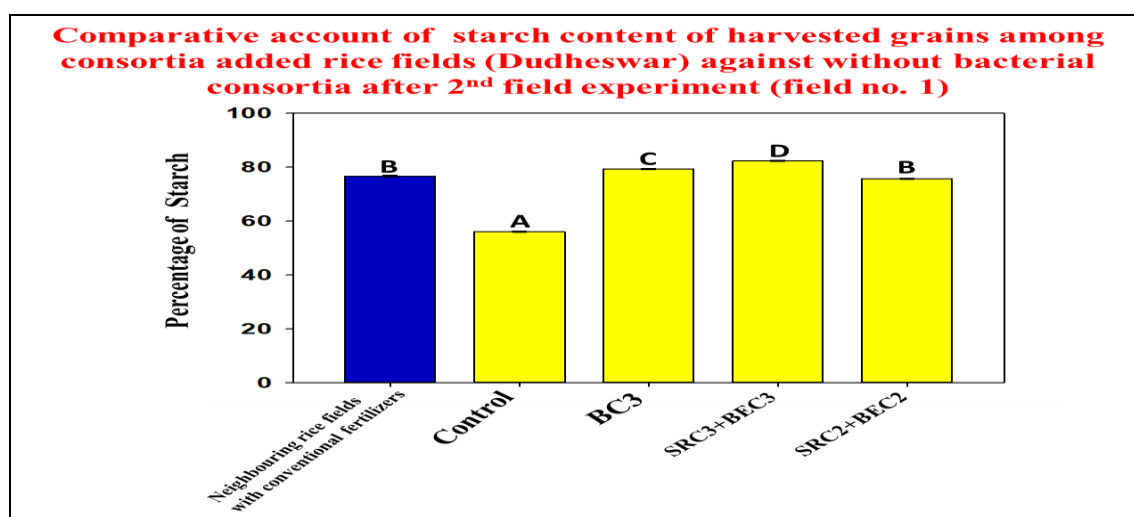


Figure 9.22: The above figure depicts a comparative study of starch content analysis from rice grains of neighbouring rice fields cultivated with conventional fertilizers, control (without bacteria) and different consortia-added plots of the 2nd field experiment at field no. 1. Data were plotted as mean \pm standard error (n=3) in the graph.

Observations:

Major significant improvement in starch% observed for all bacterial consortia-added rice plots especially BC3 and SRC3+BEC3 consortia added plots (~80% starch content). Neighbouring rice fields with conventional fertilizers and SRC2+BEC2 consortia added plots showed more or less identical starch% content.

9.3.e. Protein content analysis in harvested rice grains:

Calibration curve of protein to be followed was described in the figure 9.9.

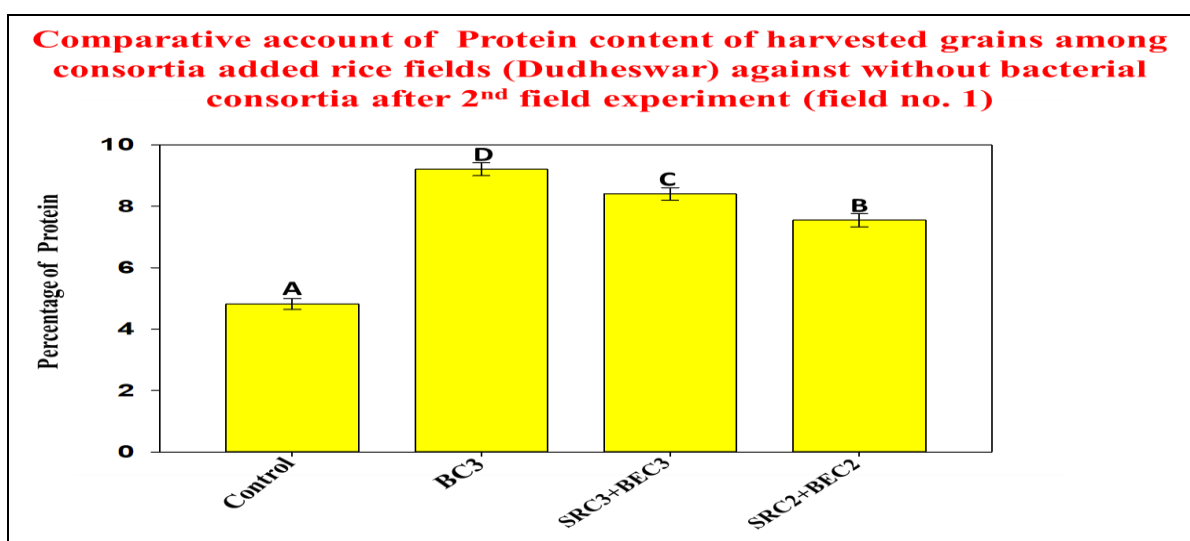


Figure 9.23: The above figure depicts a comparative study of protein content analysis from rice grains of control (without bacteria) and different consortia-added plots of the 2nd field experiment at field no. 1. Data were plotted as mean \pm standard error (n=3) in the graph.

Observations:

Major significant improvement in protein% was observed for harvested rice grains from all bacterial consortia-added rice plots especially, BC3 and SRC3+BEC3 consortia-added plots (~8-9%) against that of control plots (~4-5%).

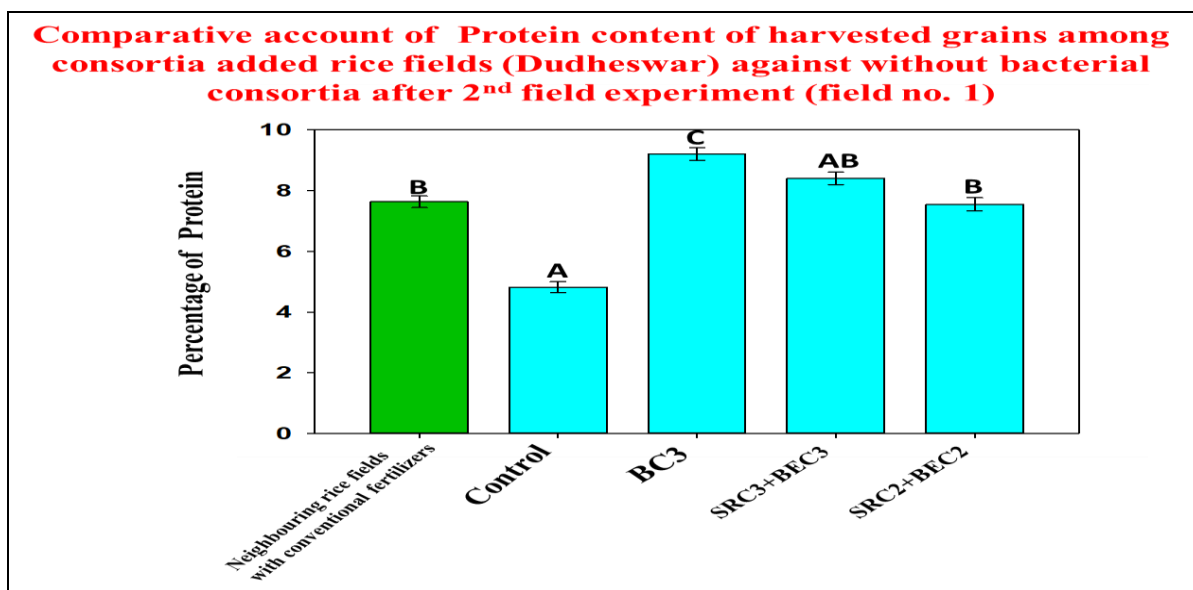


Figure 9.24: The above figure depicts a comparative study of protein content analysis from rice grains of neighbouring rice fields cultivated with conventional fertilizers, control (without bacteria) and different consortia-added plots of the 2nd field experiment at field no.1. Data were plotted as mean \pm standard error (n=3) in the graph.

Observations:

Major significant improvement in protein% was observed in harvested rice grains from bacterial consortia-added rice plots, especially BC3 consortia-added plots (~9%). Neighbouring rice fields cultivated with conventional fertilizers and SRC2+BEC2 consortia-added plots demonstrated more or less comparable protein content (~7-8%).

Soil physical parameters and nutrient profiling in Sundarbans cultivated rice field soil (0-15 cm cores) before and after the 2nd field experiment (Field no. 1):

9.3.f. Analysis of soil pH during the experimental period:

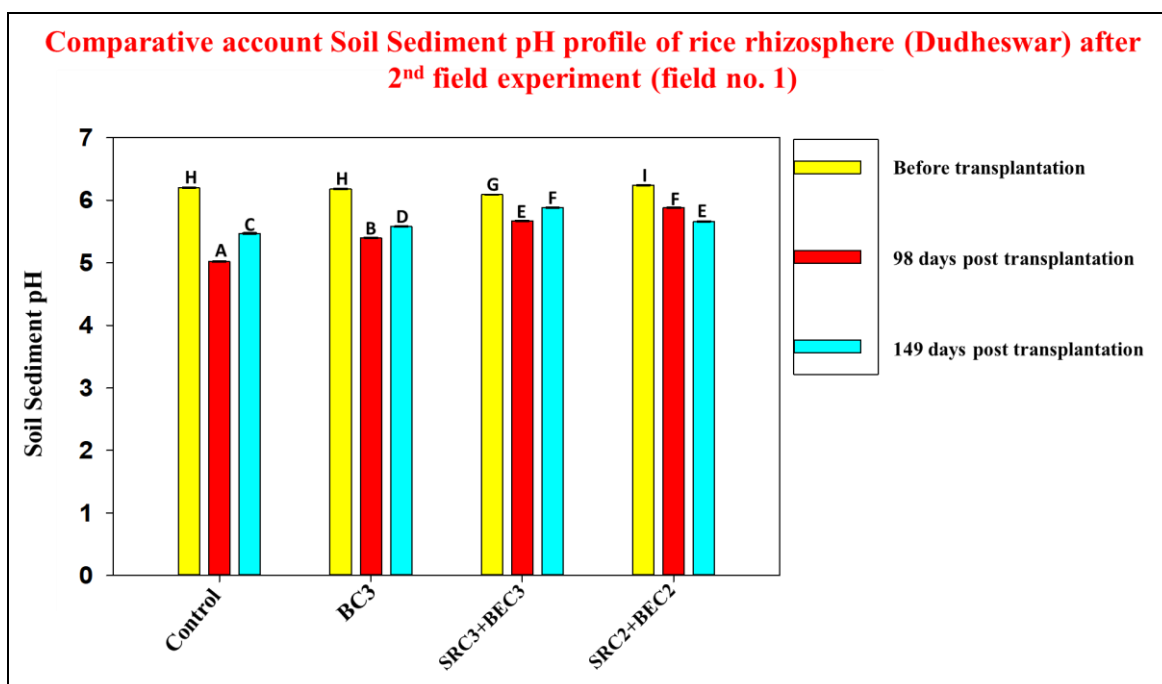


Figure 9.25: The above figure depicts the soil pH studied from control (without bacteria) and different consortia (prepared by mixing endophytic and rhizospheric bacterial strains) added rhizospheric soil for rice varieties Dudheswar. Data were plotted as mean \pm standard error (n=3) after 2nd field experiment (field number 1) in the graph.

Observations:

The soil pH was found to decrease significantly for all consortia-added plots as well as control plots (without bacteria) in the 2nd field (field no. 1) experiment. Data were collected on 149 days post-transplantation.

9.3.g. Analysis of soil electrical conductivity (EC) during the experimental period:

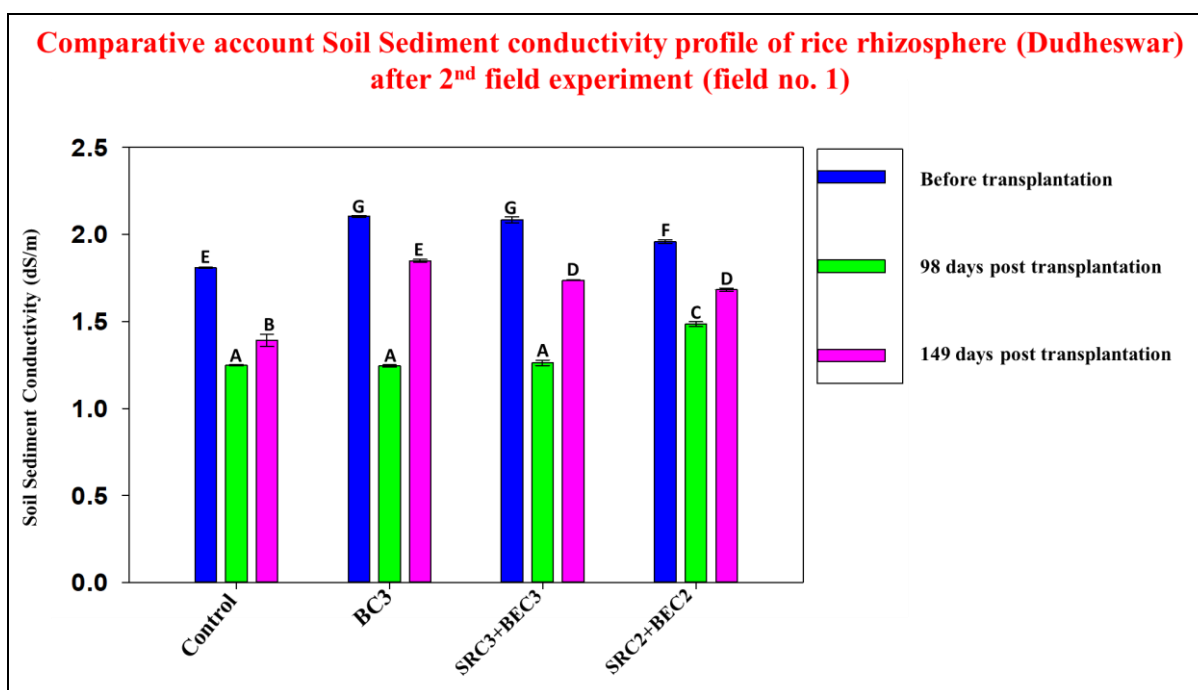


Figure 9.26: The above figure depicts the soil conductivity studied from control (without bacteria) and different consortia (prepared by mixing endophytic and rhizospheric bacterial strains) added rhizospheric soil for rice varieties Dudheswar. Data were plotted as mean \pm standard error (n=3) after 2nd field experiment (field no. 1) in the graph.

Observations:

The soil conductivity was found to significantly decrease for all consortia-added plots as well as control plots (without bacteria) up to 98 days post-transplantation with slight increase observed at 149 days post-transplantation in the 2nd field (field no.1) experiment. Data were collected till 149 days post-transplantation. This decrease in soil EC was caused by heavy rains during monsoon.

9.3.h. Analysis of soil organic carbon (SOC) during the experimental period:

Calibration curve of organic carbon followed was described in the figure 7.6.

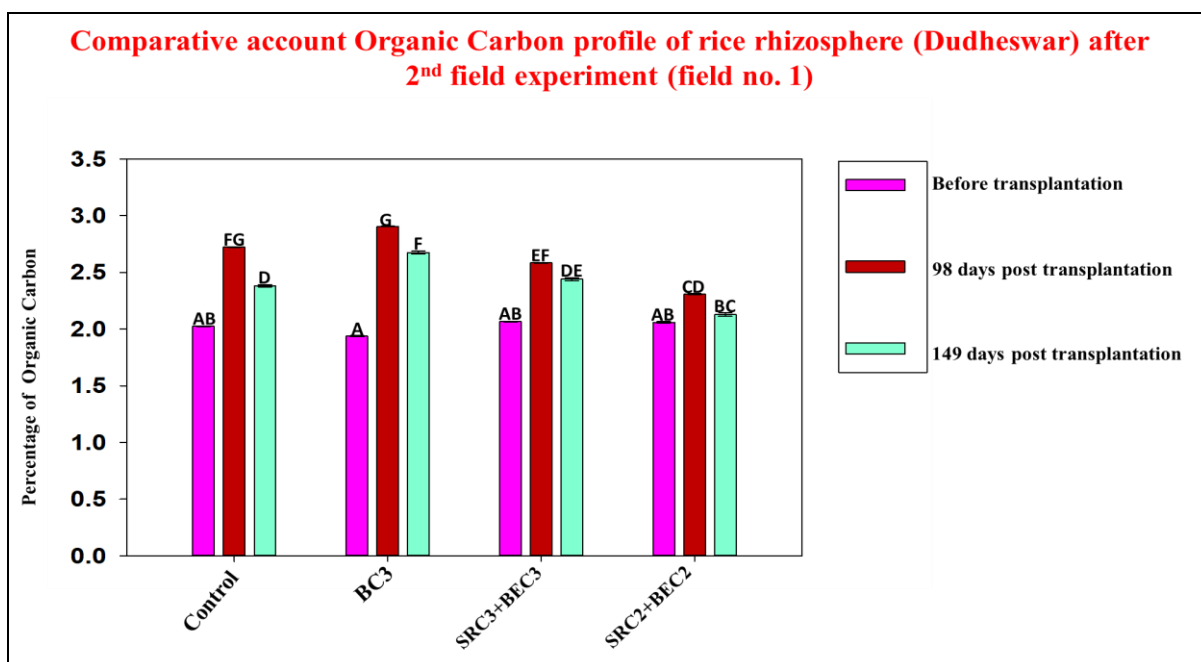


Figure 9.27: The above figure depicts the soil organic carbon studied from control (without bacteria) and different consortia (prepared by mixing endophytic and rhizospheric bacterial strains) added rhizospheric soil for rice varieties Dudheswar. Data were plotted as mean \pm standard error ($n=3$) after 2nd field experiment (field no. 1) in the graph.

Observations:

The organic carbon content increased for consortia-added plots and control (without bacteria) plots as compared to before transplantation in the 2nd field (field no.1) experiment. Organic carbon content was found to be higher in 98 days post-transplantation as compared to the 149 days post-transplantation.

9.3.i. Analysis of soil nitrate-nitrogen during the experimental period:

Calibration curve of nitrate-nitrogen followed was described in the figure 7.8.

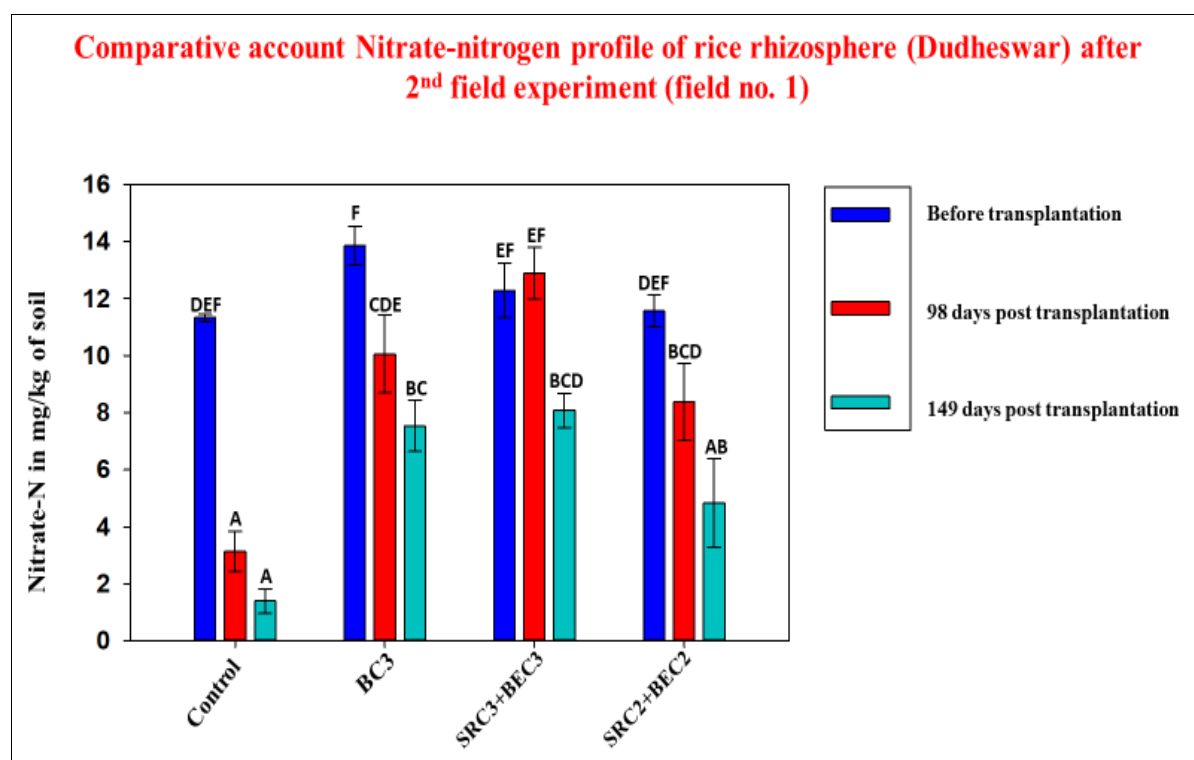


Figure 9.28: The above figure depicts the soil nitrate-nitrogen studied from control (without bacteria) and different consortia (prepared by mixing endophytic and rhizospheric bacterial strains) added rhizospheric soil for rice varieties Dudheswar. Data were plotted as mean \pm standard error (n=3) after the 2nd field experiment (field no. 1) in the graph.

Observations:

The nitrate-nitrogen content gradually decreased over 149 days post-transplantation for consortia added plots and control (without bacteria) as compared to before transplantation in the 2nd field (field no.1) experiment. This decline in nitrate-N was observed to be the highest for the control plots. In consortia added plots the nitrate-nitrogen consumed by rice plants was assumed to be replenished by the bacterial consortia added in the rhizosphere soil.

9.3.j. Analysis of soil ammonia-nitrogen during the experimental period:

Calibration curve of ammonia-nitrogen to be followed was described in the figure 7.10.

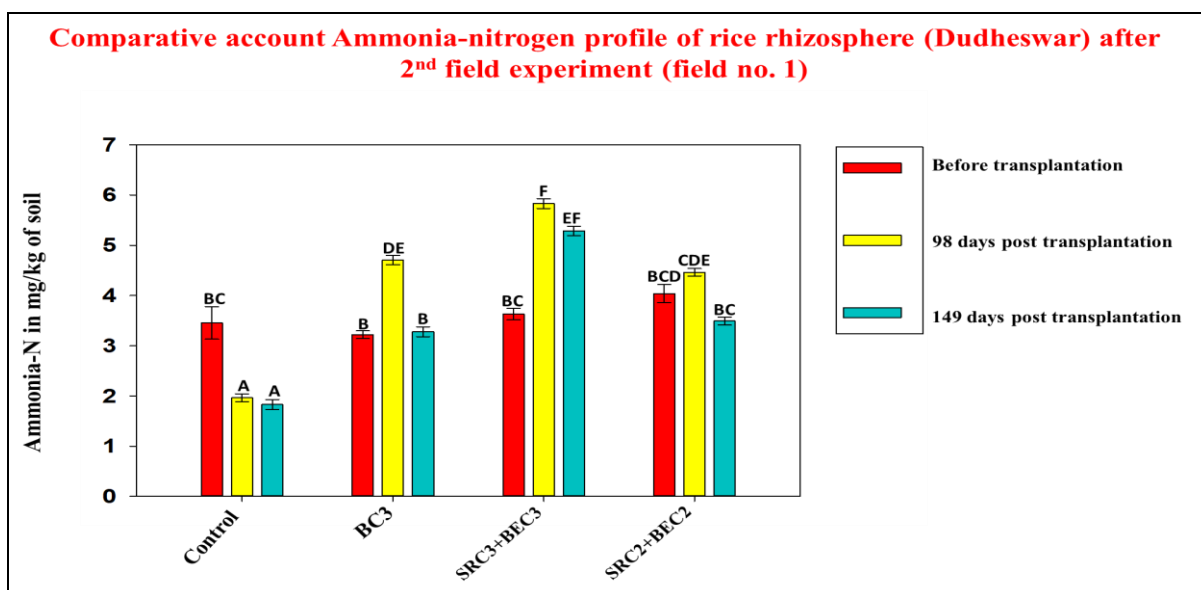


Figure 9.29: The above figure depicts the soil ammonia-nitrogen studied from control (without bacteria) and different consortia (prepared by mixing endophytic and rhizospheric bacterial strains) added rhizospheric soil for rice varieties Dudheswar. Data were plotted as mean \pm standard error (n=3) after the 2nd field experiment (field no. 1) in the graph.

Observations:

The ammonia-nitrogen content increased for consortia added plots as compared to before transplantation in the 2nd field (field no.1) experiment across 149 days post-transplantation. However, decline in ammonia-N was observed for the control plots where no bacterial consortia was added. In consortia-added plots the ammonia-nitrogen consumed by rice plants was assumed to be replenished by the bacterial consortia with free-N₂-fixing bacterial members added in the rhizosphere soil.

9.3.k. Analysis of plant-available phosphorus in soil during the experimental period:

Calibration curve of plant-available phosphorus followed was described in the figure 7.12.

P-solubilization profile at rhizospheres of experimental plots as indicator/metric of growth promotion/enrichment of consortia

Taking P-solubilization profile at rhizospheres of experimental plots as indicator/metric of growth promotion/enrichment of consortia, in the 2nd field experiment (field no. 1), data were recorded at 38 days, 66 days, 98 days and 149 days post-transplantation from cultivated rice rhizosphere (Dudheswar). The data were represented in the following figure:

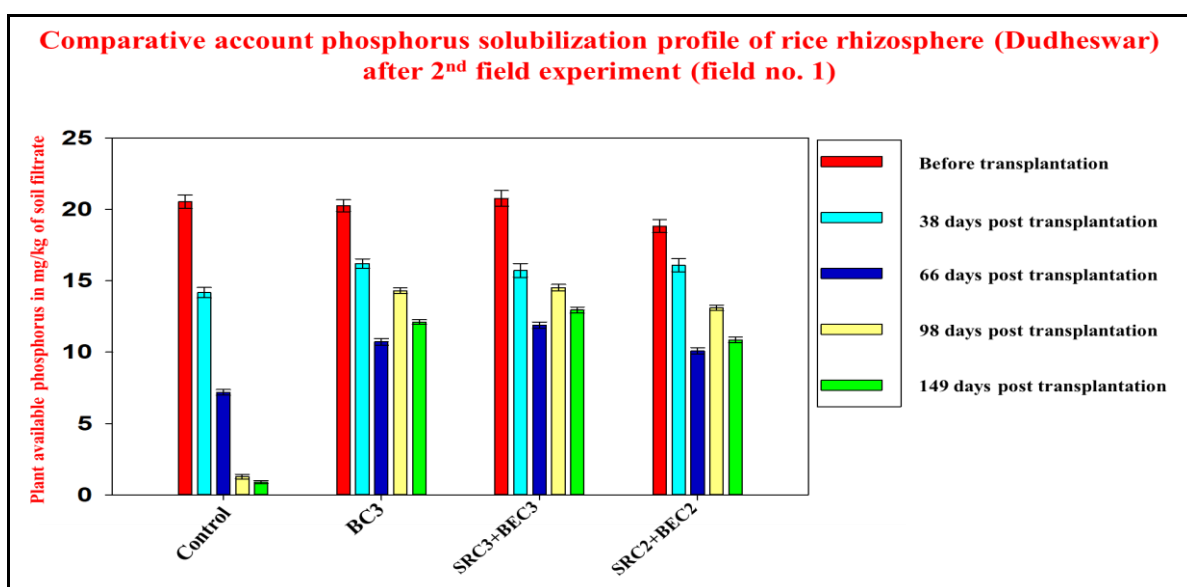


Figure 9.30: The above figure depicts the comparison study of plant available phosphorus from control (without bacteria), and different consortia (prepared by mixing endophytic and rhizospheric bacterial strains) added rhizospheric soil, till 149 days post-transplantation at a specific time interval in the 2nd field experiment (field no. 1) for cultivated **Dudheswar** rice. Data were plotted as mean \pm standard error (n=3) in the graph.

Observations:

- In almost all consortia added rhizospheres, the lowest level of soluble plant available phosphorus (P) is found to be at **66** days post-transplantation after which it gradually increased as observed at **98 days** and **149 days** post-transplantation rhizosphere soils. This increase in soluble plant-available phosphorus (P) can be attributed to the enrichment of PGP consortia at rice rhizosphere which have many a constituent member as high P-solubilizer
- In contrast, control (no bacteria added) rice rhizospheres, showed no significant increase in level of soluble plant available phosphorus (P) even after 66 days post transplantation.
- Many of the consortia added rhizospheres of experimental rice plants showed presence of higher level of soluble plant available phosphorus (P) as compared to control (no bacteria added) rice rhizospheres even at **66** days post-transplantation, when the rice plants showed maximum utilization of soil-P.
- P-solubilization seems to be a promising growth promotion potential of the selected/added consortia (most members in each consortium were high P-solubilizers as observed earlier in laboratory experiments).
- **Significant increase in solubilized-P was observed in consortia added rhizospheres as compared to control (no bacterial addition) rhizospheric soils after 98 days post transplantation in all the above represented figures. Generally, we observed that in our greenhouse pot experiment solubilized-P content increased after 89 days of post-transplantation. Similar results are observed in our rice field experiments also.**

9.4. 2nd field experiment details in Sundarban rice field (Field no. 2):

Details of field no. 2 rice fields in Sundarban are described below-

9.4.a. Field no. 2 details:

- ☐ The rice cultivar: **Dudheswar IC 593998**
- ☐ Seeds sown on the seedbed: **24-06-2022**
- ☐ Seedlings transplantation: **07-08-2022**
- ☐ Age of the seedlings when transplantation was done: **43 days**
- ☐ Initial height of roots at the time of transplantation: **10cm to 15cm**
- ☐ Initial height of seedlings at the time of transplantation: **60cm to 70cm**
- ☐ Distance between the seedlings transplanted: **approx. 30cm**
- ☐ Seedlings transplanted per replica: **100**
- ☐ Seedlings transplanted per consortium: **400**
- ☐ Leaf width at the time of plantation: **0.2-0.5 cm**
- ☐ Number of tillers transplanted in a cluster: **5 to 8**
- ☐ 1st addition of bacterial culture: **05-09-2022**
- ☐ 2nd addition of bacterial culture: **13-10-2022**
- ☐ Conductivity of the water where rice seedlings had been transplanted
mS/cm=1.3 ppt
- ☐ Conductivity of the soil where rice seedlings had been transplanted
mS/cm=1 ppt
- ☐ Conductivity of water by which seedbed was maintained: **0.817 mS/cm=0.4 ppt**
- ☐ Conductivity of soil where seedbed was prepared = **0.817 mS/cm=0.4 ppt**
- ☐ Soil sediment pH: **7.38-7.48**
- ☐ **8 Control rice plots of 4 m² each** (no bacterial culture added) used.
- ☐ **8 replica rice plots of 4 m² each** used for each bacterial consortium.

9.4.b. Different growth parameters of cultivated rice observed in the 2nd field experiment, field no. 2 at Sundarbans:

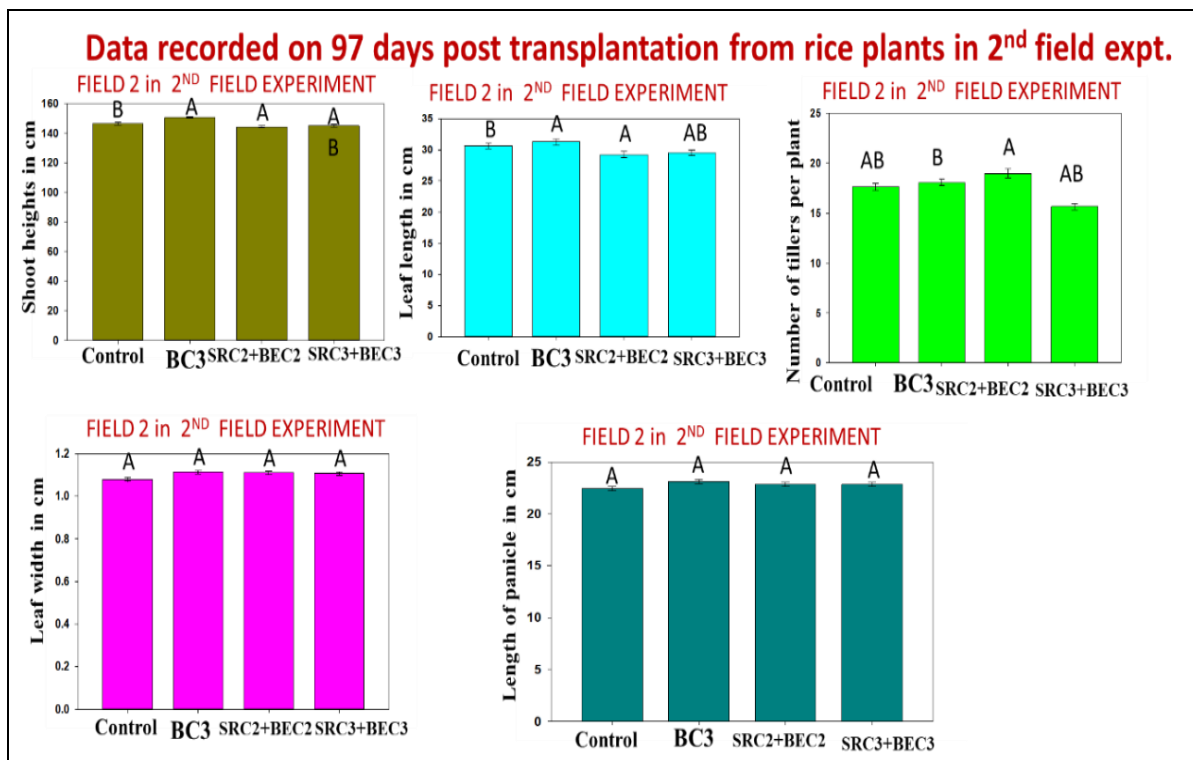


Figure 9.31: The above figure depicts the growth parameters of rice plants (Dudheswar) after 2nd field experiment, field no. 2 on 97 days post-transplantation. A comparison study of shoot height, leaf length, number of tillers, leaf width and length of panicle across control (without bacteria) and consortia-added plots was made. Data were plotted as mean \pm standard error (n=80 per category) in the graph.

Observations:

No significant difference was observed as compared to control at vegetative stages in **field no. 2.**

9.4.c. Different yield parameters of cultivated rice in the 2nd field experiment, field no. 2 at Sundarbans:

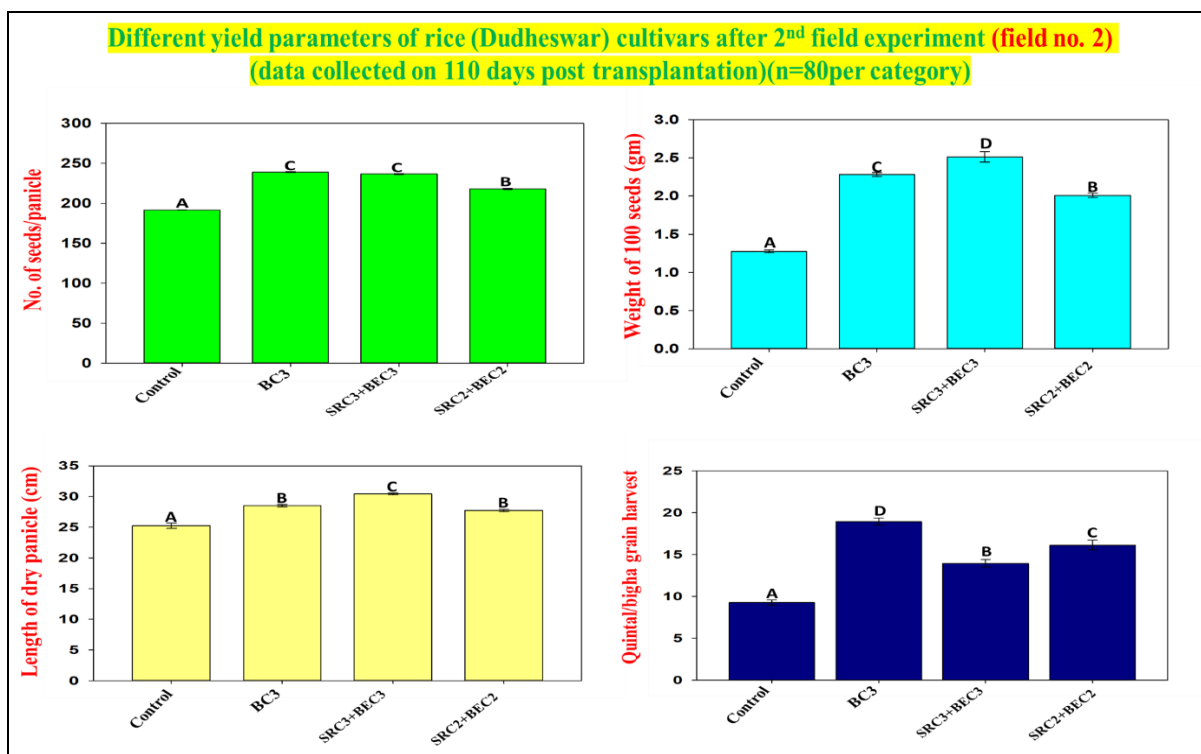


Figure 9.32: The above figure depicts the yield parameters of rice plants (Dudheswar) in the 2nd field experiment, (field no. 2) on 110 days post-transplantation. A comparison study of no. of seeds/panicles, weight of 100 seeds, length of dry panicle and quintal/bigha grain harvest across control (without bacteria) and consortia-added plots was presented. Data were plotted as mean \pm standard error (n=80 per category) in the graph.

Observations:

The significant increase is observed in all the above yield parameters such as number of seeds per panicle, weight of 100 seeds in gm and length of dry panicle in cm in harvested grains of all the consortia-added plots in comparison to control plots where no bacteria was added. However, major significant increase is observed in yield in quintal per bigha in consortia-added plots in the 2nd field (field no. 2) experiment. While control plots yielded ~10 quintal/bigha, the BC3 consortia added plots yielded up to 20 quintal/bigha, with SRC3+BEC3 and SRC2+BEC2 consortia-added plots yielding in the range of 14-17 quintal/bigha.

9.4.d. Starch content analysis in the harvested rice grains:

Calibration curve of starch followed here was already depicted in the figure 9.7.

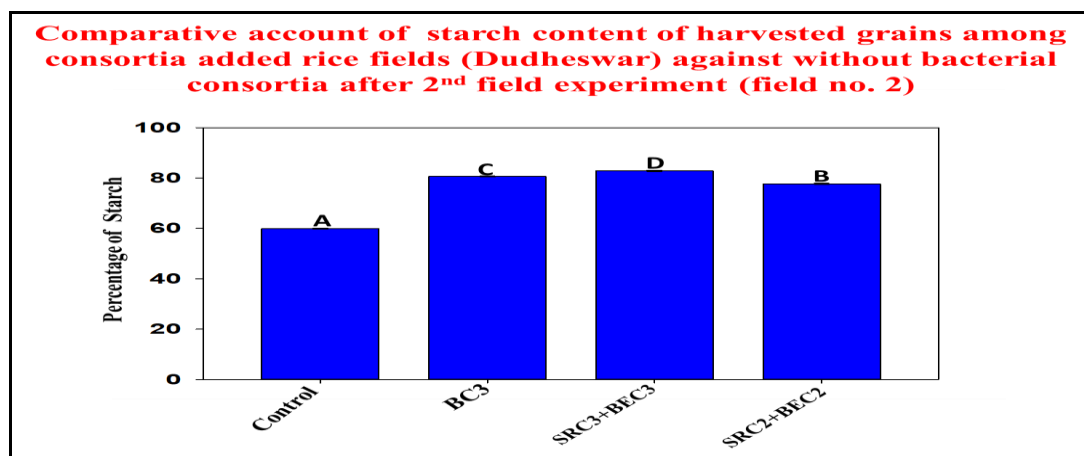


Figure 9.33: The above figure depicts a comparative study of starch content analysis from rice grains of control (without bacteria) and different consortia-added plots of the 2nd field experiment at field no. 2. Data were plotted as mean \pm standard error (n=3) in the graph.

Observations:

Major significant improvement in starch% was observed for the harvested grains of all bacterial consortia-added rice plots especially BC3 and SRC3+BEC3 consortia-added plots (~80%) in comparison to the ~60% starch content in the grains harvested from control plots where no bacteria was added in the 2nd field experiment at field no. 2.

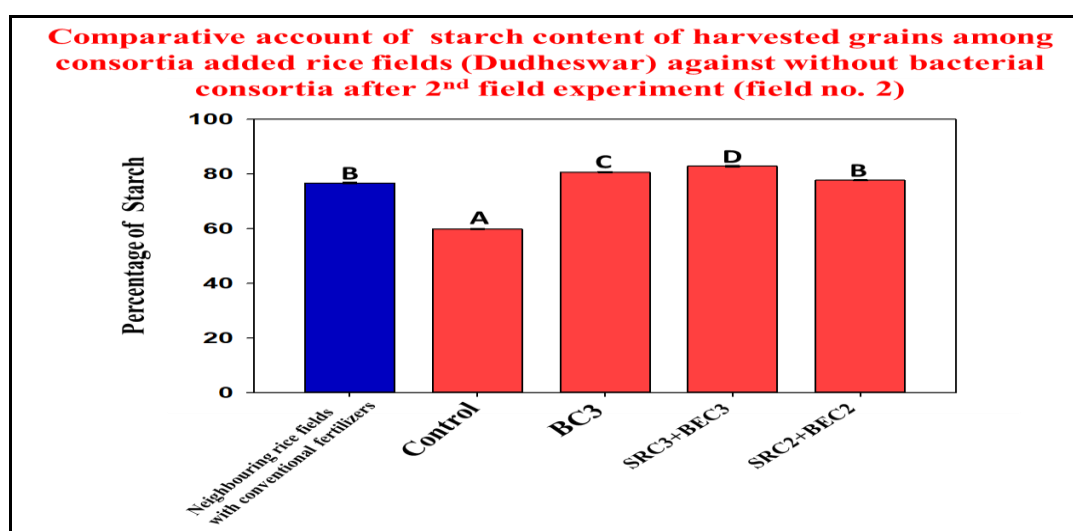


Figure 9.34: The above figure depicts a comparative study of starch content analysis from rice grains of neighbouring rice fields cultivated with conventional fertilizers, control (without bacteria) and different consortia-added plots of the 2nd field experiment at field no. 2. Data were plotted as mean \pm standard error (n=3) in the graph.

Observations:

Major significant improvement in starch% in harvested rice grains was observed for all bacterial consortia-added rice plots especially BC3 and SRC3+BEC3 consortia-added plots (~80%) in the 2nd field experiment at field number no. 2 as compared to that of control. Harvested grains from neighbouring rice fields cultivated with conventional fertilizers and SRC2+BEC2 consortia-added plots demonstrated comparable starch content (slightly below 80%).

9.4.e. Protein content analysis in harvested rice grains:

Calibration curve of protein followed was depicted in the figure 9.9.

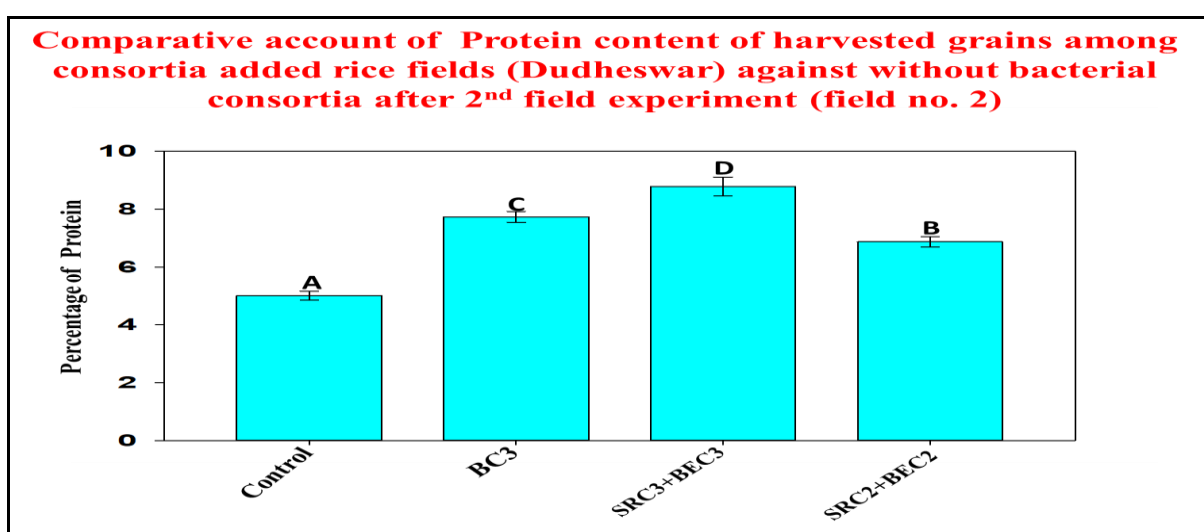


Figure 9.35: The above figure depicts a comparative study of protein content analysis from rice grains of control (without bacteria) and different consortia-added plots of the 2nd field experiment at field no. 2. Data were plotted as mean \pm standard error (n=3) in the graph.

Observations:

Major significant improvement in protein% was observed for the harvested grains from all the bacterial consortia-added rice plots especially BC3 and SRC3+BEC3 consortia-added plots (~7-8%) of the 2nd field experiment at field no. 2. In comparison to that of the control plots (~4-5%).

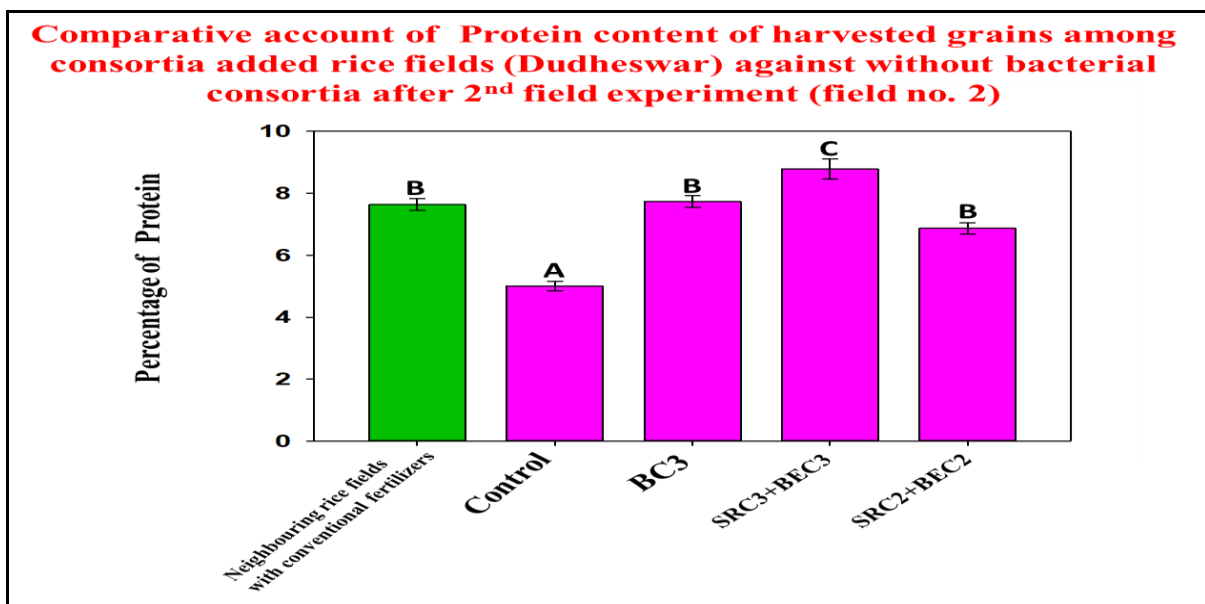


Figure 9.36: The above figure depicts a comparative study of protein content analysis from rice grains of neighbouring rice fields cultivated with conventional fertilizers, control (without bacteria) and different consortia-added plots of the 2nd field experiment at field no. 2. Data were plotted as mean \pm standard error (n=3) in the graph.

Observations:

Major significant improvement in protein% was observed for all the bacterial consortia-added rice plots especially BC3 and SRC3+BEC3 consortia added plots of the 2nd field experiment at field no. 2 (~7-8%). Neighbouring rice fields cultivated with conventional fertilizers and SRC2+BEC2 consortia-added plots yielded rice grains with comparable protein% content (slightly below 8%).

9.4.f. Analysis of soil pH during the experimental period:

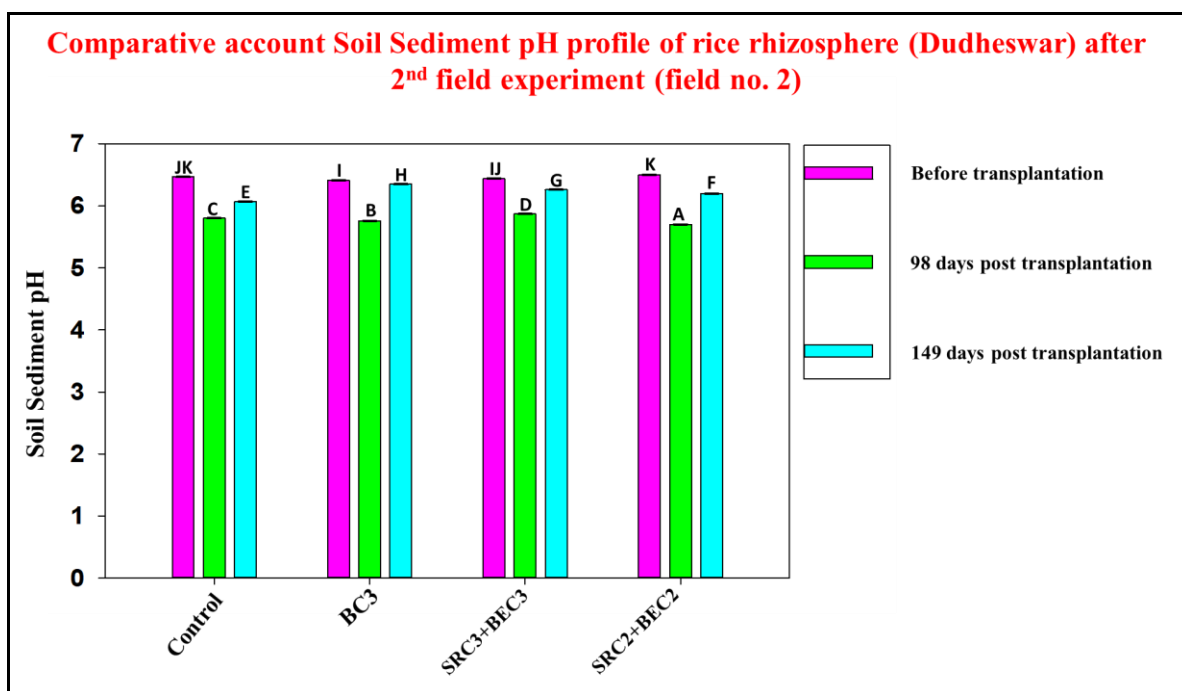


Figure 9.37: The above figure depicts the soil pH studied from control (without bacteria) and different consortia (prepared by mixing endophytic and rhizospheric bacterial strains) added rhizospheric soil for rice varieties Dudheswar. Data were plotted as mean \pm standard error (n=3) after 2nd field experiment (**field no. 2**) in the graph.

Observations:

The soil pH decreased significantly for all consortia added plots and control plots (without bacteria) also when compared to that of before transplantation in the 2nd field (field no. 2) experiment. Data were collected till 149 days post-transplantation.

9.4.g. Analysis of soil electrical conductivity (EC) during the experiment time:

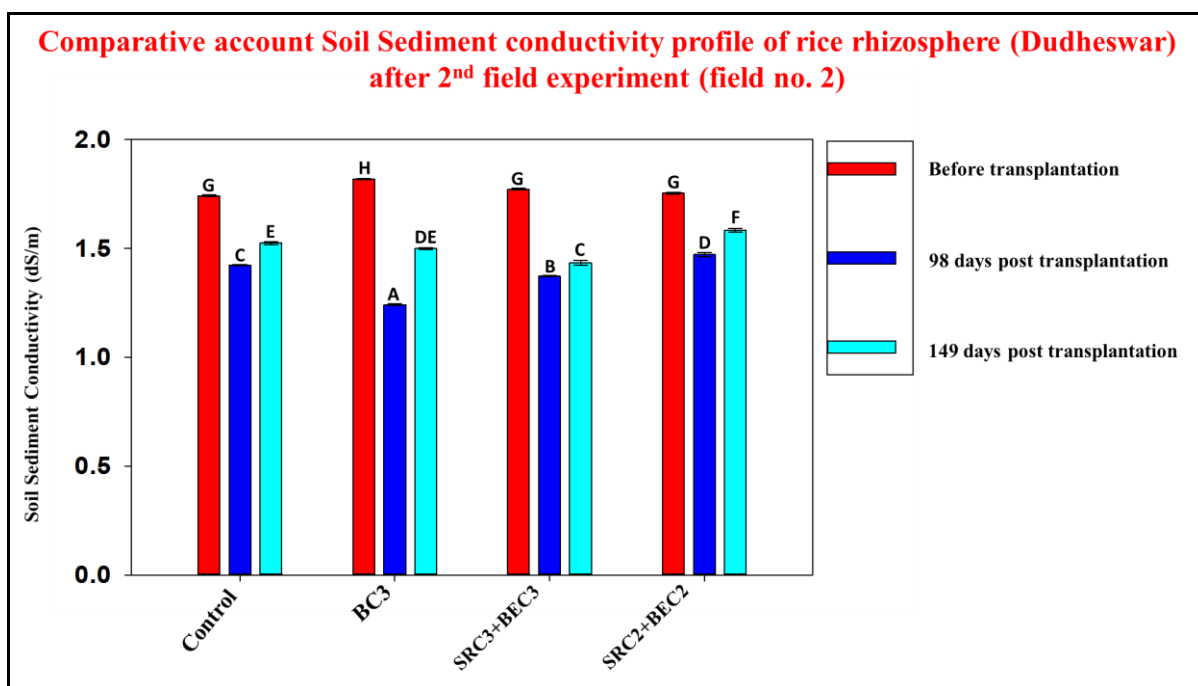


Figure 9.38: The above figure depicts the soil conductivity studied from the control (without bacteria) and different consortia (prepared by mixing endophytic and rhizospheric bacterial strains) added rhizospheric soil for rice varieties Dudheswar. Data were plotted as mean \pm standard error (n=3) after 2nd field experiment (field number 2) in the graph.

Observations:

The soil conductivity decreased for all consortia-added plots and control plots (without bacteria) also when compared to that of before transplantation due to heavy monsoon rains. At 98 days post-transplantation the decline in EC was the highest, however slightly increased at 149 days post-transplantation in the 2nd field (field no. 2) experiment.

9.4.h. Analysis of soil organic carbon (SOC) during the experimental period:

Calibration curve of organic carbon followed was depicted in the figure 7.6.

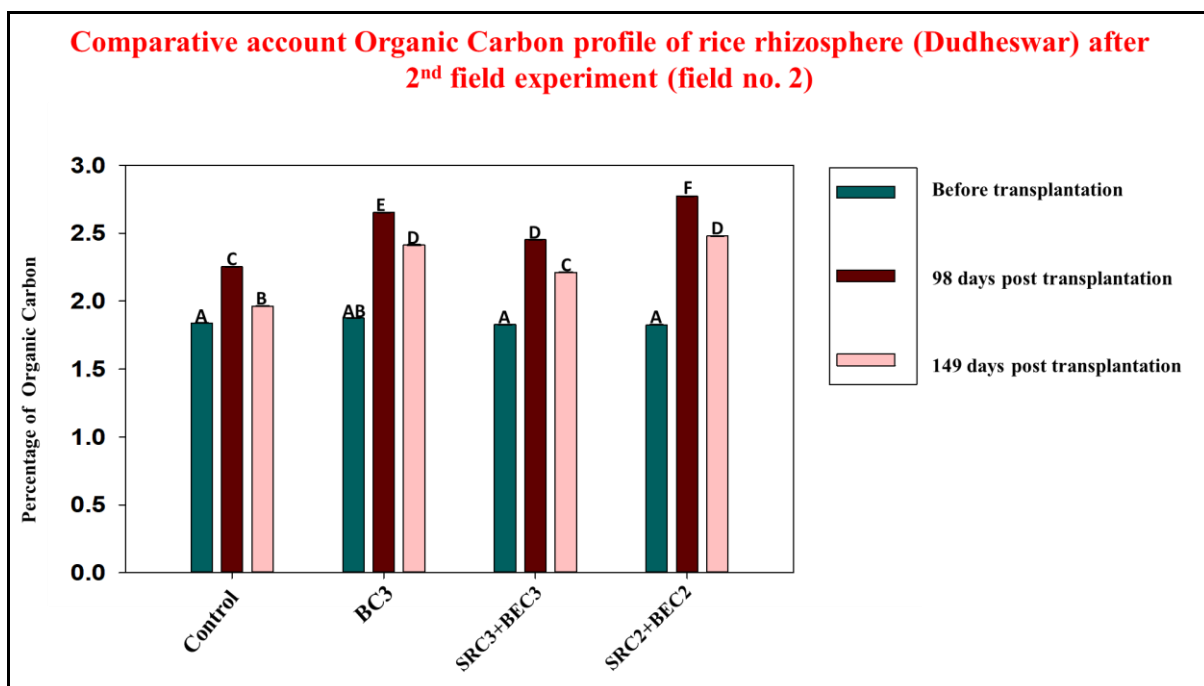


Figure 9.39: The above figure depicts the soil organic carbon studied from the control (without bacteria) and different consortia (prepared by mixing endophytic and rhizospheric bacterial strains) added rhizospheric soil for rice varieties Dudheswar. Data were plotted as mean \pm standard error (n=3) after 2nd field experiment (field number 2) in the graph.

Observations:

The organic carbon content increased for consortia added plots and control (without bacteria) plots as compared to that before transplantation in the 2nd field (field no. 2) experiment. Organic carbon content was found to be the highest at 98 days post-transplantation with slight decline at 149 days post-transplantation.

9.4.i. Analysis of soil nitrate-nitrogen during the experimental period:

Calibration curve of nitrate-nitrogen followed was depicted in the figure 7.8.

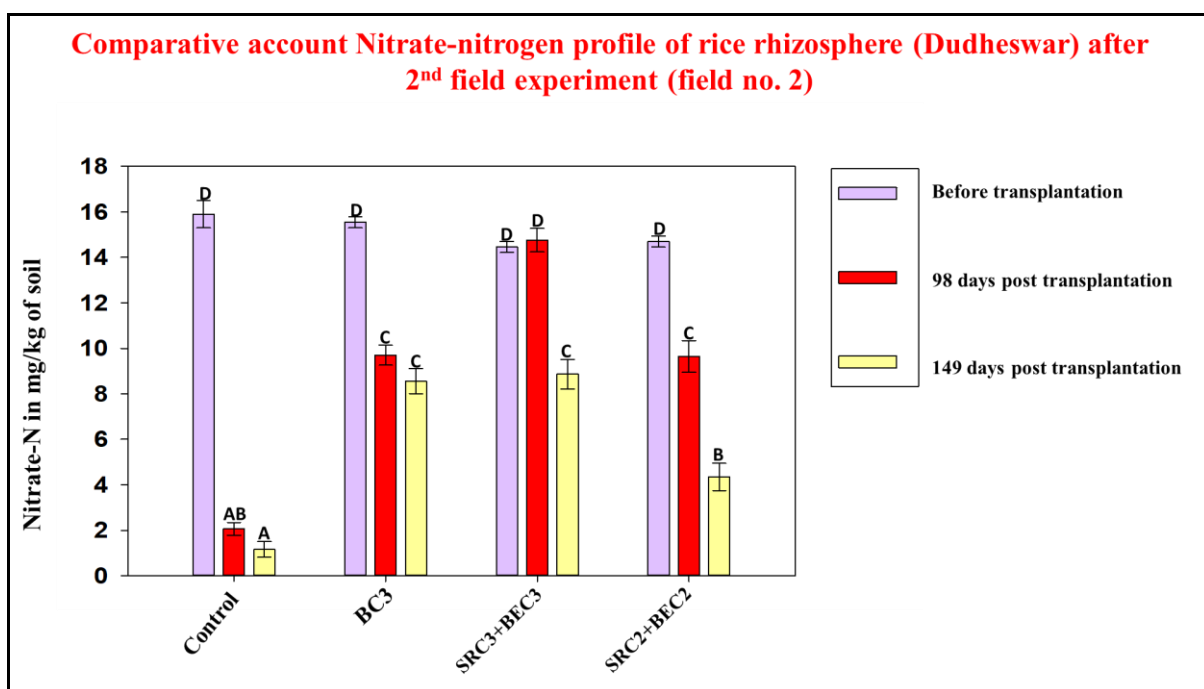


Figure 9.40: The above figure depicts the soil nitrate-nitrogen studied from control (without bacteria) and different consortia (prepared by mixing endophytic and rhizospheric bacterial strains) added rhizospheric soil for rice varieties Dudheswar. Data were plotted as mean \pm standard error (n=3) after the 2nd field experiment (field no. 2) in the graph.

Observations:

The nitrate-nitrogen content gradually decreased significantly for consortia added plots and control (without bacteria) also as compared to that of before transplantation in the 2nd field (field no. 2) experiment. However, this decline was found to be the highest for the control plot soil where no bacterial consortia was added. In all other consortia added soil, replenishment of nitrate-nitrogen must have occurred via the microbial processes of the added consortia, while consumption of nitrate-N by rice plants continued. Interestingly, SRC3+BEC3 consortia added plots demonstrated decline in nitrate-nitrogen only at 149 days post-transplantation.

9.4.j. Analysis of soil ammonia-nitrogen during the experimental period:

Calibration curve of ammonia-nitrogen followed was described in the figure 7.10.

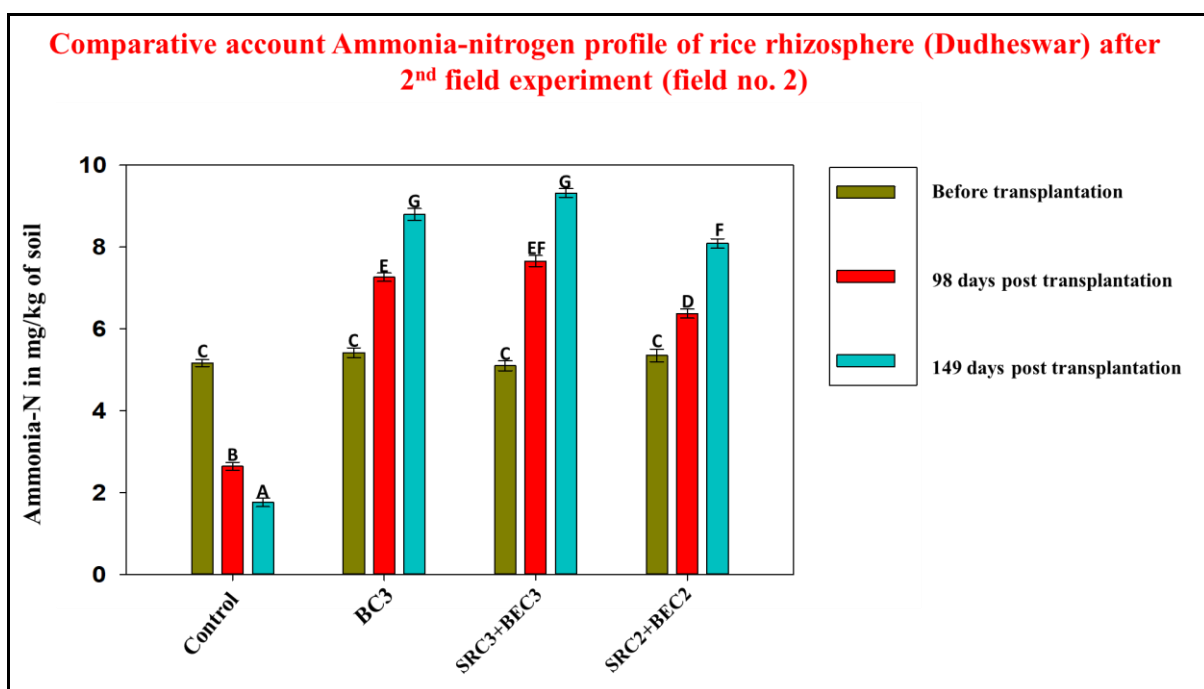


Figure 9.41: The above figure depicts the soil ammonia-nitrogen studied from control (without bacteria) and different consortia (prepared by mixing endophytic and rhizospheric bacterial strains) added rhizospheric soil for rice varieties Dudheswar. Data were plotted as mean \pm standard error (n=3) after the 2nd field experiment (field no. 2) in the graph.

Observations:

The ammonia-nitrogen content increased significantly over the 149 days pot-transplantation period for all consortia-added plots only as compared to before transplantation in the 2nd field (field no. 2) experiment, demonstrating higher rate of accumulation of ammonia-N in soil in compared to its consumption rate by the rice plants. This efficient replenishment of ammonia-N was made possible in the consortia-added plot soil because of the efficient free N₂-fixing bacterial members present in the added consortia. In contrast, in the control plots the ammonia-nitrogen content gradually decreased significantly as observed till 149 days post-transplantation.

9.4.k. Analysis of plant-available phosphorus in soil during the experimental period:

Calibration curve of plant-available phosphorus followed was depicted in the figure 7.12.

P-solubilization profile at rhizospheres of experimental plots as indicator/metric of growth promotion/enrichment of consortia

Taking P-solubilization profile at rhizospheres of experimental plots as indicator/metric of growth promotion/enrichment of consortia, in 2nd field experiment (field number 1), data were recorded at 38 days, 66 days, 98 days and 149 days post-transplantation of rice rhizosphere (Dudheswar). The data were represented in the following figure:

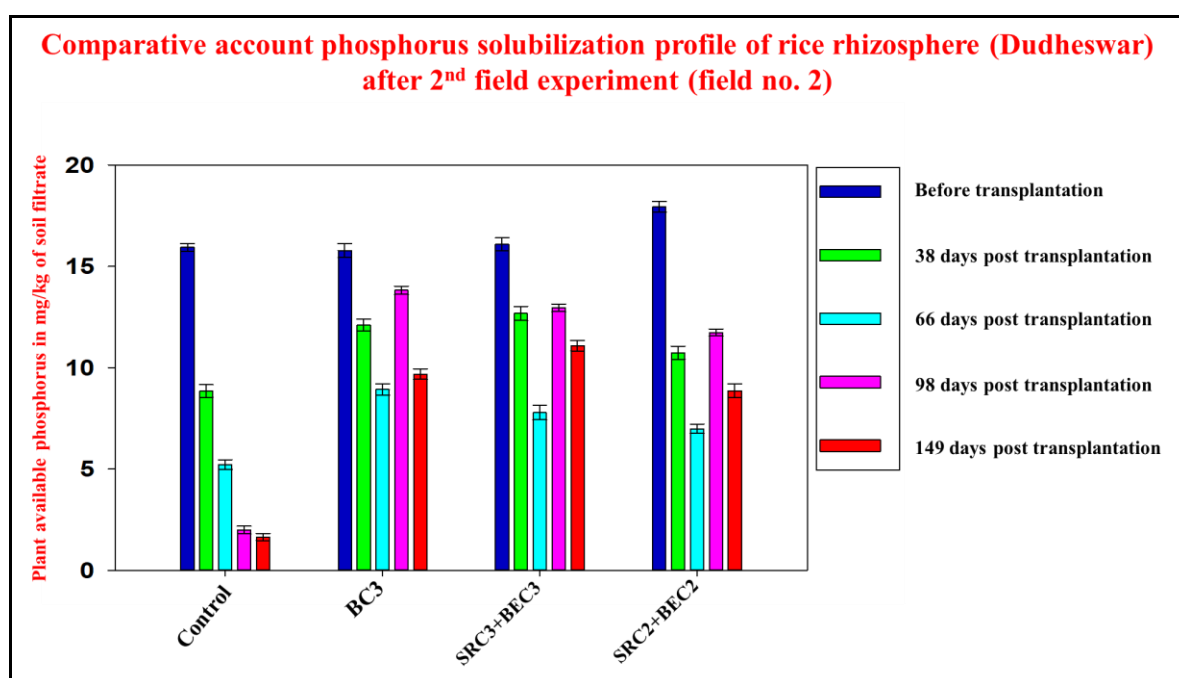


Figure 9.42: The above figure depicts the comparison study of plant-available phosphorus from control (without bacteria), and different consortia (prepared by mixing endophytic and rhizospheric bacterial strains) added rhizospheric soil, up to 149 days post-transplantation at a specific time interval in the 2nd field experiment (field no. 2) for **Dudheswar** cultivar of rice. Data were plotted as mean \pm standard error (n=3) in the graph.

Observations:

- In almost all consortia-added rhizospheres, the lowest level of soluble plant-available phosphorus (P) is found to be at **66** days post-transplantation after which it gradually increased as observed at **98 days** and **149 days** post-transplantation rhizosphere soils. This increase in soluble plant-available phosphorus (P) can be attributed to the enrichment of PGP consortia at rice rhizosphere which have many a constituent member as high P-solubilizer.
- In contrast, control (no bacteria added) rice rhizospheres, showed no significant increase in level of soluble plant available phosphorus (P) even after 66 days post-transplantation.
- Many of the consortia added rhizospheres of experimental rice plants showed presence of higher level of soluble plant available phosphorus (P) as compared to control (no bacteria added) rice rhizospheres even on **66** days post-transplantation, when the rice plants showed maximum utilization of soil-P.
- P-solubilization seems to be a promising growth promotion potential of the selected/added consortia (most members in each consortium were high P-solubilizers as observed earlier in laboratory experiments).
- **Significant increase in solubilized-P was observed in consortia added rhizospheres as compared to control (no bacterial addition) rhizospheric soils even after 98 days post-transplantation in all the above represented figures. Earlier, we observed that in our greenhouse pot experiment solubilized-P content increased even after 89 days of post-transplantation when the same stopped at control pot soils without any bacterial consortia added and NPK-added pot soils. Identical trends in P-solubilization could be observed in our rice field experiments also.**

9.5. Data collected from neighbouring rice fields of Sundarban cultivated with conventional fertilizers after harvest:

9.5.a. Starch content analysis in harvested grains:

Calibration curve of starch followed was described in the figure 9.7.

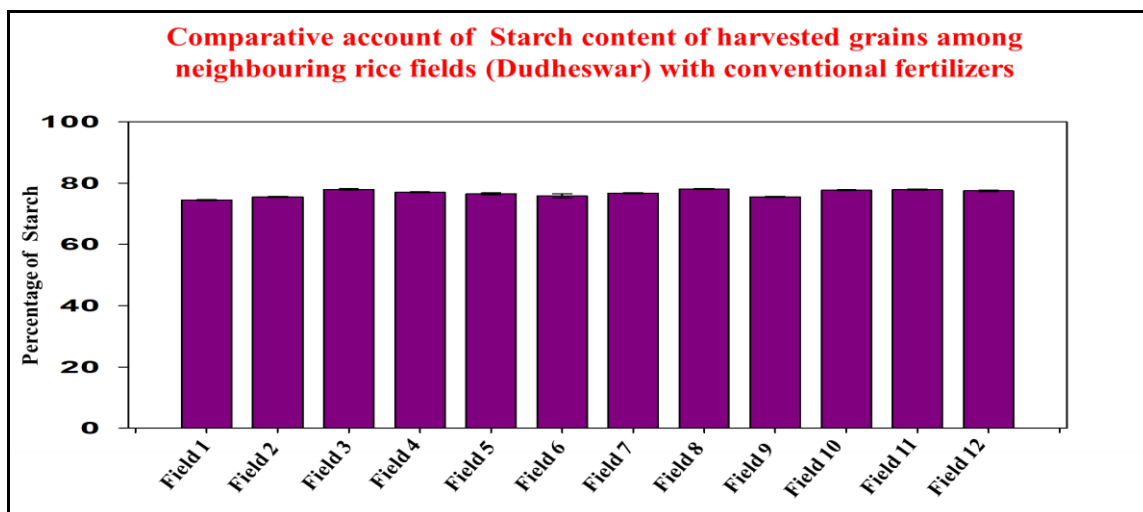


Figure 9.43: The percentage of starch (ranges 74.52-78.11% percent) observed was overall the same for the harvested grains 12 different neighbouring rice fields at Sundarbans cultivated with conventional fertilizers. Data were plotted as mean \pm standard error in the graph.

9.5.b. Protein content analysis in harvested grains:

Calibration curve of protein followed was described in the figure 9.9.

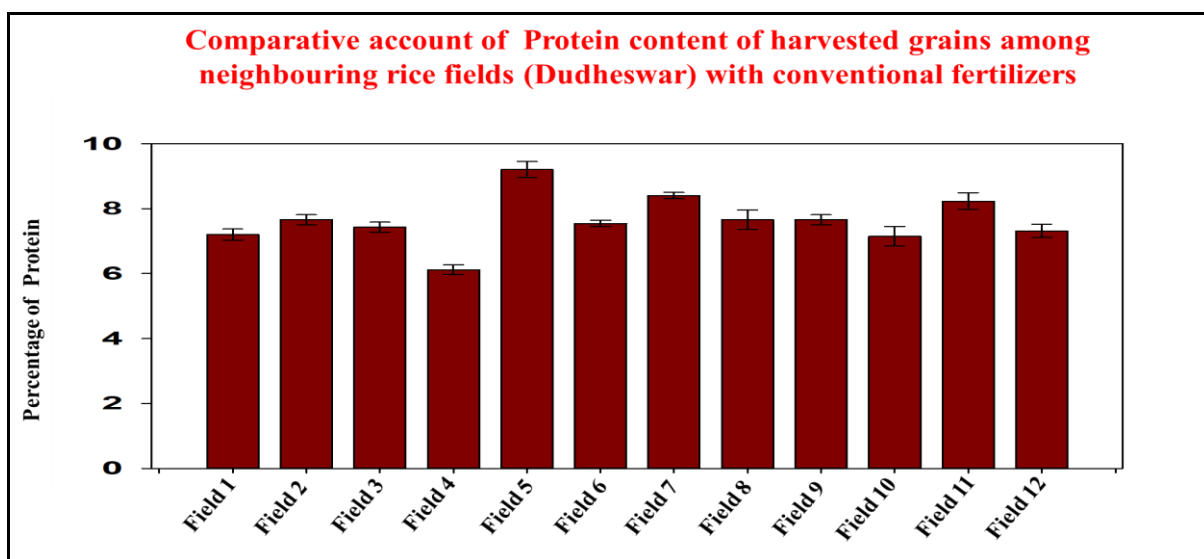


Figure 9.44: The percentage of protein (ranges 6.12- 8.4%) observed was more or less the same in harvested grains for 12 different neighbouring rice fields at Sundarbans cultivated with conventional fertilizers. Data were plotted as mean \pm standard error in the graph.

9.5.c. Analysis of soil pH in neighboring rice fields:

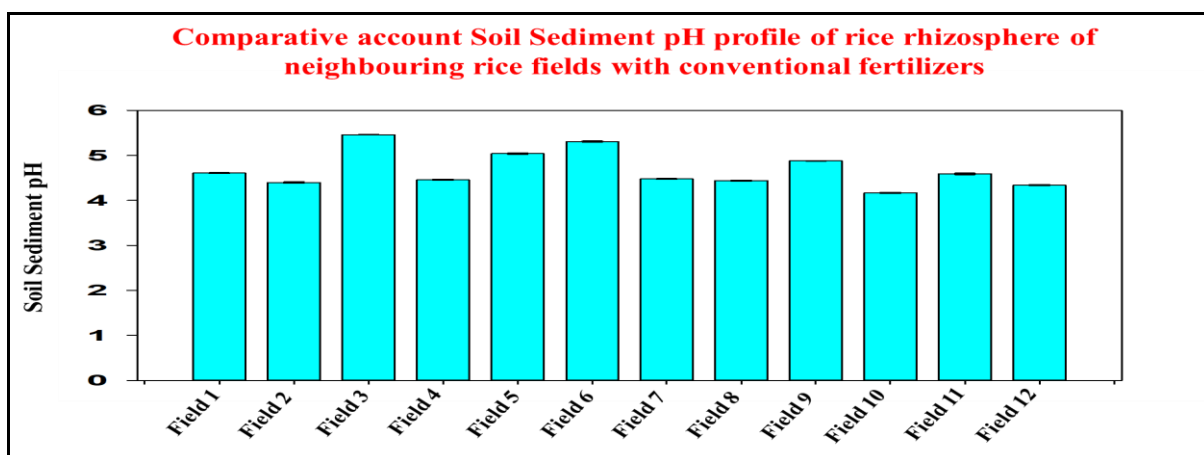


Figure 9.45: The soil pH varied (4.17-5.46) for 12 different neighbouring rice fields at Sundarbans cultivated with conventional fertilizers. **The pH was found to be more acidic as compared to the experimental rice fields described earlier at Sundarbans.** Data were plotted as mean \pm standard error in the graph.

9.5.d. Analysis of soil electrical conductivity (EC):

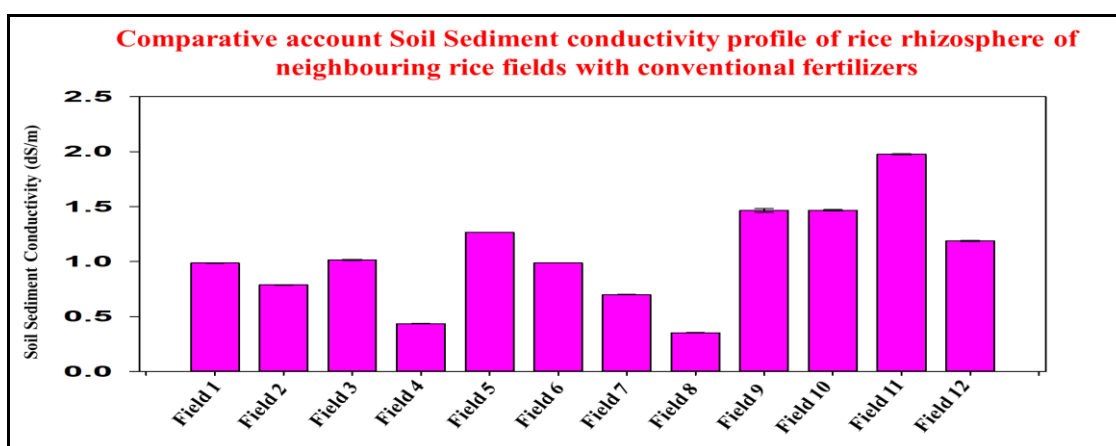


Figure 9.46: The soil conductivity varied (0.353-1.976 ds/m) for 12 different neighbouring rice fields at Sundarbans cultivated with conventional fertilizers. **The salinity of these neighbouring rice fields was observed to be much lower in comparison to our experimental rice field soil at Sundarbans.** Data were plotted as mean \pm standard error in the graph.

9.5.e. Analysis of soil organic carbon (SOC):

Calibration curve of organic carbon followed was described in the figure 7.6.

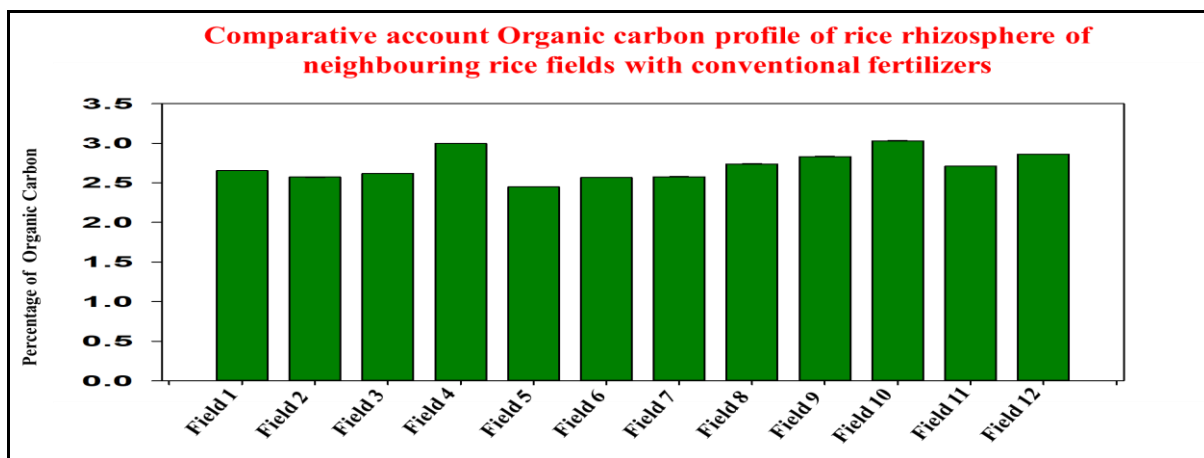


Figure 9.47: The percentage of organic carbon (ranges 2.45- 3.03%) observed across 12 different neighbouring rice fields at Sundarbans cultivated with conventional fertilizers. **The observed SOC is almost comparable with that of our experimental fields at Sundarbans.** Data were plotted as mean \pm standard error in the graph.

9.5.f. Analysis of soil nitrate-nitrogen in neighbouring rice fields at Sundarbans:

Calibration curve of nitrate-nitrogen followed was described in the figure 7.8.

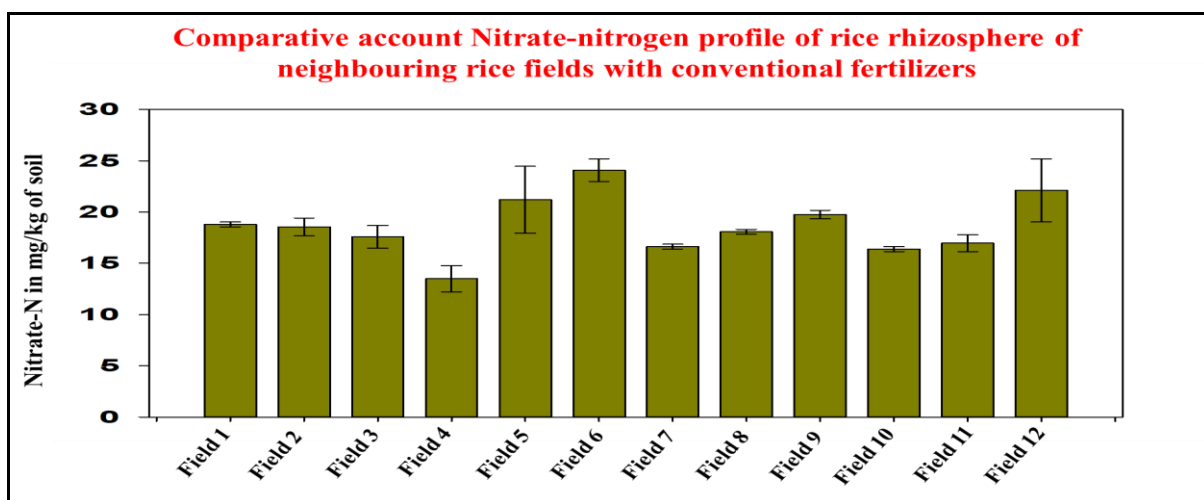


Figure 9.48: The nitrate-nitrogen content (ranges 13.50- 24.09 mg/kg of soil) varied for 12 different neighbouring rice fields at Sundarbans cultivated with conventional fertilizers. **The observed nitrate-N content of these fields was found to be much higher than that observed in the experimental rice fields at Sundarbans, most probably due to over-use of synthetic chemical fertilizers, even when the crop was harvested. This remaining high nitrates will be eventually washed off as agricultural run-off and will eventually pollute the hinterland aquatic bodies.** Data were plotted as mean \pm standard error in the graph.

9.5.g. Analysis of soil ammonia-nitrogen in the neighbouring rice fields at Sundarbans:

Calibration curve of ammonia-nitrogen followed was depicted in the figure 7.10.

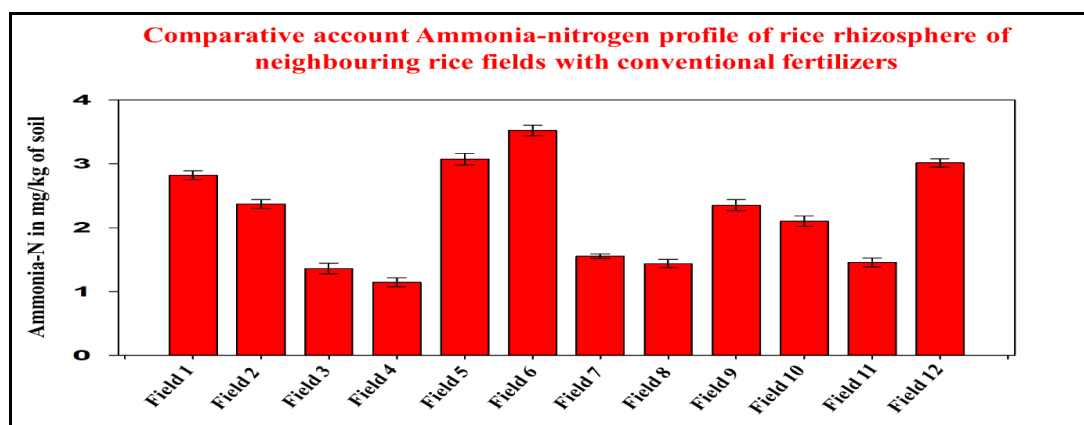


Figure 9.49: The ammonia-nitrogen content (ranges 1.14- 3.52 mg/kg of soil) varied for 12 different neighbouring rice fields at Sundarbans cultivated with conventional fertilizers. **Surprisingly, the observed ammonia-N content of these fields after crop harvest was found to be much lower in comparison to the experimental rice fields at Sundarbans, even after excessive use of synthetic chemical fertilizers.** Data were plotted as mean \pm standard error in the graph.

9.5.h. Analysis of plant-available phosphorus from the neighbouring rice fields at Sundarbans:

Calibration curve of plant-available phosphorus followed was depicted in the figure 7.12.

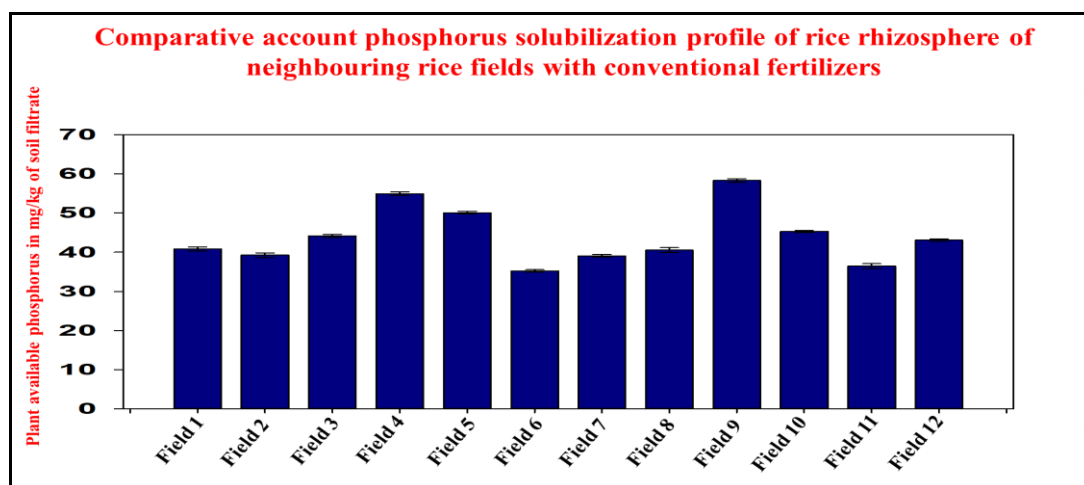


Figure 9.50: The solubilized-P content (ranges 35.25- 58.30 mg/kg of soil) varied for 12 different neighbouring rice fields at Sundarbans cultivated with conventional fertilizers. **The observed solubilized-P content of these fields was found to be much higher than that observed in the experimental rice fields at Sundarbans, most probably due to over-use of synthetic chemical fertilizers, even when the crop was harvested. This residual high phosphates will be eventually washed off as agricultural run-off and will eventually pollute the hinterland aquatic bodies.** Data were plotted as mean \pm standard error in the graph.

Objective 8

10. Observation of bacterial community abundances by Next Generation Sequencing (NGS) from rice fields before and after rice cultivation with PGP endophytic bacterial consortia.

1. Soil samples were collected from rhizospheres of rice field from control (no bacterial culture added) and for each root endophytic consortium added plots from the 1st field experiment and DNA was isolated from these soil samples and sent for amplicon based 16S abundance metagenome sequencing by next generation sequencing.
2. Results of the NGS metagenome data were submitted to NCBI
3. Analyses of these sequencing data is utilized here to validate the enrichment of selective bacterial biome at the rhizosphere site of application and to correlate the growth parameters and yield data obtained as a result of PGP attributes of selected and applied bacterial consortia.

Table 26: The details of the accessioned NGS data are enlisted in the following table:

Bioproject Accession no.	Name of the Bioproject	Biosample accessions	Name of the Biosamples	SRA (Sequence Read Archive) accessions
PRJNA824796	Sundarban cultivated rice rhizosphere microbiome	SAMN27478637	Sundarban cultivated rice rhizosphere 01	SRR18726894
		SAMN30789297	Sundarban cultivated rice rhizosphere 02	SRR21541564
		SAMN30885898	Sundarban cultivated rice rhizosphere 03	SRR21607174
PRJNA878939	Experimental plot cultivated rice rhizosphere soil microbiome from Sundarbans	SAMN30762289	Experimental plot cultivated rice rhizosphere root endophyte BC1 added soil microbiome from Sundarbans	SRR21519017
		SAMN30789041	Experimental plot cultivated rice rhizosphere root endophyte	SRR21520002

Bioproject Accession no.	Name of the Bioproject	Biosample accessions	Name of the Biosamples	SRA (Sequence Read Archive) accessions
			BC2 added soil microbiome from Sundarbans	
		SAMN30789042	Experimental plot cultivated rice rhizosphere root endophyte BC3 added soil microbiome from Sundarbans	SRR21523264
		SAMN30789144	Experimental plot cultivated rice rhizosphere root endophyte BC1, BC2, BC3 added soil microbiome from Sundarbans	SRR21527972
		SAMN30789227	Experimental cultivated rice-rhizosphere microbiome enriched with root-endophytic & halo-grass rhizobacteria from Sundarbans	SRR21541159

The root endophytic consortia added to the rice field in first field experiment comprised of these 7 genera viz. *Aeromonas*, *Mangrovibacter*, *Pseudomonas*, *Bacillus*, *Serratia*, *Pseudocitrobacter*, *Enterobacter* spp. The enrichment of these members at rice rhizosphere was attempted to be validated by the relative abundances of respective phyla, class, family and genus in the analysed NGS data in the following way below:

10.a. Comparative account of relative abundances at phylum level:

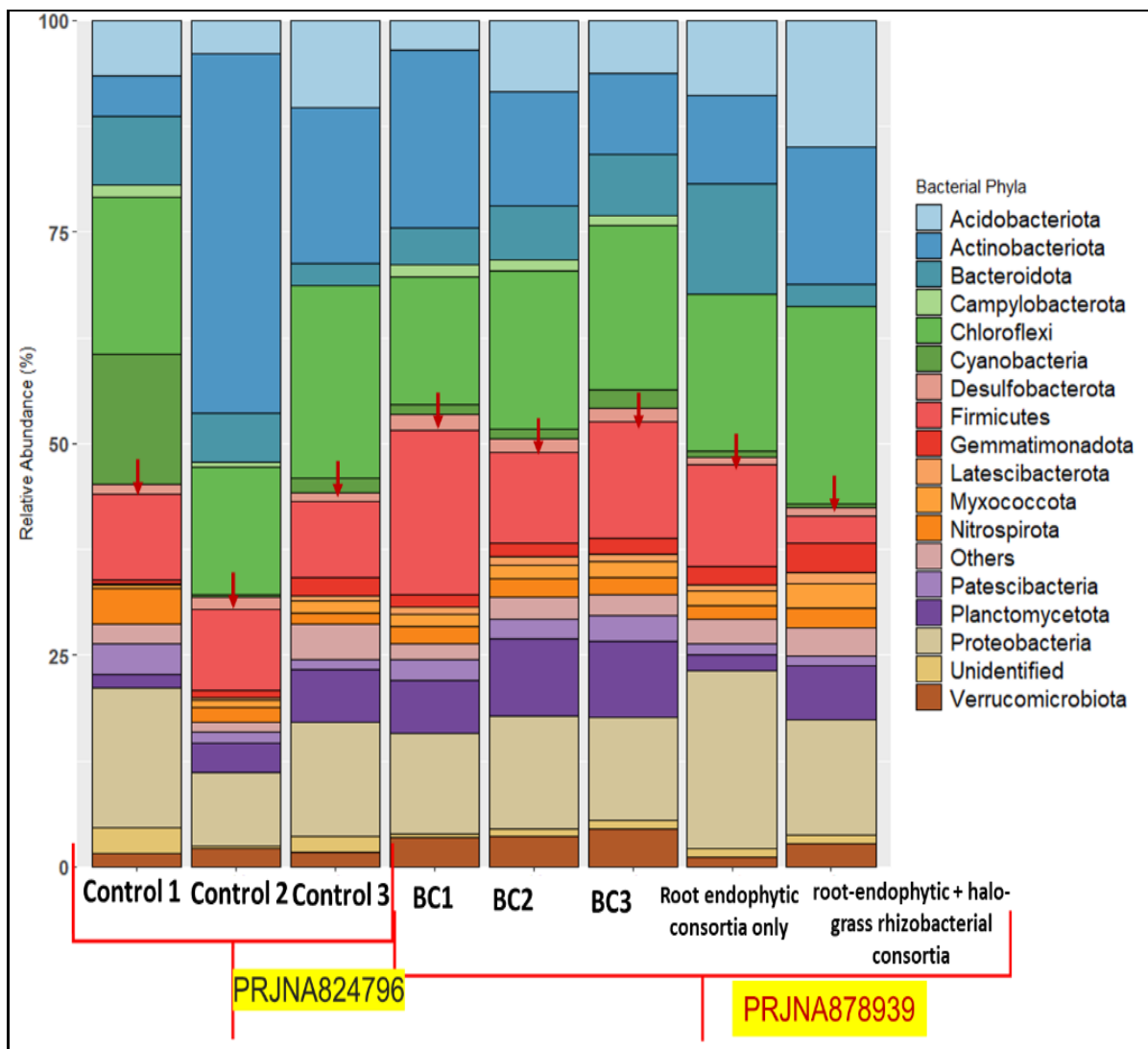


Figure 10.1: Comparative account of relative abundances at phylum level

Comparative account of relative abundances at phylum level shows enrichment of **Firmicutes** at **BC1, BC2, BC3** consortia added soil as well as when **all root endophyte consortia** added soil was sampled in a **mixed** way. Abundance of Firmicutes is denoted with **red down-arrows**. The constituent genus of root endophyte consortia *Bacillus* spp. belongs to the phylum Firmicutes.

10.b. Comparative account of relative abundances at class level:

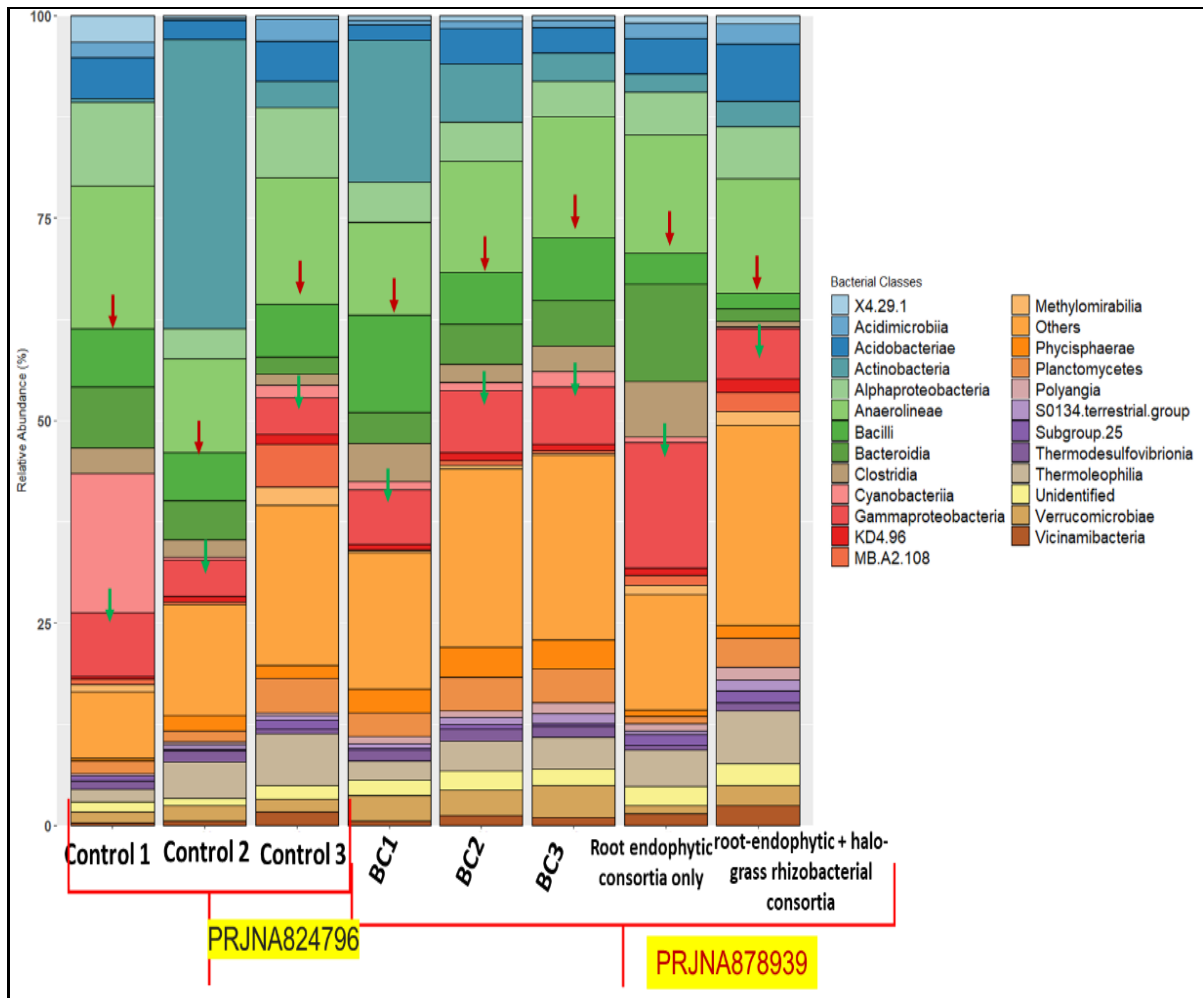


Figure 10.2: Comparative account of relative abundances at class level

Comparative account of relative abundances at class level shows enrichment of **Bacilli** (denoted with red down-arrows) at BC1, BC2, BC3 consortia added soil as well as enrichment of **Gammaproteobacteria** (denoted with green down-arrows) at BC1, BC2, BC3 consortia added soil and when all root endophyte consortia added soil was sampled in a mixed way. The constituent genus of root endophyte consortia *Bacillus* spp. belongs to the class Bacilli, whereas *Aeromonas*, *Mangrovibacter*, *Pseudomonas*, *Serratia*, *Pseudocitrobacter*, *Enterobacter* spp. all belong to the class Gammaproteobacteria

10.c. Comparative account of relative abundances at family level:

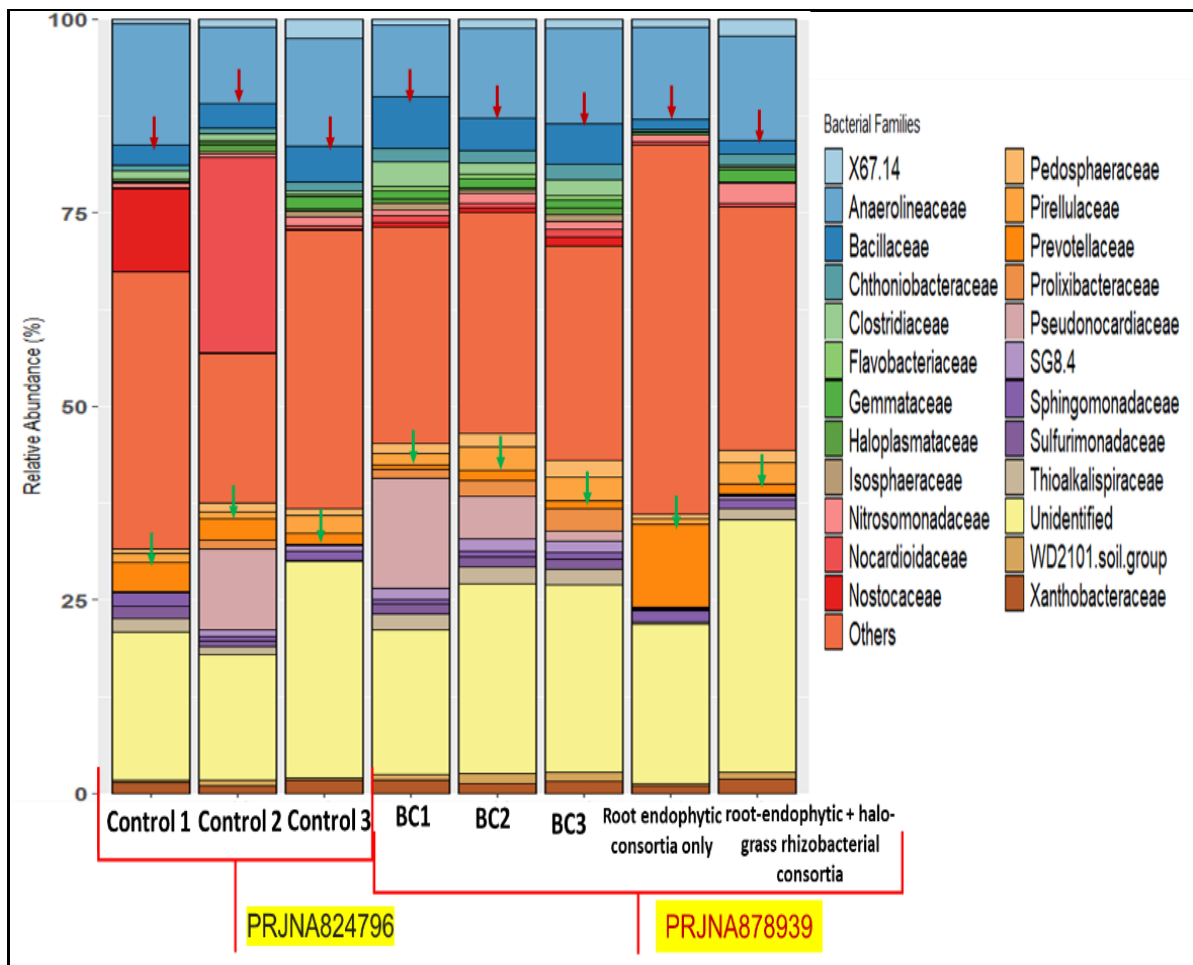


Figure 10.3: Comparative account of relative abundances at family level

Comparative account of relative abundances at family level shows enrichment of **Bacillaceae** (denoted with red down-arrows) at **BC1**, **BC2**, **BC3** consortia-added soil. The family **Prevotellaceae** possesses the genus *Prevotella_9* and *Prevotella* which are signature sequences of soil manured with cow-dung as *Prevotella_9*/ *Prevotella* has been reported to be present in gut microbiome of these animals. Relative abundance of **Prevotellaceae** (denoted with green down-arrows) was observed to be high in control rhizosphere as compared to **BC1**, **BC2**, **BC3** consortia added soil. However, the referred abundance is observed to be very high when **all root endophyte consortia added soil** was sampled in a mixed way (might be due to sampling error).

10.d. Comparative account of relative abundances at genus level:

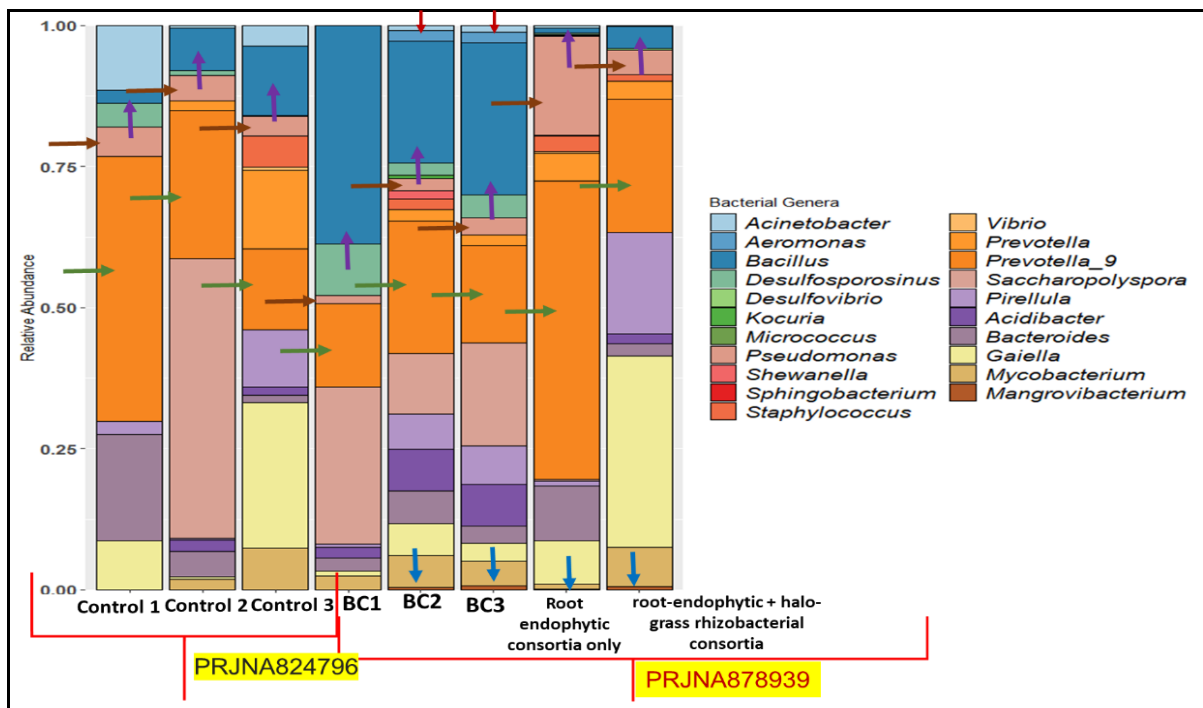


Figure 10.4: Comparative account of relative abundances at genus level

Comparative account of relative abundances at genus level shows the following features:

- Abundance enrichment of *Aeromonas* (denoted with red down-arrows) at BC2, BC3 consortia-added soil
- Noticeable abundance enrichment of *Bacillus* (denoted with violet up-arrows) at BC1, BC2, BC3 consortia added soil
- Consistent relative abundance of *Pseudomonas* (denoted with chocolate-brown side-arrows) observed in all the samples with highest abundance observed when all root endophyte consortia added soil was sampled in a mixed way
- Decrease in abundance of *Prevotella_9* (denoted with green side-arrows) at BC1, BC2, BC3 consortia added soil. However, the referred abundance is observed to be very high when all root endophyte consortia added soil was sampled in a mixed way (might be a cause of sampling error).
- Noticeable abundance of *Mangrovibacterium* (denoted with blue down-arrows) at BC2, BC3 consortia added soil, all root endophyte consortia added soil as well as all halo-grass rhizosphere bacterial consortia added soil.
- The constituent genera of root endophyte consortia are *Aeromonas* spp., *Bacillus* spp. *Pseudomonas* spp., *Mangrovibacter* spp.

IV. Conclusion

Conclusion:

From this study it can be concluded that the mangrove trees share out a greater proportion of net primary production for their root growth as compared to other terrestrial tree communities. The mangrove trees possess higher below-ground biomass as compared to above-ground biomass for their environmental and waterlogged conditions. They maintain this extensive root network for their survival, growth, and development. The root growth and development of mangroves depends upon essential nutrients which can be provided by both rhizospheric and endophytic bacteria. The term 'rhizophagy cycle' is one of the nutrient acquisition processes where endophytic bacteria expend a part of life within plant root and rest part of their life expend as free-living microorganism in the soil. In this cycle, soil microorganisms used by the plants to achieve nutrients in soils, attract them to return to the plant by various process like root exudates secretion, internalize the microorganisms, oxidatively extract nutrients from them and next throw out them back into soil from tips of root hairs to achieve extra nutrients. Root endophytic bacteria makes a symbiotic relationship with plants and provides them with water, nutrients, protection from herbivory and systemic resistance with various abiotic and biotic stress factors. It is also established that nutrients solubilization and transformation occurs by endophytes including phosphorous, nitrogen, potassium and other micro elements in their easily obtainable forms to the plants. It also was shown that root endophytes increase the elemental formation especially phosphorous and nitrogen in roots of root endophyte-inoculated plants.

In this study I have selected various mangrove species from degraded and non-degraded mangrove ecosystems and collected their root and pneumatophore samples from Indian Sundarbans. I have been successful in the establishment of 78 pure isolates of cultivable endophytic bacteria (NCBI Accession no. MT421976 to MT422053). The root endophytic bacterial growth was observed on different nutrient cycling media viz. for sulfur oxidation, cellulose degradation, free nitrogen fixation, phosphorous solubilization, iron oxidation.

Plant growth promotion profiling was carried out on the basis of IAA production (Indole -3-acetic acid), siderophore production, phosphate solubilization, free nitrogen fixation (**acetylene reduction assay for demonstration of nitrogenase activity *in vitro* for free nitrogen fixer endophytes**), assay of 1-aminocyclopropane-1- carboxylate deaminase (ACC) synthesis. Many bacteria were found to be good IAA producer such as *Pseudomonas sp.*, *Aeromonas sp.*, *Staphylococcus sp.* and *Bacillus sp.* and their range of IAA production was between 9-17

µg/ml. Some were found to be good phosphate solubilizer such as *Pseudomonas* sp., *Aeromonas* sp., *Staphylococcus* sp., *Gallacimonas* sp., *Vibrio* sp., and *Serratia* sp. and their range of P-solubilization existed between 90-160 µg of plant-available P released/ml of PSM. The best siderophore producing strains are *Pseudomonas* sp., *Aeromonas* sp., *Staphylococcus* sp., *Bacillus* sp., *Mangrovibacter* sp., and *Citrobacter* sp. and their siderophore productivity ranged between 80%-95% in iron-free media.

The best ACC deaminase producing strains are *Pseudomonas* sp., *Aeromonas* sp., *Staphylococcus* sp., *Bacillus* sp. and *Citrobacter* sp. and their range of ACC deaminase production units ranged between 1.8-9 units.

The best free nitrogen-fixing strains established are *Pseudomonas* sp., *Aeromonas* sp., *Staphylococcus* sp., *Bacillus* sp., *Pseudocitrobacter* sp. and *Citrobacter* sp. and their reduced ethylene synthesis spanned in the range of 0.4-14 nmole/100 µl/24 hour.

The best PGP endophytic bacteria were selected for formulation of PGP consortia on the basis of their growth promotion criteria and growth curves. Then these consortia were applied on nursery/greenhouse/field applications. From these experiments we observed a significant improvement in growth and yield parameters of the experimental plants. From greenhouse the growth modulations of rice are much better on consortia applied pots as compared to the control pots. In case of field application of these consortia on the rice field of Dudheswar landrace (IC No. 593998), the yield modulation was much improved on consortia applied plants as compared to the control plots from 1st and 2nd successful rice field applications. The application of those same consortia on the *Avicennia officinalis* saplings in mangrove nursery in Indian Sundarbans was also carried out. The observed increase of shoot height in saplings after bacterial application was significant as compared to the control (without bacteria).

This observed growth and yield improvement of the plant species on which these PGP endophytic consortia were applied was validated when bacterial community abundances were examined through Next Generation Sequencing (NGS) from rice field before and after rice cultivation with PGP endophytic bacterial consortia. The bacterial community abundances demonstrated the enrichment of the consortial members at the rhizosphere soil after rice cultivation with PGP endophytic bacterial consortia and therefore the growth and yield improvement of the experimental plant species could be successfully correlated with the applicability of these plant growth promoting root endophytic bacterial consortia established from roots and pneumatophores of mangrove and mangrove associate species of Indian Sundarbans.

References

References

- Ahemad, M., & Kibret, M. (2014). Mechanisms and applications of plant growth promoting rhizobacteria: current perspective. *Journal of King saud University-science*, 26(1), 1-20. doi: 10.1016/j.jksus.2013.05.001
- Ali, S. Z., Sandhya, V., & Venkateswar Rao, L. (2014). Isolation and characterization of drought-tolerant ACC deaminase and exopolysaccharide-producing fluorescent *Pseudomonas* sp. *Annals of microbiology*, 64, 493-502. doi: 10.1007/s13213-013-0680-3
- ALKahtani, M. D., Fouda, A., Attia, K. A., Al-Otaibi, F., Eid, A. M., Ewais, E. E. D., ... & Abdelaal, K. A. (2020). Isolation and characterization of plant growth promoting endophytic bacteria from desert plants and their application as bioinoculants for sustainable agriculture. *Agronomy*, 10(9), 1325. doi: 10.3390/agronomy10091325
- Alongi, D. M., Christoffersen, P., & Tirendi, F. (1993). The influence of forest type on microbial-nutrient relationships in tropical mangrove sediments. *Journal of experimental marine Biology and Ecology*, 171(2), 201-223. doi: 10.1016/0022-0981(93)90004-8
- Anand, R., & Chanway, C. (2013). N₂-fixation and growth promotion in cedar colonized by an endophytic strain of *Paenibacillus polymyxa*. *Biology and Fertility of Soils*, 49, 235-239. doi: 10.1007/s000374-012-0735-9
- Andrews, M. Y., & Duckworth, O. (2016). A universal assay for the detection of siderophore activity in natural waters. *Biometals*, 29, 1085-1095. doi: 10.1007/s10534-016-9979-4
- Bhattacharyya, P. N., & Jha, D. K. (2012). Plant growth-promoting rhizobacteria (PGPR): emergence in agriculture. *World Journal of Microbiology and Biotechnology*, 28, 1327-1350. doi: 10.1007/s11274-011-0979-9
- Bent, E., & Chanway, C. P. (1998). The growth-promoting effects of a bacterial endophyte on lodgepole pine are partially inhibited by the presence of other rhizobacteria. *Canadian Journal of Microbiology*, 44(10), 980-988. doi: 10.1139/cjm-44-10-980
- Berg, G., Krechel, A., Ditz, M., Sikora, R. A., Ulrich, A., & Hallmann, J. (2005). Endophytic and ectophytic potato-associated bacterial communities differ in structure and antagonistic function against plant pathogenic fungi. *FEMS Microbiology Ecology*, 51(2), 215-229. doi: 10.1016/j.femsec.2004.08.006
- Biswas, S., Saber, M. A., Tripty, I. A., Karim, M. A., Islam, M. A., Hasan, M. S., ... & Hasan, M. N. (2020). Molecular characterization of cellulolytic (endo-and exoglucanase) bacteria from the largest mangrove forest (Sundarbans), Bangladesh. *Annals of microbiology*, 70, 1-11. doi: 10.1186/s13213-020-01606-4
- Biswas, S., Zaman, S., & Mitra, A. (2017). Soil Characteristics of Indian Sundarbans: The Designated World Heritage site. *Sci J Biomed Eng Biomed Sci*, 1(2), 053-059.
- Boddey, R. M., De Oliveira, O. C., Urquiaga, S., Reis, V. M., De Olivares, F. L., Baldani, V. L. D., & Döbereiner, J. (1995). Biological nitrogen fixation associated with sugar cane and rice: contributions and prospects for improvement. In *Management of Biological Nitrogen Fixation for the Development of More Productive and Sustainable Agricultural Systems: Extended versions of papers presented at the Symposium on Biological Nitrogen Fixation for Sustainable Agriculture at the 15th Congress of Soil Science, Acapulco, Mexico, 1994* (pp. 195-209). Springer Netherlands. doi: 10.1007/BF00032247
- Boruah, J. (2020). Effect of 0.1% HgCl₂ on surface sterilization of som (*Persea bombycina* King) explant during tissue culture-a major host plant of muga silkworm. *Int J Curr Microbiol App Sci*, 9, 954-958. doi: 10.20546/ijcmas.2020.907.111

- Brooks, R. A., & Bell, S. S. (2005). A multivariate study of mangrove morphology (Rhizophora mangle) using both above and below-water plant architecture. *Estuarine, Coastal and Shelf Science*, 65(3). doi: 10.1016/j.ecss.2005.06.019
- Burd, G. I., Dixon, D. G., & Glick, B. R. (1998). A plant growth-promoting bacterium that decreases nickel toxicity in seedlings. *Applied and Environmental Microbiology*, 64(10), 3663-3668. doi: 10.1128/AEM.64.10.3663-3668.1998.
- Calvo-Polanco, M., Ribeyre, Z., Dauzat, M., Reyt, G., Hidalgo-Shrestha, C., Diehl, P., ... & Boursiac, Y. (2021). Physiological roles of Casparian strips and suberin in the transport of water and solutes. *New Phytologist*, 232(6), 2295-2307. doi: 10.1111/nph.17765
- Canene-Adams, K. (2013). Preparation of formalin-fixed paraffin-embedded tissue for immunohistochemistry. In *Methods in enzymology* (Vol. 533, pp. 225-233). Academic Press. doi: 10.1016/B978-0-12-420067-8.00015-5.
- Chanway, C. (1996). Endophytes: they're not just fungi! CP Chanway. *Can. J. Bot*, 74(3), 321-322. doi: 10.1139/b96-040
- Chen, T., Cai, X., Wu, X., Karahara, I., Schreiber, L., & Lin, J. (2011). Casparian strip development and its potential function in salt tolerance. *Plant signaling & behavior*, 6(10), 1499-1502. doi: 10.4161/psb.6.10.17054
- Conrath, U., Beckers, G. J., Flors, V., García-Agustín, P., Jakab, G., Mauch, F., ... & Mauch-Mani, B. (2006). Priming: getting ready for battle. *Molecular plant-microbe interactions*, 19(10), 1062-1071. doi: 10.1094/MPMI-19-1062
- Datta, N. P., Khera, M. S., & Saini, T. R. (1962). A rapid colorimetric procedure for the determination of organic carbon in soils. *Journal of the Indian Society of Soil Science*, 10(1), 67-74.
- Deivanai, S., Bindusara, A. S., Prabhakaran, G., & Bhore, S. J. (2014). Culturable bacterial endophytes isolated from Mangrove tree (Rhizophora apiculata Blume) enhance seedling growth in Rice. *Journal of natural science, biology, and medicine*, 5(2), 437. doi: 10.4103/0976-9668.136233
- Dhayanithy, G., Subban, K., & Chelliah, J. (2019). Diversity and biological activities of endophytic fungi associated with Catharanthus roseus. *BMC microbiology*, 19, 1-14. doi: 10.1186/s12866-019-1386-x
- Dheeman, S., Maheshwari, D. K., & Baliyan, N. (2017). Bacterial endophytes for ecological intensification of agriculture. *Endophytes: Biology and Biotechnology: Volume I*, 193-231. doi: 10.1007/978-3-319-66541-2_9
- Dobereiner, J., & Boddey, R. M. (1981). Nitrogen fixation in association with Gramineae.
- Dorich, R. A., & Nelson, D. W. (1983). Direct colorimetric measurement of ammonium in potassium chloride extracts of soils. *Soil Science Society of America Journal*, 47(4), 833-836. doi: 10.2136/SSSAJ1983.03615995004700040042X
- Dubois, M., Gilles, K. A., Hamilton, J. K., Rebers, P. A., & Smith, F. A. J. N. (1951). A colorimetric method for the determination of sugars. *Nature*, 168(4265), 167-167. doi: 10.1038/168167a0
- Edwards, A. C., Hooda, P. S., & Cook, Y. (2001). Determination of nitrate in water containing dissolved organic carbon by ultraviolet spectroscopy. *International Journal of Environmental Analytical Chemistry*, 80(1), 49-59. doi: 10.1080/03067310108044385
- El-Deeb, B., Bazaid, S., Gherbawy, Y., & Elhariry, H. (2012). Characterization of endophytic bacteria associated with rose plant (Rosa damascena trigintipeta) during flowering stage and their plant growth promoting traits. *Journal of plant interactions*, 7(3), 248-253. doi: 10.1080/17429145.2011.637161

- Emilio, O. (1997). Majagual: The tallest mangroves in the world. *International News Letter of Coastal Management-Intercoast Network*, 1, 1-17.
- Farooqui, A., & Joshi, Y. (2016). Low Na/K ratio in the leaves of mangroves mitigates salinity stress in estuarine ecosystem. *Tropical Plant Research*, 3(1), 78-86.
- Gartley, K. L. (2011). Recommended methods for measuring soluble salts in soils. *Recommended soil testing procedures for the northeastern United States. Northeastern Regional Publication*, 493, 1864-2.
- Ghosh, U. D., Saha, C., Maiti, M., Lahiri, S., Ghosh, S., Seal, A., & MitraGhosh, M. (2014). Root associated iron oxidizing bacteria increase phosphate nutrition and influence root to shoot partitioning of iron in tolerant plant *Typha angustifolia*. *Plant and soil*, 381, 279-295. doi: 10.1007/S11104-014-2085-X
- Glick, B. R., Cheng, Z., Czarny, J., & Duan, J. (2007). Promotion of plant growth by ACC deaminase-producing soil bacteria. *New perspectives and approaches in plant growth-promoting Rhizobacteria research*, 329-339. doi: 10.1007/s10658-007-9162-4
- Glick, B. R., Todorovic, B., Czarny, J., Cheng, Z., Duan, J., & McConkey, B. (2007). Promotion of plant growth by bacterial ACC deaminase. *Critical reviews in plant sciences*, 26(5-6), 227-242. doi: 10.1080/07352680701572966
- Gordon, S. A., & Weber, R. P. (1951). Colorimetric estimation of indoleacetic acid. *Plant physiology*, 26(1), 192.
- Gupta, P., Jain, V., Pareek, A., Kumari, P., Singh, R., Agarwal, P., & Sharma, V. (2017). Evaluation of effect of alcoholic extract of heartwood of *Pterocarpus marsupium* on in vitro antioxidant, anti-glycation, sorbitol accumulation and inhibition of aldose reductase activity. *Journal of traditional and complementary medicine*, 7(3), 307-314. doi: 10.1016/j.jtcme.2016.11.001
- Hallmann, J., Quadts-Hallmann, A., Mahaffee, W. F., & Kloepper, J. W. (1997). Bacterial endophytes in agricultural crops. *Canadian journal of microbiology*, 43(10), 895-914. doi: 10.1139/m97-131
- Hossain, M. Z., Aziz, C. B., & Saha, M. L. (2012). Relationships between soil physico-chemical properties and total viable bacterial counts in Sunderban mangrove forests, Bangladesh. *Dhaka Univ. J. Biol. Sci*, 21(2), 169-175.
- Ish-Shalom-Gordon, N., & Dubinsky, Z. (1993). Diurnal pattern of salt secretion in leaves of the black mangrove, *Avicennia marina*, on the Sinai coast of the Red Sea.
- Jain, P., & Pundir, R. K. (2017). Potential role of endophytes in sustainable agriculture-recent developments and future prospects. *Endophytes: biology and biotechnology: volume I*, 145-169. doi: 10.1007/978-3-319-66541-2_7
- Jha, Y., Subramanian, R. B., & Patel, S. (2011). Combination of endophytic and rhizospheric plant growth promoting rhizobacteria in *Oryza sativa* shows higher accumulation of osmoprotectant against saline stress. *Acta physiologiae plantarum*, 33, 797-802. doi: 10.1007/s11738-010-0604-9
- Kaneko, S., Inagaki, M., & Morishita, T. (2010). A simple method for the determination of nitrate in potassium chloride extracts from forest soils.
- Keeney D.R., & Nelson, D.W. (1987). Nitrogen--Inorganic Forms, sec. 33-3, Extraction of Exchangeable Ammonium, Nitrate, and Nitrite. In: *Methods of Soil Analysis: Part 2, Chemical and Microbiological Properties*, Page A.L. (Ed.), *Agronomy*, 9(2), 648-649.
- Kifle, M. H., & Laing, M. D. (2016). Isolation and screening of bacteria for their diazotrophic potential and their influence on growth promotion of maize seedlings in greenhouses. *Frontiers in plant science*, 6, 147315. doi: 10.3389/fpls.2015.01225

- Kim, J., & Rees, D. C. (1994). Nitrogenase and biological nitrogen fixation. *Biochemistry*, 33(2), 389-397. doi: 10.1021/bi00168a001
- Krishnamurthy, P., JYOTHI-PRAKASH, P. A., Qin, L. I. N., He, J. I. E., Lin, Q., LOH, C. S., & Kumar, P. P. (2014). Role of root hydrophobic barriers in salt exclusion of a mangrove plant *Avicennia officinalis*. *Plant, Cell & Environment*, 37(7), 1656-1671. doi: 10.1111/pce.12272
- Krishnaswamy, U., Muthusamy, M., & Perumalsamy, L. (2009). Studies on the efficiency of the removal of phosphate using bacterial consortium for the biotreatment of phosphate wastewater. *European Journal of Applied Sciences*, 1(1), 06-15.
- Kristensen, E., Bouillon, S., Dittmar, T., & Marchand, C. (2008). Organic carbon dynamics in mangrove ecosystems: a review. *Aquatic botany*, 89(2), 201-219. doi: 10.1016/j.aquabot.2007.12.005
- Kuklinsky-Sobral, J., Araújo, W. L., Mendes, R., Geraldi, I. O., Pizzirani-Kleiner, A. A., & Azevedo, J. L. (2004). Isolation and characterization of soybean-associated bacteria and their potential for plant growth promotion. *Environmental microbiology*, 6(12), 1244-1251. doi: 10.1111/j.1462-2920.2004.00658.x
- Lally, R. D., Galbally, P., Moreira, A. S., Spink, J., Ryan, D., Germaine, K. J., & Dowling, D. N. (2017). Application of endophytic *Pseudomonas fluorescens* and a bacterial consortium to *Brassica napus* can increase plant height and biomass under greenhouse and field conditions. *Frontiers in Plant Science*, 8, 299946. doi: 10.3389/fpls.2017.02193
- Liu, Y., Xu, Z., Chen, L., Xun, W., Shu, X., Chen, Y., ... & Zhang, R. (2024). Root colonization by beneficial rhizobacteria. *FEMS Microbiology Reviews*, 48(1), fuad066. doi: 10.1093/femsre/fuad066
- Machungo, C., Losenge, T., Kahangi, E., Coyne, D., Dubois, T., & Kimenju, J. W. (2009). Effect of endophytic *Fusarium oxysporum* on growth of tissue-cultured Banana plants.
- Mahansaria, R., Choudhury, J. D., & Mukherjee, J. (2015). Polymerase chain reaction-based screening method applicable universally to environmental haloarchaea and halobacteria for identifying polyhydroxyalkanoate producers among them. *Extremophiles*, 19, 1041-1054. doi: 10.1007/S00792-015-0775-9
- Maheshwari, D. K., Dheeman, S., & Agarwal, M. (2015). Phytohormone-producing PGPR for sustainable agriculture. *Bacterial metabolites in sustainable agroecosystem*, 159-182. doi: 10.1007/978-3-319-24654-3_7
- Mangalassery, S., Dayal, D., & Patel, S. (2017). Salinity characteristics of soils supporting halophyte vegetation in saline desert ecosystems in Western India.
- Marella, S. (2014). Bacterial endophytes in sustainable crop production: Applications, recent developments and challenges ahead. *Int. J. Life Sci. Res*, 2(2), 46-56.
- Mariano, R.L.R., Silveira, E.B., & Assis, S.M.P. (2004). Importance of growth promoting bacteria and biocontrol of plant disease for sustainable agriculture. *Annals of the Pernambuco Academy of Agricultural Science*, 1, 89-111.
- McIntosh, J. L. (1969). Bray and Morgan soil extractants modified for testing acid soils from different parent materials 1. *Agronomy Journal*, 61(2), 259-265.
- Miliute, I., Buzaitė, O., Baniulis, D., & Stanys, V. (2015). Bacterial endophytes in agricultural crops and their role in stress tolerance: a review. *Zemdirbyste-Agriculture* 102(4), 465-478.
- Minz, D., Ofek, M., & Hadar, Y. (2013). Plant rhizosphere microbial communities. *The prokaryotes*, 56-84. doi: 10.1007/978-3-642-30123-0_38

- Moore, E.R.B., Arnscheidt, A., Krüger, A., Strohm, C., & Mau, M. (2004). Simplified protocols for the preparation of genomic DNA from bacterial cultures. *Molecular Microbial Ecology Manual, Second Edition*, 1 (01), 3–18.
- Msimbira, L. A., & Smith, D. L. (2020). The roles of plant growth promoting microbes in enhancing plant tolerance to acidity and alkalinity stresses. *Frontiers in Sustainable Food Systems*, 4, 106. doi: 10.3389/fsufs.2020.00106
- Mukherjee, A., Bhattacharjee, P., Das, R., Pal, A., & Paul, A. K. (2017). Endophytic bacteria with plant growth promoting abilities from *Ophioglossum reticulatum* L. *AIMS microbiology*, 3(3), 596. doi: 10.3934/microbiol.2017.3.596
- Nautiyal, C.S. (1999). An efficient microbiological growth medium for screening phosphate solubilizing microorganisms. *FEMS Microbiology Letters*, 170 (1), 265-270. doi: 10.1111/J.1574-6968.1999.TB13383.X
- Sahadevan, N., Vishnupriya, S., & Mathew, J. (2016). Isolation and functional characterisation of endophytic bacterial isolates from *Curcuma longa*. *International Journal of Pharma and Bio Sciences*, 7(1), 455 – 464.
- Okello, J.A., Kairo, J.G., Dahdouh-Guebas, F., & Beeckman, H. (2020). Mangrove trees survive partial sediment burial by developing new roots and adapting their root, branch and stem anatomy. *Trees* 34, 37–49. doi: 10.1007/s00468-019-01895-6.
- Okon, Y., & Labandera-Gonzalez, C. A. (1994). Agronomic applications of Azospirillum: an evaluation of 20 years worldwide field inoculation. *Soil Biology and Biochemistry*, 26(12), 1591-1601. doi: 10.1016/0038-0717(94)90311-5
- Ola, A., Gauthier, A. R., Xiong, Y., & Lovelock, C. E. (2019). The roots of blue carbon: responses of mangrove stilt roots to variation in soil bulk density. *Biology Letters*, 15(4), 20180866. doi: 10.1098/rsbl.2018.0866
- Ong, J. E., Gong, W. K., & Wong, C. H. (2004). Allometry and partitioning of the mangrove, *Rhizophora apiculata*. *Forest Ecology and Management*, 188(1-3), 395-408. doi: 10.1016/j.foreco.2003.08.0002
- Pallavi, Mishra, R. K., Sahu, P. K., Mishra, V., Jamal, H., Varma, A., & Tripathi, S. (2023). Isolation and characterization of halotolerant plant growth promoting rhizobacteria from mangrove region of Sundarbans, India for enhanced crop productivity. *Frontiers in Plant Science*, 14, 1122347. doi: 10.3389/fpls.2023.1122347
- Park, G., Oh, H.N., & Ahn, S. (2009). Improvement of the ammonia analysis by the phenate method in water and wastewater. *Bulletin of the Korean Chemical Society*, 30(9), 2032–2038. doi: 10.5012/BKCS.2009.30.9.2032.
- Park, K. H., Lee, O. M., Jung, H. I., Jeong, J. H., Jeon, Y. D., Hwang, D. Y., ... & Son, H. J. (2010). Rapid solubilization of insoluble phosphate by a novel environmental stress-tolerant *Burkholderia vietnamiensis* M6 isolated from ginseng rhizospheric soil. *Applied microbiology and biotechnology*, 86, 947-955. doi: 10.1007/s00253-009-2388-7
- Patel, M. V., & Patel, R. K. (2014). Indole-3-acetic acid (IAA) production by endophytic bacteria isolated from saline desert, the little Runn of Kutch. *CIBTech Journal of Microbiology*, 3(2), 2319-3867.
- Penrose, D. M., & Glick, B. R. (2003). Methods for isolating and characterizing ACC deaminase-containing plant growth-promoting rhizobacteria. *Physiologia plantarum*, 118(1), 10-15. doi: 10.1034/J.1399-3054.2003.00086.X
- Pineda, A., Zheng, S.J., van Loon, J.J., Pieterse, C.M., & Dicke, M. (2010). Helping plants to deal with insects: the role of beneficial soilborne microbes. *Trends in Plant Science* 15 (9), 507–514. doi: 10.1016/j.tplant.2010.05.007

- Prihatiningsih, N., Djatmiko, H. A., & Lestari, P. (2023). Consortium of endophytic bacteria application improves grain yield of rice. In *3rd International Conference on Sustainable Agriculture for Rural Development (ICSARD 2022)* (pp. 244-250). Atlantis Press. doi: 10.2991/978-94-6463-128-9_25
- Puri, A., Padda, K. P., & Chanway, C. P. (2017). Plant growth promotion by endophytic bacteria in nonnative crop hosts. *Endophytes: Crop Productivity and Protection: Volume 2*, 11-45. doi: 10.1007/978-3-319-66544-3_2
- Rahman, S.A., Sukenda, S., Widanarni, W., Alimuddin, A., & Ekasari, J. (2019). Isolation and identification of endophytic bacteria from the mangrove leaves of *Avicennia marina* and evaluation of inhibition to bacterium causing ice-ice disease. *AACL Bioflux*, 12, (3).
- Rahman, S.M., Donoghue, D.N.M., & Bracken L.J. (2021). Is soil organic carbon underestimated in the largest mangrove forest ecosystems? Evidence from the Bangladesh Sundarbans. *Catena* 200, 105159. doi: 10.1016/j.catena.2021.105159
- Rajkumar, M., Ae, N., Prasad, M. N. V., & Freitas, H. (2010). Potential of siderophore-producing bacteria for improving heavy metal phytoextraction. *Trends in biotechnology*, 28(3), 142-149. doi: 10.1016/j.tibtech.2009.12.002
- Ray, R., Majumder, N., Das, S., Chowdhury, C., & Jana, T. K. (2014). Biogeochemical cycle of nitrogen in a tropical mangrove ecosystem, east coast of India. *Marine Chemistry*, 167, 33-43. doi: 10.1016/j.marchem.2014.04.007
- Reef, R., Feller, I. C., & Lovelock, C. E. (2010). Nutrition of mangroves. *Tree physiology*, 30(9), 1148-1160. doi: 10.1093/treephys/tpq048
- Rivera-Monroy, V. H., & Twilley, R. R. (1996). The relative role of denitrification and immobilization in the fate of inorganic nitrogen in mangrove sediments (Terminos Lagoon, Mexico). *Limnology and Oceanography*, 41(2), 284-296. doi: 10.4319/lo.1996.41.2.0284
- Rizaludin, M. S., Stopnisek, N., Raaijmakers, J. M., & Garbeva, P. (2021). The chemistry of stress: understanding the 'cry for help' of plant roots. *Metabolites*, 11(6), 357. doi: 10.3390/metabo11060357
- Rodriguez, R. J., Henson, J., Van Volkenburgh, E., Hoy, M., Wright, L., Beckwith, F., ... & Redman, R. S. (2008). Stress tolerance in plants via habitat-adapted symbiosis. *The ISME journal*, 2(4), 404-416. doi: 10.1038/ismej.2007.106
- Rojas, A., Holguin, G., Glick, B. R., & Bashan, Y. (2001). Synergism between *Phyllobacterium* sp.(N₂-fixer) and *Bacillus licheniformis* (P-solubilizer), both from a semiarid mangrove rhizosphere. *FEMS Microbiology Ecology*, 35(2), 181-187. doi: 10.1111/j.1574-6941.2001.tb00802.x
- Rolfe, S. A., Griffiths, J., & Ton, J. (2019). Crying out for help with root exudates: adaptive mechanisms by which stressed plants assemble health-promoting soil microbiomes. *Current opinion in microbiology*, 49, 73-82. doi: 10.1016/j.mib.2019.10.003
- Rollins, D. M. (2000). The Gram Stain BSCI 424 PATHOGENIC MICROBIOLOGY, university of Maryland. *Department of cell biology and molecular genetics*.
- Ryan, R. P., Germaine, K., Franks, A., Ryan, D. J., & Dowling, D. N. (2008). Bacterial endophytes: recent developments and applications. *FEMS microbiology letters*, 278(1), 1-9. doi:10.1111/j.1574-6968.2007.00918.x
- Sadaiah, K., Veronica, N., Nagendra, V., Niharika, G., Neeraja, C. N., Surekha, K., ... & Sanjeeva, R. D. (2018). Methods of protein estimation and the influence of heat stress on Rice grain protein. *International Journal of Pure and Applied Bioscience*, 6, 159-168. doi: 10.18782/2320-7051.5733
- Saintilan, N. (1997). Above-and below-ground biomass of mangroves in a sub-tropical estuary. *Marine and Freshwater Research*, 48(7), 601-604. doi: 10.1071/MF97009

- Santoyo, G., Moreno-Hagelsieb, G., del Carmen Orozco-Mosqueda, M., & Glick, B. R. (2016). Plant growth-promoting bacterial endophytes. *Microbiological research*, 183, 92-99. doi: 10.1016/j.micres.2015.11.008
- Saravanakumar, D., & Samiyappan, R. (2007). ACC deaminase from *Pseudomonas fluorescens* mediated saline resistance in groundnut (*Arachis hypogea*) plants. *Journal of Applied Microbiology*, 102(5), 1283–1292. doi: 10.1111/J.1365-2672.2006.03179.X
- Shabanamol, S., Varghese, E.M., Thampi, M., Karthika, S., Sreekumar, J., & Jisha, M.S. (2020). Enhancement of Growth and Yield of Rice (*Oryza Sativa*) by Plant Probiotic Endophyte, *Lysinibacillus sphaericus* under Greenhouse Conditions. doi: 10.1080/00103624.2020.1751190
- Shakeel, M., Rais, A., Hassan, M. N., & Hafeez, F. Y. (2015). Root associated *Bacillus* sp. improves growth, yield and zinc translocation for basmati rice (*Oryza sativa*) varieties. *Frontiers in Microbiology*, 6, 166077. doi: 10.3389/fmicb.2015.01286
- Shiomi, H.F., Silva, H.S.A., de Melo, I.S., Vieira, N.F., & Bettiol, W. (2006). Bioprospecting endophytic bacteria for biological control of coffee leaf rust. *Scientia Agricola*. 63(1), 32-39. doi: 10.1590/S0103-90162006000100006
- Singh, R. P., & Jha, P. N. (2015). Plant growth promoting potential of ACC deaminase rhizospheric bacteria isolated from *Aerva javanica*: A plant adapted to saline environments. *Int. J. Curr. Microbiol. Appl. Sci*, 4, 142-152.
- Singh, N., & Raijin, P.S. (2004). Free radical scavenging activity of an aqueous extract of potato peel. *Food chemistry* 85(4), 611–616. doi: 10.1016/j.foodchem.2003.07.003
- Solo´rzano, L. (1969). Determination of ammonia in natural waters by the phenolhypochlorite method. *Limnology and Oceanography*, 14(5), 799–801. doi: 10.4319/lo.1969.14.5.0799
- Srikanth, S., Lum, S. K. Y., & Chen, Z. (2016). Mangrove root: adaptations and ecological importance. *Trees*, 30, 451-465. doi: 10.1007/s00468-015-1233-0
- Strobel, G., & Daisy, B. (2003). Bioprospecting for microbial endophytes and their natural products. *Microbiology and Molecular Biology Reviews* 67(4), 491–502. doi: 10.1128/MMBR.67.4.491-502.2003
- Takarina, N. D. (2020). Mangrove Root Diversity and Structure (cone, pencil, prop) Effectiveness in Accumulating Cu and Zn in Sediments and Water in River Blanakan. In *IOP Conference Series: Earth and Environmental Science* (Vol. 550, No. 1, p. 012009). IOP Publishing. doi: 10.1088/1755-1315/550/1/012009
- Tatongjai, S., Kraichak, E., & Kermanee, P. (2021). Comparative anatomy and salt management of *Sonneratiacaseolaris* (L.) Engl. (Lythraceae) grown in saltwater and freshwater. *PeerJ*, 9, e10962. doi: 10.7717/peerj.10962
- Thatoi, H., Behera, B. C., Dangar, T. K., & Mishra, R. R. (2012). Microbial Biodiversity in Mangrove soils of Bhitarkanika, Odisha, India. *International Journal of Environmental Biology*, 2, 50-58.
- Toledo, G., Bashan, Y., & Soeldner, A. (1995). In vitro colonization and increase in nitrogen fixation of seedling roots of black mangrove inoculated by a filamentous cyanobacteria. *Canadian Journal of Microbiology*, 41(11), 1012-1020.
- Tomlinson, P.B. (1986). *The Botany of Mangroves*. Cambridge University Press, Cambridge, 419. doi: 10.1017/S0266467400002017
- Tomlinson, P. B. (2016). *The botany of mangroves*. Cambridge University Press.
- Toth, S. J., & Prince, A. L. (1949). Estimation of cation-exchange capacity and exchangeable Ca, K, and Na contents of soils by flame photometer techniques. *Soil science*, 67(6), 439-446. doi: 10.1097/00010694-194906000-00003

- Usuki, F., & Narisawa, K. (2007). A mutualistic symbiosis between a dark, septate endophytic fungus, *Heteroconium chaetospora* and a nonmycorrhizal plant, Chinese cabbage. *Mycologia*, 99(2), 175–184. doi: 10.3852/mycologia.99.2.175
- Verma, S. K., Sahu, P. K., Kumar, K., Pal, G., Gond, S. K., Kharwar, R. N., & White, J. F. (2021). Endophyte roles in nutrient acquisition, root system architecture development and oxidative stress tolerance. *Journal of Applied Microbiology*, 131(5), 2161-2177. doi: 10.1111/jam.15111
- Vinoth, R., Kumaravel, S., & Ranganathan, R. (2019). Anatomical and physiological adaptation of mangrove wetlands in east coast of Tamil Nadu. *World Scientific News*, (129), 161-179.
- Vovides, A. G., Wimmeler, M. C., Schrewe, F., Balke, T., Zwanzig, M., Piou, C., ... & Berger, U. (2021). Cooperative root graft networks benefit mangrove trees under stress. *Communications Biology*, 4(1), 513. doi: 10.1038/s42003-021-02044-x
- Walia, A., Guleria, S., Chauhan, A., & Mehta, P. (2017). Endophytic bacteria: role in phosphate solubilization. *Endophytes: Crop Productivity and Protection: Volume 2*, 61-93. doi: 10.1007/978-3-319-66544-3_4
- Waller, F., Achatz, B., Baltruschat, H., Fodor, J., Becker, K., Fischer, M., ... & Kogel, K. H. (2005). The endophytic fungus *Piriformospora indica* reprograms barley to salt-stress tolerance, disease resistance, and higher yield. *Proceedings of the National Academy of Sciences*, 102(38), 13386-13391. doi: 10.1073/pans.0504423102
- Zabalgogezcoa, Í., Ciudad, A. G., de Aldana, B. R. V., & Criado, B. G. (2006). Effects of the infection by the fungal endophyte *Epichloë festucae* in the growth and nutrient content of *Festuca rubra*. *European journal of agronomy*, 24(4), 374-384. doi: 10.1016/j.eja.2006.01.003

Publications

1. List of publications:

- 1.1** The book chapter titled “An account of coastal diverse mangroves of North Indian Ocean countries with a focus to species richness in relation to sediment biogeochemical cycling: Case study from Indian Sundarbans mangrove” co-authored by Krishna Ray, Sandip Kumar Basak, Chayan Kumar Giri, Anup Mandal, Hemendra Nath Kotal, Subhajit Saha, Sumana Mondal, **Biswajit Biswas**, Bhanumati Sarkar, Ipsita Das, Rudranil Sengupta, Anjali Ghosh, Rajojit Chowdhury, Mst. Momtaj Begam, Chandan Mukherjee and Tapan Sutradhar has been accepted for publication in the book titled ‘Biogeochemistry of the coastal Indian Ocean’ to be published by Springer Nature as part of Book Series Atmosphere, Earth, Ocean and Space. **Biogeochemistry of coastal Indian Ocean, AEONS Series (print ISSN 2524-440X).**
- 1.2** Manuscript titled “Estuarine mangrove niches select cultivable heterotrophic diazotrophs with diverse metabolic potentials - A prospective cross-dialogue for functional diazotrophy” co-authored by Sumana Mondal[†], **Biswajit Biswas[†]**, Rajojit Chowdhury[†], Rudranil Sengupta[†], Anup Mandal, Hemendra Nath Kotal, Chayan Kumar Giri, Subhajit Saha, Mst. Momtaj Begam, Chandan Mukherjee, Ipsita Das, Sandip Kumar Basak, Mahasweta Mitra Ghosh, Krishna Ray has been communicated to Frontiers in Microbiology and under revision at present.

REVIEW FORUM Corresponding Author [Need Help ? Contact us](#)

✓ 1. Initial Validation

✓ 2. Editorial Assignment

✓ 3. Independent Review

7. Final Decision

4. Interactive Review

Estuarine mangrove niches select cultivable heterotrophic diazotrophs with diverse metabolic potentials -A prospective cross-dialogue for functional diazotrophy

Sumana Mondal , Biswajit Biswas , Rajojit Chowdhury , Rudranil Sengupta , Anup Mandal , Hemendra Nath Kotal , CHAYAN KUMAR GIRI , Subhajit Saha , Mst Momtaj Begam , Chandan Mukherjee , Ipsita Das , Sandip Kumar Basak , Mahasweta Mitra Ghosh and Krishna Ray *

Original Research, Front. Microbiol. - Aquatic Microbiology


Received on: 19 Oct 2023, Edited by: [Camila Fernandez](#) ✉


Manuscript ID: 1324188


Research Topic: [Women in Aquatic Microbiology: 2023](#)


Scope Statement: This manuscript is aimed for the Frontiers in ... [more](#)


Keywords: biological nitrogen fixation, Free-living heterotrophic diazotroph, Estuarine mangrove ecosystem, Indian Sundarbans, stringent narrow niche, multidimensional specialization


 Download latest manuscript

 Supplementary materials

 View submitted files history

 Request extension

 View invoice

 **ON TIME**

Submit your comments to the Reviewer(s) and re-submit a new version of your manuscript. Manuscript quality indicators are available to all participants in the [AIRA](#) tab to facilitate the peer review process.

You are pending to respond to Reviewer 2 and Reviewer 3 and/or resubmit a new version of your manuscript.



भारतीय विज्ञान शिक्षा एवं अनुसंधान संस्थान कोलकाता

(भारत सरकार के मानव संसाधन विकास मंत्रालय द्वारा स्थापित एक स्वायत्तशासी संस्थान)

INDIAN INSTITUTE OF SCIENCE EDUCATION AND RESEARCH KOLKATA

(An autonomous Institute established by Ministry of Education, Government of India)

Date: 11th May, 2023.

TO WHOM IT MAY CONCERN

The chapter titled '**An account of coastal diverse mangroves of North Indian Ocean countries with a focus to species richness in relation to sediment biogeochemical cycling: Case study from Indian Sundarbans mangrove**' co-authored by Krishna Roy, Sandip Kumar Basak, Chayan Kumar Giri, Anup Mandal, Hemendra Nath Kotal, Subhajit Saha, Sumana Mondal, Biswajit Biswas, Bhanumati Sarkar, Ipsita Das, Rudranil Sengupta, Anjali Ghosh, Rajojit Chowdhury, Mst. Momtaj Begam, Chandan Mukherjee and Tapan Sutradhar has been accepted for publication in the book titled '**Biogeochemistry of the coastal Indian Ocean**' to be published by Springer Nature as part of Book Series Atmosphere, Earth, Ocean and Space.

Professor Punyasloke Bhadury,
Editor, Biogeochemistry of the coastal Indian Ocean.

Estuarine mangrove niches select cultivable heterotrophic diazotrophs with diverse metabolic potentials -A prospective cross-dialogue for functional diazotrophy

Sumana Mondal¹, Biswajit Biswas^{2, 1}, Rajojit Chowdhury¹, Rudranil Sengupta¹, Anup Mandal¹, Hemendra N. Kotal¹, CHAYAN K. GIRI¹, Subhajit Saha¹, Mst Momtaj Begam¹, Chandan Mukherjee¹, Ipsita Das¹, Sandip Kumar Basak³, Mahasweta Mitra Ghosh², Krishna Ray^{1*}

¹West Bengal State University, India, ²St. Xavier's College, India, ³Sarat Centenary College, India

Submitted to Journal:
Frontiers in Microbiology

Specialty Section:
Aquatic Microbiology

Article type:
Original Research Article

Manuscript ID:
1324188

Received on:
19 Oct 2023

Revised on:
04 Nov 2023

Journal website link:
www.frontiersin.org

Papers presented in National Seminars:

1. “Culturable community of root endophytic bacteria in Indian Sundarban mangrove species demonstrate high potential for plant growth promoting activities under laboratory conditions” Biswajit Biswas, Sumana Mondal, Mahasweta Mitra Ghosh, Sandip Kumar Basak and Krishna Ray. National Virtual Conference on “Genomics to Phenomics: A New Horizon in Plant Science Research” (NVC-2021), Department of Botany, University of Calcutta, 28th February -1st March, 2021.

2. “Halophytic grasses and rice rhizosphere in Indian Sundarbans are habitat of nutrient cycling bacteria having high potential of plant growth promotion”

Sumana Mondal, Biswajit Biswas, Sandip Kumar Basak and Krishna Ray. National Virtual Conference on “Genomics to Phenomics: A New Horizon in Plant Science Research” (NVC-2021), Department of Botany, University of Calcutta, 28th February -1st March, 2021.

3. “Diversity of root endophytic bacteria of mangroves, plant growth promotion at lab and at rice fields of Indian Sundarbans”. Biswajit Biswas, Sumana Mondal, Chayan Kumar Giri, Mahasweta Mitra Ghosh, Sandip Kumar Basak and Krishna Ray. National Seminar on “Biodiversity Conservation & Sustainable Development-with a sense of urgency to combat desertification and climate change”. April 22-23, 2022. Sarat Centenary College, Dhaniakhali, Hooghly, WB, PIN-712302.